

# Indian Journal of Physics

Vol. IX

AND

PROCEEDINGS

OF THE

Indian Association for the Cultivation of Science

Vol. XVIII.



Board of Editors

D. M. BOSE, Ph.D.

P. N. GHOSH, Ph.D.

S. K. MITRA, D.Sc., *Secretary*.

(With Ten Plates).

Printed at the Calcutta University Press, Senate House,  
Calcutta, by Bhupendralal Banerjee and published  
by the Secretary, Indian Association  
for the Cultivation of Science,  
210, Bow-Bazar Street, Calcutta.

1934-35

Price 12 Rupees or 16 Shillings or 4·5 Dollars.





### 1. *Magnetic Studies.*

In the last Report we gave a detailed account of some magne-crystallic measurements made in this laboratory. These measurements have been widely extended, and more than eighty single crystals, both diamagnetic and paramagnetic, have been studied by Messrs. Santilal Banerjee and Asutosh Mookherjee. A new method has been developed for the purpose, which is quite as simple and accurate as the oscillational method previously adopted by us, but has the further advantage of being applicable to even such small crystals as weigh less than a milligram.

The results of these magnetic studies are in course of publication in the Philosophical Transactions of the Royal Society, and a review of this work will appropriately belong to the next Report ; we will confine ourselves here to a few of the results which have already been published. Taking for example *s*-triphenylbenzene, earlier X-ray measurements suggested that all the benzene rings in the crystal are oriented parallel to one of the crystallographic planes, whereas, from a later and more complete X-ray analysis, Mrs. Lonsdale and Orelkin concluded that the benzene planes cannot all be parallel to one another. This point is easily settled by the magnetic measurements, which, besides confirming the latter conclusion, further enable us to calculate the actual inclinations of the benzene rings.

The orientations of the  $\text{CO}_3$  groups in ammonium carbonate crystal have also been determined by Mr. Mookherjee in the same manner from the magnetic data. These data further show that the structure of the  $\text{CO}_3$  group in this crystal is practically the same as in the normal carbonates like calcite and aragonite.

The magnetic measurements on single crystals of graphite by Messrs. B. C. Guha and B. P. Roy deserve special mention here. Graphite crystal occurs in nature in the form of thin

## PART I.

### REPORT ON SCIENTIFIC INVESTIGATIONS.

The investigations carried out during the year may be classed under the following heads :—

1. Magnetic studies on single crystals of diamagnetic substances in relation to the orientations of molecules in the crystal lattice, and of paramagnetic salts in relation to crystalline fields.
2. Studies on the physics and chemistry of crystals : polarized absorption by aromatic hydrocarbons containing condensed benzene nuclei, preferential orientations of included molecules in crystals, photodissociation in crystals in relation to their pleochroism, etc.
3. Other optical investigations, e.g., optical properties of thin films, the screening constants and optical polarizabilities of molecules, etc.
4. X-ray analysis of the structure of organic crystals.
5. Studies on the Raman effect in its various aspects, e.g., the measurement of the intensities of the scattered lines and of their polarizations and the influence of electric field on them, their dependence on the frequency of the exciting light ; applications of the Raman effect to the study of chemical reactions and to the elucidation of the structure of simple molecules.
6. Extensive studies, both theoretical and experimental, on the light scattering and X-ray diffraction by binary liquid mixtures, in relation to their constitution.

hexagonal plates. Some exceptionally well developed single crystals from Ceylon were available, and were found to exhibit remarkable magnetic properties. Whereas along directions in the cleavage plane of the crystal its diamagnetic susceptibility is only  $-0.4$  to  $-0.5 \times 10^{-6}$  per gm, that along the normal to the plane is abnormally large, being as high as  $-22 \times 10^{-6}$ , i.e., more than 40 times the value in the former directions. This abnormal unidirectional diamagnetism can be traced to its peculiar structure, and some recent unpublished experiments by Mr. Ganguli throw interesting light on its origin.

*Solutions of Manganous Salts* :—Some accurate measurements on the magnetic susceptibilities of aqueous solutions of manganous salts of different concentrations and at various temperatures, have been made by Mr. Akshayananda Bose. The special interest of these solutions is that the magnetic moment of the  $Mn^{+2}$  ion is due wholly to the spin moments of the electrons in its incomplete shell, their resultant orbital moment being nothing. For such ions the theory is very simple: their susceptibilities should be inversely proportional to the absolute temperature, and the constant of proportionality can also be calculated theoretically. But curiously, the available experimental data on temperature variation of susceptibility of  $Mn^{++}$  ions in aqueous solution do not conform to the theory.

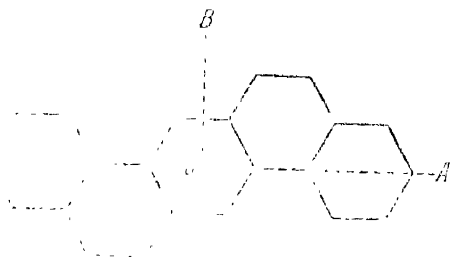
Bose's measurements were undertaken with a view to explain this discrepancy. He finds that the susceptibilities of the manganous ions in aqueous solution do obey the inverse temperature law, and further that their absolute values are exactly as predicted by theory.

## 2. *Physics and Chemistry of Crystals.*

*Polarized absorption by single crystals*.—One characteristic feature of organic crystals is that its constituent molecules retain their individuality, i.e., they are present in the crystal as separate entities. (This is not, however, the case with many

inorganic crystals.) This circumstance enables us to get an insight into the properties of individual molecules from a study of the corresponding properties of the crystal. In particular, those properties of the molecule which are strikingly different for different directions in the molecule, are conveniently studied in this manner.

We shall take as an example the well-known cancer producing substance, 1, 2; 5, 6—dibenzanthracene. From X-ray studies on this substance, which crystallizes in the form of extremely thin flakes, Iball and Robertson of the Royal Institution of London, have fixed the structure of the molecule. It consists of five plane hexagonal rings arranged as in the figure,



The X-ray studies further show that in the crystal all the molecules of dibenzanthracene are orientated parallel to one another, with their long axes OA perpendicular to the plane of the crystal flake. Magnetic measurements made in this laboratory by Mr. Santilal Banerjee and the present writer also point out to the same conclusion. Thus in the plane of the crystal flake there are two mutually perpendicular directions one of which, say  $a$ , is parallel to the breadth OB of the molecules, while the other, say  $b$ , is along the normal to the molecular planes. By allowing polarized white light to traverse the crystal, and analyzing the transmitted light with a spectroscope, it is found by Mr. P. K. Seshan and the present writer (1) that the *positions* of the absorption

shows some extra bands as compared with that of specially purified specimens. According to Winterstein, these extra bands can be identified, from their positions, and from other evidence, as due to the presence of extremely small quantities, of the order of 1 part in a hundred thousand, of the compound naphthacene.

It would be of interest to find how the flat long molecules of this impurity are accommodated in the crystal lattice. The absorption measurements with polarized light supply a definite answer, and they show that the parasitic naphthacene molecules take up orientations practically parallel to those of the main substance.

Inclusions of naphthacene in chrysene, and of fluorene in diphenyl, have also been studied, and we again find a similar parallism in orientation of the impurity molecules and those of the main substance that accommodates them.

*Photo-dissociation of crystals* : The theoretical explanation of the absorption spectra of organic crystals presents serious difficulties in view of their complexity. From this point of view some of the inorganic salts are much simpler. Taking for example the nitrates, it is found that they all have two absorption bands, one very strong, having its long wave-length limit at about  $235m\mu$ , and the other, much feebler, having its long wave-length limit at  $350 m\mu$ . The fact that the positions of these two bands are practically the same in aqueous solutions, in the fused state, and in the solid state, suggests that the absorptions should be characteristic of the nitrate ion. Following the explanation of Henri, Datta and others of the continuous absorption of some oxides, these two absorption bands have been attributed by Mr. A. C. Guha and the present writer to the photo-dissociation of the nitrate into the corresponding nitrite and an oxygen atom in

bands for vibrations along the  $a$  and the  $b$  axes are practically identical, and are nearly the same as in the absorption spectrum of dilute solutions of the substance. This is a further proof that the molecules in the crystal retain their identity. (2) Though the *positions* of  $a$  and  $b$  absorptions are identical, the  $a$  absorption is considerably more intense than  $b$ . It is thus plain that the molecule of dibenzanthracene is capable of absorbing vibrations along its width much more strongly than vibrations along the normal to their planes.

A large number of aromatic hydrocarbons containing condensed benzene nuclei and having more or less a plane structure, have been studied similarly as single crystals for the polarization of their absorption bands, e.g., naphthalene, anthracene, phenanthrene, chrysene, pyrene, fluoranthene, etc. The orientations of the molecules in these crystals are known from X-ray and magnetic studies. Interpreting the results in the same manner as before, we obtain the interesting result that in all these molecules light vibrations along the normal to the molecular planes are much less absorbed than vibrations in the plane. The former vibrations correspond also to a smaller refractive index.

*Orientations of parasitic molecules included in crystals:* Conversely, in aromatic crystals for which the molecular orientations are not already known from X-ray or magnetic data, the above property can be conveniently utilized for obtaining information regarding the orientations of the benzene rings in the crystal lattice. This method has been used by us to find out the orientations of foreign molecules which are sometimes included as impurities in crystals. Taking for example the well-known substance anthracene, ordinarily pure crystals of this substance show three strong absorption bands at the blue end of the spectrum, which are almost absent from very carefully purified specimens. The fluorescence of ordinarily pure anthracene also

the normal and in the excited state respectively. Doing so we find that the long wave-length limits of the two absorption bands correspond to (1) a heat of dissociation of the oxygen molecule into two normal oxygen atoms, equal to 114 k. cal. per gm. molecule, which is in good agreement with 114.6 k. cal. obtained by other methods ; (2) an energy of excitation of the oxygen atom to its D level, equal to 43 k. cal. per gm. atom, as compared with 45.1 k. cal. obtained from spectroscopic data. That the value for these two quantities come out of the proper magnitude lends support to the photo-chemical origin of the bands suggested above.

Accepting then the photo-chemical explanation for the absorptions in the crystalline state also, the observation made by Mr. Dasgupta and the present writer that in single crystals of sodium and potassium nitrates, in which the nitrate ions are all orientated parallel to one another, light-vibrations in the plane of the  $\text{NO}_3$  ions are much more strongly absorbed than vibrations along the normal to the plane, immediately suggests that the former vibrations should be photo-chemically more efficient than the latter. This result has recently been verified by Mr. Narayanaswamy, who has studied the dissociation of other crystals also, under the action of polarized light. These experimental studies are in course of publication, and will be reviewed in the next report.

### 3. *Other Optical Investigations.*

#### *Interference phenomena observed with crystal plates :*

Among other optical studies we should mention here an interesting interference phenomenon observed with crystal plates. The Haidinger rings obtained with a thin optically worked glass plate in mono-chromatic light are very familiar to students of physics. If instead of glass, a plate of mica is substituted, due to double-refraction by the mica plate, there appear

two sets of elliptic rings, which are slightly differently spaced. These fringes were first studied in this laboratory by Mr. Chinmayanandam several years ago. Owing to this unequal spacing the fringes will be very distinct in regions where they are exactly in step and indistinct in regions where they are out of step. These regions of maxima or minima of visibility lie on certain geometrical curves, which are the same as the regions of dark or bright bands observed with a plate of double the thickness under the microscope between crossed nicols.

In these experiments of Chinmayanandam the incident light is monochromatic, and the variation in the path retardation introduced by the plate arises from the direction of observation being different for the different fringes. There is an interesting variation of this experiment, made recently by Mr. Sundararajan, viz., to allow polarized white light to be incident normally on the crystal plate and analyze the transmitted light after passing through a nicol with a spectroscope. Here the actual distance traversed in the crystal is the same for all the wave-lengths, but the differences in optical path arise from variation of the refractive index with wave-length; so that the spectrum will be crossed by a number of bright and dark interference bands. Here again, due to the double-refraction of the plate, there will be two sets of fringes of different spacing, and consequently positions of maxima and minima of visibility, which again will be the same as the usual birefringence fringes obtained with a plate of double the thickness between crossed nicols. For the details, which are rather technical, the reader is referred to the original paper in the "Indian Journal of Physics."

*Optical constants of the naphthalene molecule:* Any precise data for individual molecules are always of interest. The principal optical constants of some symmetric molecules



like oxygen, carbon dioxide, benzene, etc., have been calculated from their light scattering and refraction. When the molecule has no axis of symmetry, the calculation is difficult and requires a knowledge of other physical constants, e.g., electric or magnetic double-refraction. The constants for the naphthalene molecule have been calculated in this manner, and they are strikingly different for different directions in the molecule. For example, along the length of the molecule the optical polarizability is more than double that along the normal to its plane.

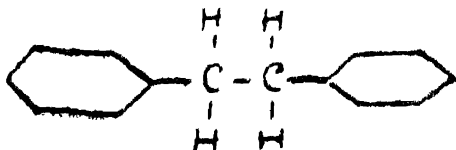
Before closing this section on molecular optics we should refer to an interesting paper by Dr. P. Das in the "Indian Journal of Physics"; from certain simple structural considerations, Dr. Das has been able to calculate the screening constants of molecules, which agree with those calculated by more elaborate methods..

*Thin Films* : Prof. Wood recently discovered some remarkable optical properties exhibited by thin films of alkali metals in the ultra-violet. These phenomena have been explained on the basis of the electron theory, but it was found that the number of effective electrons required for quantitative explanation is less than the actual number. Mr. Mukhopadhyaya points out that the theory concerns with an extensive medium, and it is known that as the linear dimensions of the medium are gradually diminished so as to approach the mean free path of the electrons, the influence of the limiting boundaries is in effect equivalent to diminishing the number of electrons per unit volume. When this is taken into account, Mr. Mukhopadhyay finds that the discrepancy referred to above between the calculated and the observed values disappears.

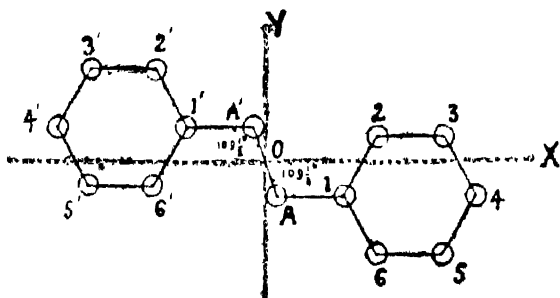
#### 4. *X-Ray Analysis of the Structure of Organic Crystals.*

Investigations are also being carried on in the laboratory on the structural analysis of organic crystals by X-ray methods

by Dhar, Guha and Mukhopadhyaya. We shall mention here only the recent analysis by Dhar of the structure of the interesting crystal dibenzyl. The molecule of dibenzyl is generally assigned, on the basis of chemical evidence, the structure,



A preliminary X-ray study of this crystal was first made by Hengstenberg and Mark, who found that the molecule possesses a centre of symmetry. Magnetic studies by Banerjee gave some useful information on the orientation of the benzene rings in the crystal-lattice. From intensity measurements on reflections from about ten planes, Mr. Dhar obtained the following results. The six carbon atoms of each benzene ring form a regular hexagon, with its sides equal to  $1.41 \text{ \AA}$ .



One of the aliphatic carbon atoms, viz., C, lies on the prolongation of the line joining the atoms 4 and 1, and the other on the

line joining 4' and 1' (adopting the usual notation). The line joining C and C' makes with each of the above lines the usual tetrahedral angle of  $109\frac{1}{2}^\circ$ . The two benzene rings are practically, but not quite, in the same plane.

As regards the orientations of the molecules in the unit cell, it is found that the OX axes of both the molecules in the cell lie in the (010) plane, at  $32^\circ$  to 'a' axis in the obtuse angle  $\beta$ . The OY axes are inclined at plus and minus  $60^\circ$  respectively to the b(010) plane. These orientations are almost the same as those given by the magnetic data.

At about the same time, and quite independently, Dr. Robertson, working at the Royal Institution, London, with much more extensive data for the intensities of X-ray reflections has arrived at a different conclusion regarding the shape of the molecule. As before the atoms 4, 1 and C are collinear, as also the atoms C', 1' and 4'; the angles at C and C' are also tetrahedral as before. But the plane containing the lines 4, 1, C and C', 1', 4' is perpendicular to the planes of the benzene rings instead of being parallel to the benzene planes as in Dhar's model. The molecular orientations in the unit cell suggested by him are also naturally different from those obtained by Dhar.

Using the more extensive experimental data of Dr. Robertson, Dhar finds that the configuration suggested by him fits with the new values almost, but not quite, as satisfactorily as Robertson's molecule. Dhar's analysis has, however, the advantage of being in conformity with the magnetic results, whereas Robertson's orientations definitely disagree with them.

The work is being continued with a view to remove the discrepancy between Robertson's results and Dhar's.

*List of Papers published during the year 1934.*

## Indian Journal of Physics.

1. Studies in Light-Scattering by Binary Liquid Mixtures : By S. Parthasarathy.
2. The Principal Magnetic Susceptibilities of Graphite : By B. C. Guha and B. P. Roy.
3. The Effect of Electric Field on the Polarisation of Raman Lines : By S. C. Sirkar.
4. On the Dispersion of Polarisation of Raman Lines : By S. C. Sirkar.
5. The Principal Optical Polarizabilities of the Naphthalene Molecule : By K. S. Krishnan.
6. X-Ray Analysis of the Structure of Dibenzyl : By Jagattaran Dhar.
7. On Molecular Screening Constants : By Panchanon Das.
8. The Valency Angles of Oxygen and Sulphur : By N. Gopala Pai.
9. A New Interference Phenomenon observed with Crystalline Plates : By K. S. Sundararajan.
10. The Relative Intensities of the Raman and the Rayleigh Lines in Light Scattering : By Jagattaran Dhar.

*Nature,*

11. The Magnetic Anisotropy of Graphite : By K. S. Krishnan.
12. The Weiss Constant of Paramagnetic Ions in the S-State : By Akshayananda Bose.
13. Crystal Structure of 1,3,5-Triphenylbenzene : By K. S. Krishnan and S. Banerjee.

*Current Science.*

14. The Valency Angle of Oxygen in Ethylene Oxide : By N. Gopala Pai.
15. Photo-Dissociation of the  $\text{NO}'_3$  Ion and its Dependence on the Polarisation of the Exciting Light-Quantum : By K. S. Krishnan and A. C. Guha.
16. X-Ray Analysis of the Crystal Structure of Dibenzyl : By Jagattaran Dhar.
17. Absorption Spectra of Single Crystals of Polynuclear Hydrocarbons : By K. S. Krishnan and P. K. Seshan.
18. Refractive Index of Thin Films of Potassium : By B. Mukhopadhyaya-

*Philosophical Magazine.*

19. The Raman Effect in Study of Chemical Reactions : By S. Parthasarathy.
20. X-Ray Diffraction in Liquid Mixtures : By S. Parthasarathy.

*Proceedings of the Indian Academy of Sciences.*

21. Raman Effect in Selenic Acid and Some Selenates : By A. S. Ganesan.
22. Absorption Spectra of Nitrates and Nitrites in Relation to their Photo-Dissociation : By K. S. Krishnan and A. C. Guha.

*Physical Review.*

23. Large Artificial Crystals of Graphite: By K. S. Krishnan.
24. The Orientations of the  $\text{CO}_3$ -Groups in Ammonium Bicarbonate Crystal: By Asutosh Mookherjee.

*Zeitschrift für Kristallographie.*

25. Orientations of Impurity Molecules in Crystals: By K. S. Krishnan and P. K. Seshan.

## PART II.

## ADMINISTRATIVE REPORT.

*Our Research Workers.*

Facilities for research were provided during the year to 28 research scholars from various parts of India. Mr. S. W. Chinchalkar, one of our research scholars was awarded the Doctorate Degree in Science of the Nagpur University for his work on magneto-optics. Mr. Jagattaran Dhar was appointed as acting Professor of Physics in St. Paul's College.

In addition to the usual colloquium lectures, courses of special lectures were delivered by the late Dr. Panchanon Das on Band Spectra, by Dr. Sukumar Chandra Sircar on Mathematical Crystallography, and by Dr. Satya Prakash on the Physics and Chemistry of Colloids.

*Lecture Arrangements.*

Regular courses of lectures in Physics and Chemistry for the benefit of students were delivered at the Association with the aid of our apparatus and demonstrators.

*Laboratory Equipments.*

The following additions have been made during the year to our stock of Apparatus :—

1. One Hartmann and Braun Zelton scale for galvanometer.
2. Three small achromatic objectives.
3. Three Ramsden eye-pieces.
4. Three micrometer eye-piece scales.
5. One Baly absorption tube.
6. One quartz-window lamp with spiral filament.
7. One pair X-ray protective goggles.
8. Two Bench type ammeters.
9. One oil-immersed transformer, primary 150 volts, secondary 3000 and 5000 peak voltages.
10. 16" Pressure gauge 4000 for liquid air machine.
11. 1 Hilger photo-measuring micrometer with stainless steel slides.
12. 1 Quartz Wollaston prism, 25 mm.  $\times$  25 mm.

*Workshop.*

The following apparatus were made during the year under report by the Mechanics in the Workshop of the Association :—

1. One safety red lamp with electric fittings.
2. One vessel with electric motor driven stirrer.
3. One pair solenoids.
4. One pair angular, and one pair plane pole pieces, for electromagnet.
5. One solid brass stand with two special boss heads.
6. One small rotating sector photometer.
7. Three short-focus telescopes, with graduated circles (lenses purchased).
8. Two special stands for the short focus telescopes.

9. One circular lamp and scale arrangement.
10. One brass boss head special.
11. Two air ovens with long burners.
12. One X-ray tube stand.
13. One X-ray target for Shearer tube.
14. Two search coils.
15. One big size attracted disc electrometer.
16. One pair brass disc electrodes for above.
17. One pair brass electrodes for inhomogeneous field.
18. An arrangement for mounting crystals on spectro-scope table.
19. A set of six metal tubes for grinding crystals into spheres.
20. Adapter for filling air at high pressure to cylinders from liquid air machine.
21. Three torsion heads with graduated circles.
22. One big size electromagnet.
23. One apparatus fitted with electric motor for rotation and oscillation arrangement combined, for X-Ray crystal work.
24. One crystal holder for testing pyro-electric effect.

Besides the above instruments, several laboratory fittings repairing of instruments, and valve seats, and setting up pressure gauges of the liquid air machine were taken up and executed by the mechanics of the Workshop.

#### *Library and Reading Room.*

The following publications were subscribed for as usual:—

1. Scientific American.
2. Nature.
3. Science Abstracts, A & B.
4. American Journal of Science.
5. Philosophical Magazine.



6. Astrophysical Journal.
7. Proceedings of the Royal Society A.
8. Proceedings of the Royal Institution of Great Britain.
9. Transactions of the Royal Society A.
10. Physical Review.
11. The Review of Scientific Instruments.
12. Physikalische Berichte.
13. Zeitschrift für Physik.
14. Annalen der Physik.
15. Physikalische Zeitschrift.
16. Journal of the American Chemical Society.
17. Journal of Physical Chemistry.
18. Proceedings of the National Acedemy of Sciences, Washington.
19. Zeitschrift für Physikalische Chemie, A & B.
20. Zeltschrift für Kristallographie A & B.
21. Annales de Physique.
22. Comptes Rendus.
23. Chemical Abstracts.
24. Revue de Optique.
25. Science Progress.
26. Naturwissenschaften.
27. Journal of the Chemical Society of London.
28. British Chemical Abstracts, A.
29. Transactions of the Faraday Society.
30. Zeitschrift für Astrophysik.

The following is addition and in

31. Journal of Chemical Physics.
32. Physics.
33. Review of Modern Physics.

We acknowledge with thanks the presentation of journals and periodicals in exchange for our Proceedings from the following Societies and Institutions.—

1. The Smithsonian Institution, Washington.
2. Cambridge Philosophical Society.
3. Physico-Mathematical Society, Tokyo.
4. Manchester Literary and Philosophical Society.
5. American Philosophical Society.
6. University of Illinois.
7. Academie der Wissenschaften, Leipzig.
8. The Franklin Institute,
9. South African Association for the Advancement of Science.
10. The Prussian Academy of Sciences, Berlin.
11. University of Philadelphia.
12. The Physical Society of France.
13. Bureau of Standards, Washington.
14. University of Iowa.
15. University of Calcutta.
16. Calcutta Mathematical Society.
17. Indian Chemical Society.
18. Reale Accademia Nazionale dei Lincei, Rome.
19. Societe de Physique et d'Histoire-Naturelle, Geneva.
20. Bayrischen Akademie der Wissenschaften, Munchen,
21. Der Gesellschaft der Wissenschaften, Gottingen.
22. Imperial Agricultural Institute, Pusa,
23. The Asiatic Society of Bengal.
24. The Indian Institute of Science, Bangalore
25. The Geological Survey of India.
26. Academy of Sciences, Cracow.
27. University of Brazil.
28. University de la Bruera.
29. Academy of Sciences, Leningrad.

30. University of Durham.
31. Royal Academy of Sciences, Amsterdam.
32. Imperial Academy, Tokyo.
33. Royal Meteorological Society, London.
34. University of Frankfurt-a-Main.
35. Royal Dublin Society.
36. Tohoku Imperial University.
37. Institute of Physical and Chemical Research, Japan.
38. Royal Academy of Sciences, Copenhagen.
39. Kodaikanal Observatory.
40. College of Science, Kyoto.
41. National Research Council, Japan.
42. Academy of Sciences, Vienna.
43. Society Chimique, Zagreb.
44. Hungary University (Szeged).
45. Ungarische Akademie, Budapest.
46. American Chemical Society (Industrial & Engineering Chemistry, Industrial Edition).
47. Della Societa Italianna di Fisica.
48. Societe de Chimie-Physique, Paris,
49. Mathematikaies Physikai Akademia, Budapest.
50. National Physical Laboratory of London.
51. Nederlandsch Tijdschrift Voor Naturkunde.
52. Physical Society of London.
53. Comite de Revue General des Science,
54. Editor of 'Physique Theorique'.
55. University of Upsala.
56. University of California.
57. Wissenschaftliche Veroffentlichungen aus dem Siemens Konzern.
58. Societe Polanaise de Physique, Warszawa.
59. Societo Vaudoise des Sciences Naturelles, Lausanne.
60. United States Department of Agriculture.

61. The Editor of 'Terrestrial Magnetism and Atmospheric Electricity'.
62. De L' Institute Pasteur, Paris.
63. Swiss Physical Society.
64. Canada Geological Survey.
65. Society Polonaise des Naturalistes Kopernik.
66. Deutschen Naturwissenschaftlich-Medizinischen Verein für Böhmen "Lotos" (Prag).
67. The Institute of Physics, London.
68. The National Research Council, Washington.
69. The Chinese Chemical Society.
70. National Tsing Hua University, Peiping.
71. The Shanghai Science Institute, Shanghai.
72. The Editors, Current Science.
73. The Massachusetts Institute of Technology, Cambridge, Massachusetts.
74. The Marine Biological Laboratory, Lancaster Pr.
75. The Royal Society of Canada, Ottawa.
76. The American Institute of Physics, New York.
77. Institut des Recherches Biologiques, Saimka, Perm.
78. Societati Romane de Fizica, Bucarest.
79. Societatis Scientiarum Fennica, Gelsingfors.
80. Natur und Volk, Frankfurt a.M.
81. The Academy of Sciences of the U. S. S. R. (For "Bulletin of the Far Eastern Branch of Academy of Sciences of the U. S. S. R." & "Physikalische Zeitschrift der Sowjetunion").
82. Tokyo University of Literature & Science, Koishikawa, Tokyo.
83. The Indian Academy of Sciences, Bangalore.
84. University of Leiden.
85. Technical Physics of the U. S. S. R. (Leningrad).

*List of Books purchased during 1934.*

1. The Metallic State—By W. Hume Rothery.
2. The Covalent Link in Chemistry—By Sidgwick.
3. The Crystalline State—By Sir W. H. Bragg & W. L. Bragg.
4. The Theory of Atomic Collisions—By Mott & Massey.
5. Resonance Radiation & Excited Atoms—By Mitchell & Zemansky.
6. Molekulstruktur—By H. A. Stuart.
7. Grundlagen der Photo-Chemie—By Bonhoeffer & Harteck.

## OBITUARY.

It is with a deep sense of regret and sorrow that we announce the loss the Association has sustained by death of the following members.

1. Dr. Ganesh Prasad, D.Sc.

*Vice President.*

2. Dr. S. K. Mookerjee, D.Sc.

*Member of the Committee of Management.*

3. Dr. Panchanon Das, D.Sc.

*Life Member.*

### Number of Members.

At the commencement of session, we had 126 Life members, 9 Ordinary Resident and 8 Ordinary Non-resident members. Total 143.

At the end of the session we had 123 Life Members, 8 Ordinary Resident and 7 Ordinary Non-resident members. Total 138.

— o —

### Meetings.

During the session under review, besides the Annual General Meeting, 12 Meetings of the Committee of Management were held.

*Financial Statement*

During the year under report, the Government of India continued their grant of Rs. 20,000/- less 5% in aid of an scientific researches and our grateful thanks are due to them.

## Government Securities in Bank—31st December, 1934.

		Rs.	A.	P.
General Fund	...	81,100	0	0
Veharilala Mitra Fund	..	1,32,000	0	0
Nikunja Garabini Prize Fund	..	500	0	0
Jatindra Ch. Prize Fund	..	600	0	0
Joykissen Medal Fund	.	9,000	0	0
Woodburn Medal Fund	.	500	0	0
Dr. Sircar Research Medal Fund	.	3,000	0	0
Mahendralal Sircar Memorial Research				
Professorship Fund		1,47,200	0	0
Floating Balance in the Bank		26,682	5	10
Cash in Office	...	1,251	1	6

## Government Securities in Bank 31st December, 1933.

General Fund	...	81,100	0	0
Veharilala Mitra Fund		1,32,000	0	0
Nikunja G. Prize Fund		500	0	0
Jatindra Chandra Prize Fund		600	0	0
Joykissen Medal Fund		9,000	0	0
Woodburn Medal Fund		500	0	0
Dr. Sircar Research Medal Fund	...	3,000	0	0
Mahendralal Sircar Research Memorial Professor-				
ship Fund	...	1,47,200	0	0
Floating Balance in the Bank	...	1,665	0	9
Cash Balance in the office	...	906	0	0

*Acknowledgments.*

The thanks of the Association are due to the Honorary Engineer Mr. J. N. Mukherjee, the Honorary Legal Advisers Babu Nirmal Chunder Chunder and Babu Jyotish Chandra Pal, the Honorary Secretary Dr. S. K. Mitra for their gratuitous services, the University of Calcutta for printing Indian Journal of Physics free of charges, and the Corporation of Calcutta for exemption of Municipal Taxes.

*Balance Sheet*  
*Liabilities & Funds.*

			Rs.	AS.	P.
General Fund	...	...	2,21,272	10	8
Investment Reserve Fund	...	..	35,764	0	0
Depreciation Reserve Fund	...	...	1,50,034	10	3
Government of India Grant	...	...	15,018	4	0
Joykissen Medal Fund	...	...	9,000	0	0
Woodburn Medal Fund	...	..	500	0	0
Dr. Sircar Research Medal Fund	...	...	3,000	0	0
Nikunja Garabini Prize Fund	...	...	500	0	0
Jatindra Chandra Prize Fund	...	...	600	0	0
Veharilala Mitra Fund	...	...	1,00,000	0	0
Building Fund	...	...	7,580	0	0
Mahendralal Sircar Memorial Research					
Professorship Fund	...	...	1,64	500	0 0
Employees' Provident Fund	...	...	6,922	4	0
Joykissen Medal Fund Interest	...	...	2,544	0	0
Woodburn Medal Fund Interest	...	...	299	0	0
Dr. Sircar Research Medal Fund Interest	...	...	1,365	0	0
Nikunja Garabini Prize Fund Interest	...	...	386	9	2
Jatindra Chandra Prize Fund Interest	...	...	270	11	0
Suspense	...	...	9	5	0
			Rs. 7,19,566	6	1

Examined and found correct.

S. N. Mukherji, R.A..

Incorporated Accountant,

*and Auditor.*



as at 31st December, 1934.

*Property & Assets.*

			Rs.	AS.	P.
Land & Building	...	..	31,680	11	9
Lecture Hall & Gallery	...	...	23,465	5	3
Vizianagram Laboratory	...	...	40,900	14	0
Observatory Room	...	...	3,320	9	9
Range of Shops (East)	...	...	2,516	10	9
„ „ „ (West)	...	...	2,308	5	0
Servants' Quarters	...	...	1,024	0	0
Durwan's Quarter	...	..	303	13	9
Scientific Instruments (K. K. Tagore Fund)			25,000	0	0
„ „ (General Fund)	...	...	90,597	5	2
Botanical Instruments	...	...	2,329	6	0
Workshop Instruments	...	..	9,861	5	9
Tools & Implements	...	...	209	11	3
Furniture	...	...	17,712	12	3
Library	...	..	55,037	9	1
Suspense Establishment	...	...	9,243	15	0
Investments in G. P. Notes (At Face Value)					
General Fund	...	...	81,100	0	0
Veharilala Mitra Fund	..		1,32,000	0	0
Nikunja Garabini Prize Fund	...		500	0	0
Jatindra Chandra Prize Fund	...		600	0	0
Joykissen Medal Fund	..		9,000	0	0
Woodburn Medal Fund	...		500	0	0
Dr. Sircar Research Medal Fund			3,000	0	0
Mahendralal Sircar Memorial Research					
Professorship Fund	...		1,47,200	0	0
Balance at P. O. Savings Bank	...		2,220	8	0
Imperial Bank of India	...		26,682	5	10
„ „ Office	...		1,251	1	6
			<hr/>		
			Rs. 7,19,566	6	1

S. K. Mitra,

*Honorary Secretary.*

## Statement of Accounts for 1934.

*Receipts and Payments for**Receipts*

			Rs.	AS.	P.
Suspense	...	...	17,595	6	0
Provident Fund	..	...	2,733	15	11
P. O. Savings Bank withdrawn		...	60	0	0
Subscriptions	...	...	369	0	0
Rent from shops	...	...	4,354	0	0
Miscellaneous Receipts	...	...	940	12	9
Sale of Publication	...	...	1,778	12	6
Advertisement Receipts	...	...	77	12	0
Old Material Sold	...	...	6	8	0
Mahendralal Sircar Memorial Research					
Professorship Fund	...	...	300	0	0
Interest Account :					
Joy Kissen Medal Fund	...	...	315	0	0
Dr. Sircar Research Medal Fund	...	...	105	0	0
Woodburn Medal Fund	...	...	17	8	0
Jatindia Chandra Prize Fund	...	...	21	0	0
Nikunja Garabini Prize Fund	...	...	17	8	0
General Fund	...	...	12,691	5	0
Government of India Grant	...	...	36,000	0	0
Imperial Bank of India withdrawals	...	...	43,138	14	5
Opening Balance on 1-1-34	...	...	906	0	0
			1,21,428	6	7

Examined and found correct.

S. N. Mukherji, R.A.,

*Incorporated Accountant,  
and Auditor.*

*the year ended 31st December, 1934.**Expenditure*

	Rs.	As.	P.
Suspense Account—Staff Income-Tax	550	6	0
Provident Fund—S. Ramiah Paid Off	180	0	0
P. O. Savings Bank Deposited	1,393	7	11
Commission Account :			
General Fund	39	5	0
Nikunja Garabini Prize Fund	0	3	0
Establishment	7,596	9	0
Municipal Tax	685	12	0
Electric Charges	1,827	12	3
Gas Charges	326	2	6
Telephone Charges	277	8	8
Workshop Charges	1,480	7	0
Electric Accessories	310	13	0
Electric Installation	441	1	6
Building Repairs	2,539	11	3
Printing Charges	2,461	10	3
Postage & Telegrams	1,306	5	0
Miscellaneous Expenses	1,965	12	9
Research Scholarship	5,715	6	0
Laboratory Charges	4,301	7	9
Suspense Establishment	9,243	15	0
Contribution to Staff Provident Fund	1,190	8	0
Scientific Instruments—General Fund	2,638	7	9
Tools & Implements	6	8	0
Furniture	1,938	3	0
Library	3,603	11	0
Imperial Bank of India (Remittances)	68,156	3	6
Cash Balance as on 31-12-34	1,251	1	6
	1,21,428	6	7

S. K. Mitra,

*Honorary Secretary*

## Statement of Accounts for 1934.

*Receipts and Payments for**Receipts*

				Rs.	As.	P.
Suspense	...	...	...	17,595	6	0
Provident Fund	..	...	...	2,733	15	11
P. O. Savings Bank withdrawn			...	60	0	0
Subscriptions	...	...	...	369	0	0
Rent from shops		...	...	4,354	0	0
Miscellaneous Receipts		...	...	940	12	9
Sale of Publication		...	...	1,778	12	6
Advertisement Receipts		...	...	77	12	0
Old Material Sold		...	...	6	8	0
Mahendralal Sircar Memorial Research						
Professorship Fund	...	...	...	300	0	0
Interest Account :						
Joy Kissen Medal Fund		...	...	315	0	0
Dr. Sircar Research Medal Fund		...	...	105	0	0
Woodburn Medal Fund		...	...	17	8	0
Jatindra Chandra Prize Fund		...	...	21	0	0
Nikunja Garabini Prize Fund		...	...	17	8	0
General Fund	...	...	...	12,691	5	0
Government of India Grant	...	...	...	36,000	0	0
Imperial Bank of India withdrawals		...	...	43,138	14	5
Opening Balance on 1-1-34	...	...	...	906	0	0
				1,21,428	6	7

Examined and found correct.

S. N. Mukherji, R.A.,

*Incorporated Accountant,  
and Auditor.*

*the year ended 31st December, 1934.*

*Expenditure*

		Rs.	AS.	P.
Suspense Account—Staff Income-Tax	...	550	6	0
Provident Fund—S. Ramiah Paid Off	...	180	0	0
P. O. Savings Bank Deposited	...	1,393	7	11
Commission Account :				
General Fund	...	39	5	0
Nikunja Garabini Prize Fund	...	0	3	0
Establishment	...	7,596	9	0
Municipal Tax	...	685	12	0
Electric Charges	...	1,827	12	3
Gas Charges	...	326	2	6
Telephone Charges	...	277	8	8
Workshop Charges	...	1,480	7	0
Electric Accessories	...	310	13	0
Electric Installation	...	441	1	6
Building Repairs	...	2,539	11	3
Printing Charges	...	2,461	10	3
Postage & Telegrams	...	1,306	5	0
Miscellaneous Expenses	...	1,965	12	9
Research Scholarship	...	5,715	6	0
Laboratory Charges	...	4,301	7	9
Suspense Establishment	...	9,243	15	0
Contribution to Staff Provident Fund	..	1,190	8	0
Scientific Instruments—General Fund	..	2,638	7	9
Tools & Implements	...	6	8	0
Furniture	...	1,938	3	0
Library	...	3,603	11	0
Imperial Bank of India (Remittances)	..	68,156	3	6
Cash Balance as on 31-12-34	..	1,251	1	6
		1,21,428	6	7

S. K. Mitra,

*Honorary Secretary*



# X-Ray Analysis of the Structure of Dibenzyl

By

JAGATTARAN DHAR, M.Sc.

*Research Scholar, Indian Association for the Cultivation  
of Science, Calcutta.*

*(Received for publication, June 12, 1934).*

## ABSTRACT.

The paper gives an account of a detailed X-ray analysis of the structure of dibenzyl crystal. The benzene rings in the molecule are found to have a plane hexagonal structure, and they lie in parallel planes separated by about 0.23 A. U. One of the aliphatic carbon atoms in the molecule lies in the prolongation of the line L joining the atoms 4 and 1, and the other on the line L' joining 4' and 1'. The line joining the two aliphatic carbon atoms themselves is found to be inclined at  $103\frac{1}{2}^{\circ}$  to each of the above two lines, L and L'.

## 1. Introduction.

In a previous communication<sup>1</sup> was given an analysis of the structure of diphenyl by X-ray methods. It was found that the benzene rings constituting the molecule have a plane hexagonal structure, and the two rings are in the same plane, the lines joining the carbon atoms 4 and 1, and 1' and 4', on the usual chemical notation, being coincident. More recently Dr. Lucy Pickett<sup>2</sup> has published results of a complete X-ray analysis

<sup>1</sup> 'Ind. Jour. Phys.,' Vol. 7, p. 43 (1932).

<sup>2</sup> 'Nature,' Vol. 131, p. 513 (1933); 'Proc. Roy. Soc.' A, Vol. 142, p. 333 (1933).

of terphenyl (*p*-diphenyl benzene) and also some preliminary X-ray studies on quaterphenyl (*p*-diphenyldiphenyl). She finds that in these compounds also, the benzene rings have a plane structure and that the different benzene rings constituting the molecule are in a line and lie in the same plane.

Diphenyl derivatives of methane, ethane etc., will be of interest particularly in reference to the question how the introduction of the aliphatic carbon atoms between the two benzene rings will affect the disposition of the rings, or the structure of the rings themselves. Diphenyl methane is a liquid at ordinary temperatures and is not so convenient as diphenyl ethane (dibenzyl). The latter compound was therefore selected for X-ray studies. The present paper gives an account of the X-ray analysis of this crystal by the usual methods.

## 2. *Earlier Measurements on Dibenzyl Crystal.*

Preliminary X-ray investigations on the dibenzyl crystal have been made by Hengstenberg and Mark.<sup>3</sup> They assign it to the monoclinic prismatic class with the space-group  $C_{2h}^5$  ( $P2_1/a$ ). The unit cell is, according to them, of dimensions  $a=12.82\text{\AA}$ ;  $b=6.18\text{\AA}$ ;  $c=7.74\text{\AA}$  and  $\beta=116^\circ$ . (The axial ratios are in agreement with those from goniometric measurements by Boeris,<sup>4</sup> namely  $a:b:c=2.0806:1:1.2522$ ;  $\beta=115^\circ 54'$ .) The unit cell is found to contain two molecules, the molecules possessing a centre of symmetry. In their X-ray measurements the 'b' axis was directly determined from a rotation photograph with the help of a Weissenberg camera, but the 'c' and 'a' axes were calculated out of reflections from the *c* (001) and the *a* (100) faces respectively, using the value of  $\beta$ .

<sup>3</sup> 'Zeit. f. Kryst.,' Vol. 70, p. 292 (1929). The unit cell was also determined by Becker and Rose 'Zeit. f. Phys.,' Vol. 14, p. 369 (1923).

<sup>4</sup> Quoted in 'Groth's Chemische Krystallographie,' Vol. 5, p. 191.



### 3. *Dibenzyl Crystal.*

Dibenzyl was crystallised out of acetic ether solution by the process of slow evaporation. The crystals grow generally in the form of hexagonal plates parallel to the  $c(001)$  face and the bounding faces are  $m(110)$ ,  $m'(\bar{1}10)$  or  $w(11\bar{1})$ ,  $w'(\bar{1}11)$  and  $\sigma(20\bar{1})$  or  $a(100)$ . The long edge of the six-sided plate is generally the '  $b$  ' axis. The faces were identified in the usual manner by mounting the crystal on a goniometer head, and measuring the various interfacial angles. The goniometer head carrying the crystal with any desired axis made vertical, is then bodily removed and placed on the stirrup of a rotating crystal arrangement. Rotation photographs were then taken in a cylindrical-film camera of 4 cm. radius by passing X-rays from a Shearer tube with copper target run by a transformer.

Since the  $c(001)$  face is well developed, no difficulty was experienced in mounting the crystal with its '  $a$  ' or '  $b$  ' axis vertical, for the rotation photographs. In order to place the '  $c$  ' axis vertical the  $c(001)$  plane was first adjusted horizontal and then rotated suitably about the '  $b$  ' axis.

### 4. *The Unit Cell and its Dimensions.*

Three separate rotation photographs about the '  $a$  ', '  $b$  ' and '  $c$  ' axes were taken. The axial lengths followed directly from the mean  $\zeta$  values of the layer lines in each of the rotation photographs, read with the help of Bernal's<sup>5</sup> chart II. In this way the following lengths were found.

$a = 12.65\overset{\circ}{\text{\AA}}$ ,  $b = 6.35\overset{\circ}{\text{\AA}}$ ,  $c = 7.665\overset{\circ}{\text{\AA}}$  and  $\beta = 116^\circ$  (calculated from higher orders of reflection from  $(001)$  face). Taking the density of the crystal<sup>6</sup> as 1.11, the number of molecules per unit cell comes out as 2.03, *i. e.*, 2. The above data regarding the unit cell agree with those obtained by Hengstenberg and Mark.<sup>7</sup>

<sup>5</sup> 'Proc. Roy. Soc.' A, Vol. 113, p. 117 (1927).

<sup>6</sup> 'Ind. Jour. Phys.', Vol. 8, p. 149 (1933).

<sup>7</sup> *Loc. cit.*

### 5. *Indexing the Reflecting Planes and the Determination of Space Group.*

In order to decipher the various diffracted spots a few oscillation photographs about the 'a,' 'b,' 'c' axes were taken at intervals of  $15^\circ$  and sometimes of  $5^\circ$ , using a nickel filter to monochromatise the X-ray beam. The basal nets were drawn from a, b, c oscillations with (i)  $b^* = 0.243$ ;  $c^* = 0.201$ ;  $a^* = 90^\circ$ , (ii)  $a^* = 0.122$ ;  $c^* = 0.201$ ;  $\beta^* = 64^\circ$ , (iii)  $a^* = 0.122$ ;  $b^* = 0.243$ ;  $\gamma^* = 90^\circ$  and the oscillation diagrams were prepared in the manner outlined by Bernal in his paper. The values of  $\xi$  for all possible reflecting planes within the range of oscillation, were measured. They were then compared after the appropriate magnification of the photographs with those of the diffracted spots as read directly from Bernal's chart II and thereby the planes were assigned. There is found to be a good agreement between the calculated and the observed values.

The reflecting planes ascertained in this way are embodied in Table I, where the intensities of the diffracted spots are also indicated.

From Table I, it appears that all planes of the type  $\{h0l\}$  are absent if  $h$  is odd as well as those of the type  $\{0k0\}$  if  $k$  is odd. These two halvings assign the dibenzyl crystal to the space group  $C_{2h}^5$  ( $P2_1/a$ ).

### 6. *Integrated Intensities of Reflection and the Observed Structure-Factor.*

Crystals were made to oscillate by means of a cam arrangement. For intensity measurements a fairly thin and small crystal was completely bathed in the X-ray beam and oscillation photographs were taken through a nickel filter. The spots which appeared as sharp lines and which could be uniquely ascertained, were microphotometered. A blackness scale for the X-ray tube used, was prepared. From the blackness scale (calibration curve) the peak value of the intensity for the spots microphotometered, was obtained. The intensity of any peak multiplied by its width gives a relative estimate of the integrated intensity.

TABLE I.

Axial planes.	Prism planes.	General planes.	
001 ( <i>s.</i> )	011 ( <i>v.s.</i> )	111 ( <i>m.</i> )	532 ( <i>w.</i> )
002 ( <i>m.</i> )	012 ( <i>m.</i> )	121 ( <i>w.m.</i> )	512 ( <i>s.</i> )
003 ( <i>v.w.</i> )	013 ( <i>w.</i> )	121̄ ( <i>m.</i> )	613̄ ( <i>w.</i> )
004 ( <i>w.</i> )	014 ( <i>w.</i> )	112 ( <i>s.</i> )	611̄ ( <i>m.</i> )
005 ( <i>v.w.</i> )	021 ( <i>m.</i> )	114 ( <i>v.w.</i> )	612 ( <i>w.</i> )
200 ( <i>v.s.</i> )	201̄ ( <i>v.s.</i> )	115̄ ( <i>v.w.</i> )	632̄ ( <i>w.</i> )
400 ( <i>w.</i> )	201 ( <i>s.</i> )	211̄ ( <i>v.s.</i> )	631 ( <i>v.w.</i> )
600 ( <i>w.</i> )	202̄ ( <i>m.</i> )	212 ( <i>s.</i> )	651 ( <i>v.w.</i> )
800 ( <i>v.w.</i> )	203̄ ( <i>w.m.</i> )	213̄ ( <i>v.w.</i> )	713̄ ( <i>v.w.</i> )
020 ( <i>w.m.</i> )	205̄ ( <i>v.w.</i> )	215̄ ( <i>v.w.</i> )	712̄ ( <i>v.w.</i> )
040 ( <i>v.w.</i> )	401 ( <i>w.</i> )	223 ( <i>m.</i> )	721̄ ( <i>w.</i> )
	401̄ ( <i>w.</i> )	214 ( <i>v.w.</i> )	722̄ ( <i>v.w.</i> )
	402̄ ( <i>v.w.</i> )	215̄ ( <i>w.</i> )	851 ( <i>v.w.</i> )
	404̄ ( <i>w.</i> )	311̄ ( <i>v.w.</i> )	832 ( <i>v.w.</i> )
	601̄ ( <i>v.w.</i> )	312 ( <i>w.</i> )	833 ( <i>w.</i> )
	603̄ ( <i>w.</i> )	323 ( <i>m.</i> )	841̄ ( <i>v.w.</i> )
	604̄ ( <i>w.</i> )	313 ( <i>m.</i> )	832̄ ( <i>v.w.</i> )
	110 ( <i>m.</i> )	411 ( <i>m.</i> )	842̄ ( <i>w.</i> )
	120 ( <i>w.</i> )	412 ( <i>m.</i> )	852̄ ( <i>v.w.</i> )
	140 ( <i>w.</i> )	411̄ ( <i>v.w.</i> )	941 ( <i>v.w.</i> )
	310 ( <i>s.</i> )	421 ( <i>w.m.</i> )	952 ( <i>v.w.</i> )
	320 ( <i>w.</i> )	423 ( <i>w.</i> )	
	410 ( <i>w.</i> )	422 ( <i>w.</i> )	
	420 ( <i>m.</i> )	413̄ ( <i>w.m.</i> )	
	510 ( <i>s.</i> )	513̄ ( <i>w.</i> )	
	620 ( <i>w.</i> )	515̄ ( <i>v.w.</i> )	
	730 ( <i>v.w.</i> )		
	740 ( <i>v.w.</i> )		

The symbols used have the following meanings :—

*v.s.* very strong, *s.* strong, *m.* medium, *w.m.* weak medium, *w.* weak, *v.w.* very weak.

It should be remarked here that in calculating the integrated intensity due attention was paid to the structure of the lines in the microphotometer curves. The same procedure was repeated with another small crystal and the average of the integrated intensities was taken.

With the integrated intensities thus found, the relative molecular structure-factors were calculated with the help of the formula

$$\frac{F}{F_1} = \sqrt{\frac{\sin 2\theta (1 + \cos^2 2\theta_1) \times P}{\sin 2\theta_1 (1 + \cos^2 2\theta) \times P_1}},$$

where  $F$  is the molecular structure-factor for the plane in question,

$\theta$  is the glancing angle for the plane,

$P$  is the integrated intensity.

The terms with suffix 1 refer to reflection  $\{001\}$ .

TABLE II.

Planes.	Integrated Intensity.	Molecular Structure-factor observed.	Molecular Structure-factor calculated.
001	16	1	1
002	12	1.26	1.47
003	1	.45	.26
004	2.5	.89	.69
005	1	.66	.4
200	84	2.3	3.1
011	100	3.0	2.3
012	8	1.11	1.59
121	3	.71	.43
$\bar{1}12$	16	1.21	.95
111	12	1.12	.95
114	2	.87	.59

TABLE III.

Planes.	Remarks on Intensity.	Molecular Structure-factor observed.	Molecular Structure-factor calculated.
110	medium	1.05	.76
120	weak	.62	.28
020	weak medium	.85	.53
040	very weak	.59	.32
600	weak	1.39	1.72
021	medium	1.43	1.65
410	weak	.6	.28
400	weak	.7	.78
401	weak	2.95	2.67
201	very strong	1.82	1.99
203	weak medium	1.14	.78
201	strong	1.75	1.28
510	strong	1.82	1.51
730	very weak	.22	.1
740	very weak	.26	.21
12 $\bar{1}$	medium	1.15	1.11

In Table II only those planes whose intensities were *measured*, are given. In Table III, the intensities were recorded by eye-estimation and comparison. So in the second column remarks on intensity are given. In each case, the integrated intensity of the  $\{011\}$  reflection is taken as 100 and other reflections are expressed in terms of it. In the third and the fourth column, the structure-factor of  $\{001\}$  reflection is taken as unity.

The process of analysis in all structure determinations involves the comparison of the calculated structure-factor with the observed structure-factor. The observed structure-factor is computed from the integrated intensities, as measured, of the

spots. The calculated structure-factor follows from the positions of the atoms in a particular molecular configuration tentatively assumed in conformity with the symmetry of the space-group. The method employed in the present case is the method of trial and error.

### 7. *A priori Considerations regarding the Structure of the Molecule.*

The dibenzyl crystal has two molecules in the unit cell and belongs to the space-group  $C_{2h}^5$ . This space-group requires four asymmetric crystal units for the unit cell, and so each crystal unit here is one-half of the chemical molecule, *i.e.*, the molecule has a centre of symmetry. Let us now consider the possible configurations for the molecule consistent with its having a centre of symmetry. In the first place, as has been mentioned in the introduction, the benzene rings in diphenyl and terphenyl molecules are now known definitely to have a plane hexagonal structure. It is, therefore, very probable that in dibenzyl as well, the benzene rings are planar hexagons. The C—C distance in the hexagon can be taken to be  $1.41 \text{ \AA}$ .<sup>8</sup> (In the later parts of this section the planes of two benzene rings in the molecule will be called for brevity P and P' respectively.) We can further assume that the carbon atom A lies on the prolongation of the line joining the carbon atoms 4 and 1 and similarly A' lies on the line 4' and 1'. (See Fig. 2.) For brevity again, we shall call these lines joining 4, 1, A and A', 1', 4' as L and L' respectively. The distance between A and 1 or A' and 1' may be taken to be the same as between the atoms 1 and 1' in diphenyl, namely  $1.48 \text{ \AA}$ . Similarly, the A to A' distance may be assumed to be the same as the C—C distance in diamond or in the aliphatic compounds, *i.e.*, it lies within the range,  $1.54 \text{ \AA}$  to  $1.48 \text{ \AA}$ .

<sup>8</sup> Robertson—'Proc. Roy. Soc.,' A, Vol. 140, p. 94 (1933).

Consistent with the centre of symmetry of the molecule, only the following relative orientations of the planes  $P$  and  $P'$  and the lengths  $L$  and  $L'$  of the two benzene rings in the molecule are possible.

Case I :— $P$  and  $P'$  are coincident :—

(a)  $L$  and  $L'$  are also coincident.

(b)  $L$  and  $L'$  are parallel to each other, but are not coincident.

Case II :— $P$  and  $P'$  are parallel to each other, but are not coincident.

Before proceeding to find which of these structures represents the actual molecule, we shall describe how the structure-factors can be calculated for a given orientation of the molecules in the unit cell, so as to be able to compare the value of the structure-factor for any proposed orientation, with its experimental value.

### 8. *The Atomic Parameters and the Calculation of the Structure-Factor.*

Suppose that  $M_1$  and  $M_2$  are the two molecules in the unit cell of the substance in question. The molecule  $M_1$  is placed with its centre of symmetry at the origin of reference (taking any lattice point of the unit cell as origin) and the other molecule  $M_2$  with its centre of symmetry at  $\frac{1}{2}a, \frac{1}{2}b, 0$ . The molecule  $M_1$  is first placed with its plane coincident with the  $c$  (001) plane of the unit cell and then brought to the correct position by the following successive rotations :—

- (i) through an angle  $\lambda$  about the ' $a$ ' axis with the direction ' $c$ ' to ' $b$ ' taken as positive ;
- (ii) through an angle  $\mu$  about the ' $b$ ' axis with the direction ' $a$ ' to ' $c$ ' taken as positive ;

(iii) through an angle  $\nu$  about the normal to the plane containing the 'b' axis and the length of the molecule after rotations (i) and (ii) have been performed.

As  $M_2$  is derived from  $M_1$  by a glide plane reflection it would have rotations of  $-\lambda$ ,  $\mu$  and  $-\nu$  respectively.

To start with, a rectangular system of axes was adopted and the final co-ordinates of the atoms of the molecule after the successive rotations, were obtained in terms of them. They were afterwards changed to the oblique system of axes. In the dibenzyl crystal the positions of the atoms in only one half of the chemical molecule would have to be determined; that is, it is required to find out here 21 parameters only.

Let 'a,' 'b,' 'c' be the axes of the unit cell—'b' axis lying in the plane of the paper and 'a,' 'c' lying in a perpendicular plane with an angle  $\beta$  between them. Draw  $c'$  in the plane containing 'a' and 'c' but at right angles to 'a' so that the angle included between 'c' and  $c'$  is  $\alpha$ . (See fig. 1.)

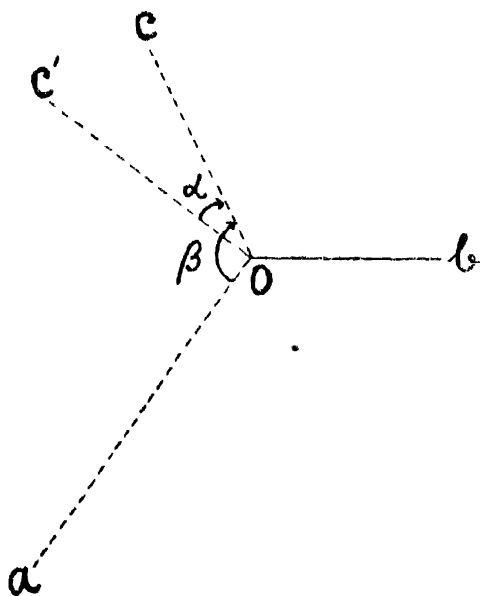


FIG. 1.



As we shall see in the next section,  $\nu=0$ , and in this case, if  $x, y, z$  are the co-ordinates of any atom in  $M$ , and  $X_1, Y_1$  and  $Z_1$  the final co-ordinates of the same atom after rotations (i) and (ii) have been made, we have

$$X_1 = x \cos \mu + y \sin \lambda \sin \mu - z \cos \lambda \sin \mu$$

$$Y_1 = z \sin \lambda + y \cos \lambda$$

$$Z_1 = x \sin \mu - y \sin \lambda \cos \mu + z \cos \lambda \cos \mu$$

$X_1, Y_1, Z_1$  are then changed to axial co-ordinates  $X, Y, Z$  by the use of the relations

$$X = X_1 + Z_1 \tan \alpha$$

$$Y = Y_1$$

$$Z = Z_1 \sec \alpha,$$

$X, Y, Z$  being of course expressed in terms of the respective axial lengths.

The structure-factor of the molecule is then calculated from the simplified form of the expression for the space group  $C_{2h}^{16}$  containing two molecules, which is given as

$$F_m = 4 \Sigma F_c \cos 2\pi \left( \frac{hx_p}{a} + \frac{lz_p}{c} \right) \cos 2\pi \frac{ky_p}{b}.$$

when  $h+k$  is even :

$$F_m = 4 \Sigma F_c \sin 2\pi \left( \frac{hx_p}{a} + \frac{lz_p}{c} \right) \sin 2\pi \frac{ky_p}{b},$$

when  $h+k$  is odd :

the summation extending over one crystal unit.  $F_c$  represents the scattering power of carbon which is obtained from the curve of graphite constructed by Mrs. Lonsdale.<sup>9</sup>

<sup>9</sup> 'Proc. Roy. Soc.,' A, Vol. 123, p. 494 (1929).

9. *Structure of Dibenzyl.*

Values of  $\lambda$ ,  $\mu$  and  $\nu$  :—The orientations of the benzene rings of the dibenzyl molecule have been determined by Krishnan and Banerjee<sup>10</sup> by the magnetic method. By a correlation of the principal magnetic susceptibilities of the crystal with those of the molecules they have shown that the line containing the carbon atoms 4, 1 and A and the one containing A', 1' and 4' lie in the  $b$  (010) plane in the obtuse angle  $\beta$ , inclined at  $32^\circ.0$  to the  $a$ -axis and at  $83^\circ.9$  to the  $c$ -axis. The planes of the benzene rings of the two molecules in the unit cell are shown by them to be inclined at  $+60^\circ$  and  $-60^\circ$  respectively to the  $b$ (010) plane. These values given by Krishnan and Banerjee correspond in our rotation to  $\lambda=30^\circ$ ,  $\mu=32^\circ$  and  $\nu=0$ . We shall adopt these values for  $\lambda$  and  $\mu$  in our preliminary trials and vary the other parameters and then find how far any variation of the orientations themselves affect the agreement between the calculated and the observed structure-factors.

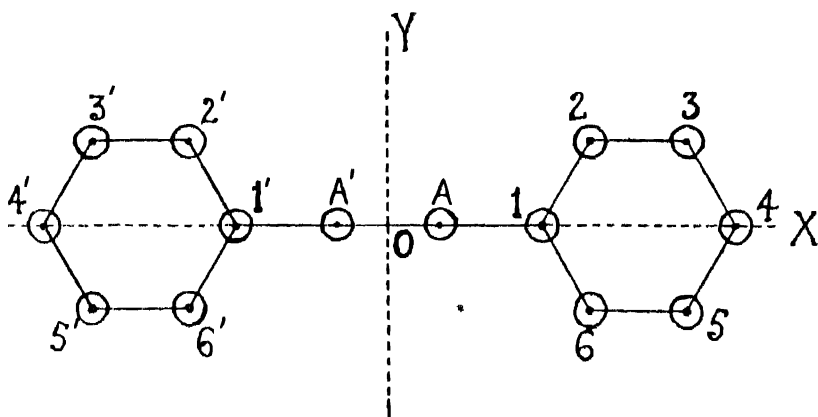


FIG 2.

<sup>10</sup> 'Phi: Trans.,' A, Vol. 231, p. 235 (1933).

We can now find out which of the possible structures for the molecule given at the end of section 7 conforms to the actual one. Let us consider the simplest configuration, *viz.*, that corresponding to Case I (a) (see Sec. 7), where the planes of the two benzene rings and also their lengths coincide. All the carbon atoms will lie in a plane in the positions indicated in figure 2.

The calculated structure-factors for some of the planes are given in the Table IV. It is clear from the Table that there is no agreement at all between the calculated and the observed structure-factors, so that this configuration is not tenable.

TABLE IV.

Planes.	$A-A'=1.48\text{\AA}$ $A-1=1.48\text{\AA}$ $F_{hkl}$	$A-A'=1.54\text{\AA}$ $A-1=1.48\text{\AA}$ $F_{hkl}$	$A-A'=1.54\text{\AA}$ $A-1=1.54\text{\AA}$ $F_{hkl}$	Observed molecular structure-factor.
001	1	1	1	1
002	35.44	14.44	3.89	1.26
003	2.72	.57	.07	.45
004	20.41	8.2	2.01	.89
005	11.11	4.53	1.41	.66
200	47.75	18.71	4.74	2.3
011	10.08	4.46	1.43	3.08

We may next try the alternative configuration corresponding to Case I (b), in which the planes of the two benzene rings are identical, but the lines L and L' instead of being coincident are parallel to each other. The line AA' joining the two aliphatic carbon atoms will now be inclined to both L and L'. The value of this angle would naturally be the tetrahedral valency angle of the aliphatic carbon atom, *viz.*,  $109\frac{1}{2}^\circ$ . The positions of the atoms under these assumptions will be as shown in fig.3.

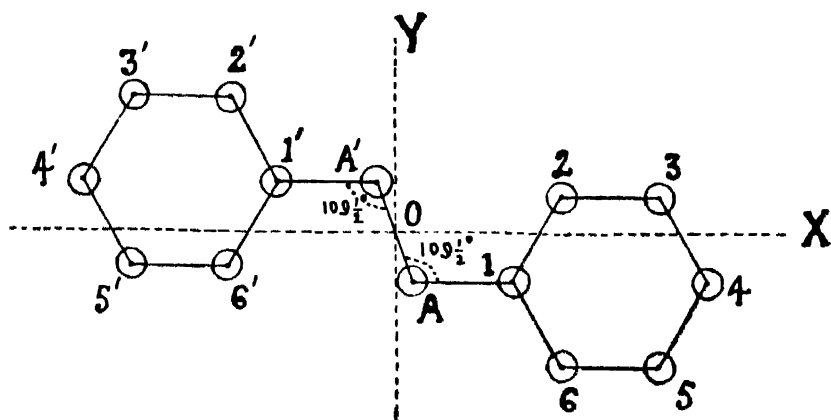


FIG. 3.

All the carbon atoms lie in the plane and the angles  $1' A' A$  and  $A' A 1$  will be each  $109\frac{1}{2}^\circ$ . When initially the molecule is placed parallel to the  $c$  (001) plane (before the rotations through angles  $\lambda$  and  $\mu$  about the 'a' and 'b' axes respectively are made) the orientations of the line  $A A'$  and of the lines  $L$  and  $L'$  with reference to the positive directions of the 'b' and 'a' axes are taken to be as indicated in fig. 3.

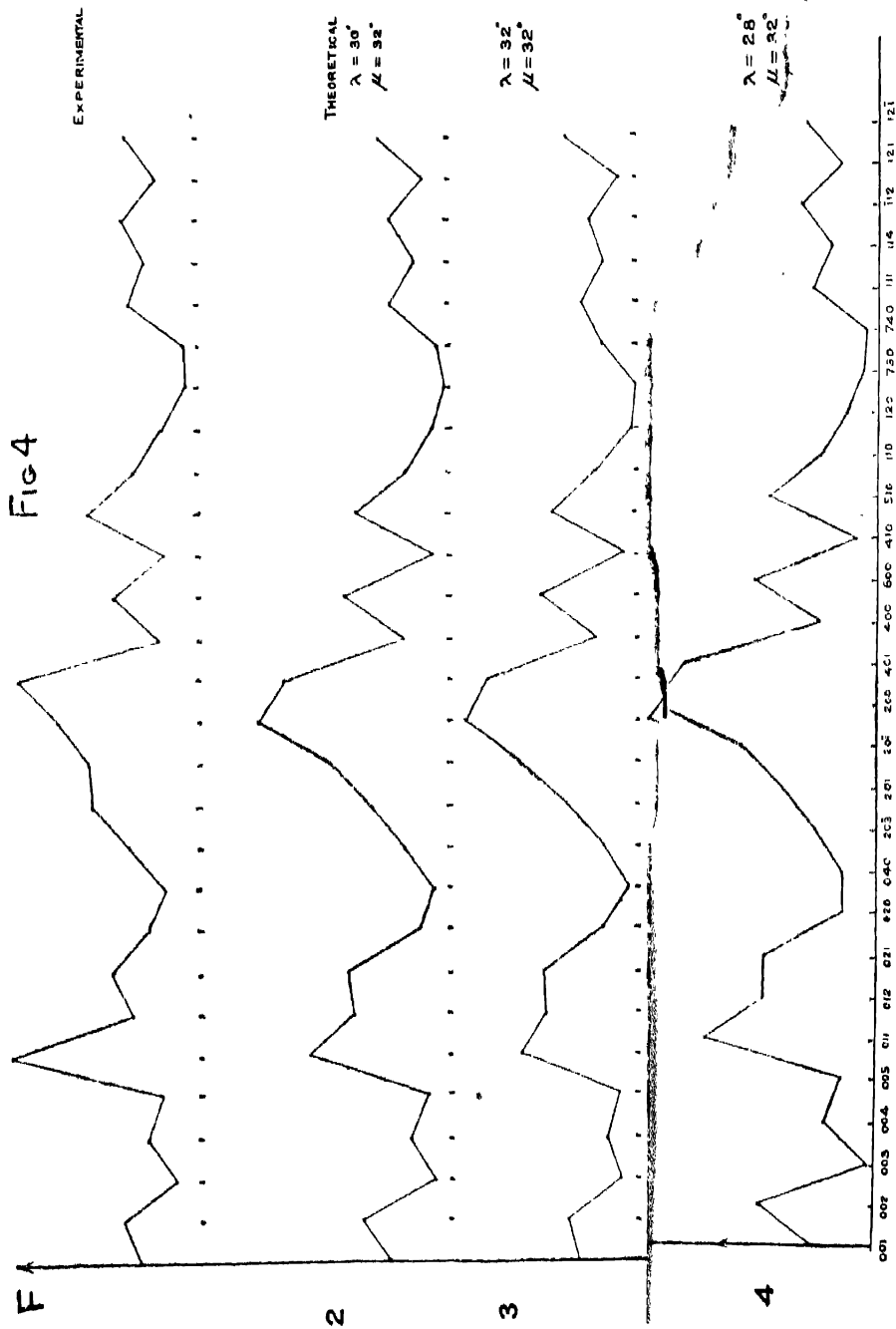
The calculated structure-factors for this case are given in Table V. The calculated values are much closer to the experimental values of the structure-factor than in Case I (a) considered in the previous paragraph. The agreement, however, is still far from satisfactory. The deviations are consistently in one direction, the calculated values being uniformly higher. Since neither (a) nor (b) of Case I fits, we can conclude that *the two benzene rings cannot lie in the same plane.*

If they are not in the same plane, we have to consider the various configurations obtained by allowing the line  $A A'$  (see fig. 3) to describe a cone about the 'a' axis of semi-vertical angle  $(180^\circ - 109\frac{1}{2}^\circ)$  that is  $70\frac{1}{2}^\circ$ , *the planes of the benzene rings remaining all the time parallel to the plane of the paper* (the plane of the paper would correspond to the  $c(001)$  plane in the initial

position of the molecule). In the process of this rotation of OA about the 'a' axis, the  $x$  co-ordinate (using the system of co-ordinate axes as defined earlier) will naturally remain unaltered, while the  $y$  and  $z$  co-ordinates will continually vary,  $y^2 + z^2$  being constant. When the point A lies in the plane of the paper  $z$  will be zero, while, when the point A has reached its maximum height above the plane of the paper,  $y$  will be zero. Starting from the plane of the paper, as OA rotates, the ratio  $z/y$  will increase from zero to infinity. For any given value of  $z/y$  the co-ordinates of all the other carbon atoms can be easily calculated; whence using the values of  $\lambda$ ,  $\mu$  and  $\nu$  given already, the structure-factors of reflections can be calculated also. The calculated structure-factors for various values of  $z/y$  of the point A are given in Table V. Any given value of  $z/y$  uniquely determines the height of the plane of the first ring (123456) above the plane of the paper, and consequently of the second ring (1'2'3'4'5'6') below it.

TABLE V.

Planes.	$\frac{z_A}{y_A} = 0$ $F_{hkl}$	$\frac{z_A}{y_A} = -\frac{1}{\sqrt{3}}$ $F_{hkl}$	$\frac{z_A}{y_A} = -\frac{1}{2}$ $F_{hkl}$	$\frac{z_A}{y_A} = -\frac{1}{6}$ $F_{hkl}$	$\frac{z_A}{y_A} = -\frac{1}{2}$ $F_{hkl}$	$\frac{z_A}{y_A} = -1$ $F_{hkl}$	$\frac{z_A}{y_A} = \infty$ $F_{hkl}$	Observed molecular structure- factor.
001	1	1	1	1	1	1	1	1
002	3.7	1.8	1.5	1.25	.94	.39	.52	1.26
003	.13	.25	.27	.29	.31	.33	.32	.45
004	2.0	.93	.7	.56	.37	.02	.1	.89
005	.81	.52	.4	.32	.21	.001	.05	.66
200	7.6	3.88	3.17	2.69	2.1	1.08	1.29	2.3
012	8.99	2.02	1.64	1.38	1.05	.44	.38	1.11
114	1.32	.71	.45	.5	.39	.11	.17	.87



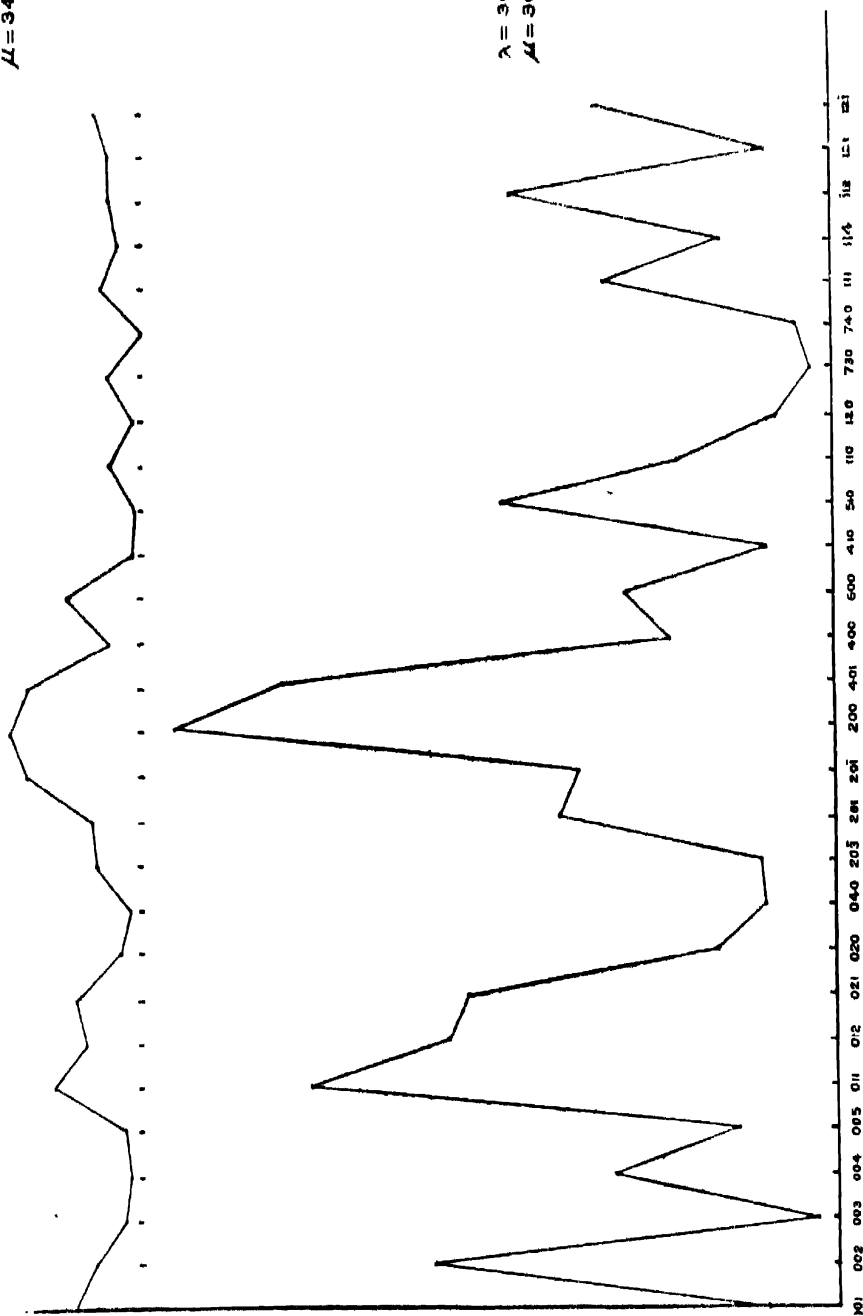
$\lambda = 30^\circ$   
 $\mu = 34^\circ$ 
 $\lambda = 30^\circ$   
 $\mu = 30^\circ$ 


FIG. 4a.

TABLE VI.

Planes.	Observed molecular structure-factor	$A-1=1.48\overset{\circ}{\text{\AA}}$ $A-A'=1.54\overset{\circ}{\text{\AA}}$ $\angle OAl=109^\circ$ $F_{hkl}$	$A-1=1.48\overset{\circ}{\text{\AA}}$ $A-A'=1.5\overset{\circ}{\text{\AA}}$ $\angle OAl=109^\circ$ $F_{hkl}$
011	3.08	1.97	2.3
114	.87	.5	.6
111	1.12	.81	.97
001	1	1	1

The molecular structure-factors included in Table V are all calculated by taking the  $C-C$  distance in the ring as  $1.42\overset{\circ}{\text{\AA}}$ , the aliphatic  $C-C$  distance ( $AOA'$  in Fig. 3) as  $1.54\overset{\circ}{\text{\AA}}$  and the distance between the carbon atoms at A and 1 or between  $A'$  and  $1'$  as  $1.48\overset{\circ}{\text{\AA}}$ . These were next altered and we get the best agreement when the aliphatic  $C-C$  distance in the ring is  $1.50\overset{\circ}{\text{\AA}}$  and the length A to 1 is  $1.48\overset{\circ}{\text{\AA}}$ . The results of the variation are shown in Tables VI and VII.

TABLE VII.

Planes.	Observed molecular structure-factor	$A-1=1.5\overset{\circ}{\text{\AA}}$ $A-A'=1.5\overset{\circ}{\text{\AA}}$ $\angle OAl=109\frac{1}{2}^\circ$ $F_{hkl}$	$A-1=1.48\overset{\circ}{\text{\AA}}$ $A-A'=1.5\overset{\circ}{\text{\AA}}$ $\angle OAl=109\frac{1}{2}^\circ$ $F_{hkl}$
011	3.08	2.0	2.3
114	.87	.56	.6
111	1.12	.88	.96
001	1	1	1

In Tables VI and VII only those planes which are much affected by changing the lengths of the carbon bonds outside the rings, are entered.



It is seen from Table V that for  $\frac{z_A}{y_A}=0$ , the calculated values are uniformly too high, and for  $\frac{z_A}{y_A}=\infty$  they are too low. The best fit obtains for the configuration corresponding to  $\frac{z_A}{y_A}=-\frac{1}{6}$ . Now  $OA (= \sqrt{y_A^2 + z_A^2})$  is half of the distance between A and A', i.e.,  $\frac{1}{2} \times 1.5\text{\AA}$  or  $0.75\text{\AA}$ . The above value of  $z_A/y_A$  adopted, viz.,  $-\frac{1}{6}$ , corresponds to  $z=0.12$  A.U., i.e., the plane of the two benzene rings are separated from each other by a distance equal to  $0.23\text{\AA}$ .

The agreement between the observed and the calculated structure-factors for this case shows that the assumptions with which we started, regarding the plane hexagonal structure of the benzene ring and its dimensions, as well as regarding the values of  $\lambda$ ,  $\mu$  and  $\nu$ , which define the orientations of the benzene rings in the lattice, are justified. In any case, the actual structure cannot be far from that finally arrived at here.

In order, however, further to confirm the above values that were adopted for  $\lambda$  and  $\mu$ , slight variations of these angles from the values chosen were tried, and as will be seen from the graphs given in Fig. 4., and Fig. 4a the new values weaken the agreement between the observed and the calculated structure-factors.

The first two curves give the experimental and theoretical values respectively of the structure-factors and the latter conforms to the former as best as possible. The four other curves that follow, are drawn by changing  $\lambda$  or  $\mu$  with the values noted against them.

## 10. Conclusion.

We may here sum up the final results obtained for the structure of dibenzyl. Considering, first, the molecule, the 6 carbon atoms of each benzene ring form a regular hexagon.

The aliphatic carbon atom A (see Fig. 3) lies on the prolongation of the line joining the atoms 4 and 1, and the other A' on the line joining 4' and 1'. The line AOA' makes with either of the above lines (*viz.*, 4 1 and 4' 1'), an angle of  $109\frac{1}{2}^{\circ}$ . Further, the two benzene rings do not lie in the same plane, but in parallel planes slightly separated from each other. Thus in Fig. 3, all the carbon atoms on the right-hand side of OY may be supposed to be raised above the plane of the paper by about 0.12Å and all the atoms on the left side to be pushed below the plane by the same distance.

In order to define the orientations of the molecules, consider in Fig. 3 the two perpendicular axes OX and OY lying in the plane of the paper, and fixed to the molecule. It is found that the OX axes of both the molecules in the unit cell lie in the *b* (010) plane in the obtuse angle  $\beta$ , making an angle of  $32^{\circ}$  with the '*a*' axis (and  $84^{\circ}$  with the '*c*' axis). The OY axes of the two molecules are inclined at plus and minus  $60^{\circ}$  respectively to the *b* (010) plane.

The author desires to express his grateful thanks to Prof. K. S. Krishnan, D.Sc., for the keen interest he took throughout the course of the work.

## 2

# On Some Considerations of Sputtering Applied to Purification of Mercury by Electric Arc Still

By

R. K. COWSIK, M.Sc.

(Received for publication, October 10, 1933.)

Mercury is generally found impure as a result of amalgamation with dissolvable impurities like Cd, Zn, Ag, Cu, Pb, etc. In such cases it is usual to prescribe a simple distillation of the alloyed mercury to get the pure mercury. To facilitate the process various are the stills used. Fig. 1 illustrates a directly gas-heated still and Fig. 2 illustrates an arc

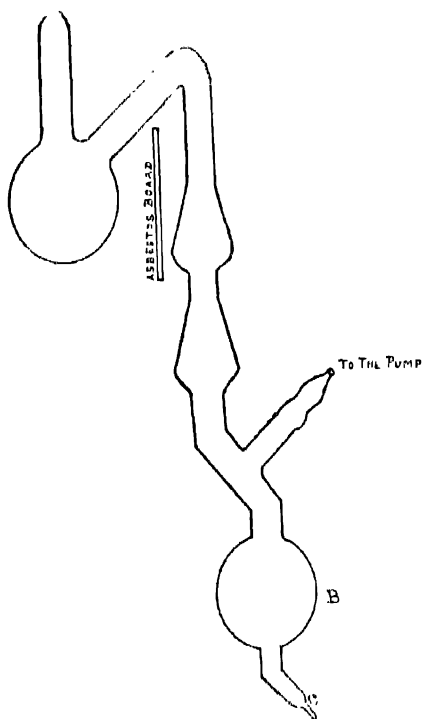


FIG. 1.

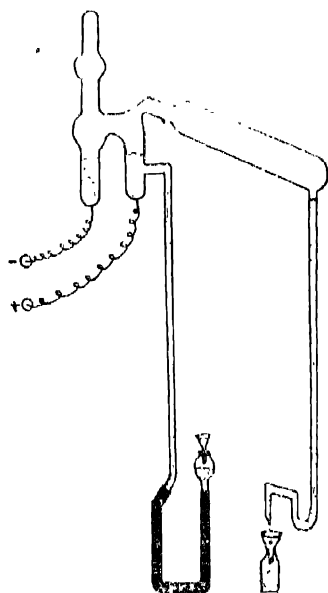


FIG. 2.

still as has been described by H. P. Waran in *Phil. Mag.*, Vol. 2, pp. 317-320, 1926.

In both cases the mercury is given the usual preliminary process of cleaning. The curious fact to note however is that in such attempts to get pure distilled mercury, the arc distilled mercury seems to be less pure than the simple gas heated and distilled mercury.

This point appeared surprising and worthy of further examination and hence a complete study of the methods of purification of mercury so as to be in a position to trace the origin of the impurities finally found associated with the arc distilled mercury, was undertaken.

The methods of cleaning mercury generally suitable for laboratory purposes may be classified as under :—

Mechanical separation of undissolved impurities.

Methods of oxidation and reduction of the impurities.

Treatment with mercurous nitrate solution.

Distillation at low pressure and in vacuo.

None of these processes is complete in itself and to get very pure mercury it is necessary to treat the mercury under all the processes. The first and foremost operation is to remove all the undissolved and free impurities from it by some mechanical process. The most suitable of all the methods is to squeeze it through folds of clean chamois leather or fine muslin.

In any chemical method of cleaning mercury the chemical reagent must come in contact with a large surface of the mercury. But if the mercury is contaminated with grease or oil the thin layer of grease or oil on the surface of the mercury will prevent the mercury reacting with the chemical reagent. Hence it is necessary to free the mercury from oil or grease. For this purpose a concentrated solution of KOH has been found to be the most suitable. Caustic potash is without action on mercury and yet removes grease efficiently.

Yet another advantage in using caustic potash to remove grease is that, metallic impurities like Zn, Pb, and Sn are acted upon by KOH and these impurities go into solution leaving mercury pure.

After cleaning it with caustic potash it is necessary to clean it by treating it with a concentrated solution of mercurous nitrate acidified with dilute  $\text{HNO}_3$ . This is done by making mercury fall in the form of a fine spray through mercurous nitrate solution. As this process has to be repeated a number of times to make the reaction of the mercury with mercurous nitrate complete it is necessary to devise an

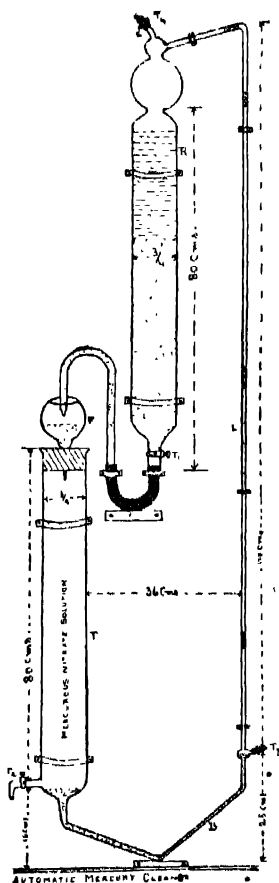


FIG. 3.

apparatus in which the mercury repeatedly circulates automatically in the form of a fine spray through the mercurous nitrate solution, over and over again. This can easily be achieved by an apparatus of the automatic type illustrated in Fig. 3. This has been found to work very satisfactorily.

R is a reservoir of mercury  $\frac{3}{4}$ " in diameter and 80 cms. long. There is a glass stop-cock (which must not be greased) at the bottom of this reservoir and by adjusting the tap the flow of mercury through the glass jet into the funnel F can be controlled. From the funnel F mercury in the form of a fine spray falls through the tube T which is  $\frac{3}{4}$ " in diameter and 80 cms. long and contains a concentrated solution of mercurous nitrate acidified with dilute  $\text{HNO}_3$ . This height of solution is kept balanced by a small quantity of mercury in the bent tube B which is connected by means of a narrow tube L, 2 mm. in diameter, to the top of the reservoir R. It is necessary that this tube must not be greater than 2 mm. in diameter as otherwise the mercury pellet will be broken up before it reaches the height of the tube. The top of this reservoir R is also connected by means of a pinch cock  $T_1$  and rubber tubing to a filter pump. At the end of the bent tube B there is a small bulb blown in the tube L to which is attached a side tube V open to the atmosphere. This tube is provided with a rubber tube and pinch cock  $T_3$ . The level of mercury in the bent tube must just stand near the side tube V without closing it. The whole apparatus is firmly clamped to a vertical wooden board fixed to the wall.

Working of the apparatus :—To begin with, the glass stoppers  $T_1$  and  $T_2$  are completely closed. The pinch cock  $T_1$  is completely opened and the rubber tube C is connected to the filter pump which is worked. Mercury that has been freed from suspended impurities by a preliminary filtration is poured in the funnel F. Mercury falls in a fine spray through the mercurous nitrate solution in tube T. The pinch cock  $T_2$  is kept partially open when the mercury in the

bent tube B rises in the limb L and closes the side tube V, the filter pump sucks a vacuum above it and the atmospheric pressure acting below the pellet of mercury carries it up the narrow tube L and drops into the reservoir R. Mercury is allowed to accumulate in the reservoir to about three-fourth of its height and then the tap  $T_1$  is slightly opened and the rate of flow of mercury from the reservoir to the funnel adjusted so that the rate is not at least greater than the rate of flow of mercury from the funnel into the tube T containing the mercurous nitrate solution. When once this is adjusted the whole process is continuous and automatic.

It is advisable to have a small column of distilled water above the mercury in the reservoir. Mercury after passing through the mercurous nitrate solution is contaminated with the solution and hence it is necessary to wash it before it goes into the reservoir. By having water above the mercury in the reservoir, the mercury pellets that are carried up the vertical tube L will fall through the column of water before reaching the mercury in the reservoir. The water could be got above the level of mercury in the reservoir by dipping the nozzle  $T_2$  in a very small quantity of water held in a beaker while the apparatus is working.

The apparatus is very easy to clean. All the mercurous nitrate solution is tapped off through the stop cock  $T_2$  and the clean mercury from the jet by opening the stop cock  $T_1$ . Water is made to circulate through the whole system by dipping the nozzle  $T_3$  in clean water held in a beaker. The dirty water is drawn off through the nozzle and fresh water is made to circulate again three or four times. It is essential to keep the apparatus clean like this when not in use.

An apparatus of this type set up in the Presidency College, Physics Laboratory at Madras is working very satisfactorily for the past one year and with very little care, yielding about 5 lbs. of clean mercury in about 6 hours during

which time the mercury falls through the mercurous nitrate solution at least about a dozen times.

The above process of cleaning mercury is very necessary for the preliminary removal of all the more volatile metals before distillation. In cleaning with mercurous nitrate solution the more electro-negative metals like Mg, Zn, Cd, Ni, Pb, Sn, and Cu displace mercury from the mercurous nitrate solution and thereby are easily eliminated as soluble nitrates of these metals. Of course the process is not complete. But this helps to reduce the amount of the impurities present in the mercury before distillation, since when these impurities are present in large quantities a single distillation is not found to be enough to complete the purification. There is an advantage in preferring treatment with mercurous nitrate, for other chemical processes of oxidation of the impurities. The order of removal of metals by oxidation from amalgams is Zn, Cd, Sn, Pb, Cu, Hg and Ni.<sup>1</sup> On the other hand the order of removal of metals by displacement of mercury in the mercurous nitrate is Mg, Zn, Cd, Ni, Sn, Pb and Cu. We thus see that some metals that are difficult to remove by the method of oxidation are easily removed by treatment with mercurous nitrate. Mercury after being treated with mercurous nitrate is well washed with distilled water repeatedly until free from any trace of acid. Then it is completely dried by slowly heating it, out of contact with air.

Mercury thus obtained is very nearly pure for all practical purposes. But for obtaining the mercury of the highest purity it has first to be distilled and here comes the problem. Two ways are recommended for the distillation.

1. By ordinary gas flame heated still, Fig. 1.
2. By the mercury arc still, Fig 2.<sup>2</sup>

<sup>1</sup> J. Russel, "Jour. Chem. Soc.," Vol. 127, p. 2221 (1925); Vol. 128, p. 1872 (1926) and p. 2398 (1929).

<sup>2</sup> H. P. Waran, Phil. Mag., Vol. 2, p. 317 (1926).



To test the relative efficiency of the two stills the following distillations were done and the samples of the distillate analysed chemically.

Dirty laboratory mercury which on chemical analysis was found to contain Cd, Ni, Sn, Pb, Ag and Zn all in fair proportions was divided into two parts and distilled separately by the two stills. The distillate from the ordinary still was found to contain a fair proportion of Cd, Zn and Pb while the distillate from the arc still contained in addition fair proportions of Cd, Sn, Ag and traces of Cu.

Again the same laboratory mercury after being subjected to the preliminary processes of purification detailed above was distilled by the two stills separately and the samples of the distillates from the two stills were again analysed. It was found that in the ordinary still all the impurities were eliminated by a single stage of distillation. In the arc still traces of impurities like Ag, Cu and Sn continued to occur in the distillate. To examine this difference further clean mercury that contained known impurities of Ag, Cu, Ni and Mg was distilled by the arc still and it was found that while Ni and Mg were eliminated Cu and Ag continued to be present in the distillate.

Thus we see that the behaviour of the two forms of stills is distinctly different. Certain metals like Ag and Cu that are eliminated by the gas heated still are not eliminated by the arc still. Again in the arc still metals like Ag and Cu have a greater tendency to distill over than metals like Ni and Mg. Also it was found that best results were obtained with the arc still if the mercury to begin with is very pure and specially free from particular impurities like Ag, Cd and Cu. It is common experience that the distillate from a highly contaminated mercury is indeed not pure.<sup>8</sup> But why when samples of mercury when distilled by the arc still of the Waran type and

<sup>8</sup> Hullet, *Phy. Rev.*, Vol. 21, p. 388 (1905) and Vol. 33, p. 307 (1911).

by an ordinary gas heated still should yield mercury with different impurities in the two cases and why certain metals alone and others are not eliminated in the Waran's mercury arc still, it is not easy to explain.

It occurred to me while investigating the phenomenon of cathodic sputtering that the metals irremovable from mercury by distillation in the arc still were exactly those that sputter greatly in the discharge tube and it suggested itself to me whether the phenomenon of sputtering could be the cause of the observed peculiarity in the arc still. Assuming the arc discharge to be of the same nature as discharge through rarefied gases, the only difference being in the high current density of arc, it is natural to suppose that the metals found as impurities in the distillate of an arc still are sputtered along with the mercury from the cathode of the arc and are condensed in the condenser tube along with the vapour of mercury from the anode. If we assume that in the mercury arc phenomenon there is cathodic sputtering taking place at the negative pool of mercury, the impurities are accounted for on that account. In the ordinary vacuum still the whole mass of mercury is raised to a temperature slightly below the boiling point of mercury and necessarily very much below even the melting point of most of the metal impurities. Hence vaporisation takes place over the whole of the exposed surface of the liquid, enabling the mercury to distill over leaving the impurities behind. Traces of impurities may be carried mechanically along with the mercury vapour. But in the case of the mercury arc the phenomenon seems to be different. Here the evaporation at the cathode is by sputtering. According to the thermal theory<sup>4</sup> sputtering is caused by a small mass of the metal  $1$ , probably a few molecules of the metal in the neighbourhood of the point of impact of the positive ion taking up the energy of impact and vaporising on that account. Unlike

<sup>4</sup> R. K. Cowdik, *Ind. Jour. Phys.* Vol. 8, p. 209 (1933).

ordinary vaporisation the effect is instantaneous and localised. On the impact of the positive ion if the energy is sufficient the whole of the amalgam molecule that is struck by the ion is vaporised and thus the impurities reach the condenser and come as an impurity in the distillate. So the distinction between an ordinary gas heated still and the mercury arc still is one of general vaporisation and cathodic sputtering. In both a process of fractional distillation takes place. But since the process of vaporisation in the two cases are different, the products of distillation are also different. In the mercury arc the current density being greater than in the discharge tube the sputtering effects at the cathode can be expected to be greater than in the discharge tube. Hence it looks as if sputtering at the cathode of the arc is the cause of the impurity in the distillate from the arc still.

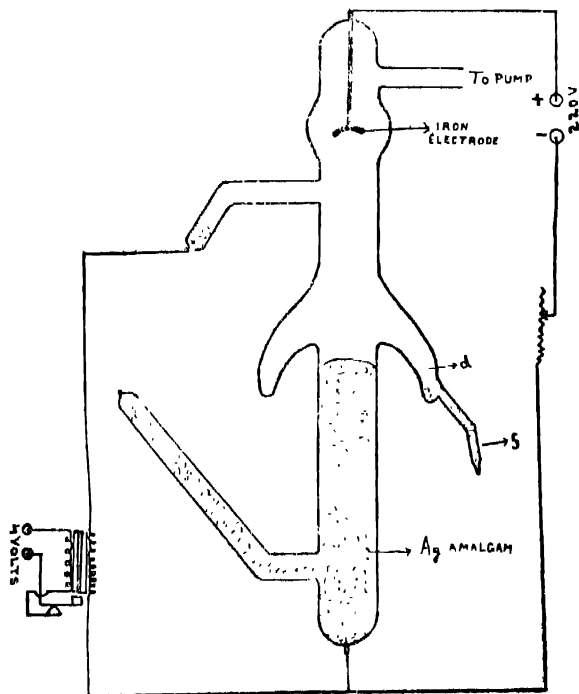


FIG. 4.

To experimentally investigate the point further a mercury arc as shown in Fig. 4 was constructed in which the anode was of metallic iron.

By making the anode of metallic iron and the cathode the pool of mercury, we are able to find out quantitatively the amount of metal sputtered from the cathode. If the anode were also of mercury the estimation of the amount of metal distilled over from the cathode will become difficult as we will have to estimate the same quantity of the metal in a larger mass of distilled mercury from the anode. Now silver has a boiling point as high as  $1955^{\circ}\text{C}$  and a sputtering value next only to gold which is taken as 100. Hence if an amalgam of silver is distilled by the arc shown in Fig. 4 and by an ordinary gas heated still we should be able to see the contrast in the performance of the two very clearly. But if an amalgam of Cd, Sn, or Zn be used the difference will not be so marked since the boiling point of these metals is low and their sputtering value is not also high. Another test is provided by an amalgam of Mg. Since its boiling point is high and sputtering value practically zero, it ought not to occur as an impurity in either still. It is necessary to use a concentrated solution of the amalgams to accentuate the result.

To examine this point the arc illustrated in Fig. 4 is used after being filled with the concentrated amalgam using specially purified mercury. The arc is exhausted by a Cenco pump. The tube is held vertically and the arc struck by connecting the terminals of the secondaries of an induction coil temporarily to *b* and *c* while a permanent D. C. potential is applied across *a* and *b* in series with a resistance as shown in Fig. 4. The distillate from the cathode collects in the annular ring '*d*' and flows into the side tube *f*. When sufficient amount of mercury collects in the tube it is drawn off by breaking the tip of the tube and the amount of silver in it is estimated quantitatively.

The same sample of amalgam as was used in the above experiment is distilled in an ordinary gas heated still as shown in Fig. 1. The apparatus is kept exhausted to the same degree of vacuum as in the arc shown in Fig. 4 and a slow heat applied from a Bunsen burner. The distilled mercury which collects in the bulb B is drawn out through the end c and the quantity of silver in it estimated.

A third sample of the same amalgam is distilled in the Waran's arc still and the silver in the sample of the distillate estimated.

The quantity of silver in all cases is estimated by separating the silver from the mercury and weighing it in the form of pure silver chloride. It was found that the mercury from the arc shown in Fig. 4 contained 6.5032% of silver by weight. The mercury from the Waran's arc still contained 60.32% of silver while the distillate from the ordinary gas heated still yielded only a qualitative test for the presence of silver but no quantitative estimation was possible as the percentage of silver in it was too low.

The above experiments were repeated using an amalgam of magnesium in the place of the silver. It was found that there was a slight trace of magnesium in the distillate from the ordinary gas heated still but there was no trace even in the distillate of the Waran's arc still and the distillate from the arc with the iron anode shown in Fig. 4.

The above experiments seem to confirm the idea that the impurity in the distillate from an arc still must be due to sputtering at the cathode. Silver is not an easily volatile metal but its rate of sputtering is next only to that of gold. Hence it is that we get only a trace of silver in the distillate from the ordinary gas heated still while in the case of mercury arc with an iron anode there is a large percentage of metal in the distillate. But in the case of the Waran's arc still the effect is masked by the vaporisation of the anode also and the percentage of silver in the distillate is lowered. In the case

of magnesium whose sputtering value is zero and boiling point fairly high we see that in the Waran's arc still and the special mercury arc distillate, magnesium does not occur. Slight traces of silver and magnesium occur in the distillate from the ordinary gas heated still likely being carried mechanically along the mercury vapour from the highly concentrated amalgams. This shows that the difference in the behaviour of the arc still and the ordinary gas flame heated still is not that due to a higher temperature of the arc as compared with the ordinary still heated at the bottom. If that were so whether the impurity was Ag or Mg should make little difference in the performance of the arc still. But we find that in the arc still Ag distills over and not Mg. Since the process of heat vaporisation and sputtering are different the order of removal of metals by ordinary distillation and arc distillation are different. The following table gives the order in which the different metals are removed by the different processes of cleaning

Metals removed by treatment with KOH.	Order of removal of metals by mer- curous nitrate.	Order of removal of metals by Oxidation. <sup>5</sup>	Order of removal of metals by heat vaporisa- tion.	Order of removal of metals by Waran's Arc still.
Sn	Mg	Zn	Au	Mg
Zn	Al	Cd	Pt	Al
Pb	Cr	Sn	Ag	Ni
—	Mn	Pb	Cu	Cu
—	Cd	Cu	Sn & Pb	Sn
—	Ni	—	Zn	Pt
—	Sn	—	Cd	Ag
—	Pb	—	—	Au
—	Cu	—	—	—

<sup>5</sup> Russel, *loc. cit.*

mercury. It will be seen from the table that to get mercury of the highest purity, it has to be treated under all the processes, since none of them can remove all the impurities with the same degree of efficiency and by a single trial. But when mercury contains one or more known impurities it will be advantageous to prefer one method of treatment to another. For instance if Au is an impurity it will be advisable to distill the mercury by ordinary distillation than by the Waran's Arc still. If magnesium, nickel, etc., are the known impurities it will be better to use the Arc distiller. Hence the Waran's Arc distiller has certain preferences over the ordinary gas heat distiller, although mercury to be distilled in it must not contain impurities in great proportion.

I have great pleasure in acknowledging my indebtedness to Dr. H. Parameswaran, M. A., Ph.D., D.Sc., F.I.P., Professor of Physics, Presidency College, Madras for all the guidance that he has given me in this work.

PHYSICS LABORATORY,  
PRESIDENCY COLLEGE,  
MADRAS, S. INDIA.





# On Molecular Screening Constants

By

PANCHANAN DAS.

(Received for publication, May 26, 1934.)

## ABSTRACT.

Assuming that in a diatomic molecule with two electrons, the inner one screens the charge on each nucleus by  $\frac{1}{2}e$ , the term values and the heat of dissociation of the molecules occurring in the following table are calculated by Hylleraas's method.

	LiH.	BeH.	Li <sub>2</sub> .
Heat of Dissoc*. (Calc.) (in electron volts.) ...	2.30	2.30	1.08
Heat of Dissoc*. (Obs.) (in electron volts.) ...	2.56	2.21	1.14

	$1s2p^1\Sigma.$	$1s2s^3\Sigma.$	$\frac{1}{2}\{1s2p(^1\pi + ^3\pi)\}.$	$1s1s^1\Sigma.$
Term value of H <sub>2</sub> (Calc.) (in Rydberg unit) ...	-1.490	-1.416	-1.442	-2.32
Term value of H <sub>2</sub> (Obs.) (in Rydberg unit) ...	-1.499	-1.469	-1.439	-2.33

The Ritz method of finding the characteristic energy values of atoms very often yields a useful collateral result, *viz.*, the value of the screening constant of the atomic nucleus. By a combination of the Ritz method and the method of

separation of variables Hylleraas<sup>1</sup> has almost exactly calculated the term values of the  $H_2$ -molecule in the lowest few states. The advantage he has had over his predecessors appears to lie in the fact that as a first approximation he regards the outer electron as moving in a field due to half the actual charge of each nucleus. It will be shown in the present paper that if the idea of nuclear screening to the extent of  $\frac{1}{2}e$  is applied to slightly more complex molecules, that leads to a fair agreement between the observed and calculated values of the electronic terms and the heat of dissociation, the calculation being extremely simplified by the fact that certain tables prepared by Hylleraas can be directly made use of.

Let the two nuclei in the molecule be denoted by  $a$  and  $b$ , and the electrons by the numbers 1 and 2; then  $r_{1a}$  stands for the distance between the nucleus  $a$  and the electron 1; similar meanings attach to  $r_{2b}$ ,  $r_{12}$ , etc. The potential energy of the electrons in Hylleraas's units is

$$V = -4 \left( \frac{1}{r_{1a}} + \frac{1}{r_{1b}} + \frac{1}{r_{2a}} + \frac{1}{r_{2b}} - \frac{1}{r_{12}} \right),$$

and the energy operator of the system is  $H = \Delta_1 + \Delta_2 + V$ , where  $\Delta_1$ ,  $\Delta_2$  are Laplacian operators with a constant factor. Then the total energy is

$$\int \bar{\psi} H \psi d\tau / \int \bar{\psi} \psi d\tau,$$

where

$$\psi = \psi_1 \psi_2$$

and

$$d\tau = d\tau_1 d\tau_2,$$

$\psi_1$  being the wave function of the electron 1,  $\psi_2$  being that of 2.

Now if we write

$$E' = \int \bar{\psi} \left( \Delta_1 - \frac{4}{r_{1a}} - \frac{4}{r_{1b}} \right) \psi d\tau / \int \bar{\psi} \psi d\tau, \quad \dots \quad (1)$$

$$E = \int \bar{\psi} \left( \Delta_2 - \frac{2}{r_{2a}} - \frac{2}{r_{2b}} \right) \psi d\tau / \int \bar{\psi} \psi d\tau, \quad (2)$$

and

$$E_s = 4 \int \bar{\psi} \left( -\frac{1}{2r_{2a}} - \frac{1}{2r_{2b}} + \frac{1}{r_{12}} \right) \psi d\tau / \int \bar{\psi} \psi d\tau \quad (3)$$

the total energy is  $E' + E + E_s$ .

It is evident from (1) and (2) that  $E'$  is the total energy of an electron in a field of two nuclei each of charge unity, while  $E$  (without prime) is the energy in a field of half the charge;  $E_s$  is a perturbation term involving exchange integrals of the Sugiura types which Hylleraas evaluates numerically. The notion of screening is thus implicit in a treatment where  $E_s$  is regarded as mere perturbation energy.

The energy values  $E$ ,  $E'$  of the individual electrons are found by Hylleraas by the use of elliptic coordinates. If  $2R$  be the internuclear distance and  $Z_a$ ,  $Z_b$  be the respective nuclear charges, the potential of an electron in terms of the elliptic coordinates

$$\xi = (r_a + r_b) / 2R$$

and

$$\eta = (r_a - r_b) / 2R$$

is easily seen to be

$$V = -\frac{2}{R} \frac{\xi(Z_a + Z_b) + \eta(Z_a - Z_b)}{\xi^2 - \eta^2}$$

When the variables have been separated in the resulting wave equation, the equation involving the variable  $\xi$  is found to be

$$\frac{\partial}{\partial \xi} \left\{ (\xi^2 - 1) \frac{\partial X}{\partial \xi} \right\} - \frac{n^2 X}{\xi^2 - 1} + \left[ -C\xi^2 + B\xi - A \right] X = 0 \quad \dots \quad (4)$$

where

$$B = R(Z_a + Z_b), \quad C = -\frac{1}{4} ER^2 \quad (5)$$

and  $A$  is another eigen value parameter determined by the corresponding equation in  $\eta$ .  $E$  is the energy parameter.

Before proceeding further we explain that in Hylleraas's notation  $E_{nlm}$  stands for the energy of an electron with quantum numbers  $n, l, m$ . For instance, an electron in the  $2p$  state with quantum numbers  $2, 1, 0$  has energy  $E'_{210}$ , under full nuclear charge.

In the case of hydrogen  $Z_a = Z_b = 1$ , and Hylleraas solves the equation (4) for the  $1s$ -state of the electron and tabulates the value of  $E'_{100}$  for different  $R$  values which is reproduced here :—

TABLE I.

$E'_{100}$	-3.470	-2.905	-2.683	-2.498	-2.341	-2.205	-2.089	-1.988	-1.899	-1.822
$R$	0.5	1	1.25	1.5	1.75	2	2.25	2.5	2.75	3

Table No 2 of his paper gives the values of  $E_{200}$ , the energy of a  $2s$ -electron in a nuclear field  $Z_a = Z_b = \frac{1}{2}$ . This is our table II.

TABLE II.

$E_{200}$	-0.250	-0.233	-0.227	-0.222	-0.216	-0.211	-0.207	-0.202	-0.194
$R$	0	1	1.25	1.5	1.75	2	2.25	2.5	3

We shall presently describe a method whereby the energy value  $E$  for any value  $Z_a, Z_b$  can be readily calculated by the use of the foregoing tables.

The equation corresponding to (4) for an electron on nuclei of charges  $Z'_a, Z'_b$  and at a distance  $2R'$  apart is

$$-\frac{\partial}{\partial \xi} \left\{ (\xi^2 - 1) \frac{\partial \chi'}{\partial \xi} \right\} - \frac{m^2 X'}{\xi^2 - 1} + \left[ -C'\xi^2 + B'\xi - A' \right] X' = 0 \quad \dots (6)$$

where

$$B' = R'(Z'_a + Z'_b), \quad C' = -\frac{1}{4} E/R^2 \quad \dots \quad (7)$$

Then (4) and (6) would constitute the same eigen value problem, if  $A' = A$ , which means that  $Z_a - Z_b = Z'_a - Z'_b$  and  $B' = B$ ,  $C' = C$ , which give from (5) and (7)

$$E(R) = \left( \frac{Z_a + Z_b}{Z'_a + Z'_b} \right)^2 E' \left( R, \frac{Z_a + Z_b}{Z'_a + Z'_b} \right) \quad \dots \quad (8)$$

Hence if a table of values of  $E(R)$  be given we can construct a table for  $E'(R)$  and *vice versa*, graphically by means of the formula (8).

We first take up the LiH molecule. We assume, as Hutchisson and Muskat<sup>2</sup> have done, that the Li-nucleus along with its K-electrons constitutes a simple nucleus of charge unity. The problem is to find the energy of a 1s-electron and a 2s-electron in the field of two nuclei, each of unit charge. The energy  $E'_{100}$  of the 1s-electron is already given in table I. This electron screens the nuclei to the extent of half the charge, so that the energy  $E_{200}$  of the 2s-electron is to be read from table II. Table III below gives the values of  $E_{LiH} = E'_{100} + E_{200} + 2/R$  which represents the total energy of the molecule LiH.

Table III

$E_{LiH}$	-1.137	-1.386	-1.414	-1.417	-1.407	-1.390
R	1	1.5	1.75	2	2.25	2.5

From a graph of  $E$  against  $R$  we find the minimum value of  $E_{LiH}$  to be -1.42 Rydberg units roughly. When this hypothetical molecule dissociates, the products are a hydrogen-like

<sup>2</sup> Hutchisson and Muskat, Phys. Rev., 40, 340 (1932).

atom in the  $1s$ -state and another in the  $2s$ -state, the total energy of which is  $-1.25$  units. Hence the heat of dissociation of the  $\text{LiH}$  molecule is  $-0.17$  units  $= 2.3$  electron-volts, which is the same as Hutchisson and Muskat's calculated value. The experimental value<sup>3</sup> is  $2.56$  volts.

In finding the heat of dissociation of the more complex  $\text{BeH}$  molecule Ireland<sup>4</sup> assumes that the  $\text{Be}$  nucleus along with its two  $\text{K}$ -electrons constitutes a simple nucleus of charge 2, so that the problem of the  $\text{BeH}$  molecule is that of two electrons, of which either both are in the  $2s$ -state or one is in the  $2s$ -state and the other in the  $2p$ -state, and a third electron in the  $1s$ -state in a field of two nuclei of charges 1 and 2 units. He shows that there is a  $^2\Sigma$  state and a  $^2\pi$  state in which  $E$  as a function of  $R$  has a minimum and the heats of dissociation calculated by him are  $3.5$  and  $1.5$  volts respectively while the experimental values are  $2.22$  and  $2.21$  volts. Admittedly the agreement is poor; but if we take a simplified model of the  $\text{BeH}$  molecule, in which the  $\text{Be}$  nucleus with its  $\text{K}$ -electrons and the third electron in the  $2s$ -state is regarded as a simple nucleus of charge 1, then  $\text{BeH}$  and  $\text{LiH}$  present identical problems; then the heat of dissociation of  $\text{BeH}$  also is  $2.3$  volts which is in better accord with the observed value than Ireland's.

We next consider the  $\text{Li}_2$  molecule. Effectively it has two electrons each in the  $2s$ -state in a field of two nuclei each of unit charge. The energy  $E'_{200}$  of a  $2s$ -electron in a field  $Z'_a = Z'_b = 1$  has not been given by Hylleraas; but we can apply the formula (8) and utilise the table II for  $E_{200}$  in finding  $E'_{200}$ . We get the following values:—

$E'_{200}$	-1	-0.930	-0.846	-0.777
$R$	0	0.5	1	1.5

<sup>3</sup> Nakamura, *Zs., f. Phys.*, 59, 218 (1930).

<sup>4</sup> Ireland, *Phys. Rev.*, 43, 331 (1933).

By graphical extrapolation we extend the table further :—

$E'_{200}$	-0.70	-0.62	-0.55	-0.47	-0.40
R	2	2.5	3	3.5	4

We assume that the 2s-electron of one Li atom effectively reduces the nuclear charges by  $\frac{1}{2}e$ ; then the energy of the 2s-electron of the second atom must be  $E_{200}$  of table II. Then the total energy of the molecule is  $E_{Li_2} = E'_{200} + E_{200} + 2/R$ . The values of  $E_{Li_2}$  are given below :—

$E_{Li_2}$	2.82	0.92	0.33	0.09	-0.02	-0.07	-0.08	-0.07
R	.5	1	1.5	2	2.5	3	3.5	4

$E_{Li_2}$  has thus a minimum value -0.08 units, which is the same as Furry<sup>5</sup> and Bartlett's. A Morse formula fits into the above table easily. If in the formula  $E = D e^{-2a(R-R_0)} - 2D e^{-a(R-R_0)}$ , we put  $D = 0.08$ ,  $R_0 = 3.5$  and  $a = 0.59$ , we get the following table of values :—

$E_{Li_2}$ (Morse)	0.92	0.33	0.083	-0.028	-0.070	-0.080	-0.075
R	1	1.5	2	2.5	3	3.5	4

The heat of dissociation  $D = .08 \times 13.53 = 1.08$  volts as against the observed value 1.14 volts.

We finally consider the hydrogen terms. If one electron be in the 1s-state while the other is in the 2p-state with quantum numbers (2, 1, 0) the resulting molecular terms are 1s2p  $^1\Sigma$ . Hylleraas's table No. 3 gives the value  $E_{210}$  of a (2, 1, 0) electron in a field of half the nuclear charges. Adding  $E_{210}$ ,  $E'_{100}$  and  $2/R$  we get the energy in the 1s2p  $\Sigma$  state,

<sup>5</sup> Furry and Bartlett, Phys. Rev., 38, 1615 (1931).

and the minimum value is found to be  $-1.490$  against the observed value  $-1.4989$  of the  $1s2p^1\Sigma$  term.

If the second electron is in the  $(2, 0, 0)$  state, the molecular term are  $1s2s^1\Sigma$ , and the energy value  $E_{200} + E'_{100} + 2/R$  has a minimum  $-1.416$  as against the observed value  $-1.4645$  of the  $1s2s^1\Sigma$  term. The difference is a little marked here, showing that the amount of screening is not exactly half on the  $2s$ -electron because of its penetrative character.

If the second electron is in the  $(2, 1, 1)$  state the molecular terms are  $1s2p^1\Sigma$ , and the calculated value has a minimum  $-1.442$ . The observed mean value

$$(1s2p^1\pi + 1s2p^3\pi)/2 \text{ is } -(1.4176 + 1.4600)/2 = -1.4388$$

which nearly agrees with the calculated term.

If both the electrons are in the  $1s$ -state, the molecular term is  $1s1s^1\Sigma$ , but in this case the amount of screening is found to be about  $\frac{3}{8}$  and not  $\frac{1}{2}$ . Thus putting  $Z_a = Z_b = \frac{5}{8}$  and  $Z'_a = Z'_b = 1$ , we get from (8)

$$E_{100}(R) = \left(\frac{5}{8}\right)^2 E'_{100}\left(\frac{5R}{8}\right) \quad (9)$$

The value of the total energy

$$E_{100} + E'_{100} + \frac{2}{R} = E_{H_2}$$

is calculated with the help of (9) and tabulated below :

$E_{H_2}$	$\infty$	$-0.90$	$-2.205$	$-2.31$	$-2.32$	$-2.30$	$-2.25$
$R$	$0$	$0.5$	$1$	$1.25$	$1.5$	$1.75$	$2$

The experimental value of  $E_{H_2}$  is  $-2.3262$ , and  $R_0 = 1.42$ . From the foregoing table we get  $E_{H_2} = -2.32$  and  $R_0 = 1.5$ .



It is obvious that all the labour involved in the numerical computation made by the writers referred to, when the atomic wave functions are used and the exchange integrals have to be evaluated, is reduced to a minimum here, principally because the use of elliptic co-ordinates gives a nearly exact eigen value, and secondly because of the consideration of the proper amount of screening.



# Ellipsoidal Wave-Functions

By

S. L. MALURKAR.

(Received for publication, May 24, 1934.)

## *Introduction.*

The wave equation

$$\Delta\phi - \frac{1}{c^2} \frac{\partial^2 \phi}{\partial t^2} = 0$$

occurs widely and normal functions suitable for different boundary conditions have been studied for a long time. In this paper an attempt has been made to obtain and study the properties of normal functions suitable for boundary conditions over ellipsoids or other central quadrics. The normal functions bear a relation to Lamé functions similar to that existing between Mathieu functions and the circular functions. During the course of this work, which was undertaken at widely separated intervals and completed by 1929, a memoir by F. Moeglich, dealing partially with the problem of obtaining functions which could be used for ellipsoidal boundaries, was published in 1927. The normal functions obtained by him are functions of two variables. His method simplifies much of the preliminary work and does not raise the question regarding the existence of solutions for nonlinear integral equations, which looms prominently in the present work.

Also neither the methods employed nor the results obtained bring out the analogy with the Mathieu and Lamé functions as, *e.g.*, the various species of normal functions corresponding to the species of Lamé functions.

The first section deals with the derivation of the differential equation in algebraical form and its uniformisation. The boundary conditions are also specified. In the form involving Jacobean elliptic functions the fundamental differential equation is

$$\frac{d^2 U}{d\xi^2} + (a_0 - a_1 k^2 sn^2 \xi - n^2 k^4 sn^4 \xi) U = 0$$

where  $n$  is a constant and  $a_0$  and  $a_1$  have to be characteristic constants.

The next section is devoted to properties common to all the characteristic functions. It is seen that the solutions can be written in the form

$$(sn\xi)^{\sigma_1} (cn\xi)^{\sigma_2} (dn\xi)^{\sigma_3} \psi(sn^2\xi)$$

where  $\psi$  is an integral function of  $sn\xi$  and  $\sigma_1$ ,  $\sigma_2$ , and  $\sigma_3$  have values equal to 0 or 1. The functions are therefore continuously differentiable for finite values of  $sn\xi$ . From the usual form of the second solution of a second order differential equation in the normal form the symmetry character of the second solution is found.

The second half of the section is concerned with orthogonal relations. By the usual methods it is shown that the characteristic constants are real so long as we deal with real Cartesian space. The wave functions can be normalised. The linear independence of the characteristic functions follows easily. A third orthogonal relation that will prove of use is also given.

Section III deals with integrals connected with the equations. From an analogue to Whittaker's integral for a wave equation, the integral equations of the characteristic functions

are deduced. The integral equations are non-linear. The convention is therefore made that the solutions are always dealt with in their normal form.

Then the actual form of the nuclei for the four species and eight types are given. By ordinary methods the integral equation can be solved for small values of  $n$ .

The method of stationary phase gives us the asymptotic expressions for large values of  $sn\xi$ . It follows simply from the asymptotic expressions for large and positive values of  $sn\xi$  that the second solution behaves differently from the characteristic functions.

The work involved is rather heavy for the calculation of the functions. The method of Horn used by Jeffreys was applied to the present problem for large values of  $n$ . It is possible that this is the first application of the method for a differential equation with two characteristic constants. The method adopted in the section requires a slight explanation. The condition for determining the various constants that occur is first given and at the end a review is made by comparing the asymptotic solution obtained in this section with the one got by using the method of stationary phase. This is possible as the asymptotic expressions have a common region of validity. Considering formally, the Horn and Jeffreys method is a re-arrangement of the Hamburger approximation about the irregular point. Probably this formal relation may be extended so as to facilitate the identification of solutions in their variant forms. For large values of  $n^2$  no approximations of the third and fourth species have been derived.

I. The fundamental system of confocal quadrics which define the elliptic co-ordinates are taken here to be

$$1 = x^2/(\lambda - e_3) + y^2/(\lambda - e_2) + z^2/(\lambda - e_1)$$

where

$e_1, e_2, e_3$  are real,  $e_1 > e_2 > e_3$  and  $e_1 + e_2 + e_3 = 0$ .

This choice saves symbols. The quadric is an ellipsoid, a hyperboloid of one sheet or a hyperboloid of two sheets according as  $\lambda > c_1$ ,  $e_1 > \lambda > c_2$ , or  $e_2 > \lambda > c_3$ . The co-ordinates corresponding to the three quadrics are denoted by  $\lambda$ ,  $\mu$ ,  $\nu$ . The ranges of values given above for them are useful. As is well-known, the following relation holds :

$$x^2 = (\lambda - c_3)(\mu - c_3)(\nu - c_3)/(e_3 - c_1)(c_3 - c_2)$$

$$y^2 = (\lambda - c_2)(\mu - c_2)(\nu - c_2)/(c_2 - c_1)(c_2 - c_3)$$

$$z^2 = (\lambda - c_1)(\mu - c_1)(\nu - c_1)/(c_1 - e_2)(c_1 - c_3).$$

Denoting for shortness

$$\Delta_{\lambda}^2 = (\lambda - c_1)(\lambda - c_2)(\lambda - c_3)$$

and similar symbols for other variables ( $\mu$ ,  $\nu$ ) and  $\sum_{\lambda\mu\nu}$  for the sum of cyclically permuted terms, the wave equation

$$\Delta\phi - 1/c^2 \cdot \partial^2\phi / \partial t^2 = 0$$

reduces to

$$-4/(\lambda - \mu)(\mu - \nu)(\nu - \lambda) \cdot \left[ \sum_{\lambda\mu\nu} \Delta_{\lambda} (\mu - \nu) \partial (\Delta_{\lambda} \partial \phi / \partial \lambda) / \partial \lambda \right] \\ - 1/c^2 \cdot \partial^2\phi / \partial t^2 = 0. \quad \dots (1.0)$$

Without loss of generality it is assumed that  $\phi$  is proportional to  $\exp(ipt)$  and so we replace  $-1/c^2 \cdot \partial^2\phi / \partial t^2$  by  $p^2\phi^2/c^2$ .

The equation (1.0) becomes

$$\sum \Delta_{\lambda} (\mu - \nu) \partial (\Delta_{\lambda} \partial \phi / \partial \lambda) / \partial \lambda - p^2 (\lambda - \mu)(\mu - \nu)(\nu - \lambda) \phi / 4c^2 = 0. \dots (1.1)$$

The equation is separable and we may assume as usual that the solution is of form  $\Lambda(\lambda) M(\mu) N(\nu)$ . The three functions  $\Lambda(\lambda)$ ,  $M(\mu)$  and  $N(\nu)$  satisfy the same differential equation as for  $\Lambda$ ; the equation is

$$\Delta_{\lambda} d(\Delta_{\lambda} d\Lambda/d\lambda)/d\lambda = (a_0 + a_1\lambda - p^2\lambda^2/4c^2)\Lambda \quad \dots (1.2)$$

where  $a_0$  and  $a_1$  are arbitrary constants. A priori their values are not known. They have to be restricted by a choice as in the case of Mathieu or Lamé functions. In the problems that we come across  $\phi$  is of the nature of a varying potential or like quantity. The simplest assumption would be that it is single valued in space. The derivatives of  $\phi$  are of the nature of velocity or force or the like. As we deal with finite magnitudes of these quantities, and much less frequently with infinite values, we make the following restrictions.  $\phi$  is a one valued function of  $x, y, z$  with bounded derivatives everywhere in the finite region. This would mean that  $\Lambda$  has to be one-valued in  $(\lambda - e_1)^{\frac{1}{2}}, (\lambda - e_2)^{\frac{1}{2}}$  and  $(\lambda - e_3)^{\frac{1}{2}}$  with one or more factors of the type  $(\lambda - e_1)^{\frac{1}{2}}, (\lambda - e_2)^{\frac{1}{2}}$  and  $(\lambda - e_3)^{\frac{1}{2}}$ . It will be seen later that apart from these factors the main function is an integral function of any of the three quantities

$$(\lambda - e_1)^{\frac{1}{2}}, (\lambda - e_2)^{\frac{1}{2}}; \text{ and } (\lambda - e_3)^{\frac{1}{2}}$$

The equation (1.2) written in full is

$$(\lambda - e_1)(\lambda - e_2)(\lambda - e_3)[d^2 \Lambda / d\lambda^2 + 1/2 \{1/(\lambda - e_1) + 1/(\lambda - e_2) + 1/(\lambda - e_3)\} d\Lambda / d\lambda]$$

$$-(a_0 + a_1 \lambda - p^2 \lambda^2 / 4c^2) \Lambda = 0.$$

This equation has singularities at  $e_1, e_2$  and  $e_3$  with exponents 0 and 1/2, and an irregular singularity at infinity. The equation is therefore a confluent form of differential equation with six regular singularities.\*

The form of the equation suggests that

$$\Lambda = (\lambda - e_1)^{\sigma_1/2} (\lambda - e_2)^{\sigma_2/2} (\lambda - e_3)^{\sigma_3/2} \Lambda_1(\lambda)$$

where  $\sigma_1, \sigma_2, \sigma_3$  could be 0 or 1, and  $\Lambda_1(\lambda)$  is some function of  $\lambda$  which is one valued and bounded and which in a variant form will be shown to be integral in  $(\lambda - e_1)^{\frac{1}{2}}, (\lambda - e_2)^{\frac{1}{2}}$  and  $(\lambda - e_3)^{\frac{1}{2}}$  and the like.

\* Cf. L. Ince., Ordinary Differential Equations, p. 502.

As every finite point except  $\lambda = e_1, e_2$  or  $e_3$  is an ordinary point of the differential equation no such point could be a multiple zero of  $\Lambda_1$  unless the function is identically zero, which case we bar out. The finite zeros of  $\Lambda_1$  have to be different from  $e_1, e_2$  or  $e_3$  as otherwise the exponents at these points could not be 0 or 1/2.

The presence of the radicals in the algebraic form of the differential equation prevents an easy handling of it. The limiting or boundary conditions are combrous for use. This difficulty can be overcome by uniformising the variables. The two possible forms of the equations corresponding to the Weirstrassian and the Jacobean elliptic functions are both easily derivable and could be solved in a more elegant way.

The invariants of an elliptic function (Weirstrassian) are so determined that the semi-periods  $\omega_1, \omega_2, \omega_3$ ; ( $\omega_1 + \omega_2 + \omega_3 = 0$ ) satisfy  $\mathfrak{E}(\omega_r) = e_r$ ; ( $r=1, 2$  or  $3$ ). The variables  $\alpha, \beta, \gamma$  are found so that  $\lambda = \mathfrak{E}(\alpha)$ ;  $\mu = \mathfrak{E}(\beta)$ ; and  $\nu = \mathfrak{E}(\gamma)$ . The equation (1.1) becomes

$$\sum_{\alpha\beta\gamma} [\mathfrak{E}(\beta) - \mathfrak{E}(\gamma)] \partial^2 \phi / \partial \alpha^2 - p^2 \{ \mathfrak{E}(\beta) - \mathfrak{E}(\gamma) \} \{ \mathfrak{E}(\gamma) - \mathfrak{E}(\alpha) \} \{ \mathfrak{E}(\alpha) - \mathfrak{E}(\beta) \} \phi / c^2 = 0. \quad \dots (1.3)$$

This equation gives rise to a one-variable equation in the form

$$d^2 A / d\alpha^2 + \{ p^2 / c^2 [\mathfrak{E}(\alpha)]^2 - a_1 \mathfrak{E}(\alpha) - a_0 \} A = 0. \quad \dots (1.4)$$

where  $a_1, a_0$  are arbitrary constants which vary according to the form of the equation employed.

The Jacobean form is obtained by taking

$$\begin{aligned} \lambda = \mathfrak{E}(\alpha) &= e_1 - (e_1 - e_3) k^2 \operatorname{sn}^2 \xi \\ \mu = \mathfrak{E}(\beta) &= e_1 - (e_1 - e_3) k^2 \operatorname{sn}^2 \eta \\ \nu = \mathfrak{E}(\gamma) &= e_1 - (e_1 - e_3) k^2 \operatorname{sn}^2 \zeta \end{aligned} \quad \dots (1.5)$$



where  $k^2 = (c_1 - c_2)/(c_1 - c_3)$ ;

and  $k'^2 = (c_2 - c_3)/(c_1 - c_3)$

which is possible if  $\alpha = (\xi + iK')/\sqrt{(c_3 - c_1)}$

with similar relations for  $\beta$  and  $\gamma$ .  $iK'$  is the quarter period in the usual notation.\*

As the explicit relations between the Cartesian and the Jacobean elliptic co-ordinates may be useful they are collected below :

$$\left. \begin{aligned} x &= q/k' \operatorname{dn} \xi \operatorname{dn} \eta \operatorname{dn} \zeta \\ y &= -iqk^2/k' \operatorname{cn} \xi \operatorname{cn} \eta \operatorname{cn} \zeta \\ z &= -iqk^2 \operatorname{sn} \xi \operatorname{sn} \eta \operatorname{sn} \zeta \end{aligned} \right\} \quad \dots \quad (1.6)$$

where  $q = \sqrt[4]{(e_1 - e_3)}$ .

The equation (1.1) reduces to

$$\sum_{\xi \eta \zeta} (sn^2 \eta - sn^2 \zeta) \partial^2 \phi / \xi \partial^2 + n^2 k^4 (sn^2 \xi - sn^2 \eta) (sn^2 \eta - sn^2 \zeta) (sn^2 \zeta - sn^2 \xi) \phi = 0 \quad \dots \quad (1.7)$$

where  $n = pq/c$ . The corresponding single variable equation is

$$d^2 U / d\xi^2 + (a_0 - a_1 k^2 sn^2 \xi - n^2 k^4 sn^4 \xi) U = 0 \quad \dots \quad (1.8)$$

This is the generalised Lamé equation as denoted by L. Ince. When  $n=0$  it passes to the usual Lamé form and with proper conditions leads to Lamé functions.

The limiting conditions for the arbitrary constants are that they should be so chosen that

(i)  $U$  or  $A$  is a doubly periodic function of  $\xi$  or  $\alpha$  as the Jacobean or the Weierstrassian form is used.

(ii)  $U$  or  $A$  has bounded derivatives at all points except possibly at  $\xi = iK'$  or  $2K + iK'$  and congruent points in the Jacobean form or  $\alpha = 0$  in the Weierstrassian form.

\* See, e.g., Whittaker and Watson, Modern Analysis, p. 501.

We may confine ourselves to the Jacobean form as being simpler to deal with in spite of the fact that the formulae are unsymmetrical. When  $n=0$  the above conditions would lead to the Lamé functions, with  $a_1 = l(l+1)$  where  $l$  is an integer and  $a_0$  has one of  $2l+1$  discrete characteristic values. In the memoir by Moeglich\* already referred to he has proved the existence of the characteristic constants with the help of linear integral equations for the above equation. And they correspond to the characteristic constants of Lamé functions.

II. It is necessary to have and to utilize the general properties of the functions which can be derived without evaluating their particular values.

A comparison with the algebraic form or a simple examination of the Jacobean form of the equation shows that the form of the solution should be

$$U(\xi) = (sn\xi)^{\sigma_1} (cn\xi)^{\sigma_2} (dn\xi)^{\sigma_3} \psi(sn^2\xi),$$

where  $\sigma_1, \sigma_2$  or  $\sigma_3$  may be 0 or 1, and the nature of  $\psi$  is to be determined. By the limitations imposed already its derivatives exist at all points with the possible exception of points congruent to  $\xi = iK'$  or  $\xi = 2K + iK'$ .

As the differential equation is unchanged by changing  $\xi$  to  $-\xi$ ,  $U(-\xi)$  is also a solution of the same differential equation. Hence it is enough if we consider solutions of type

$$(sn\xi)^{\sigma_1} (cn\xi)^{\sigma_2} (dn\xi)^{\sigma_3} \psi(sn^2\xi). \quad \dots \quad (2.1)$$

If the characteristic constants  $a_1, a_0$  be real and  $n^2$  is real  $\psi$  may be taken to be a real function of the argument, *i.e.*,  $sn^2\xi$ .

Let us consider the solution valid about the point  $\xi=0$ . Here  $\psi(sn^2\xi)$  can be expanded as a power series in terms of

\* F. Moeglich, *Annalen der Physik*, Band 83, p. 609; *Beugungserscheinungen an Körpern von ellipsoidischer Gestalt*, 1927.

$sn^2\xi$ . Ordinarily this power series ceases to converge as the singular points are approached.

As  $\psi(sn^2\xi)$  is unchanged when  $\xi$  is replaced by  $(2K - \xi)$ ,  $K = \xi$  is a point of symmetry for the function and as the derivatives of  $U(\xi)$  and hence  $\psi$  exist unless  $|sn\xi|$  is infinite;

so  $d\psi/d\xi = 0$ ; at  $\xi = K$ .

Similarly  $d\psi/d\xi = 0$  at  $\xi = K + iK'$ .

Any solution of the differential equation (1.8) about the point  $\xi = K$  may be written as

$$AF_1(1-\theta^2) + B\sqrt{(1-\theta^2)}F_2(1-\theta^2)$$

where  $\theta$  denotes  $sn\xi$  and  $F_1, F_2$  are power series of their arguments.

$$\text{Hence } \psi(\theta^2) = \theta^{-\sigma_1} (1-\theta^2)^{-\sigma_2/2} (1-k^2\theta^2)^{-\sigma_3/2} \times [AF_1(1-\theta^2) + B\sqrt{(1-\theta^2)}F_2(1-\theta^2)].$$

$$\text{As } d\psi/d\xi = \sqrt{(1-\theta^2)(1-k^2\theta^2)} \cdot d\psi/d\theta$$

$$\text{and } d\psi/d\xi = 0 \text{ at } \xi = K \text{ or } \theta = 1,$$

$$\text{it follows that } A=0 \quad \text{if } \sigma_2=1$$

$$B=0 \quad \sigma_2=0,$$

i.e.,  $\psi$  considered as a function of  $\theta$  or  $sn\xi$  has no singularity at  $\theta = 1$  or  $\xi = K$ . Similarly  $\psi$  has no singularity at  $\xi = K + iK'$  or  $\theta = 1/k$ . But  $\psi$  can have no other singular points for finite values of  $|sn\xi|$ . Hence  $\psi(sn^2\xi)$  is an integral function of  $sn\xi$ .  $\psi$  can similarly be considered as integral functions of  $cn\xi$  or  $dn\xi$ . This property is useful.

A second solution of the differential equation could be taken to be as

$$U(\xi) \int_{dt}^{\xi} / \{U(t)\}^2.$$

It follows easily that this would have the form

$$(sn\xi)^{1-a_1} (cn\xi)^{1-a_2} (dn\xi)^{1-a_3} \psi_1(sn^2\xi). \quad \dots (2.2)$$

where  $\psi_1$  is not necessarily an integral function of  $sn^2\xi$ . But from the form of the solution, it follows that when  $\xi$  is real, the origin ( $\xi=0$ ) is a point of symmetry for one solution, while it is the point of anti-symmetry for the other solution of the differential equation. Also when  $\xi=K+i\sigma$ , i.e., when  $\xi$  lies along a line parallel to the imaginary axis through  $\xi=K$ , the point  $\xi=K$  is a point of symmetry for one solution and the point of anti-symmetry for the other.

*Orthogonal relations.* Corresponding to the two characteristic constants of the differential equation two important orthogonal relations are obtainable.

For clearness  $U(\xi | a_1 a_0)$  will be written to show that  $a_1 a_0$  are the two characteristic constants.

Let us consider the case, when the constant  $a_1$  is the same for two characteristic functions and the other constants are  $a_0$  and  $a'_0$ .

The respective functions are  $U(\xi | a_1 a_0)$  and  $U(\xi | a_1 a'_0)$ .

From their differential equations it follows

$$\int \left\{ U(\xi | a_1 a'_0) \partial^2 U(\xi | a_1 a_0) / \partial \xi^2 - U(\xi | a_1 a_0) \partial^2 U(\xi | a_1 a'_0) / \partial \xi^2 \right\} \\ \int U(\xi | a_1 a_0) U(\xi | a_1 a'_0) d\xi = 0 \quad \dots (2.3)$$

where the integrals are taken over the same range. The first integral vanishes when the initial and final limits of integration differ by a whole number of periods which do not contain points congruent to  $iK'$  or  $2K+iK'$ . Hence if  $a_0 \neq a'_0$

$$\int U(\xi | a_1 a_0) U(\xi | a_1 a'_0) d\xi = 0,$$

the range of integration being from  $\xi = \xi_1$  to  $\xi = \xi_1 + 4mK + 4m'iK'$  where  $m$  and  $m'$  are integers. Preferably we may take the whole range of integration to be from  $-2K$  to  $+2K$ .

Now let us consider the case when the characteristic constants are all different, and let  $a_1 a_0$  and  $a'_1 a'_0$  be the constants. Now the product function  $U(\xi | a_1 a_0) U(\eta | a_1 a_0)$  satisfies the differential equation

$$\begin{aligned} & \{ \partial^2 / \partial \xi^2 - \partial^2 / \partial \eta^2 \} U(\xi | a_1 a_0) U(\eta | a_1 a_0) \\ & - \{ a_1 k^2 + a_0 k'^2 (sn^2 \xi + sn^2 \eta) \} (sn^2 \xi - sn^2 \eta) U(\xi) U(\eta) = 0. \end{aligned}$$

Hence it follows that

$$\begin{aligned} & U(\eta | a_1 a_0) U(\eta | a'_1 a'_0) [ U(\xi | a'_1 a'_0) \partial^2 U(\xi | a_1 a_0) / \partial \xi^2 \\ & \quad - U(\xi | a_1 a_0) \partial^2 U(\xi | a'_1 a'_0) / \partial \xi^2 ] \\ & - U(\xi | a_1 a_0) U(\xi | a'_1 a'_0) [ U(\eta | a'_1 a'_0) \partial^2 U(\eta | a_1 a_0) / \partial \eta^2 \\ & \quad - U(\eta | a_1 a_0) \partial^2 U(\eta | a'_1 a'_0) / \partial \eta^2 ] \\ & - k^2 (a_1 - a'_1) (sn^2 \xi - sn^2 \eta) U(\xi | a_1 a_0) U(\eta | a_1 a_0) U(\xi | a'_1 a'_0) U(\eta | a'_1 a'_0) = 0. \end{aligned}$$

Integrating with respect to  $\xi$  and  $\eta$  so that the limits of integration of each of these integrals differ by a whole number of periods, the first two terms integrate to zero. Of course, these ranges exclude points congruent to  $iK'$  or  $2K + iK'$ . The ranges for the two integrals need not be the same.

Hence

$$\begin{aligned} & (a_1 - a'_1) \iint (sn^2 \xi - sn^2 \eta) U(\xi | a_1 a_0) U(\eta | a_1 a_0) U(\xi | a'_1 a'_0) \times \\ & \quad U(\eta | a'_1 a'_0) d\xi d\eta = 0. \end{aligned}$$

The anti-symmetry of the integrand with respect to  $\xi$  and  $\eta$  prevents us from taking congruent ranges for the two integrals. The integration ranges may be mutually perpendicular to each other, not passing through  $iK'$  or  $2K + iK'$ . The convenient choice is for  $\xi$  from  $-2K$  to  $+2K$ , and for  $\eta$  from

$K-2iK'$  to  $K+2iK'$ . If  $a_1 \neq a'_1$  the integral is zero over these ranges. If  $a_1 = a'_1$  but  $a_0 \neq a'_0$  from (2.3) it follows that the integral is still zero. Hence

$$\iint (sn^2\xi - sn^2\eta) U(\xi | a_1 a_0) U(\eta | a_1 a_0) U(\xi | a'_1 a'_0) U(\eta | a'_1 a'_0) d\xi d\eta = 0 \dots (2.4)$$

if  $a_1 \neq a'_1$ ; or if  $a_1 = a'_1$  but  $a_0 \neq a'_0$ .

From the above equation it can easily be deduced that in the infinitesimally narrow strip where  $n^2$  and  $sn^2\xi$  are real, the characteristic constants are real.

If possible, let  $a_1$  and  $a_0$  be complex characteristic values and let  $\bar{a}_1$  and  $\bar{a}_0$  be their imaginary conjugates. From the differential equation it follows that if  $\psi_1$  and  $\psi_2$  are real functions of their arguments such that

$$U(\xi | a_1 a_0) = (sn\xi)^{\sigma_1} (cn\xi)^{\sigma_2} (dn\xi)^{\sigma_3} \{\psi_1(sn^2\xi) + i\psi_2(sn^2\xi)\},$$

the differential equation with constants  $\bar{a}_1$  and  $\bar{a}_0$  has a solution

$$U(\xi | \bar{a}_1 \bar{a}_0) = (sn\xi)^{\sigma_1} (cn\xi)^{\sigma_2} (dn\xi)^{\sigma_3} \{\psi_1(sn^2\xi) - i\psi_2(sn^2\xi)\},$$

and as this function satisfies the conditions of a characteristic function, the constants  $\bar{a}_1$  and  $\bar{a}_0$  are also characteristic constants. From (2.4) it follows that

$$(a_1 - \bar{a}_1) \iint (sn^2\xi - sn^2\eta) U(\xi | a_1 a_0) U(\eta | a_1 a_0) U(\xi | \bar{a}_1 \bar{a}_0) U(\eta | \bar{a}_1 \bar{a}_0) d\xi d\eta = 0.$$

$$-2K < \xi < 2K; \text{ and } \eta \text{ is from } K-2iK' \text{ to } K+2iK';$$

but

$$U(\xi | a_1 a_0) U(\xi | \bar{a}_1 \bar{a}_0) = (sn\xi)^{2\sigma_1} (cn\xi)^{2\sigma_2} (dn\xi)^{2\sigma_3} + \{[\psi_1(sn^2\xi)]^2 + [\psi_2(sn^2\xi)]^2\},$$

this quantity has a constant sign (positive) in the range  $-2K < \xi < 2K$ . Similarly,  $U(\eta | a_1 a_0) U(\eta | \bar{a}_1 \bar{a}_0)$  preserves the same sign throughout its range, positive, if  $\sigma_2 = 0$  and negative, if  $\sigma_2 = 1$ , and  $(sn^2\xi - sn^2\eta)$  is negative throughout the ranges of  $\xi$  and  $\eta$ . Hence the value of the integrand is real and has the

same sign throughout the ranges of integrations. The factor  $i$  is introduced owing to the fact that the range of integration for  $\eta$  is parallel to the imaginary axis. It follows that unless the value of the integrand is everywhere zero  $(a_1 - \bar{a}_1) = 0$  or  $a_1$  is real. We definitely bar out the null solution. Similarly from the other orthogonal relation it can be proved that  $a_0$  is also real.

Let us consider the integral

$$\iint (sn^2\xi - sn^2\eta) \{U(\xi | a_1 a_0) U(\eta | a_1 a_0)\}^2 d\xi d\eta$$

taken over the ranges  $-2K < \xi < 2K$  and  $\eta$  from  $K - 2iK'$  to  $K + 2iK'$ .

As before

$$\{U(\xi | a_1 a_0)\}^2 = (sn\xi)^{2\sigma_1} (cn\xi)^{2\sigma_2} (dn\xi)^{2\sigma_3} [\psi(s^2\xi)]^2$$

$\psi$  being a real function of  $sn^2\xi$  has a positive sign in the range of  $\xi$ . And  $\{U(\eta | a_1 a_0)\}^2$  is also real in the integration range for  $\eta$  and preserves the same sign positive, if  $\sigma_2 = 0$  and negative, if  $\sigma_2 = 1$ , and  $(sn^2\xi - sn^2\eta)$  is negative and hence as before the integral cannot be zero unless the characteristic functions identically vanish. This last possibility we ignore. As the value of the integral is not zero its value could be fixed arbitrarily. Owing to the presence of an imaginary factor it would not be possible to normalise the integral to unity and yet preserve the real nature of  $\psi(sn^2\xi)$  in the required range. The normalisation which commends itself most is the one when the value of the integral is  $\pm i$ . The ambiguity in signs is necessary as  $cn\eta$  is purely imaginary on the line  $K + i\sigma$ . This causes no confusion.

The ranges of integration being the narrow strip  $sn^2\xi$  and  $n^2$  real, it is not possible to study the characteristic constants when  $sn^2\xi$  is complex. The work would be prohibitive. All the quadrics which are real in the Cartesian co-ordinates are fully accounted for by the real values of  $sn^2\xi$ . Of course

this would be no reason to treat the complex values of  $sn^2\xi$  with indifference. In fact, it is only by considering the asymptotic nature of the characteristic functions when  $sn^2\xi$  is large and real, *i.e.*, when the quadric has all its axes imaginary, that we can deduce the difference between the two solutions of the differential equation.

The corresponding orthogonal relations are well known for Lamé functions and form the basis of Liouville and Klein expansion of an arbitrary function in terms of Lamé products.

Finally, we need a third orthogonal relation. Considering the differential equations for

$$U(\xi \mid a_1 a'_0; U(\eta \mid a_1 a_0); U(\zeta \mid a_1 a_0)$$

the  $a_1 a_0; a_1 a'_0$  being two pairs of characteristic constants with one common member  $a_1$ ; and writing for simplicity

$$F(\xi, \eta, \zeta) = U(\xi \mid a_1 a'_0)U(\eta \mid a_1 a_0)U(\zeta \mid a_1 a_0)$$

we have

$$\begin{aligned} (sn^2\eta - sn^2\zeta) \frac{\partial^2 F}{\partial \xi^2} + (sn^2\zeta - sn^2\xi) \frac{\partial^2 F}{\partial \eta^2} + (sn^2\xi - sn^2\eta) \frac{\partial^2 F}{\partial \zeta^2} \\ + n^2 k^4 (sn^2\xi - sn^2\eta)(sn^2\eta - sn^2\zeta)(sn^2\zeta - sn^2\xi)F \\ + (a'_0 - a_0)(sn^2\eta - sn^2\zeta)F = 0. \end{aligned} \quad \dots (2.5)$$

Let  $f(\xi\eta\zeta)$  be a symmetrical, doubly periodic bounded and continuously differentiable but not necessarily separable solution of (1.7), *i.e.*,

$$\begin{aligned} \sum_{\xi\eta\zeta} (sn^2\eta - sn^2\zeta) \frac{\partial^2 f}{\partial \xi^2} \\ + n^2 k^4 (sn^2\xi - sn^2\eta)(sn^2\eta - sn^2\zeta)(sn^2\zeta - sn^2\xi)f = 0. \end{aligned} \quad \dots (17b \text{ is})$$

By the usual process it is seen that

$$(a'_0 - a_0) \iiint F(\xi\eta\zeta) f(\xi\eta\zeta) (sn^2\eta - sn^2\zeta) d\xi d\eta d\zeta = 0 \quad \dots (2.6)$$



ranges

$$-2K < \xi < 2K; \quad -2K < \eta < 2K \quad \text{and} \quad \xi \text{ from } K-2iK' \text{ to } K+2iK'.$$

Hence if  $a'_0 \neq a_0$  the integral is zero.

The first two orthogonal relations provide us with proofs of linear independence of the various combinations of the characteristic functions.

For a given  $a_1$  and different values of  $a_0$  all being characteristic constants, the functions  $U(\xi | a_1 a_0)$  are all linearly independent. It may be recalled that for a given finite value of  $a_1$  the number of possible  $a'_0$ s are finite. If the linear independence did not exist we would have

$$U(\xi | a_1 a_0) = \sum'_{a'_0} \Lambda(a_1 a'_0) U(\xi | a_1 a'_0)$$

$\Sigma'$  denotes that in the summation with respect to  $a'_0$ ,  $a'_0 = a_0$  is excluded. Multiplying by  $U(\xi | a_1 a''_0)$  and integrating for  $\xi$  over a whole number of periods as, e.g.,  $-2K$  to  $+2K$  it is found that  $\Lambda(a_1 a'_0) = 0$  for all values of  $a'_0$ , whence the theorem follows.

Let

$$\begin{aligned} & U(\xi | a_1 a_0) U(\eta | a_1 a_0) \\ &= \sum'_{a'_1 a'_0} \Lambda(a'_1 a'_0) U(\xi | a'_1 a'_0) U(\eta | a'_1 a'_0) \end{aligned}$$

$\Sigma'$  denoting that in the summation,  $a_1 = a'_1$  and  $a_0 = a'_0$  are excluded, and that only a finite number of  $a_1$  and  $a_0$ s are taken.

Multiplying by

$$(sn^2 \xi - sn^2 \eta) U(\xi | a''_1 a''_0) U(\eta | a'_1 a''_0)$$

and integrating between the limits  $-2K < \xi < 2K'$   
and  $\eta$  between  $K-2iK'$  to  $K+2iK'$

we obtain  $\Lambda(a'_1 a'_0) = 0$  for all values of  $a'_1$  and  $a'_0$  included in the summation.

Let  $f(\xi\eta\zeta)$  be defined as before and let

$$\iiint f(\xi\eta\zeta)(sn^2\eta - sn^2\zeta)U(\eta | a_1a_0)U(\zeta | a_1a_0)d\eta d\zeta = \pm B(\xi | a_1a_0) \\ -2K \leq \eta \leq 2K \quad \text{and } \zeta \text{ is from } K-2iK' \text{ to } K+2iK'$$

it follows that over the same range

$$\iiint \{f(\xi\eta\zeta) - B(\xi | a_1a_0)U(\eta | a_1a_0)U(\zeta | a_1a_0)\}(sn^2\eta - sn^2\zeta) \\ \times U(\eta | a_1a_0)U(\zeta | a_1a_0)d\eta d\zeta = 0.$$

The symmetry of  $f(\xi\eta\zeta)$  and a repeated application of (2.6) shows that  $B(\xi | a_1a_0) = A(a_1a_0)U(\xi | a_1a_0)$ . The  $\pm$  are used as before to keep the functions real; -ve if there be a factor of type  $cn\xi$  in  $U(\xi | a_1a_0)$  and +ve otherwise.

It is possible to break up  $f(\xi\eta\zeta)$  as a sum of terms like  $A(a_1a_0)U(\xi | a_1a_0)U(\eta | a_1a_0)U(\zeta | a_1a_0)$  and a remainder which is orthogonal to any finite number of characteristic functions  $U(\eta | a_1a_0)U(\zeta | a_1a_0)$  as we like.

If  $f(\xi\eta\zeta)$  be representable as

$$(sn\xi)^{\sigma_1}(cn\xi)^{\sigma_2}(dn\xi)^{\sigma_3} \times \text{a function of } sn^2\xi;$$

$\sigma_1, \sigma_2$  or  $\sigma_3$  being 0 or 1, all the  $A(a_1a_0)$ 's which do not correspond to the particular characteristic functions with the same factor

$$(sn\xi)^{\sigma_1}(cn\xi)^{\sigma_2}(dn\xi)^{\sigma_3}$$

are easily seen to be zero. As it is possible to arrange any  $f(\xi\eta\zeta)$  as a sum of functions of the above form, the ambiguity due to  $\pm$  signs need not trouble us.

III. (a) *Integral Equations.\** The integral equations for the characteristic functions, which are naturally more complicated than usual, may now be deduced.

\* Communicated first at the Bangalore Session of the Conference of the Indian Mathematical Society, April, 1926.

The method adopted here is analogous to the one used by E. T. Whittaker in the case of Mathieu functions.\* We start from a modified expression of his general solution for the wave equation †

$$\Delta\phi - 1/c^2 \cdot \frac{\partial^2 \phi}{\partial t^2} = 0$$

when the solution is bounded at the origin. Whittaker's solution is

$$\iint F(x \cos u \cos v + y \cos u \sin v + z \sin u + ct; u; v) du dv.$$

As we are using the Jacobean elliptic functions, the modified expression can be put as

$$\iint F\left(\frac{1}{k'} \cdot xdnudnv + \frac{ik}{k'} ycnucnv + kzsusnv + ct; u; v\right) du dv \quad \dots \quad (3.0)$$

ranges

$$-2K < u < 2K; v \text{ from } K - 2iK' \text{ to } K + 2iK'.$$

The moduli  $k$  and  $k'$  are at our disposal. It may be supposed that they are equal to the values used in the previous sections.

If the solution of the wave equation in Jacobean elliptic functional form of the last section be a particular case of this integral, *i.e.*, if

$$U(\xi|a_1a_0)U(\eta|a_1a_0)U(\zeta|a_1a_0)\exp(ipt)$$

a particular value of this integral, it may be supposed without much sophistication that in the above integral the form of  $F(X, u, v)$  may be  $\exp(iX/c) S(u, v)$ , where  $S(u, v)$  is some function of  $u$  and  $v$  only.

\* E. T. Whittaker, Proc. of the Vth International Congress of Mathematics, 1912, Cambridge, also Modern Analysis. Whittaker and Watson, pp. 407 *et seq.*

† E. T. Whittaker, Math. Annalen, 1902, Vol. 57, pp. 353 *et seq.*

Replacing the values of  $x, y, z$  by their equivalents in terms of  $\xi\eta\zeta$  we obtain.

$$\begin{aligned}
 & U(\xi|a_1a_0)U(\eta|a_1a_0)U(\zeta|a_1a_0) \\
 &= \iint \exp \left[ in \left\{ \frac{1}{k'^2} \, dnu \, dnv \, dn\xi \, dn\eta \, dn\zeta \right. \right. \\
 &\quad \left. \left. + \frac{k^3}{k'^2} \, cnu \, cnv \, cn\xi \, cn\eta \, cn\zeta \right. \right. \\
 &\quad \left. \left. - ik^3 \, snu \, snv \, sn\xi \, sn\eta \, sn\zeta \right\} \right] S(u, v) du dv \quad \dots \quad (3.1)
 \end{aligned}$$

The integration limits for  $u$  and  $v$  are the same as before. As  $\xi\eta\zeta$  are independent of each other, any two of them may assume arbitrary values. Omitting all constant factors we get:

for

$$\eta=K; \zeta=0$$

$$U(\xi) = \iint \exp(in/k' \, dn\xi \, dnu \, dnv) S(u, v) du dv;$$

for

$$\eta=-K+iK'; \zeta=0$$

$$U(\xi) = \iint \exp(nk^2/k' \, cn\xi \, cnu \, cnv) S(u, v) du dv;$$

for

$$\eta=K+iK'; \zeta=K.$$

$$U(\xi) = \iint \exp(nk^2 \, sn\xi \, snu \, snv) S(u, v) du dv.$$

These three integrals suggest to us the types met with. We may replace the various exponential functions by cos, sin, cosh, and sinh functions, according to the requirements of symmetry about the points 0 and K. Though it is possible to deal individually with the three integrals, a slightly generalised form simplifies much of the work. It is evident that every one of the exponential or cos, sin, cosh, and sinh

functions is a symmetrical in  $\xi uv$ , doubly periodic, bounded and continuously differentiable (except at points congruent to  $iK'$  and  $2K + iK'$ ) solution of

$$\sum_{\xi uv} (sn^2 u - sn^2 v) \frac{\partial^2 f}{\partial \xi^2}$$

$$+ n^2 k^4 (sn^2 \xi - sn^2 u)(sn^2 u - sn^2 v)(sn^2 v - sn^2 \xi) f = 0.$$

The exponential and circular functional solutions of the integrals satisfy exactly the same conditions postulated for  $f$  on page 58. The additional condition of symmetry about the point 0 and  $K$  may be introduced as it is useful.

We may also write

$$(sn^2 u - sn^2 v) S(u, v)$$

instead of  $S(u, v)$ .

Hence the integral can be written as\*

$$U(\xi) = \iiint f(\xi uv) (sn^2 u - sn^2 v) S(u, v) du dv$$

the limits of integration are as before

$$-2K < u < 2K \text{ and for } v, K - 2iK' \text{ to } K + 2iK'.$$

As

$$d^2 U(\xi | a_1 a_0) / d\xi^2 - (n^2 k^4 sn^4 \xi + a_1 k^2 sn^2 \xi - a_0) U(\xi | a_1 a_0) = 0$$

and supposing that the conditions of differentiation under the integral sign are satisfied we get

$$\iint (sn^2 u - sn^2 v) S(u, v) \{ \partial^2 f / \partial \xi^2 - (n^2 k^4 sn^4 \xi + a_1 k^2 sn^2 \xi - a_0) f \} du dv = 0.$$

Utilising the differential equation satisfied by  $f(\xi uv)$  this may be written as :

$$\iint S(u, v) [(sn^2 v - sn^2 \xi) \{ \partial^2 f / \partial u^2 - (n^2 k^4 sn^4 u + a_1 k^2 sn^2 u - a_0) f \}$$

$$+ (sn^2 \xi - sn^2 u) \{ \partial^2 f / \partial v^2 - (n^2 k^4 sn^4 v + a_1 k^2 sn^2 v - a_0) f \}]$$

$$du dv = 0.$$

\* Cf. L. Ince., *loc. cit.*, p. 197.

And by partial integration we have

$$\begin{aligned}
 & \iint f(\xi uv) [(s^2 v - sn^2 \xi) (\partial^2 / \partial u^2 - n^2 k^4 sn^4 u - a_1 k^2 sn^2 u + a_0) S(u, v) \\
 & \quad + (sn^2 \xi - sn^2 u) (\partial^2 / \partial v^2 - n^2 k^4 sn^4 v - a_1 k^2 sn^2 v + a_0) S(u, v)] \times dudv. \\
 & + \int dv \left( sn^2 v - sn^2 \xi \right) \left( S \frac{\partial f}{\partial u} - f \frac{\partial S}{\partial u} \right) \\
 & + \int du \left( sn^2 \xi - sn^2 u \right) \left( S \frac{\partial f}{\partial v} - f \frac{\partial S}{\partial v} \right) \Big|_v \\
 & = 0.
 \end{aligned}$$

This equation can be satisfied if in particular  $S(u, v)$  is doubly periodic, bounded function of type  $U_1(u) U_2(v)$  where

$$d^2 U_1(u) / du^2 - (n^2 k^4 sn^4 u + a_1 k^2 sn^2 u - a_0) U_1(u) = 0$$

and

$$d^2 U_2(v) / dv^2 - (n^2 k^4 sn^4 v + a_1 k^2 sn^2 v - a_0) U_2(v) = 0.$$

As  $a_1$  and  $a_0$  are characteristic constants, if it be assumed that two characteristic solutions cannot exist for the same pair of characteristic constants,  $U_1(u)$  and  $U_2(v)$  may be identified with  $U(u | a_1 a_0)$  and  $U(v | a_1 a_0)$ . Otherwise we can also proceed as follows :

The symmetry character of  $f(\xi uv)$  is the same as that of  $U(\xi | a_1 a_0)$  for the variable  $\xi$ . (It is assumed that we use  $f(\xi uv)$  in the cos, sin, etc., form). Hence if we assume that  $U_1(u)$  is equal to  $AU(u|a_1 a_0) + BV(u|a_1 a_0)$  where  $V(u|a_1 a_0)$  is the second solution of the differential equation, and as the ranges are symmetrical about 0 and  $K$ , and the symmetry characters are different for the two solutions at each of these points, it is seen easily that the second solution need not appear in the integrals. So we obtain an integral equation in the form

$$U(\xi | a_1 a_0) = \text{const} \iint U(u | a_1 a_0) U(v | a_1 a_0) (sn^2 u - sn^2 v) f(\xi uv) dudv \dots \quad (3.8)$$

the ranges of integration which have to be different for the two variables are as before

$$-2K < u < 2K ; \quad v \text{ from } K - 2iK' \text{ to } K + 2iK'.$$

The integral equation is not necessarily the most general one possible, but it is sufficient for our purpose. The constant in the integral equation is indefinite as the latter is nonlinear. The value of the constant may be made definite by assuming that if  $U(\xi)$  is a possible solution, then the following relation should be satisfied :

$$i \iint \{U(u) U(v)\}^2 (sn^2 u - sn^2 v) du dv = \pm 1.$$

In other words it may be said that the solution should always be used in its normal form. The ambiguity of signs is retained as before to keep the functions real and need not trouble us. Corresponding to this identity the integral equation may be written as

$$U(\xi) = \pm ic \iint f(\xi uv) (sn^2 u - sn^2 v) U(u) U(v) du dv,$$

where  $c$  is a constant of the integral equation. It is found that the integral equation has solutions which satisfy all our previous conditions only for certain discrete values of  $c$ .

The integral equation in the Weirstrassian form is easily obtainable as

$$U(\alpha) = \text{const} \iint U(\beta) U(\gamma) \{ \mathfrak{E}(\beta) - \mathfrak{E}(\gamma) \} \phi(\alpha\beta\gamma) d\beta d\gamma \quad \dots \quad (3.4)$$

$$\beta \text{ from } (\omega_1 - \omega_2) \text{ to } (\omega_1 + \omega_2)$$

$$\gamma \text{ from } (\omega_2 - \omega_1) \text{ to } (\omega_1 + \omega_2)$$

where  $\phi$  satisfies the following differential equation and where  $\phi$  is symmetrical, doubly periodic and bounded and has bounded derivatives,

$$\sum_{\alpha\beta\gamma} [\mathfrak{E}(\beta) - \mathfrak{E}(\gamma)] \partial^2 \phi / \partial \alpha^2 \\ - [\mathfrak{E}(\beta) - \mathfrak{E}(\gamma)] [\mathfrak{E}(\gamma) - \mathfrak{E}(\alpha)] [\mathfrak{E}(\alpha) - \mathfrak{E}(\beta)] p^2 \phi / c^2 = 0,$$

*i.e.*, the same wave equation in the Weirstrassian form with which we started.

In both these integral equations the nucleus satisfies, except for a trivial factor, the partial differential equation from which we started. This is analogous to the integral equations for Mathieu and Lamé functions.\*

III. (b) Till now the integral equation has been treated in a general form. It is easy to specify the nuclei. We have eight and only eight distinct forms corresponding to the four species of Lamé functions or in other words to the various possible modes of symmetry character about the two points 0 and K. As the characteristic function consists of two portions one being

$$(sn\xi)^{\sigma_1} (cn\xi)^{\sigma_2} (dn\xi)^{\sigma_3}$$

and the other an integral function of  $sn^2\xi$  a tabular arrangement of the first factor may be useful.

	$sn \xi,$	$sn \xi \, cn \xi,$	
1,	$cn \xi,$	$cn \xi \, dn \xi,$	$sn\xi \, cn\xi \, dn\xi$
	$dn \xi,$	$dn \xi \, sn \xi,$	

The corresponding integral equations are :

factor            1.

$$U(\xi) = ic \iint \cosh (nk^2 sn\xi \, sn\eta \, sn \zeta) (sn^2\eta - sn^2\zeta) U(\eta) U(\zeta) \, d\eta d\zeta \quad \dots \quad (3.51)$$

factor             $sn\xi.$

$$U(\xi) = ic \iint \sinh (nk^2 sn\xi \, sn\eta \, sn\zeta) (sn^2\eta - sn^2\zeta) U(\eta) U(\zeta) \, d\eta d\zeta \quad \dots \quad (3.52)$$

factor             $cn \xi.$

$$U(\xi) = -ic \iint \sinh (nk^2/k' \cdot cn\xi \, cn\eta \, cn\zeta) (sn^2\eta - sn^2\zeta) U(\eta) U(\zeta) \, d\eta d\zeta \quad (3.53)$$

\* E. T. Whittaker, *loc. cit.* and Proc. Lond. Math. Soc. (2), Vol. XIV, pp. 260 *et. seq.*  
See also Modern Analysis, p. 564.



factor  $dn \xi$ .

$$U(\xi) = ic \iint \sin(n/k' \cdot dn \xi \, dn \eta \, dn \zeta) (sn^2 \eta - sn^2 \zeta) U(\eta) U(\zeta) \, d\eta d\zeta \quad \dots \quad (3.54)$$

factor  $sn \xi \, cn \xi$ .

$$U(\xi) = -ic \iint cn \xi \, cn \eta \, cn \zeta \sinh(nk^2 sn \xi \, sn \eta \, sn \zeta) (sn^2 \eta - sn^2 \zeta) U(\eta) U(\zeta) \, d\eta d\zeta \quad \dots \quad (3.55)$$

factor  $cn \xi \, dn \xi$ .

$$U(\xi) = -ic \iint dn \xi \, dn \eta \, dn \zeta \sinh(nk^2/k' \cdot cn \xi \, cn \eta \, cn \zeta) (sn^2 \eta - sn^2 \zeta) \\ \times U(\eta) U(\zeta) \, d\eta d\zeta \quad \dots \quad (3.56)$$

factor  $dn \xi sn \xi$ .

$$U(\xi) = ic \iint sn \xi \, sn \eta \, sn \zeta \sin(n/k' \cdot dn \xi \, dn \eta \, dn \zeta) (sn^2 \eta - sn^2 \zeta) U(\eta) U(\zeta) \\ d\eta d\zeta \quad \dots \quad (3.57)$$

factor  $sn \xi \, cn \xi \, dn \xi$ .

$$U(\xi) = -ic \iint sn \xi \, sn \eta \, sn \zeta \, cn \xi \, cn \eta \, cn \zeta \sin(n/k' \cdot dn \xi \, dn \eta \, dn \zeta) \\ (sn^2 \eta - sn^2 \zeta) U(\eta) U(\zeta) \, d\eta d\zeta \quad \dots (3.58)$$

In addition every characteristic function satisfies the normalising condition that

$$\iint (sn^2 \eta - sn^2 \zeta) [U(\eta) U(\zeta)]^2 \, d\eta d\zeta = \pm 1 \quad \dots \quad (3.6)$$

according as the characteristic function has not or has a factor of type  $cn \zeta$ .

The limits of integration are same for all the integrals.

$$-2K < \eta < 2K; \text{ and } \zeta \text{ is from } K - 2iK' \text{ to } K + 2iK'.$$

We might of course make the ranges smaller owing to symmetry considerations.

The integral equations can be solved in the usual fashion for small values of  $n$  and  $sn^2 \xi$ . An example is given for the function which reduces to a constant when  $n$  is zero.

We assume the following expansions in powers of  $n$  :

$$U(\xi) = (8\pi/k^2)^{-\frac{1}{2}} \{1 + n^2 U_2(\xi) + n^4 U_4(\xi) + \dots\} / (1 + n^2 b_2 + n^4 b_4 + \dots) \\ (8\pi c/k^2)^{-1} = (8\pi/k^2)^{-\frac{1}{2}} (1 + n^2 a_2 + n^4 a_4 + n^6 a_6 + \dots); \quad \dots \quad (3.7)$$

after substituting these values in the two integrals we obtain the following equations :—

$$\{U_2(\xi) + a_2 + b_2\} \\ = ik^2/8\pi \iint (sn^2\eta - sn^2\zeta) \left\{ \frac{k^4 sn^2\xi}{2} \frac{sn^2\eta sn^2\zeta}{2} + U_2(\eta) + U_2(\zeta) \right\} d\eta d\zeta \\ 2b_2 = ik^2/8\pi \iint (sn^2\eta - sn^2\zeta) \{U_2(\eta) + U_2(\zeta)\} d\eta d\zeta. \\ U_4(\xi) + (a_2 + b_2)U_2(\xi) + a_4 + a_2b_2 + a_4 \\ = ik^2/8\pi \iint (sn^2\eta - sn^2\zeta) \left[ \frac{k^8 sn^4\xi}{4!} \frac{sn^4\eta sn^4\zeta}{4!} \right. \\ \left. + \{U_2(\eta) + U_2(\zeta)\} \frac{k^4 sn^2\xi sn^2\eta sn^2\zeta}{2!} \right. \\ \left. + U_4(\eta) + U_2(\eta) U_2(\zeta) + U_4(\zeta) \right] d\eta d\zeta.$$

These equations lead to the following values provided we assume that  $U_2(\xi)$ ,  $U_4(\xi)$ , etc., have no constant term :

$$U_2(\xi) = k^2 sn^2\xi/6; \quad a_2 = (1 + k^2)/18 = b^2.$$

$$U_4(\xi) = k^4 sn^4\xi/5! + (1 + k^2)k^2 \cdot \frac{1}{2!} \cdot \frac{1}{6} \cdot sn^2\xi.$$

Much of the work is reduced by using Legendre's equality :

$$EK' + E'K - KK' = \pi/2$$

in the usual notation, or in the integral form as used here

$$i \iint (sn^2\eta - sn^2\zeta) d\eta d\zeta = 8\pi/k^2.$$

### III. (c) : Asymptotic Expansions for large values $|sn\xi|$ .

It is possible to obtain the asymptotic expansions for characteristic functions with the help of the integral equations for large values of  $|sn\xi|$ . At present we shall confine ourselves to real values of  $sn^2\xi$ . In the integral equations the nucleus is a rapidly oscillating function if  $sn^2\xi$  is large and negative. The method of stationary phase introduced by Kelvin would be necessary to evaluate the integral. When  $sn^2\xi$  is large and positive we deal with exponentials of real quantities and simpler calculations lead to the asymptotic expression.

For the purpose of this subsection it may be assumed that the values of the characteristic function for small values of  $sn^2\xi$  and the values of the characteristic constant are known. The integral limits may conveniently be taken as  $0 < \eta < K$  and  $\zeta$  from  $K$  to  $K+iK'$  and suitable factors of 2 are introduced.

Let us consider the first integral equation

$$U(\xi) = 16ic \iint \cosh(nk^2 sn\xi \, sn\eta \, sn\zeta)(sn^2\eta - sn^2\zeta) U(\eta) U(\zeta) d\eta d\zeta.$$

The points  $sn\eta=1$  and  $sn\zeta=1$ , or  $sn\zeta=1/k$  are stationary points. Of these it can be seen that owing to the factor  $(sn^2\eta - sn^2\zeta)$  the dominant term of the integral would be contributed from the neighbourhood of the point  $sn\eta=1$ ;  $sn\zeta=1/k$ . The line of integration for  $\zeta$  may be divided into two sections at  $sn^2\zeta = \frac{1+k^2}{2k^2}$ , so that the contributions about the two stationary points may be considered separately. The integral is therefore

$$\begin{aligned} & 16ic \int_0^K \int_{K+iG}^{K+iK'} \cosh(nk^2 sn\xi \, sn\eta \, sn\zeta)(sn^2\eta - sn^2\zeta) U(\eta) U(\zeta) d\eta d\zeta \\ & + 16ic \int_0^K \int_K^{K+iG} \cosh(nk^2 sn\xi \, sn\eta \, sn\zeta)(sn^2\eta - sn^2\zeta) U(\eta) U(\zeta) d\eta d\zeta \\ & = I_1 + I_2, \quad \text{where } sn^2(K+iG) = (1+k^2)/2k^2. \end{aligned}$$

We can also find the asymptotic value of the characteristic function when  $sn\xi$  is real and large. As far as physical applications are concerned it is unnecessary as it corresponds to a quadric with all its axes imaginary. But it proves useful for the demonstration that the differential equations have only one characteristic solution. It is sufficient to derive only the dominant terms.

Let  $sn\xi$  be positive. In the integral

$$16ic \iint \cosh (nk^2 sn\xi sn\eta sn\zeta) (sn^2\eta - sn^2\zeta) U(\eta) U(\zeta) d\eta d\zeta.$$

$nk^2 sn\xi sn\eta sn\zeta$  has a maximum value equal to  $nk sn\xi$ . We can write the cosh expression as a sum of two exponentials. The term with the factor  $\exp(-nk^2 sn\xi sn\eta sn\zeta)$  is seen to be of a far smaller order than the term with the factor

$$\exp(nk^2 sn\xi sn\eta sn\zeta).$$

In

$$U(\xi) = 16ic \exp(nk sn\xi) \iint \exp(-nk sn\xi sn\eta sn\zeta) \cosh(nk^2 sn\xi sn\eta sn\zeta) (sn^2\eta - sn^2\zeta) U(\eta) U(\zeta) d\eta d\zeta$$

the important contribution is from the neighbourhood of  $\eta = K$ ;  $\zeta = K + iK'$  and very simple calculation gives the leading term as

$$\frac{32C}{k^2} U(K)U(K+iK') \frac{\exp(nk sn\xi)}{nk sn\xi}$$

When  $sn\xi$  is real and negative we use the other exponential term which we neglected in the above case, and we obtain a similar dominant term.

It is sufficient to give only the dominant terms for the other functions when  $sn^2\xi$  is large and negative.

factor  $sn\xi$  is  $iv = nk^2 sn\xi$ .

$$16 ck'^2/k^2. U(K)U(K+iK') \frac{\pi k \sin v/k}{2vk'^2}.$$

Factor  $cn$   $\frac{\sin (nkc n\xi)}{nc n\xi}$  omitting all constants

Factor  $dn$   $\sin (ndn\xi/h)/ndn\xi$

Factor  $cn$   $cn\xi \sin v K_2/4 \sin (v-vK^2/4-\pi/4)/v^{\frac{3}{2}}$

where  $v=nksn\xi$ .

The other functions are not given here as they are quite similar. When  $sn^2\xi$  is large and positive, i.e.,  $\xi$  is on the line  $iK'$  it would be convenient to express all elliptic functions in terms of  $sn\xi$  as  $|sn\xi| \sim |cn\xi| \sim \frac{1}{k} |dn\xi|$ . For simplicity, we may suppose that  $sn\xi$  is positive, without losing the generality.

The characteristic functions of the first species have the asymptotic form leaving off all constant factors :

$$\exp (nk sn\xi)/sn\xi.$$

Second species :

$$\exp (nk sn\xi)/sn\xi.$$

Third species :

$$\exp (nk sn\xi)/\sqrt{sn\xi}.$$

Fourth species :

$$\exp (nk sn\xi).$$

Let us consider the value of the function on the line  $iK'+\epsilon$ . Let  $\epsilon > 0$ , and be small. All the functions have the dominant term given by an expression of type  $\exp(nk sn\xi)$ .  $(sn\xi)^{-s}$  where  $s$  is some constant depending on the species. The corresponding asymptotic expression for the second solution of the differential equation would be given by

$$V(\xi) = U(\xi) \int_{iK'+0}^{\xi} dt' \{U(t')\}^2$$

where  $+0$  is put to show distinctly that  $sn\xi$  is large and positive. The behaviour when  $sn\xi$  is large and negative could be obtained from considerations of symmetry. The order of the above integral can be obtained as

$$V(\xi) \sim \text{const.} \exp(-nk sn\xi) \cdot (sn\xi)^{2-k}.$$

This asymptotic expression for the second solution is bounded as  $sn\xi$  tends to  $+\infty$  while all the characteristic functions become infinite for the same values of  $sn\xi$ . Hence the second solution of the differential equation must be falling in a separate category, quite apart from the characteristic functions.

#### IV. Asymptotic expansion when $n$ is large.

The methods developed by Horn and Jeffreys\* for the determination of the asymptotic solutions of differential equations have been so fruitful in many instances that it appeared worth while to apply similar methods in the present investigation, and obtain asymptotic expressions for large values of  $n^2$ . It may be remarked incidentally that the calculation involved in this method is considerably less than for the other methods.

$$\text{In } d^2U/d\xi^2 - (n^2k^4 sn^4\xi + a_1 k^2 sn^2\xi - as)U = 0$$

we assume

$$U = \exp(nX) \cdot Y \{1 + f_1/n + f_2/n^2 + \dots\} \quad \dots \quad (4.10)$$

where  $X$ ;  $Y$ ;  $f_1$ ;  $f_2$ ; ..... are functions of  $\xi$  only. We also assume that

$$a_1 = \alpha_{-2}n^2 + \alpha_{-1}n + \alpha_0 + \alpha_1/n + \alpha_2/n^2 + \dots$$

$$a_0 = \beta_{-2}n^2 + \beta_{-1}n + \beta_0 + \beta_1/n + \beta_2/n^2 + \dots$$

(4.11 & 4.12)

\* Horn, Math. Annalen, Vol. 52, p. 342, 1899. Jeffreys, Proc. Lond. Math. Soc., Vol. XXIII (Ser. 2), p. 428; see also Goldstein, Trans. Phil. Soc. of Cambridge, 1927.

Substituting in the differential equation and comparing the coefficients of the powers of  $n$ , we have the following equations :

$$X'^2 - k^4 sn^4 \xi - \alpha_{-2} k^2 sn^2 \xi + \beta_{-2} = 0; \quad (4.21)$$

$$2X'Y' + YX'' - (\alpha_{-1} k^2 sn^2 \xi - \beta_{-1})Y = 0; \quad (4.22)$$

$$Y'' + 2X'Y' - (\alpha_0 k^2 sn^2 \xi - \beta_0)Y = 0; \quad (4.23)$$

where the primes denote derivatives with respect to  $\xi$ . The first equation is solved by choosing  $\alpha_{-2}$  and  $\beta_{-2}$  so that  $X$  is doubly periodic. The other equations are then treated similarly.

From (4.11)

$$X' = \pm \int \sqrt{(k^4 sn^4 \xi + \alpha_{-2} k^2 sn^2 \xi - \beta_{-2})} d\xi.$$

It is seen that  $X$  has three and only three forms when it could be doubly periodic. Each of the three forms leads to an asymptotic expression and to corresponding constants

For  $X = \pm k sn\xi$ ;

$$\left. \begin{aligned} X'^2 - k^4 sn^4 \xi + k^2(1 + k^2)sn^2 \xi - k^2 &= 0 \\ \text{So } \alpha_{-2} &= -(1 + k^2); \beta_{-2} = -k^2 \end{aligned} \right\} \quad (4.31)$$

For  $X = \pm ikcn\xi$ .

$$\left. \begin{aligned} \alpha_{-2} &= -1; \quad \beta_{-2} = 0 \end{aligned} \right\} \quad (4.32)$$

For  $X = \pm idn\xi$

$$\left. \begin{aligned} \alpha_{-2} &= -k^2; \quad \beta_{-2} = 0 \end{aligned} \right\} \quad (4.33)$$

From (4.22)

$$\log (YX'^{\frac{1}{2}}) - \frac{1}{2} \int (\alpha_{-1} k^2 sn^2 \xi - \beta_{-1}) d\xi / X' = \text{const.} \quad (4.41)$$

We may choose the most appropriate constant by its simplicity. Its value multiplies the whole function by a

constant, and hence would not be very important for the form of the asymptotic expression.

If  $X = \pm ksn\xi$

Then

$$\log [Y(cn\xi dn\xi)^{\frac{1}{2}}]$$

$$= \frac{1}{2kk'^2} [a_{-1}k^2 - \beta_{-1}] \log \{(1 + sn\xi)/cn\xi\} \\ - (a_{-1} - \beta_{-1})k \log \{(1 + ksn\xi)/dn\xi\}]$$

Hence

$$Y = (cn\xi dn\xi)^{-\frac{1}{2}} \left( \frac{1 + sn\xi}{cn\xi} \right)^{\pm(l + \frac{1}{2})} \left( \frac{1 + ksn\xi}{dn\xi} \right)^{\mp(m + \frac{1}{2})} \dots$$

provided

$$\begin{aligned} a_{-1}k^2 - \beta_{-1} &= 2kk'^2(l + \tfrac{1}{2}) \\ a_{-1} - \beta_{-1} &= 2k'^2(m + \tfrac{1}{2}) \end{aligned} \quad \} \quad \dots \quad (4.43)$$

It is easily seen that  $Y$  is doubly periodic and symmetrical or anti-symmetrical about the various points only if  $l$  and  $m$  are integers. Let  $Y_1$  and  $Y_2$  be the values of  $Y$  with +ve and -ve signs. We have for large values of  $n$  compared with  $f_1$ .

$$U(\xi) \sim A \exp(nk sn\xi) \cdot Y_1 + B \exp(-nksn\xi) Y_2$$

$$Y_1(\xi) = Y_2(-\xi)$$

$$\text{If } U(\xi) = \pm U(-\xi); \text{ then } B = \pm A.$$

$$U(\xi) \sim A [Y_1 \exp(nksn\xi) \pm Y_2 \exp(-nksn\xi)]$$

giving the even and odd functions. The solutions fail completely at  $\xi \equiv K$  or  $K + iK'$  and Stoke's phenomena occur at these points.



We may obtain the next approximation as follows :

From (4.23) we have

$$2f_1 + Y''/YX' - (\alpha_0 k^2 sn^2 \xi - \beta_0)/X' = 0$$

$$\text{Or } 2f_1 + Y'/YX' + \int \{Y'/Y \cdot (Y'/Y + X''X) - \alpha_0 k^2 sn^2 \xi + \beta_0\} \frac{d\xi}{X'} = 0 \dots (4.51)$$

We leave off the constant of integration as before. The above partial integration simplifies the calculation.

In particular for  $X = \pm ksn\xi$

we have :

$$\begin{aligned} & 2f_1 + 1/k \cdot [(l + \frac{1}{2})/cn^2 \xi - (m + \frac{1}{2})k/dn^2 \xi] \\ & \pm sn\xi(dn^2 \xi + k^2 cn^2 \xi)/2k \cdot cn^2 \xi dn^2 \xi \\ & \pm sn\xi/2k \cdot [(l^2 + l)/cn^2 \xi + (m^2 + m)/dn^2 \xi] \\ & \pm 1/kk'^2 \cdot \{\beta_0 - 2k(l + \frac{1}{2})(m + \frac{1}{2}) - (\alpha_0 + \frac{1}{2})k^2 + \frac{1}{2}k'^2(l^2 + l + \frac{1}{2})\} \\ & \pm \log\{(1 + sn\xi)/cn\xi\} \\ & \pm 1/k'^2 \cdot \{\beta_0 - 2k(l + \frac{1}{2})(m + \frac{1}{2}) - (\alpha_0 + \frac{1}{2}) - \frac{1}{2}k'^2(m^2 + m + \frac{1}{2})\} \\ & \pm \log\{(1 + ksn\xi)/dn\xi\} \\ & = 0. \end{aligned}$$

We determine  $\alpha_0$  and  $\beta_0$  as follows : Let  $f_{1+}$  and  $f_{1-}$  be the values corresponding to  $nksn\xi$  and  $-nksn\xi = X$  respectively. Then to a second approximation the asymptotic expansion is (neglecting terms of order  $1/n^2$ )

$$U(\xi) \sim A \exp(nksn\xi)(1 + f_{1+}/n)/Y + B \exp(-nksn\xi)(1 + f_{1-}/n)/Y.$$

Consider the solution for points on the line  $K + i\sigma$  where  $\sigma$  is real and  $K' > |\sigma|$ . On the half line below the real axis the constants may be taken as  $A'$  and  $B'$ . We find the relation between the two sets of constants by the symmetry about  $K$ . But it will be found that it is not possible to have non-zero values of  $A$ ,  $B$ ,  $A'$  and  $B'$  with the symmetrical property unless the logarithmic term  $\log\{(1 + sn\xi)/cn\xi\}$  has its

co-efficient zero. Hence we equate the co-efficient to zero. Again considering the symmetry about  $K+iK'$  for points lying parallel to the real axis the co-efficient of the other logarithmic term is found to be zero. The required criteria are that the co-efficients of the logarithmic terms must be equated to zero. Similarly in the higher stages of approximations also we successively put the co-efficients of logarithmic terms to zero and also determine the successive approximations of the characteristic constants.

Hence

$$\alpha_0 + 1/2 = -\frac{1}{2}(l^2 + l + m^2 + m)$$

$$\beta_0 = +(\alpha_0 + 1/2) + 2k(l + 1/2)(m + 1/2) + 1/2k'^2(m^2 + m + 1/2).$$

The case of  $X = \pm ksn\xi$  has been given in more detail than the other two cases as it appears to be the more important one. The other two functions can be written down without much explanation

For  $X = \pm ikcn\xi$

$$Y = (sn\xi dn\xi)^{-\frac{1}{2}} \left( \frac{1 + cn\xi}{sn\xi} \right)^{\pm(l+1/2)} \left( \frac{k' + ikcn\xi}{dn\xi} \right)^{\mp(m+1/2)} \quad (4.44)$$

$$\beta_{-1} = -2ik(l+1/2); \alpha_{-1} = 2k'(m+1/2) - 2ik(l+1/2) \quad (4.45)$$

$$\beta_0 = 2(l+1/2)(m+1/2)ikl' - 1/2(l^2 + l + k^2 + 1/2)$$

$$\alpha_0 = -(l^2 + l)/2 - (m^2 + m)/2$$

$$f_1 = i/2k[(l+1/2)/sn^2\xi - (m+1/2)ikl'/dn^2\xi]$$

$$\pm cn\xi(dn^2\xi - k^2sn^2\xi)/4iksn^2\xi dn^2\xi$$

$$\mp cn\xi[(l^2 + l)/sn^2\xi - (m^2 + m)k^2/dn^2\xi]/2ik$$

for  $X = \pm idn\xi$ .

$$Y = (sn\xi cn\xi)^{-\frac{1}{2}} \left( \frac{1 + dn\xi}{ksn\xi} \right)^{\pm(l+1/2)} \left( \frac{k' + dn\xi}{kcn\xi} \right)^{\pm(m+1/2)}$$

$$\beta_{-1} = -2ik^2(l+1/2); \alpha_{-1} = -2ik'(m+1/2) - 2i(l+1/2)$$

$$f_1 = i\{(l+1/2)/sn^2\xi - (m+1/2)k'/cn^2\xi\}/2k^2$$

$$\begin{aligned} & \pm dn\xi(cn^2\xi - sn^2\xi)/4ik^2sn^2\xi cn^2\xi \\ & \mp dn\xi\{(l^2+l)/sn^2\xi - (m^2+m)/cn^2\xi\}/4ik^2 \\ \beta_0 &= 2k'(l+1/2)(m+1/2) - 1/2(l^2+l+3/2) \\ \alpha_0 k^2 &= -(l^2+l+k^2)/2 - (m^2+m)/2. \end{aligned}$$

There is an important point yet to be noticed. In the choice for  $X$  it has been said that it should be doubly periodic, and we obtained three possible values for it. Given the value of  $X$  the rest of the steps follow simply from considerations of symmetry or doubly periodic property of the resulting functions. Consider  $U(\xi)$  for a given value of  $n$ . Its asymptotic expression for large values of  $sn^2\xi$  has been found by the application of the method of stationary phase. In every case we found that we had the asymptotic expression in terms of  $nksn\xi$ ,  $nkc n\xi$  or  $ndn\xi$ . Hence the method of stationary phase would be quite applicable even when  $|sn\xi|$  is large. The Horn-Jeffreys approximation gives the asymptotic expressions in terms of the same values for large values of  $n$ . Hence the asymptotic expression derived from large values of  $n$  becomes better applicable for large values of  $|sn\xi|$ . Hence for sufficiently large values of  $|sn\xi|$  and  $n$  the asymptotic expression derived from the method of stationary phase must approximate to that obtained in this section for large values of  $n$ . And at least the dominant terms must be identical.

Leaving off all constant factors the dominant term obtained by the method of stationary phase is

$$\frac{\cos}{\sin} inksn\xi/nksn\xi$$

when  $sn^2\xi$  is large and negative, and

$$\exp(nksn\xi)/nsn\xi; \quad \exp(-nksn\xi)/nsn\xi$$

when  $sn\xi$  is large and positive, and negative respectively. To the same order of approximation, the expression derived in this section is

$$\exp(\pm nksn\xi)/sn\xi.$$

The other functions like those having a factor  $cn\xi$  and  $dn\xi$  give dominant terms with expressions of form

$$\exp(\pm ink\, cn\xi)/cn\xi$$

$$\exp(\pm indn\xi)/dn\xi.$$

As

$$|sn\xi| \sim |cn\xi| \sim |dn\xi| \sim 1/k$$

when  $sn^2\xi$  is large these expressions are not different from those already obtained. We may start with any of the three possible values for the expression X, namely,

$$= \pm ksn\xi, \pm ikcn\xi \text{ or } \pm idn\xi.$$

All the three possible values for X are doubly periodic functions of  $\xi$ . These three expressions exhaust the possible values for X. The relations between these three possible asymptotic expressions to the other functions obtained in this essay can be obtained by comparing the asymptotic expressions obtained for large values of  $n$  and  $sn^2\xi$  in this and previous section.

From the three possible asymptotic forms it can easily be seen that the characteristic constants of the differential equation and asymptotic expressions are real only when (i) when  $n$  is purely real  $X = \pm ksn\xi$ , (ii) when  $n$  is purely imaginary  $X = \pm idn\xi$ . The third case when  $X = \pm ikcn\xi$  the characteristic constants are always complex.

But we know that in the infinitesimally narrow strip when  $n$  and  $sn^2\xi$  are real the characteristic constants are real. Hence we need consider only  $X = \pm ksn\xi$  when  $n^2$  is positive and  $X = \pm idn\xi$  when  $n^2$  is negative. In such cases the asymptotic expressions are also real.

It gives me great pleasure to acknowledge the encouragement I received from Prof. J. E. Littlewood, Cambridge, and Dr. E. P. Metcalfe, then Principal, Central College, Bangalore, during the course of the work.

# Transport Phenomena in Degenerate Gases and their Bearing on White Dwarfs.

By

A. GANGULI AND P. MITRA.

(Received for publication, March 22, 1934.)

## ABSTRACT.

Methods for the study of transport problems due to Maxwell and Chapman have been extended to the degenerate gases by applying the new statistics due to Fermi and Dirac. In order to apply this to an assembly of electrons and ions, Perisco's method has been adopted using known data for white dwarfs. Calculations are given for the companion of Sirius and  $\epsilon_2$ -Eridani for different central temperatures.

Recently Kothari studied the transport phenomena in degenerate gases by applying Boltzman's method<sup>1</sup> and considered the case of inverse square law according to the method due to Chapman.<sup>2</sup> In a later paper<sup>3</sup> he indicates the possibility of the application of his result to white dwarfs. Since the problem is of vital interest not only to dwarf stars but even to the ordinary giant stars, which according to Milne<sup>4</sup> possess a degenerate core, in the present investigation we shall study the problem afresh after the more powerful method due to Maxwell and Chapman<sup>5</sup> and in the application to stellar models we shall

<sup>1</sup> Kothari, Phil. Mag., **13**, 361 (1932); see also Uehling and Uhlenbeck, Phys. Rev., **43**, 552 (1933).

<sup>2</sup> Chapman, M. N., **32**, 291 (1922).

<sup>3</sup> Kothari, *ibid*, **93**.

<sup>4</sup> Milne, *ibid*, **91**, 4 (1930).

Maxwell, Collected Works, II; Chapman, Phil. Trans., **216A**, 279.

adopt the more rigid method of Perisco<sup>6</sup> instead of Chapman's approximation of the inverse square law.

In the new statistics the number of molecules per unit vol. is given by the well-known formula

$$n = \frac{m^3}{h^3} \iiint F(\dot{x}, \dot{y}, \dot{z}) d\dot{x}d\dot{y}d\dot{z} \quad \dots (1)$$

the distribution function  $F = \frac{1}{\Lambda^3 e^{u/kT} \pm 1}$ , the symbols  $\Lambda$ ,  $u$ ,  $k$  and  $T$  having their usual significance and plus or minus sign is to be taken according as the Fermi-Dirac or Bose-Einstein statistics is followed.

The average value of any property  $P$  is

$$\bar{P} = \frac{\iiint F P d\dot{x}d\dot{y}d\dot{z}}{\iiint F d\dot{x}d\dot{y}d\dot{z}}. \quad (2)$$

### *Hydrodynamical Equation of Continuity.*

With our new value of  $P$  and following Maxwell's method we obtain the usual hydrodynamical equation of continuity,<sup>7</sup> viz.,

$$\frac{dn}{dt} = - \left[ \frac{\partial}{\partial x} (n\dot{x}_0) + \frac{\partial}{\partial y} (n\dot{y}_0) + \frac{\partial}{\partial z} (n\dot{z}_0) \right] \quad \dots (3)$$

for the steady state, where  $\dot{x}_0$  etc. are the velocities due to mass-motion and  $n$  the number density.

For the gas not in the steady state we have the general equation

$$\begin{aligned} \frac{d}{dt} (n\bar{P}) = & - \left[ \frac{\partial}{\partial x} (n\dot{x}\bar{P}) + \frac{\partial}{\partial y} (n\dot{y}\bar{P}) + \frac{\partial}{\partial z} (n\dot{z}\bar{P}) \right] \\ & + \frac{n}{m} \left[ X \frac{\partial \bar{P}}{\partial \dot{x}} + Y \frac{\partial \bar{P}}{\partial \dot{y}} + Z \frac{\partial \bar{P}}{\partial \dot{z}} \right] + \triangle P. \end{aligned} \quad \dots (4)$$

<sup>6</sup> Perisco, M. N., **86**, 93 (1926).

<sup>7</sup> Jeans, D. *Mathematical Theory of Gases* (Cambridge), 4th Ed., Chap. IX, p. 231.

The second term in the above expression is due to the external force and the last one due to collision.

By usual methods of transformation we obtain finally

$$n \frac{D\bar{P}}{Dt} = \sum \left[ - \frac{\partial}{\partial x} (n \bar{\xi} \bar{P}) + \frac{n}{m} X \frac{\partial \bar{P}}{\partial \dot{x}_0} \right] + \triangle P \quad \dots \quad (5)$$

where

$$\frac{D}{Dt} = \frac{d}{dt} + \dot{x}_0 \frac{\partial}{\partial x} + \dot{y}_0 \frac{\partial}{\partial y} + \dot{z}_0 \frac{\partial}{\partial z}.$$

$\sum$  denotes the summation with respect to  $x, y, z$ ;  $\bar{\xi}, \bar{\eta}, \bar{\zeta}$  are the components of the molecular velocity.

In the case of transfer for a single gas  $\triangle P = 0$  and eqn. (5) reduces to

$$n \frac{D\dot{x}_0}{Dt} = - \left[ \frac{\partial}{\partial x} (n \bar{\xi}^2) + \frac{\partial}{\partial y} (n \bar{\xi} \bar{\eta}) + \frac{\partial}{\partial z} (n \bar{\xi} \bar{\zeta}) \right] + \frac{n}{m} X \quad \dots \quad (6)$$

and corresponding equations for  $y$  and  $z$ , putting  $P$  equal to  $\dot{x}, \dot{y}$ , and  $z$  respectively.

Eliminating  $X, Y$  and  $Z$  from the equations (5) and (6) we have the final equation

$$\begin{aligned} & n \left[ \frac{D\bar{P}}{Dt} - \frac{\partial \bar{P}}{\partial \dot{x}_0} \frac{D\dot{x}_0}{Dt} - \frac{\partial \bar{P}}{\partial \dot{y}_0} \frac{D\dot{y}_0}{Dt} - \frac{\partial \bar{P}}{\partial \dot{z}_0} \frac{D\dot{z}_0}{Dt} \right] \\ &= \sum \left[ - \frac{\partial}{\partial x} (n \bar{\xi} \bar{P}) + \frac{\partial \bar{P}}{\partial \dot{x}_0} \left\{ \frac{\partial}{\partial x} (n \bar{\xi}^2) + \frac{\partial}{\partial y} (n \bar{\xi} \bar{\eta}) + \frac{\partial}{\partial z} (n \bar{\xi} \bar{\zeta}) \right\} \right] + \triangle P. \end{aligned} \quad \dots \quad (7)$$

Taking  $P = \dot{x}^2$  we have equation (7) in the following form

$$\begin{aligned} n \frac{D}{Dt} (\bar{\xi}^2) &= - \frac{\partial}{\partial x} (n \bar{\xi}^3) - \frac{\partial}{\partial y} (n \bar{\xi}^2 \bar{\eta}) - \frac{\partial}{\partial z} (n \bar{\xi}^2 \bar{\zeta}) \\ &\quad - 2n \left( \bar{\xi}^2 \frac{\partial \dot{x}_0}{\partial x} + \bar{\xi} \bar{\eta} \frac{\partial \dot{x}_0}{\partial y} + \bar{\xi} \bar{\zeta} \frac{\partial \dot{x}_0}{\partial z} \right) + \triangle \dot{x}^2. \quad \dots \quad (8) \end{aligned}$$

Now

$$\dot{\xi}^2 = \overline{\eta}^2 = \zeta^2 = \lambda \quad \text{and} \quad \overline{\xi\eta} = \overline{\eta\zeta} = \overline{\xi\zeta} = 0.$$

Substituting these in equation (7) we have

$$\begin{aligned} & n \left[ \frac{D\overline{P}}{Dt} - \frac{\partial \overline{P}}{\partial \dot{x}_0} \frac{D\dot{x}_0}{Dt} - \frac{\partial \overline{P}}{\partial \dot{y}_0} \frac{D\dot{y}_0}{Dt} - \frac{\partial \overline{P}}{\partial \dot{z}_0} \frac{D\dot{z}_0}{Dt} \right] \\ &= \sum \left[ -\frac{\partial}{\partial x} (n\xi\overline{P}) + \frac{\partial \overline{P}}{\partial \dot{x}_0} \frac{\partial}{\partial x} (n\lambda) \right] + \triangle P \quad \dots \quad (9) \end{aligned}$$

and from equation (8) we have

$$n \frac{D\lambda}{Dt} = -2n\lambda \frac{\partial \dot{x}_0}{\partial x} + \triangle \dot{x}^2 \quad \dots \quad (10)$$

and two other similar equations.

Adding these and remembering that  $\triangle(\dot{x}^2 + \dot{y}^2 + \dot{z}^2) = 0$  we have

$$3 \frac{D\lambda}{Dt} = -2\lambda \left( \frac{\partial \dot{x}_0}{\partial x} + \frac{\partial \dot{y}_0}{\partial y} + \frac{\partial \dot{z}_0}{\partial z} \right). \quad \dots \quad (11)$$

On eliminating  $\frac{D\lambda}{Dt}$  between equations (10) and (11),

$$n\lambda \left[ 2 \frac{\partial \dot{x}_0}{\partial x} - \frac{2}{3} \left( \frac{\partial \dot{x}_0}{\partial x} + \frac{\partial \dot{y}_0}{\partial y} + \frac{\partial \dot{z}_0}{\partial z} \right) \right] = \triangle \dot{x}^2. \quad \dots \quad (12)$$

Incidentally we may note that from equations (3) and (11) we get

$$\lambda n^{-\frac{2}{3}} = 0$$

since  $\lambda = \frac{p}{m}$  for the classical as well as for the degenerate case, we have the general law of adiabetic motion

$$p\rho^{-\frac{5}{3}} = \text{Const.} \quad \dots \quad (13)$$



We now proceed to calculate the average values of  $\triangle P$  for  $P = \dot{x}\dot{y}$  and obtain finally

$$\triangle(\dot{x}\dot{y}) = n\lambda \left( \frac{\partial \dot{y}_0}{\partial x} + \frac{\partial \dot{x}_0}{\partial y} \right). \quad \dots (14)$$

We next consider the case of  $P = \dot{x}^2 + \dot{y}^2 + \dot{z}^2$

$$\begin{aligned} \bar{P} &= \dot{x}_0^2 + \dot{y}_0^2 + \dot{z}_0^2 + 5\dot{x}_0\lambda \\ \xi\bar{P} &= (3\dot{x}_0^2 + \dot{y}_0^2 + \dot{z}_0^2)\lambda + \xi^2(\xi^2 + \eta^2 + \zeta^2) \\ \eta\bar{P} &= 2\dot{x}_0\dot{y}_0\lambda, \quad \zeta\bar{P} = 2\dot{x}_0\dot{z}_0\lambda \end{aligned}$$

$\xi^4 = \frac{15}{7}\lambda^2$  for the degenerate case. (It may be noted that for classical case  $\xi^4 = 3\lambda^2$ )

$$\begin{aligned} \overline{\xi^2\eta^2} &= \overline{\xi^2\zeta^2} = \frac{5}{7}\lambda^2 (= \lambda^2 \text{ for the classical case}) \\ \overline{\xi^2(\xi^2 + \eta^2 + \zeta^2)} &= \frac{25}{7}\lambda^2 (= 5\lambda^2 \quad \text{,,} \quad \text{,,} \quad \text{,,}). \end{aligned}$$

Hence we have

$$\begin{aligned} &\triangle \dot{x}(\dot{x}^2 + \dot{y}^2 + \dot{z}^2) \\ &= -2n\dot{x}_0\lambda \left[ 2\frac{\partial \dot{x}_0}{\partial x} - \frac{2}{3} \left( \frac{\partial \dot{x}_0}{\partial x} + \frac{\partial \dot{y}_0}{\partial y} + \frac{\partial \dot{z}_0}{\partial z} \right) \right] + 2n\lambda\dot{y}_0 \left( \frac{\partial \dot{y}_0}{\partial x} + \frac{\partial \dot{x}_0}{\partial y} \right) \\ &\quad + 2n\lambda\dot{z}_0 \left( \frac{\partial \dot{x}_0}{\partial z} + \frac{\partial \dot{z}_0}{\partial x} \right) + \frac{15}{7}n\lambda \frac{\partial \lambda}{\partial x}. \quad \dots (15) \end{aligned}$$

For the classical case the last term in the above equation (right-hand side) has for its numerical coefficient 5 instead of  $15/7$ .

### Calculation of $\triangle P$ .

The dynamics of collision according to the new statistics<sup>8</sup> takes the form

$$\begin{aligned} \triangle_{12}P &= \int \dots \int F_1 \left( 1 \pm \frac{F_1}{Z_1} \right) F'_2 \left( 1 \pm \frac{F'_2}{Z_2} \right) d\dot{x}_1 d\dot{y}_1 d\dot{z}_1 d\dot{x}_2 d\dot{y}_2 d\dot{z}_2 \\ &\quad V[P] p dp d\epsilon \quad \dots (16) \end{aligned}$$

<sup>8</sup> Nordheim, P. R. S., 117A, 258 (1927).

$$p dp d\epsilon = \left[ (m_1 + m_2) K \right]^{\frac{2}{s-1}} \frac{4}{V^{s-1}} a da d\epsilon \quad \dots (17)$$

the symbols having their usual meanings.

In the case of interaction between electrons and atoms the additional correction term in the distribution functions may be neglected.

Proceeding by a method analogous to that of Maxwell and Chapman we get the following expressions for the coefficient of viscosity ( $\kappa$ ), conductivity ( $\mathfrak{S}$ ) and diffusion (D) considering the inverse fifth power law.

$$\kappa = \frac{p}{\mu n} \quad \dots (18)$$

where  $p$  is pressure and  $\mu = \frac{3}{2} \sqrt{2mK} A_2$ ;  $A_2 = \pi \int \sin^2 \theta' a da$  and  $\theta'$  is the angular deflection after collision.

$$\mathfrak{S} = \frac{15}{14} \kappa C_v \quad (\text{degenerate case})$$

$$\mathfrak{S} = \frac{5}{2} \kappa C_v \quad (\text{non-degenerate case})$$

$$D_{12} = \frac{p}{n} \cdot \frac{1}{m_1 m_2 A_1 (n_1 + n_2)} \frac{\sqrt{m_1 + m_2}}{K} \quad \dots (19)$$

For a single gas

$$D = \frac{3A_2 p}{\mu n^2 m A_1}$$

where

$$A_1 = 4\pi \int \cos^2 \frac{\theta'}{2} a da.$$

*Inverse Square Law*:—In the case of an assembly electrons and ions the attractive force varies according to the inverse square law and the above results are to be modified as follows:—

Instead of equations (16) we have

$$\Delta P = \int \dots \int F_1 F_2 dx_1 dy_1 dz_1 dx_2 dy_2 dz_2 V \cdot J_p,$$

where

$$J_p = 2\pi \int [P] p dp.$$

For all practical purposes we may take  $V$  out of the integration sign as  $\bar{V}$  (average  $\bar{V} = \frac{\sqrt{2}V}{m}$ ) as are done by Chapman and by Perisco. Strictly however this is not permissible.

We then have

$$\Delta P = \bar{V} \int \dots \int F_1 F_2 dx_1 dy_1 dz_1 dx_2 dy_2 dz_2 J_p.$$

Proceeding as before we have

$$\Delta \dot{x} = \bar{V} n_1 n_2 A_1 (\dot{x}_{02} - \dot{x}_{01})$$

where

$$A_1 = 4\pi \int \cos^2 \theta' p dp$$

$$\Delta \dot{x}^2 = \frac{1}{3} n^2 \mu_1 (-2\bar{\xi}^2 + \bar{\eta}^2 + \bar{\zeta}^2)$$

$$\Delta \dot{x} \dot{y} = -n^2 \mu_1 \bar{\xi} \eta$$

$$\Delta \dot{x} (\dot{x}^2 + \dot{y}^2 + \dot{z}^2) = \frac{2}{3} \mu_1 n^2 \{ \dot{x}_0 (\bar{\xi}^2 + \bar{\eta}^2 + \bar{\zeta}^2) - 3(\dot{x}_0 \bar{\xi}^2 + \dot{y}_0 \bar{\xi} \eta + \dot{z}_0 \bar{\xi} \zeta) \\ - \bar{\xi} (\xi^2 + \eta^2 + \zeta^2) \}$$

where

$$\mu_1 = \frac{1}{2} \bar{V} A_2$$

and

$$A_2 = \pi \int \sin^2 \theta' p dp.$$

We then have the same old forms for co-efficients of viscosity and conductivity as before with the modified values of  $\mu_1$ ,  $A_1$  and  $A_2$ .

*Numerical Calculations.*

In order to calculate  $A_1$  and  $A_2$  instead of taking the law of inverse square for the point charge as was done by Chapman we considered a distribution of charge according to Debye and Hückel as assumed by Perisco. We then proceeded to find out the potential and evaluate the integral

$$\theta_0(V, \rho) = \int_0^{\eta_1} \frac{d\eta}{\sqrt{1 + \eta^2 - \frac{2c_1}{V^2} \cdot \frac{m_1 + m_2}{m_1 m_2} \phi\left(\frac{\rho}{\eta}\right)}}$$

by a graphical method for the cases of Sirius B assuming the central temperature to be of the orders  $10^7$ ,  $10^8$  and  $10^9$  and for  $\epsilon_2$ -Eridani with central temperature  $10^8$  assuming that the stellar matter is composed of completely ionised Ca-atoms.<sup>9</sup> The integrations involved in  $A_1$  and  $A_2$  were subsequently carried on graphically. The physical constants for the two white dwarfs are given in Table I<sup>10</sup> and the computed results in Table II.

TABLE I.

Name of the star.	Density $\times 10^{-4}$	Electron number density.	Velocity $\times 10^{-9}$	Probable central temp.
$\epsilon_2$ -Eridani	9.8	$2.55 \times 10^{28}$	8.174	$10^8$
Sirius B	5.0	1.303	6.536	$10^9$
"	"	"	"	$10^8$
"	"	"	"	$10^7$

<sup>9</sup> Ganguli, Current Science, Dec., 1932, also Jan., 1934.

<sup>10</sup> Jeans, Astronomy and Cosmogony. In calculating  $n$  the average mol. wt. was taken to be 2.2.

TABLE II.

Name of the star.	Temp.	$\mu, \times 10^{-23}$	Diffusion D.	Viscosity $\kappa$ .	Conductivity $\mathfrak{g} \times 10^{16}$ .
$\epsilon_2$ Eridani	$10^8$	2.55	$3.621 \times 10^{-2}$	1.466	2.458
Sirius B	$10^9$	1.303	1.937	52.05	2.95
"	$10^8$	"	1.071	28.73	1.629
"	$1.37 \times 10^7$	"	1.121	69.02	3.819

The densities of the two other known white dwarfs Procyon B and Van Mannen's star are so high that these lead to velocities comparable with that of light and relativistic consideration are to be introduced for these. We intend to discuss these cases in a subsequent paper.

From Table II it is interesting to note that D,  $\kappa$  and  $\mathfrak{g}$  are affected but little by the variation of temperature for the same star. The density however has a marked effect and this is the decisive factor in the degenerate state. For instance  $\kappa$  in contrast to the classical case is found to decrease with the number but slightly increases with temperature as in the classical case. A detailed discussion of the bearing of these on stellar structure will be given elsewhere.

COLLEGE DUPLIX LABORATORY,  
CHANDERNAGORE.

1st March, 1934.



## The Budde Effect in Halogens

By

T. S. NARAYANA.

*(Received for publication, March 10, 1934.)*

### ABSTRACT.

Experiments on the Budde effect in Halogens  $\text{Cl}_2$  and  $\text{Br}_2$  were made under varied conditions. Budde effect was found absent in dry gases. Experiments were made on pure dry  $\text{Cl}_2$  enclosed in a pyrex bulb where all heat losses from the glass walls were arrested; and photo-expansion was observed. Dry air + dry halogen mixtures showed expansion on illumination. The Budde effect was found absent in the band absorption region. All the existing theories are reviewed and discussed. A mechanism based on the theory put forward by Born and Franck for the formation of a homopolar diatomic molecule is given and the divergent results of the various workers are reconciled.

In 1871 Budde<sup>1</sup> observed that chlorine and bromine suffer an expansion, when exposed to rays of high refrangibility; and he explained it as due to some loosening of the binding forces in the molecule. The experiments of Mellor,<sup>2</sup> Shenstone,<sup>3</sup> Bevan,<sup>4</sup> Baker,<sup>5</sup> as well as those of Caldwell,<sup>6</sup> Richardson,<sup>7</sup> and Pringsheim<sup>8</sup> on this Budde effect in chlorine, have disclosed the fact that dry chlorine showed no expansion inspite of its absorbing the radiations of visible spectrum. On the contrary, the recent work of Kistiakowsky,<sup>9</sup> Martin, Cole and Lent<sup>10</sup> showed that the dry chlorine also exhibits the so-called Budde effect, or photo-expansion. Likewise the Budde effect was

studied by Ludlam,<sup>11</sup> Brown and Chapman,<sup>12</sup> Matthews<sup>13</sup> and in a more quantitative manner by Lewis and Rideal,<sup>14</sup> in the case of bromine. The results obtained by Brown and Chapman<sup>12</sup> as well as by Matthews<sup>13</sup> in the case of dry bromine and dry air mixture differ entirely from that of Ludlam<sup>11</sup> and Lewis and Rideal,<sup>14</sup> who observed no expansion. Recent work of Kistiakowsky<sup>15</sup> showed a definite expansion in the case of bromine even on drying.

It is generally assumed in all the photo-chemical reactions of chlorine, that moist chlorine absorbs light energy which is subsequently converted into translational energy, while in dry chlorine, the absorbed energy is given out as isochromatic fluorescence. This was the explanation given by Weigert<sup>10</sup> for the absence of Budde effect in dry chlorine. A similar explanation was offered by Lewis and Rideal in the case of dry bromine, who claim to have found a difference in the absorption spectra and the light-scattering power of moist and dry bromine. But the experiments of Kistiakowsky<sup>15</sup> and Ludlam<sup>17</sup> in search of isochromatic fluorescence or resonance radiation gave negative results. Moreover, no difference in the absorption spectra or in the light-scattering power of moist and dry gases was found.

If the dry halogens absorb light, one of the following must take place :

(1) The absorbed radiant energy must be converted into thermal energy, about which there is a controversy.

(2) The absorbed light must be re-emitted as isochromatic fluorescence or resonance radiation for which there is no experimental proof.

(3) The absorbed light energy must bring about a change in the physical properties of the halogens for which there is not the slightest evidence.

Thus the cause of the Budde effect remains unknown. Especially, in view of the divergent experimental results, the present investigation was undertaken to know exactly the mechanism of the light action on moist and dry halogens.



*Experimental.*

Preparation of Materials :—(1) Pure phosphorus pentoxide was prepared by purifying Kahlbaum's pure phosphorus pentoxide according to the method of Finch and Fraser (Journ. Chem. Soc., p. 117, 1926). It satisfied Beck and Shenston's criteria for purity.

(2) Preparation of chlorine :—For experiments on pure moist chlorine, gas from the steel cylinder was passed through potassium permanganate washers and fractionally distilled. The middle fraction was used for the experiments. For experiments on pure, dry chlorine, it was prepared by the action of pure hydrochloric acid on Kahlbaum's pure potassium permanganate. The chlorine thus liberated is passed through potassium permanganate washers and heated calcium oxide to free it from hydrochloric acid. It was afterwards purified by a series of fractionations in vacuum using liquid air to condense. The middle fraction was retained each time. This fraction was finally liquefied over phosphorus pentoxide prepared as above ; and dried perfectly.

(3) Bromine :—Pure bromine was prepared by distilling Kahlbaum's pure liquid bromine over zinc oxide.

*Apparatus and mode of operation.*—Experiments on moist chlorine were made in an all-glass apparatus, shown in Fig. 1. The pressure increase on illumination was observed by means of an all-glass spring manometer—sensitivity 0.1 mm. The manometer was made by blowing a very thin-walled bulb and collapsing one side as symmetrically as possible.

The whole apparatus was evacuated by means of a Töpler pump. Care was taken to maintain pressure inside and outside the manometer nearly same (as the manometer cannot stand large pressure differences). The pressure inside the apparatus was qualitatively known by the length of the dark space in the discharge tube to be less than  $10^{-4}$  mm. Hg. The condensable gases were condensed by a liquid air trap, and the uncondensable

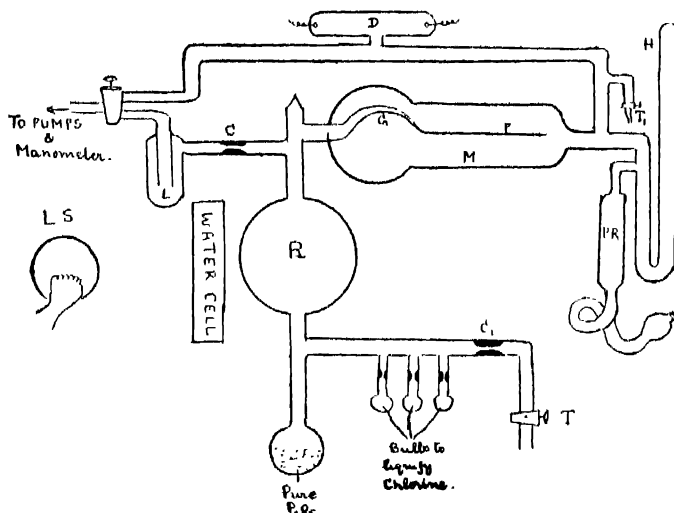


FIG. 1.

- D = Discharge tube ;  
 L. S = Light source ;  
 P.R. = Pressure regulator ;  
 L = Liq. air trap ;  
 H = Mercury manometer ;  
 M = Manometer casing ;  
 P = Pointer (glass) ;  
 G = Glass spring manometer.

gases were pumped out. After this operation was finished, the pump line was cut off by sealing the constriction C.

Chlorine was introduced through the tap T (which is lubricated with  $P_2O_5$  grease as chlorine attacks the organic tap grease), the tap  $T_1$  being opened to atmosphere in such a way that the rate of pressure increase inside the glass manometer is the same as the rate of pressure increase in the manometer casing M. When the chlorine pressure in R was approximately 1 atm., the chlorine line was cut off by sealing constriction  $C_1$ .

### Results.

Light from a 1000 watt Tungsten filament lamp kept at 40 cms. distance from R, after traversing a water cell 15 cms.

long to cut off the less refrangible heat rays, was allowed to fall on the reaction vessel R; and the pressure increase was observed by the movement of the manometer pointer, which was viewed through a microscope. Pressure outside the casing M was regulated, and the pointer was brought to its initial position; and the reading on the mercury manometer was taken. Thus by using the glass manometer as a null instrument the pressure change was directly read in terms of mms. Hg. The results for the photo-expansion in moist chlorine are given below.

TABLE 1.

Pressure of chlorine 1 Atm.

Sensitivity of manometer 0.1 mm.

No. of hours dried.	Time of exposure.	Expansion.	Contraction time (light off) <sub>b</sub>	Remarks.
0 hrs.	Secs.	mm. Hg.	55 seconds	The data were reproduced five times without any deviations.
	0	0.0		
	2	0.1		
	6	0.2		
	15	0.3		
	25	0.4		
	40	0.6		
	60	0.6		
	70	0.6		
		Steady		

Chlorine was allowed to dry on the  $P_2O_5$  kept at the bottom of the reaction vessel by liquefying, before taking readings; and the following results were obtained.

TABLE 2.

No. of hours dried.	Time of exposure in seconds.	Expansion in mm Hg.	Contraction time (light off) seconds.	Remarks.
48	30-40	0.5	43	Data reproduced five times.
96	60-70	0.3	75	„
144	60-70	0.2	68	„
192	60-70	0.1	65	„
384	60-80	0.1	68	„
408	70-80	0.1	70	„

*Influence of pressure on the photo-expansion in chlorine.*—This was studied by liquefying chlorine in the small bulbs and sealing them off at the constrictions (care was taken to reduce the pressure in M simultaneously at the same rate as in R).

Sensitivity of manometer 0.1 mm.

Light source 1000 watt lamp.

Distance between lamp and reaction vessel is 40 cms.

Length of water cell 15 cms.

TABLE 3.

Pressure.	Time of Exposure.	Expansion.
1 atmosphere	40 seconds	0.6 mm.
$\frac{1}{2}$ „	40 „	0.3 „
$\frac{1}{3}$ „	40 „	> 0.1 „

At every pressure, the results were produced three times.

*Influence of wave-length.*—Wratten light filters were interposed between the reaction vessel R and the water cell in the

path of the light beam. Pressure changes were observed as before.

TABLE 4.

Wave-length region $\mu\mu$ — $\mu\mu$	Time of Exposure Seconds.	Expansion. mm. Hg.	Remarks.
300-570	40	0.3 mm.	At every wave-length the results were reproduced thrice.
340-620	„	0.3 „	
480-600	„	0.2 „	
500-600	„	Zero	
600-700	„	Zero	

Above 490  $\mu\mu$  on the long wave side, the Budde effect is found to be absent.

*Influence of light intensity.*—This was studied by varying the distance between the light source and the reaction vessel R.

TABLE 5.

Distance.	Time of Exposure.	Expansion.
40 cms.	40 seconds	0.6 mm
60 „	„ „	0.4 „
80 „	„ „	0.25 „

From Table 5, it is shown that the Budde effect is proportional to  $\sqrt{\text{light intensity}}$ .

#### A STUDY OF THE PHOTO-EXPANSION IN PURE DRY CHLORINE.

As there was always 0.1 mm. expansion in the first experiments carried out in chlorine, in unbaked soft glass apparatus, it

is of interest to see what exactly would happen if the chlorine is perfectly dry. So an all glass† pyrex apparatus was constructed (see Fig. 2). All taps were avoided; instead, internal seals operated by electromagnets were used.

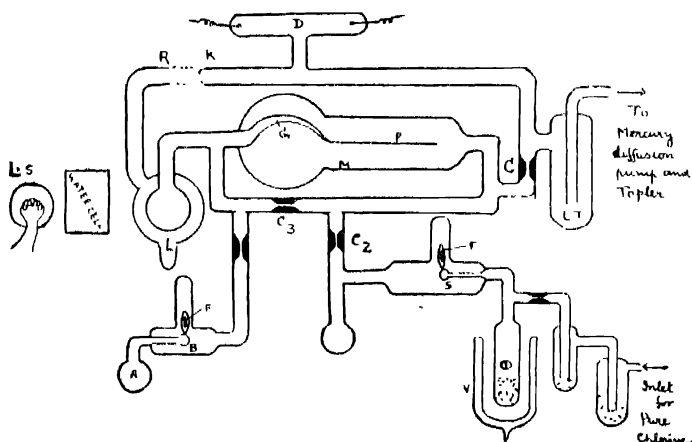


FIG. 2.

- D=Discharge tube;  
 L.S=Light source;  
 F=Iron core sealed in glass;  
 L.T=Liq. air trap;  
 A=Bulb containing air at very low pressure;  
 V=Dewar vessel;  
 $\phi$ =Pure  $\text{Cl}_2$  liquefied over pure  $\text{P}_2\text{O}_5$ .

The reaction vessel including the glass manometer was baked in high vacuum produced by mercury diffusion pump backed by Töpler pump for two days, at a temperature of  $450^\circ\text{C}$ . All the gases evolved were condensed by a liquid air trap put in series with the pump line. The vacuum inside was qualitatively measured by the length of the dark space in the discharge tube. A vacuum less than  $10^{-5}$  mm. was in the apparatus for two days. After this operation was done, the pump line was cut off by sealing at the constriction C. The seal S was then broken by operating the magnet, and perfectly pure, dry chlorine, prepared as described before, was let into the apparatus. After taking the

required amount, the apparatus was sealed off first at the constriction  $C_2$ . After the pressure equilibrium inside the apparatus was reached, the by-pass was cut off at  $C_3$ . This chlorine was exposed to light, and pressure changes were recorded as in the case of moist chlorine.

## BUDDE EFFECT IN DRY CHLORINE.

TABLE 6.

Time of Exposure	Expansion.	Remarks.
10 seconds	Zero	
20 "	"	
30 "	"	This experiment was repeated thrice.
40 "	"	
50 "	"	"Budde Effect" was found to be completely absent in pure dry chlorine.
60 "	"	
100 "	"	

Kistiakowsky <sup>9</sup> in trying to explain the absence of the Budde effect in pure, dry chlorine assumes that the chlorine molecules are dissociated into atoms on absorption of light quanta of the continuous absorption region, irrespective of the presence of moisture or foreign molecules. Radiant energy is thus primarily converted into chemical energy, and the warming up of the gas or the Budde effect must be due to a secondary process, the recombination of chlorine atoms. Kistiakowsky <sup>9</sup> opines that in dry gas the recombination of atoms takes place on the wall; and the heat of the recombination is dissipated away by the glass walls, as such the homogeneous gas is not warmed up; and hence the absence of the Budde effect in dry chlorine. If this explanation is correct, Budde effect must occur even in a perfectly pure, dried system, provided the heat losses from glass walls are

perfectly arrested by constructing a reaction vessel of the Dewar type. So, an all-glass pyrex apparatus was constructed as shown in Fig. 2. The tubes K & R were joined and the outer bulb was perfectly evacuated by means of a mercury diffusion pump backed by a Töpler pump. The reaction vessel was exposed to light as before and the following interesting results were obtained.

TABLE 7.

Light source 1000 Watt : Tungsten filament lamp.

Distance between reaction vessel and the lamp—40 cms.

Length of water cell—15cms.

Sensitivity of the manometer—1/10mm.

Time of Exposure.	Expansion when there is vacuum in L.	Expansion when there is no vacuum in L.
50 secs.	2.5 div.	Zero.
"	3.0 "	"
"	3.0 "	"
"	3.0 "	"
"	3.0 "	"

*Influence of foreign gases on the photo-expansion in dry chlorine.*—Air perfectly dried over pure phosphorus pentoxide obtained as described before was allowed into the apparatus containing dry chlorine, by breaking the internal seal B by an electro-magnet. After letting in a very small amount, the air-line was cut off and the system was exposed to light. Following results were obtained :—



TABLE 8.

Time of Exposure.	Expansion.
5 seconds	0.1 mm
10 "	0.2 "
20 "	0.2 "
30 "	0.2 "

*The Case of bromine.*—For studying the Budde effect in bromine an all-glass apparatus was constructed as shown in Fig. 3. Brominated wax was successfully used as a grease for the taps. After the whole apparatus was evacuated by means of a Töpler pump using a

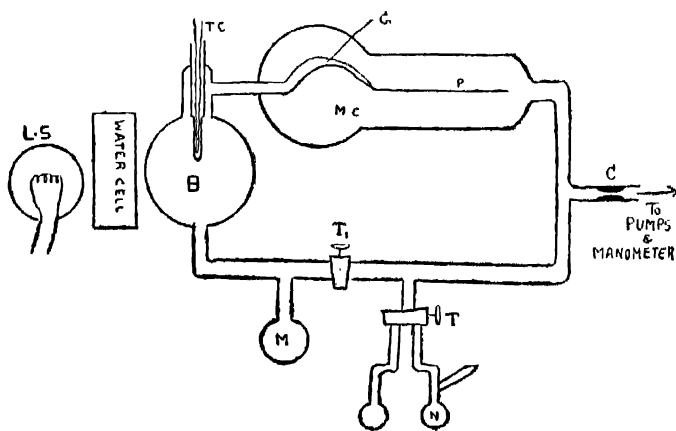


FIG. 3.

L.S = Light source ; T.C = Thermo couple ;  
M =  $\text{P}_2\text{O}_5$  bulb ;  
N =  $\text{Br}_2$  bulb ;  
B = Reaction vessel ;  
P = Pointer ;  
G = Glass manometer ;  
M.C = Manometer casing.

liquid air trap, the pump line was cut off at C. Bromine prepared as described before was allowed into the apparatus by opening the three-way tap T towards the reaction vessel ; the tap  $T_1$  used for closing and opening the bi-pass being kept open. Bromine was at a pressure of 250 mm. in the apparatus. After the equilibrium was established the three-way tap T and bi-tap  $T_1$  were closed. The bulb B was exposed to light; and pressure changes were observed as in the case of chlorine. The glass manometer used in this experiments was calibrated first with mercury manometer and so the pressure changes given by the glass manometer were directly converted into mms. Hg.

### BUDDE EFFECT IN MOIST BROMINE.

TABLE 9.

Light source 500 watt. tungsten filament lamp.

Distance between light source and the bromine bulb B 40 cms

Length of water cell 15cms.

Sensitivity of the manometer 1/14 mm.

Time of exposure.	Expansion in mm. Hg.	Contraction time light off.
2 Seconds	0.14 mm	55 Seconds.
5 "	0.30 "	
10 "	0.40 "	
20 "	0.64 "	
30 "	0.85 "	
40 "	0.92 "	
50 "	Steady	

*Influence of drying on the Budde effect in bromine*—The bi-pass tap  $T_1$  was opened, and bromine was condensed on the phosphorus pentoxide in the bulb M. After keeping it in contact with  $P_2O_5$  for some hours the cooling bath was removed,

and the gaseous bromine filled the whole apparatus. When equilibrium was established the bi-pass tap  $T_1$  was closed, and the bulb B was exposed to light. This was done a number of times. The following results were obtained :—

TABLE 10.

Time of drying in hrs.	Time of contact. liq. $Br_2$ with $P_2O_5$ hrs.	Time of exposure seconds.	Expansion in mm. Hg.	Contraction time (Light off).
144 hrs	4	50	0.7 mm	55 seconds
172 „	3	„	0.7 „	„ „
384 „	4	„	0.3 „	„ „
432 „	3	„	0.3 „	„ „
504 „	3	„	0.2 „	„ „
696 „	4	„	0.2 „	50 „
		„	Steady.	50 „

The above results were produced five times without any deviation. From this it can be shown that the Budde effect in bromine also decreases on drying.

*Influence of wave length on the Budde effect.*—This was studied as in the case of chlorine with the help of Wratten light filters and the following results were obtained.

TABLE 11.

Spectral Region. $\mu\mu$ -	Exposure time, Seconds	Expansion in mm. Hg.	Contraction time (light off).
300-500	40	0.3	49 seconds
540-570	„	0.2	45 „
560-600	„	Zero	—
580-700	„	Zero	—

Above 540  $\mu\mu$  the Budde effect is found absent.

*Effect of Light Intensity.*—This was studied by varying the distance between the light source and the bulb B.

TABLE 12.

Distance between B and lamp.	Time of exposure. in seconds.	Expansion. in mm. Hg.	Contraction time (light off).
40 cms.	50	0.9	52 secs
60 „	50	0.5	52 „
70 „	50	0.25-0.3	53 „

This shows that the Budde effect is proportional to  $\sqrt{\text{light intensity}}$ .

*Effect of Pressure.*—This was studied by putting in cooling baths and condensing some bromine in the bulb N. The vapour pressure of bromine was taken at that particular temperature of the bath. When the equilibrium was established, the three-way tap T was closed, and then the bi-way tap T<sub>1</sub> was closed. As usual the bromine vapour was exposed to light and the following results were obtained. A thermo-couple calibrated against a Beckman was taken, and put into the thin walled sealed capillary, which passes through the centre of the bromine bulb B. The following results were obtained :—

TABLE 13.

Pressure in mm. Hg	Exposure time, seconds	Expansion. in mm. Hg.	Temperature rise.	
			Galvanometer deflection.	Temperature.
250 mm.	50	0.9	170 div.	0.85° C
250 „	50	0.92	175 „	0.86° C
100 „	50	0.4	—	—

It can be seen from the above table that the Budde effect in bromine is proportional to the pressure of bromine. Also the expansion is accounted by the temperature rise of the system. Assuming the coefficient of expansion of bromine gas to be 0.0037

$$p = 250 (1 + 0.0037 \times t).$$

The pressure increase was found at 250 mm. to be 0.9 mm.

$$\begin{aligned} p &= 250 (1 + 0.0037 \times 0.85). \\ &= 250.8. \end{aligned}$$

$$\therefore p_{\text{calc.}} = 250.8 - 250 = 0.8 \text{ mm.}$$

Observed pressure increase 0.9 mm.

This slight difference of  $0.9 - 0.8 = 0.1$  may be due to heat losses through the capillary.

### *Discussion of Results.*

It is inferred from Tables 2 and 10 that the Budde effect undoubtedly diminishes on drying in the case of chlorine and bromine. Experiments on pure dry chlorine have established beyond doubt (Table 6) the results of Baker,<sup>5</sup> Richardson,<sup>7</sup> Pringsheim,<sup>8</sup> Mellor<sup>2</sup> and Shenstone,<sup>9</sup> as well as those of Lewis and Rideal<sup>14</sup> and Ludlam.<sup>11</sup>

From spectroscopic and thermochemical data the energy of dissociation of  $\text{Cl}_2$  and  $\text{Br}_2$  is given as 57000 cal and 46200 cal respectively. For optical dissociation to take place, the gases must absorb light on the short wave side of the convergence limit (for  $\text{Cl}_2$  below 4785Å and for bromine below 5000Å). Above this limit according to Franck,<sup>19</sup> dissociation in elementary act of absorption is an impossibility. As the Budde effect in chlorine and bromine was absent above 5000Å on the long wave side of the convergence limit, we can safely suppose that the Budde effect is entirely due to dissociation of the molecule into atoms. The expansion that was observed slightly above the convergence limit on the long wave side, may be due to the

dissociation taking place as a result of collisions between the active and the inactive molecules. Thermal effects may be observed because of the high pressure of the system. So beyond doubt we can assume that for the Budde effect to occur, the molecule must undergo dissociation, and the atoms so formed must recombine in the homogeneous gas phase. In such a case, the heat of recombination heats the gas, and hence the Budde effect, or the warming of the gas.

Various theories have been put forward to explain the mechanism of the Budde effect in dry halogens, but none of them is satisfactory. In the light of the experiments made by Kistiakowsky<sup>16</sup> and Ludlam,<sup>17</sup> any theory which assumes emission of the absorbed energy by the dry halogen to explain the absence of the Budde effect cannot be taken as correct.

The theory put forward by Kistiakowsky also completely breaks down, when the question of explaining the presence of the Budde effect in dry chlorine mixed with minute traces of dry air, observed in the present work; and a similar observation made by Brown and Chapman<sup>14</sup> and Matthews<sup>18</sup> in the case of dry bromine and dry air mixture.

To elucidate fully the mechanism of the Budde effect in halogens, one has to suppose that the molecule dissociates on absorption of the light quanta of its continuous absorption. The atoms so formed, must combine in the homogeneous gas phase. According to the theory of Born and Franck<sup>20</sup> for the formation of a homopolar di-atomic molecule, a three body collision is necessary. They have proved on the basis of quantum mechanics, that only neutral bodies can function as a third body in the triple collision processes. Applying this to the case of halogens, the recombination of the atoms is brought about by collision with neutral water molecules in the gas phase, as such the heat of recombination manifests itself in the gas phase. Hence Budde effect occurs. In the case of a dry gaseous system the recombination of atoms takes place on the dry glass walls which function as a third body. In such a case the heat of

recombination is dissipated away to the outside; as such no Budde effect occurs. (In the case of hydrogen R. W. Wood<sup>21</sup> has observed in the hydrogen discharge tube, that dry glass walls catalyse the recombination of atoms, and that a thin monomolecular layer of water is sufficient to poison the wall reaction.)

According to the theory put forward here one can expect the Budde effect to take place (i) if the dissipation of heat by the glass walls is arrested; and (ii) if a dry foreign gas molecule, which acts as a third body, is present in the dry gas. Experiments were done to verify these two conclusions; and actually an expansion of 0.2mm. in the case of dry chlorine contained in a vessel where all heat losses through walls were arrested (results of Table 7) was observed.

Pure dry chlorine gave no expansion (Table 6); but when minute traces of dry air were present, expansion was observed (Table 8). Similar results were obtained in the case of dry bromine and dry air by Matthews and Brown and Chapman. The magnitude of the Budde effect in dry halogens + dry air, or foreign molecules, will be less than in moist, because of the two following reasons:—(1) In moist, apart from the wall reaction being poisoned, the homogeneous reaction, namely, the recombination of the halogen atoms, is catalysed due to the high dipole nature of water molecules (J. J. Thomson, "The Electron in Chemistry"). On the other hand, in the dry gas + the dry air mixtures, some of the atoms combine in the homogeneous gas phase due to triple collisions with the foreign gas molecule, and some atoms on the walls of the vessel; as such part of the energy is always lost through walls. Hence the Budde effect in moist gases is always more than in dry gases.

If one assumes\* that the unilluminated  $\text{Cl}_2$  molecules are also efficient in bringing about the recombination of chlorine atoms (just as dry glass walls, moisture and foreign gas molecules bring about) it is easy to explain the discrepancy in the results obtained by Kistiakowsky<sup>16</sup> on the one hand and Baker,<sup>5</sup> Pringsheim,<sup>8</sup>

Richardson,<sup>7</sup> Lewis and Rideal<sup>14</sup> and Ludlam<sup>11</sup> on the other. Kistiakowsky<sup>15</sup> observed the Budde effect in dried chlorine and bromine. He has illuminated the central part of the reaction vessel. In the light of the above assumption it may be argued out, that the recombination of the halogen atoms is brought about by the unilluminated chlorine molecules in the homogeneous gas phase, as such the heat of recombination heats the gas and hence the observed Budde effect even on drying.

The contraction observed by Venkataramiah, on illuminating chlorine by an iron arc, was never noticed in these experiments on chlorine. He argues out the possibility of a complex  $\text{Cl}_3$  molecule. A  $\text{Cl}_6$  molecule may be assumed in interpreting the chain reactions in the  $\text{CoCl}_2$  formation, but the existence of it cannot be so easily proved experimentally.

### *Summary.*

(1) The Budde effect was observed in moist chlorine and bromine.

(2) The Budde effect was absent in  $\text{Cl}_2$  and  $\text{Br}_2$  above  $500\mu\mu$  and  $550\mu\mu$  respectively.

(3) The Budde effect was found proportional to pressure and to  $\sqrt{\text{light intensity}}$  in chlorine and bromine.

(4) In dry chlorine photo-expansion was observed when the heat losses from the walls were arrested. Dry chlorine and dry air mixture showed the Budde effect

(5) The theories that were put forward to explain the mechanism of the Budde effect were discussed. A new mechanism was suggested in the light of Born and Franck's theory for the formation of a homopolar diatomic molecule. From the theory put forward here, the divergent results of the various workers were reconciled.

(6) It is assumed that unilluminated chlorine molecules function as efficient third bodies in the recombination of  $\text{Cl}$  atoms.



(7) The existence of a  $\text{Cl}_2$  molecule is questioned.

The author takes this opportunity of thanking Prof. Dr. H. E. Watson for his interest during the course of this investigation.

*Bibliography.*

1. Budde, "J. f. Prakt. Chem.," vol. 7, p. 376 (1873); also "Phil. Mag.," vol. 42, p. 290 (1891) and "Pogg Ann.," vol. 6, p. 477 (1873).
2. Mellor, "Trans. Chem. Soc.," vol. 81, p. 1280 (1902).
3. Shenstone, "Jour. Chem. Soc.," vol. 71, p. 471 (1897).
4. Bevan, "Proc. Roy. Soc.," A, vol. 72, p. 5 (1903); also "Phyl. Trans.," p. 91 (1903).
5. Baker, "British Assn. Reports," p. 496 (1894).
6. "Amer. Chem. Jour.," vol. 31, p. 51 (1904).
7. Richardson, "Phil. Mag.," vol. 32, p. 277 (1892).
8. Pringsheim, "Weid. Ann.," vol. 30, p. 413 (1887).
9. Kishakowsky, "Jour. Amer. Chem. Soc.," vol. 49, p. 2194 (1927).
10. "Jour. Phys. Chem.," vol. 33, p. 148 (1929).
11. "Proc. Roy. Soc." (Edin.), vol. 44, pp. 97-102 (1924).
12. "Jour. Chem. Soc.," p. 560 (1928).
13. "Trans. Faraday Soc.," p. 41 (1929).
14. "Jour. Chem. Soc.," vol. 96, p. 583 (1926).
15. "Jour. Amer. Chem. Soc.," vol. 51, p. 1395 (1929).
16. Weigert, "Zeit. f. Physikal. Chem.," vol. 106, p. 42 (1923).
17. "Proc. Roy. Soc." (Edin.), vol. 49, p. 256 (1929).
18. Finch and Fraser, "Jour. Chem. Soc.," p. 117 (1926).
19. Franck, "Trans. Faraday Soc.," Oct., 1925.
20. "Zeit. f. Physik," vol. 31, p. 411 (1925).
21. "Proc. Roy. Soc.," A, vol. 102, p. 1 (1922).

\* Such specific properties to the unilluminated  $\text{Cl}_2$  molecule can be assumed; as Wicke and Stenzen recently (Phys. Rev., 1933) have shown that while  $\text{H}_2$  is efficient in bringing about the recombination H atoms, hydrogen atoms are not at all efficient.

† The pyrex glass tubes were cleaned by washing; and then dried, according to Baker, *Journ. Chem. Soc.*, p 1661 (1929); also Proc. Roy. Soc., 110A 624 (1926); 123 A. 285 (1929). All the glass tubes used in constructing the apparatus were melted thoroughly and the capillaries and the occluded air bubbles were completely removed.



# **GAERTNER SCIENTIFIC CORPORATION, CHICAGO.**

**X-Ray Spectrometers** -Single and double crystal.

**Precision Research Spectrometers** of all kind.

**Astronomical Instruments**

**Calorimeters.**

**Chronographs and Accessories.**

**High Grade Optical parts**—Lenses, Parallel plates, Prisms,  
Test planes etc.

**Instruments of Precision**—Measuring Microscopes, Micro-  
meter slides, Comparators, Cathetometers, etc.

**Interferometers and Accessories.**

**Polariscopes.**

**Quartz Spectrographs and Accessories.**

**Universal Laboratory Supports.**

For detailed literature and price lists, please write to

***SOLE REPRESENTATIVES***

**THE ANDHRA SCIENTIFIC CO.,  
MASULIPATAM.  
(S. INDIA.)**



# The Budde Effect in Iodine, Part I. A General Study of the Photo-Expansion

By

T. S. NARAYANA.

*(Received for publication, March 10, 1934.)*

## ABSTRACT.

On the basis of the mechanism put forward in the paper entitled "The Budde Effect in Halogens" (See this Journal, p. 91) it was predicted that all homopolar diatomic gases should show this so-called "Budde Effect" on absorption of light quanta of the continuous absorption (provided the energy of recombination is given out as thermal energy). Experiments to verify this conclusion were carried out in iodine, and a phenomenon similar to the Budde effect in  $\text{Cl}_2$  and  $\text{Br}_2$  was observed. The photo-expansion was found to be proportional to the light intensity and to the vapour pressure of iodine. It was found to be a maximum in the violet and orange regions of the spectrum when the iodine vapour pressure was 70 mm. and it is very difficult to explain this by our present knowledge of "absorption in diatomic molecules."

A mechanism of the Budde effect or the expansion of chlorine and bromine on exposure to rays of high refrangibility was put forward on the basis of Born and Franck's<sup>1</sup> theory for the formation of a homopolar diatomic molecule in a paper entitled "The Budde Effect in Halogens,"<sup>2</sup> according to which any homopolar diatomic molecule on absorbing light quanta of the short wave side of the convergence limit must exhibit the so-called "Budde Effect."

<sup>1</sup> Born and Franck, 'Z. f. Physik' ; Vol. 31, p. 411 (1926).

<sup>2</sup> Narayana, Ind. Jour. Phys., Vol 9, p. 91 (1934).

To verify the validity of the theory put forward, experiments were made in the case of iodine ; and a phenomenon similar to the "Budde Effect" was observed in iodine, a report of which was made in "Current Science," Vol. 1, No. 11, p. 348 (1933).

### *Experimental.*

An all glass apparatus as shown in Fig. 1 was constructed.

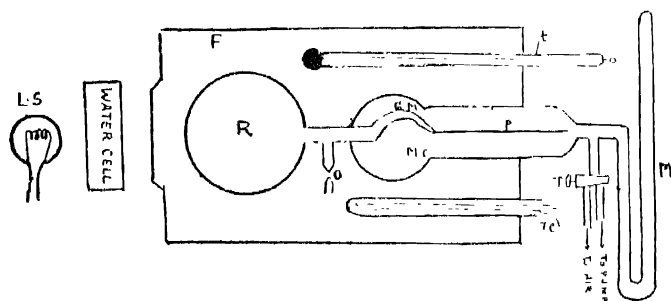


FIG. 1.

- L.S = Light source ; F = Furnace ;  
 R = Reaction bulb containing iodine vapour ;  
 M = Mercury manometer ;  
 M. C = Manometer casing ;  
 G. M = Glass spring manometer ;  
 t = Thermometer ;  
 T-C = Thermo-couple ;  
 O = Constriction to cut off pump line ;  
 p = Glass pointer ;  
 T = Tap to control pressures outside (G. M).

It was evacuated by means of a Töpler pump, and the pump line was cut off at o. The reaction vessel was enclosed in a furnace the temperature of which was controlled by means of a rheostat. The manometer used in these experiments was made by blowing a thin glass bulb and collapsing one side as symmetrically as possible. It has a sensitivity of 0.1 mm. It was used as a null instrument, as such the pressure of iodine vapour was directly read on the mercury manometer M. (As the manometer cannot

stand large pressure differences, all pressure changes inside were accordingly counterbalanced from outside.) When the pointer was steady for some time the bulb containing iodine vapour was exposed to light from a 500 watt tungsten filament lamp and the pressure change was observed by viewing the glass pointer through a microscope. The following results were obtained :—

*Results.*

Distance between the light source and the reaction bulb—50 cms. Length of water cell—15 cms.

Sensitivity of the glass manometer—0.1 mm.

TABLE I.

Time of exposure in seconds.	Expansion in mm. Hg.	Contraction time (Light off).
3	0.7	9 secs.
5	0.9	
6	0.9	
10	0.9	

*Influence of pressure* :—Pressure changes inside the reaction bulb were brought about by changing the temperature of the furnace. The pressure of the iodine vapour was measured directly on the mercury scale (when the temperature of the furnace was steady and the glass pointer was brought to a zero position).

TABLE II.

Pressure of iodine.	Exposure time.	Expansion.	Contraction time (Light off).
20 mm.	3 secs.	>1 div.	5 secs.
50 "	3 "	0.9 mm.	"
60 "	3 "	1.1 "	"

The above table shows that the Budde effect in iodine is proportional to the pressure of iodine vapour.

*Influence of wave length* :—This was studied by interposing Wratten light filters in the path of the light beam.

TABLE III.

Pressure of iodine—70 mm.

Spectral region $\mu\mu$ — $\mu\mu$ .	Exposure time.	Expansion.
Whole of the visible region.	5 secs.	1.3 mm.
360-520	"	0.2 "
480-700	"	0.7 "
500-580	"	0.2 "
545-700	"	0.7 "
560-700	"	0.7 "
580-700	"	0.7 "
800-860	"	0.3 "
900-480	"	0.4 "

From the results of the above table, it is evident that the Budde effect is a maximum in the violet and orange regions of the spectrum, the green region having little effect.

*Effect of light intensity* :—This was studied by varying the distance between the light source and the reaction vessel.

TABLE IV.

Distance	Exposure time	Expansion.
30 cm.	5 secs.	1.6 mm.
40 "	"	0.9 "
60 "	"	0.4 "
80 "	"	0.2 "



Thus it is found that in iodine the Budde effect is proportional to the light intensity (unlike chlorine and bromine where it is proportional to  $\sqrt{\text{the light intensity}}$ ).

In conclusion, the author takes the opportunity of thanking Prof. Dr. H. E. Watson for the kind interest he has taken during the course of this investigation.



# The Budde Effect in Iodine, Part II. The Influence of Temperature on the Photo-Expansion

By

T. S. NARAYANA.

*(Received for publication, March 10, 1934.)*

## ABSTRACT.

A study of the influence of temperature on the photo-expansion was made. It was found to diminish with temperature. The results were interpreted on the basis of R. W. Wood's results on the influence of moist and dry glass walls on the recombination of hydrogen atoms. A probable explanation for the rate of fall in the formation of phosgene at high temperatures was given.

The mechanism of the Budde effect or the photo-expansion in chlorine and bromine was explained by the author (see this Journal, page 91). It is due to the diatomic molecule dissociating on absorption of light in the continuous region, and subsequent ternary collisions of the atoms with foreign neutral molecules present in the body of the gas. According to this, any homopolar diatomic molecule on absorbing light in its continuous region, should show the so-called "Budde Effect," provided the gas molecules do not undergo any change in molecular structure, *e.g.*, the transformation of  $O_2 + h\nu = O_3$ . It was predicted on this theory that a molecule like iodine should exhibit the so-called Budde effect. To verify this, experiments on the photo-expansion of iodine were carried out and a phenomenon similar to the Budde effect in chlorine and bromine was observed in iodine, "Current Science," Volume 1, No. 11, p. 348

(1933). In the present paper the influence of temperature on the photo-expansion in iodine is studied.

### *Experimental.*

An all glass apparatus as shown in Fig. 1 (the Budde Effect in Iodine, Part I, see this Journal, page 112) was constructed. The whole apparatus was evacuated by means of a Töpler pump, and the constriction sealed off. The whole apparatus was kept in a furnace and the temperature was controlled by means of a rheostat. As the pressure increased inside the reaction vessel R and and manometer GM, air was left slowly through the tap T to bring the manometer pointer to its original position. Thus as the glass spring manometer was used here as a null instrument the pressure of iodine inside was given by directly reading on the mercury manometer.

When the temperature of the furnace remained steady at 200°C, light from a 500 watt tungsten filament lamp was focussed on the reaction vessel after traversing through a water cell, and the movement of the pointer was observed through a microscope.

### *Results.*

Light source—500 watt lamp.

Distance between R and light source—50 cms.

Length of water space—15 cms.

Sensibility of manometer—0.1 mm.

### Temperature 200°C.

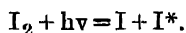
Exposure time in seconds.	Expansion in mm. Hg.	Contraction time (light off).	Remarks.
2	0.5	10 secs.	The result was reproduced five times.
5	0.7		
7	0.7		
10	0.7		
	steady		

Temperature 350°C.

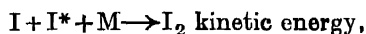
Exposure time in seconds.	Expansion in mm. Hg.	Contraction time (light off).	Remarks.
2	0.3	8 secs.	The result was reproduced five times.
5	0.4		
7	0.45		
10	0.45 steady		

*Discussion of Results.*

The photo-expansion of iodine was found to be 0.7 mm. at 200°C and 0.45 mm. at 350°C. From the observations made it is definite that the photo-expansion falls with rise in temperature. The iodine molecule dissociates first on absorbing light quanta of the visible region



The two iodine atoms collide with neutral water molecules present in the body of the vapour to form an iodine molecule



and the heat of recombination of iodine atoms heats the gas and hence the observed pressure increases (R. W. Wood<sup>1</sup> has shown that while a dry glass wall catalyses the recombination of atoms, a moist glass wall inhibits). In the present case, as the adsorbed monomolecular film of water vapour is not given off at 200°C, the wall process is poisoned. At higher temperatures the monomolecular film loosens itself and the wall process also comes into play. In such a case, at higher temperatures, the recombination of iodine atoms takes place partly in the gaseous

<sup>1</sup> R. W. Wood, Proc. Roy. Soc., A, Vol. 102, p. 1 (1922).

phase, and partly on the walls. The heat of recombination of the atoms on the wall is dissipated away, and so the magnitude of the photo-expansion falls. From this it is evident that the walls have got a definite influence on the recombination of the atoms when they are dry.

It is evident from the above results that at higher temperatures, as a consequence of the wall process coming into prominence, the concentration of iodine atoms in the body of the gas falls down. From this it can be inferred that whenever the rate of a reaction is controlled by  $[x]^2$  or  $[x]$  atoms, the rate should roughly be same, when the reaction is carried in perfectly dry glass vessels or moist glass vessels raised to higher temperatures, as both tend to reduce the concentration of atoms in the homogeneous gas phase. This may be the probable cause for the rate of formation of phosgene falling down at high temperatures.

In conclusion, the author takes the opportunity of thanking Prof. Dr. H. E. Watson for the kind interest he has taken during the course of this investigation.

# The Valency Angles of Oxygen and Sulphur

By

N. GOPALA PAI, M.A.

*Research Scholar, Indian Association for the Cultivation  
of Science, Calcutta.*

*(Received for publication, July 2, 1934.)*

## ABSTRACT.

The valency angles of oxygen and sulphur atoms are calculated for a number of simple molecules from their fundamental frequencies of oscillation, and their dipole moments.

### 1. Introduction.

The determination of the relative orientations of the different valency bonds connecting an atom to its neighbours in a molecule is a problem of importance in chemistry. In certain favourable cases, the determination presents no difficulty. For example, in cyclopropane, the angles between any two C—C bonds can be shown from direct considerations of symmetry to be  $60^\circ$ , and similarly in methane or carbon tetrachloride the valency bonds can be shown to make with one another angles of  $109^\circ 5'$ . In other cases, however, the problem presents difficulties, and one has to deduce the angles by indirect methods.

One of the methods in general use for finding the valency angle is based on a knowledge of the permanent dipole moment

of the molecule. As is well-known, with each chemical bond may be associated a definite dipole moment characteristic of the bond. The resultant moment of the molecule as a whole will be the vectorial sum of the moments of the constituent bonds. When the moments of these bonds are known, the magnitude of the resultant moment gives one an idea of the relative orientations of these various bonds. In simple cases, such a correlation may give definite information regarding the angles between the valency bonds.

In the case of simple molecules, there is another method which has been used with success. It has been shown by Bjerrum,<sup>1</sup> Dennison<sup>2</sup> and others that the natural oscillation frequencies of a simple molecule can be calculated from the known dispositions of the atoms and the binding forces between them. Conversely, a knowledge of the oscillation frequencies of a molecule derived from infra-red absorption measurements, or more conveniently from its Raman spectrum, enables one to deduce, in favourable cases, the binding forces and the relative orientations of the chemical bonds.

Both the methods have their natural limitations. The latter method can be applied conveniently in particular to simple triatomic molecules. For more complicated ones the identification of the different observed frequencies as due to a particular mode of oscillation of the molecule becomes increasingly difficult, and the method, therefore, ceases to be of practical value. In the dipole method, on the other hand, a knowledge of the dipole moments characteristic of the constituent chemical bonds is presumed. In most cases, this is not available, and even under favourable conditions, only rough estimates of the characteristic moments of the bonds can be made. The valency angles calculated from these data are naturally uncertain. By a suitable combination of the two methods, it is possible, however, to deduce

<sup>1</sup> N. Bjerrum, *Verh. D. Phys. Ges.*, Vol. 16, p. 737 (1914).

<sup>2</sup> D. M. Dennison, '*Phil. Mag.*,' Vol. I, p. 195 (1926).



the valency angles with definiteness. In the present paper, the valency angles of oxygen and sulphur are calculated in this manner for a number of simple compounds.

## 2. Oscillations of a Triatomic Molecule.

The calculation of the valency angles from the Raman frequencies is particularly simple in the case of symmetrical triatomic molecules of the type  $XY_2$ , for which the theory has been worked out in great detail by Bjerrum, Dennison and others. The angle between the two  $X-Y$  bonds gives directly the valency angle of the atom  $X$ . From this point of view, several of the molecules considered in this paper have been so chosen that in effect they may be treated as triatomic molecules of the above type.

The simplest molecule of this type has three fundamental oscillation frequencies, say  $\nu_1$ ,  $\nu_2$  and  $\nu_3$  corresponding to oscillations represented in Fig. 1.

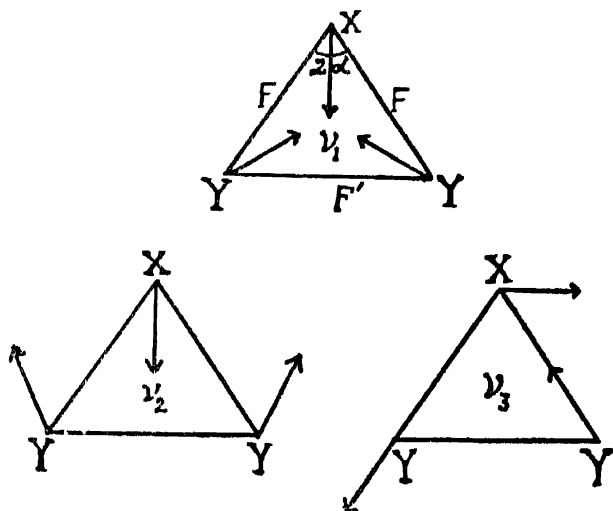


FIG. 1.

Let us denote by  $F$  the binding force between the  $X$  and  $Y$  atoms, and by  $F'$  the force between  $Y$  and  $Y$ , and let  $2\alpha$  be the angle between the two  $X-Y$  bonds. Also let the mass of  $X$  be

M and of Y be  $m$ . Then it can be shown that

$$n_1 = \frac{F}{m} \left[ p + (1-p) \cos^2 \alpha \right] \quad \dots \quad (1)$$

$$n_2 n_3 = \frac{2F'}{m} \times \frac{F}{m} \times p \cos^2 \alpha \quad \dots \quad (2)$$

$$n_2 + n_3 = \frac{2F'}{m} + \frac{F}{m} \left[ 1 - (1-p) \cos^2 \alpha \right] \quad \dots \quad (3)$$

$$\text{where } p = \frac{M+2m}{M}; \quad n^2 = \frac{4\pi^2 c^2}{L} \nu^2. \quad \dots \quad (4)$$

If the three fundamental frequencies  $\nu_1$ ,  $\nu_2$  and  $\nu_3$  are known, the three equations enable us to calculate  $F$ ,  $F'$  and  $2\alpha$ .

### 3. Dimethyl Ether.

We shall first consider dimethyl ether. In view of the small mass of the three hydrogen atoms in the methyl groups, we may treat the methyl groups as single units of mass 15. The molecule of dimethyl ether can then be considered as a tri-atomic molecule of the type discussed above.  $2\alpha$  in this compound will naturally denote the angle between the two C—O bonds, and will, therefore, give the valency angle of the oxygen atom in the compound. In order to calculate  $\alpha$ , we require to know the three  $\nu$ 's. From the Raman spectrum the three fundamental frequencies of the  $(\text{CH}_3)_2\text{O}$  molecule are found to be

$$1106 \text{ (3)}; \quad 921 \text{ (4)}; \quad 267 \text{ (1)}.$$

From these frequencies, using the relations (1) to (3) we obtain, in the first place, for  $F$ , *i.e.*, for the binding force between C and O, the value 4.52 dyn/cm., and for  $F'$ , the binding force between C and C, the value 0.68 dyn/cm.  $F'$  is naturally much smaller than  $F$  since there is no chemical binding, in the ordinary sense, between the C atoms.

The same equations give for  $2\alpha$ , *i.e.*, for the valency angle of the O atom, the value  $118^\circ$ .

#### 4. Dipole Moment of the C—O Bond.

The dipole moment of  $(\text{CH}_3)_2\text{O}$  has been measured by Sanger and Steiger,<sup>3</sup> and Stuart,<sup>4</sup> and they obtain the value 1.32D and 1.29 D respectively ( $\text{D} = 10^{-18}$  c.g.s. e.s.u.). Since we know from the previous section the inclination of the two C—O bonds to each other, we can calculate the value of the permanent moment characteristic of either of the C—O bonds. Thus, we obtain

$$\mu_{\text{C-O}} = \frac{1.29 \times 10^{-18}}{2 \cos 59^\circ} = 1.25 \text{ D.}$$

#### 5. Diethyl, Dipropyl and Diphenyl Ethers.

The calculation of the valency angle of O in these compounds from their Raman frequencies is not rigorous in view of the complicated structure of the  $(\text{C}_2\text{H}_5)$  group, which we cannot treat as a single oscillating unit. However, since we know the dipole moment of  $(\text{C}_2\text{H}_5)_2\text{O}$  and also the moment of the C—O bond we can readily calculate the angle between the two C—O bonds. We thus obtain

$$2\alpha = 2 \cos^{-1} \cdot \frac{1.14}{2 \times 1.25} = 126^\circ.$$

This value is larger than that obtained for  $(\text{CH}_3)_2\text{O}$ , and is evidently due to the larger size of the  $(\text{C}_2\text{H}_5)$  groups, which would tend to open out the two C—O bonds.

The dipole moment<sup>5</sup> of  $(\text{C}_6\text{H}_7)_2\text{O}$ , *viz.*, 1.16 D, gives in the same manner for the valency angle of oxygen  $124^\circ.8$ , which is practically the same as the value in  $(\text{C}_2\text{H}_5)_2\text{O}$ . No dipole moment data are available for higher members of this series.

<sup>3</sup> 'Helv. Phys. Acta,' Vol. 2, p. 136 (1929).

<sup>4</sup> Z. Physik, Vol. 51, p. 490 (1928).

<sup>5</sup> Meyer and Buchner, 'Physikal. Z.,' Vol. 33, p. 390 (1932).

We may consider in this section also the case of diphenyl ether  $(C_6H_5)_2O$ , whose permanent moment has recently been measured by Bergmann and Tschudnowsky,<sup>6</sup> and is found to be 1.12 D. If the characteristic dipole strength of the C—O bond in this compound is the same as in the aliphatic ethers considered in the previous paragraphs, this value of the dipole moment of  $(C_6H_5)_2O$  would correspond to a valency angle of

$$2 \cos^{-1} \left( \frac{1.12}{2 \times 1.25} \right) \text{ or } 127^\circ$$

for the O atom. This is the same as in the other compounds considered.

## 6. Water.

In order to make the series of triatomic molecules of the type  $OY_2$  complete, we shall include also the simplest molecule of this type, *viz.*,  $OH_2$ . The structure of this molecule has been discussed in detail by a number of workers from various independent points of view, among whom may be specially mentioned Debye,<sup>7</sup> Hund<sup>8</sup> and Mecke<sup>9</sup> and his collaborators. By an extensive critical analysis of the rotation vibration spectrum of this molecule, Mecke has recently determined accurately the three moments of inertia of the molecule in the ground state, *viz.*,  $I = 0.995 \times 10^{-40}$ ,  $L = 1.908 \times 10^{-40}$  and  $K = 2.980 \times 10^{-40}$ . The relation  $I + L = K$  is nearly satisfied. For the oscillationless state, Mecke obtains by extrapolation the values  $I = 1.009 \times 10^{-40}$ ,  $L = 1.901 \times 10^{-40}$  and  $K = 2.908 \times 10^{-40}$ . These values satisfy accurately the relation  $I + L = K$ . From these data, the valency angle of oxygen comes out as  $104^\circ$ - $106^\circ$ .

On the other hand, Plyler,<sup>10</sup> who has discussed in great detail the infra-red absorption bands of water, adopts the follow-

<sup>6</sup> 'Z. Phys. Chem.,' B, Vol. 17, p. 107 (1932).

<sup>7</sup> "Polar Molecules," The Chemical Catalog Co., Inc., 1929, Chap. IV.

<sup>8</sup> Hund, 'Z. Physik,' Vol. 31, p. 81 (1925); Vol. 32, p. 1 (1925).

<sup>9</sup> 'Z. Physik,' Vol. 81, p. 465 (1933).

<sup>10</sup> Plyler, 'Physic. Rev.,' Vol. 39, p. 77 (1932).

ing three as the fundamental frequencies of oscillation of the  $\text{H}_2\text{O}$  molecule, *viz.*,  $\nu_1=5309\text{ cm}^{-1}$ ,  $\nu_2=1597\text{ cm}^{-1}$  and  $\nu^3=3742\text{ cm}^{-1}$ . From these frequencies, using Dennison's formulae (1), (2) and (3) above, he obtains for the valency angle  $2\alpha$  of the oxygen atom the value  $115^\circ$ .

### 7. The Valency Angle of Oxygen.

We may collect in this place the values obtained for the valency angle of oxygen in various compounds. They are given in Table I.

TABLE I.

Molecule.	Method.	Valency Angle of Oxygen.
$\text{H}_2\text{O}$	Plyler from oscillation frequencies	$115^\circ$
	Mecke from Rotation-Vibration Spectra	$104^\circ\text{--}106^\circ$
$(\text{OH}_3)_2\text{O}$	From Raman frequencies	$118^\circ$
$(\text{C}_2\text{H}_5)_2\text{O}$	From $\mu=1.12\text{ D}$	$125^\circ.8$
$(\text{C}_3\text{H}_7)_2\text{O}$	From $\mu=1.16\text{ D}$	$124^\circ.8$
$(\text{C}_6\text{H}_5)_2\text{O}$	From $\mu=1.12\text{ D}$	$126^\circ.9$

The values group about  $120^\circ$ .

### 8. Ethylene Oxide.

We next consider the simple heterocyclic compound containing oxygen, *viz.*, ethylene oxide, which also can be treated as a symmetrical triatomic molecule of the type  $\text{AX}_2$ . The heterocyclic nature of this compound in contrast with the open structure of dimethyl ether, is plainly responsible for the wide difference in properties of these two compounds. Let us first consider their Raman spectra. The scattering of ethylene oxide

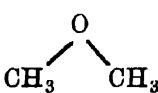
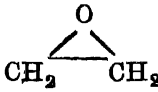
has been studied by the present writer,<sup>11</sup> and its Raman lines are found to be much more intense than those of  $(\text{CH}_3)_2\text{O}$ . Further the fundamental oscillation frequencies are found to be 865, 810 and  $1123\text{ cm}^{-1}$ , from which the binding force  $F$  between C and O atoms, and the force  $F'$  between two C atoms as also the valency angle  $2\alpha$  of O can be calculated as before. Doing so, we obtain

$$F = 4.2 \times 10^5 ; \quad F' = 3.4 \times 10^5 ;$$

$$\text{and } 2\alpha = 64^\circ.$$

These values are of interest, especially when viewed in relation to the corresponding values for  $(\text{CH}_3)_2\text{O}$ . The values for the two compounds are placed together in the following Table for comparison :—

TABLE II.

Compound.	$F \times 10^{-5}$ .	$F' \times 10^{-5}$ .	Valency Angle.
	4.5	0.68	118°
	4.2	3.4	64°

$F$  is practically the same for the two compounds.  $F'$ , however, is much larger in  $(\text{CH}_2)_2\text{O}$  than in  $(\text{CH}_3)_2\text{O}$ . This is what we should expect because of the presence of a chemical bond between the two C atoms in  $(\text{CH}_2)_2\text{O}$ , which is absent in  $(\text{CH}_3)_2\text{O}$ . This C—C bond in  $(\text{CH}_2)_2\text{O}$  will naturally tend to bring the two C atoms close together, so that the valency angle of O should be much smaller in this compound than in  $(\text{CH}_3)_2\text{O}$ . This, as we see from Table II, is actually the case, the valency

<sup>11</sup> To be published elsewhere.

angles of O in the two compounds being  $64^\circ$  and  $118^\circ$  respectively.

This large difference in the valency angle in the two compounds will also mean a corresponding difference in their dipole moments. The dipole moment of  $(\text{CH}_2)_2\text{O}$  is not only much greater than that of  $(\text{CH}_3)_2\text{O}$ , but the ratio between the two moments, *viz.*,  $\frac{1.88}{1.29} = 1.5$ , has nearly the same value as

$\frac{\cos 32}{\cos 59} = 1.6$ . This shows that the characteristic dipole moment of the C—O bond is practically the same in the two compounds in spite of differences in the nature of the C—O bonds in the two compounds.

### 9. *Dimethyl Sulphide.*

Among the simple sulphur compounds  $(\text{CH}_3)_2\text{S}$  would be very suitable for direct calculation of the valency angle. The Raman Spectrum of this compound has been recently studied by the present writer. Treating this molecule as a triatomic one of the type  $\text{AX}_2$ , the natural frequencies of oscillation as given by their Raman spectra are as follows :

$$\nu_1 = 694 \text{ (8)} \quad \nu_2 = 745 \text{ (5)}, \quad \nu_3 = 284 \text{ (6)}.$$

From these values, the valency angle of S, *viz.*,  $2\alpha$ , comes out as  $100^\circ$ .

### 10. *Other Sulphur Compounds.*

From the above value of  $2\alpha$ , and the known dipole moment<sup>12</sup> of  $(\text{CH}_3)_2\text{S}$ , *viz.*, 1.41, the value of the moment characteristic of C—S bond comes out as 1.09 D (which is practically the same as for the C—O bond). Using this value, we can now

<sup>12</sup> Hunter and Partington, J. C. S., p. 2812 (1932).

calculate in the same manner as we did for the ethers, the valency angle of S in diethyl, dipropyl and other sulphides. The following table gives the values so obtained :—

TABLE III.

Compound.	Method.	Valency angle of S.
H <sub>2</sub> S	From infra-red frequencies	90°
(CH <sub>3</sub> ) <sub>2</sub> S	From Raman frequencies	100°
(C <sub>2</sub> H <sub>5</sub> ) <sub>2</sub> S	From dipole moment	87°·8
(C <sub>3</sub> H <sub>7</sub> ) <sub>2</sub> S	"	89°·4
(C <sub>4</sub> H <sub>9</sub> ) <sub>2</sub> S	"	87°·8
(C <sub>6</sub> H <sub>5</sub> ) <sub>2</sub> S	"	95°·2

Thus in all the compounds, the angle is near about 90°, and is considerably smaller than that of O in the corresponding oxygen compounds.

The author desires to express his grateful thanks to Prof. K. S. Krishnan, D.Sc., for the keen interest he took during the progress of this work.



## Susceptibility Constants for Co-ordinate Linkage in Addition Compounds, Part I

By

S. S. BHATNAGAR, MULK RAJ VERMA AND PYARA LAL KAPUR.

*(Received for publication, July 2, 1934.)*

The determination of the constitutive correction factor  $\lambda$  in the additivity formula for magnetic susceptibility

$$\chi_M = \sum d \chi_A + \lambda \text{ (Pascal)}$$

requires careful investigation. Pascal, in his classical researches, was able to affix certain definite values of the correction constant for many of the valency linkages, like double bond, triple bond, etc. and showed that the constant retains its identity in a large number of organic compounds. But so far no measurements seem to have been made for the constant  $\lambda$ , when a co-ordinate linkage is established. Such a case is provided when two substances react in simple stoichiometrical ratios to give products known as molecular or addition compounds.

Different workers have put forward different views to account for the formation of such compounds. Lowry<sup>1</sup> and Bennet and Wills<sup>2</sup> postulate that it is very probable that one of the components acts as a donor and the other as an acceptor so that co-ordination linkage is established. On the electronic theory of valency, the donor molecule possesses a lone pair which under

the electron repelling forces is transferred to the acceptor molecule and is thus shared by both as  $A : + B = A \rightarrow B$ .

In the present investigation we have studied the magnetic susceptibility of those molecular compounds only in which the existence of co-ordinate linkage has been shown to be a probability from an examination of various physical properties. The compounds studied are those formed between (i) *m*-dinitrobenzene and (a) benzidine, (b) naphthalene and (c)  $\alpha$ -naphthylamine ; (ii) picric acid and (a) naphthalene, (b) anthracene, (c) phenanthrene and (d)  $\alpha$ -methyl naphthalene.

### *Experimental.*

The original components were purified by the following methods and finally repeatedly crystallised from the solvents until the melting points as indicated against each were obtained. These melting points were comparable to the standard ones given in International Critical Tables, Vol. I.

*m*-Dinitrobenzene. Recrystallised extra pure *m*-dinitrobenzene from absolute alcohol, m. p. 90°C. (given m. p. 90°C.).

Benzidine. Dissolved in hydrochloric acid and then precipitated the sulphate ; decomposed by caustic soda, washed and recrystallised from benzene, m. p. 126° ; given 128·7°C.

Naphthalene. Recrystallised from aldehyde-free alcohol ; m. p. 80°C., given 80°C.

$\alpha$ -naphthylamine. Steam distilled with superheated steam ; filtered and recrystallised from benzene, m. p. 50°C., given 50°C.

Picric acid. Recrystallised from hot water ; m. p. 119°C., given 120°C.

Anthracene. Recrystallised extra pure anthracene from benzene ; m. p. 218°C ; given 218°C.

Phenanthrene. Recrystallised from benzene, m. p. 100°C., given 99°·6C.

$\alpha$ -methyl naphthalene. Distilled twice, boiling point 241°C., given b. p. 243°C.

The various molecular compounds were prepared by mixing the components in molecular proportions, dissolving in a suitable solvent and recrystallising. They were further purified by recrystallisation from the same solvent.

*m*-dinitrobenzene-benzidine and *m*-dinitrobenzene- $\alpha$ -naphthylamine compounds were prepared in absolute alcohol.<sup>9</sup>

*m*-dinitrobenzene-naphthalene compound was prepared in benzene.<sup>4</sup>

Naphthalene picrate was prepared in ether,<sup>5</sup> anthracene picrate in benzene<sup>6</sup> and phenanthrene<sup>7</sup> and  $\alpha$ -methyl naphthalene<sup>8</sup> picrates in absolute alcohol.

In the following table are given the melting points and densities of the compounds prepared along with the corresponding data given in literature :—

TABLE I.

Substance.	Molecular weight.	Colour.	Molecular ratio.	Density.	Melting Point Found. °C	Melting Point Given. °C.
<i>m</i> -Dinitrobenzene-benzidine	352	Deep violet	1 : 1	1.394	127-128	127.6 to 128
<i>m</i> -Dinitrobenzene-naphthalene	296	Yellowish green	1 : 1	1.313	51.4	50.7 to 51.6
<i>m</i> -Dinitrobenzene- $\alpha$ -naphthylamine	311	Blood red	1 : 1	1.35	65.0	65.1 to 65.7
Picric acid-naphthalene	357	Yellow	1 : 1	1.510	149	149
Picric acid-anthracene	407	Red	1 : 1	1.502	141	138 ; 139
Picric acid-phenanthrene	407	Orange yellow	1 : 1	1.46	142.5	143
Picric acid- $\alpha$ -methyl naphthalene	371	Yellow	1 : 1	1.466	140.5	141-142

The magnetic susceptibilities of the original components and the molecular compounds were determined by a Curie-Wilson

balance<sup>9</sup> slightly modified as described in previous communications from this laboratory.<sup>10</sup> A constant weight of substance (0.1000 gm.) was used in each determination. Water was used as a standard of comparison and its susceptibility was taken as  $-7.25 \times 10^{-7}$ . The accuracy of the balance was further tested by determining the susceptibilities of some other well known substances like KCl, NaCl,  $C_6H_6$ , etc. It was found that this balance gives results within  $\pm 1/2\%$ .

In the following table are given the values for magnetic susceptibilities of the original components as determined. Column III gives the values of the components as found in the International Critical Tables, Vol. VI. In the last column have been gathered together the computed values for molar susceptibilities :—

TABLE II.

Substance.	$-\chi \times 10^7$ Observed.	$-\chi \times 10^7$ Given in Int. Crit. Tables.	$-\chi M \times 10^7$ Observed.
m-Dinitrobenzene	3.96	3.98	665
Benzidine	6.03	...	1109
Picric acid	3.53	...	807
Anthracene	7.46	7.26	1927
Phenanthrene	7.22	7.18	1285
$\alpha$ -Methyl naphthalene	7.17	...	1017
Naphthalene	7.24	7.17	927
$\alpha$ -Naphthylamine	6.50	...	929.4

The values for the magnetic susceptibility of molecular compounds are given in the following table. In Columns III and V are given the observed gram and gram molecular susceptibilities and in Columns IV and VI the corresponding calculated values assuming the additivity law to hold good. In the last column

are given the differences between the observed and the calculated susceptibilities per gram molecule :—

TABLE III.

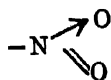
Compound.	Molecular weight.	$-\chi \times 10^7$		$-\chi_M \times 10^7$		$-\delta\chi_M \times 10^7$ (a-b)
		Obs.	Calc.	Obs. (a)	Calc. (b)	
m-Dinitrobenzene. benzidine.	352	5.26	5.04	1851	(665 + 1109) = 1774	77
„ naphthalene	296	5.73	5.38	1696	(665 + 927) = 1592	104
„ $\alpha$ -naphthylamine	311	5.35	5.13	1674	(665 + 929) = 1594	80
Picric acid-naphthalene.	357	5.25	4.86	1874	(807 + 927) = 1734	140
„ „ anthracene	407	5.54	5.24	2255	(807 + 1327) = 2134	121
„ „ -phenanthrene.	407	5.43	5.14	2209	(807 + 1285) = 2092	117
„ „ $\alpha$ -methyl-naphthalene	371	5.21	4.916	1933	(807 + 1017) = 1824	109

It may be thus seen that the addition compound becomes more diamagnetic than should be expected on the additivity law. This increase in diamagnetic susceptibility has a value varying between  $77 \times 10^{-7}$  and  $140 \times 10^{-7}$  per gram molecule.

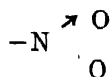
### Summary and Discussion.

All the compounds studied are the addition compounds formed by the interaction of a nitro-compound and an amine or a hydrocarbon, and the co-ordination linkage is established in these through  $-\text{NO}_2$  group as shown below.

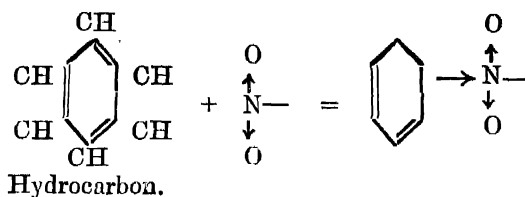
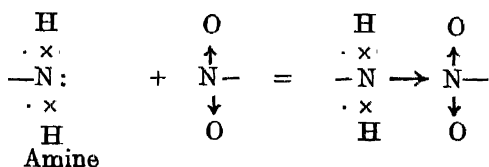
Parachor measurements of the nitro-compounds establish the following structure of the nitro-group<sup>11</sup> :—



Under proper conditions of activation the nitro-group acquires the structure<sup>12</sup>

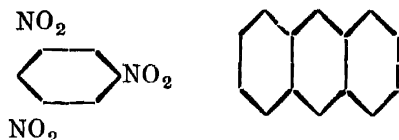


with the result that there are only six electrons in N's orbit and as such it can accept two more electrons from suitable donor molecules like amines or hydrocarbons, and a co-ordination linkage be established



The presence of such a linkage has also been established experimentally by Sahai<sup>13</sup> by parachor measurements in the case of the molecular compounds of *m*-dinitrobenzene- $\alpha$ -naphthylamine and *m*-dinitrobenzene-naphthalene. The presence of a similar co-ordinate linkage in the compound of *m*-nitrophenol and *p*-toluidine has also been established by him, the union taking place through a nitro-group. Though no measurements are available on the molecular compounds of picric acid and hydrocarbons, the presence of a similar linkage may be assumed on analogy. If this assumption be correct, the hydrocarbon or any other donor molecule should lie adjacent to the nitro-group. This has been shown to be so by the study of the crystal structure of trinitrobenzene-anthracene compound by X-ray methods.<sup>14</sup>

The two molecules lie with respect to one another as shown below :



The formation of the addition compound involves an increase in the diamagnetic susceptibility as shown in Table III, the increase varying between  $77 \times 10^{-7}$  and  $140 \times 10^{-7}$  per gram molecule. Value of about the same order is obtained if the susceptibility of the inorganic molecular compounds is subtracted from the one calculated on the additive law. The figures incorporated in the following table are taken from the International Critical Tables, Vol. VI, and are illustrative of the above point of view :—

TABLE IV.

Components.	Molecular susceptibility observed.	Molecular compound.	Molecular susceptibility		$-d\chi_M \times 10^7$
	$-\chi_M \times 10$		Obs.	Calc.	
$\text{Al}_2\text{O}_3$	100.0	$\text{Al}_2\text{O}_3 \cdot \text{H}_2\text{O}$	404.4	$(100 + 129.6)$ $= 229.6.$	174.8
$\text{H}_2\text{O}$	129.6				
$\text{K}_2\text{SO}_4$	701.2	$\text{K}_2\text{SO}_4 \cdot \text{Al}_2(\text{SO}_4)_3.$	2425.2	$(701.2 + 1641.6)$ $= 2342.8.$	82.4
$\text{Al}_2(\text{SO}_4)_3$	1641.6				

The inorganic molecular compounds are perhaps similarly constituted, there being respectively a donor and an acceptor molecule. The increase in diamagnetism may therefore be explained as arising out of the establishment of a co-ordination linkage, with the result that the octet of the acceptor molecule is completed.

Magnetic susceptibility of binary mixtures of liquids, which when mixed in particular molecular concentration ratios are also known to form addition compounds by the study of various

physical properties such as freezing point curves,<sup>15</sup> dipole moments,<sup>16</sup> absorption spectra,<sup>17</sup> etc., has been studied by various workers and has yielded conflicting results. Some authors have reported great deviations from the additive law,<sup>18</sup> a few observe no change<sup>19</sup> and still others have reported deviations to the extent of 3-4%. From the study of other physical properties molecular compounds have been shown to be formed at these concentrations<sup>20</sup>. Cabrera and Madinaveitia<sup>21</sup> observed an increase in the diamagnetic susceptibility of the mixture of  $\text{CHCl}_3$  and acetone and the value found was  $38 \times 10^{-7}$  units per gram molecule. This value is much less than the one obtained by us. It may be due to the fact that in liquid mixtures after some time a sort of an equilibrium is established between the components and the compound and therefore the magnetic susceptibility value obtained is the sum of  $\chi_A + \chi_B + \chi_C$  where  $\chi_A + \chi_C$  = molecular susceptibility of the components and  $\chi_C$  is that of the compound.

In the case of solid organic compounds studied by us, although the addition compound formation is complete yet the increase in the magnetic susceptibility value varies. If the establishment of a co-ordinate linkage be the only change involved during the formation of an addition compound the change in susceptibility should be a constant quantity. But as it is not, it suggests that besides the establishment of this linkage, there are other factors such as change in the radius of the molecule, influence of other groups present in the molecule, etc., which influence the change in susceptibility.

The influence of the groups is manifested on a loose perusal of the data given in Table III. The increase in susceptibility, when hydrocarbons form molecular compounds with nitro-compounds, is about  $120 \times 10^{-7}$  units per gram molecule, whereas, when amines react with nitro compounds, the increase in value is about  $80 \times 10^{-7}$  units per gram molecule.

The exact influence of various groups on the magnetic property of the molecular compounds is being studied and the results will be communicated later on.



*References.*

- <sup>1</sup> Lowry : Chemistry and Industry, 43, 218 (1924).
- <sup>2</sup> Bennet and Willis : Jour. Chem. Soc., p. 256 (1929).
- <sup>3</sup> Buehler and Heap : Jour. Amer. Chem. Soc., 48, 3168 (1926).
- <sup>4</sup> Hepp : Ann., 215, 379 (1882).
- <sup>5</sup> Beilstein Band, 6, S. 272.
- <sup>6</sup> Fritzsche : J. Pr. (1) 73, 288 ; Ann., 109, 247 (1859).
- <sup>7</sup> Fittig : Ostarmeyer Ann., 166, 361 (1873).
- <sup>8</sup> Meyer and Fricke : Ber., 47, 2770 (1914).
- <sup>9</sup> Wilson : Proc. Roy. Soc., A, 96, 429 (1920).
- <sup>10</sup> Bhatnagar and Kapur : Jour. Indian Chem. Soc., 9, 347 (1932).
- <sup>11</sup> Glasstone : 'Recent Advances in Physical Chemistry,' Churchill, 1931.
- <sup>12</sup> Bennet and Willis : *loc. cit.*
- <sup>13</sup> Sahai : Thesis, Punjab University, 1933.
- <sup>14</sup> Hertel : Zeit. Physikal. Chemie, B, 11, 77 (1930).
- <sup>15</sup> Wyatt : Trans. Faraday Soc., 25, 43 (1929).
- <sup>16</sup> Ebert : *Vide* Glasstone, *loc. cit.*
- <sup>17</sup> Riuz : Anales Soc. Espan. fis. quim., 30, 561 (1932).
- <sup>18</sup> Trew and Spencer : Proc. Roy. Soc., A, 131, 209 (1931).
- <sup>19</sup> Ramachandra Rao and Sivarama Krishnan : Nature, 128, 875 (1931) ; Indian Jour. Phys., 6, 509 (1931) ; K. Kido : Sc. Rep. Tohoku Imp. Univ., 1st series, 21, 385 (1932).
- <sup>20</sup> Buchner : Nature, 128, 301 (1931) ; Ranganadham : Nature, 127, 975 (1931).
- <sup>21</sup> Cabrera and Madinaveitia : Anales Soc. Espan. fis quim., 30, 528 (1932).

UNIVERSITY CHEMICAL LABORATORIES,  
LAHORE.



# A New Interference Phenomenon Observed with Crystalline Plates

By

K. S. SUNDARARAJAN.

*Research Scholar, Indian Association for the Cultivation of Science, Calcutta.*

*(Received for publication, September 10, 1934.)*

(Plates II and III.)

## 1. Introduction.

It is well known that when a crystalline plate, placed between two crossed Nicols, is viewed through a spectroscope, and a parallel beam of white light is allowed to traverse the optical system, the spectrum would be crossed by a number of dark and bright bands. The positions of these bands are defined by the relation  $(\mu_1 - \mu_2)d = n\lambda/2$ , where  $\mu_1$  and  $\mu_2$  are the principal refractive indices of the plate in its plane and  $d$  is the thickness, and  $n$  is any integer; the dark bands correspond to even values of  $n$  and the bright bands to odd values. The intensities at the minima would be zero and hence the visibility of the fringes would be best when the principal planes of the polarising and analysing Nicols make  $45^\circ$  with the two extinction directions of the crystalline plate. When the analyser, instead of being crossed with the polariser, is parallel to it, the fringe system observed through the spectroscope would be very similar, only the previous positions of maxima would now correspond to

positions of minima of intensity, and *vice versa*. Such an optical arrangement is frequently used for studying the dispersion of birefringence of crystals.<sup>1</sup> In these experiments, the thickness of the plates is naturally so chosen as to give a closely spaced system of fringes, since the values of birefringence can then be determined accurately.

While conducting similar experiments with organic crystals where because of the very high double refraction thin crystals only had to be used, the writer came across a second set of fringes more closely spaced than, and quite different from, the birefringence fringes, described above. This subsidiary set of interference fringes, superposed on the interference system due to the birefringence, is not contemplated in the usual treatment of the subject. The purpose of the paper is to present an account of the experimental observations made in connection with this phenomenon together with a complete theory.

## 2. *Elementary Theory of the Birefringence Fringes.*

The explanation of the birefringence fringes described in the previous section is simple. Let us consider the case where the crystalline plate is placed between two parallel Nicols with its principal axes at  $45^\circ$  to those of the Nicols. The vibration incident on the crystal plate will resolve into two of equal amplitudes (*viz.*,  $1/\sqrt{2}$  of that of the incident vibration), vibrating respectively along the two principal axes of the crystal. On emergence from the crystal plate, they will have a phase difference

$\delta = \frac{2\pi}{\lambda}(\mu_1 - \mu_2)d$ , and for such wave-lengths for which

$\delta$  is a multiple of  $2\pi$ , they will compound into a vibration in the principal plane of the analyser, and will be wholly transmitted. On the other hand, whenever  $\delta$  is an odd multiple of  $\pi$ , the re-

1. See for example K. S. Krishnan and A. C. Das Gupta, 'Ind. Jour. Phys.,' Vol. 8, p. 49 (1938).

sulting vibration will be completely cut out by the analyser. These two conditions define the positions of the bright and dark birefringence fringes observed through the spectroscope.

### 3. *Requirements of a More Complete Theory.*

In the above treatment, the amplitude of either of the vibrations transmitted by the crystal plate is taken to be  $1/\sqrt{2}$  of the incident amplitude, which involves the tacit assumption that the amplitude is independent of wave-length. But actually, due to multiple reflections, the amplitude of each of these vibrations will vary with the wave-length, fluctuating rapidly through a series of maxima and minima. It is this that gives rise to the well known interference fringes observed with thin films placed in front of the slit of a spectroscope. Further the frequency of these fluctuations will be different for the two vibrations. When these vibrations pass through the analyser and interfere, there will naturally appear in the spectrum of the transmitted light, in addition to the birefringence fringes arising from the fluctuations with wavelength of the *phase difference*  $\delta$  between the two vibrations, a system of secondary maxima and minima arising from the fluctuations in their *amplitudes*. Since these fluctuations of amplitude are very rapid, the latter set of maxima and minima in the spectrum will be more closely spaced than the former arising from the fluctuations of  $\delta$  with wave-length. As a prelude to the theoretical investigation of these two sets of fringes, let us consider the simple case where the polariser alone is present, the analyser being removed, and the crystal plate is rotated in its plane so as to have one of its principal axes parallel to the incident vibrations.

### 4. *Incident Vibration Parallel to One of the Principal Axes of the Crystal.*

Let a wave of unit amplitude represented by the expression *cos*  $\omega t$  be incident normally on the crystal plate. The expres-

sion for the transmitted wave just on emergence from the plate, will then be given by the usual expression

$$y = \frac{(1-r^2) e^{i(\omega t - \epsilon_1)}}{1-r^2 e^{-2i\epsilon_1}} \quad \dots (1)$$

(which is obtained by taking into consideration, in addition to the directly transmitted wave, also those that are transmitted after suffering 2, 4, 6, etc., internal reflections), where  $r^2$  is the reflecting power, i.e., the ratio of the intensities of the reflected and incident waves,

$2\epsilon_1 = \frac{2\pi}{\lambda} \times 2\mu_1 d$  is the phase difference between two successive transmitted waves and  $\mu_1$  is the refractive index of the crystal corresponding to the particular direction of vibration of light. The intensity of the complete transmitted wave will evidently be given by

$$I = \frac{(1-r^2)^2}{1+r^4-2r^2\cos 2\epsilon_1} \quad (2)$$

I will be a maximum or a minimum according as  $2\epsilon_1 = 2n\pi$  or  $(2n+1)\pi$ , i.e.,  $2\mu_1 d = n\lambda$  or  $(2n+1)\lambda/2$ . Hence the spectrum will be crossed by alternate bright and dark fringes. The intensities at the minima will of course be finite.

If the polarising Nicol is rotated by  $90^\circ$  so as to make the incident vibration parallel to the other principal axis of the crystal plate, the system of bands observed will be similar to the one described, being however differently spaced, the positions of the bright and dark fringes being now given by the conditions  $2\mu_2 d = n\lambda$  and  $2\mu_2 d = (2n+1)\lambda/2$  respectively.

### 5. Incident Vibrations at $45^\circ$ to the Principal Axes.

If the incident vibrations are at  $45^\circ$  to the principal axes of the crystal, the intensity of the transmitted light would be given by the expression

$$I = (1-r^2)^2 \frac{1+r^4-2r^2\cos(\epsilon_1+\epsilon_2)\cos(\epsilon_1-\epsilon_2)}{(1+r^4-2r^2\cos 2\epsilon_1)(1+r^4-2r^2\cos 2\epsilon_2)} \quad \dots (3)$$

and hence the interference system observed will be the same as that obtained by a simple superposition of the two separate sets of fringes described in the previous section. Due to the difference in spacing of the two sets of fringes, there will naturally be alternating positions of maxima and minima of *visibility*, given by the relations  $2(\mu_1 - \mu_2)d = n\lambda$  and  $2(\mu_1 - \mu_2)d = (2n+1)\lambda/2$  respectively, these  $n$ 's being of course different from the previous  $n$ 's.

It may be mentioned here that the same system of fringes can also be obtained with incident *unpolarised* light.

### 6. Transmitted Wave analysed by a Second Nicol.

The results obtained when in addition to the first Nicol inclined at  $45^\circ$  to the principal axes of the crystal, there is introduced an analyser after the crystal, either parallel or crossed with the first Nicol, are highly interesting. Let us first consider the case when the Nicols are parallel.

Let us suppose that the incident wave is represented by  $e^{i\omega t}$ . The two vibrations in the crystal are then represented separately by  $e^{i\omega t}/\sqrt{2}$ , just when they enter the crystal. The first wave after transmission through the crystal plate and the analyser will be given by  $\frac{1}{2} \frac{(1-r^2)e^{i(\omega t - \epsilon_1 + \phi)}}{1-r^2e^{-2i\epsilon_1}}$  and the second wave by  $\frac{1}{2} \frac{(1-r^2)e^{i(\omega t - \epsilon_2 + \phi)}}{1-r^2e^{-2i\epsilon_2}}$ , both vibrating in the same direction;  $\phi$  is a constant which will depend on the path traversed after leaving the crystal.

It can be easily shown that the resultant intensity of the light emerging from the analyser, obtained by compounding the above two vibrations, is equal to

$$(1-r^2)^2 \cos^2 \frac{\epsilon_1 - \epsilon_2}{2} \frac{1+r^4-2r^2 \cos(\epsilon_1 + \epsilon_2)}{(1+r^4-2r^2 \cos 2\epsilon_1)(1+r^4-2r^2 \cos 2\epsilon_2)} \dots \quad (4)$$

The first factor  $\cos^2 \frac{\epsilon_1 - \epsilon_2}{2}$  varies very slowly with wavelength. Considering the second factor

$$\frac{1 + r^4 - 2r^2 \cos(\epsilon_1 + \epsilon_2)}{(1 + r^4 - 2r^2 \cos 2\epsilon_1)(1 + r^4 - 2r^2 \cos 2\epsilon_2)},$$

and comparing it with the expression

$$\frac{1 + r^4 - 2r^2 \cos(\epsilon_1 + \epsilon_2) \cos(\epsilon_1 - \epsilon_2)}{(1 + r^4 - 2r^2 \cos 2\epsilon_1)(1 + r^4 - 2r^2 \cos 2\epsilon_2)}$$

in equation (3), it is seen the two expressions are practically the same, except for the presence of a slowly varying factor  $\cos(\epsilon_1 - \epsilon_2)$  multiplying one of the terms in the numerator, so that the *positions* of the maxima and minima will be practically the same as those given by expression (3), *i.e.*, those obtained by the superposition of the two sets of interference fringes considered already. The positions of the maxima and minima of *visibility* will also be the same. But due to the presence of the first term, *viz.*,  $\cos^2 \frac{\epsilon_1 - \epsilon_2}{2}$ , the effect of which will be considered presently, the relative *intensities* at the different maxima will now be different from those given by (3).

Let us proceed to consider the effect of the first term, namely,  $\cos^2 \frac{\epsilon_1 - \epsilon_2}{2}$ . It is easily seen that whenever the visibility of the fringe system is a maximum,  $2(\epsilon_1 - \epsilon_2) = 2n\pi$  and hence  $\cos^2 \frac{\epsilon_1 - \epsilon_2}{2}$  is either a maximum or a minimum according as  $n$  is even or odd, the minimum value being zero. There will thus be absolute darkness whenever  $(\epsilon_1 - \epsilon_2) = (2n + 1)\pi$ , *i.e.*,  $(\mu_1 - \mu_2)d = (2n + 1)\lambda/2$ .

When the thickness of the crystal is large, the maxima and minima arising from the fluctuations in the second factor, may



be too closely spaced to be resolved by the spectroscope, in which case, only the maxima and minima determined by the fluctuations of the first factor (which are much slower) will appear; these will be the birefringence fringes that are observed under normal conditions and that are explained by the elementary theory given in §2.

To sum up, there are closely spaced interference fringes, whose visibility fluctuates, the alternate positions of maximum visibility being completely dark.

The problem when the Nicols are crossed, can be treated similarly and the expression for the intensity of the transmitted light in this case comes out as

$$(1-r^2)^2 \sin^2 \frac{\epsilon_1 - \epsilon_2}{2} \cdot \frac{1+r^4+2r^2 \cos (\epsilon_1 + \epsilon_2)}{(1+r^4-2r^2 \cos 2\epsilon_1)(1+r^4-2r^2 \cos 2\epsilon_2)} \dots \quad (5)$$

It can be shown that the positions of maxima and minima arising from the fluctuation of the second factor

$$\frac{1+r^4+2r^2 \cos (\epsilon_1 + \epsilon_2)}{(1+r^4-2r^2 \cos 2\epsilon_1)(1+r^4-2r^2 \cos 2\epsilon_2)}$$

with wave-length will be practically the same as in the case of parallel Nicols considered before. The absolute minima of intensity, will now be very different since they are defined

by the condition  $\sin^2 \frac{\epsilon_1 - \epsilon_2}{2} = 0$ , instead of by the condition

$\cos^2 \frac{\epsilon_1 - \epsilon_2}{2} = 0$  of the previous case. This will correspond, in the

case of observations with plates that are sufficiently thick to obliterate the interference system arising from the second term in (5), to an interchange of the positions of the bright and dark birefringence fringes, when the analyser is rotated from the position of parallelism with the polariser to the crossed position.

### 7. *Experimental Observations.*

The crystal plate was mounted suitably between two Nicols and white light from point source, collimated by an achromatic lens, was allowed to traverse the optical system axially. The crystal was mounted on a graduated turn-table, capable of rotation both about a vertical and a horizontal axis. The plate was adjusted to be normal to the path of light by the usual method. The transmitted light was allowed to fall on the slit of a spectrograph.

A thin plate of the monoclinic crystal chrysene (1, 2 benzo-phenanthrene) parallel to its (001) face was used to obtain the spectrograms reproduced in Figs. 1 to 5 in Plate II. Fig. 1 corresponds to the case where the incident light vibrations are parallel to one of the principal axes of the crystal plate (namely, the 'b' axis) and the analyser is removed from the path of the transmitted light. Fig. 2 is a similar spectrogram obtained with the incident vibrations along the other principal axis, *viz.*, the 'a' axis, of the crystal. The refractive index and also the dispersion of the crystal for vibrations along the 'b' axis are much larger than for vibrations along 'a'; consequently, the first fringe system is more closely spaced than the second, besides also having a slightly better visibility, since due to the higher value of the refractive index the reflectivity is also higher.

Fig. 3 was obtained with incident unpolarised light, which may be taken to be equivalent to two vibrations of equal intensity along the first and the second principal axes, respectively, of the crystal. The fringes obtained may therefore be treated as though they were obtained by superposing those in Figs. 1 and 2. The frequent alternation in the degree of visibility are clearly brought out. Fig. 4 was obtained with the crystal between parallel Nicols, at  $45^\circ$  to the crystal axes, and Fig 5 corresponds to the Nicols crossed. In both the figures, namely, 4 and 5, the positions of maximum and minimum visibility are clearly the same as in Fig. 3, and further every alternate posi-

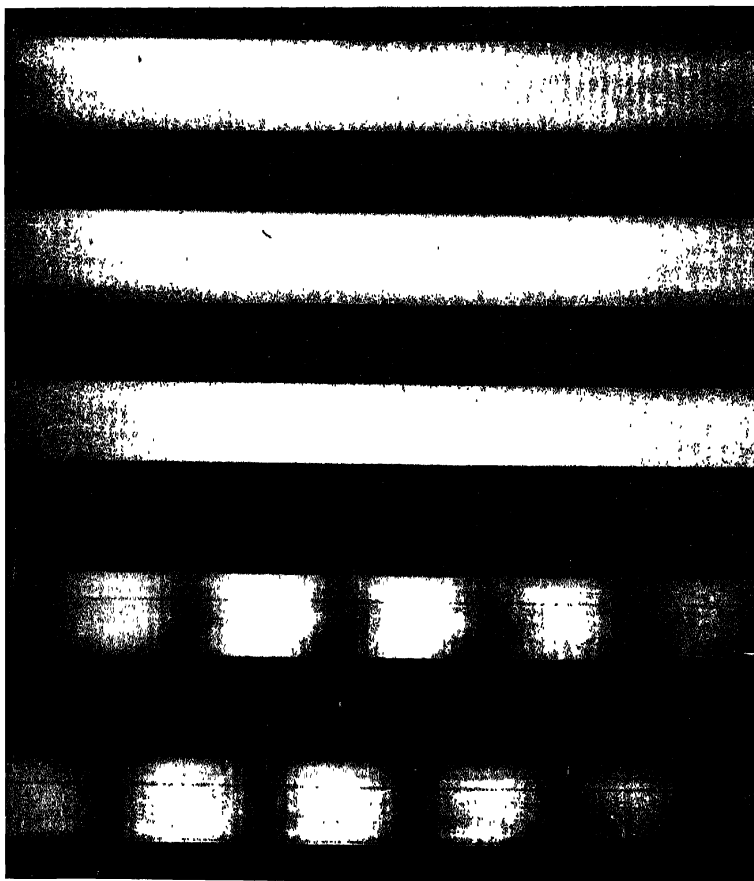


Fig. 1.

Fig. 2.

Fig. 3

Fig. 4.

Fig. 5.



tion of maximum visibility is dark, as required by theory. For all the figures, a Cu arc spectrum has been given for reference. Fig. 6 (Plate III) is a microphotometric record of a small portion of the negative corresponding to Fig 3. The regions of maximum and minimum visibility are brought out even more clearly than in Fig. 3. Fig. 7 is similarly a microphotometric record corresponding to Fig. 4. The figure shows clearly that the regions of maximum visibility are alternately dark and bright.

Observations were also made with other crystals, *e.g.*, potassium chlorate, mica, which can be obtained in the form of natural thin plates, and similar results were obtained.

#### 8. *Comparison with the Observations of Chinmayanandam on Haidinger's Rings in Crystalline Plates.*

Following Lord Rayleigh<sup>2</sup> who first drew attention to the complication in the Haidinger rings observed with mica, arising from its doubly refracting properties, Chinmayanandam<sup>3</sup> and later, Schaefer<sup>4</sup> have studied the phenomenon in great detail, both theoretically and experimentally. They find in the observed interference system, there are curves of minimum visibility (which may be considered as arising from the superposition of two sets of Haidinger fringes), coinciding with the isochromatic lines that would be obtained with a plate of double the thickness under crossed nicols in "convergent light." It is easily seen that the phenomenon treated in this paper is complementary to that observed by these authors. In their experiments, the incident light is monochromatic and the interference system observed arises from the different points in the field of view corresponding to different angles of observation and therefore to different

<sup>2</sup> Lord Rayleigh, 'Phil. Mag.', Vol. 12, p. 186 (1906).

<sup>3</sup> T. K. Chinmayanandam, 'Proc. Roy. Soc.', A, Vol. 95, p. 175 (1919).

<sup>4</sup> O. Schaefer and K. Fricke, 'Zeits. f. Physik,' Vol. 14, p. 253 (1923); O. Schaefer, *ibid*, Vol. 17, 1 (1923).

lengths of path in the crystal. On the other hand in the present experimental arrangement, the direction of observation is always the same, namely, normal to the crystal plate, and hence the distance traversed inside the crystal is the same for all the rays. The differences in optical path that give rise to the interference system in this case arise from *the differences in refractive index for different wave-lengths*, the incident light being now white. In both Chinmayanandam's experiments and in ours, because of the *double refraction* of the plate, there will be two sets of interference fringes which would have different spacings and the occurrence of maxima and minima of visibility in both the cases has a similar explanation. Indeed the analogy will be even closer if the Haidinger fringe system of the crystalline plate is observed in the transmitted light instead of by reflection as in Chinmayanandam's experiments. The curves of maximum visibility in this case would coincide with the isochromatic lines that would be observed between crossed nicols with a plate of the same crystal of double the thickness. The birefringence fringes in the present experiment will be analogous to the isochromatic curves described above. Further their positions are the same as the positions of maxima of visibility obtained with the crystal plate, when its thickness is halved. With crystal plates of sufficiently large thickness, the individual fringes may be too close to be resolved by the spectroscope, and only the birefringence fringes may then be visible.

### 9. *Analogy with Other Phenomena.*

According to the theory developed in this paper, the birefringence fringes are viewed as arising from the superposition of the two sets of closely spaced fringes having a small difference in spacing every alternate position of maximum visibility of the superposed system corresponding to the dark band of the birefringence system. The frequency of occurrence of the







birefringence fringes in the spectrum will therefore be much smaller than that of either of the two original systems which give rise to it, by superposition (actually half the difference between the two original frequencies). Thus it is possible to observe the birefringence fringes even under conditions where the original systems of fringes may be too closely spaced to be resolved by the spectroscope. The analogy with the 'heterodyne' beats in wireless, which are detectable, while the individual waves that continue to produce the beats are not, is obvious.

It should be mentioned here that the above view of the birefringence fringes as arising from the differential combination of two sets of closely spaced fringes is again analogous to the explanation suggested some years back by Schuster<sup>5</sup> for the origin of Brewster's bands as due to the superposition of two sets of Haidinger rings due respectively to the two plates. The analogy may be easily followed in detail.

In conclusion, I express my heartfelt thanks to Prof. K. S. Krishnan, for his valuable suggestions and the keen interest he has taken in my work throughout. My thanks are also due to Mr. P. K. Seshan for helping me in many of the experiments.

<sup>5</sup> Sir Arthur Schuster, 'Phil. Mag.,' Vol. 48, p. 609 (1924).



## Are not Liquid Sodium-Amalgams Colloidal ?

(A reply to the criticism of Henry E. Bent)

By

R. M. JOSHI.

(Received for publication, May 27, 1934.)

### ABSTRACT.

All the important arguments raised by Bent in his discussion of the paper of Paranjpe and Joshi are considered and it is attempted to show that the probability of dilute liquid sodium-amalgams being colloidal systems is greater than Bent admits.

Henry E. Bent (*J. Phys. Chem.*, **37**, 431-436, 1933) has recently criticised the views published in this journal by Paranjpe and the present author (*J. Phys. Chem.*, **36**, 2474, 1932) and has tried to refute the arguments given there in support of the colloid view of dilute liquid sodium-amalgams. He has also adduced facts which in his opinion either prove or constitute strong evidence that sodium-amalgams are true solutions. I have corresponded with Dr. Bent and having clarified the points at issue now endeavour to give a detailed reply to what has been cited against the colloid view of dilute liquid sodium-amalgams.

It is not claimed that any of the points under discussion cannot be explained on the true solution theory but it is submitted that the simplest and the most direct explanations are obtained from the colloid theory. In fact Bent agrees with the possibility of a "lyophillic reversible colloid in rather concentrated liquid amalgams"; what I strive to prove is the probability even in dilute amalgams.

ing upon the method of preparation should be given a fair trial. Since the methods of preparation adopted by Hine and Bohariwalla and co-workers were nearly the same and their results agreed between themselves and since the method of preparation followed by Davies and Evans has been different the disagreement must in the first instance be attributed to the difference in the method of preparation.

The argument of Bent that Willstatter's results are due to impurities seems to be unnecessarily conservative. It is true that Willstatter and co-workers thought that they might attribute the differences in properties to the possible presence of impurities from the walls of the vessels. But the following references will show that the probability is not high. Thus Rabinovitsch (*Koll. Zeits.*, **52**, 31, 1930) has shown that iron is hardly soluble in mercury and that it is very difficult to amalgamate iron with mercury. Again porcelain does not dissolve in either mercury, or sodium or a sodium-amalgam. This leaves the possibility of the Hessian Crucible yielding impurities. Willstatter's results show that the properties of amalgams prepared in these three types of vessels vary one from the other in all cases. An easier explanation, however, lies in the direction of a "wall-effect" as suggested by Paranjpe and the present author.

Let us now turn to the evidence which according to Bent points towards true solutions. The most convincing according to him is to be found in the vapour-pressure data of Bent and Hildebrand (*J. Am. Chem. Soc.*, **49**, 3011, 1927). These were obtained at temperatures between 554 to 651°K. while the case discussed is of amalgams at room temperatures, i.e., about 300°K. It is possible for lyophilic solutions to be highly peptized at such high temperatures and thus resemble true solutions in certain respects (Cf. Freundlich, 'Colloid and Capillary Chemistry,' translated by Hatfield, 805, 1926). Now, even with true solutions the deviation as expressed by  $\beta$  in the equation  $\log a/N_1 = \beta N_2^2$  decreases with rise of temperature. In

the work of Bent and Hildebrand  $\beta$  decreases from 20 for 298°K. to 12·82 for 648°·1 K. The question is not so much the interpretation of the change in  $\beta$  as of  $\beta$  itself. Can such deviations be caused by the formation of colloid micellæ in the system? The answer seems to be in the affirmative since among the factors that bring about deviations from ideal behaviour are included association of the solute and complex formation between the solute and the solvent. Bent and Hildebrand explain these deviations by assuming the simultaneous presence of five (or perhaps more) different compounds between sodium and mercury each obeying Raoult's law, but they also add, "Doubtless other compounds are present and other factors would have to be considered for an exact treatment of the behaviour of these amalgams." It is suggested that the colloid hypothesis makes matters simpler and affords a more direct explanation of the deviations.

The other piece of evidence advanced by Bent is the freezing point data. Since the experimental and the theoretical values of freezing point depression agree for very dilute amalgams as pointed out by Bent, and since the results of Bent and Hildebrand suggest a compound of the formula  $\text{NaHg}_{10}$  to be present in very dilute amalgams, evidently we are dealing with an instance of what Kendall (*J. Chem. Soc.*, **127**, 1778, 1925) describes as pseudo-ideal. Also the difference in the internal pressures of sodium and mercury is not small (*cf.* Hildebrand, "Solubility," Chemical Catalog Company, U.S.A., 1924). The effect of the internal pressure difference seems to be counterbalanced by the other factors such as micellæ formation, tending to bring about an opposite kind of deviation.

The third piece of evidence advanced in this connection by Bent is the crystalline structures exhibited by Vanstone's microphotographs. The fact that the structures are crystalline is no evidence against the colloid hypothesis. It is possible to obtain crystalline solids by freezing colloidal solutions. Freundlich (*loc. cit.*, p. 582) while summarizing the influence of freezing on

the stability of lyophillic sols mentions the following fact. "Upon freezing we observe.....that the micellæ are forced together by the ice in crystallizing out and finally separate in the form of flakes or of a fine net work with many meshes." The changes experienced by a potassium stearate coagel in the course of time are known to involve various stages of coarsening and resulting in the formation of crystals.

Finally there remains to discuss one more point raised by Bent in connection with transference of sodium with an electric current. He suggests that conductance data would have to be precise to one part in one hundred thousand in order to give much information regarding the behaviour of sodium since the conductivity is practically all electronic and the transference number of sodium in these amalgams is less than  $10^{-5}$ . No doubt all conductivity is electronic and the data available do not have the precision required by Bent, but it is known that the conductivity concentration curves do show discontinuities at approximately the same concentrations and the endeavour is to interpret them. If on the compound formation theory the migration of sodium is to be referred to be slight ionisation of the compounds (at least five according to Bent) the transference number of sodium would have to be more than  $10^{-5}$  and the current densities in the electrolytic experiments would not be high. The low transference number and the high current densities suggest, on the other hand, that the migrating ions which contain sodium are very heavy and encounter great resistance to motion. This means that the ions going towards the cathode are very large and have large amounts of mercury associated with them. The largeness of these ions is enough to impress colloid properties on the system (*Cf.* the colloid properties exhibited by many true solutions of some of the more complex organic dyes).

Thus in the light of what has been said above it would appear that the probability of dilute liquid sodium-amalgams being colloidal systems is greater than Bent admits.

My thanks are due to Dr. T. S. Wheeler and Professor G. R. Paranjpe of this Institute for the interest they took in the preparation of this paper.

*13th October, 1933.*  
ROYAL INSTITUTE OF SCIENCE,  
BOMBAY, INDIA.





# Thermionic Emission and Catalytic Activity, Part III. A Mechanism of Activation of Gases at Hot Metallic Surfaces

By

B. S. SRIKANTAN.

*(Received for publication, January, 1933 ; revised  
September, 1934.)*

## *Abstract.*

A parallelism between thermionic emission and catalysis has been drawn. A view is advanced that in a hot metallic catalyst the process of activation is primarily due to the collision of the adsorbed molecule with the freely moving electrons ; and an expression is derived, connecting the velocity constant and the temperature co-efficient, which is tested by experimental data available. This is shown to be a more general equation than that of Arrhenius.

Langmuir<sup>1</sup> found that chemically indifferent gases have no effect on the electron emission from tungsten but poisons suppressed the emission of electrons from it. Briner<sup>2</sup> and collaborators have shown that in the oxidation of nitrogen by platinum and other catalysts, the catalytic efficiency bears a constant ratio to their power to emit electrons. Further Thompson<sup>3</sup> and Srikantan<sup>4</sup> find that chemical activation of gases at

<sup>1</sup> Langmuir, Trans. Faraday Soc., **17**, 641 (1921).

<sup>2</sup> Briner, Helv. Chem. Acta., **9**, 634 (1926).

<sup>3</sup> Thompson, Phy. Zeit., **14**, 11 (1913).

<sup>4</sup> Srikantan, Ind. Jour. Phys., **5**, 685 (1930).

catalytic surfaces is perceptible at the temperature at which thermionic emission commences. Taylor<sup>5</sup> claims that catalysis is not due to the entire surface of the catalyst but is confined to certain active patches or centres on it. Experiments by Richardson<sup>6</sup> on thermionic emission from metal surfaces have shown the interesting fact that the emission of electricity from a hot surface does not occur uniformly over the surface but from localised patches. The author's work<sup>7</sup> has shown that thermionic emission from a filament coated with mixtures of ceria and thoria is maximum with that containing about 1% ceria. It has been already observed by Swan<sup>8</sup> that the catalytic activity of wires coated with ceria-thoria mixtures is maximum with one containing 0.96%<sup>3</sup> ceria. It is the object of this paper to associate the two sets of observations by claiming the catalytically active patches to be the same as those that are thermionically active.

Further, Arrhenius' equation<sup>9</sup> is usually taken as a guide in finding the relation between the velocity constant and temperature. But it is purely empirical. It gives us a measure of the energy of activation in any reaction but does not give us any idea as to the mechanism of activation in catalytic processes.

"In gases the accumulation of energy is due to collisions among the molecules of the gas."<sup>10</sup> But the accumulation of energy in a film of gas adsorbed at a solid surface is more complicated than that in a gaseous phase. Due to the presence of the residual affinities on the surface and their tendency to build up a continuation of the lattice arrangement, the adsorbed film of gas forms a part of the surface also.<sup>11</sup> In a thesis submitted

<sup>5</sup> Taylor, Proc. Roy. Soc., **105A**, 105 (1925).

<sup>6</sup> Richardson, Proc. Roy. Soc., **107A**, 377 (1925).

<sup>7</sup> To be published shortly in the Journal of the Indian Chemical Society.

<sup>8</sup> Swan, Jour. Chem. Soc., **125**, 780 (1924).

<sup>9</sup> Arrhenius, Zeitsch. Physik. Chem., **4**, 226 (1889).

<sup>10</sup> J. J. Thomson, Phil. Mag., **37**, 378 (1924).

<sup>11</sup> Cf. F. H. Constable, Proc. Roy. Soc., **108A**, 359 (1925).

to the Dacca University by the author (1930) while considering the various factors contributing to the accumulation of energy in a film of gas adsorbed on a catalyst material, attention was drawn to the fact that the atoms of the solid (characterised by the existence of specific heat) might share their energy of vibration with the adsorbed molecule of the gas and thus help to accumulate energy in the adsorbed film. Evidence has also been brought forward for such a view.<sup>12</sup> It was also suggested that the freely moving electrons in a metallic catalyst<sup>13</sup> might, under suitable conditions, come into collision with the adsorbed gas and thus activate it, just as is likely to happen in free space.<sup>14</sup>

Here, if one assumes that the velocity of any gaseous reaction on a hot metallic surface is due to and is proportional to the saturation current at that temperature, then one obtains an interesting relation between the velocity constant and the temperature. This new equation is shown at the end of this paper to be equally applicable as that of Arrhenius and in fact more general than the other. Further, it serves to connect the two sets of observations on thermionic emission and catalysis and shows that the little understood mechanism of catalytic activation of gases at hot metallic surfaces is mainly due to the collision between the thermions and the adsorbed gas. However under simplifying conditions the equation reduces to that of Arrhenius.

Thus the kinetic energy of an electron is  $\frac{1}{2} m \mathbf{v}^2$ , where  $m$  = mass and  $\mathbf{v}$  = the mean velocity in cms. per sec.

In time  $\theta$ , the space travelled by  $N$  electrons is  $N \mathbf{v} \theta$ .

If  $E$  is the energy of activation at temperature  $T$  and it is solely derived from a collision with an electron, then an electron

<sup>12</sup> Ind. Jour. Phys., **4**, 539 (1930).

<sup>13</sup> J. J. Thomson, Applications of Dynamics to Physics and Chemistry, p. 296. Riecke and Drude, Annal. d. Physik, **66**, 353 and 1193 (1898); **1**, 566 (1900); **2**, 835 (1900).

<sup>14</sup> J. J. Thomson, *British Ass. Rep.*, Sheffield (1910), p. 501.

travels before activation of the gas through impact with an adsorbed molecule, a distance of  $2vE/mv^2$  or  $2E/mv$  cms.

Then the number of collisions of an electron on the surface per cm. of its path, which terminate the free path equal to or greater than  $2E/mv$  is given by  $Ce^{-2E/mv}$  where  $C$  = total number of collisions per cm. of its path and  $l$  = mean free path.

If every collision is effective, the number of gas molecules chemically activated per unit area of active surface in time  $\theta$  is

$$Nv\theta C e^{-2E/mv}$$

or  $K = NvC e^{-2E/mv}$ , where  $K$  is the velocity constant.

But  $C \propto T$  and  $Nv = i/e$  where  $i$  is the current,

$$\text{or } K = \frac{k_1}{e} \times i \times T e^{-2E/mv} \text{ where } k_1 \text{ is a constant.}$$

$$\text{But } l \propto 1/c \quad \text{or } l/k_1 T$$

Therefore

$$K/T = \frac{k_1 i e^{-2k_1 ET/mv}}{e}$$

Since  $T_1/v_1 = T_2/v_2$ ,  $2k_1 ET/mv = X$ , a constant, and the equation becomes

$$K = \frac{k_1 T i e^{-X}}{e}$$

It has been shown (*loc. cit.*) that the emission of electricity is perceptible at the temperature when catalysis also begins. Therefore for  $i$  in the above equation one can put the value of the saturation current at  $T$ ,

$$\text{i.e., } i = AT^{1/2} e^{-b/T}$$

Therefore

$$K = \frac{k_1}{e} A T^{3/2} e^{(-b/T + K)}, \text{ where } b \text{ is a constant ;}$$

$$\text{or } K = Y T^{3/2} e^{-(b/T + X)} \quad \text{as } \frac{k_1}{e} A = Y, \text{ a constant.}$$

The validity of the above equation is tested by plotting  $(-\log K + 3/2 \log T)$  against  $(1/T)$  which ought to be a straight line in the case of a single reaction. It is found to be so. The accompanying graphs from the data of Hinshelwood and his collaborators<sup>15</sup> on the thermal decompositions of ammonia on a

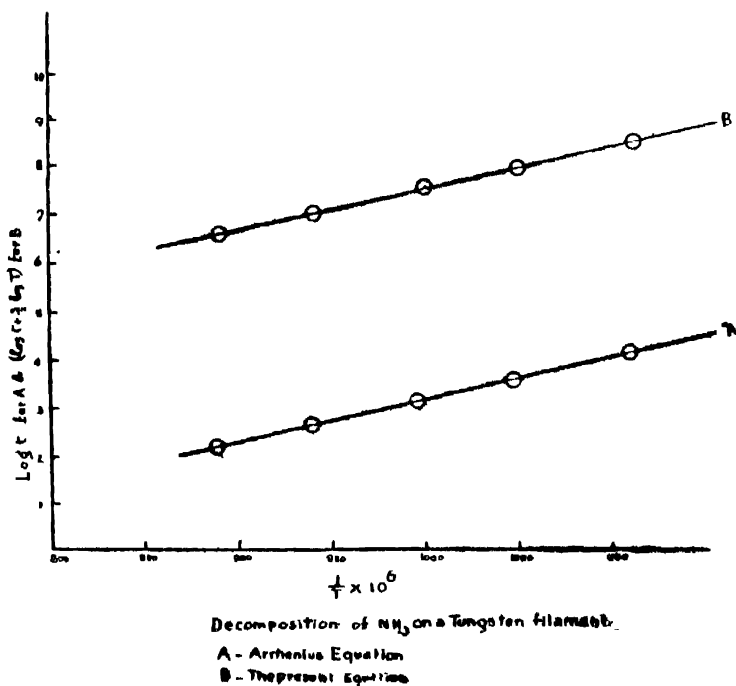


FIG. 1.

<sup>15</sup> Hinshelwood and collaborators, Jour. Chem. Soc., 127, 327 and 1116 (1925).

travels before activation of the gas through impact with an adsorbed molecule, a distance of  $2vE/mv^2$  or  $2E/mv$  cms.

Then the number of collisions of an electron on the surface per cm. of its path, which terminate the free path equal to or greater than  $2E/mv$  is given by  $Ce^{-2E/mvl}$  where  $C$  = total number of collisions per cm. of its path and  $l$  = mean free path.

If every collision is effective, the number of gas molecules chemically activated per unit area of active surface in time  $\theta$  is

$$Nv\theta Ce^{-2E/mvl}$$

or  $K = NvCe^{-2E/mvl}$ , where  $K$  is the velocity constant.

But  $C \propto T$  and  $Nv = i/e$  where  $i$  is the current,

$$\text{or } K = \frac{k_1}{e} \times i \times T e^{-2E/mvl} \text{ where } k_1 \text{ is a constant.}$$

But  $l \propto 1/c$  or  $1/k_1 T$

Therefore

$$K/T = \frac{k_1 i e^{-2k_1 ET/mv}}{e}$$

Since  $T_1/v_1 = T_2/v_2$ ,  $2k_1 ET/mv = X$ , a constant, and the equation becomes

$$K = \frac{k_1 T i e^{-X}}{e}$$

It has been shown (*loc. cit.*) that the emission of electricity is perceptible at the temperature when catalysis also begins. Therefore for  $i$  in the above equation one can put the value of the saturation current at  $T$ ,

$$i.e., i = AT^{1/2} e^{-b/T}$$

Therefore

$$K = \frac{k_1}{e} \Lambda T^{3/2} e^{-(b/T + K)}, \text{ where } b \text{ is a constant ;}$$

$$\text{or } K = Y T^{3/2} e^{-(b/T + K)} \quad \text{as } \frac{k_1}{e} \Lambda = Y, \text{ a constant.}$$

The validity of the above equation is tested by plotting  $(-\log K + 3/2 \log T)$  against  $(1/T)$  which ought to be a straight line in the case of a single reaction. It is found to be so. The accompanying graphs from the data of Hinshelwood and his collaborators<sup>15</sup> on the thermal decompositions of ammonia on a

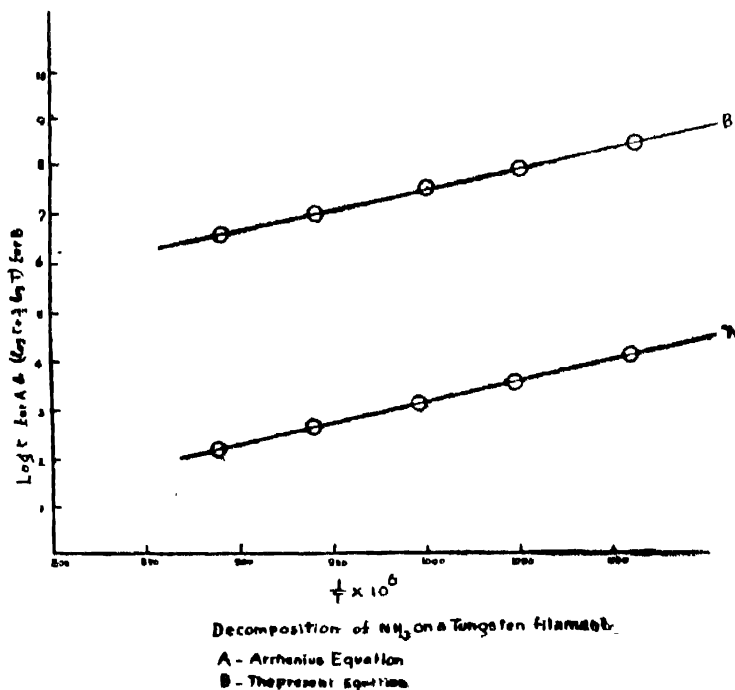


FIG. 1.

<sup>15</sup> Hinshelwood, and collaborators, Jour. Chem. Soc., 127, 327 and 1116 (1925).

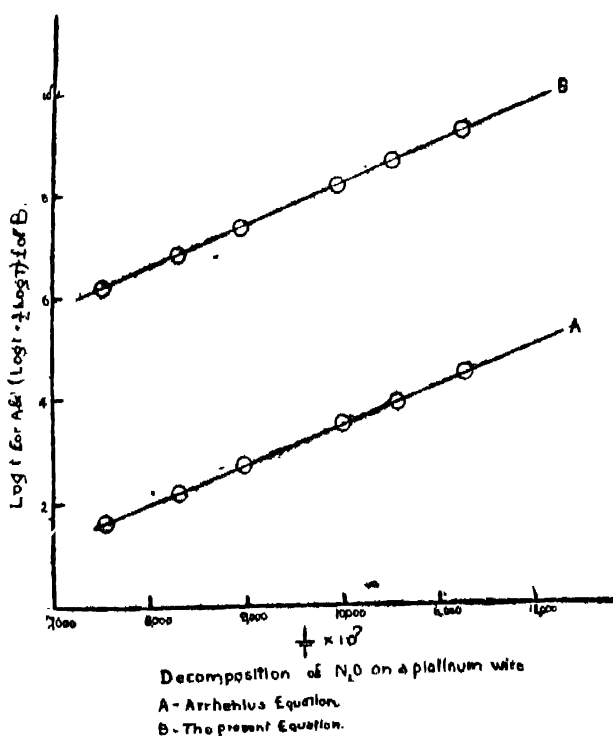


FIG. 2.

tungsten filament and that of nitrous oxide on platinum, show the applicability of the present equation as that of Arrhenius.\* If however the temperature considered is only over a limited range in any set of observations, the term  $(3/2 \log T)$  can be almost considered to be a constant and the equation reduces to that of Arrhenius.

DEPARTMENT OF TECHNICAL CHEMISTRY,  
 COLLEGE OF ENGINEERING, GUINDY (MADRAS)  
 AND ANDHRA UNIVERSITY, WALT AIR.

\* Note.—Instead of  $-\log k$  the values plotted are those of  $\log t$ , where  $t$  is the time required for a definite fraction of the reaction to proceed at a given pressure. (Cf. Hinshelwood: *The Kinetics of Chemical Change in Gaseous Systems*, 1929, p. 43.)



## On the Determination of the Absorption Coefficient of Sound

By

R. N. GHOSH AND HAJI GHULAM MOHAMED.

*Physics Department, University of Allahabad.*

*(Received for publication, June 2, 1934.)*

### *Introduction.*

This paper forms a preliminary report of the investigations into the acoustic properties of certain materials which are easily available in different parts of India. It is likely, however, that the climatic conditions might have an important effect on the sound-absorbing properties of materials so much so that the results of the tests carried out, say in America, might be very much different from those that could be obtained in India. Humidity, for instance, might considerably change the very nature of the acoustic substance by filling its pores with water particles and thus seriously affecting the sound-absorption. Secondly, dust in India is also an important factor in determining sound-absorption co-efficient of any material. With this in view, it was considered desirable to carry out such tests afresh with materials which have already been tested elsewhere.

The method employed in these investigations was the stationary-wave method which had previously been used by E. T. Paris. <sup>1</sup>

*Theory.*

The theory of the method is briefly as follows:—

When one end of a long cylindrical pipe is closed by means of a perfect reflector, the other end remaining open to a source of sound of constant pitch and intensity, sound waves from this source travel down the pipe and are completely reflected back from the perfect reflector. The amplitudes of the incident and reflected waves in this case would be equal and thus a stationary wave would be formed in the pipe so that there would be maximum pressure variation at the nodes and zero pressure-variation at the anti-nodes. If, however, we replace the perfect reflector by a specimen that absorbs part of the incident sound-energy, the amplitude of the reflected wave will be less than that of the original incident wave so that we would have within the pipe two stationary waves of amplitudes  $A+B$  and  $A-B$  respectively which might be regarded as super-imposed upon each other in such a way that the nodes and anti-nodes of the first are one quarter of a wave-length away from those of the second system of stationary waves. Here  $A$  is the amplitude of the incident wave and  $B$  that of the reflected one.

Now  $\alpha$  the co-efficient of sound-absorption is defined by

$$\alpha = \frac{E_i - E_r}{E_i} \quad (1)$$

where  $E_i$  is the energy-flux in the incident waves,  $E_r$  that in the reflected waves and these are proportional to  $A^2$  and  $B^2$  respectively. If now we determine  $a/b$ , the ratio of the maximum pressure-amplitude to the minimum pressure-amplitude we can readily calculate  $\alpha$  in terms of the ratio  $a/b$ . Thus, since

$$\alpha = \frac{A^2 - B^2}{A^2} \quad \text{and} \quad \frac{a}{b} = \frac{A+B}{A-B}$$

we have,

$$\bar{a} = \frac{4}{2 + \frac{a}{b} + \frac{b}{a}} \quad \dots \quad (2)$$

For details see E. T. Paris, (*loc. cit.*) p. 270.

### *Description of the Apparatus.*

The apparatus employed in the present investigation does not differ much from that used by E. T. Paris. It consists of an experimental pipe made from three earthen-ware glazed drain-pipes (5 cms. wall thickness) cemented together. The dimensions of the pipe are about 30 cms. internal diameter and 180 cms. length. Since it was placed in a sequestered place in the laboratory, far away from the traffic, all such precautions to prevent the communication of the external vibration to its walls which might effect the hot-wire microphone readings, were quite unnecessary. At one end of the pipe a wooden box of dimensions 3 ft. length,  $2\frac{1}{2}$  ft. breadth and  $2\frac{1}{2}$  ft. height, served the purpose of the sound-chamber.

The perfect reflector was merely a disc of 37 cms. diameter cut out of a brass sheet 0.25 inch thick and was solidly mounted on a wooden disc of the same size and about  $1\frac{1}{2}$  inch thick. The specimens to be tested were also made in the form of discs of 37 cms. diameter and were mounted on the perfect reflector. This whole system was placed in the open end of the pipe and made air-tight by means of a rubber-washer and cotton-waste filling all round the rim. The surface of the specimen was always kept normal to the axis of the experimental pipe. In the sound-chamber and opposite to the open end of the pipe was placed a moving coil type loud-speaker about 50 cms. away from the open end and the stationary wave produced by it was tested by the detecting apparatus. A diagram (Fig. 1) is appended here to show the velocity amplitude along the axis of the pipe. The

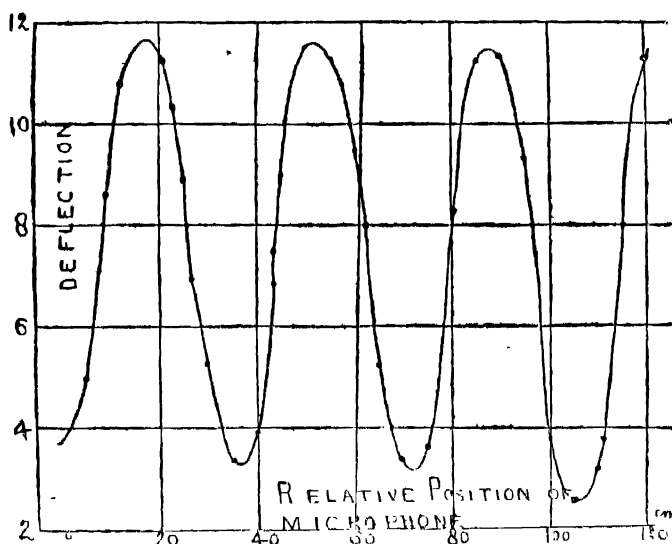


FIG 1.

microphone used as the detecting apparatus in these experiments was, in all essential detail, the ordinary selective hot-wire microphone used by Tucker<sup>2</sup> and Paris, but was made as small as possible so as to avoid any perceptible disturbances by its presence in the sound pattern inside the experimental pipe.

This microphone was mounted rigidly on a stand fixed in an iron rod about 350 cms. long and the height of the stand was so adjusted that the centre of the orifice of the microphone lay on the axis of the pipe. A short piece of brass rod bent in the shape of a semi-circle of radius equal to the internal radius of the clay-pipe and rivetted normally to the iron rod served well to keep the microphone always on the axis of the pipe in all its positions throughout the entire length. In order to avoid jerky motion, noise and friction, the semi-circular brass rod was encased in a piece of rubber tubing.

To measure the changes in the resistance of the hot-wire grid, Wheatstone's bridge method was employed. By including a

part of Callendar and Griffith's bridge in one of the arms of a post office box, the changes in the resistance of the order of 0.1 ohm could be easily ascertained. Smaller values of resistance changes could be directly read from the galvanometer deflections which indicated a resistance change of 0.001 ohm for one mm. deflection. We had only one microphone at our disposal and so we could not use a compensating microphone. This gave us much trouble in the beginning because of the fact that we passed a steady current of 37 m. amps. through the microphone and the resistance of the post-office box, which got heated on account of such heavy current, rendered the balance unsteady. To remedy this we constructed a special resistance coil of thick wire about 260 ohms resistance and thus by avoiding the use of high resistance coils (greater than 20 ohms) in the post-office box obtained the desirable steadiness of the balance. In this arrangement the balance became quite steady after about half an hour. When exposed to the sound, the fall in resistance of the hot wire grid was somewhat about 25 ohms at a maximum depending upon the accuracy of the tuning, the strength of the current to heat the grid and the intensity of the sound. This order of resistance change was found by experience to be very convenient for our purpose. A diagrammatic representation of the change of resistance with the relative positions of the microphone inside the pipe for a particular tuning and the heating current 37 m. amps. is shown in Fig. 1. After the balance has been obtained with no sound and a steady heating current of 37 m. amps. and the microphone having been kept at one of the maxima it was found that whenever the sound was switched on, the milliammeter in series with the grid showed a rise in the heating current due to the fall in the resistance of the grid. To obtain the balance then with the sound it was necessary to adjust the heating current to its original value correctly, because an error of about 0.1 m. amp. in the heating current introduced an error of about 0.6 ohms in the value of the change of resistance in the grid. That this is very important might be seen from Fig. 2,

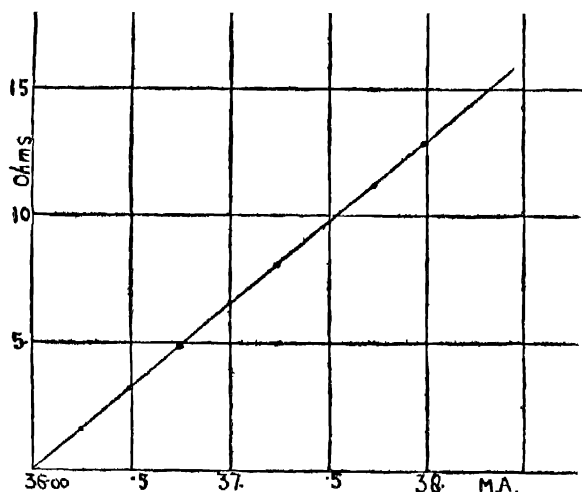


FIG. 2.

in which the resistance changes are plotted against the heating current for a particular constant intensity of the source of sound for the same position of microphone. In order to avoid this source of error it was necessary to read the milliammeter as accurately as possible through a microscope and always adjust the current by means of a sliding resistance to the original value before taking readings.

The source of sound which was a moving coil type<sup>3</sup> loud-speaker was actuated by means of a Numan's Oscillator\* of a fairly constant pitch and intensity. The oscillations from this oscillator were first amplified by an audio-frequency one-stage amplifier and then sent to the loud speaker. The microphone itself was a good indicator of the constancy of the intensity, because unless the intensity of the source was constant the

\* Now we have placed a copper oxide rectifier in the L. S. circuit to ensure the constancy of the intensity by observing the deflection of a galvanometer. For success with the type of oscillator used, it is very necessary that all the batteries should be fully charged, specially the low tension ones. This has also been changed to a valve maintained tuning fork oscillator.

balance could not remain steady. Complete electrical diagram of the sound-producing apparatus is shown in Fig. 3.

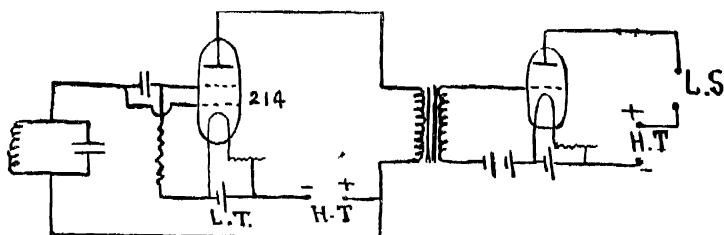


FIG. 3.

### *Procedure.*

The experimental procedure was as follows :—The microphone was moved roughly in the position of a maximum and then tuned to the frequency of the note of the loud-speaker by slowly altering the volume of the container until the fall of resistance of the grid observed was maximum for the same note and the same position of the microphone. Very accurate tuning of the instrument for these experiments was not at all necessary. The specimen under observation was then mounted on the perfect reflector and placed at the end of the pipe. The source of sound was switched on and the microphone was then moved to the position of maximum resistance change by a very slow motion of the sliding rod keeping eye on the spot of light from the galvanometer. The turning point of the spot of light which would be located within one millimeter movement of the iron rod indicated the exact position of a minimum. After reading the milliammeter, and adjusting the sliding resistance to make the heating current exactly 37 m. amps., the deflection  $\rho_1$  was noted down with sound; the balance-point without sound having already been noted down. Several reading of  $\rho_1$  were taken. Then the microphone was moved to the position of maximum, the current adjusted to 37 m. amps. and the balance obtained without sound,

and change in resistance say  $\rho_2$  due to sound was also noted down. After this the specimen was removed and the perfect reflector alone was placed in position.

Then the position of the microphone for a minimum change of resistance (in terms of galvanometer deflection) was recorded. As a matter of fact there should be absolutely no change of resistance with and without sound if the reflections from the surface of the reflector were perfect. But it was never the case; there being always a change of resistance of the order of about 0.005 ohms. This at present was neglected. The rod was then moved very slowly in one direction until the deflection was  $\rho_1$ , and the position of the microphone was noted down. The difference between these two positions of the microphone say  $y_1$ , was thus obtained. The same process was repeated by a slow motion of the rod in the reverse direction and the value of  $y'_1$ , on the opposite side of the position of minimum to give the same fall of resistance  $\rho_1$ , as before, was also determined. This process was repeated several times. The same process was repeated and  $y_2$  and  $y'_2$  the respective displacements of the microphone from the position of the minimum to one required to give a fall of resistance equal to  $\rho_2$ , were determined.

It is clear that the pressure-amplitudes in the system of stationary waves which produced the resistance changes  $\rho_1$  and  $\rho_2$  must be proportional to  $\sin ky_1$ , and  $\sin ky_2$  where  $k=2\pi/\lambda$ ,  $\lambda$  being the wave-length. The value of  $k$  thus obtained was 0.091.

Hence the ratio  $a/b$  comes out to be equal to  $\sin ky_2/\sin ky_1$  and thus  $a$  can be calculated from equation (2).

The half wave-length was found by observing the position of the microphone at the two successive nodes. The frequency of the note from the source of sound was determined correctly from the knowledge of the velocity of sound in air at that temperature and humidity to be equal to 512. The results are set down in details in tables below.



Specimen.	$i_{11}$ , m. amps.	Defect. $\rho_0$ , mms.	$t_1$	$y_1$ , cms.	$y_1'$ , cms.	Mean $y_1$ , cms.	$y_2$ , cms.	$y_2'$ , cms.	Mean $y_2$ , cms.	$k y_1$	$k y_2$	$\alpha$
Hair felt $\frac{1}{4}$ inch thick.	37.0	40.0	17.9	1.0	1.05	1.02	11.7	11.8	11.75	5°-12'	61°-0	0.34
	37.0	40.5	17.85	1.05	1.05	1.05	11.7	11.7	11.7			
	37.0	40.0	17.9	1.0	1.0	1.0	11.8	11.8	11.8			
	37.0	40.0	17.9	1.0	1.0	1.0	11.7	11.8	11.75			
	37.0	39.5	17.8	1.0	1.0	1.0	11.7	11.7	11.7			
Plaster about 4 mms. thick on a brick- wall specimen. The surface of this specimen had many cracks.	37.0	17	7.1	0.35	0.4	0.35	5.7	5.8	5.75	2°-6'	29°-42'	0.25
	37.0	18	7.1	0.4	0.4	0.4	5.8	5.8	5.8			
	37.0	18	7.2	0.4	0.4	0.4	5.8	5.8	5.8			
	37.0	17	7.2	0.4	0.45	0.42	5.7	5.7	5.7			
	37.0	16	7.1	0.4	0.4	0.4	5.7	5.7	5.7			
Asbestos sheet 3 mms. thick.	37.0	10.0	12.7	0.65	0.6	0.62	13.3	13.2	13.25	3°-24'	69°-0'	0.22
	37.0	10.0	12.8	0.65	0.6	0.62	13.2	13.2	13.2			
	37.0	10.0	12.7	0.65	0.65	0.65	13.2	13.3	13.25			
	37.0	10.0	12.7	0.65	0.65	0.65	13.3	13.2	13.25			
	37.0	9.5	12.7	0.65	0.7	0.67	13.3	13.3	13.3			
	37.0	10.0	12.8	0.65	0.65	0.65	13.2	13.3	13.25			
	37.0	8.5	12.7	0.65	0.65	0.65	13.3	13.2	13.25			

$i_{11}$  = heating current on the acid

Specimen.	$i_s$ , m. amps	Deflect. $P_2$ , mms.	$\rho_1$ , ohms.	$y_1$ , cms.	$y'_1$ , cms.	Mean $y_1$ , cms.	$y_2$ , cms.	$y'_2$ , cms.	Mean $y_2$ , cms.	$k y_1$	$k y_2$	$\alpha$
Khaddar, dry and coarsely woven; about 1 mm. thick.	37.0	8.0	20.5	0.55	0.50	0.52	14.9	14.8	14.85	2°.36'	77°.42'	0.17
	37.0	9.0	20.6	0.5	0.5	0.5	14.9	14.9	14.9			
	37.0	8.0	20.5	0.5	0.55	0.52	14.9	14.9	14.9			
	37.0	9.0	20.5	0.5	0.5	0.5	14.9	14.8	14.85			
	37.0	7.5	20.5	0.5	0.5	0.5	14.9	14.9	14.9			
	37.0	8.0	20.5	0.5	0.5	0.5	14.8	14.9	14.85			
Cotton-waste loosely packed; about 1½ inches thick.	37.0	88.0	3.30	1.8	1.8	1.8	7.1	7.1	7.1	9°.24'	37°.2	0.67
	37.0	88.0	3.31	1.8	1.8	1.8	7.2	7.1	7.15			
	37.0	89.0	3.33	1.8	1.8	1.8	7.1	7.1	7.1			
	37.0	88.0	3.30	1.8	1.8	1.8	7.1	7.1	7.1			
	37.0	89.0	3.29	1.8	1.8	1.8	7.1	7.2	7.15			
	37.0	89.0	3.31	1.8	1.8	1.8	7.2	7.1	7.15			
	37.0	88.0	3.32	1.7	1.8	1.75	7.1	7.1	7.1			
	37.0	87.0	3.31	1.8	1.8	1.8	7.2	7.1	7.1			
	37.0	88.0	3.30	1.8	1.8	1.8	7.1	7.1	7.1			

*Discussions.*

The greatest disadvantage of this method of determining sound absorption co-efficient of materials having a low value for  $\alpha$  is due to the fact that the so-called perfect reflector never fulfils the conditions of the perfect reflector demanded by the theory of the method and hence the results thus obtained are always higher than what they ought to be. To neglect the small sound-energy absorption by the system and the reflector will be serious in the case of materials having a low absorption co-efficient.

The other prominent sources of error found by the authors were as follows :—

1. A slight carelessness in placing either the specimen or the perfect reflector in an airtight way influences the result appreciably. The value of  $\alpha$  thus obtained is always higher than what it should be.

2. Avoiding altogether the use of a sound chamber to keep the source of sound insulated, so to say, from the moving objects (for instance the experimenter himself) inside the room where the apparatus is installed, has a very uncertain effect on the quantity of sound-energy entering the experimental pipe.

3. To keep any object inside the chamber in such a way that this object occupies different positions inside the chamber during one experiment is also a serious source of error. In such cases too, the sound energy entering the pipe is affected.

4. A slight carelessness in closing the door of the sound-chamber has also some slight measurable effect on the results.

5. Changes in either the frequency or the intensity of the note impairs the accuracy of the results greatly.

6. Unevenness in the surface of the pipe or displacing the orifice from the axis is also an uncertain source of error.

7. The presence of the microphone inside the pipe is also a small source of error but may be neglected.

In the present investigation, though some of the most prominent sources of error have been eliminated, still we think our results to be a little too high. The work is still in progress and we hope to report the results concerning the effect of humidity on the absorption co-efficient of materials shortly.

### *Summary.*

This is a preliminary report on the determination of the co-efficients of sound-absorption of a few specimens by the stationary-wave method.

The stationary waves were produced in a long clay pipe by a source of sound which was kept in a sound chamber and the sound intensities at different places in the pipe were measured by a movable hot-wire microphone tuned to the frequency of the source of sound (a Numan's Oscillator) having a fairly constant frequency and intensity.

The specimens so far tested were :—1. Hair-felt. 2. Cotton-waste. 3. Plaster on bricks. 4. Asbestos 5. Khaddar.

The apparatus is very sensitive. The work is still in progress.

### *References.*

1. E. T. Paris, Proc. Phys. Soc., Vol. 39, p. 269, (1926-27).
2. Tucker and Paris, Phil. Trans. Roy. Soc. A., Vol. 221, p. 389 (1921).
3. K. C. Van Ryn., Exp. Wireless, Vol. 2, p. 134 (1925).

## Spark Spectrum of Iodine

BY

P. N. KALIA, M.Sc.

*Research Scholar, University of the Punjab ;  
Department of Physics, Government College, Lahore.*

*(Received for publication, September 19, 1934.)*

### ABSTRACT

123 new lines of ionised iodine have been measured between  $\lambda 1275$  and  $\lambda 2376$ , using a one-metre vacuum grating. The spectrum was excited by electrodeless discharge in tubes filled with iodine vapour at less than  $0.05$  mm. pressure.

The earliest measurements of the arc and spark spectra of iodine in the visible and ultra-violet regions are due to Konen and Exner and Haschek<sup>1</sup>. Later, Wood and Kimura<sup>2</sup> measured a large number of lines between  $\lambda 7468$  and  $\lambda 4682$  in Geissler tubes, and showed that several of these lines possessed hyperfine structures. Still later, L. Bloch and E. Bloch<sup>3</sup> in an interesting work excited the spectra of iodine by electrodeless discharge, and succeeded in sorting out the lines due to various stages of ionisation. Their observations extended from  $\lambda 7350$  to  $\lambda 2220$  and are obviously of great help to work of classification. The most recent and also the most accurate measurements are due to W. Kerris,<sup>4</sup> who measured 687 lines lying between  $\lambda 7486$  and

<sup>1</sup> Kayser's 'Handbuch der Spektroskopie.'

<sup>2</sup> 'Astrophys. Jour.,' Vol. 46, p. 181 (1917).

<sup>3</sup> 'Ann. de phys.,' Vol. 11, p. 141, (1929); Vol. 16, p. 503 (1931)

<sup>4</sup> 'Zeits. f. Phys.,' Vol. 60, d. 20 (1930).

$\lambda$  2562 in Geissler tube condensed discharge. In the Schumann region, evidently the only observations available so far have been by L. A. Turner<sup>5</sup> who has restricted his experiments to the excitation of the arc spectrum of iodine in the fluorite region. In the present work, an attempt has been made to measure the arc and spark lines of iodine from  $\lambda$  2376 up to the transmission power of fluorite.

### *Experimental.*

The spectrum of iodine was excited by electrodeless discharge in a pyrex tube 25 cms. long and 1.5 cms. in diameter with about 50 turns of copper wire wound round it. The energy was supplied by a 30 KV transformer taking 3 amps. at 100 volts in the primary, and having a small glass plate condenser and a spark gap in the secondary circuit. The tube was sealed on in front of the slit of a one-meter vacuum spectrograph of Sawyer type, provided with a grating having 14403 lines per inch ruled on speculum metal. A small fluorite plate was always fixed before the slit to stop the iodine vapour from going into the body of the spectrograph. Small desired quantities of iodine vapour could be put into the discharge tube by regulating a stop-cock attached to a side tube, leading to reservoir of iodine. The evacuation was carried out through another side tube connected to a quartz mercury diffusion pump backed by an oil pump. A liquid air trap was introduced between the pumping system and the discharge tube to absorb mercury vapour as also to prevent the iodine vapour from going to the pump and spoiling its working. As an extra precaution a tube containing calcium oxide was also inserted. The pressure in the discharge tube was always kept at a value below 0.5 mm. of mercury and was maintained by regulating the stop-cock leading to the pumps. When the discharge was passed and the pressure was regulated the whole tube was filled with a very strong pale bluish green glow and it was this

<sup>5</sup> 'Phys. Rev.,' Vol. 27, p. 397 (1926).

light which was photographed. The spectrum was obtained on plates prepared by the author according to Schumann's directions and the lines extended from  $\lambda$  2400 to  $\lambda$  1250. Several spectrograms were taken with varying exposures, and to bring out the weakest lines in one case a sixteen hour exposure was also given. Carbon lines appeared strongly as impurity. The dispersion was determined with the nitrogen standards given by Bowen and Ingram,<sup>1</sup> but for actual calculation of wave lengths the carbon line 1931.027 was taken as standard. It is believed that the error in measurement is less than .1A.

### Results.

In all 143 lines were measured. Twenty (20) of them are the arc lines which have already been obtained by Turner.<sup>2</sup> The table of lines which follows contains all the lines measured by the author as well as those obtained by Turner in order to complete the observation in the fluorite region.

$\lambda$ (I. A.) (Kalia)	Int.	$\lambda$ (I. A.) Turner	Int.	$\nu$
		1234.2	3	81024
		1259.4	2	79400
1275.6	00	*1275.7	2	78390
		1277.4	0	78281
1285.9	0			77770
		†1286.3	2	77742
		1289.6	1	77541
		1291.4	1	77437
		1296.6	0	77127
		*1300.6	2	76888

<sup>1</sup> 'Phys Rev..' Vol. 28, p. 444 (1926).

<sup>2</sup> *loc. cit.*

$\lambda$ (I. A.) (Kalia)	Int.	$\lambda$ (I. A.) Turner	Int.	$\nu$
		1303.2	1	76735
		1313.6	0	76124
		1314.1	1	76099
		1317.7	3	75893
1325.1	$\frac{1}{2}$			75465
1329.1	1			75239
		1330.4	2	75167
		1336.7	6	74810
		1339.9	0	74631
		1340.9	2	74579
		1343.7	1	74420
		1349.0	1	74128
		1350.3	1	74055
		1352.4	00	73942
1354.3	1	1354.3	00	73841
		1355.5	6	73775
		1358.1	3	73631
		1361.2	5	73465
		1366.6	0	73173
		1367.7	2	73114
		1368.3	3	73084
		1382.3	0	72342
		1383.4	3	72286
		1390.9	5	71897
		1393.3	2	71769
		1395.0	00	71685
		1400.2	3	71421
1403.7	$\frac{1}{2}$			71242
1415.6	4			70644



$\lambda$ (I. A.) (Kalia)	Int.	$\lambda$ (I. A.) Turner.	Int.	$\nu$
		1421.6	4	70345
		1425.7	8	70143
		1429.7	0	69947
1436.6	$\frac{1}{2}$			69607
		1446.5	5	69181
		1455.4	4	68806
		1457.6	4	68606
1458.1	3	1458.2	6	68580
		1459.2	6	68528
		1466.0	5	68210
		1466.7	00	68179
1482.2	0			67467
		1486.1	1	67289
1486.6	0			67269
1490.5	4			67093
...	...	1493.2	5	66971
1495.8	$\frac{1}{4}d$	.....	...	66854
1505.2	0	.. ...	...	66486
1507.4	0	1507.3	3	66340
1511.5	0	.....	...	66159
1514.9	2	1514.8	9	66012
1518.1	2	1518.3	7	65868
1523.3	0	.....	...	65649
.....	...	1526.6	4	65505
1531.5	00	.....	...	65294
1532.5	$\frac{1}{2}$	.....	...	65252
1535.4	$\frac{1}{2}$	.....	...	65130
1537.7	0	.....	...	65032
1543.7	1d	.....	...	64779
1545.6	1d	1545.9	1	64690

$\lambda$ (I. A.) (Kalia)	Int.	$\lambda$ (I. A.) Turner.	Int.	$\nu$
1547.6	1d	.....	...	64615
1550.5	$\frac{1}{8}$	.....	...	64497
1553.6	$\frac{1}{2}$	.....	...	64365
1565.5	1	.....	...	63877
1567.7	$\frac{1}{2}$	.....	...	63789
1569.8	2	.....	...	63703
1572.2	1	.....	...	63606
1574.6	0	.....	...	63510
1577.7	3	.....	..	63383
1579.0	0d	.....	...	63332
1581.1	3	.....	...	63247
1582.8	2	1582.8	1	63179
1585.8	1	.....	...	63058
1589.3	1	.....	...	62922
1593.8	3	1593.8	6	62742
1596.5	2d	.....	...	62638
1597.9	2d	.....	...	62581
1599.5	2d	.....	...	62522
1608.3	4	.....	...	62176
1613.7	4	.....	...	61971
1617.8	4	1617.9	6	61809
1620.6	1d	.....	...	61707
1623.7	0	.....	...	61587
1626.0	$\frac{1}{2}$	.....	...	61503
1628.4	0	.....	...	61410
1630.9	3	.....	...	61314
1634.1	$\frac{1}{8}$	.....	...	61197
1636.8	0	.....	...	61094
1639.0	$\frac{1}{2}$	1639.2	1	61008
1641.1	4	1641.1	7	60934

# SPARK SPECTRUM OF IODINE

$\lambda$ (I. A.) (Kalia)	Int.	$\lambda$ (I. A.) Turner.	Int.	$\nu$
1642.4	6	1642.5	7	60886
1648.8	1	.....	...	60649
1653.9	3	.....	...	60464
1655.0	2	.....	...	60424
1670.6	1d	.....	...	59859
.....	...	1675.3	1	59690
1678.6	0	.....	...	59573
1682.8	1	.....	...	59424
1690.6	00	.....	...	59150
1695.9	1	.....	...	58966
1702.3	7	1702.3	8	58745
1705.9	00	.....	...	58620
1713.3	2d	.....	...	58367
1726.5	1	.....	...	57920
1730.5	7	.....	...	57787
1747.9	00	.....	...	57212
1752.1	$\frac{1}{2}$	.....	...	57075
1753.4	2	.....	...	57032
1760.6	$\frac{1}{2}$	.....	...	56799
1765.2	1	.....	...	56650
1772.0	1	.....	...	56433
1776.8	$\frac{1}{2}$ d	.....	...	56282
1782.9	9	1782.9	9	56088
1784.3	5	.....	...	56045
1788.5	$\frac{1}{2}$ d	.....	...	55913
.....	...	1789.6	00	55879
1793.7	2d	.....	...	55752
1799.2	7	1799.2	7	55580
1807.3	$\frac{1}{2}$	.....	...	55331
1811.9	1d	.....	...	55189

$\lambda$ (I. A.) (Kalia)	Int.	$\lambda$ (I. A.) Turner.	Int.	$\nu$
1814.4	$\frac{1}{2}$	.....	...	55114
1830.5	9	1830.4	10	54631
1844.5	8	1844.5	9	54216
1850.3	4	.....	...	54046
1863.1	7	.....	...	53675
1868.9	7	.....	...	53507
1872.3	8	.....	...	53410
1873.9	7	.....	...	53364
1876.5	7	1876.4	7	53292
1879.1	1d	.....	...	53218
1882.1	6	.....	...	53134
1894.9	6	.....	...	52872
1896.9	6	.....	...	52719
1905.8	4	.....	...	52471
1911.3	3	.....	..	52. 20
1914.7	7	.....	...	52227
1932.6	4	.....	...	51743
1944.4	2	.....	...	51429
1971.6	7	.....	...	50721
1978.5	5	.....	...	50543
1980.5	3	.....	...	50492
1982.1	$\frac{1}{2}$	.....	...	50451
2023.6	5	.....	...	49416
2034.5	5	.....	...	49152
2038.6	0	.....	...	49054
2041.7	2	.....	...	49979
2049.2	6	.....	...	48799
2053.9	$\frac{1}{2}$	.....	...	48689
2062.1	10	2062.1	10	48493
2068.9	1	.....	...	48336

$\lambda$ (I. A.) (Kalia)	Int.	$\lambda$ (I. A.) Turner.	Int.	$\nu$
2074.9	$\frac{1}{2}$	.....	...	48196
2080.9	2	.....	...	48057
2087.2	1	.....	...	47911
2094.0	$\frac{1}{2}$	.....	...	47755
2097.4	0	.....	...	47677
2109.7	0	.....	...	47400
2122.5	00	.....	...	47114
2150.4	$\frac{1}{2}$	.....	...	46502
2182.6	2	.....	...	45817
2203.5	$\frac{1}{2}$	.....	...	45382
2213.2	0	.....	...	45183
2219.7	0	.....	...	45051
2224.2	2	.....	...	44959
2229.2	5	.....	...	44859
2237.8	0	.....	...	44686
2239.4	00	.....	...	44656
2249.2	3	.....	...	44461
2265.7	3	.....	...	44137
2287.7	0	.....	...	43712
2292.3	3	.....	...	43625
2293.4	2	.....	...	43604
2299.6	00	.....	...	43487
2307.9	$\frac{1}{2}$	.....	...	43330
2319.5	0	.....	...	43114
2331.2	1	.....	...	42896
2335.1	2	.....	...	42825
2341.9	2	.....	...	42700
2344.1	1	.....	...	42661
2345.9	1	.....	...	42628
2376.0	2	.....	...	42087

The lines due to Turner, excepting those marked with an asterisk, are arc lines. The lines measured by the present writer with the exception of those that are common with Turner's arc lines are considered to be spark lines.

The author is very thankful to Dr. P. K. Kichlu for his help and guidance in the course of this work.

# The Relative Intensities of the Raman and the Rayleigh Lines in Light Scattering

By

JAGATTARAN DHAR, M.Sc.

*Research Scholar, Indian Association for the Cultivation  
of Science, Calcutta.*

*(Received for publication January, 1934)*

## ABSTRACT.

The paper gives an account of measurements on the relative intensities of the Rayleigh and the Raman lines in the scattering by some typical liquids, namely,  $C_6H_6$ ,  $CCl_4$ ,  $SiCl_4$ ,  $CHCl_3$  and  $CHBr_3$ .

## 1. Introduction.

Considerable amount of theoretical work has recently been done by Manneback,<sup>1</sup> Placzek,<sup>2</sup> Bhagavantam<sup>3</sup> and others on the relative intensities of the Raman and Rayleigh lines in light scattering. The experimental data, however, on the subject are very meagre, and it is proposed in the present paper to give the results of an experimental investigation on the intensities of the different lines in the light scattering by some liquids.

<sup>1</sup> 'Zeit. f. Phys.', Vol. 62, p. 224 (1930).

<sup>2</sup> 'Zeit. f. Phys.', Vol. 70, p. 84 (1931).

<sup>3</sup> 'Ind. Jour. Phys.', Vol. 6, p. 340 and p. 557 (1931).

## 2. *Experimental.*

The liquids were of Kahlbaum's extra-pure variety, further purified by repeated redistillation in vacuo in the usual double-bulbs. The liquids were contained in a Wood's tube of about 3.5 cms. diameter and 20 cms. length. One end of the tube was fitted with a plane glass window and the other end was bent in the form of a horn in the usual manner in order to offer a dark background for observation. The tube was blackened except for a narrow portion along its length for letting in the incident light, and another rectangular portion in the plane glass window for the purpose of observation. With this arrangement, the stray light was practically eliminated. Light from a quartz mercury lamp was allowed to fall on the Wood's tube from one side, and the scattered radiations coming through the plane window were focussed by means of a sphero-cylindrical lens on the slit of a Hilger E<sub>2</sub> spectrograph so as to give a magnification 1:1. A Hilger neutral-tint wedge of about 7 mms. length, placed in contact with the slit of the spectrograph with its direction of maximum gradient parallel to the length of the slit, served for the measurements of the relative intensities of the various lines appearing in the scattered spectrum.

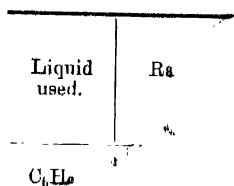
In order to be sure that the scattered light was falling uniformly over the whole area of the wedge, a preliminary short exposure was given without the wedge, and the photographic plate after development was examined. If the lines appearing in the spectrum, were found to be *uniformly* black along their length, the final exposure for the scattered radiations from the liquid, with the wedge inserted in its proper place, was started; otherwise, the optical parts were readjusted so as to secure uniformity of illumination tested in the manner described above.

After careful adjustment, a blue circular patch of light due entirely to the scattered radiations from the liquid, was obtained on the slit of the spectrograph, and it was quite sufficient to



#### 4. Results.

The results obtained are given in .



between the whole length of the wedge covered the window of the Wood. As the scattered radiations were of extent of about three times the length to get Raman lines, the window was covered.

The intensities of the Raman lines were determined by comparing the heights of the lines with those of the Rayleigh lines. The wedge was calibrated for different wave-lengths and then the lines to be compared were photographed through the wedge. The relative intensities would then be determined by (a) the heights of the lines, (b) the wedge constant for particular wave-lengths in question, and (c) the magnification of the spectrograph. Now, if the limiting intensity that is just visible towards the feeble end of the lines be  $I_c$ , and the lengths of the lines  $Y_1$  and  $Y_2$ , then

$$I_c = I_{\lambda_1} 10^{-\frac{K_1 Y_1}{m_1}}$$

$$= I_{\lambda_2} 10^{-\frac{K_2 Y_2}{m_2}}$$

where  $K_1, K_2$  denote the wedge constants per mm., and  $m_1$  and  $m_2$  the magnifications, for wave-lengths  $\lambda_1$  and  $\lambda_2$  respectively. Hence

$$\frac{I_{\lambda_1}}{I_{\lambda_2}} = 10^{-\left[\frac{K_2 Y_2}{m_2} - \frac{K_1 Y_1}{m_1}\right]}$$

\* 'Phil. Trans.', A. Vol. 217, p. 287 (1918).

The heights of the lines were measured with the help of a comparator of large magnification. The magnification of the spectrograph was obtained by using a known length of the slit and measuring the lengths of the lines photographed through it. As all the quantities on the right-hand side are known, the relative intensities can be calculated.

It should be remarked here that the sensitivity of the photographic plate is not the same for all wave-lengths, and hence even for the small spectral region concerned, the sensitivity of the plate for different wave-length has to be determined. At first the spectrum of the liquid was taken, and then below it on the same plate, intensity marks for calibration were recorded with the standard tungsten-filament lamp by varying the width of the slit of the spectrograph already calibrated.

The positions of the Raman lines of the liquid in question were then marked in the continuous spectra, and the region required in each continuous spectrum was microphotometered. From these microphotometric records, blackening-log intensity graphs were drawn for the wave-length of each Raman line and of the exciting line. The ratio of the intensities for two wave-lengths (one referring to the Raman line and the other to the exciting line) was then experimentally found by the method of parallel displacement.<sup>5</sup> From the calibration chart supplied along with the standard lamp, the colour temperature corresponding to the current used was read off. Then with the help of Wien's law of radiation, the ratio of actual intensities for the two wave-lengths under consideration was computed. The latter computed ratio divided by the former experimental one determines, therefore, the relative sensitivities of the plate for these two wave-lengths. The intensity-ratio as observed was then multiplied by this ratio in order to get the result quite independent of the plate-sensitivity.

<sup>5</sup> 'Physik. Zeits.', Vol. 26, p. 764 (1925).

# 4. Results.

The results obtained are given in the following table :—

TABLE I.

Liquid used.	Raman lines $\Delta\nu$ .	$\frac{I_R}{I_T} \times 10^3$ .	Carrelli and Went <sup>6</sup> $\frac{I_R}{I_T} \times 10^3$ .	Dnure <sup>7</sup> $\frac{I_R}{I_T} \times 10^3$ .
<chem>C6H6</chem>	605	3.5	1.28	
	849	1.9	0.93	
	992	9.5	10.9	5
	1176	4.5	2.4	1.5
	1605	3.8	1.8	2.5
	3060		6.6	7
<chem>CCl4</chem>	217	1.9	18	10
	313	3.1	23	13
	459	3.0	16	6.0
	770	1.2	6	7.5
	790			
<chem>SiCl4</chem>	150	1.8		
	221	1.0		
	423	4.1		
<chem>CHCl3</chem>	262	5.4		
	367	4.0		
	667	2.4		
	762	1.7		
<chem>CHBr3</chem>	154	4.2		
	222	6.0		
	538	2.9		
	654	3.2		

$I_R$  indicates the intensity of the Raman lines.

$I_T$  indicates the intensity of the Rayleigh lines.

The 4358 Hg line was used for excitation.

<sup>6</sup> 'Zeit. f. Phys.,' Vol. 76, p. 236 (1932).

'Ann. de phys.,' Vol. 12, p. 375 (1929)-

### 5. *Discussion of Results.*

In the case of benzene and carbon tetrachloride, for which data are available from the earlier work of Carrelli and Daure, it will be seen that our present values agree, at any rate as regards the order of magnitude, with their values.

We shall only remark here that the most intense line in the scattering by  $\text{CCl}_4$  is not the  $459\text{ cm}^{-1}$  line, which corresponds to the inactive symmetrical oscillations of the four chlorine atoms with respect to the central carbon, but the line  $313\text{ cm}^{-1}$ . In the case of  $\text{SiCl}_4$ , however, the most intense line is the inactive line corresponding to  $423\text{ cm}^{-1}$ . The cause of the discrepancy for the former substance, namely  $\text{CCl}_4$ , is not clear. As regards  $\text{CHCl}_3$  and  $\text{CHBr}_3$ , again, there is a reversal of the order of intensities in the case of the first two lines (see Table I).

The author expresses his grateful thanks to Sir C. V. Raman, Kt., and Prof. K. S. Krishnan, D.Sc., for their keen interest in the work.

## Constitution of Water in Solutions of Electrolytes as studied by the Raman Effect

By

C. S. SIVA RAO, M.A.,

*Research Scholar, Andhra University, Waltair.*

*(Received for publication, September 25, 1934.)*

### ABSTRACT

To arrive at a clear conception of the behaviour of water in solutions of electrolytes the results of a more thorough and systematic investigation of the subject than has hitherto been attempted, are described in this paper. The results obtained may be briefly summed up as follows :

(1) The water band obtained in the Raman spectra of solutions of electrolytes is sharper than for pure water.

(2) While with aqueous solutions of nitric acid, sulphuric acid and sodium nitrate the band gets sharper with increasing concentration and shifts as a whole towards greater frequency, the portion of the intensity curve on the smaller frequency side becoming less convex, just the opposite results have been observed with solutions of hydrochloric acid in water.

(3) Whereas there is a progressive shift towards larger frequency in the water band in solutions of electrolytes at the same concentration as we pass from lithium chloride to sodium nitrate and from hydrochloric to sulphuric and nitric acids, these differences tend to vanish when their water content is equalized.

The probable cause of the results observed—hydration of the ions of the dissolved substance or change in the water equilibrium due to variations in the proportions of monohydrate, dihydrate and trihydrate—is discussed in detail and conclusions arrived at.

(4) The cation appears to exert little influence on the behaviour of the solvent, as can be inferred from the similarity of results obtained with acids and salts.

(5) The intensity curves for sodium nitrate are in general much sharper than those for nitric acid, even when the latter is taken at a much higher concentration. This result is explained as partly due to the formation of more complex hydrates and partly due to the superposition of the  $\text{NO}_2\text{OH}$  band at  $3420\text{ cm}^{-1}$  over the band due to water in solutions of nitric acid.

### 1. Introduction.

For a proper understanding of the nature of solution it is necessary to have a clear conception of the behaviour as much of the solvent as of the solute, when one is in combination with the other. And, water being the most important and universal solvent, a detailed study of its nature and constitution in solutions of different characteristic groups of substances, *e.g.*, strong electrolytes, weak electrolytes and non-electrolytes, will lead us a long way in arriving at some clear and definite ideas regarding the nature of solution and the characteristic function that the solvent plays therein. It is therefore proposed to deal in this communication with the author's investigations on the subject with reference to the first characteristic group, *viz.*, the strong electrolytes.

There are several methods of attack of the problem. In general, any physical property of the system, *e.g.*, specific gravity, electrical conductivity, absorption spectrum, g-point determination of the binary system, solubility at different concentrations, will provide with information on the subject, and these were the methods employed by the workers in the field. But in recent years the Raman effect has been applied with advantage to the investigation of the nature of solution on account of the simpler and at the same time more definite information that is provided by a study of the Raman spectra of solutions. In fact, on account of the very simple relations that exist between the intensity of the Raman lines or bands and the numbers of molecules or ions that give rise to them, the possibility of arriving by this method at very

clear ideas on electrolytic dissociation, particularly in concentrated solutions has been demonstrated by Ramakrishna Rao and others ; <sup>1</sup> and now the author has applied the method to study the other aspect of the problem, namely, that concerning the behaviour of the solvent in solution.

## 2. *Earlier Work on the Raman Spectra of Solutions.*

Whereas, on the one hand, it is definitely established that electrolytes dissociate into their constituent ions in their aqueous solutions, there is, on the other hand, evidence to show that an entirely different process takes place with respect to the solvent. The water molecules generally combine with the dissociated ions of the solute to form, what are called, hydrates. Mendeleeff<sup>2</sup> was the first to give definite ideas as regards the formation of hydrates in solution. By plotting specific gravities of solutions of sulphuric acid and calcium chloride in water against their respective concentrations he found that the curves exhibited a number of maxima, which he interpreted as being due to the formation of hydrates.

Jones and his collaborators<sup>3</sup> arrived at similar conclusions from their work on the freezing-point measurements with mixtures of acetic acid and sulphuric acid, acetic acid and water, and of acetic acid, water and sulphuric acid. They found that the total lowering of the freezing point of the mixture was less than the sum of the lowerings due to the individual constituents.

<sup>1</sup> I. Ramakrishna Rao : (i) Proc. Roy. Acad., Amsterdam, Vol. 33, No. 6, p. 632 (1930).

" " (ii) Roy. Soc. Proc. A, Vol. 127, p. 279 (1930).

" " (iii) Indian Journ. Phys., Vol. 8, p. 123 (1933).

" " (iv) Roy. Soc. Proc. A, Vol. 144, p. 159, (1934).

L. A. Woodward : (i) Physikal. Zeits., Vol. 32, p. 212, (1931).

" " " Vol. 32, p. 777 (1931).

L. A. Woodward and R. G. Horrer (iii) Roy. Soc. Proc. A, Vol. 144, p. 120

(1934).

L. Simmons : Soc. Scient. Fenn., Comm. Phys.—Math. VII. 9. (1933).

<sup>2</sup> Ber. d. Chem. Gesell., Vol. 1, p. 379 (1886).

<sup>3</sup> Publication 210 of the Carnegie Institution of Washington (1915).

This was a phenomenon just opposite to that observed with electrolytes and must therefore be ascribed to an association of the molecules of the solvent with the ions of the solute thus reducing the number of independent molecules which lower the freezing-point.

Later, during the course of their work on water and solutions by a study of their Raman spectra, it was found by the earlier workers that water, unlike other substances which give more or less sharp lines, gives rise to a broad and diffuse band extending over  $750\text{ cm}^{-1}$  from about  $3000\text{ cm}^{-1}$  to  $3750\text{ cm}^{-1}$ , corresponding to the infra-red absorption at  $2.97\text{ }\mu$  and resolvable by an analysis of its intensity curves into three individual components with maxima of intensities at  $3610\text{ cm}^{-1}$  ( $2.77\text{ }\mu$ ),  $3413\text{ cm}^{-1}$  ( $2.93\text{ }\mu$ ), and  $3195\text{ cm}^{-1}$  ( $3.13\text{ }\mu$ ).<sup>4</sup> Notable changes are noticed<sup>5</sup> in the distribution of intensity in the band with change of temperature and with addition of electrolytes to water. Ramakrishna Rao<sup>6</sup> found that the changes observed in the intensity and relative position of the maxima in the band with change of temperature could be best explained on the hypothesis of the presence in water of three types of molecules corresponding to  $\text{H}_2\text{O}$ ,  $(\text{H}_2\text{O})_2$  and  $(\text{H}_2\text{O})_3$ , the relative proportions of which alter with change of temperature. He found that an increase of temperature results in the shift of the maximum of the band to the greater frequency side and is due to a diminution in the proportion of the triple molecules corresponding to the maximum at  $3195\text{ cm}^{-1}$  and a proportionate increase in the number of the single molecules corresponding to the maximum at  $3610\text{ cm}^{-1}$ . He also noted that the addition of the electrolyte, nitric acid, causes a shift in the position of the intensity maximum of the band towards the larger frequency side similar to the effect of a rise of temperature and interprets it as being due to a change in the proportion of the three types of molecules. He attributes the development of

<sup>4</sup> I. Ramakrishna Rao : Roy. Soc. Proc. A, Vol. 145, p. 489 (1934).

<sup>5</sup> " Roy. Soc. Proc. A, Vol. 130, 489 (1931).

<sup>6</sup> *loc. cit.*



a second maximum in solutions of nitric acid in water at concentrations higher than 76% to the formation of hydrates. A similar observation was recorded by Meyer<sup>7</sup> about the appearance of a second maximum on the short wave-length side in solutions of nitric acid at high concentrations, its intensity exceeding that of the original peak at 14 mols per litre.

Ganesan and Venkateswaran<sup>8</sup> studied the Raman Spectrum of concentrated nitric acid in which they obtained two bands resolved from one another in the position of the usual broad and diffuse band observed with pure water.

Gerlach<sup>9</sup> worked with water and solutions of dissolved salts and found that water gives rise to a double band ranging over  $35 \pm 5 \text{ \AA}$  and that addition of nitrates shifts the short wave band to the violet, while the chlorides tend to blot it out.

Pringsheim and Schlivitch<sup>10</sup> on the one hand, and Brunetti and Ollano<sup>11</sup> on the other, disagree with the observations of the earlier workers as regards the changes in the intensity of the water band with addition of salts. The former, in their work on water and lithium chloride solution, observe that the relative changes in intensity of the water band with change of temperature and with addition of salts noticed by others are spurious. But it has been demonstrated by the recent work of Ramakrishna Rao that the changes observed in the intensity distribution of the water band with rise of temperature are really genuine and are due to changes in the relative proportions of the single  $(\text{H}_2\text{O})_1$  double  $(\text{H}_2\text{O})_2$  and triple  $(\text{H}_2\text{O})_3$  molecules which are supposed to exist in water.

Hatley and Callihan<sup>12</sup> worked with solutions of KCl, NaOH and KOH in water at various concentrations and observed that

<sup>7</sup> Phys. Zeit., Vol. 31, p. 690. (1930).

<sup>8</sup> Ind. Jour. Phys., Vol. 4, p. 236 (1929).

<sup>9</sup> Phys. Zeits., Vol. 31, p. 695 (1930).

<sup>10</sup> Zs. für Phys., Vol. 60, 9-10, p. 581 (1930).

<sup>11</sup> Accad. Lincei, Atti., Vol. 12, p. 522 (1930).

<sup>12</sup> Phys. Rev., Vol. 38, p. 909 (1931).

in all cases the energy appears to shift towards the long wavelength side and that the top of the curve gets sharper with increasing concentration.

Rafalowski<sup>13</sup> working with solutions of hydrochloric acid and nitric acid in water at various concentrations reported that the water band became less sharp with increasing concentration in the case of hydrochloric acid while with nitric acid it became sharper.

Hulubei<sup>14</sup> claimed to have obtained, besides the double band at  $3233\text{--}3443\text{ cm}^{-1}$ , ten other bands with wave-number shifts lying between  $6747\text{--}10944\text{ cm}^{-1}$  from the original exciting line. These were found to disappear with addition of salts, which he interpreted as being connected with association in water.

Silveira<sup>15</sup> obtained the Raman spectra of solutions of  $\text{MgCl}_2$ ,  $\text{Mg}(\text{ClO}_3)_2$ ,  $\text{Mg}(\text{NO}_3)_2$ , which gave lines with small frequency shifts,  $1655$  and  $376\text{ cm}^{-1}$ , the former being attributed to the Mg ion complex with water and the latter to  $\text{ClO}_3$  and  $\text{NO}_3$  ion complexes with water. In two later communications<sup>16</sup> his observations with other solutions revealed a large number of lines with small frequency shifts.

Embirikos<sup>17</sup>, in continuation of the work of Gerlach referred to above, worked with a number of univalent and divalent chlorides and nitrates and his results, are in agreement with those of Gerlach. Nitrates are, however, noticed to give rise to a second band, the distance between the two components increasing with concentration. The nature of the cation is found to exert no influence on the structure of the Raman band of water. The second band with ammonium nitrate solution, which he wrongly attributed to water, is really due to the  $\text{NH}_4^+$  group, as has been shown in a previous communication.<sup>18</sup>

<sup>13</sup> Acad. Polonaise Sci. et Lettres, Bull. 7-10 A, p. 623 (1931).

<sup>14</sup> Comptes Rendus, Vol. 194, p. 1474 (1932).

<sup>15</sup> Comptes Rendus, Vol. 194, p. 1336 (1932).

<sup>16</sup> Comptes Rendus, Vol. 195, p. 416 and p. 521 (1932).

<sup>17</sup> Phys. Zeits., vol. 33, p. 946 (1932).

<sup>18</sup> Zs. für Physik., Vol. 88, p. 127 (1934).

Cabannes and Riols<sup>10</sup> found that the water band was triple and that the addition of sodium nitrate causes shifts in the intensity of the band to higher frequencies and the disappearance of the component at  $3625\text{ cm}^{-1}$  due to the  $\text{H}_2\text{O}$  molecules.

In spite of all this varied amount of work with reference to the behaviour of water in solutions of electrolytes, especially by a shift of its Raman band, there has been so far no attempt at a thorough and systematic investigation of the nature of the changes noticeable in the structure of the water band and to give a satisfactory interpretation thereof.

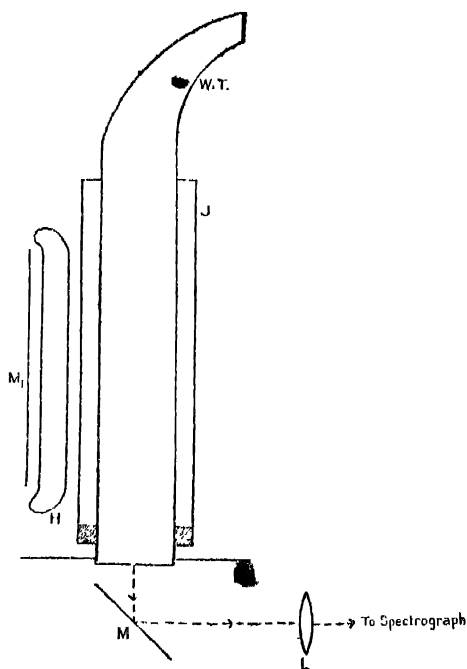
The present work is, therefore, undertaken with the idea of systematically studying the behaviour and constitution of water in solutions of some of the typical electrolytes, both acids and salts, under conditions easily comparable, and to arrive at a satisfactory understanding of the cause of the variations observed in the structure of the Raman band of water—namely, whether the effect is due to the hydration of the ions of the solute by combination with the molecules of the solvent, water, or whether the effect is similar to that observed with change in temperature, *viz.*, a mere change in the proportions of different types of molecules supposed to exist in water.

### 3. *Experimental Procedure.*

(a) *Experimental arrangement* : The experimental arrangement employed in these investigations is represented in Fig 1. It consists of the vertical Wood's tube W. T. containing the liquid to be studied, close to which is placed the illuminating mercury lamp H, and the light scattered by the liquid along W. T. through the plane quartz window at the bottom of the tube is reflected on to the slit of the spectrograph through the condensing lens L by means of a plane mirror M held at an inclination of  $45^\circ$  to the vertical. The light from the mercury lamp is concentrated on the Wood's tube containing the liquid by means of an

<sup>10</sup> Comptes Rendus, Vol. 198, p. 90 (1934).

FIG. 1.



elliptical mirror  $M_1$  made out of a polished sheet of aluminium and held on the side away from the tube. All extraneous light from the lamp is cut off by suitable screens. Further, the light from the lamp is filtered through a solution of cobalt chloride, which transmits the  $3650\lambda$  group and the  $4047\lambda$  line of the mercury arc, but effectively cuts off the  $4358\lambda$  group and the  $4916\lambda$  line and its accompanying group of faint lines, so that the water bands excited by the former two have been obtained, that due to the  $3650\lambda$  group being usually the stronger. The filtering solution is contained in the interspace between the Wood's tube and a wider pyrex glass jacket,  $J$ , concentric with it and held in position by rubber bands which close the tube water-tight at the bottom. On account of the small depth of the filtering liquid it has to be made somewhat concentrated. Although this arrangement requires rather long exposures, it permits of an easy removal and replacement of the observation tube ( $W. T.$ ) without disturbing any other arrangement, another advantage

is that a small quantity of filter will suffice and it can be re-filled when necessary from the top during the course of an exposure without disturbing either the tube or the lamp. During the course of exposure the lamp and the tube are cooled by means of a table fan.

Another arrangement, due to Wood,<sup>20</sup> has also been employed in some cases. In this, a cylindrical pyrex glass condenser containing the filtering solution is placed right above the horizontal Wood's tube with the liquid under investigation. In cases where no filter is necessary it is filled with water and placed in position, and a Hewittic mercury lamp of the horizontal type is situated above the cylindrical condenser as close to it as possible. Two elliptical mirrors, one of them placed above the mercury lamp and the other placed below Wood's tube, serve to reflect back the light from the arc on the condenser and the Wood's tube respectively, so that maximum use is made of the light from the arc. This arrangement has been found to be very efficient in practice and permits of comparatively short exposures.

(b) *Continuous spectrum and colour filters*: As it is the Raman band due to *water* that is the subject of study in these investigations, there is no difficulty as regards its proper assignment to its corresponding exciting line. Thus there is no necessity for using light filters for obtaining perfectly monochromatic light. But a constant source of trouble encountered during the work on the Raman spectra of solutions is the presence in the scattered light of a large amount of continuous spectrum, which gets superposed on the water band, thus rendering difficult any accurate investigation of the distribution of intensity along the band.

This continuous spectrum may be attributed to many causes. Firstly, it is due to the presence of a feeble continuous spectrum in the light from the mercury arc itself, its intensity increasing

<sup>20</sup> Phys. Rev., Vol. 37, p. 1022 (1931).

with increasing temperature of the arc. Thus it can be reduced to a minimum by running the arc at a low temperature and hence at a low intensity and cooling it, at the same time, by means of a table fan. This, of course, necessarily involves long exposures. A second source of this continuous spectrum is the presence of fluorescent impurities in the substance under investigation. This is eliminated by employing throughout Merck's or Kahlbaum's extra pure chemicals manufactured for analytical purposes and using pure grease-free distilled water for dissolving the chemicals. In some cases, exposure of the substance under study to ultraviolet radiation from the lamp produces photochemical reactions which result in the formation of foreign substances, which may produce a continuous spectrum; but most of the substances studied in the present investigations do not undergo photochemical decomposition, and so one cause of the trouble does not arise. Yet another cause of this continuous spectrum, which seriously handicaps the work on solutions, is that in the case of a freshly prepared solution the fluctuations in its density and concentration are considerable and since the Rayleigh scattering is dependent on these fluctuations, a freshly prepared solution scatters the continuous spectrum present in the light from the mercury arc much more than does a solution kept for a sufficiently long time, so as to allow it to become perfectly homogeneous and its fluctuations to appreciably vanish. Hence, in all these experiments the solutions are allowed to lie over for some time before their Raman spectra are taken to ensure a perfectly homogeneous distribution of the molecules of the dissolved substances in the solution.

Notwithstanding all these precautions, a faint continuous spectrum still persists in most of the solutions. When it is appreciable, it becomes necessary to suppress it by the use of suitable filters. Generally it extends from  $4000\text{\AA}^\circ$  to  $5500\text{\AA}^\circ$ , and its maximum lies between  $4500\text{\AA}^\circ$  and  $5000\text{\AA}^\circ$ , a region where the water band excited by the  $4047$ , line is

situated. The best filter to eliminate this continuous background is a solution of iodine in carbon tetrachloride, but, on account of its volatility, a solution of cobalt chloride is generally employed in these investigations as it is found to be nearly as good and to be extremely stable towards the ultraviolet radiation from the arc.

There is one advantage in the work on the Raman band of water owing to the fact that it has a very large frequency shift and as such the Raman lines due to the anions present in solution and excited by the same mercury line do not generally get superposed on the band, as they usually have small frequency shifts. But, in some cases, the Raman lines due to the anion, like the  $\text{NO}_3^-$  and  $\text{SO}_4^{2-}$  ions, excited by strong mercury are lines other than the line used to excite the band get superposed on the water band and so it becomes imperative in such cases to eliminate such superposition by effectively cutting off such lines by means of suitable filters.

(c) *Choice of substances and exciting lines* : All the previous work on the Raman band of water in solutions was qualitative, no systematic study being made of its changes with special reference either to the amount of solute or solvent contained in the solution. In an investigation of the changes in the structure of the water band under the influence of dissolved substances it is always desirable to take the different substances under the same molar concentration, so that the number of molecules of the solute in a definite volume of the solution remains the same in all cases. Then it is easier to interpret the mutual influence of the solute and the solvent in terms of the number of molecules and the results for different substances become readily comparable with one another. Further the second aspect of the problem, wherein a certain volume of the solution in each case contains the same water content, thereby making the same number of molecules of the solvent influence the solute in the different solutions, is also equally interesting and provides additional valuable

information on the subject. Both aspects of the problem, outlined above, have been investigated by the author and the results given below.

Again, for observations on the influence of ions on the structure of the Raman water-band, it is necessary to work at as high a concentration as possible, *c.g.* of the order of about 12N, and comparatively few electrolytes dissolve to such a large extent. Further, the appearance of a large amount of continuous spectrum at high concentrations in some cases renders the work with them rather difficult and uncertain, as has been found, for example, in the case of zinc chloride solution at 12N concentration. As pointed out before, this is much more so for the band excited by the  $4047\text{ \AA}$  line of the mercury arc inasmuch as the maximum of the continuous background falls in the same region of the spectrum in which the band due to this line is formed. Also, most of the electrolytes absorb the ultraviolet thus restricting the work to only a few exciting lines in the visible region or in the near ultraviolet.

Again, a difficulty in using the  $4358\text{ \AA}$  line as the exciting line is that the band excited by this falls in a region in which most photographic plates are not sufficiently sensitive. Hence the only band which can be studied in most cases is that excited by the  $3650\text{-}63\text{ \AA}$  group of lines, and this also happens to be more intense than that excited by the  $4047\text{ \AA}$  line. Also the dispersion of the Fuess's spectrograph which is about  $16\text{ A}^\circ$  per m.m. in this region, is larger in the region of this band thus enabling greater accuracy to be attained in the estimation of frequencies. But there is one drawback with regard to the use of this band: whereas the band excited by the  $4047\text{ \AA}$  line is due to a single exciting line, that excited by the  $3650\text{-}63\text{ \AA}$  group is due to a group of three lines, situated close together although of unequal intensity, so that in the latter case there is to some extent a partial superposition of the bands excited by the individual lines of the group. But from a comparative



study of the intensity curves of the water band excited by the  $4047\text{ \AA}$  line as well as by the  $3650\text{--}63\text{ \AA}$  group in a number of cases, it has been found that the curves agree with one another to a close approximation if the value for the frequency of the exciting line in the case of the  $3650\text{--}63\text{ \AA}$  group is taken to be  $27340\text{ cm}^{-1}$ , a value very nearly the mean for the group. Although the band due to the  $4047\text{ \AA}$  line is to be preferred on account of its inherent purity, originating as it does in a single exciting line, it had to be given up for the reasons mentioned above and the band excited by the  $3650\text{--}63\text{ \AA}$  group has been studied almost throughout these investigations.

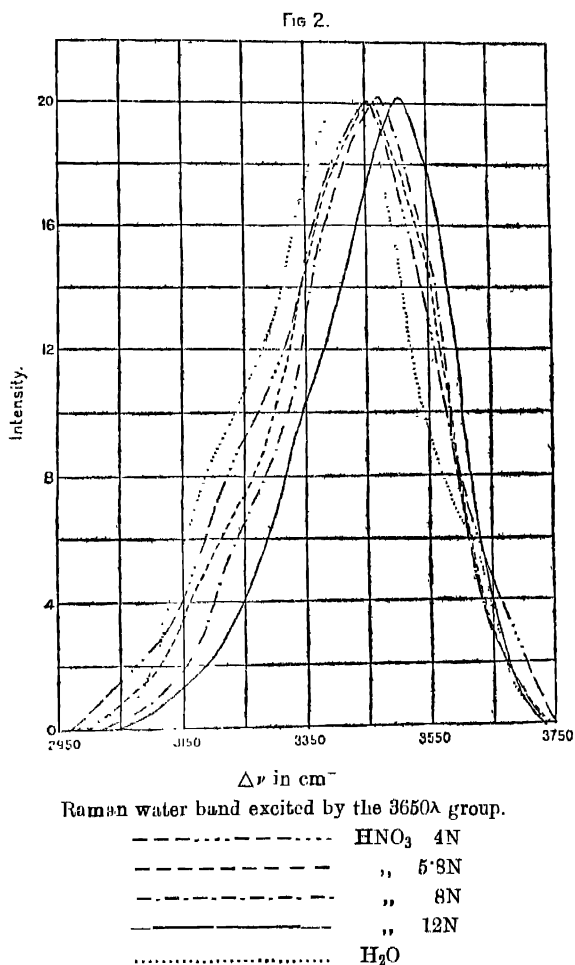
To make a study of the variations that take place in the structure of the water band with addition of other substances it is necessary to examine its intensity curves rather than the band itself, as the latter by itself cannot furnish much useful information. Therefore, the microphotometric curves of the band in each case are taken and by taking on each plate comparison exposures with a calibrated Zeiss step-filter and a straight filament lamp fed under constant voltage, the density-log intensity curve is drawn for each plate in the particular position of the spectrum in which the band is formed, and from this the intensity curve for each band is calculated, density at different points along the band being given by its microphotometric curve. One difficulty experienced in obtaining fairly smooth microphotometric curves of the water band is that on account of the large grain of the plates used owing to their high speed—Ilford golden iso-zenith plates, H and D 1400, being invariably used throughout—the outline of the curve is always very coarse, and this necessarily involves large errors in estimating the actual shape of the curve. The curves were found to improve (1) by making the slit of the thermopile of an optimum width, neither too large nor too narrow, (2) by using a comparatively short deflection between the zero line taken with no light falling on the slit of the thermopile and the blank

plate line taken with the light passing through the unexposed portion of the plate, and (3) finally by adjusting the spectrum slightly out of focus.

Although it is very necessary that the spectrum should be adjusted in perfect focus for the measurement of intensities of spectral lines, its adjustment a little out of focus in the present case, where it is a band and not a line that is studied, does not affect the results very much. This is more so, as it is only the relative distribution of the intensities along the band in the several cases that we are concerned with, and not the absolute values. Further to make the results obtained more reliable, all the plates with the different spectra are developed and fixed under identical conditions, as far as practicable, by using the same strength of the developer and always developing for the same interval of time at the same mean temperature, *viz.*, 18°C. Also, the plate is developed sufficiently along (4.5 minutes) to properly bring out the continuous back-ground of the spectrum without any appreciable fogging of the plate. The intensity values are always corrected for this continuous background.

#### 4. Results.

To begin with, the results for each electrolyte are given. Fig. 2 represents the intensity curves for the water band excited by the 3650-63 $\mu$  group in the Raman spectra of solutions of nitric acid at four different concentrations, *viz.*, 4.04N, 5.86N, 8N and 12N. The curve for pure water is also given for comparison. The intensity at each point in the band is marked against the corresponding frequency shift. The band being very diffuse, it is not possible to measure wave-lengths by means of a micrometer. Hence to determine the Raman frequencies corresponding to every point in the band, the dispersion curve for the region of the spectrum between 4017  $\mu$  and 4358  $\mu$  mercury lines



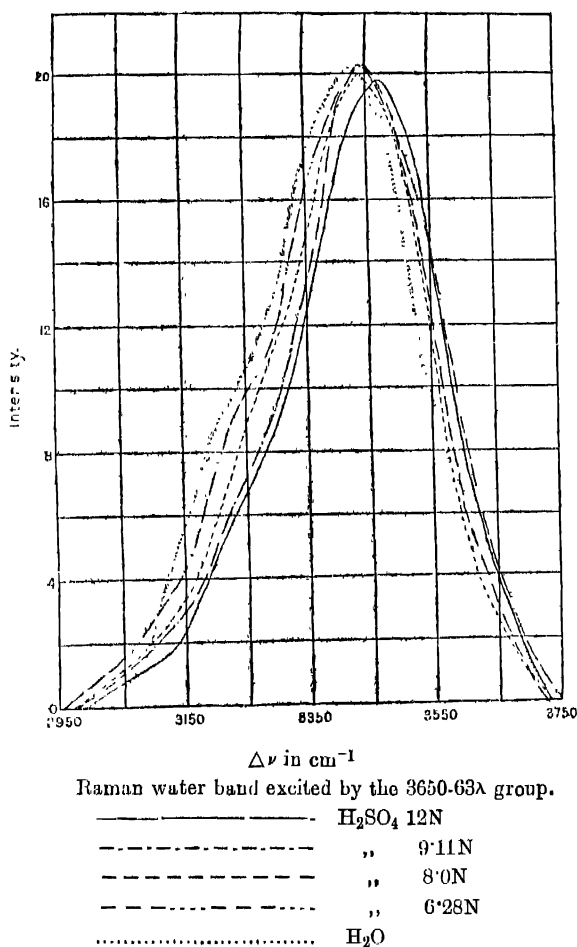
is drawn. The distance of each point on the microphotometric curve of the band from the  $4078\text{\AA}$  line is measured and the corresponding wave-length at this point is determined from the above dispersion curve. From an examination of the intensity curves the following results are clear :—

(i) The water band in nitric acid solutions is invariably sharper than for pure water.

From fig. 2 it follows that with increasing concentration of the acid,

(ii) the band becomes sharper;

FIG. 3.

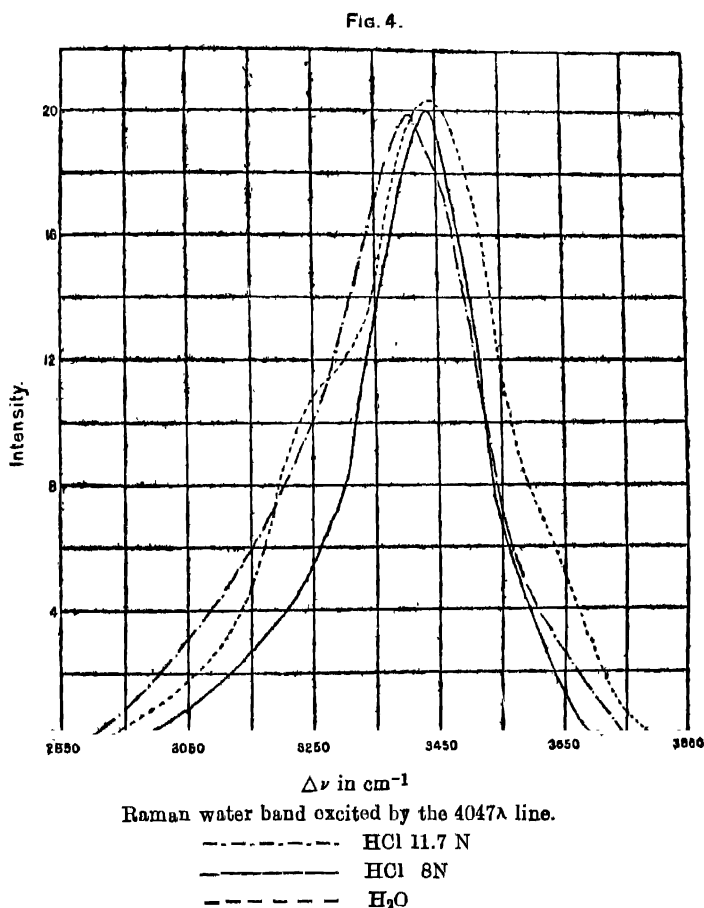


(iii) there is a progressive shift in the maximum of the band as well as in the position of the band as whole towards larger frequency ;

(iv) the curves become less and less convex on the side of smaller frequency.

In fig. 3 are given the intensity curves for the water band in solutions of sulphuric acid at four different concentrations, *viz.*, 6.28N, 8N, 9.11N and 12N. Results very similar to those observed in the case of nitric acid are found with increasing concentration of sulphuric acid also.

The intensity curves for hydrochloric acid at two different concentrations, 8N and 11.7N, are represented in fig. 4 along with that for water. While the band in solutions of hydrochloric

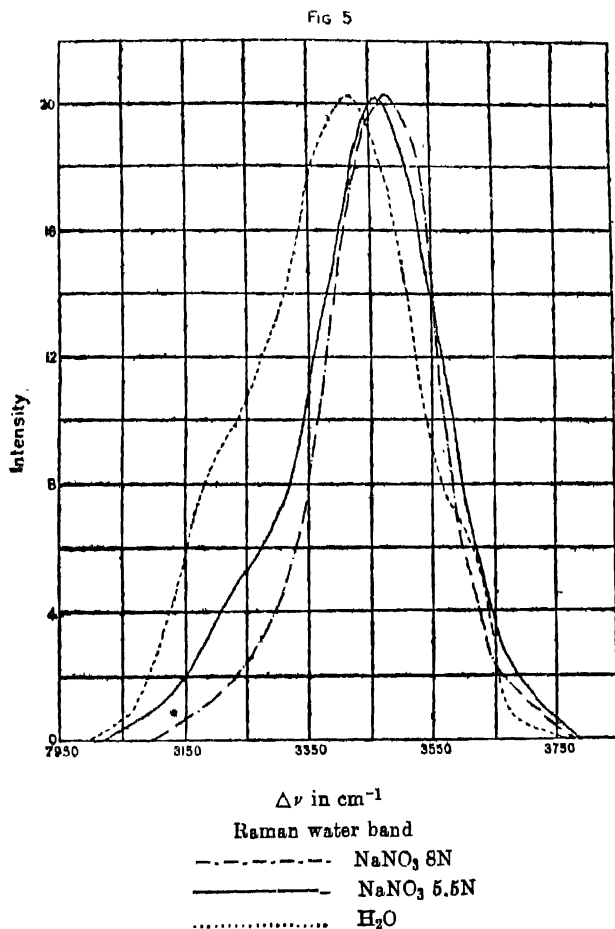


acid in water is sharper than for the pure solvent, the positions of the maxima almost coinciding, as contrasted with nitric and sulphuric acids, the results obtained with water solutions of hydrochloric acid with increasing concentration of the acid content are as follows :

(i) the band gets broader ;

(ii) there is a relative shift in the maximum of the band as well as in the position of the band as a whole towards the smaller frequency side.

Fig. 5 represents the intensity curves for the water band in solutions of sodium nitrate at two different concentrations, 5.5N and 8N, together with the curve for pure water. While the curves for sodium nitrate are shifted to the side of greater frequency shift relative to that for water, in this case again the



same results are obtained with regard to the relative shift and shape and positions of the bands as are observed in the case of nitric and sulphuric acids under different concentrations.

Table I contains the positions of the maximum of the band at different concentrations of all the above electrolytes.

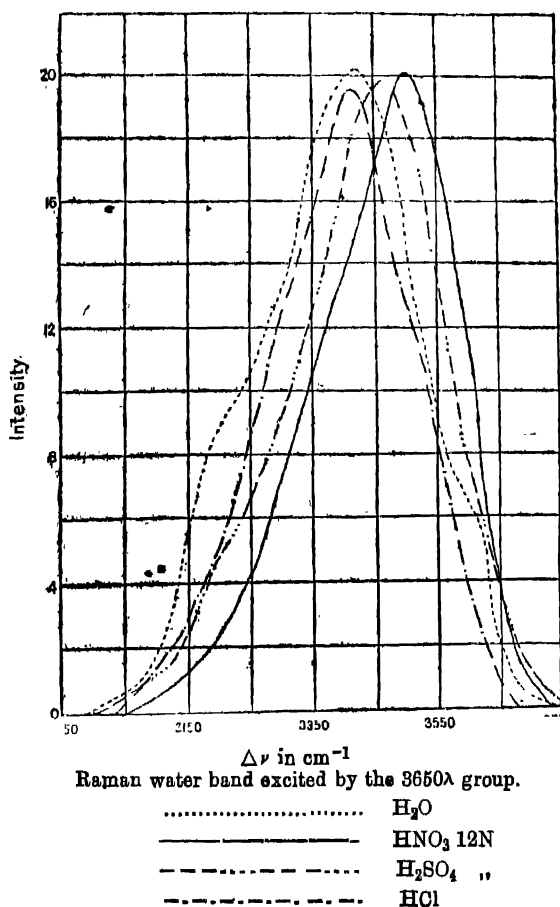
TABLE I

Substance.	Concentration.	Position of the maximum.
1. $\text{H}_2\text{O}$	—	3424 $\text{cm}^{-1}$
2. $\text{HNO}_3$	4.04N	3450 „
„	5.86N	3460 „
„	8.0 N	3474 „
„	12.0 N	3504 „
3. $\text{H}_2\text{SO}_4$	6.28N	3433 „
„	8.0 N	3436 „
„	9.11N	3440 „
„	12.0 N	3468 „
4. $\text{HCl}$	8.0 N	3435 „ (4047 $\lambda$ excit)
„	11.7 N	3415 „
5. $\text{NaNO}_3$	5.5 N	3463 „
„	8.0 N	3480 „

Thus, while with increasing concentration of the electrolyte in water in the case of nitric acid, sulphuric acid and sodium nitrate there is a sharpening of the band and a progressive shift to the larger frequency side, just the contrary results of a broadening of the band with a relative shift to the smaller frequency side have been obtained with increasing concentration in the case of hydrochloric acid. Again, the appearance of convexity, though slight, observed in the shape of the intensity curves at higher dilutions in the case of sulphuric acid, nitric acid and sodium nitrate does not seem to be present in the case of hydrochloric acid. On the contrary, it even appears that there is a slightly greater concavity on the smaller frequency side at the smaller concentration in the case of hydrochloric acid.

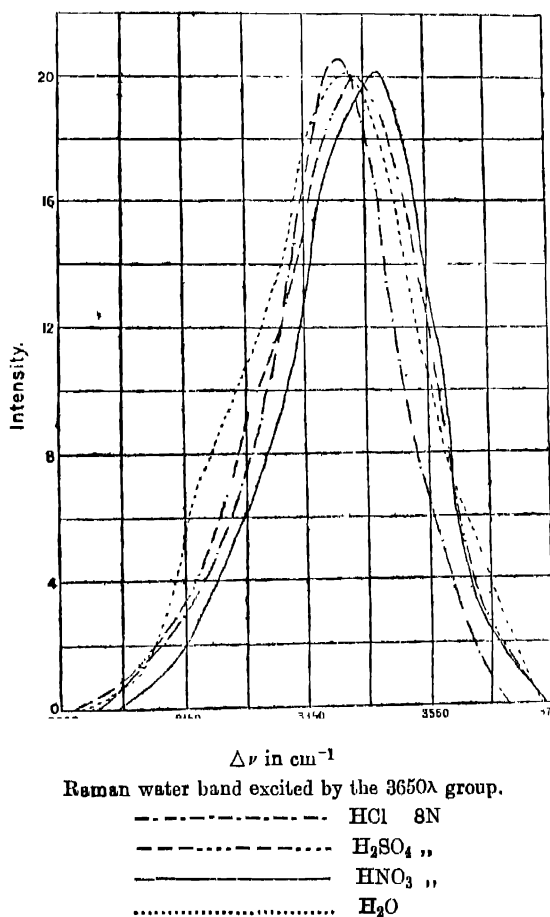
Thus far a study has been made of the changes in the structure of the water band at different concentrations only of each electrolyte separately. To determine if there is any relationship between the bands obtained with the same concentration of different electrolytes, their Raman spectra are taken as far as possible under identical conditions of illumination from the mercury lamp, etc. The work is undertaken to examine the nature of the dependence of the constitution of water on the electrolyte dissolved in it.

Fig. 6 gives the intensity curves for the three acids, nitric, sulphuric and hydrochloric, at the same concentration, *viz.*, 12N, and for pure water. One very striking feature that is at once





noticeable in the curves is the relative shift in the positions of the maxima to the larger frequency side as we pass from hydro-



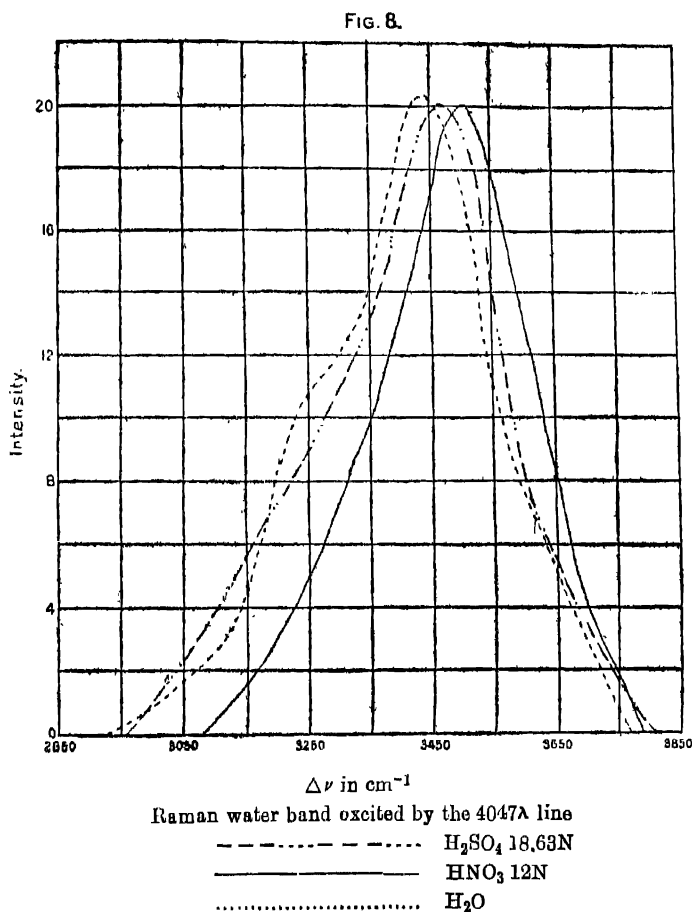
chloric acid to sulphuric and nitric acids, the shift in the case of nitric acid being the greatest. The same relative shift in the band as a whole is also very conspicuous from the intensity curves, the shift of the band gradually increasing from hydrochloric to sulphuric and nitric acids, being a maximum for the last.

Fig. 7 gives the intensity curves for the same three acids at another concentration, viz., 8N. The same results noticed above with 12N concentration of the acids are observed in the

present case also, although to a less conspicuous degree. Also, at the smaller concentration the bands are in general less sharp (except in the case of hydrochloric acid where the opposite result has been observed) than at the higher concentration, a result one might naturally expect by reason of the increased proportion of water.

Having investigated the water band for different electrolytes at the same concentration and each of them under different concentrations, further work was found necessary in order to arrive at a more satisfactory conclusion as to the observed effect of the dissolved substances on the constitution of water, namely, whether it is due to an association of the molecules of water with the ions of the dissolved electrolyte in the form of water of hydration, or whether it is simply due to a change in the water equilibrium due to a change in the proportion of the single, double and triple molecules, an effect similar to that observed with change of temperature. If the cause of the observed results is mainly the second, then it is to be expected, when the amount of water content in the different electrolytes is equalized, that there would be a close similarity in the intensity curves of the water band in the different substances. This will also lead us to infer that the nature of the electrolyte has little to do with the observed phenomenon. Therefore, the above acids were next studied with the same water content, the same number of molecules of the solvent being influenced by those of the solute in each case.

Fig. 8 represents the intensity curves for pure water, sulphuric acid at 18.63 N concentration, and nitric acid at 12 N concentration, the last two containing the same water content. Hydrochloric acid could not be studied with this water content, as the highest concentration of the acid available, about 12 N, contains more water than nitric acid of 12 N concentration. The above curves are for the Raman water band excited by the 4047 $\lambda$  line, as, on account of the very high concentration of sulphuric acid necessary in this case, some of the Raman lines due

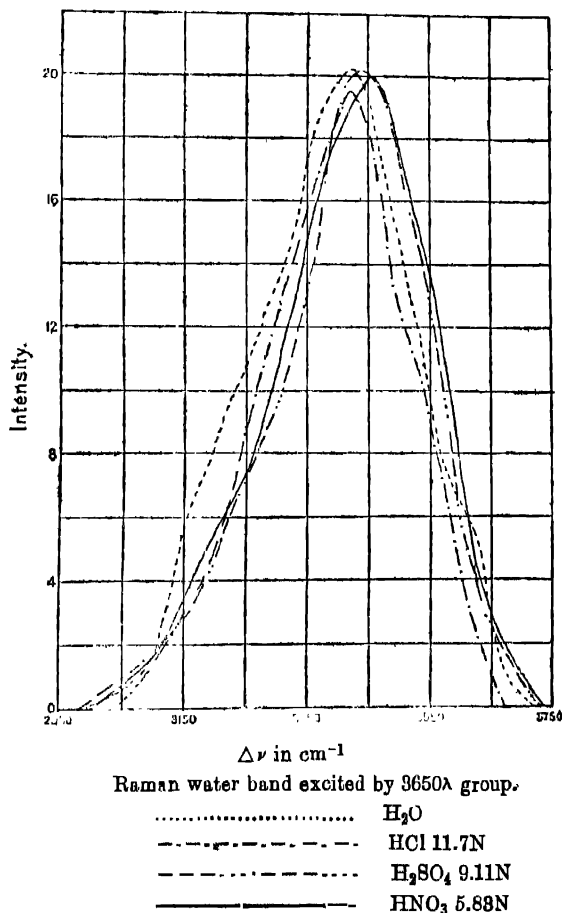


to the  $\text{SO}_4$  ion and excited by the 4047  $\lambda$  line got superposed over the band excited by the 3650-63 $\lambda$  group and so this band could not be used. The shift between the curves for  $\text{H}_2\text{SO}_4$  and  $\text{HNO}_3$  noticed before at the same concentration still remains considerable and the increased similarity between the curves observed with the same water content at smaller concentrations is not so obvious in the present case.

In fig. 9 are given the intensity curves for pure water, and for nitric, sulphuric and hydrochloric acids, all of them with the same water content as 12 N concentration of hydrochloric acid. When the proportion of water content is equalised in the three

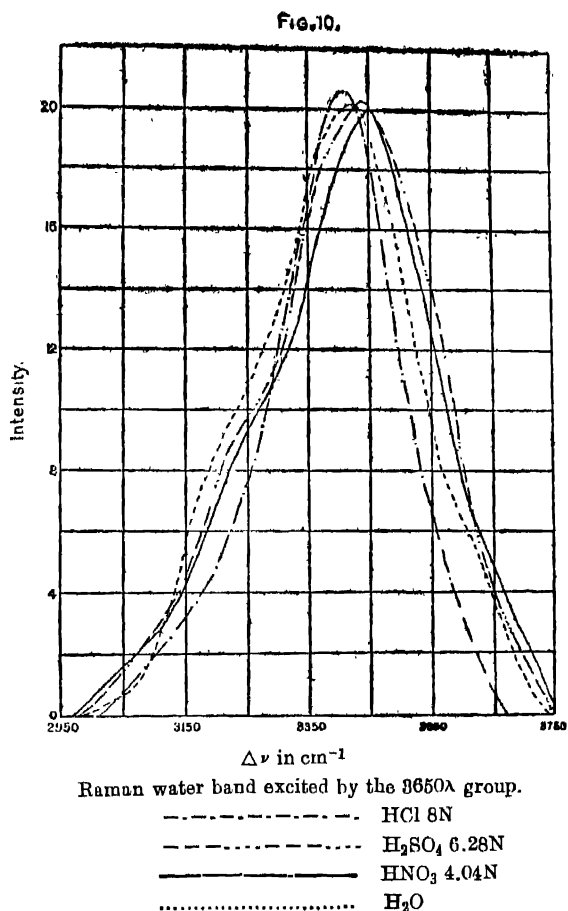
acids a remarkable change is noticed in the relative positions of their intensity curves. The relative shifts between the curves tend to vanish, the curves get closer to each other and they become more and more similar, except for some minor differences which still persist.

FIG. 9.



The same result is also noticed from the intensity curves given in fig. 10 for the same three acids and pure water, the former being taken with the same water content as 8 N solution of hydrochloric acid.

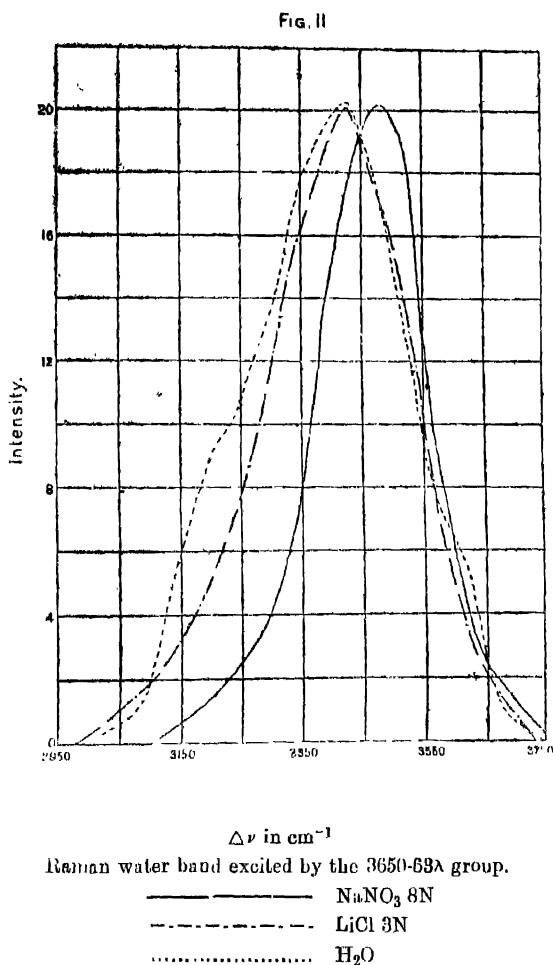
Thus, while the three acids, when studied at the same concentration, exhibit marked differences in the shape and position



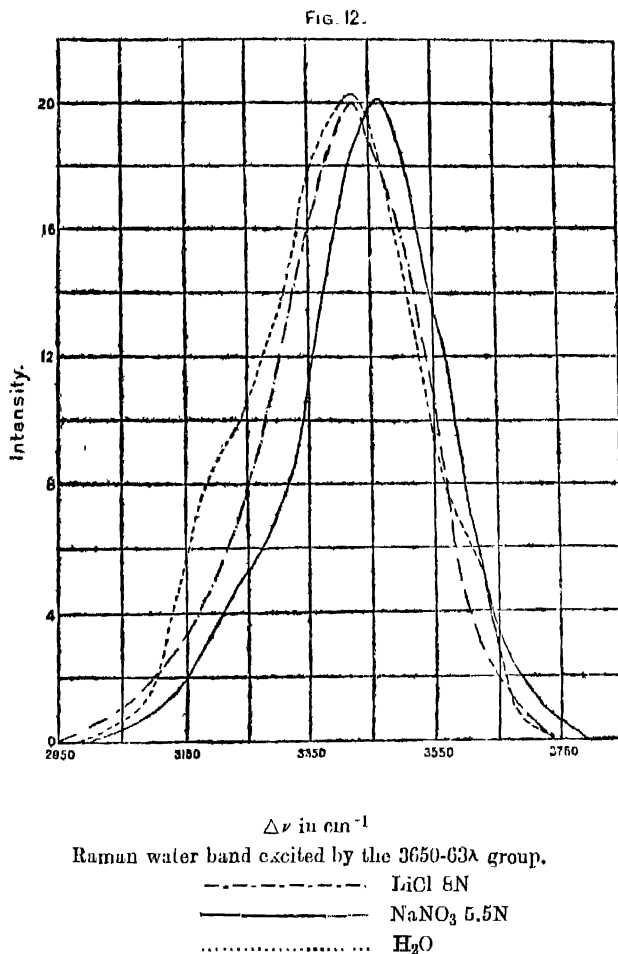
of the water band in their solutions, when studied with the same water content these differences tend to disappear and the intensity curves and hence the bands themselves become increasingly similar.

Fig. 11 gives the intensity curves for pure water and the two salts, sodium nitrate and lithium chloride, both of them being of the same concentration, *viz.*, 8N. Not many salts dissolve even to such high concentrations as 8N and above, and of the few that do so, ammonium salts had to be rejected on account of the partial overlapping of the  $\text{NH}_4^+$  band<sup>21</sup> at about

<sup>21</sup> Zs. für Physik, Vol. 88, 1-2, p. 127 (1934).



$3220\text{ cm}^{-1}$  over that of water, thus rendering very difficult any correct estimation of the intensity distribution in the latter : and in the case of salts like zinc chloride and lithium nitrate the presence of the continuous spectrum, in spite of the filter, was so great that here again no correct estimation of the intensity distribution in the band could be made. Hence, only these two salts,  $\text{NaNO}_3$  and  $\text{LiCl}$ , have been studied. In the case of the salts also the same relative shifts are observed in the positions of the bands as in the case of hydrochloric and nitric acids in fig. 6. When the quantity of water content in the two salts



is equalized it is found, as can be seen from fig. 12, that the curves tend to get closer and become more similar, although the effect does not seem to be so great as with the acids.

Table 2 gives the positions of the maximum of the water band in acids and salts at the same concentration and same water content.

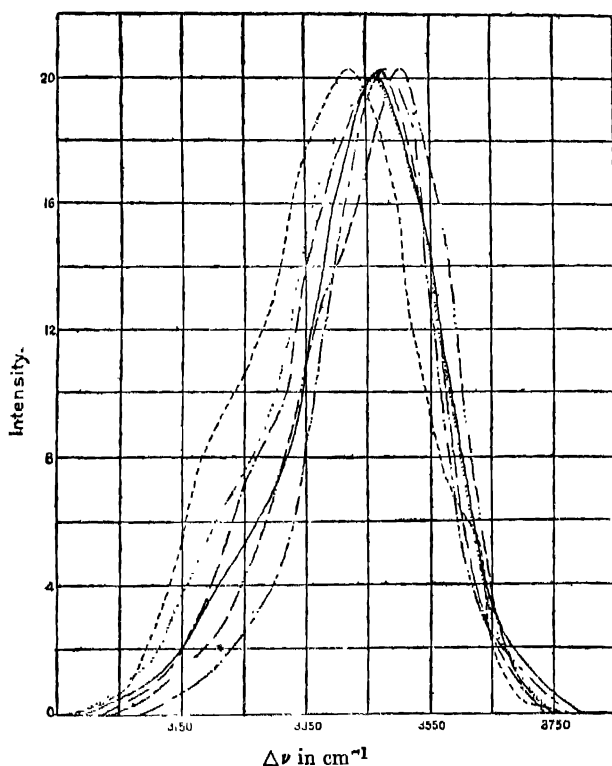
Finally, in fig. 13 are given, for purposes of mutual comparison, the intensity curves for water and for nitric acid and sodium nitrate at different concentrations. It is at once apparent that the curves for sodium nitrate are, in general, much sharper than

TABLE II.

Position of maximum.

Substance.	at 12 N concentration.	at 8N concentration.	At the same water conten	
			as 11.7N HCl	as 8NHCl (or LiCl)
1. H <sub>2</sub> O	3424 cm <sup>-1</sup>	3424 cm <sup>-1</sup>	3424 cm <sup>-1</sup>	3424 cm <sup>-1</sup>
2. HCl	3418 "	3425 "	3418 "	3425 "
3. HNO <sub>3</sub>	3504 "	3474 "	3460 "	3450 "
4. H <sub>2</sub> SO <sub>4</sub>	3468 "	3486 "	3440 "	3433 "
5. LiCl	—	3427 "	—	3427 "
6. NaNO <sub>3</sub>	—	3480 "	—	3463 "

FIG. 13.



Raman water band excited by the 3650-63λ group

- HNO<sub>3</sub> 12N
- · - · - HNO<sub>3</sub> 8N
- ..... HNO<sub>3</sub> 5.86N
- NaNO<sub>3</sub> 8N
- NaNO<sub>3</sub> 5.5N
- H<sub>2</sub>O



those for nitric acid. In fact, the curves for the 8N nitrate solution, the maximum concentration under which it has been studied, are sharper than even the curve for nitric acid at a much higher concentration, namely 12 N.

### 5. *Summary of the Results.*

The following is a generalized summary of the results obtained from a study of the intensity curves of the different electrolytes under different conditions which permit of an easy comparison of the results.

(1) The water band in solutions of electrolytes is invariably sharper than for pure water.

In the case of nitric and sulphuric acids and sodium nitrate,

(2) the band gets sharper with increasing concentration ;

(3) there is a clear shift in position of the maximum as also of the band as a whole towards the side of greater frequency with increasing concentration.

(4) there is the appearance of a certain amount of concavity, though slight, in the shape of the curve on the side of smaller frequency at higher concentrations.

In the case of hydrochloric acid, **however,**

(5) the band is sharper with 8N acid than at 11.7 N, although in both cases the band is sharper than for pure water ;

(6) there is a shift in the band towards the smaller frequency side as the concentration is increased; and

(7) the shorter frequency side of the intensity curve appears to be less concave at the higher concentration.

(8) In the case of acids, as well as salts, at the same concentration, there is a progressive relative shift in the positions of the maximum of the band, as well as in the band as a

whole, towards the greater frequency side as we pass from lithium chloride to sodium nitrate and from hydrochloric to sulphuric and nitric acids, that in the case of nitric acid being the greatest.

(9) With the same water content, both with acids and salts, the bands become more and more similar, the differences noticed in (8) tending to vanish.

(10) The water band in solutions of sodium nitrate is much sharper than that for nitric acid, even when the latter is taken at a much higher concentration.

## 6. Discussion.

These changes in the intensity distribution of the Raman band of water with addition of electrolytes are similar to those observed by Ramakrishna Rao<sup>22</sup> with change of temperature. To explain the latter phenomena, Ramakrishna Rao put forward the hypothesis that the three components in the water band corresponding to Raman frequencies equal to 3610, 3413 and 3195  $\text{cm}^{-1}$  are due respectively to the three types of molecules, namely  $(\text{H}_2\text{O})$ ,  $(\text{H}_2\text{O})_2$  and  $(\text{H}_2\text{O})_n$ , which are supposed to be present in water. The change with temperature in the intensity distribution of the band is attributed by him to changes in their relative proportions.

On account of the close similarity between the two sets of phenomena, *viz.*, changes in the structure of the water band with temperature on the one hand and with addition of electrolytes on the other, the explanation of the latter appears, to a large extent, to be most probably the same as for the former. The predominance of the central component at about 3400  $\text{cm}^{-1}$  in the water band in most electrolytic solutions and the general weakening of the other two components, compared to the band for pure water, shows that, on the above hypothesis, the double

$(\text{H}_2\text{O})_2$  molecules in water increase in proportion when an electrolyte is added to it, the number of the other two types at the same time diminishing.

This is at once clear from the greater sharpness of the curves for the solutions of dissolved electrolytes than that for pure water as well as from the slightly concave nature of their intensity curves, as compared with the curve for pure water which has a decidedly convex shape, particularly on the side of greater frequency shift: also the positions of the maxima in all the cases very nearly correspond to that of the double molecules in the water band. This indicates that the  $(\text{H}_2\text{O})_2$  molecules persist in solutions of electrolytes while the  $\text{H}_2\text{O}$  and  $(\text{H}_2\text{O})_3$  type molecules are comparatively unstable, particularly at the higher concentrations of the electrolytes, and as such tend to gradually disappear, the triple molecules perhaps dissociating and recombining amongst themselves or with the single molecules to form the simpler type,  $(\text{H}_2\text{O})_2$  molecules. Thus the increased sharpness of the water band in solutions of electrolytes and the relative shift in the shape and position of the band to different degrees in the different cases to the side of greater frequency may be due to a change in the water equilibrium, consequent upon the partial dissociation and recombination of the more complex  $(\text{H}_2\text{O})_3$  molecules amongst themselves and with the single molecules to form the stabler type of  $(\text{H}_2\text{O})_2$  molecules.

Bancroft and Gould in a recent paper,<sup>23</sup> made a similar suggestion as to the possibility of a more satisfactory explanation of the phenomena, so far ascribed to ionic hydration, on the basis of a displacement in the water equilibrium between the monohydrol, dihydrol and trihydrol. This explanation of the observed effect as due to a change in the proportion of the three types of water molecules appears, at least in part, to be the true interpretation when one considers the observed result of an increasing similarity and blending together of the intensity

<sup>23</sup> Jour. Phys. Chem., Vol. 38, 2, p. 197 (1934).



exhibit a sharpening of the band in the region where the component due to the  $(\text{H}_2\text{O})_2$  molecules is found to be present, it may be that, in many of them, hydrates with an even number of associated molecules predominate. But in cases where hydrates with an odd number of molecules are present it may happen that the band due to the water of hydration shifts either to the side of greater or smaller frequency depending on the number of molecules of hydration, whether single or triple. Thus the appearance of a slight convexity noticed in the shape of the intensity curves on the smaller frequency side with increasing dilution in the case of nitric and sulphuric acids is perhaps due to the formation of complex hydrates, particularly those with three associated molecules of water, that is,  $\text{H}_2\text{SO}_4 \cdot 3\text{H}_2\text{O}$  and  $\text{HNO}_3 \cdot 3\text{H}_2\text{O}$ . This is also supported by the observations of the earlier workers on the freezing point curves of the acid water mixtures referred to before.

The effect may be also partly due to an increase in the proportion of triple molecules that results with increased water content in the solution. Again, the decreasing sharpness is observed in the shape of the band with increasing dilution in the case of sulphuric acid, nitric acid and nitrates, as indicated in their intensity curves, figs. 2, 3, 5 and the slight shift noticeable in the curves to the smaller frequency side as dilution of the acid increases appears to be also due to the same two causes. Both these effects, namely, the formation of complex hydrates (particularly those with three molecules of water of hydration) and the formation of an increased proportion of triple molecules at higher dilutions, tend to shift the resultant curve to the smaller frequency side, the region corresponding to the component of the triple molecules in the band for pure water.

The anomalous results observed in the case of hydrochloric acid, *viz.*, an increased broadening of the band at the higher concentration of the acid, a slight shift in the band to the smaller frequency side at the larger concentration as compared

with that at the smaller concentration, do not seem to be easily explicable on the above hypotheses, as it is very improbable that more complex hydrates, which alone could shift the band to the short frequency side, could form at greater concentrations of the acid or with less quantity of water present. This problem is expected to be cleared by further work, which is in progress at present.

The greater sharpness in the intensity curves of sodium nitrate as compared with those of nitric acid, fig. 13, even when the latter is taken at much higher concentrations seems to be partly due to the formation of more complex hydrates in nitric acid and partly due to the superposition of the narrow diffuse band at  $3420\text{ cm}^{-1}$  due to  $\text{NO}_2\text{OH}$  molecule, found by Kohlrausch<sup>27</sup> to be present in pure nitric acid, over that due to water. The latter cause also appears to be the real explanation of the appearance of a second band observed by Ramakrishna Rao<sup>28</sup> in nitric acid solutions at concentrations higher than 76%, and not the formation of hydrates as put forward by him.

Passing on to the curves for the same concentration of the different electrolytes, figs. 6 and 7, the shift in the position of the band to the larger frequency side, as we pass from hydrochloric to sulphuric and nitric acids indicates the gradual decrease in the proportion of triple molecules and at the same time a slight increase in the proportion of single molecules. These results are, to some extent, in conflict with the hypothesis of Bancroft and Gould,<sup>29</sup> who postulate, from their observations on the Hofmeister series of certain anions, that for equivalent concentrations the amount of monohydrate is less with nitrate ion than with chloride ion. If that were the case, the intensity curve for hydrochloric acid must be shifted *more* to the larger frequency side than that of nitric acid, indicating thereby a

<sup>27</sup> Naturwiss., Vol. 19, p. 690 (1931).

<sup>28</sup> Roy. Soc., Proc., A, Vol. 130, p. 489 (1931).

<sup>29</sup> *loc. cit.*

greater preponderance of the single molecules or monohydrol in hydrochloric acid than in nitric acid, but actually the reverse is found to be the case. Again, their assumption in the same connection that the sulphate ion tends to convert trihydrol and monohydrol into dihydrol must lead one to expect that the water band in sulphuric acid would be narrower than in the other cases, thus indicating the comparatively low proportion of the single and triple molecules, but this again is found to be at variance with the experimental results obtained by the author.

Thus, the changes in the intensity distribution of the water band with addition of electrolytes may be not only due to changes in the relative proportions of the three types of molecules present in water, but may also arise out of formation of hydrates by combination of the ions with the water molecules.

The striking similarity of the curves with solutions of the three acids when the amount of water they contain is equalized, figs. 9 and 10, leads one to the conclusion that the differences noticed in the curves for different electrolytes are only due to a difference in their water content, and when it is the same in all the cases the nature of the electrolyte has not much influence anyway on the constitution of water and in consequence on the structure of its band. This is quite an unexpected result.

Thus the marked similarity between the several intensity curves taken with solutions having the same water content, leads one to expect that the effect of dissolved electrolytes is similar to that of a change of temperature of water, *viz.*, a change in the water equilibrium due to variation in the proportions of the three types of water molecules. Otherwise the result is not easily explained unless one makes the highly improbable assumption that at the same water content the amount and nature of hydrates formed are identical for the several substances.

Though the above curves are very similar, there are small but yet definite secondary differences between them which cannot be explained away as arising out of experimental errors, as they

are much more than the probable differences which may arise in the estimation of intensities. They therefore remain to be explained. These differences are to be attributed either to variations in the water equilibrium to different amounts for the different electrolytes or to formation of hydrates which may be different for the different electrolytes. That the latter cause explains the differences between the curves of sodium nitrate and lithium chloride (fig. 12), that still persist even when their water content is equalized, as also the greater sharpness of the band in sodium nitrate solution than in that of lithium chloride, can also be inferred from the fact that lithium salts are known to crystallize with a large amount of water of crystallization while sodium salts do not; and it is but natural that those salts, which crystallize with a larger amount of water, also associate with water molecules to a much greater extent in solution. With the results thus far available it is difficult to decide more definitely between the two alternatives set forth above as to the probable cause of the observed results. Both, however, seem to be equally probable and co-existent.

Finally, the cation seems to exert little characteristic influence on the constitution of water as can be inferred from the similarity of results obtained with acids and salts.

In conclusion, it is a pleasure to express my best thanks to Dr. I. Ramakrishna Rao for his very keen interest and helpful guidance throughout the progress of the work.



## The Raman Spectra of Dimethyl and Diethyl Trisulphides

By

N. GOPALA PAI, M.A.,

*Research Scholar, Indian Association for the Cultivation of Science.*

*(Received for publication, July 30, 1934.)*

### ABSTRACT.

The results of a study of the Raman spectra of certain organic trisulphides are discussed in relation to the structure of the molecules.

#### 1. Introduction.

The Raman spectra of the organic mono- and di-sulphide derivatives have been studied by Venkateswaran,<sup>1</sup> and various interesting results have been deduced. For example from the spectra of the alkyl monosulphides, he has been able to calculate uniquely the frequency characteristic of the C-S bond ( $694 \text{ cms.}^{-1}$ ). From the characteristic Raman frequencies of the simplest member of this series, *viz.*, dimethyl sulphide, the present writer<sup>2</sup> has calculated the valency angle of the sulphur atom and also the energy of binding of the C-S linkage. From the results for the disulphides, which are naturally more difficult to interpret, Venkateswaran has calculated the S-S frequency to be about  $509 \text{ cms.}^{-1}$ . The trisulphides have not been studied so far for their Raman effect. In view of the controversies regarding their molecular structure from the purely chemical point of view, it was hoped that a study of the Raman spectra of these compounds would throw light on the problem. The present paper gives an account of the measurements on the Raman spectra of these compounds and a discussion of the experimental results in relation to their molecular structure.

<sup>1</sup> 'Ind. Jour. Phys.,' Vol. 6, p. 51 (1931).

<sup>2</sup> 'Ind. Jour. Phys.,' Vol. 9, p. 121 (1934).

2. *Experimental.*

Both the trisulphides were obtained from the Palit Chemical Laboratories through the kindness of Sir P. C. Ray. A preliminary purification was effected by a fractionation under reduced pressure and the purified compound was sealed in the usual bulb and tube arrangement. This as usual was sealed off after evacuation, and the liquid to be experimented upon was distilled into the experimental tube. After the final purification about 4 c.c. were available and it had a strong yellow tint. The usual type of optical arrangement was used. The liquid showed strong absorption of the  $\lambda 4046$  mercury line and only the Raman lines excited by the  $\lambda 4358$  were recorded after long exposures.

3. *Results.*

TABLE I.

I	$\nu$	$\Delta\nu$	I	$\nu$	$\Delta\nu$
1d	22754	F-184	1	21980	F-958
1d	22398	F-240	1	21786	F-1152
1d	22656	F-282	0	21713	F-1225
2d	22492	F-446	0	21626	F-1312
3	22149	F-489	3	21503	F-1435
3	22125	F-513	2d	19953	F-2985
5d	22238	F-700	2	19894	F-3044

$\Delta\nu = 184(1d), 240(1d), 282(1d), 446(2d), 489(3), 513(3), 700(5d), 958(1), 1152(1), 1225(0), 1312(0), 1435(3), 2985(2d), 3044(2).$

TABLE II.

I	$\nu$	$\Delta\nu$	I	$\nu$	$\Delta\nu$
3d	22781	F-157	2	21888	F-1050
3d	22735	F-203	1	21739	F-1199
1	22567	F-371			D-2966
2	22499	F-439	1	21672	F-1266
4d	22151	F-487	2	21520	F-1418
2	22294	F-644	2	21482	F-1456
1	22268	F-670	1	21360	F-1578
2	21968	F-970	0	19968	F-2970

$\Delta\nu = 157(3d), 203(3d), 371(1), 439(2), 487(4d), 644(2), 670(1), 970(2), 1050(2), 1199(1), 1266(1), 1418(2), 1456(2), 1578(1), 2970(0).$

The data are given in Tables I and II. The collected Raman frequencies for the two compounds are given in Table III along with those for the mono- and disulphides for comparison. The numbers appearing as subscripts in the table indicate the intensities in arbitrary units.

TABLE III.

S	$(\text{CH}_3)_2\text{S}$ .	$\begin{array}{c} \text{CH}_3-\text{S} \\   \\ \text{CH}_3-\text{S} \end{array}$	$\begin{array}{c} \text{CH}_3\text{S} \\ \diagup \quad \diagdown \\ \text{CH}_3\text{S} \end{array} \text{S}$	$\begin{array}{c} \text{C}_2\text{H}_5\text{S} \\ \diagup \quad \diagdown \\ \text{C}_2\text{H}_5\text{S} \end{array} \text{S}$	$\begin{array}{c} \text{C}_2\text{H}_5\text{S} \\   \\ \text{C}_2\text{H}_5\text{S} \end{array}$	$(\text{C}_2\text{H}_5)_2\text{S}$ .
84 152 st 183			184 <sub>1</sub>	157 <sub>3d</sub> 203 <sub>3d</sub>	197 <sub>3</sub>	
216 st 242 ft	284 <sub>6</sub>	237 <sub>3</sub> 275 <sub>2</sub>	240 <sub>1</sub> 282 <sub>1</sub>			
433 ft 470 st		509 <sub>5</sub>	446 <sub>2</sub> 489 <sub>3</sub> 513 <sub>3</sub>	371 <sub>1</sub> 439 <sub>2</sub> 487 <sub>4d</sub>	382 <sub>2</sub> 372 <sub>2</sub>	366 <sub>1</sub> 333 <sub>1</sub> 386 <sub>1</sub>
				644 <sub>2</sub>	506 520 641 <sub>5</sub>	636 <sub>3</sub> 659 <sub>3</sub>
724 [from absorption spectrum of vapour]	604 <sub>8</sub> 743 <sub>5</sub>	696 <sub>6</sub> 740 <sub>0</sub>	700 <sub>5</sub>	670 <sub>1</sub>	672 <sub>5</sub>	694 <sub>3</sub>
					759 <sub>1d</sub>	
	1031 <sub>0</sub> 1073 <sub>1</sub>	956 <sub>2</sub> 1073 <sub>1</sub>	958 <sub>1</sub>	970 <sub>2</sub> 1050 <sub>2</sub>	974 <sub>4</sub> 1026 <sub>1</sub> 1055 <sub>3</sub>	971 <sub>3</sub> 1020 <sub>0</sub> 1044 <sub>1</sub>
			1162 <sub>1</sub> 1225 <sub>0</sub>	1199 <sub>1</sub> 1266 <sub>1</sub>	1255 <sub>1</sub>	
	1336 <sub>2</sub> 1428 <sub>5</sub> 1445 <sub>5</sub>	1307 <sub>0</sub> 1429 <sub>3d</sub>	1312 <sub>0</sub> 1435 <sub>3</sub>	1418 <sub>2</sub> 1456 <sub>2</sub> 1578 <sub>1</sub>	1353 <sub>2d</sub> 1421 <sub>3</sub> 1456 <sub>3</sub>	1429 <sub>1</sub> 1456 <sub>3</sub>
	2836 <sub>2</sub> 2850 <sub>2</sub> 2914 <sub>7</sub> 2965 <sub>4</sub> 2987 <sub>4</sub> 3046 <sub>1</sub>	2811 <sub>1</sub> 2910 <sub>8</sub> 2982 <sub>5</sub>	2985 <sub>2d</sub>	2970 <sub>0</sub>	2870 <sub>2</sub> 2924 <sub>4d</sub> 2971 <sub>4d</sub>	2879 <sub>2</sub> 2925 <sub>4</sub> 2967 <sub>2</sub>
			3044 <sub>2</sub>			

#### 4. *Discussion of Results.*

The simplest member, dimethyl trisulphide, gives about 14 frequencies in all, some of which can be identified as being due to the methyl group present in the compound. In the same manner some of the frequencies in the higher homologue, diethyl trisulphide, can be attributed to the  $C_2H_5$  group and these are naturally more numerous than those due to the  $CH_3$  group, owing to the greater complexity of the structure of the former. If we exclude these frequencies due to the  $CH_3$  and  $C_2H_5$  group respectively, there are others, as will be seen from Table III, common to both the compounds and may be attributed to the S-S and C-S bonds of the molecule.

Considering first the intense frequency at  $\Delta\nu = 700\text{cm.}^{-1}$  present in dimethyl trisulphide it is to be associated with the presence of the C-S group in the compound. Its continued presence in more or less the same position in the methyl derivatives of the mono- and disulphides decidedly points to its origin from this group. In the case of the ethyl derivatives a significant difference is noted in the fact that in the place of this single strong line, two or more lines are observed. This effect of the influence of the complexity of the molecule on the multiplicity of some of the characteristic frequencies is well known. For example, the frequency at  $\Delta\nu = 509\text{ cms.}^{-1}$  present in dimethyl disulphide has been attributed to the S-S group. In diethyl disulphide this frequency appears double at  $\Delta\nu = 508\text{ cms.}^{-1}$  and  $\Delta\nu = 526\text{ cms.}^{-1}$  respectively. As will be seen from the table, the same frequencies appear also in dimethyl trisulphide corresponding to an intense line at  $\xi 13$ . In diethyl trisulphide, however, there are no lines near about this region. This is surprising. This is the only particular in which these two derivatives show a difference, whereas in all other respects the similarity between the two groups of frequencies is marked.

### 5. *The Molecular Structure of the Polysulphides.*

Most of the theories regarding the constitution of the polysulphides are based mainly on the following two considerations :—

(a) The general behaviour of the polysulphides towards inorganic substances is in conformity with a structural formula of the type  $R_2SS_x$ , one of the S atoms in the compound behaving differently from the others.

(b) On the other hand the reactions of the polysulphides with alkyl halides are more in accordance with a formula of the type  $R_2S_2S_x$ , which differentiates two of the sulphur atoms from the rest.

The simplest theory consistent with the above considerations is that put forward by Spring and Demarteau<sup>3</sup> among others, which considers the polysulphides to be merely solutions of sulphur in the corresponding monosulphide (in which case one of the sulphur atoms will be different from the rest) or in the corresponding disulphide (in which case two of the sulphur atoms will stand differentiated, and the formula will be of the type (b) *viz.*,  $R_2S_2S_x$ ). They prefer, however, the latter alternative, *i.e.*, solution in the disulphide.

This solution theory has been criticised on chemical grounds by Küster and Heberlein.<sup>4</sup> If the polysulphides were mere solutions of suitable amounts of sulphur in the disulphide one should expect the various polysulphides to be hydrolysed in solution to nearly the same extent, which is not the case.

Let us now consider the solution theory on the evidence of the Raman effect. There are some low Raman frequencies in the trisulphides which have nearly the same positions and relative intensities as the Raman frequencies of sulphur; for example, the lines at  $\Delta\nu = 433$  and  $470 \text{ cms.}^{-1}$  present in sulphur appear at  $446$  and  $489 \text{ cms.}^{-1}$  in dimethyl trisulphide and at  $439$

<sup>3</sup> 'Bull. Soc. Chem.,' [3], 1, p. 311.

<sup>4</sup> 'Zeit. anorg. Chem.,' Vol. 45, p. 53 (1905).

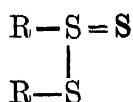
" " " Vol. 44, p. 481 (1905).

and  $487 \text{ cms.}^{-1}$  in diethyl trisulphide. At first sight this observation appears to lend support to the solution theory of the structure of the trisulphide. A more careful consideration however does not justify such a conclusion. Because according to this view the Raman spectrum of the trisulphide should be expected to be a superposition of the spectra of sulphur and of the mono- or the di-sulphide. Actually this is not the case; in the first place some of the strong frequencies present in sulphur for example, at 84, 216, are absent in the trisulphides. Secondly even though corresponding to the frequencies of the trisulphide some nearly equal frequencies can be found, either in the spectrum of sulphur or of the disulphide, the difference between the frequencies so correlated are too great to be attributed to influence of solution.

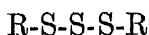
The trisulphide should therefore be treated as a definite compound, and not as mere solution of sulphur in the corresponding disulphide.

Among the structural formulæ suggested for the trisulphide, two deserve special mention :—

(a) The one proposed by Thomas and Rule,<sup>5</sup> namely



(b) That proposed by Mandeléeff<sup>6</sup> and Blanksma<sup>7</sup> by analogy with the structure of the long chain hydrocarbons



A preliminary objection may be raised against (a) since it makes all the sulphur atoms in the trisulphide different; whereas (b)

<sup>5</sup> 'J. O. S.,' Vol. 111, p. 1063 (1917).

<sup>6</sup> The Principles of Chemistry, St. Petersburg, p. 617 (1908).

<sup>7</sup> 'Rec. Trav. Chim. Pays. Bas.,' Vol. 20, p. 146 (1900).

differentiates two of the sulphur atoms from the third as required by the considerations set forth in an earlier part of this section.

The evidence of the Raman effect also is in favour of the latter formula, *viz.*, (b). From the point of view of the Raman effect the essential difference between the formula (a) and (b) lies in the fact that while in (a) there is an S=S bond, in (b) both the bonds between the sulphur atoms are S—S. Since there is difference between the characteristic frequencies of the S=S and S-S bonds we are enabled from the Raman effect data to decide between the formulæ (a) and (b).

The frequency corresponding to S=S has been deduced from the absorption and fluorescence spectra of sulphur vapour to be equal to  $725 \text{ cms.}^{-1}$ , while, as we have already remarked in a previous section, the frequency of the S-S bond is equal to  $509 \text{ cms.}^{-1}$ . These values for S=S and S-S bonds can also be seen to be interconsistent, since their ratio  $725 : 509$  is nearly equal to  $\sqrt{2}$ , as we should expect to a first approximation.

From an examination of the Raman frequencies given in Table III it will be seen that the  $725 \text{ cms}^{-1}$  frequency is absent from the spectrum of either of the trisulphides; the nearest frequency that appears in the spectrum of methyl trisulphide is  $700 \text{ cms.}^{-1}$ , which is present also in the spectrum of dimethyl disulphide and is evidently due to the C-S bond; while in the diethyl trisulphide the frequency nearest to  $725 \text{ cms.}^{-1}$  is only  $670 \text{ cms.}^{-1}$ , which again appears in diethyl sulphide. We can therefore conclude that there is no S=S bond in either of the trisulphides, and their formula cannot correspond to (a), and are presumably given by (b), *viz.*, 'R-S-S-S-R. The Raman spectra of  $\text{H}_2\text{S}_2$  and  $\text{H}_2\text{S}_3$  are also being studied with a view to determine their structure, and the results will be published in due course.

### Summary.

The Raman spectra of dimethyl and diethyl trisulphides have been studied and the results are discussed with reference to

the constitution of these molecules. It is shown on the evidence of the Raman effect data that the theory which considers the polysulphides as mere solutions of sulphur in the corresponding disulphides is untenable. The formula  $\text{R}-\text{S}=\text{S}$



proposed by Thomas and Rule also is not supported by the Raman effect data, since the characteristic  $\text{S}=\text{S}$  frequency at about  $725 \text{ cm}^{-1}$  does not appear in the Raman spectra of the two trisulphides. The evidence is generally in favour of the Mandeléeff Blanksma formula  $\text{R}-\text{S}-\text{S}-\text{S}-\text{R}$  analogous to that of the saturated hydrocarbons.

The author's best thanks are due to Prof. Dr. K. S. Krishnan for his keen interest and kind guidance in the work.



# An X-Ray Investigation of the Crystals of Anthranilic Acid

By

MATA PRASAD AND M. R. KAPADIA

(Received for publication, August 15, 1934.)

## ABSTRACT.

The paper describes the preliminary results of an X-ray investigation of the crystals of anthranilic acid. The substance crystallises in two modifications which differ in density. The dimensions of the unit cell have been found to be different in the two cases and while one belongs to the space group  $Q_h^1$ , the other belongs to  $Q_h^2$ . The number of molecules per unit cell in each case is eight.

Crystals of anthranilic acid were prepared by the slow evaporation of the solution of the substance in alcohol. Anthranilic acid crystallises in two types of crystals both of which belong to the rhombic bipyramidal class. These two types of crystals are obtained simultaneously from the same solution under identical conditions. Both these crystals were studied by the rotating crystal method using a Shearer tube fitted with copper anticathode.

## *First Modification.*

The prominent faces developed are  $a$  (100),  $b$  (010),  $c$  (111),  $i$  (122). The axial ratio is

$$a:b:c=0.6877:1:0.6161 \text{ (cf., Groth, Vol. IV, pp. 508).}$$

The lengths of the three axes were found to be

$$a=16.16 \text{ \AA} ; \quad b=11.77 \text{ \AA} ; \quad c=7.17 \text{ \AA}.$$

These give the ratio

$$a:b:c=1.373:1:0.609.$$

This shows that the  $a$  axis is of twice the length found by the crystallographic methods.

Oscillation photographs were taken about  $a$  and  $c$  axes at an interval of  $15^\circ$  and were worked out by the aid of Bernal's chart. The list of planes observed is given in Tables I and II. The intensities of the planes were determined by eye estimation and the symbols used have the usual meaning.

TABLE I.

Axial planes.	Prism planes ( <i>h</i> <i>o</i> <i>l</i> ).	Prism planes ( <i>o</i> <i>k</i> <i>l</i> ).	Prism planes ( <i>h</i> <i>k</i> <i>o</i> ).
002 m.	102 s.	022 s.	210 w.
020 v.s.	103 s.	023 w.	220 s.
040 v.s.	202 w.	041 w.	230 s.
060 m.s.	203 w.m.	042 w.	240 m.s.
200 s.	302 w.m.	043 w.	250 m.s.
400 s.	401 s.	061 w.	260 m.
800 w.m.	402 s.		410 s.
	501 m.s.		420 w.m.
	502 m.		430 w.m.
	601 w.		450 m.
	602 s.		620 w.m.
			630 w.m.
			640 w.

TABLE II.  
*General Planes.*

111 v.s.	211 m.	311 v.s.	411 v.s.	511 s.	611 m.	711 v.w.
113 m.s.	212 w.m.	312 w.m.	412 w.m.	512 v.w.	612 w.m.	722 v.w.
122 w.	213 m.s.	313 w.m.	413 w.	521 m.	621 w.	
131 m.s.	214 w.m.	321 s.	421 s.	522 w.	641 w.	
132 v.w.	221 m.	322 w.	422 w.	523 w.	651 m.s.	
133 w.m.	222 w.m.	331 m.	423 m.	531 v.w.		
141 w.m.	231 w.	332 w.	431 w.m.	533 w.		
142 m.	232 w.m.	341 w.	441 m.	541 w.m.		
151 m.s.	242 w.	342 m.	442 v.w.	542 v.w.		
152 w.m.	251 v.w.	351 m.	451 v.w.	551 w.		
161 m.			461 m.			
162 w.						

It will be seen from this list that the planes (*okl*) are halved when *k* is odd and the planes (*hko*) are halved when *h* is odd. These halvings correspond to the space group  $Q_h^{II}$ . The number of molecules in the unit cell required by the space group is 8. The number of molecules in the unit cell, calculated from the dimensions of the cell and the specific gravity of the crystals, which was redetermined and found to be 1.355, is also nearly 8. This shows that the molecules of anthranilic acid in the crystal are asymmetric.

### *Second Modification.*

The prominent faces developed in the crystal are *b* (010), *a* (100) and *o* (111). The ratio of the axes is

$$a:b:c=0.6066:1:0.8751 \text{ (Groth, loc. cit.)}.$$

The lengths of the axes were found to be

$$a=12.77 \text{ \AA} ; \quad b=10.8 \text{ \AA} ; \quad c=9.403 \text{ \AA}.$$

and these give the axial ratio

$$a:b:c=1.197:1:0.8812.$$

Thus again in this case the length of the *a* axis is doubled.

Oscillation photographs taken about  $a$  and  $c$  axes at an interval of  $15^\circ$  indicated the planes given in Tables III and IV.

TABLE III.

Axial planes.	Prism planes ( $h0l$ ).	Prism planes ( $okl$ ).	Prism planes ( $hko$ ).
002 s.	102 m.s.	012 m.s.	110 s.
004 s.	104 w.	014 m.s.	130 w.m.
020 s.	202 s.	022 s.	140 v.w.
200 v.s.	204 m.	024 m.s.	150 m.s.
400 v.s.	304 m.	031 m.s.	220 s.
	402 s.	032 w.m.	240 w.
		034 w.	310 m.s.
		041 w.	330 w.
		042 v.w.	410 w.
		051 v.w.	420 m.s.
		052 s.	440 w.m.

TABLE IV.  
*General Planes.*

111 v.s.	211 v.s.	311 v.s.	411 s.	511 w.	612 m.	711 v.w.
113 s.	212 s.	312 m.s.	412 m.	512 w.		
121 s.	213 w.	313 s.	413 m.s.	532 m.s.		
122 s.	221 s.	321 m.s.	414 w.	593 w.m.		
123 w.m.	222 w.m.	323 m.s.	421 m.s.			
124 m.	223 m.s.	332 w.m.	422 m.			
131 s.	231 w.	333 m.	423 m.			
133 m.s.	233 m.	334 v.w.	432 m.s.			
134 v.w.	241 m.s.	341 v.w.	433 w.m.			
141 m.	243 w.		441 w.m.			
142 v.w.	251 m.					
143 m.s.	252 m.s.					
152 w.						

In this case the planes (*h*0*l*) are halved when *l* is odd. This corresponds to the space group  $Q_h^{\bar{2}}$ . The number of molecules in the unit cell required by the space group is 8 and that found from the dimensions of the unit cell and the specific gravity of the crystals (redetermined and found to be 1.422) is also nearly 8. The molecules of this modification are, as well, asymmetric in the unit cell.

It will be interesting to work out how a change in the crystalline nature of anthranilic acid is brought about by a change in the orientation of the molecules. But the difficulties involved are many and attempts are being made to find a way out of them.

One of the authors (M.P.) desires to express his thanks to the University of Bombay for a grant which defrayed part of the expenses of this investigation.

CHEMICAL LABORATORIES,  
THE ROYAL INSTITUTE OF SCIENCE,  
BOMBAY.



# Lines or Bands in the Spectrum of the Night Sky.

By

J. V. KARANDIKAR, B.Sc.

(Received for publication, October 21, 1934.)

Plate IV.

## 1. Introduction.

In a previous paper <sup>1</sup> K. R. Ramanathan described the general spectrum of the night sky as observed in India and pointed out that, besides the green auroral line 5577Å originating from atomic oxygen, there are many other "lines" or bands which have also to be considered as characteristic of the spectrum of the night sky. As was first emphasised by Lord Rayleigh <sup>2</sup> the spectrum is quite distinct from the spectrum of the polar aurora.

During the dry season of the early part of 1933, Dr. Ramanathan and the present author obtained strongly exposed and better dispersed spectra of the light of the night sky which showed many more "lines" than the previous photographs. A short note on this has already appeared in *Nature*.<sup>3</sup> The present paper contains a list of these "lines" and a comparison of them with those obtained by Dufay <sup>4</sup> and by Cabannes and Dufay <sup>5</sup> in France and by Slipher <sup>6</sup> in America.

<sup>1</sup> 'Ind. J. Phys.', Vol. 7, p. 405 (1932).

<sup>2</sup> 'Proc. Roy. Soc.', A, Vol. 103, p. 45 (1923).

<sup>3</sup> 'Nature', Vol. 132, p. 749 (1933).

<sup>4</sup> 'Journal de Physique', Ser. 7, Vol. 4, p. 221 (1933).

<sup>5</sup> J. Cabannes and Dufay, 'Compt. Rendus', Vol. 198, p. 306 (1934).

<sup>6</sup> 'M.N.R.A.S.', Vol. 93, p. 657 (1933).

## 2. *Spectrographs used and Exposures.*

Two spectrographs were used both of which were constructed locally. One of them was the same as that used in the earlier work. The second spectrograph was also a single-prism instrument, but the camera lens had a longer focal length (41") and a smaller aperture ratio  $F/2.9$ . Both the spectrographs were exposed towards the north sky at an angle of about  $20^\circ$  to the horizon during moonless hours of the night after the cessation and before the beginning of twilight.

With the first instrument a good plate was obtained with an exposure of 75 hours between the 12th and 29th April, 1933 (Fig. 1b). By means of a diaphragm in front of the slit an exposure of the zodiacal light was also made on the same plate, the duration of exposure being  $25\frac{1}{2}$  hrs. (Fig. 1a). By an oversight in obtaining the latter spectrum, the spectrograph remained exposed for  $5\frac{3}{4}$  hrs. towards the north sky also.

With the second spectrograph a good plate was obtained between 17-3-33 and 1-5-33 with a total exposure of 181 hours. As in the previous work, *Mimosa Extrema-ortho* and *Finogran* plates were used. Fig. 2 shows this spectrum; the comparison spectrum of helium is superposed.

## 3. *Results.*

The following table (Table 1) gives the wave-lengths of the lines and their relative intensities (estimated). For comparison, the wave-lengths of the lines as listed by Dufay and Cabannes and Dufay are also given in the table. The wave-lengths given in Dufay's paper were based on a large number of plates taken by him in 1931 and 1932. Those given in Cabannes' and Dufay's paper (*Comptes Rendus*) were obtained from a plate exposed at Pic du Midi in August, 1933. Slipher has also published some beautifully exposed spectra (M.N.R.A.S 93, 657, 1933) especially in the red and near infra-red—but a full list of the lines is not yet available.





Fig. 1.

(a) Spectrum of the Zodiacal light ( exposure  $25\frac{1}{2}$  hrs ).

This had an additional exposure of  $5\frac{3}{4}$  hrs. towards night sky

(b) Spectrum of night sky ( exposure 75 hrs.).



Fig. 2

Night sky spectrum obtained with the larger spectrograph  
( exposure 181 hrs.).

Comparison spectrum is that of helium.



TABLE 1.

$\bar{A}$  } Lines in the night-sky spectrum observed at Poona  
 $B$  } by K. R. Ramanathan and J. V. Karandikar.

A—Smaller dispersion spectrograph

B—Larger „ „

C Lines in the night-sky spectrum observed in France by Dufay.

D „ „ „ „ observed in France by Cabannes and Dufay.

A	B	C	D
5890	5913	6315	
5783	5745	5892	
5577			
5446	5577	5662	
		5577	
		5316	
		5162	
	5123(1)		5162(1)
			5181(?)
			5092(1)
			5030(3)
	4997(1)		5003(2)
			4965(2)
			4984(3)
			4916(?)
		4866	4904(3)
			4968(3)
4827(6)	4840(5)	4837	4838(4)
			4825(3)
			4808(3)
			4781(2)
			4767(1)
			4730(?)
			4726(0)
			4712(1)
		4708	4700(?)
4675(7)	4681(7)		4693(3)
		4679	4669(4)
			4649(?)
		4615	4632(?)
			4617(3)
			4592(1)
4576(6)		4576	4582(2)
			4573(0)

A	B	C	D
4636(8)	4553(8)	4554	4554(4) 4636(4)
		4512	4519(2)
		4500	4495(1)
		4478	4480(?)
			4472(1)
	4443	4447	4419(3)
4419(9)	4427(9)	4421	4431(5) 4419(4)
			4402(1)
		4382	4386(2)
4357	4350	4351	4370(3) 4360(?) 4345(1) 4337(1)
4324	4321(4)	4330	4328(3) 4313(?)
			4301(0)
4266	4268(1)	4270	4288(2) 4279(2) 4269(2) 4259(2) 4236(0)
		4237	
	4216(2)		4225(?) 4221(3) 4214(0)
4200(1)			4199(1) 4193(1)
	4179(8)	4180	4181(1)
	4166(9)		4173(5) 4160(2) 4153(1) 4144(2) 4135(3)
4129(3)	4126(3)		4122(2)
		4100	4110(1) 4101(1) 4091(2)
4085(6)	4085(5)	4082	4073(4) 4067(?)
4062(6)	4064		4061(0) 4052(2)
		4044	4044(?) 4038(1)
	4022(5)	4031	4029(0)
4002(4)	4005(3)	4026	4022(2) 4014(1) 4002(1) 3995(1) 3989(1)

A	B	C	D
		3980	3980(0) 3974(?) 3966(3) 3964(?) 3950(2) 3935(0) 3924(?) 3916(3) 3901(?) 3903(1) 3891(0)
3945(3)	3951(2)	3952 3911	
3910(1)	3918(1)	3916	
3864(1)	3871		
3844	3844		
3777			
3732			

It will be seen from the above table and the photographs given by Dufay that, keeping in mind the necessarily small dispersion, the spectra obtained by the French investigators are practically identical with those obtained in India both as regards the position of the lines and their relative intensities. Cabannes and Dufay used an extraordinarily powerful spectrograph with a corrected objective of focal length 8 cm. and aperture ratio  $F/0.7$ . The length of the spectrum between 3900 and 5200 Å was 5.71 mm. As this spectrum which revealed 44 new lines was obtained by Cabannes and Dufay during the course of a single night, the sky on that night should have been exceptionally bright. The relative intensities of the usual lines do not appear to differ much from the normal.

#### 4. Identification of the Night-Sky Radiations.

The green line 5577 Å being the most prominent characteristic of the night-sky spectrum, and being present at all times, the attention of investigators was naturally directed first towards its identification. The line was traced to its source by the searching investigations of McLennan and Shrum (Proc. Roy. Soc. A, 120, 327, 1928) who showed that the line was due to atomic oxygen. Except the 5577 line and the two lines in the red 6300 Å and 6360 Å discovered by Slipher, all of which are ascribed to

atomic oxygen corresponding to the transitions from the metastable state  $^1S_0 - ^1D_2$ ,  $^1D_2 - ^3P_2$  and  $^1D_2$  and  $^3P_1$  respectively, the other lines or bands in the night-sky spectrum have not been definitely identified. Positive and negative bands of nitrogen, atomic lines of N, O, Ar and He have been suggested but with the poorly dispersed spectra that are so far available and the richness in lines of the spectra of the possible sources a confident and conclusive identification has not been possible so far.

## Continued Fractions Associated with Ellipsoidal Wave-Functions.

BY

S. L. MAJUMKAR, POONA.

(*Received for publication, October 23, 1934.*)

In a previous memoir <sup>1</sup> the fundamental equation for an ellipsoidal wave-function in the Jacobean elliptic form has been derived as

$$d^2U/d\xi^2 + (a_0 - a_1 k^2 sn^2 \xi - n^2 k^4 sn^4 \xi) U = 0 \quad \dots \quad \dots \quad (1)$$

where  $U(\xi)$  is of form

$$(sn \xi)^{\sigma_1} (cn \xi)^{\sigma_2} (dn \xi)^{\sigma_3} \psi(sn^2 \xi)$$

$\psi$  being an integral function of  $sn \xi$  and  $a_1$  and  $a_0$  are characteristic constants.

By the transformation  $sn \xi = v$  the above equation reduces to

$$(1 - v^2)(1 - k^2 v^2) d^2U/dv^2 - v(1 + k^2 - 2k^2 v^2) dU/dv \\ + (a_0 - a_1 k^2 v^2 - n^2 k^4 v^4) U = 0 \quad \dots \quad (2).$$

We may use either of these equations for the purposes of this paper. The values of  $\sigma$  throughout this paper are 0 or 1.

<sup>1</sup> See 'Ind. Journal of Physics,' Vol. IX, p. 45 *et seq.*, 1934.

I. Let us assume that

$$U(\xi) = \Sigma A_\nu (sn\xi)^{2\nu + \sigma};$$

then

$$(2\nu + 2 + \sigma)(2\nu + 1 + \sigma)A_{\nu+1} - \{(1 + k^2)(2\nu + \sigma)^2 - a_0\}A_\nu + \{(2\nu - 2 + \sigma)(2\nu - 1 + \sigma) - a_1\}k^2A_{\nu-1} - n^2k^4A_{\nu-2} = 0 \quad \dots \quad (3)$$

$$(4 + \sigma)(3 + \sigma)A_2 - \{(1 + k^2)(2 + \sigma)^2 - a_0\}A_1 + \{\sigma(1 + \sigma) - a_1\}k^2A_0 = 0 \quad \dots \quad (4)$$

$$(2 + \sigma)(1 + \sigma)A_1 - \{(1 + k^2)\sigma^2 + a_0\}A_0 = 0 \quad \dots \quad \dots \quad \dots \quad (5)$$

If we put

$$B_\nu = A_{\nu+1}/A_\nu$$

then

$$(2\nu + 2 + \sigma)(2\nu + 1 + \sigma)B_\nu - \{(1 + k^2)(2\nu + \sigma)^2 - a_0\} + \{(2\nu - 2 + \sigma)(2\nu - 1 + \sigma) - a_1\}k^2/B_{\nu-1} - n^2k^4/B_{\nu-1}B_{\nu-2} = 0 \quad \dots \quad (6)$$

It is seen that the value of  $B_\nu$  tends for large values of  $\nu$  either to unity or zero. As  $U(\xi)$  is an integral function of  $sn\xi$  the value of  $B_\nu$  must necessarily be zero ultimately.

The value of  $B_\nu$  can be put in the form of a continued fraction of Fürstenau's type.

$$B_\nu = n^2k^4 / [\{(2\nu + 2 + \sigma)(2\nu + 3 + \sigma) - a_1\}k^2 - \{(1 + k^2)(2\nu + 4 + \sigma)^2 - a_0\}B_\nu + \{(2\nu + 5 + \sigma)(2\nu + 6 + \sigma) - a_1\}k^2/B_{\nu+1}B_{\nu+2}] \dots \quad (7)$$

The values of  $B_0$  and  $B_1$  obtained in the form of continued fractions have to be equal to their values given by the equations

$$(\sigma + 4)(\sigma + 3)B_1 - \{(1 + k^2)(2 + \sigma)^2 - a_0\} + \{\sigma(\sigma + 1) - a_1\}k^2/B_0 = 0$$

$$(\sigma + 2)(\sigma + 1)B_0 = (1 + k^2)\sigma^2 - a_0$$

Just as in the problems dealt by Kelvin, Darwin and Goldstein, it is necessary to point out that the coefficients  $A$  can be determined with the relations 3, 4 and 5 only if we know the value of  $a_0$  and  $a_1$  exactly and we make no approximation at any



stage.<sup>2</sup> Otherwise the value of  $B_\nu$  will inevitably tend to unity instead of zero. Similar remarks will apply to functions of other species also.

II. Let

$$U(\xi) = \Sigma A_\nu (sn\xi)^{2\nu + \sigma} cn\xi ;$$

then

$$(2\nu + 2 + \sigma)(2\nu + 1 + \sigma)A_{\nu+1} - \{(2\nu + 1 + \sigma)^2 + (2\nu + \sigma)^2 k^2 - a_0\} \cdot A_\nu \\ + \{(2\nu - 1 + \sigma)(2\nu + \sigma) - a_1\} k^2 \cdot A_{\nu-1} - n^2 k^4 A_{\nu-2} = 0 \quad \dots \quad (8)$$

$$(4 + \sigma)(3 + \sigma)A_2 - \{(3 + \sigma)^2 + (2 + \sigma)^2 k^2 - a_0\} A_1 \\ + \{(1 + \sigma)(2 + \sigma) - a_1\} k^2 \cdot A_0 = 0 \quad \dots \quad (9)$$

$$\text{and } (1 + \sigma)(2 + \sigma)A_1 \{(1 + \sigma)^2 + \sigma^2 k^2 - a_0\} A_0 = 0 \quad \dots \quad (10)$$

putting  $B_\nu = A_{\nu+1}/A_\nu$  we get

$$B_\nu = n^2 k^4 / [\{(2\nu + \sigma + 3)(2\nu + 4 + \sigma) - a_1\} k^2 - \{(2\nu + 5 + \sigma)^2 + (2\nu + 4 + \sigma)^2 k^2 \\ - a_0\} B_{\nu+1} + (2\nu + 6 + \sigma)(2\nu + 5 + \sigma) B_{\nu+1} B_{\nu+2}] \quad \dots \quad (11)$$

III. If

$$U(\xi) = \Sigma A_\nu (sn\xi)^{2\nu + \sigma} dn\xi ;$$

then

$$(2\nu + 2 + \sigma)(2\nu + 1 + \sigma)A_{\nu+1} - \{(2\nu + 1 + \sigma)^2 k^2 + (2\nu + \sigma)^2 - a_0\} \cdot A_\nu \\ + \{(2\nu + \sigma)(2\nu - 1 + \sigma) - a_1\} k^2 \cdot A_{\nu-1} - n^2 k^4 A_{\nu-2} = 0 \quad \dots \quad (12)$$

$$(4 + \sigma)(3 + \sigma)A_2 - \{(3 + \sigma)^2 k^2 + (2 + \sigma)^2 - a_0\} A_1 \\ + \{(2 + \sigma)(1 + \sigma) - a_1\} k^2 A_0 = 0 \quad \dots \quad (13)$$

$$\text{and } (2 + \sigma)(1 + \sigma)A_1 - \{(1 + \sigma)^2 k^2 + \sigma^2 - a_0\} A_0 = 0 \quad \dots \quad (14)$$

If

$$B_\nu = A_{\nu+1}/A_\nu ;$$

<sup>2</sup> See the references in Lamb's *Hydrodynamics*, pp. 335, sixth edition, 1932. See also Goldstein on Mathieu Functions. *Trans. of the Cambridge Phil. Soc.*, Vol. XXXIII, No. XI, pp. 303-36, 1927.

then

$$B_\nu = n^2 k^4 / [\{(2\nu+4+\sigma)(2\nu+3+\sigma) - a_1\} k^2 - \{(2\nu+5+\sigma)^2 k^2 + (2\nu+4+\sigma)^2 - a_0\} B_{\nu+1} + (2\nu+6+\sigma)(2\nu+5+\sigma) B_{\nu+1} B_{\nu+2}]. \quad \dots \quad (15)$$

IV. If

$$U(\xi) = \Sigma A_\nu (sn\xi)^{2\nu+\sigma} \cdot cn\xi \cdot dn\xi ;$$

then

$$(2\nu+2+\sigma)(2\nu+1+\sigma) A_{\nu+1} - \{(2\nu+1+\sigma)^2(1+k^2) - a_0\} A_\nu + \{(2\nu+\sigma)(2\nu+1+\sigma) - a_1\} k^2 A_{\nu-1} - n^2 k^4 A_{\nu-2} = 0 \quad \dots \quad (16)$$

$$(4+\sigma)(2+\sigma) A_2 - \{(3+\sigma)^2(1+k^2) - a_0\} A_1 + \{(2+\sigma)(1+\sigma) - a_1\} k^2 A_0 = 0 \quad \dots \quad (17)$$

$$\text{and} \quad (2+\sigma)(1+\sigma) A_1 - \{(1+\sigma)^2(1+k^2) - a_0\} A_0 = 0 \quad \dots \quad (18)$$

if  $B_\nu = A_{\nu+1}/A_\nu$  then it is equal to

$$n^2 k^4 / [\{(2\nu+5+\sigma)(2\nu+4+\sigma) - a_1\} k^2 - \{(2\nu+5+\sigma)^2(1+k^2) - a_0\} B_{\nu+1} + (2\nu+6+\sigma)(2\nu+5+\sigma) B_{\nu+1} B_{\nu+2}] \quad \dots \quad (19)$$

All the possible species and types of characteristic functions are included in the above as in each instance  $\sigma$  could be either one or zero.

## **Investigations on the Rectification of Alternating Current by Crystals.**

By

S. R. KHASTGIR, D.Sc. (EDIN.)

AND

ANIL KUMAR DAS GUPTA, M.Sc.,

*Dacca University.*

*(Received for publication, November 12, 1934.)*

### *Introduction.*

Various theories have been put forward to explain the action of the crystal detectors. Eccles<sup>1</sup> gave a complete theory based on thermo-electric action at the contact point of the crystal. The passage of current across the high resistance junction of the metal and the crystal causes heat to be produced and the local heating leads to the generation of thermo-electric force which involves both the contact electromotive force (Peltier E.M.F.) at the junction and the Thompson effect in the metal and the crystal. Briefly speaking, this thermo-electric force occurs during both the positive and the negative half of the applied voltage producing the current, during one of which it assists and during the other opposes, giving thereby a rectified current.

<sup>1</sup> 'Proc. Phys. Soc.,' Vol. 25 (1915).

Dowsett <sup>2</sup> mentioned two other causes, besides the thermo-electric cause for the phenomena of rectification in crystals, *viz.*, (1) the electro-chemical nature of the elements comprising the crystal and (2) the crystal structure.

James <sup>3</sup> suggested an electrolytic theory. Schlegel and Buggisch <sup>4</sup> maintained a theory based on arrangements of parts approximating a point and a plane.

It was Schottky <sup>5</sup> who first put forward an electronic theory of rectification. The existence of a work function at the boundary of a material makes it possible, if the work functions are different at the boundaries of the two materials in contact, to show that there should be a difference in the conductance across the boundary in the two opposite directions. According to Schottky, the rectified current is a purely electronic flow which takes place between two electrodes separated by a dielectric interlayer.

Pelabon <sup>6</sup> in a similar way worked out a formula for the rectified current which seemed to agree with his experimental results. Similar theories have been worked out by Frenkel and Joffe <sup>7</sup> and Van Geel.<sup>8</sup>

Ogawa's <sup>9</sup> theory is based on the cold electron emission. The rectification according to Ogawa is brought about by the difference of the electron emissions from the two electrodes forming the contact. The crystal, in effect, is a cold vacuum tube operating as a detector by the difference in the electronic emissions.

<sup>2</sup> 'Wireless Telephony & Broadcasting,' Vol. 2, pp. 14-44.

<sup>3</sup> 'Phil. Mag.,' Vol. 49, pp. 681-695 (1925).

<sup>4</sup> 'Phys. Zeits.,' Vol. 28, pp. 174-179 (1927).

<sup>5</sup> 'Zeits. f. Physik,' Vol. 14, pp. 63-106 (1923).

<sup>6</sup> 'Comptes Rendus,' Feb. 25, pp. 620-622 (1929).

<sup>7</sup> 'Phys. Rev.,' Vol. 39, pp. 530-531 (1932).

<sup>8</sup> 'Zeits. f. Physik,' Vol. 69, pp. 765-785 (1931).

<sup>9</sup> 'Phil. Mag.,' Vol. 6, pp. 175-178 (1928).

L. Reglar <sup>10</sup> suggested that the rectification phenomenon could be traced to the piezo-electric effect.

R. de L. Krönig <sup>11</sup> showed in a general way that the crystal rectification could be due to asymmetrical binding of the ions into positions of equilibrium by restoring forces, not symmetrical for equal and opposite displacements.

### *Scope of the present investigation.*

The object of the present investigation has been to experimentally study and collect facts about crystal rectification in view of the existing theories of rectification.

Our experiments have revealed two different kinds of rectification. One is always associated with point contacts and this we have called the "point"—rectification. The other kind—the volume rectification—has been found to be independent of any point effect. This has been attributed to the asymmetry in crystal structure. In crystals which have no centres of symmetry such as carborundum (SiC), zincite (ZnO) and silicon, a very marked asymmetry in current conductivity has been observed which is quite independent of any point action, whereas symmetrical crystals like galena, iron pyrites, molybdenite, etc., have shown no trace of such asymmetric conductance when tested with L. F. alternating current.

Although more crucial tests have to be made before this asymmetric conductance is established beyond doubt, these experiments have strongly suggested its existence in crystals having no centres of symmetry. We have accordingly classified the crystal detectors into two groups: (1) crystals having centres of symmetry and (2) crystals having no such symmetry.

It should be mentioned here that Tissot <sup>12</sup> showed that with a certain group of crystals, even relatively large polished plates

<sup>10</sup> 'Phys. Zeits.,' Vol 29, pp. 429-436 (1928).

<sup>11</sup> 'Nature,' March 2, 1929.

<sup>12</sup> 'L'Electrician,' Vol. 39, p. 331 (1910).

between two metallic electrodes made very sensitive detectors. G. W. Pierce<sup>13</sup> also concluded that carborundum, anatase and brookite are better conductors in one direction than in the opposite.

According to our classification, there exists only the "point" rectification in the symmetrical crystals and in the crystals having no centres of symmetry there is, in addition, volume rectification due to the asymmetric conductance which is generally very pronounced in comparison with the "point" rectification.

Seven symmetrical natural crystals have been studied *viz.*, iron pyrites ( $\text{FeS}_2$ ), galena ( $\text{PbS}$ ), magnetite ( $\text{Fe}_3\text{O}_4$ ), molybdenite ( $\text{MoS}_2$ ), pyrolusite ( $\text{MnO}_2$ ), cassiterite ( $\text{SnO}_2$ ) and bornite ( $\text{Cu}_2\text{S}$ ,  $\text{CuS}$ ,  $\text{FeS}$ ).

The experiments conducted with these crystals are grouped as follows :

- I. Study of the asymmetric conductance or volume rectification in carborundum, zincite and silicon.
- II. Study of rectification with different crystals having the same metal contact.
- III. Study of rectification with crystals in contact with pointed crystals of the same composition.
- IV. Study of the effect of heating the contact point on the rectifying action.
- V. Study of the effect of heat, ultra-violet light and X-rays on the rectifying action.

#### 1. *Asymmetric Conductance or Volume Rectification in Carborundum, Zincite and Silicon.*

A narrow glass tube has been made narrower at one end and the crystal under examination, after having been thoroughly cleaned is fixed at that end by sealing wax so that one-half of the crystal

<sup>13</sup> 'Electrician,' 69, 66, 1912, *vide* Zenneck's 'Wireless Telegraphy,' p- 282.

projects out. The tube is then filled with clean mercury. The tube with its contents is then fixed inside a wider glass tube containing mercury so that the projecting part of the crystal is under mercury. Leads are then taken from the mercury in both the tubes. [See Fig. 1 (a).] Another way of mounting the crystal has also been tried. Two pointed brass teeth have been soldered each to the middle of each edge of a metal paper-clip as shown in Fig. 1 (b). One end of the crystal under examination is held tightly between the pointed ends of the two teeth.

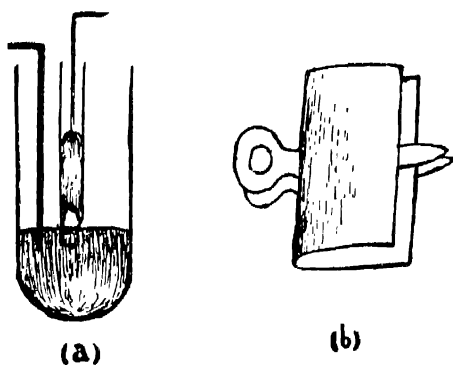


FIG. 1.

The other end is also held in a similar way by another similar clip attached with two similar brass teeth.

Carborundum, zincite and silicon crystals mounted in both ways have revealed marked asymmetry in the current-voltage curves. The curves for carborundum and zincite are shown in Fig. 2. The calculated resistances in arbitrary units in the two opposite directions for different voltages are also shown in the figures. The rectification ratio which is taken as the ratio of the difference of the two currents in the two opposite directions to the larger current has been calculated for each voltage. The calculated values of the rectification ratio for different voltages are also illustrated. The experimental results are given in Table I.

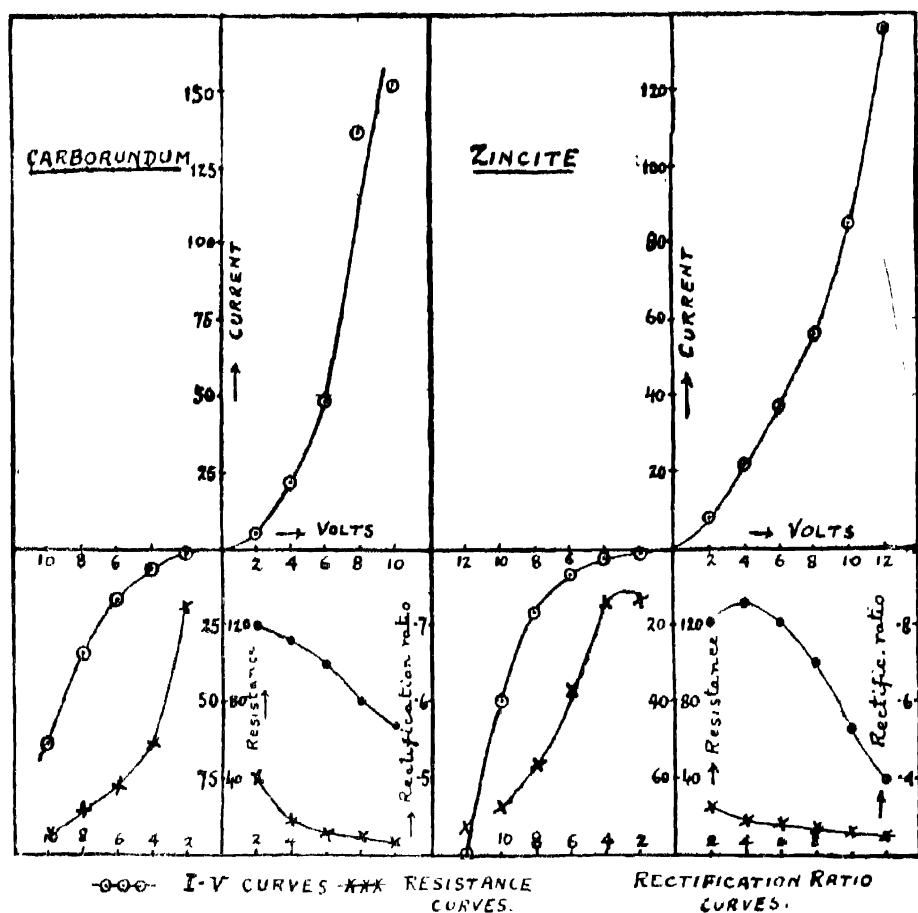


Fig. 2.

These results have been corroborated by directly passing a low-frequency alternating current through the crystal so mounted. It should be mentioned that when tested with low-frequency A. C., the symmetrical crystals have shown no such asymmetry. Copper pyrites (in the form of a lump of irregular shape) which is a crystal having no centre of symmetry, has not also shown any asymmetry.\*

\*The rectification effect with copper-pyrites and a silver point is also extremely small.



TABLE I.

Voltage (volts)	$I_1$ (Galv. scale divisions.)	$I_2$ (Galv. scale divisions.)	$R_1$	$R_2$	Rectification Ratio.
Carborundum. (good crystal).					
2	05	1.5	40	133	.7
4	22	7	18	57	.68
6	48	17	12.5	35	.65
8	136	34	9.3	24	.6
10	151	64	6.7	10	.57
Zincite.					
2	8	1.5	25	133	.81
4	22	3	18	133	.86
6	37	7	16	86	.81
8	56	17	14	47	.7
10	85	40	12	25	.53
12	136	8.1	9	15	.4

*N.B.*— $I_1$  and  $I_2$  are the values of the currents in the two opposite directions.  $R_1$  and  $R_2$  represent corresponding resistances (in arbitrary units).

Actual measurements of the resistances in the two opposite directions have also been made for specific directions in the case of a good carborundum crystal.

If ABCD represents the (111) face of the carborundum crystal, the actual resistances along directions (AB, BA), (AD, DA) and (BD, DB) have been determined by the Callendar Griffiths bridge method. The results are shown in Table II.

TABLE II.

Directions.		Resistances in two directions.	
(1)	(2)	(1)	(2)
(AB)	(BA)	145 M $\Omega$	1075 M $\Omega$
(AD)	(DA)	780 $\Omega$	256 $\Omega$
(BD)	(DB)	625 M $\Omega$	105 M $\Omega$

## II. Rectification with Different Crystals having the same Metal Contact.

### Experimental details :

The circuit diagrams for the construction of the characteristic curves are shown in Fig. 3. G represents the galvanometer shunted, when necessary, with a low resistance S. In Fig. 3 (a) is shown the circuit arrangement for crystals of low resistance *e.g.*, galena, iron pyrites, etc., where the resistance of the voltmeter is large compared with that of the crystal. The potentiometer method shown in Fig. 3(b) is meant for crystals of resistance not less than 1000  $\Omega$ , *e.g.*, zincite, carborundum, etc. In any of the two circuits, positive and negative voltages can be applied to the crystal by simply turning the commutator rocker.

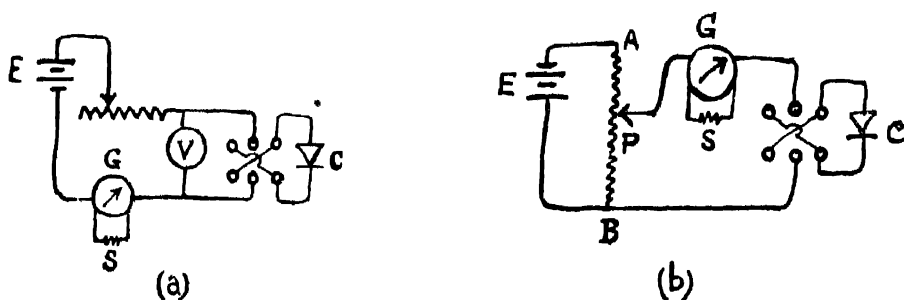


FIG. 3.

The mounting of the crystal has been carried out in the way shown in Ftg. 4. The crystal under examination is screwed or soldered to the brass ring P and the lever arrangement makes it possible to apply a constant pressure to the piece of silver wire which is screwed tightly to the bottom end of the vertical brass rod A. The upper end of the rod is screwed to a wider piece of metal D having a concave outer surface on which the lever arm rests. One end L of the lever is made the fulcrum and a weight is applied at a suitable distance on the other end.

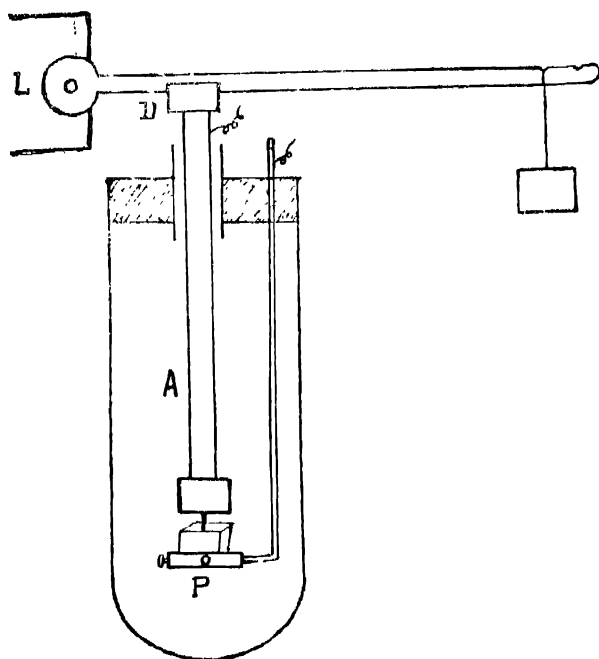


FIG 4.

*Experimental results.*—Only crystals of good crystalline form have shown rectification effect in the same direction. Natural crystals of irregular form have shown positive, negative and no rectification effects. (The rectification has been called positive when the direction of the rectified current is from the crystal to the metal contact.) In the case of the iron

pyrites,—the only symmetrical crystal we have in a good crystalline form—the sign of the rectification has been found to be negative for all contact points on the (100) faces (excepting one or two). The good carborundum crystal (which is made up of at least two or three single crystals) has shown positive rectification for many contact points. Quite a number of points on the same surface have also shown negative rectification effects. Fig. 5

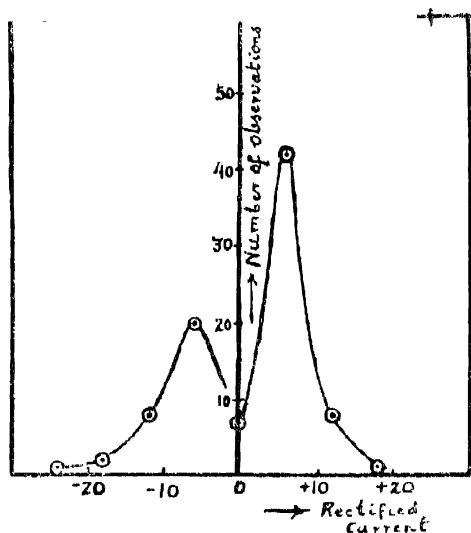


FIG. 5.

illustrates the positive and negative rectification effects observed in another lump of carborundum polycrystal. The experimental results are shown in Table III.

It is difficult to explain both positive and negative rectification effects for the same crystal on any existing theory of rectification. Maintaining the theory of plate-and-point rectification, Reisshaus<sup>14</sup> attempted to explain the arbitrary direction of the rectified current by pointing out that some points of the crystal surface are likely to be more pointed than the metal contact. The suggestion is negated by the fact that the point-and-plate effect has been found too small to account for the observed rectification effects.

TABLE III.

Rectified Current within range of 6 units. (Galv. scale divs.)	Number of observations.
12 to 18	1
6 to 12	8
0 to 6	42
0	7
0 to -6	20
-6 to -12	8
-12 to -18	2
-18 to -18	1

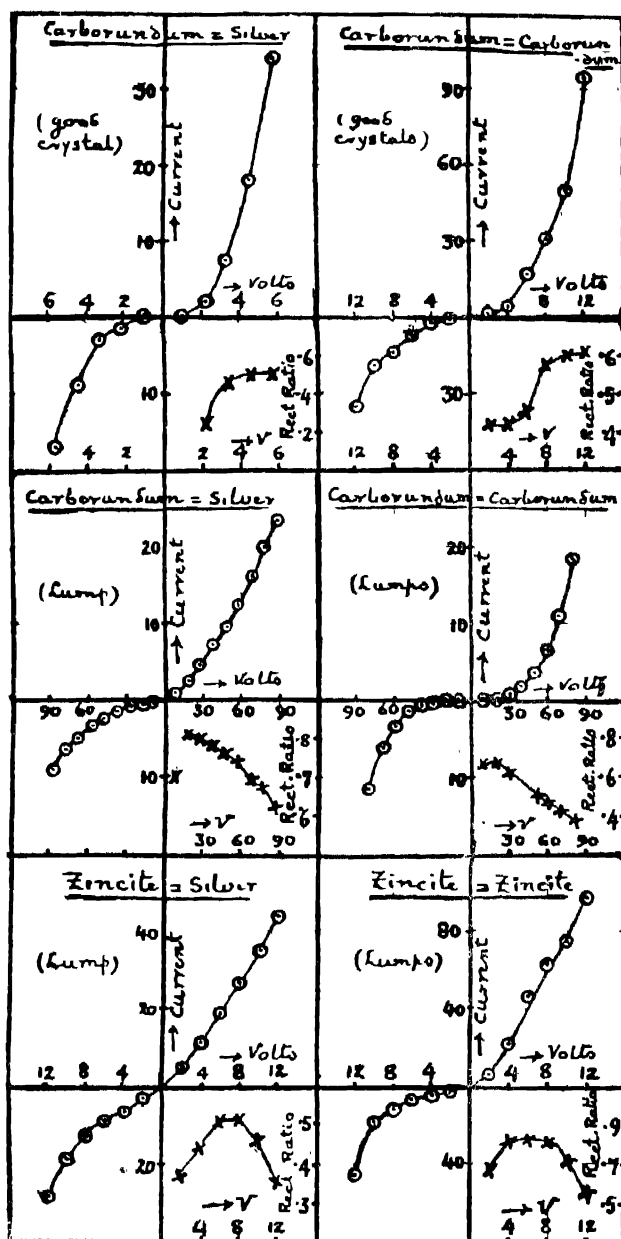
*III. Rectification with Crystals in contact with Pointed Crystals of the same Composition.*

(a) Symmetrical crystals :

Experiments with galena-galena, ironpyrites-ironpyrites, magnetite-magnetite, molybdenite-molybdenite, pyrolusite-pyrolusite, cassiterite-cassiterite and bornite-bornite have all shown rectification effects. The direction of rectification has been found either way and the magnitude for many contact points very small and for many others moderate.

(b) Crystals having no centres of symmetry :

Experiments with carborundum-carborundum, zincite-zincite and silicon-silicon have shown rectification effects as pronounced as in the case of these crystals with a metal point. This is evident from a comparison of the characteristic curves for crystal plane-crystal point and crystal plane-metal point. Typical curves for carborundum and zincite are shown in Fig. 6. (For experimental results see Table IV.) Exact comparison is not



I-V Curves are represented by circles and the rectification-ratio curves by crosses.

FIG. 6.

possible, since the total resistance in the circuit in the two cases has not been made the same. Nevertheless, it is clear that

whatever be the cause of the "point" rectification in the case of the symmetrical crystals, it plays a minor part in carborundum, zincite and silicon crystals. These results have been corroborated by passing both T. F. and H. F. alternating currents.

These results are definitely against the existing thermo-electric electrolytic or electronic theories of rectification.

#### *IV. The Effect of Heating the Contact Point on the Rectification Effect.*

*Experimental details.*—The junction has been heated electrically. The metal whisker in the form of a straight stout silver wire pointed at the end has been passed vertically through a spiral of a few turns of fine platinum wire. In passing currents of varying strengths through the platinum spiral, the contact has been heated to various temperatures. A small piece of thick

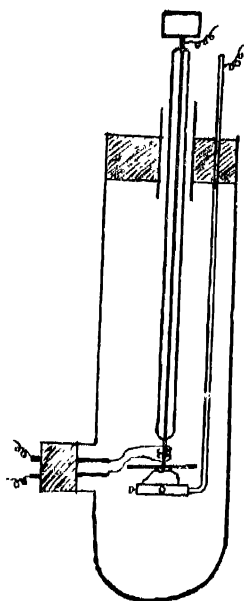


FIG. 7.

asbestos has been fixed on the top of the crystal surface and below the heating spiral with a small hole for the whisker to pass through. This has been to prevent heating the entire crystal. The arrangement of the apparatus is shown in Fig. 7.

Two different series of experiments have been performed, one with 1000 cycles/sec. A. C. from the microphone hummer and the other with H. F. current ( $\lambda = 200\text{m}$ , frequency  $= 1.5 \times 10^6$  cycles/sec.) obtained from a tuned-anode one-valve oscillator. The circuit arrangement and the mounting of the crystal in the case of H. F. current are shown in Fig. 8.

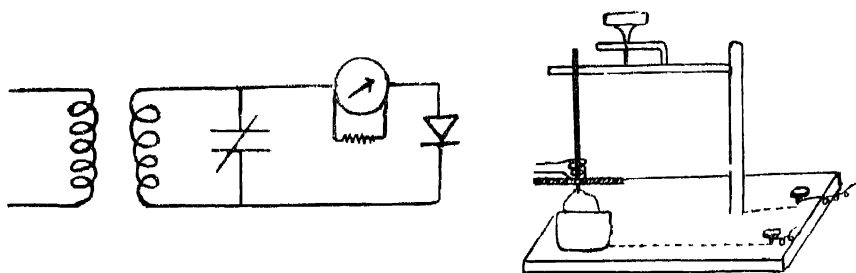


FIG. 8.

For a certain fixed value of the heating current, the current  $I_r$  as indicated by the D. C. galvanometer when an alternating current passed through the detector circuit, is not the true rectified current, for, due to the junction being heated, there must be a thermo-electric current  $I_t$ . The difference between these two currents represents the actual rectified current. Immediately after observing  $I_r$ , the leads from the A. C. supply have been shorted and the thermo-electric current  $I_t$  carefully recorded. The difference  $(I_r - I_t)$  has been found for various values of the heating current.

### *Experimental results :*

In the case of symmetrical crystals the rectified current has been usually found to decrease as the temperature of the junction



is increased. The experimental results with both L. F. and H. F. currents for iron-pyrites and magnetite are illustrated in Fig. 9. If the rectified current is small to start with, at room temperature, the value of  $(I_r - I_t)$  may fall to a zero or even a negative value as the junction is heated. This change in the

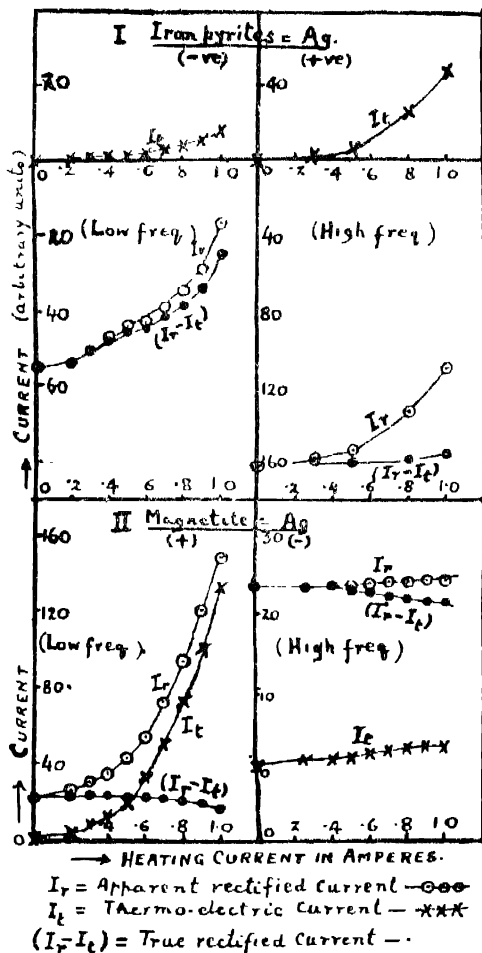


FIG. 9.

sign of the rectified current on heating the junction is shown in Fig. 10.

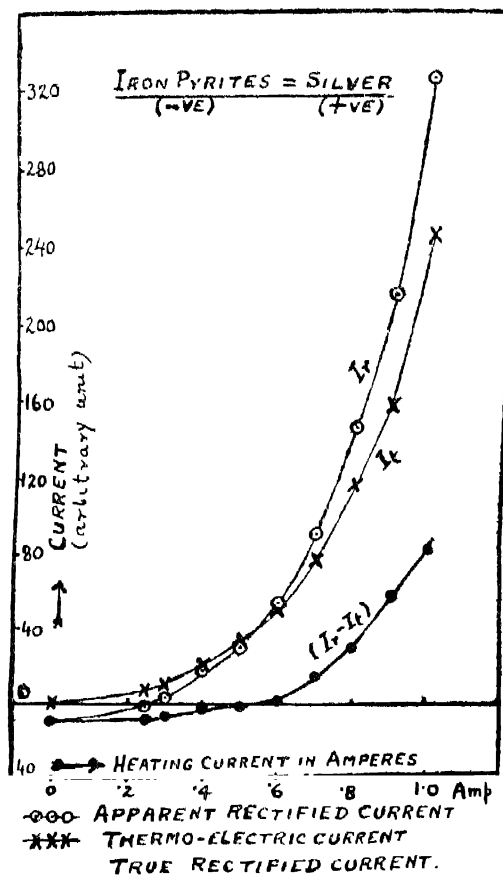


Fig. 10.

In the case of carborundum, zincite, and silicon, there has been practically no change in rectification on heating the junction between the contact point and the crystal (see Fig. 11). This is in keeping with the view that in these crystals the asymmetric conductance due to crystal asymmetry is the predominant factor in producing the total rectification effect. The experimental results are incorporated in Tables V and VI.

#### *Discussion of the results :*

Some definite statements can be made in view of these experimental results :

(1) The thermo-electric current  $I_t$  on heating the junction between the silver point and each of the crystals has been invariably found to flow *from the crystal to the point*. If the rectified current is due to this thermo-electric current, the rectified current must also flow in the same direction. We have seen that in some combinations this is so, while in some others the rectified current is opposite to the direction of the thermo-electric current. This contradicts Eccles' theory.

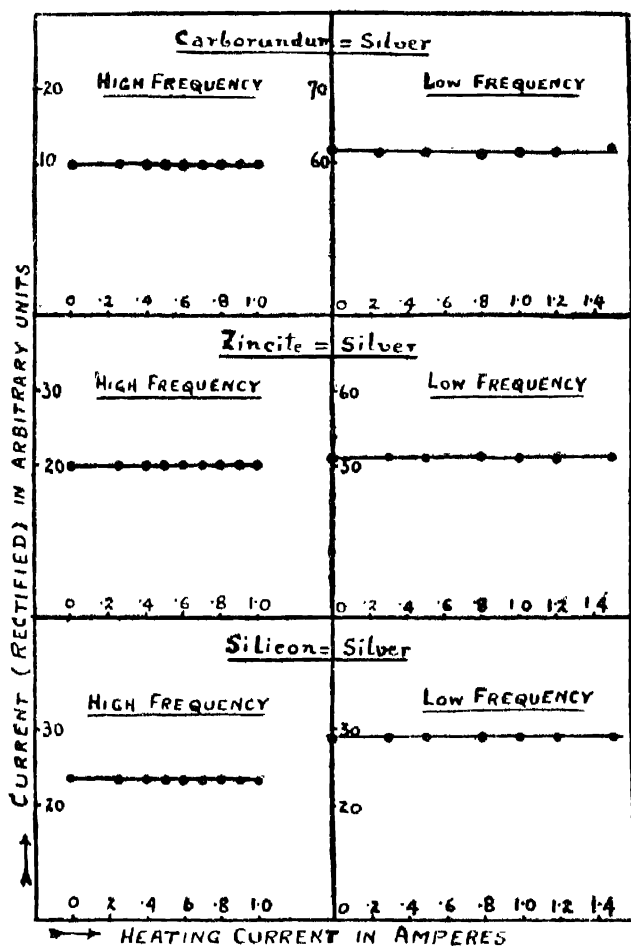


FIG. 11.

(2) The general equation for the current-voltage characteristic curve given by Eccles is

$$ax^2y^2 + cxy^2 + bxy - x + \rho y = 0$$

where  $y$  is the current,

$x$  the voltage across the variable part of the crystal resistance.

$\rho$  the contact-resistance (variable part) and

$a, b, c$  are the coefficients depending on the Thomson Effect, the Peltier Effect and the temperature coefficient of the crystal resistance respectively.

Here ' $a$ ' can be positive and negative, ' $b$ ' is positive by definition and ' $\rho$ ' is also a positive quantity. The coefficient ' $c$ ' which involves the temperature coeff. of the crystal resistance is negative for these crystals. On analysing the curve which the equation represents, it can be seen that its curvature at the origin, which is a measure of the rectification effect (without any bias voltage), depends on  $\frac{2b}{\rho^2}$ . The rectification effect, therefore,

ought to increase according to Eccles' theory when the contact point is heated, for when the temperature of the contact point is increased, ' $b$ ' which involves the Peltier E. M. F. must increase and ' $\rho$ ' the variable part of the crystal resistance must diminish. Our experiments, however, have shown that usually the rectification effect in the case of symmetrical crystals diminishes as the junction is heated.

L. S. Palmer<sup>15</sup> however, mentions that B. Hoyle observed an increase in rectification on heating the contact point.

#### V. *The Effect of Heat, Ultra-violet Light and X-rays on Crystal Rectification.*

The effect of heating the crystals has been invariably to decrease their rectifying action. Iron pyrites crystal when heated

<sup>15</sup> 'Wireless Principles and Practice', 1928, p. 304.

to 100°C. has been found to lose altogether its rectifying power. The effect of ultra-violet light is a very slight diminution in the rectifying action. The diminution is considerable when the crystals are exposed to X-rays. Flowers<sup>16</sup> studied the effect of heat on the rectifying power of galena. The effect of ultra-violet light and X-rays on the rectification has been previously studied by W. Jackson.<sup>17</sup> We have repeated the investigation and have gained some additional knowledge on the subject. The results will be published elsewhere.

### *Conclusion.*

Only the experimental results have been presented in this paper. It is clear that the existing theories of crystal rectification are unsatisfactory and in many cases not compatible with the experimental results. We have, however, developed a theory based on the existence of an unbalanced electrostatic force on the crystal surface which can satisfactorily explain the observed facts about crystal rectification in the case of ionic crystals which do not show volume rectification. The theory will be given in a subsequent paper. The experiments described in this paper have strongly suggested that in the crystals having no centres of symmetry, there is an additional amount of rectification due to asymmetric conductance. More decisive experiments have to be performed before we can associate definitely this volume rectification observed in carborundum, zincite and silicon with the crystal asymmetry. The volume rectification in the crystals having no centres of symmetry can, however, be explained according to Krönig's idea.

Our thanks are due to Prof. S. N. Bose for his kind interest in the investigation and to Prof. J. C. Ghosh and Dr. K. S. Krishnan for kindly supplying us with some crystals.

TABLE IV.

Voltage (volts)	$I_1$	$I_2$	Rect. ratio	Voltage (volts)	$I_1$	$I_2$	Rect. ratio
<i>Carborundum-silver (good crystal)</i>				<i>Carborundum-carborundum (good crystal)</i>			
0	0	0	...	2	1.75	1.0	.42
2.1	2	1.5	.25	4	6.5	3.75	.42
3.3	7.5	4	.47	6	18	9	.5
4.5	18	9	.5	8	31	13	.58
5.7	34	17	.5	10	53	21	.6
...	...	...	...	12	98	38	.61
<i>Carborundum-silver (lump)</i>				<i>Carborundum-carborundum (lumps)</i>			
10	1	.3	.7	10	.06	.02	.67
18	2.6	.5	.81	20	.3	.1	.67
28	4.7	.8	.8	30	.9	.34	.62
38	7.05	1.5	.73	40	1.95	.7	.64
48	9.7	2.3	.76	50	3.5	1.7	.51
58	12.6	3.2	.74	60	6.7	3.5	.48
68	16.2	5.0	.69	70	11.0	6.3	.43
78	20.0	6.5	.67	80	18.4	11.5	.37
88	23.5	9.0	.62	...	...	...	...
<i>Zincite-Silver</i>				<i>Zincite-Zincite</i>			
2	5.5	3.5	.37	2	6	2	.67
4	11.5	6.7	.44	4	22	4	.82
6	18.5	9.0	.51	6	47	7	.81
8	26.5	13.0	.51	8	63	12	.81
10	35.5	19.0	.46	10	75	23	.77
12	44	28.5	.35	12	97	45	.54

N. B. —  $I_1$  and  $I_2$  are currents in arbitrary units in the two opposite directions.

TABLE V.

1000 cycles per sec.					1.5 × 10 <sup>6</sup> cycles per sec.				
Heating current in amperes	Temp. (Centi-grade.)	I (Galv. divi.)	I <sub>r</sub> (scale divisions.)	I <sub>r</sub> - I <sub>t</sub>	Heating current in amperes	Temp. (Centi-grade.)	I <sub>r</sub> (Galv. divi.)	I <sub>r</sub> (scale divisions.)	I <sub>r</sub> - I <sub>t</sub>
<i>Iron Pyrites.—Ag</i>									
0	30°	-55	0	-55	0	30°	-161	0	-161
.2	32°	-51	.25	-54.25	.3	32°.5	-158	2	-160
.3	32°.5	-50.5	.5	-51	.5	33°	-153	7	-160
.4	33°	-47	.75	-47.75	.8	35°	-132	26	-158
.5	35°	-44	1.15	-45.15	1.0	60°	-109	48	-157
.6	43°	-43	1.8	-44.8					
.7	50°	-39	2.75	-41.75					
.8	60°	-34.5	4.0	-38.5					
.9	75°	-28.5	5.5	-34					
1.0	90°	-16.5	8.0	-24.5					
<i>Magnetite.—Ag.</i>									
0	30°	22	0	22	0	30°	23.5	0	23.5
.2	32°	24.5	.25	22	.25	32°	23.5	.5	23
.3	32°.5	30.5	.60	23.5	.4	33°	23.8	.8	23
.4	33°	35	1.175	23.25	.5	35°	23.8	1.0	22.8
.5	35°	43	20.5	22.5	.6	43°	24.0	1.5	22.5
.6	43°	55	32.5	22.5	.7	50°	24.25	1.8	22.45
.7	50°	73	51	22.0	.8	60°	24.25	2.25	22
.8	60°	95	73.5	21.5	.9	75°	21.5	2.5	22
.9	75°	121	101	20.0	1.0	90°	21.5	2.5	22
1.0	90°	150	133.5	16.5					
<i>Iron Pyrites.—Ag.</i>									
0	30°	-8.5	0	-8.5	I <sub>r</sub> = Apparent rectified current. I <sub>t</sub> = Thermo-electric current. (I <sub>r</sub> - I <sub>t</sub> ) = True rectified current. The negative sign indicates that the current flows from the "whisker" to the crystal.				
.25	32°	-1.0	.75	-8.5					
.3	32°.5	.5	10.75	-7.25					
.4	33°	16.5	19.75	-3.25					
.5	35°	29.75	32.5	-2.75					
.6	43°	53.5	52	1.5					
.7	50°	91	77	14					
.8	60°	146	115	31					
.9	75°	215.5	157.5	58					
1.0	90°	326	244.5	81.5					

TABLE VI.

1000 cycles per sec.					1.5 × 10 <sup>6</sup> cycles per sec.				
Heating current in amperes	Temp. (Centigrade.)	I <sub>r</sub> (Galv. divisions.)	I <sub>s</sub> (scale divisions.)	I <sub>r</sub> - I <sub>s</sub>	Heating current in amperes	Temp. (Centigrade.)	I <sub>r</sub> (Galv. divisions.)	I <sub>s</sub> (scale divisions.)	I <sub>r</sub> - I <sub>s</sub>
<i>Carborundum—Silver.</i>									
0	30°	61.75	0	61.75	0	30°	10	0	10
.25	32°	61.5	0	61.5	.25	32°	10	0	10
.5	35°	61.5	0	61.5	.4	33°	10	0	10
.8	60°	61	0	61	.5	35°	10	0	10
1.0	90°	61.5	0	61.5	.6	43°	10	0	10
1.2	110°	61.5	0	61.5	.7	50°	10	0	10
1.5	150°	62	0	62	.8	60°	10	0	10
					.9	75°	10	0	10
					1.0	90°	10	0	10
<i>Zincite—Silver.</i>									
0	30°	-51	0	-51	0	30°	-20	0	-20
.3	32°	-51	0	-51	.25	32°	-20	0	-20
.5	35°	-51	0	-51	.4	33°	-10	0	-20
.8	60°	-51	0	-51	.5	35°	-20	0	-20
1.0	90°	-51	0	-51	.6	43°	-20	0	-20
1.2	110°	-51	0	-51	.7	50°	-20	0	-20
1.5	150°	-51	0	-51	.8	60°	-20	0	-20
					.9	75°	-20	0	-20
					1.0	90°	-20	0	-20
<i>Silicon—Silver.</i>									
0	30°	29	0	29	0	30°	23.5	0	23.5
.3	32°	29	0	29	.25	32°	23.5	0	23.5
.5	35°	29	0	29	.4	33°	23.5	0	23.5
.8	60°	29	0	29	.5	35°	23.5	0	23.5
1.0	90°	29	0	29	.6	43°	23.5	0	23.5
1.2	110°	29	0	29	.7	50°	23.5	0	23.5
1.5	150°	29	0	29	.8	60°	23.5	0	23.5
					.9	75°	23.5	0	23.5
					1.0	90°	23.5	0	23.5



## Some Magnetic and Raman Spectra Evidence on the Structure of Complex Cyanides.\*

By

D. M. BOSE, CALCUTTA.

(Received for Publication, November 28th, 1934.)

*Abstract*—In a previous paper, it has been shown from magnetic evidence that in the complex cyanides, the cyanogen groups are present as double molecules  $(\text{CN})_2$ , which are linked to the central paramagnetic atom by single or double bonds. In the present paper it is shown that the Raman spectra of the complex cyanides can also be satisfactorily interpreted by means of the same structural formula.

In a previous paper <sup>1</sup> entitled "The relation between the paramagnetic properties of molecules and their chemical constitutions" the writer had, from a study of the magnetic properties, given a theory of the structure of co-ordination compounds including double salts. The starting point of the investigation was the consideration of the magnetic properties of the double cyanides of elements belonging to the first transition group, from which certain conclusions were drawn as to the detailed mechanism of the co-ordination bond, whose theory based upon electronic interaction, was first given by Sidgwick. In the paper it was shown that in the case of the double cyanides like  $\text{KCu}(\text{CN})_2$ ,  $\text{K}_2\text{Ni}(\text{CN})_4$ ,  $\text{K}_3\text{Co}(\text{CN})_6$ , etc., the unpaired electrons in the 3rd shell of the atoms Cu, Ni and Co, viz., 1, 2 and 3, were paired respectively with the free spin moments of an equal number of negatively charged double cyanogen molecules  $(\text{CN})_2^-$ , whose

\* Read before the Inaugural Meeting of the Indian Physical Society on the 29th September, 1934.

<sup>1</sup> Bose, Zeit. f. Phys., 65, p. 677, 1930.

structure can be written in the form  $(\text{NC}:\text{CN})$ .— Since the publication of this paper, the writer has been on the look out for some optical evidence of the presence of such doubly linked  $(\text{CN})_2$  molecules present in the double cyanides, *viz.*, in their Raman spectra.

The Raman spectra of simple and complex double cyanides have been studied by a large number of investigators ; the results obtained up to 1931 are included in Kohlrausch's book.<sup>2</sup> Subsequent to the publication of this book two important investigations by Damaschun<sup>3</sup> and by Samuel and Khan<sup>4</sup> have appeared. From a comparative study of the frequency shifts due to the  $\text{C}:\text{N}$  bonds in these simple and complex cyanides and also in similar compounds containing the  $\text{S. C. N}$  group, it has appeared to me that conclusions as to the existence of the  $(\text{CN}:\text{CN})$  group in the double cyanides can be reasonably inferred. It is the purpose of the present paper to show how the above conclusions can be reached.

Before proceeding to discuss the Raman spectra evidence, it will be necessary to give a short resumé of a portion of the previous paper in which the structure of the complex cyanides is discussed. As is well-known, the paramagnetic properties of the elements belonging to the first transition group and of their compounds is due to the magnetic properties of the electrons present in the incomplete d-shell of these atoms or of their ions. According to a theory proposed by the writer<sup>5</sup> the paramagnetic moment of the compounds can be calculated to a first approximation in the following way. Of the two magnetic moments of each electron present in the d-shell, *viz.*, those due to the orbital moment and to the spin-moment, the latter only is effective. Each electron contributes one Bohr magneton, and the resultant moment of the ion is equal to the algebraic sum of the

<sup>2</sup> Kohlrausch, *Stoekal-Raman Effekt*.

<sup>3</sup> Damaschun, *Zeit. f. Phys. Chem. B.*, 16, p. 81, 1932.

<sup>4</sup> Samuel and Khan, *Zeit. f. Phys.*, 84, 87 (1933).

<sup>5</sup> Bose, *Zeit. f. Phys.*, 43, p. 864, 1927.

moments due to all the electrons present in the d-shell, taking into consideration Pauli's Exclusion Principle. Therefore the magnetic moment  $n_B$  of an ion with  $Z'$  electrons in its d-shell is either

$$\begin{array}{ll} \text{equal to } Z' \text{ Bohr magnetons} & \text{if } Z' \leq 2l + 1 \\ \text{or to } 2(2l + 1) - Z' = 10 - Z' & \text{if } Z' \geq 2l + 1 \end{array}$$

where  $l = 2$  for the d-shell.

These paramagnetic elements can give rise to

(i) Cations like  $\text{Ni}^{++}$ ,  $\text{Cr}^{+++}$  etc., in which the parent atoms have lost their two 4s electrons and in the trivalent ions one d electron.

(ii) Cationic complexes like  $[\text{Co}(\text{NH}_3)_6]^{+++}$ , etc., where the ion has associated with it 4 or 6 neutral molecules like  $\text{NH}_3$ ,  $\text{H}_2\text{O}$ , etc. Some of these complexes have the same magnetic moment as the parent ions, others are either diamagnetic or have a lower paramagnetic moment. These belong to Werner's group of co-ordination compounds.

(iii) Anionic complexes, including double salts, the most important of which are, for our purpose, the cyanides, whose constitution we are going to discuss. In these complexes the paramagnetic atom does not lose any of its outer electrons, but in the majority of cases they take up electrons from their neighbours to fill the vacant places in their d-shells, and the complex becomes either diamagnetic or has a small residual paramagnetic moment.

In Table I are collected together the experimentally found values of the magneton numbers of the double cyanides of the transition elements. In column (3) are given the number of vacant places in the d-shell of the element, the magneton numbers of whose double cyanides are given in (5); (6) is obtained by subtracting (5) from (3), and represents the number of vacant places filled up in the d-shell of the paramagnetic atom in the double cyanide. This is found to be equal to the number of  $(\text{CN})^{--}$  groups present in the latter,

TABLE I.

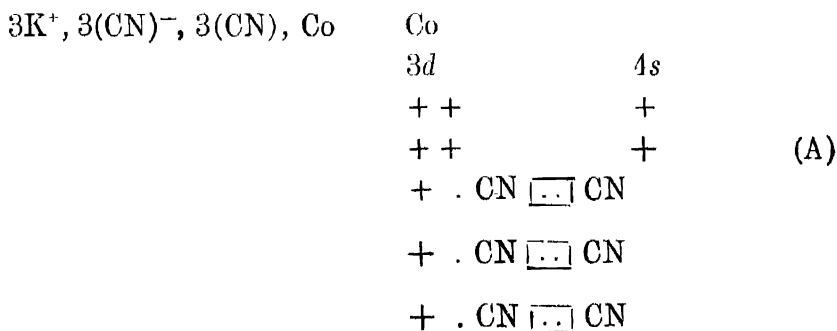
Atomic Number.	Element.	No. of Vacant places in 3d-shell.	Double Cyanides.	Magnetou number.	No. of Places filled up in d-shell.	No. of (CN) <sup>-</sup> group.
29	Cu	1	K[Cu(CN) <sub>2</sub> ]	0	1	1
28	Ni	2	K <sub>2</sub> [Ni(CN) <sub>4</sub> ]	0	2	2
27	Co	3	K <sub>3</sub> [Co(CN) <sub>6</sub> ]	0	3	3
26	Fe	4	K <sub>3</sub> [Fe(CN) <sub>6</sub> ]	1	3	3
	"	"	K <sub>4</sub> [Fe(CN) <sub>6</sub> ]	0	4	4
25	Mn	5	K <sub>3</sub> [Mn(CN) <sub>6</sub> ]	2	3	3
	"	"	K <sub>4</sub> [Mn(CN) <sub>6</sub> ]	1	4	4
24	Cr	6	K <sub>3</sub> [Cr(CN) <sub>6</sub> ]	3	3	3
	Mo	4d shell 6	K <sub>4</sub> [Mo(CN) <sub>6</sub> ] <sup>1</sup> / <sub>2</sub>	0		
	W	5d-shell 6	K <sub>4</sub> [W(CN) <sub>6</sub> ]	0		

which is shown in (7). These cyanides can be looked upon as being built of the following constituents, *viz.*,  $mK^+$  ions,  $m(CN)^-$  ions, the paramagnetic atom Me and  $n$  (CN) groups, giving rise to a compound with the formula  $K_m[Me(CN)_{m+n}]^{-m}$ . It will be seen that each one of the  $(CN)^-$  groups in a double salt contributes one electron to the d-shell of the paramagnetic atom so that if originally the atom had  $Z$  electrons in the d-shell, in the complex it has  $Z' = Z + m$  electrons and its magnetic moment  $n$  is equal to  $10 - Z'$ .

Now we shall consider in detail the mechanism by which the  $(CN)^-$  ion contributes an electron to the d-shell. In a previous paper<sup>6</sup> I have discussed the evidence for supposing that the (CN) molecule has the structure  $(1s)^2, (1s)^2, (2s)^2, (2p)^6, (3s)^1$ , *i.e.*,

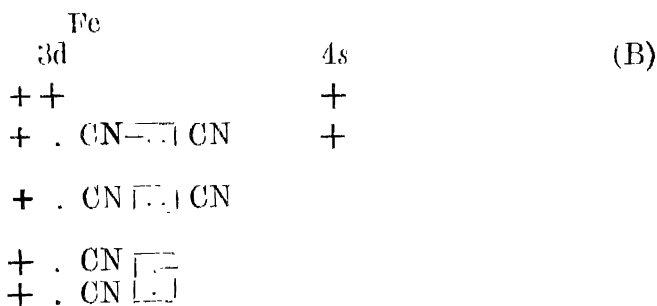
<sup>6</sup> Bose, Phil. Mag., 5, p. 1048, 1928.

in the molecule, each of the C and N atoms retain their respective shell of 1s electrons, both of which are enclosed in a common shell of 8 (2s, p) electrons, outside which there is one electron in a 3s shell,—the latter is the valency electron of the (CN) molecule. In the (CN)<sup>-</sup> ion there are 2 electrons in the 3s shell, which is then completely filled up with the spin axes of the two electrons oppositely oriented, so that the (CN)<sup>-</sup> ion is diamagnetic. Now if in these double cyanides each of the (CN)<sup>-</sup> ions contributes one electron to the d-shell of the paramagnetic atom, then the spin coupling between the two electrons in the 3s shell of the ion must be broken down, one of the electron enters the d-shell of the paramagnetic atom and the other electron has a free spin moment which, unless otherwise compensated, would go to increase the magnetic moment of the complex. But we find that the double cyanides have either zero or a greatly reduced paramagnetic moment. We have therefore to find a mechanism by which the free spin moment of the (CN)<sup>-</sup> ion in the complex is compensated. This can take place by attaching to each of the (CN)<sup>-</sup> ion a (CN) molecule, which has an unsaturated electron in its 3s-shell. In the majority of cases, the number of (CN)<sup>-</sup> and (CN) groups in the cyanides are equal, and in them we have the following structure, *viz.*, to each vacant place in the d-shell of the paramagnetic atom is attached a (NC : CN)<sup>-</sup> group. We will illustrate by writing the structural formula of K<sub>3</sub>Co(CN)<sup>6</sup>, which can be considered as being built up of the following constituents



Here + represents the electrons originally present in the d-shell of the Co atom, and · represents the electron originally in the valency shells of  $(\text{CN})^-$ , respectively of CN; the above diagram (A) shows the way they fill up the d-shell of the Co atom and saturate their own residual valencies.

We shall next consider the case of those cyanides in which the number of  $(\text{CN})^-$  group is greater than the number of CN groups, e.g.,  $\text{K}_4\text{Fe}(\text{CN})_6$ , which can be considered as being made up of  $4\text{K}^+$ ,  $4(\text{CN})^-$ ,  $2\text{CN}, \text{Fe}$ , and represented structurally as



Here the residual valencies of the last two  $(\text{CN})^-$  groups have to neutralise each other.

Thus the structural formula of  $\text{K}_3\text{Co}(\text{CN})_6$  can be written as  $\text{K}_3^+[\text{Co}(\text{NC}:\text{CN})_6^-]$  and of  $\text{K}_4\text{Fe}(\text{CN})_6$  as  $\text{K}_4^+ \left[ \frac{(\text{NC}:\text{CN})_2^-}{(\text{NC}:\text{CN})^{--}} \right]$

We have given above the structure of the double cyanides as deduced from a study of their magnetic properties. Next we shall consider what evidence in support of the above representation can be obtained from study of the Raman spectra of these complex cyanides. It is to be expected that the Raman spectra of the CN groups found in these compounds will show certain characteristic frequencies, which will be slightly different in the two cases A and B considered above.

It is known that the chemical properties of the  $(\text{CN})^-$  group is in many ways similar to those of Cl, and from analogy we can expect that the  $(\text{CN})^-$  ion will have some properties similar to

that of O, and in those cases where the mass of the radical has to be taken into account, *e.g.*, in influencing infra-red vibration frequencies, the similarity will be more with the S atom.

TABLE II.

	$\Delta\nu$	Inner Vibration $C\equiv N$ , in
Me (CN) ...	2087	(CN) <sup>-</sup>
Me S(CN) ...	2056	(S. CN) <sup>-</sup>
R. S(CN) ...	2148	(S. ON) group in covalent bond
R. (CN) ...	2250	(CN) group in covalent bond

TABLE III.

	i	ii		iii
		$\alpha$	$\beta$	
KAg (CN) <sub>2</sub> ...	290 (m)	...	...	2130 (St)
K <sub>2</sub> Ni (CN) <sub>3</sub> ...	..	...	...	2142 (m)
K <sub>2</sub> Ni (CN) <sub>4</sub> ...	...	...	...	2150 (St)
K <sub>2</sub> Zn (CN) <sub>4</sub> ...	...	2055 (w)	...	2149 2150
K <sub>2</sub> Cd (CN) <sub>4</sub> ...	...	...	...	2184 2150
K <sub>3</sub> Cu (CN) <sub>4</sub> ...	...	...	2095 2092 (St)	2176 (w) ...
K <sub>3</sub> Co (CN) <sub>6</sub> ...	340 405 (w)	2070 (w)	...	2141 (St) 2148 (m)
K <sub>3</sub> Rh (CN) <sub>6</sub> ...	593 (w)	...	...	2149 (m)
K <sub>3</sub> Cr (CN) <sub>6</sub> ...	782	...	...	2137 (w)
K <sub>4</sub> Cr (CN) <sub>6</sub> ...	619 (v.w)	...	...	2130 (m)
K <sub>4</sub> Fe (CN) <sub>6</sub> ...	...	2051 (St)	2092 (St)	2153(w), 2195(w)
K <sub>4</sub> Ru (CN) <sub>6</sub> ...	381 (w)	...	...	2068, 2107

Table II has been compiled by Samuel and Khan<sup>4</sup> from the data found in Kohlrausch's book ;<sup>2</sup> it shows how the C—N resp. the S.C≡N oscillation frequency is influenced by the presence of other groups attached by covalent or electrovalent bonds.

In Table III are collected together the principal oscillation frequencies observed in a number of double and complex cyanides. The data are collected together from Kohlrausch's book<sup>2</sup> and from the papers of Damascun<sup>3</sup> and of Samuel and Khan.<sup>4</sup>

The values of  $\Delta\nu$  found for the Raman shift, has been divided into three groups, of which those in the first are of comparatively small values, varying from  $290\text{ cm}^{-1}$  to  $782\text{ cm}^{-1}$ . They represent evidently the oscillation frequencies of the co-ordinated (CN) group with respect to the central atom. It is rather remarkable, as pointed out by Samuel and Khan,<sup>4</sup> that none of the double salts containing 4 CN groups, show the presence of a frequency shift lying in this region ; in the case of  $\text{K}_2\text{Ni}(\text{CN})_4$ , which is diamagnetic, and therefore with strong co-ordination bonds, the expected presence of frequency shifts in this region was vainly looked for by these authors. The second group of frequency shifts can be divided into two sub-groups  $\alpha$  and  $\beta$ , of which those under  $\beta$  have values very near that due to the ionised  $(\text{CN})^-$ , viz.,  $\Delta\nu = 2087\text{ cm}^{-1}$ . This shows that a portion of the double cyanides in solution are dissociated, giving rise to free  $(\text{CN})^-$  radicals.

The group of frequency shifts tabulated under  $ii(\alpha)$  have the values 2055, 2051, 2070 with a mean value of 2059, which is very near the value of 2064 found for the  $(\text{SCN})^-$  radical. In the third column, if we exclude for the present the shifts observed for the last three salts in which there are four  $(\text{CN})^-$  groups, we find their mean value is  $\Delta\nu = 2140$ , which is sufficiently near to the value of  $\Delta\nu$  found for the (SCN) group held in covalent bond to an organic radical, to permit the assumption of a similarity of structure between the (SCN) radical and the cyanogen groups present in the double cyanides.



We thus find that in the Raman spectra due to the double cyanides in solution there are two groups of frequency shifts with mean value of 2140, 2059 which are very near to the frequency shifts due to the (CN) group in the (SCN) radical present respectively in non-ionised and ionised states. We can therefore assume that in these complex salts, the (CN) groups are present in the form  $(\text{NC} : \text{CN})^-$  in which the  $\text{CN}^-$  group acts in the same way as the S atom in the radical (S.CN).

The structure which we have deduced for the cyanides from Raman spectra evidence is thus in agreement with the structure of the paramagnetic cyanides which have been obtained from a study of their magnetic properties.

We will now take up the consideration of the Raman spectra of the cyanides, containing  $\frac{1}{2}$   $(\text{CN})^-$  groups, which are placed in the bottom of Table III. As shown above, in these compounds, there are two  $(\text{CN})_2^-$  groups and one  $(\text{CN})_2^{--}$ , which are bound by covalent bond to the central atom. Corresponding to these two types of binding of the  $(\text{CN})_2$  groups with central atom, we should expect two modified frequencies of the CN vibration, one of which ought to be the same as that found for the previous group of cyanides. This expectation is fulfilled in the case of  $\text{K}_4\text{Fe}(\text{CN})_6$ . The other value of  $\Delta\nu$  is greater by about  $40\text{ cm}^{-1}$  and is due to the stronger binding of the  $(\text{CN})_2^{--}$  group to the central atom. In the case of  $\text{K}_1\text{Ru}(\text{CN})_6$  we also get two different frequencies, differing by about  $40\text{ cm}^{-1}$  which is the same as in the previous case, but their absolute values are less and come nearer to those given under (ii) for the previous compound. The presence of a low frequency shift under (i) for this compound inclines us to the assumption that the former are due to the  $(\text{CN})_2^{--}$  groups in covalent bond, rather than due to the ionised groups. The values of  $\Delta\nu$  for  $\text{K}_4\text{Cr}(\text{CN})_6$  are nearly the same as for  $\text{K}_5\text{Cr}(\text{CN})_6$ . It is known that the first named compound is rather unstable, and in solution it probably changes into the latter form.

*Concluding Remark*—The nature of the valency bond contributed by the (CN) group in the double salts is the basis of our interpretation, given in the previous paper, of Sidgwick's theory of co-ordination bond. An investigation of the Raman spectra of the hexamine salts of the iron group is being undertaken in our laboratory, and further discussion is deferred pending the conclusion of this investigation.

## Space Group and Atomic Arrangements in Anthraquinone Crystals, Part I.\*

BY

KEDARESWAR BANERJEE, D. SC., AND BHAGAWATI CHARAN GUHA, M. SC.

*Dacca University, Dacca.*

*(Received for publication, September 27, 1934.)*

### ABSTRACT.

Oscillation photographs of meso-anthraquinone have been taken by a camera of good resolving power; hko planes with  $h+k$  odd do not reflect and goniometer measurements show the existence of a centre of symmetry. The space-group is therefore  $D_{2h} p \mu \mu \nu$  ( $V_h^{13}$  according to Schönflies notation).

In recent years, a number of aromatic organic crystals have been completely studied and their atomic arrangements determined by the help of X-ray diffraction as well as from the measurements of their magnetic properties.<sup>1</sup> All the substances that have been studied have shown that the benzene ring in aromatic compounds is plane and different adjacent benzene rings in the same molecule lie in the same plane except dibenzyl where the two plane benzene rings lie parallel to each other but in two different planes. Even substitution does not change the benzene ring from its planar structure, as is shown by hexamethyl benzene, hexachlorobenzene, and p-dinitrobenzene.<sup>2</sup> In hexamethyl benzene and hexachlorobenzene the carbon and the chlorine atoms are in the same plane as in the benzene ring. But in p-dinitrobenzene it is

\* Read before the Inaugural Meeting of the Indian Physical Society on the 29th September, 1934.

not so. So it may be interesting to examine this point for other substitution products and for that in view the study of anthraquinone has been taken up.

Anthraquinone crystals belong to the orthorhombic class with axial ratios

$$a : b : c = 0.8004 : 1 : 0.1607.$$

The cell dimension has been found recently by Hertel and Römer<sup>3</sup> to be

$$a = 19.7 \text{ \AA} ; b = 24.5 \text{ \AA} ; c = 3.95 \text{ \AA},$$

and by Caspari<sup>4</sup> to be

$$a = 19.65 \text{ \AA} ; b = 24.57 \text{ \AA} ; c = 4.00 \text{ \AA}.$$

with 8 molecules per unit cell.

For crystallisation Kahlbaum's pure anthraquinone was taken. The substance was crystallised from benzene. Axial lengths as determined by us from layer line diagrams about the three crystallographic axes are

$$\begin{aligned} a &= 19.7 \text{ \AA} \\ b &= 24.6 \text{ \AA} \\ c &= 3.95 \text{ \AA} \end{aligned}$$

Oscillation photographs about the 'b' and the 'c' axes were taken with ranges of  $10^\circ$ . The exposures were fairly long such that the intense spots were heavily overexposed; this was done in order as far as possible, to avoid missing reflection from any plane. As the axial lengths along b and c are very long the spots in an ordinary camera should over-lap and render identification impossible. To avoid this, a camera with 17.19 cm. diameter was used. This was cut out of a brass cylinder and the axis of rotation of the goniometer head was fixed very accurately coinciding with the axis of the cylindrical frame for the photographic film. Thereby a very large number of reflections could be identified. In the following tables are given the indices of the reflecting planes and their estimated intensities.

TABLE I.

*Rotation about 'b' axis.*

Indices	Intensity	Indices	Intensity	Indices	Intensity
102	m	622	m	152	v. w.
401	st.	623	m	153	m
402	m	820	st.	551	m
600	st.	(10)20	m	552	w
703	m	(10)21	w	751	m
800	m	(14)21	m	951	m
803	m	(14)22	w	(11)51	st.
(10)00	w	(16)22	w	(13)51	m
(10)02	w	132	m	262	m
(12)00	m	331	v. st.	661	st.
(12)02	st.	531	st.	(10)60	st.
(15)01	w	532	w	(10)61	st.
(16)01	m	731	st.	171	w
011	st.	733	m	372	m
112	m	(11)31	w	571	st.
311	st.	(11)32	w		
312	m	(13)32	st.		
511	m	441	m		
711	w	442	w		
713	w	741	m		
811	m	840	st.		
911	st.	841	m		
(13)12	w	842	m		
(15)11	w	843	w		
221	v. st.	(12)41	m		
222	w	(12)42	w		
621	w	(16)41	w		

TABLE II.

*Rotation about 'c' axis.*

Indices	Intensity	Indices	Intensity	Indices	Intensity
040	v. st.	840	st.	(19)(15)0	v. w.
0(16)0	w	860	w	(14)20	v. w.
0(22)0	m	880	m	(14)40	v. w.
1(13)0	v. st.	8(12)0	v. w.	(14)60	w
260	st.	8(16)0	st.	(14)80	m
2(10)0	v. w.	910	v. w.	(14)(10)0	v. w.
2(14)0	m	930	v. w.	(14)(14)0	w
2(18)0	w	950	w	(16)20	m
2(20)0	w	9(11)0	v. w.	(16)40	m
400	m	9(15)0	w	(16)60	v. w.
440	x. st.	9(19)0	m	(16)80	v. w.
480	st.	(10)20	m	(16)(10)0	st.
4(12)0	v. w.	(10)60	st.	(17)50	v. w.
4(16)0	w	(10)(14)0	w	(17)70	v. w.
5(13)0	w	(10)(18)0	m	(18)20	m
620	st.	(11)10	w	(18)60	v. w.
660	w	(11)30	w		
6(10)0	m	(11)50	st.		
6(14)0	m	(11)70	st.		
6(18)0	v. w.	(11)(13)0	m		
6(22)0	w	(11)(17)0	m		
750	st.	(12)20	st.		
7(15)0	m	(12)40	v. w.		
7(17)0	st.	(12)80	w		
		(12)(12)0	w		
		(12)(16)0	m		

TABLE II (*continued*).

Indices	Intensity	Indices	Intensity	Indices	Intensity
0 (12) 1	v. w.	661	st.	(10) 61	w
0 (22) 1	v. w.	671	st.	(10) (10) 1	w
131	v. st.	681	v. w.	(10) (12) 1	w
151	m	6 (10) 1	m	(10) (14) 1	w
191	m	6 (12) 1	w	(10) (16) 1	v. w.
1 (11) 1	v. w.	6 (14) 1	w	(11) 31	m
1 (15) 1	w	6 (18) 1	m	(11) 51	m
1 (21) 1	v. w.	711	m	(11) 61	v. w.
221	v. st.	731	st.	(11) 71	v. w.
261	w	771	m	(11) 91	w
2 (12) 1	w	7 (11) 1	w	(11) (13) 1	w
2 (14) 1	v. w.	7 (13) 1	v. w.	(11) (17) 1	v. w.
311	m	7 (15) 1	m	(12) 41	v. w.
331	v. st.	7 (19) 1	st.	(12) 51	m
371	st.	811	m	(12) 81	w
3 (17) 1	v. w.	881	m	(12) (13) 1	w
3 (19) 1	v. w.	891	v. w.	(12) (16) 1	w
401	v. st.	8 (10) 1	w	(13) 21	v. w.
441	st.	8 (12) 1	v. w.	(13) 31	w
451	m	8 (14) 1	v. w.	(13) 41	v. w.
481	m	8 (16) 1	w	(13) 61	v. w.
4 (10) 1	m	8 (18) 1	w	(13) 81	m
4 (12) 1	w	8 (20) 1	w	(13) (10) 1	m
4 (16) 1	v. w.	921	st.	(13) (12) 1	w
4 (20) 1	v. w.	951	m	(14) 01	v. w.
511	st.	961	w	(14) 91	w
531	st.	971	v. w.	(15) 31	m
551	v. st.	981	v. w.	(15) 51	v. w.

TABLE II (*continued*).

Indices	Intensity	Indices	Intensity	Indices	Intensity
591	w	991	w	(15) 81	w
5 (11) 1	v.w.	9 (13) 1	v.w.	(16) 21	m
5 (13) 1	w	9 (15) 1	m	(16) 51	w
5 (19) 1	m	9 (17) 1	v.w.	(16) 81	w
621	w	(10) 21	w	(16) 91	m
				(17) 11	v.w.

Hertel and Romer<sup>3</sup> observed some reflections by the Weissenberg goniometer and Caspari<sup>4</sup> obtained a number of reflections by the oscillation method. The reflections observed by them were mostly found by the author over and above a number of other planes. It is found that the  $hko$  planes with  $h+k$  odd are systematically absent. No other systematic "ausloschungen" were observed.

Caspari observed that reflections from all planes with  $h+k$  odd were absent. But we have from our measurements definite evidence of reflection from a number of planes of the type  $hkl$  where  $h+k$  is odd, but they are absent when  $l$  is zero. A list of such planes are given below with their estimated intensities.

This shows that the molecule at the centre of the  $ab$  face is not obtained by translation but by a glide reflection, the glide being along the diagonal on  $ab$  face. Thus the third plane of reflection is to be represented by  $\nu$  and hence the space-group is  $D_{2h}p\mu\mu\nu$  ( $V_h^{18}$  according to Schönflies). The number of atoms per unit cell is 8 and therefore, the molecules do not possess any symmetry in the lattice.

From his observations Caspari came to the conclusion that the space-group is  $V^6$ . From the "ausloschungen" observed by him, the space, group corresponds to  $V_h^{19}$  if the crystal belongs to



TABLE III.

Planes that preclude the possibility of a face-centred lattice.

Indices	Intensity	Indices	Intensity
102	m	(12) 51	m
703	m	(12) (13) 1	w
(15) 01	w	(13) 21	v. w.
011	st.	(13) 41	v. w.
811	m	(13) 61	v. w.
741	m	(13) 81	m
451	m	(13) 101	m
671	st.	(13) (12) 1	w
891	v. w.	(14) 31	w
921	st.	(15) 81	w
961	w	(16) 51	w
981	v. w.	(16) 91	m
(11) 61	v. w.		

the orthorhombic bipyramidal class. But in that case the anthraquinone molecule is to be given a plane of symmetry in order that the molecules may be fitted into the cell. But from all the aromatic compounds that have so far been studied, it appears that the anthraquinone molecule can have neither a plane nor an axis of symmetry. Caspari concluded that this crystal belongs to the orthorhombic bisphenoidal class against the measurements of Fels.<sup>5</sup> To test this point, we made goniometric measurements of the faces of two crystals which were chosen for showing no sign of twinning in X-rays. The existence of the centre of symmetry was found in both the crystals, and thus its classification as bisphenoidal is precluded. The difficulties of explaining the symmetries do not however, come in if the space-group is taken to be  $V_h^{18}$  as is found by us.

The paucity of reflections of type  $hkl$  with  $h+k$  odd is due to the fact that since all the benzene rings are in one plane except for the side hydrogens and oxygens, there is a pseudo plane of symmetry of scattering matter in the molecule.

### *References.*

- <sup>1</sup> K. Banerjee, Ind. Jour. Phys., Vol. IV, p. 557, 1930.  
K. S. Krishnan, B. C. Guha and S. Banerjee, Phil. Tran. Series A., Vol, 231, pp. 235-62, 1933.  
J. Dhar, Ind. Jour. Phys., Vol. VII, p. 43, 1932  
J. M. Robertson, Roy. Soc. Proc., Vol. 140, p. 79, 1933.  
Vol. 141, p. 594, 1933.  
Vol. 142, p. 674, 1933.  
<sup>2</sup> K. Banerjee, Under publication.  
<sup>3</sup> E. Hertel and H. Romer, Zeit. f. Physik. Chemie. Bd. 11 B, p. 90, 1931.  
<sup>4</sup> W. A. Caspari, Proc. Roy. Soc. A. Vol. 136, p. 82, 1932.  
<sup>5</sup> Groth's Chemische Krystallographie, Vol. 5, p. 442.

# Rotational Raman Scattering in Benzene Vapour.<sup>1</sup>

By

S. C. SARKAR, D.Sc.

Plate V.

(Received for publication, 28th September, 1934.)

## ABSTRACT.

The rotational Raman spectrum of benzene vapour has been successfully recorded with the help of a spectrograph producing lines which are absolutely free from coma on the Stokes side in the region of  $\lambda 4046$ . It has been found that in the case of benzene vapour at  $210^{\circ}\text{C}$  and under a pressure of 16.6 atmospheres, the rotational wing is detached from the Rayleigh line, and that starting with zero intensity at about  $7\text{ cm}^{-1}$  from the centre of the Rayleigh line, the wing has a maximum intensity at a distance of about  $26\text{ cm}^{-1}$  from the said point and extends up to about  $70\text{ cm}^{-1}$  from the Rayleigh line. These observed facts are in fair agreement with the theory.

## 1. Introduction.

The theory of the rotational Raman scattering by polyatomic molecules has been put forward recently by Placzek and Teller.<sup>2</sup> According to this theory, in the case of a polyatomic molecule which can be represented by a symmetrical top, the transitions  $\Delta J = \pm 1$  are allowed besides the transitions  $\Delta = 0$  or  $\pm 2$ , which are generally observed in the case of diatomic molecules,  $J$  being the quantum number of the total rotational impulse. Also, when the polyatomic molecule is heavy, the rotational wing should start with zero intensity at the centre of the Rayleigh line and after

<sup>1</sup> Read before the Inaugural Meeting of the Indian Physical Society on the 29th September, 1934.

<sup>2</sup> G. Placzek and E. Teller, *Z. f. Phys.*, 81, 209 (1933).

having a maximum intensity at a certain distance, should extend up to a definite distance from the centre of the Rayleigh line, these distances depending on the moment of inertia and the temperature of the molecule. The facts observed in the case of gaseous ammonia by Amaldi and Placzek<sup>3</sup> are in fair agreement with the theory. In the case of liquid benzene, however, the distribution of intensity in the rotational wing observed by several authors<sup>4, 5, 6, 7</sup> is not in agreement with the prediction of the theory. Bhagavantam<sup>6</sup> has suggested that the cause of the above discrepancy in the case of liquid benzene is due to the fact that some of the benzene molecules in the liquid state are grouped together and behave as those in the solid, and the intermolecular vibrations in such groups give rise to a continuous Raman band superposed on the rotational wing. In the case of benzene vapour, however, no such complication is expected. The distribution of intensity in the rotational wing due to benzene vapour has, therefore, been investigated with suitable technique and the results are reported in the present paper.

## 2. *Experimental.*

There are two main difficulties in the experimental investigation of the rotational Raman spectra of polyatomic molecules in the gaseous state. First, the scattering in vapours is very feeble and secondly, it is difficult to eliminate stray light completely, so that the undisplaced line becomes overexposed and in the case of most of the spectrographs of large aperture a fairly intense coma is produced in the neighbourhood of the undisplaced line when the latter is very intense. The first difficulty was overcome by producing benzene vapour under high pressure so that the scattering was fairly intense. A small quantity of pure benzene distilled in vacuum was sealed inside a stout Jena glass

<sup>3</sup> E. Amaldi and G. Placzek, Z. f. Phys., 81, 259 (1933).

<sup>4</sup> J. Weiler, Z. f. Phys., 68, 782 (1931).

<sup>5</sup> S. P. Ranganadham, Ind. J. Phys., 7, 353 (1932).

<sup>6</sup> S. Bhagavantam, Ind. J. Phys., 8, 197 (1933).

<sup>7</sup> S. Bhagavantam and A. V. Rao, Ind. J. Phys., 8, 437 (1934).

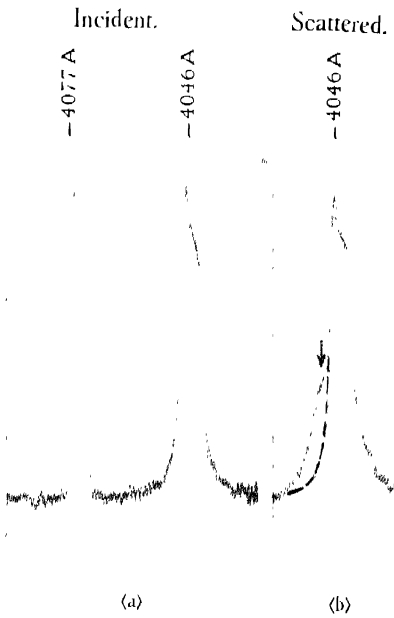


Fig. 1



tube of external diameter about 20 mm. One end of the tube served as the window through which the scattered light could be observed. The tube was heated upto  $210^{\circ}\text{C}$  in a cylindrical electric heater which was provided with two windows, one along its length through which the tube could be illuminated and the other at one of its ends through which the scattered light could be observed. Benzene vapour under a pressure of about 16.6 atmospheres was thus produced inside the tube. One of the Fuess glass spectrographs of this laboratory was found to produce lines which are absolutely free from coma on the Stokes side in the region of  $\lambda 4046$ , though there is a fairly intense coma on the anti-Stokes side. This spectrograph was used in the present investigation and therefore the presence of feeble stray light only increased a little the density of the undisplaced line, but did not produce any coma superposed on the rotational wing on the Stokes side. Precautions were also taken to cut down the intensity of the stray light by using suitable apertures in black screens and by using a condenser to focus the light from a mercury arc on the tube. The scattered spectrum was recorded with an exposure of about 10 hours on an Ilford Golden Isozenith plate, the width of the slit being 0.015 mm. Intensity marks were taken with the help of a standard tungsten ribbon lamp by varying the width of the slit of the spectrograph. The direct mercury arc spectrum was also recorded with proper density and with the same width of the slit.

### 3. *Results and Discussion.*

The microphotometric records of the mercury lines  $\lambda 4046$  and  $\lambda 4077$  in the incident and of  $\lambda 4046$  in the scattered spectrum are reproduced in Plate V in Figs. 1(a) and 1(b) respectively. The dotted portion of the curve drawn in Fig. 1(b) would be obtained in absence of the rotational wing. On measuring the distribution of intensity in the wing, the curve in continuous line shown in Fig. 2 is obtained. It is difficult to draw the theoretical curve for

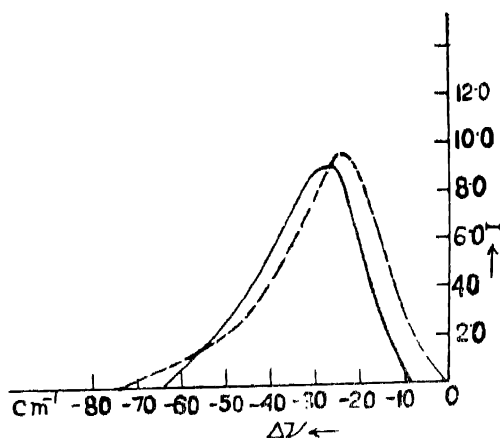


FIG. 2

benzene molecule at  $210^{\circ}\text{C}$  according to the theory of Placzek and Teller. But in Fig. 1a on page 242 of the paper by the said authors, the distribution of intensity in the rotational wing due to a plane molecule which can be represented by a symmetrical top, has been shown graphically. If the position of the maximum intensity in this curve is taken at about  $23\text{ cm}^{-1}$  from the centre of the Rayleigh line, a very rough theoretical curve is obtained which is shown by the dotted curve in Fig. 2. The following three points, however, are definitely established by the present investigation, *e.g.*, (1) the rotational wing in the case of benzene vapour is detached from the Rayleigh line and starts with zero intensity at a distance of about  $7\text{ cm}^{-1}$  from the latter, (2) the wing has a maximum intensity at about  $26\text{ cm}^{-1}$  from the centre of the Rayleigh line and (3) the wing extends only up to about  $65\text{ cm}^{-1}$  from the Rayleigh line and does not extend up to  $130\text{ cm}^{-1}$  as observed in the case of liquid benzene by previous authors.

The author is indebted to Prof. D. M. Bose for his kind interest in the work.



# On the Generalised Equation of Heat-Conduction\*

BY

M. RAZIUDDIN SIDDIQI, HYDERABAD.

(Received for publication, September 22, 1934.)

## ABSTRACT.

Solution is sought of the non-linear equations of heat-conduction for non-homogeneous bodies, i.e., of

$$\frac{\partial}{\partial x} \left\{ p(x) \frac{\partial U}{\partial x} \right\} - \frac{\partial U}{\partial t} = U^2$$

with boundary conditions

$$U(0, t) = U(\pi, t) = 0 \quad \text{for all } t \geq 0$$

$$U(x, 0) = f(x) \quad \text{for all values of } x \text{ between } 0 \text{ and } \pi.$$

The solution  $U(x, t)$  is determined in a series of Sturm-Liouville characteristic functions

$$U(x, t) = \sum_{n=1}^{\infty} v_n(t) \phi_n(x).$$

The problem of determining the co-efficients  $v_n(t)$  leads to an infinite system of non-linear integral equations which is solved by the method of successive approximations developed by the author. The uniqueness of the solution is proved.

\* Read before the Inaugural Meeting of the Indian Physical Society on the 29th September, 1934.

*Introduction.*

The equation of Heat-Conduction in a homogeneous rod on the old theory is known to be

$$\frac{\partial^2 U}{\partial x^2} - \frac{1}{a^2} \frac{\partial U}{\partial t} = 0$$

with suitable boundary and initial conditions. But in non-homogeneous bodies, and for Heat-Conduction in a deep sea, etc., the term  $\frac{\partial^2 U}{\partial x^2}$  has to be replaced by

$$\frac{\partial}{\partial x} \left\{ p(x) \frac{\partial U}{\partial x} \right\},$$

where  $p(x)$  is a positive function. Moreover, newer theories such as those of Quantum Statistics appear to show that the equation cannot be of such a simple form; there should be a term non-linear in  $U$  on the right-hand side.

Non-linear equations for homogeneous bodies have been considered by the writer in previous papers.<sup>1</sup> The present one deals with the same problem for non-homogeneous bodies. Thus we consider the equation :

$$\frac{\partial}{\partial x} \left\{ p(x) \frac{\partial U}{\partial x} \right\} - \frac{\partial U}{\partial t} = U^2$$

for the boundary conditions :

$$U(0, t) = U(\pi, t) = 0 \quad \text{for all } t \geq 0.$$

$$U(x, 0) = f(x) \quad \text{for all } x \text{ in } 0 \leq x \leq \pi.$$

We determine the solution  $U(x, t)$  in a series of the Sturm-Liouville characteristic functions :

$$U(x, t) = \sum_n v_n(t) \phi_n(x).$$

The summation over  $n$  is taken from 1 to  $\infty$  throughout this paper.

The problem of determining the co-efficients  $v_n(t)$  leads to an infinite system of non-linear integral equations which is solved by the method of successive approximations developed already by the author.<sup>2</sup> Finally the uniqueness of the solution is established.

*Existence and Uniqueness of the Solution.*

Let  $p(x)$  be an essentially positive function  $>1$  in the interval  $0 \leq x \leq \pi$ ,\* and let  $p(x)$  as well as its first two derivatives be continuous and uniformly bounded in the whole interval :

$$(1) \quad \left| p(x) \right| < M, \quad \left| \frac{dp}{dx} \right| < M, \quad \left| \frac{d^2p}{dx^2} \right| < M$$

where  $M$  is an absolute constant.

We try to determine a regular solution of the non-linear partial differential equation

$$(2) \quad \frac{\partial}{\partial x} \left\{ p(x) \frac{\partial U}{\partial x} \right\} - \frac{\partial U}{\partial t} = U^2$$

which is regular in the domain :

$$(3) \quad 0 \leq x \leq \pi, \quad 0 \leq t,$$

and which satisfies the boundary conditions :

$$(4) \quad U(0, t) = U(\pi, t) = 0 \quad \text{for all } t \geq 0.$$

$$(5) \quad U(x, 0) = f(x) \quad \text{for all } x \text{ in } 0 \leq x \leq \pi.$$

Let  $\lambda_n$  be the characteristic values and  $\phi_n(x)$  the corresponding characteristic functions of the Sturm-Liouville differential

\* For convenience we have taken the interval to be of length  $\pi$ ; obviously any other number can be taken without any essential alteration.

equation in

$$0 \leq x \leq \pi$$

$$(6) \quad \frac{d}{dx} \left\{ p(x) \frac{dy}{dx} \right\} + \lambda y =$$

or the boundary conditions

$$(7) \quad y(0) = 0, \quad y'(\pi) = 0.$$

We assume that  $\phi_n(x)$  is a complete system of normalised orthogonal characteristic functions. The asymptotic expansions of  $\lambda_n$ ,  $\phi_n(x)$  and  $\frac{d\phi_n}{dx}$  are known to be<sup>5</sup>

$$\lambda_n = n^2 \frac{\pi^2}{l_1^2} + O(1), \quad \sqrt{\lambda_n} = n \frac{\pi}{l_1} + O\left(\frac{1}{n}\right)$$

$$(8) \quad \phi_n(x) = a_n \frac{\sin nq(x)}{4 \sqrt{p(x)}} + O\left(\frac{1}{n}\right)$$

$$\frac{d\phi_n}{dx} = a_n \frac{n\pi}{l_1} \frac{\cos nq(x)}{5 \sqrt{p(x)}} + O(1),$$

where

$$l_1 = \int_0^\pi \frac{1}{\sqrt{p(x)}} dx,$$

$$(9) \quad q(x) = \frac{\pi}{l_1} \int_0^x \frac{1}{\sqrt{p(x)}} dx,$$

$$\frac{1}{a_n^2} = \int_0^\pi \frac{\sin^2 nq(x)}{\sqrt{p(x)}} dx.$$

Now we assume that the given boundary function  $f(x)$  can be expanded in a series of  $\phi_n(x)$ :

$$(10) \quad f(x) = \sum_{n=1}^{\infty} c_n \phi_n(x)$$

such that the series  $\sum_n \lambda_n |c_n|$  is convergent.

$$(11) \quad \sum_n \lambda_n |c_n| = c \quad (c \text{ is a constant}).$$

Lichtenstein<sup>4</sup> has investigated conditions under which a function  $f(x)$  can be expanded in a series of  $\phi_n(x)$ . In physical problems it is preferable to determine a solution in a Fourier Series or in the allied series of  $\phi_n(x)$ . Accordingly we set for the solution

$$(12) \quad U(x, t) = \sum_n v_n(t) \phi_n(x),$$

when the problem reduces to the determination of the co-efficients  $v_n(t)$  so that the equation (2) and the boundary condition (5) may be satisfied. We see that for any function  $v_n(t)$ , the series (12) already satisfies the boundary condition (4). If we could determine  $v_n(t)$  so that for all  $n \geq 1$

$$(13) \quad v_n(0) = c_n,$$

then the boundary condition (5) will also be satisfied. We assume for the present that the series (12) is absolutely and uniformly convergent in the domain (3).

Then we have

$$(14) \quad U^2(x, t) = \sum_n Z_n(t) \phi_n(x),$$

where

$$(15) \quad Z_n(t) = \sum_{k,l=1}^{\infty} f_n(k, l) v_k(t) v_l(t)$$

and

$$(16) \quad f_n(k, l) = \int_0^1 \phi_k(x) \phi_l(x) \phi_n(x) dx.$$

Assuming, what will be proved later that the series

$$(17) \quad \sum_n \lambda_n v_n(t) \phi_n(x) \quad \text{and} \quad \sum_n \frac{dv_n}{dt} \phi_n(x)$$

are absolutely and uniformly convergent in the domain (3) we get on substituting from (12) and (14) in (2) :

$$(18) \quad -\sum_n \lambda_n v_n(t) \phi_n(x) - \sum_n \frac{dv_n}{dt} \phi_n(x) = \sum_n Z_n(t) \phi_n(x)$$

so that for all  $n \geq 1$  we get, since all the  $\phi_n$  are independent.

$$(19) \quad \frac{dv_n}{dt} + \lambda_n v_n(t) = -Z_n(t).$$

A solution of this differential equation which satisfies the condition (13) is

$$v_n(t) = c_n e^{-\lambda_n t} - \int_0^t e^{-\lambda_n(t-s)} Z_n(s) ds$$

$$(20) \quad = c_n e^{-\lambda_n t} - \int_0^t e^{-\lambda_n(t-s)} \sum_{k,l} f_n(k,l) v_k(s) v_l(s) ds.$$

We get for all  $n \geq 1$ ,

$$(21) \quad w_n(t) = \lambda_n v_n(t); \quad \gamma_n = \lambda_n c_n,$$

then the equation (2) becomes :

$$(22) \quad w_n(t) = \gamma_n e^{-\lambda_n t} - \lambda_n \int_0^t e^{-\lambda_n(t-s)} \sum_{k,l} \frac{f_n(k,l)}{\lambda_k \lambda_l} w_k(s) w_l(s) ds$$

( $n=1, 2, 3, \dots$ ).

This is an infinite system of non-linear integral equations for the determination of  $w_n(t)$ , and consequently of the required co-efficients  $v_n(t)$  which are equal to  $\frac{1}{\lambda_n} w_n(t)$ . We solve the equation (22) by the method of successive approximations, and write for this purpose :

$$(23) \quad w_n^{(0)}(t) = \gamma_n e^{-\lambda_n t}$$

and for all  $m \geq 1$

$$(24) \quad w_n^{(m)}(t) = \gamma_n e^{-\lambda_n t} - \lambda_n \int_0^t e^{-\lambda_n(t-s)} \sum_{k,l} \frac{f_n(k,l)}{\lambda_k \lambda_l} w_k^{(m-1)}(s) w_l^{(m-1)}(s) ds$$

The question now is to prove that the sequence  $w_n^{(m)}(t)$  really converges to a limiting function for  $m \rightarrow \infty$ . This we proceed to do as follows:

First of all, we prove that the infinite series

$$(25) \quad \sum_n \lambda_n \int_0^t e^{-\lambda_n(t-s)} ds \frac{f_n(k,l)}{\lambda_k \lambda_l}$$

converges absolutely and uniformly for all  $t > 0$  and all  $k, l \geq 1$ .

In fact, we have for all  $t > 0$ ,

$$(26) \quad \int_0^t e^{-\lambda_n(t-s)} ds = e^{-\lambda_n t} \int_0^t e^{\lambda_n s} ds = \frac{1}{\lambda_n} \frac{e^{\lambda_n t} - 1}{e^{\lambda_n t}} \leq \frac{1}{\lambda_n}.$$

Therefore the series

$$\sum_n \left| \lambda_n \int_0^t e^{-\lambda_n(t-s)} ds \cdot \frac{f_n(k,l)}{\lambda_k \lambda_l} \right| \leq \sum_n \lambda_n \cdot \frac{1}{\lambda_n} \frac{|f_n(k,l)|}{\lambda_k \lambda_l} \leq \sum_n \frac{|f_n(k,l)|}{\lambda_k \lambda_l}.$$

In a previous paper,<sup>5</sup> the writer has shown that

$$\frac{\sum_n |f_n(k,l)|}{\lambda_k \lambda_l} \leq A$$

where

$$(27) \quad A = \frac{\pi}{3} (1 + M) B^3 l_1^3 > 1,$$

where  $B$  is the upper bound of  $\phi_n(x)$ , and  $l_1$  is given by (9). We see therefore that the series (25) is absolutely and uniformly convergent and that

$$(28) \quad \sum_n \lambda_n \int_0^t e^{-\lambda_n(t-s)} ds \cdot \frac{|f_n(k,l)|}{\lambda_k \lambda_l} \leq A.$$

From (24) we get then on account of (11) and (28) for all  $t$ :

$$(29) \quad \sum_n |w_n^{(m)}(t)| \leq C + A \max_n (\sum_n |w_n^{(m-1)}(t)|)^2.$$

Showing that if the series  $\sum_n |w_n^{(m)}(t)|$  is uniformly convergent then the series  $\sum_n |w_n^{(m)}(t)|$  is also uniformly convergent.

We shall prove now that the series

$$\sum_n |w_n^{(m)}(t)| < 2C,$$

for all  $t$  and all  $m \geq 1$ , provided that

$$(30) \quad C \leq \frac{1}{4A}$$

In fact, from (23), we have for all  $t$ :

$$(31) \quad \sum_n |w_n^{(0)}(t)| \leq \sum_n |\gamma_n| = C.$$

Substituting this in (29) for  $m=1$  we get

$$\sum_n |w_n^{(1)}(t)| C + AC^2 < 2C$$

since on account of (30)  $AC^2 < C$ . Substituting this again in (29) for  $m=2$ , we get

$$\sum_n |w_n^{(2)}(t)| < C + 4AC^2 < 2C.$$

And generally for all  $m \geq 1$  we get:

$$(32) \quad \sum_n |w_n^{(m)}(t)| < 2C \leq 1.$$

We have to prove now that the doubly infinite series

$$(33) \quad \sum_{m=0}^{\infty} \sum_{n=1}^{\infty} |w_n^{(m+1)}(t) - w_n^{(m)}(t)|$$

converges uniformly for all  $t \geq 0$ .



We have

$$\begin{aligned}
 w_n^{(m+1)}(t) - w_n^{(m)}(t) &= -\lambda_n \int_0^t e^{-\lambda_n(t-s)} \sum_{k,l} \frac{f_n(k,l)}{\lambda_k \lambda_l} \\
 &\quad \times \left\{ w_k^{(m)}(s) w_l^{(m)}(s) - w_k^{(m-1)}(s) w_l^{(m-1)}(s) \right\} ds \\
 &= -\lambda_n \int_0^t e^{-\lambda_n(t-s)} \sum_{k,l} \frac{f_n(k,l)}{\lambda_k \lambda_l} \\
 &\quad \times \left\{ w_k^{(m)}(s) \left[ w_l^{(m)}(s) - w_l^{(m-1)}(s) \right] + w_l^{(m-1)}(s) \right. \\
 &\quad \left. \left[ w_k^{(m)}(s) - w_k^{(m-1)}(s) \right] \right\} ds.
 \end{aligned}$$

Summing this over  $n$ , and taking account of (28) and (32), we get for all  $t$

$$(34) \quad \sum_{n=1}^{\infty} \left| w_n^{(m+1)}(t) - w_n^{(m)}(t) \right| \leq A.2.2C \max \sum_{n=1}^{\infty} \left| w_n^{(m)}(t) - w_n^{(m-1)}(t) \right|$$

Repeating the reduction process  $m$  times we get :

$$(35) \quad \sum_{n=1}^{\infty} \left| w_n^{(m+1)}(t) - w_n^{(m)}(t) \right| \leq (4AC)^m \max \sum_{n=1}^{\infty} \left| w_n^{(1)}(t) - w_n^{(0)}(t) \right|$$

Therefore

$$(36) \quad \sum_{n=0}^{\infty} \sum_{m=1}^{\infty} \left| w_n^{(m+1)}(t) - w_n^{(m)}(t) \right| \leq \sum_{m=0}^{\infty} (4AC)^m \max \sum_{n=1}^{\infty} \left| w_n^{(1)}(t) - w_n^{(0)}(t) \right|.$$

Now, from (30) we have  $4AC < 1$ , and therefore

$$(37) \quad \sum_{m=0}^{\infty} (4AC)^m = \frac{1}{1-4AC}.$$

$$\text{Also } w_n^{(1)}(t) - w_n^{(0)}(t) = -\lambda_n \int_0^t e^{-\lambda_n(t-s)} \sum_{k,l} \frac{f_n(k,l)}{\lambda_k \lambda_l} w_k^{(0)}(s) w_l^{(0)}(s) ds,$$

therefore on account of (28) and (31) we have

$$(38) \quad \max_n \sum_n \left| w_n^{(1)}(t) - w_n^{(0)}(t) \right| \leq AC^2.$$

Substituting (37) and (38) in (36), we get

$$(39) \quad \sum_{m=0}^{\infty} \sum_{n=1}^8 \left| w_n^{(m+1)}(t) - w_n^{(m)}(t) \right| \leq \frac{AC^2}{1-4AC},$$

which establishes the uniform convergence of the double series. From this uniform convergence it follows that all the limits  $\lim_{m \rightarrow \infty} w_n^{(m)}(t)$  exist, and that all the functions  $w_n(t)$ , where

$$(40) \quad w_n(t) = \lim_{m \rightarrow \infty} w_n^{(m)}(t) \quad (n=1, 2, \dots)$$

are continuous for all  $t \geq 0$ . Moreover, from (32) we get

$$(41) \quad \sum_n |w_n(t)| < 2c < 1$$

From (24) we get then on making  $m \rightarrow \infty$

$$(42) \quad w_n(t) = \gamma_n e^{-\lambda_n t} - \lambda_n \int_0^t e^{-\lambda_n(t-s)} \sum_{k,l} \frac{f_n(k,l)}{\lambda_k \lambda_l} w_k(s) w_l(s) ds.$$

Now we write again

$$(43) \quad c_n = \frac{1}{\lambda_n} \gamma_n, \quad v_n(t) = \frac{1}{\lambda_n} w_n(t),$$

and from (42) we get

$$(44) \quad v_n(t) = c_n e^{-\lambda_n t} - \int_0^t e^{-\lambda_n(t-s)} \sum_{k,l} f_n(k,l) v_k(s) v_l(s) ds$$

We see therefore that for  $n \geq 1$ ,  $v_n(t)$  satisfies the integral equation (20), and consequently the differential equation (19). Further, if in the series  $\sum_n |Z_n(t)|$  we substitute these values of  $v_n(t)$ , we see easily that the series is uniformly convergent. Since the functions  $\phi(x_n)$  are uniformly bounded for all  $n$ , we see that  $\sum_n |Z_n(t)| \phi(x)$  is uniformly convergent in the domain (3). On account of (41),

$$\sum_n \lambda_n v_n(t) \phi_n(x) = \sum_n w_n(t) \phi_n(x)$$

is also absolutely and uniformly convergent. From (18) we see then that  $\sum_n \frac{dv_n}{dt} \phi_n(x)$  is also absolutely and uniformly convergent in the domain (3).

We see thus that

$$(45) \quad u(x, t) = \sum_{n=1}^{\infty} v_n(t) \phi_n(x),$$

where the co-efficients  $v_n(t)$  are solutions of the integral equation (44), satisfies the differential equation (2) and the boundary conditions (4) and (5).

It only remains for us to show that this solution (45) is the only one of its kind which can be expanded in an absolutely and uniformly convergent series of the form  $\sum_n v_n(t) \phi_n(x)$  and which is such that also the series  $\sum_n \lambda_n |v_n(t)|$  and  $\sum_n \frac{dv_n}{dt}$  converge uniformly.

For this purpose, it is sufficient to prove that the integral equation (24) has no other solutions  $\overline{w}_n(t)$  ( $n=1, 2, \dots$ ) which are such that the series  $\sum_n |\overline{w}_n(t)|$  is uniformly convergent.

If possible, suppose that such solutions  $\overline{w}_n(t)$  exist and that

$$(46) \quad \sum_n \left| \overline{w}_n(t) \right| < 2c.$$

Now we have

$$\begin{aligned} \overline{w}_n(t) - w_n^{(m)}(t) &= -\lambda_n \int_0^t e^{-\lambda_n(t-s)} \sum_{k,l} \frac{f_n(k, l)}{\lambda_k \lambda_l} \\ &\quad \times \{ \overline{w}_k(s) \overline{w}_l(s) - w_k^{(m-1)}(s) w_l^{(m-1)}(s) \} ds \\ &= -\lambda_n \int_0^t e^{-\lambda(t-s)} \sum_{k,l} \frac{f_n(k, l)}{\lambda_k \lambda_l} \\ &\quad \times \{ \overline{w}_k(s) [\overline{w}_l(s) - w_l^{(m-1)}(s)] + w_l^{(m-1)}(s) [\overline{w}_k(s) - w_k^{(m-1)}(s)] \} ds \end{aligned}$$

Summing over  $n$ , and taking account of (28), (32) and (46), we get

$$(47) \quad \sum_n \left| \overline{w}_n(t) - w_n^{(m)}(t) \right| \leq 2.2c \max \sum_n \left| \overline{w}_n(t) - w_n^{(m-1)}(t) \right|$$

Repeating this reduction process  $m$  times, we get

$$(48) \quad \Sigma_n \left| w_n(t) - w_n^{(m)}(t) \right| \leq (4Ac)^m \cdot \max \Sigma_n \left| \bar{w}_n(t) - w_n^{(0)}(t) \right|$$

$$\text{But } \bar{w}_n(t) - w_n^{(0)}(t) = -\lambda_n \int_0^t e^{-\lambda_n(t-s)} \Sigma_{k,l} \frac{f_n(k,l)}{\lambda_n \lambda_l} \bar{w}_k(s) \bar{w}_l(s) ds,$$

therefore on account of (28) and (46), we have for all  $t$

$$\max \Sigma_n \left| \bar{w}_n(t) - w_n^{(0)}(t) \right| \leq 4Ac^2.$$

Moreover, since from (3) we have  $4Ac < 1$ , we get

$$\lim_{m \rightarrow \infty} (4Ac)^m = 0.$$

Substituting these in (48), we get

$$(49) \quad \lim_{m \rightarrow \infty} \Sigma_n \left| \bar{w}_n(t) - w_n^{(m)}(t) \right| \leq (4Ac^2) \lim_{m \rightarrow \infty} (4Ac)^m$$

So that for all  $n \leq 1$ , we get

$$(50) \quad \bar{w}_n(t) = \lim_{m \rightarrow \infty} w_n^{(m)}(t) = w_n(t),$$

i.e., the two solutions  $\bar{w}_n(t)$  and  $w_n(t)$  of the integral equation (24) are identical. This shows that the solution (45) is unique.

#### References:

1. M. R. Siddiqi: "Zur Theorie der nicht-linearen partiellen Differentialgleichungen vom parabolischen Typus." *Mathematische Zeitschrift*, Vol. 35 (1932).
2. M. R. Siddiqi: "On the Equation of Heat Conduction in Wave Mechanics." Jubilee Number of the Journal of the Indian Mathematical Society (1934).
3. M. R. Siddiqi: "The Reduction of the general non-linear parabolic equation to normal form and its solution." *Journal of the Osmania University College*, Vol. I (1933).
4. M. R. Siddiqi: "On an infinite system of non-linear Integral equations." *Bulletin of the Calcutta Mathematical Society*, Vol. 24 (1932).
5. Courant-Hilbert: "Methoden der Mathematische Physik, Vol. I (1931).
6. L. Lichtenstein: "Zu Analysis der unendlichviele Variablen." *Palermo Rendiconto*, Vol. 35 (1919).
7. M. R. Siddiqi: "On an infinite series of Integrals involving Sturm-Liouville Eigenfunctions." *Bulletin of the Academy of Sciences, U. P.*, Vol. 3 (1933).

## Magnetic Measurements on Molecular Compounds in Solution with a Modified Form of Decker's Balance\*

By

S. S. BHATNAGAR, M. B. NEVGI AND GOPALDAS TULI

*(Received for publication, September 24, 1934.)*

### ABSTRACT.

An attempt has been made to study the stability of molecular compounds in solution from magnetic standpoint, by measuring the diamagnetic susceptibility of some picrates in the solid state and in solutions in extra pure benzene over a wide range of concentrations. It is found that the susceptibility of the compounds is lowered in solutions and the value approaches that given by the law of mixtures, from which it is concluded that the molecules are dissociated in solutions.

In a paper just communicated to this journal it has been shown by Bhatnagar, Verma, and Kapur that the magnetic susceptibilities of molecular compounds in the solid conditions are quite different from the additive mixture values of their constituents. This difference has been further partially attributed to the formation of a co-ordinate linkage. Nothing is known regarding the nature of magnetic behaviour of these substances when they exist in the dissolved state.

The stability of molecular compounds in solution has been the subject of keen investigation. The molecular compounds

\* Read before the Inaugural Meeting of the Indian Physical Society on 29th September, 1934.

formed between picric acid and hydrocarbons or their derivatives are by far the largest in number and form a class by themselves. In 1894, R. Behrend<sup>1</sup> from solubility measurements on two such compounds showed that they get dissociated in solution to some extent and that their dissociation constant can be calculated. A similar indication was observed by Brown<sup>2</sup> in the case of naphthalene picrate. H. von Halban and E. Zimpelmann<sup>3</sup> examined a large number of compounds belonging to this series by the photo-electric determination of the absorption of light by their solutions at different concentrations and found them to be dissociated. This work has recently been supported by Moore, Shepherd and Goodall.<sup>4</sup>

In the present investigation an attempt has been made to test the whole matter from the magnetic standpoint, by measuring the diamagnetic susceptibility of the picrates so formed in the solid state and in solutions in extra pure benzene over a wide range of concentrations.

The apparatus employed was a modified form of Decker's<sup>5</sup> apparatus for solutions and liquids and was somewhat similar to that of Sibaiya and Venkataramiah.<sup>6</sup> The test piece was a glass cylinder of 10mm. length and 2mm. diameter. A thin glass stem was fused to this test piece and carried the mirror also. The test piece was kept at an angle of 45° with the axis of the pole pieces. This arrangement proved very satisfactory for cleaning and drying the tube after the completion of each experiment.

It was found that the position of the glass tube and consequently of the test piece changed sometimes while the torsion was being given. To remove any possibility of error liable to arise thereby a travelling vernier microscope was focussed sharply on a cross mark in the body of the tube and it enabled us

<sup>1</sup> *Zeit. Physik. Chem.*, **15**, 183 (1894).

<sup>2</sup> *Jour. Chem. Soc.*, **127**, 345 (1925).

<sup>3</sup> *Zeit. Physik. Chem.*, **117**, 461 (1925).

<sup>4</sup> *Jour. Chem. Soc.*, **1447** (1931).

<sup>5</sup> *Ann. der Physik.*, **79**, 324 (1926).

<sup>6</sup> *Indian Jour. Phys.*, **7**, 393 (1932)

to keep the tube always in the same position. Great care was taken to keep the quantity of the liquid constant throughout.

Care was also taken to keep the test piece directly between the pole pieces and not to their sides for if the piece is placed in the latter position the possibility of both the motions of rotation and of translation comes in.

Sibaiya and Venktaramiah<sup>7</sup> find the usual practice of back torsion to be trying. The authors find that it is not so if the positions of the test piece and the glass tubes are noted through the microscope before and after the application of the field, and in fact, they find this as the most satisfactory arrangement.

The readings on the torsion head can be interpreted in terms of magnetic susceptibility in the following manner :—

The moment which rotates the glass rod is given by

$$m_M = (x - x_g) \cdot H^2 A \quad \dots \quad \dots \quad (1)$$

where  $m_M$  = moment of the balancing force.

$x$  = susceptibility of the surrounding medium.

$x_g$  = susceptibility of the test piece.

$H$  = field strength.

$A$  = a constant.

If the field at the farther ends of the test piece is  $H_2$  and that  $H_1$  near the centre,  $H^2$  can be replaced by  $(H_1^2 - H_2^2)$  in the above equation. If  $H$  remains constant, then by substituting  $C_1$  for  $H^2 A$ , we get,

$$m_M = (x - x_g) \cdot C_1 \quad (2)$$

$$\text{Now} \quad \phi = M_\tau C_2 \quad (3)$$

where  $\phi$  = the torsion.

$M_\tau$  = torsion moment.

$C_2$  = a constant.

<sup>7</sup> *Loc. cit.*

When the glass rod is in equilibrium at the zero position, the moment of the back torsion must be equal to the moment of the twisting force and so

$$M_T = m_M$$

Therefore,  $\phi = \{ (x - x_g) C_1 \} \cdot C_2$

and  $\frac{\phi}{C_1 \times C_2} = x - x_g$

$$\text{Putting } C = \frac{1}{C_1 \times C_2}$$

we get,  $\phi \times C = x - x_g \quad \dots \quad \dots \quad \dots \quad (4)$

Accordingly, if  $x_w$  be the volume susceptibility of water,  $x_g$  that of glass,  $x_a$  that of air and  $x_\alpha$  that of the liquid, we have

$$(a) \quad x_w - x_g = \phi_w \times C \quad \text{for water}$$

$$(b) \quad x_a - x_g = \phi_a \times C \quad \text{for air}$$

$$(c) \quad x_\alpha - x_g = \phi_\alpha \times C \quad \text{for the liquid}$$

From (a) and (b) the value of  $x_g$  can be found as follows :

$$\frac{x_w - x_g}{x_a - x_g} = \frac{\phi_w \times C}{\phi_a \times C}$$

$$\text{or} \quad x_g = \frac{x_a \phi_w - x_w \phi_a}{\phi_w - \phi_a} \quad \dots \quad \dots \quad \dots \quad (5)$$

Similarly the apparatus constant  $C$  is given by the expression

$$C = \frac{x_w - x_a}{\phi_w - \phi_a} \quad \dots \quad \dots \quad \dots \quad (6)$$

From equation (c) we have,

$$x_\alpha = \phi_\alpha \times C + x_g$$

$$= \phi_\alpha \left( \frac{x_w - x_a}{\phi_w - \phi_a} \right) + \frac{x_a \phi_w - x_w \phi_a}{\phi_w - \phi_a}$$



And consequently,

$$\chi_{\alpha} = \phi_{\alpha} \left( \frac{x_w - x_a}{\phi_w - \phi_a} \right) + \frac{x_a \phi_w - x_w \phi_a}{\phi_w - \phi_a} \bigg/ \alpha \quad \dots \quad (7)$$

The particular precautions of taking the volume susceptibilities of air and water at the necessary temperatures and pressures and of assigning proper signs to the torsion angles must be observed.

The susceptibility of the salt from the solution was calculated with the help of the relation

$$\chi_{\text{solution}} = C_{\text{salt}} \times \chi_s + (1 - C_{\text{salt}}) \times \chi_{\text{solvent}}$$

where  $C_{\text{salt}}$  denotes the concentration of the solution.

The substances investigated were as pure as possible. Special care was taken in purifying them by repeated crystallisations and in every case before taking the magnetic measurements their physical constants were determined and compared with those given in the literature. Before actual measurements on solutions the apparatus was standardised against substances of known value and found to give very satisfactory results with an error of  $\pm 1$  per cent.

### *Results and their Discussion.*

TABLE I.

#### *Anthracene Picrate.*

Ruby Red.

m. pt. 138.5°C.

	Concentration (gms. of the substance in 100 gms. of the solvent).	$-\chi \times 10^{-6}$ .
1.	6.548	0.500
2.	6.51	0.476
3.	5.50	0.487
4.	3.557	0.492

TABLE II.

*Naphthalene Picrate.*

Golden yellow.

m. pt. 149.0°C.

	Concentration (gms. of the substance in 100 gms. of the solvent).	$-\chi \times 10^{-6}$ .
1.	11.60	0.457
2.	10.30	0.457
3.	9.05	0.486
4.	7.16	0.476

TABLE III.

 *$\alpha$ -Methyl Naphthalene Picrate.*

Orange yellow.

m. pt. 141° – 142°C.

	Concentration (gms. of the substance in 100 gms. of the solvent).	$-\chi \times 10^{-6}$ .
1.	16.50	0.479
2.	10.80	0.485
3.	8.92	0.478
4.	7.31	0.475

TABLE IV.

*Phenanthrene Picrate.*

Orange yellow.

m. pt. 142.5°C.

	Concentration (gms. of the substance in 100 gms. of the solvent).	$-\chi \times 10^{-6}$ .
1.	17.30	0.485
2.	12.59	0.470
3.	10.43	0.478
4.	7.50	0.481

The values of magnetic susceptibility obtained from different concentrations of one single substance come out to be very nearly equal to one another and considering the low solubility of the compounds and the possibility of experimental error, it can be safely said that the value is very nearly the same. As such we can take the mean value of the four observations as the value for  $\chi$  for the substance in the dissolved state. Bhatnagar, Verma and Kapur<sup>8</sup> have recently determined the values of all these substances in the solid state and in the table below the two sets of results have been compared.

TABLE V.

Substance.	$-\chi \times 10^{-6}$ in the solid state.	Observed mean value in the dissolved state.
1. Anthracene picrate	0.554	0.488
2. Naphthalene picrate	0.524	0.469
3. $\alpha$ -methyl naphthalene picrate	0.521	0.479
4. Phenanthrene picrate	0.542	0.478

It is evident that the value of  $\chi$  in the dissolved state is different from that in the solid state and while our values are considerably less as compared with the values of the abovenamed observers, they are much nearer to those obtained by the application of the mixture law showing thereby that this class of compounds do get dissociated in solution.

UNIVERSITY CHEMICAL LABORATORIES,  
LAHORE.



# An X-ray Investigation of the Crystal Structure of Meta-Azotoluene

By

MATA PRASAD AND P. H. DALAL

(Received for publication, December 3, 1934.)

(PLATE VI.)

The crystals of meta-azotoluene develop a (100), b (010) and c (111) faces, and belong to rhombic bipyramidal class and the axial ratio is <sup>1</sup>

$$a:b:c=0.8556:1:0.5438.$$

In this investigation the crystals of m-azotoluene were prepared by the slow evaporation of the solution of the substance in absolute alcohol. The crystals grow in the form of four sided plates with a (100) as a prominent face.

In order to determine the dimensions of the unit cell, rotation photographs about all the three principal axes were taken by means of a Shearer tube fitted with copper anticathode and are shown in Plate VI. The lengths of the axes were calculated from these photographs which are

$$a=11.8 \text{ \AA}, b=13.75 \text{ \AA}, c=7.52 \text{ \AA}.$$

and

$$a:b:c=0.8581:1:0.5469.$$

The axial ratios are in good agreement with those from goniometric measurements.

<sup>1</sup> Gröth, *Chemische Krystallographie*, 1919, Vol. V., p. 66.

In order to determine the space group to which the crystals belong (as this determination indicates the symmetry of the unit cell and also the symmetry elements of the molecule itself if there be any) a few oscillation photographs were taken about *b* and *c* axes at an interval of  $15^\circ$ . The indices of the various diffracted spots have been worked out by Bernal's<sup>2</sup> method of analysis and the reflecting planes have been tabulated in Tables I and II. The intensities of the spots were determined by eye estimation and the symbols employed by Robertson<sup>3</sup> have been used to indicate the intensities of the planes.

It will be seen from the above series of planes that (011), (010) and (100) are halved; also (*h* 0 *l*) are halved when *h* is odd and (*h* *k* 0) are halved when *k* is odd. These halvings correspond to the space group  $Q''_L$ . The number of molecules required by the space group is 8. The number of molecules calculated from the dimensions of the unit cell and the density of the crystals (1.05) is found to be 4.

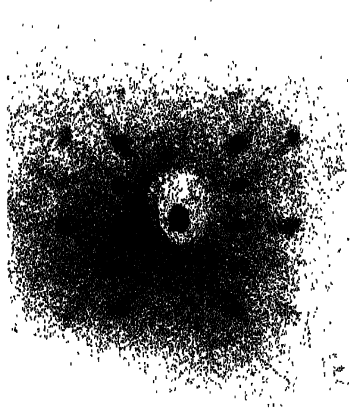
The number of molecules actually present in the unit cell being four, *i.e.*, half the number required by the space group, the molecules possess some elements of symmetry. These may be according to the space group either a plane of symmetry parallel to (100) plane or a dyad axis of symmetry perpendicular to (100) plane or a centre of symmetry. In order to examine which of these symmetrical molecular arrangements exists further work is being undertaken.

One of the authors (M.P.) has to thank the University of Bombay for a grant from which part of the expenses of this investigation was defrayed.

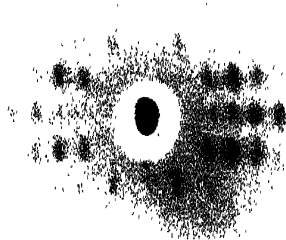
CHEMISTRY DEPARTMENT,  
ROYAL INSTITUTE OF SCIENCE,  
BOMBAY.

<sup>2</sup> Proc. Roy. Soc., A, 113, 117 (1926).

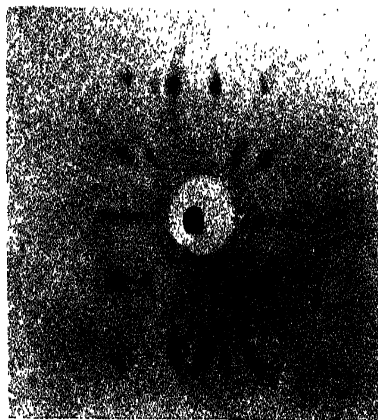
<sup>3</sup> Proc. Roy. Soc., A, 118, 712 (1928).



Rotation about  
"a" axis



Rotation about  
"b" axis



Rotation about  
"c" axis.

Rotation photographs of meta azotoluene.





TABLE I.

Axial planes.	Intensity.	Prism planes (h0l).	Intensity.	Prism planes (0kl)	Intensity.	Prism planes (hko)	Intensity.
200	v.s.	201	s.	012	v.s.	120	v.s.
400	s.	202	v.s.	062	v.w.	220	v.s.
600	v.w.	203	m.s.	023	m.	320	s.
020	s.	204	w.			520	v.w.
060	w.	401	v.w.			620	m.
002	v.s.					440	m.
						640	w.
						160	w.

TABLE II.

## General Planes.

Planes.	Intensity.	Planes.	Intensity.	Planes.	Intensity.	Planes.	Intensity.
111	v.s.	151	v.w.	251	w.	412	w.m.
112	s.	162	v.w.	271	v.w.	413	w.m.
121	w.	162	v.w.	311	w.m.	422	v.w.
122	m.	211	v.w.	313	m.	423	m.
131	w.	212	s.	321	v.w.	441	w.
132	w.	213	m.	341	w.m.	451	w.
141	v.w.	221	w.	351	w.m.	511	w.m.
142	v.w.	231	v.w.	411	w.m.	611	w.



## Rotational Raman Scattering in Benzene at Different Temperatures

By

S. C. SARKAR, D.SU. AND B. B. MAITI, M.Sc.

(Plate VII.)

*(Received for publication, Dec. 17, 1934.)*

### ABSTRACT.

The rotational Raman scattering in benzene at the room temperature and at about 210°C has been investigated with the help of a spectrograph producing lines absolutely free from coma on the Stokes side. It has been found after quantitative measurement of the distribution of intensity in the wing that even at the room temperature the rotational wing does not start with maximum intensity at the centre of the Rayleigh line as reported by previous observers, but it starts with zero intensity at the said point, and after having a maximum intensity at about 18 wave numbers from the Rayleigh line, gradually diminishes in intensity and extends up to about 120 wave numbers. When the liquid is heated up to 210°C, the position of the maximum intensity shifts away from the Rayleigh line by about 5 wave numbers and also the wing becomes narrower and extends only up to 100 wave numbers from the Rayleigh line.

### 1. Introduction.

It is well known that in the spectra of light scattered by many liquids, the Rayleigh line is accompanied by a diffuse wing extending on each side up to a few Angstrom units. This unresolved band was first observed by Raman and Krishnan<sup>1</sup> and

<sup>1</sup> C. V. Raman and K. S. Krishnan, *Nature*, 122, 882 (1929).

its origin was attributed to rotational Raman scattering. It has been observed subsequently by various observers that in the case of gases having diatomic molecules and also in the case of liquid hydrogen and a few gases having polyatomic molecules, the rotational Raman spectrum consists of closely spaced lines in the neighbourhood of the Rayleigh line. The theory of the rotational Raman scattering by diatomic molecules was given by Manneback.<sup>2</sup> According to this theory, the rotational spectrum consists of three branches Q, O and S corresponding to the transitions  $\Delta J=0$  and  $\pm 2$ , where  $J$  is the quantum number of the total rotational impulse. Also, there is a definite distribution of intensity among the different lines in the three branches. The relative intensities of different rotational Raman lines in the scattered spectrum of gaseous hydrogen observed by Bhagavantam<sup>3</sup> are in fair agreement with the theory.

The theory of the rotational Raman scattering by polyatomic molecules has been put forward recently by Placzek and Teller.<sup>4</sup> According to this theory, in the case of polyatomic molecules, the rotational Raman spectrum consists of five branches corresponding to the transitions  $\Delta J=0, \pm 1$  and  $\pm 2$ . When, however, the moment of inertia of the molecule is high, the rotational Raman spectrum consists of an unresolved band on each side of the Rayleigh line starting with zero intensity at the centre of the Rayleigh line and extending up to a few Angstrom units after having a maximum intensity at some distance depending on the temperature and the moment of inertia of the molecule. In the case of linear triatomic molecules,  $\text{CO}_2$  for example, the rotational structure of the Rayleigh line consists of lines corresponding to the transitions  $\Delta J=0, \pm 2$  only, the transitions  $\Delta J=\pm 1$  are allowed only in the case of the first excited state of the degenerate oscillation ( $\nu=675$ ), but the intensities of these

<sup>2</sup> C. Manneback, *Z. f. Phys.*, **62**, 224 (1930); **65**, 574 (1930).

<sup>3</sup> S. Bhagavantam, *Ind. J. Phys.*, **7**, 107 (1932).

<sup>4</sup> G. Placzek and E. Teller, *Z. f. Phys.*, **81**, 209 (1933).

lines at the room temperature are too small to be observed experimentally. Houston and Lewis<sup>5</sup> have resolved the rotational structure of the Rayleigh line scattered by CO<sub>2</sub> and have found the lines to correspond to the transitions  $\Delta J = 0, \pm 2$  as expected from the theory. Amaldi and Placzek<sup>6</sup> investigated very carefully the rotational structure of the Rayleigh line scattered by gaseous ammonia and have observed all the branches corresponding to the transitions  $\Delta J = 0, \pm 1, \pm 2$  as expected theoretically. Also, the relative intensities of the lines in the different branches observed by them are in fair agreement with the theory. Again, it has been found recently by one of the present authors<sup>7</sup> that in the case of benzene vapour, the distribution of intensity in the rotational wing is in fair agreement with the theory.

In the case of liquid benzene, on the other hand, there is a large discrepancy between the distribution of intensity in the rotational wing accompanying the Rayleigh line expected theoretically and that observed by Weiler,<sup>8</sup> Ranganadham,<sup>9</sup> Bhagavantam,<sup>10</sup> and Bhagavantam and Rao.<sup>11</sup> These observers find that the rotational band instead of starting with zero intensity at the centre of the Rayleigh line and having a maximum intensity at some distance from the latter, starts with maximum intensity at the centre of the Rayleigh line and the width of the band is much greater than that expected theoretically. Bhagavantam<sup>12</sup> has tried to explain this discrepancy qualitatively by assuming that some of the molecules in liquid benzene are grouped together as in the solid state, and the intermolecular vibrations give rise to a continuous Raman band superposed on the rotational wing in the neighbourhood of the Rayleigh line.

<sup>5</sup> W. V. Houston and C. M. Lewis, *Proc. Nat. Acad. Amer.*, **17**, 229 (1931).

<sup>6</sup> E. Amaldi and G. Placzek, *Z. f. Phys.*, **81**, 259 (1933).

<sup>7</sup> S. C. Sirkar, *Nature*, **139**, 859 (1934); *Ind. J. Phys.*, **9**, 295 (1935).

<sup>8</sup> J. Weiler, *Z. f. Phys.*, **68**, 782 (1931).

<sup>9</sup> S. P. Ranganadham, *Ind. J. Phys.*, **7**, 353 (1932).

<sup>10</sup> S. Bhagavantam, *Ind. J. Phys.*, **8**, 197 (1933).

<sup>11</sup> S. Bhagavantam and A. V. Rao, *Ind. J. Phys.*, **8**, 437 (1934).

<sup>12</sup> *loc. cit*

According to this hypothesis, however, one would expect a change in the distribution of intensity in the wing with the rise of temperature of the liquid, owing to the "solid molecules" being disturbed at high temperatures. But no such change was observed by Bhagavantam in the case of liquid benzene when the temperature was raised to  $75^{\circ}\text{C}$ . These facts prompted a reinvestigation of the problem and the results obtained with improved technique in the case of liquid benzene at the room temperature and at about  $210^{\circ}\text{C}$  are reported in the present paper.

## 2. *Experimental.*

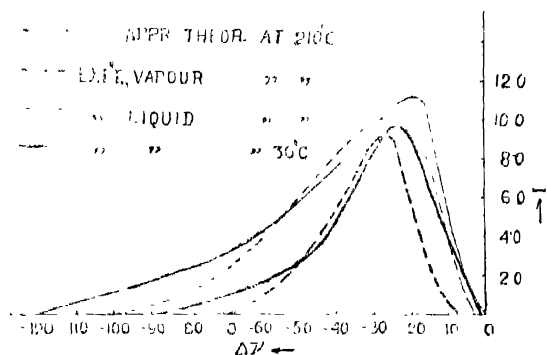
The image of the slit due to monochromatic light produced by the glass system of a spectrograph of large aperture generally consists of a sharp line and a broad and fainter coma lying very close to the line. Sometimes the most intense part of the coma lies very close to the line. If the rotational Raman spectrum due to a liquid having polyatomic molecules be recorded with such a spectrograph, the intense portion of the coma is superposed on the part of the wing close to the Rayleigh line, and there is likelihood of the results obtained for the distribution of intensity in the wing being vitiated by the presence of the coma. Therefore, a spectrograph producing lines free from coma is required in the ideal arrangement for the present investigation. One of the Fuess glass spectrographs of this laboratory was found to be suitable for the present investigation, because there is absolutely no coma on the Stokes side of the lines produced by it in the region of  $4046 \text{ \AA}$ , though there is an intense coma on the anti-Stokes side. The rotational Raman spectrum of benzene on the Stokes side at the room temperature was recorded with proper densities with the help of this spectrograph. In order to eliminate stray light, a glass condenser was used to focus the light from a mercury arc on the liquid contained in a wide tube, and also the other usual steps were taken. The width of the slit of the spectrograph was  $0.012 \text{ mm}$ . A good Zeiss lens was used to focus the scattered light on the slit of the spectrograph.

In order to record the rotational Raman spectrum of benzene at high temperatures, a stout Jena glass tube of length about 15 cm. and diameter 2 cm. was filled up to three-fourths of its volume with pure benzene distilled in vacuum and was sealed hermetically after all the air inside the tube had been drawn out. The tube was placed inside a cylindrical electric heater provided with two windows, one along its length through which the tube could be illuminated and the other at one of its ends through which the scattered light could be observed. The temperature of the liquid was raised to about  $210^{\circ}\text{C}$  by passing suitable current through the heater. The pressure inside the tube was thereby raised to about 17 atmospheres and the tube was strong enough to withstand this pressure. The scattered spectrum was recorded with proper density using the same arrangements as in the case of room temperature. In the present case, as the tube was not very wide and its window was not flat, there was feeble stray light superposed on the scattered light, but it only increased the density of the Rayleigh line slightly without producing any satellite on the Stokes side. The  $4046\text{\AA}$  group of the mercury lines in the direct mercury arc spectrum was also recorded with the same density as in the spectrograms due to scattered light, the same width of the slit of the spectrograph being used in all the cases. Intensity marks were then recorded by varying the width of the slit of the spectrograph, a standard tungsten ribbon lamp being used as the source of continuous radiation. Microphotometric records of the intensity marks as well as those of the spectrograms of scattered and incident light were obtained with the help of a Moll's self-registering microphotometer. Care was taken to utilise the maximum resolving power of this instrument. For this purpose, the slits in the instrument were made very narrow and the lines on the plates were made parallel to the slits.

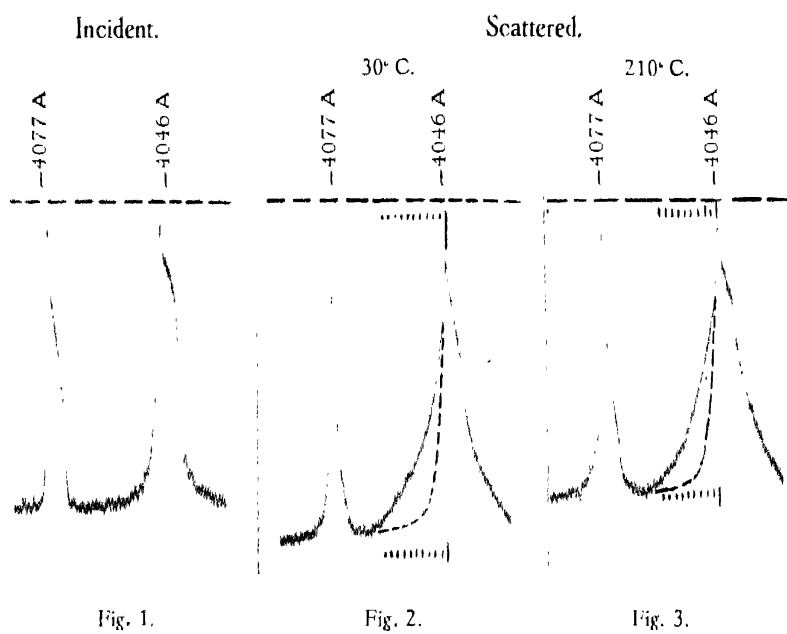
### 3. *Results and Discussion.*

The microphotometric records of the spectrograms due to the incident and scattered light in the region of  $4046\text{\AA}$  are reproduced

in Figs. 1, 2 and 3 in Plate VII. In order to measure the distribution of intensity in the wing, the densities of the background at different distances from the Rayleigh line are required. The record for the Rayleigh line free from coma would give the necessary background. For this purpose, the record for the line  $4046\text{\AA}$  in the direct mercury arc spectrum was used. When the wing is not sufficiently detached from the Rayleigh line, the background has to be determined very accurately. A curve exactly similar to the record for the line  $4046\text{\AA}$  in the incident spectrum was drawn on the record for the scattered line in the proper position. Only the part of the curve lying on the Stokes side was drawn, because there was an intense coma on the anti-Stokes side partly superposed on the wing on that side. The dotted curves in Figs. 2 and 3 have been drawn in this way. Different portions of the curve are inclined in particular ways to the straight line which is generally imprinted photographically on the record at every point where the record is started. In each of the Figs. 1, 2 and 3, such straight lines will be easily found. These lines were used as landmarks and lines parallel to them were drawn through the centres of the peaks due to scattered lines while the dotted curves were drawn in their proper positions. There was thus no chance of the dotted curves being laterally shifted or having wrong inclinations. With the help of these dotted curves, the densities of the background at different distances from the centre of the peak were determined and the









intensities of the wing at these points were measured with the help of the density-log. intensity curves as usual. The curve drawn in continuous thin line in Fig. 4 represents the results obtained in the case of benzene at the room temperature, and the dotted curve in thin line is obtained in the case of liquid benzene at about  $210^{\circ}\text{C}$ .

It will be seen from Fig. 4 that the intensity of the wing is not maximum at the centre of the Rayleigh line as reported by the previous observers. The intensity of the wing is actually zero at the centre of the Rayleigh line and the positions of maximum intensity lie at about  $18\text{ cm}^{-1}$  and  $25\text{ cm}^{-1}$  from the centre of the Rayleigh line at the room temperature and at  $210^{\circ}\text{C}$  respectively. At the room temperature there is considerable intensity of the wing at a distance of about  $5\text{ cm}^{-1}$  from the centre of the Rayleigh line and half the width of the Rayleigh line itself is about  $7\text{ cm}^{-1}$ . Therefore it is not possible to observe the separation of the wing from the Rayleigh line visually on the spectrogram, but at the high temperature the intensity of the wing at the said distance is very small so that the discontinuity in the intensity in this region can be observed visually on the spectrogram. If the intensity of the wing were maximum at the centre of the Rayleigh line, the topmost part of the peak in the microphotometric record of the scattered line ought to be much broader than that of the incident line. This was never observed even after examining the records obtained for a large number of spectrograms. In the case of the liquid at the high temperature, however, though the wing is distinctly detached from the Rayleigh line, the Rayleigh line itself seems to be broadened by about two wave numbers on each side of its centre.

Another change besides the shift in the position of maximum intensity is also observed in the rotational wing with the rise of temperature of the liquid. It will be seen from Fig. 4 that at  $210^{\circ}\text{C}$  the wing extends from a distance of  $5\text{ cm}^{-1}$  from the centre of the Rayleigh line up to about  $100\text{ cm}^{-1}$ , but at the room temperature it extends from the centre of the Rayleigh line up to

about  $120\text{ cm}^{-1}$ . It was observed by one of the present authors<sup>7</sup> that in the case of benzene vapour at  $210^{\circ}\text{C}$ , the rotational band starts from a distance of about  $7\text{ cm}^{-1}$  from the centre of the Rayleigh line and extends up to about  $70\text{ cm}^{-1}$ . Hence it seems that as the temperature of the liquid is raised, the distribution of intensity in the wing approaches that in the case of vapour. For the sake of convenience, the curve showing the observed distribution of intensity in the wing due to benzene vapour at  $210^{\circ}\text{C}$  is reproduced in Fig. 4 in thick broken line. The curve in thick line in Fig. 4 represents the approximate theoretical curve obtained for benzene molecule at  $210^{\circ}\text{C}$  on the assumption that the position of maximum intensity is at about  $22\text{ cm}^{-1}$  from the centre of the Rayleigh line. This position of the maximum intensity in the particular case is obtained according to the approximate theory put forward by Bhagavantam.<sup>13</sup>

Thus it appears from the above results that in the case of liquids having nonpolar molecules, the freedom of rotation of the molecules is not hampered very much. Some change, however, is brought about when the molecules pass from the vapour to the liquid state as can be seen from the distribution of intensities in the rotational wings shown in Fig. 4. The portion of the wing lying between  $70\text{ cm}^{-1}$  and  $100\text{ cm}^{-1}$  from the Rayleigh line observed in the case of liquid benzene at  $210^{\circ}\text{C}$  is absent in the case of benzene vapour at the same temperature. At the room temperature, again, the wing extends farther beyond  $100\text{ cm}^{-1}$ . This fact shows that this portion of the wing owes its origin to the liquid state.

The authors' thanks are due to Prof. D. M. Bose for his kind interest in the work.

<sup>13</sup> S. Bhagavantam, *Ind. J. Phys.*, **6**, 331 (1931).

# The Interpretation of the Spectra of the Mono and Dichlorides of Tin.\*

By

HRIŠHIKESHA TRIVEDI,

*Department of Physics, Allahabad University, Allahabad.*

*(Received for publication, 26th September, 1934)*

(Plate VIII.)

## ABSTRACT.

In the present paper absorption spectrum of  $\text{SnCl}_2$  vapour has been studied over the visible and quartz region. The photographs show three regions of continuous absorption having their long wave-length beginnings at  $\lambda\lambda$  4129, 3759, 2883. These results are explained by assuming the optical dissociation of  $\text{SnCl}_2$  into Cl and  $\text{SnCl}$ , the latter being in the various states designated by the author as  $^2\pi_{1\frac{1}{2}}(\text{A})$ ,  $^2\pi_{1\frac{1}{2}}(\text{B})$ ,  $\frac{1}{2}$  and  $1\frac{1}{2}$  (C, D). From the above results and other available data it is argued that the chemical binding in  $\text{SnCl}$  and  $\text{SnCl}_2$  is ionic in nature.

A fluorescence experiment was, also, tried to obtain support for the above view. The  $\text{SnCl}_2$  vapour was illuminated with the radiation 2535 A.U. of the mercury arc and fluorescence photographed. After an exposure of 50 hours, faint fluorescence patches were visible, beginning at 3480 A.U. and 3750 A.U. The experiment is still in progress.

\* Communicated by D. S. Kothari and read before the Inaugural Meeting of the Indian Physical Society on the 29th September, 1934.

1. *Introduction.*

Some years ago, Jevons<sup>1</sup> passed an uncondensed discharge through the vapour of  $\text{SnCl}_4$ , and obtained bands in the region  $\lambda 3405\text{--}\lambda 2830$ , which were carefully measured and classified by him, and interpreted as being due to tin monochloride ( $\text{SnCl}$ ). The identification rested on very satisfactory grounds, firstly as the bands could be classified according to the usual Kratzer formula for diatomic molecules, secondly as he could detect the isotope effect due to  $\text{SnCl}^{35}$  and  $\text{SnCl}^{37}$ . Ferguson<sup>2</sup> tried to analyse the other less refrangible bands between  $\lambda 3800\text{--}\lambda 3500$ , which were left unclassified by Jevons. Mulliken<sup>3</sup> wrote a short paragraph on the results in which he tried to interpret them from his theories of molecular structure.

It is well known that  $\text{SnCl}$  is only a temporary molecule, being entirely the result of the electric discharge. The structure of such a temporary molecule must have very intimate connection with that of stabler molecules  $\text{SnCl}_2$  and  $\text{SnCl}_4$ , and the present investigation was undertaken in order to trace this connection. Without entering into details, the result obtained may thus shortly be stated. When  $\text{SnCl}_2$  is illuminated by light of suitable wave-length, it decomposes into  $\text{SnCl}$  and  $\text{Cl}$ , and each of these may be in normal or excited states. The excited states of  $\text{SnCl}$  exactly agree with some of the states obtained by Jevons and Ferguson. The result is thus a further extension of Frank's<sup>4</sup> theory of absorption spectra of alkali halides, but in this case both the products of photoelectric decomposition are not atoms, but a halogen atom and a temporary diatomic halide, both of which may be in normal or excited states. I shall now describe how this result has been arrived at.

<sup>1</sup> Proc. Roy. Soc., A, Vol. 110, p. 365 (1926).

<sup>2</sup> Phys. Rev., Vol. 32, p. 607 (1928).

<sup>3</sup> Phys. Rev., Vol. 28, p. 497 (1926).

<sup>4</sup> Z. Physik., Vol. 43, p. 155 (1927).

## 2. Absorption Spectra of Tin Dichloride ( $\text{SnCl}_2$ ).

The absorption spectrum of  $\text{SnCl}_2$  was first studied with the aid of an  $\text{E}_3$  quartz spectrograph.  $\text{SnCl}_2$  is, under ordinary circumstances, a greyish white translucent substance which melts at  $246.8^\circ\text{C}$  and boils at  $622.5^\circ\text{C}$ . Its vapour pressure has been determined by Maier <sup>5</sup> between  $300^\circ\text{C}$  and  $620^\circ\text{C}$ . Juliusberger <sup>6</sup> has given a Rankine type formula for vapour pressures.

$$\log P = A - \frac{B}{T} - C \log T$$

where  $T$  is the temperature in absolute degrees. For  $\text{SnCl}_2$ , the various constants have the following values

$$A = 17.5792\ 292; \quad B = 2416.68$$

$$\text{and } C = 3.276919.$$

The substance is diamagnetic, having a mass-susceptibility of  $-0.055 \times 10^{-6}$  per mole.

As vapour sufficient for showing absorption can be obtained only at comparatively high temperatures, an opaque quartz tube about an inch in diameter was taken. It was provided with water jackets for preventing the hot vapour from coming from inside of the tube and depositing on the transparent quartz windows. The substance could be introduced through a side tube which also served for the connection to the vacuum pump. The furnace was heated by winding nichrome wire round it and passing high current through the nichrome winding.

The vapour pressures could be measured by noting the temperature to which the furnace was raised and finding out the saturation vapour pressure of the substance at that temperature either from the values of Maier or from the formula of Juliusberger. The temperature of the furnace was roughly estimated

<sup>5</sup> C. G. Maier, 'Vapour pressures of common metallic chlorides', Washington, p. 38, (1925).

<sup>6</sup> Ann. Physik, Vol. 3, p. 618 (1900).

by calibrating it in terms of the heating current when it had come to a steady state of temperature. In practice, the steady state was brought about by heating it for at least one hour and a half with constant current. Each photograph was taken only when the furnace had been heated by a definite electric current for two hours. The source for the continuous absorption was the hydrogen tube run by a high current transformer (2 K.W.) at a current density of 100 m.A. Ilford process plates were used. A photograph of the absorption spectrum is shown in Fig 1. With a view to obtain accurately the long wave-length limits of absorption, a series of microphotograms of the negatives were taken with the microphotometer at the department of Physics of the Muslim University, Aligarh, by Dr. R. Asundi and I wish to express my thanks at this place to Dr. Asundi for his trouble and to Prof. R. Samuel for his kindness in allowing the use of the apparatus. The cuts were very sharp in all the photographs taken at different temperatures and the limits obtained from the microphotograms of these were not much different from limits obtained from visual examination.

### 3. *The Results of the Experiment.*

It was found that the absorption spectrum of  $\text{SnCl}_2$  showed no trace of bands in the region between  $\lambda 6000$ - $\lambda 2000$ . There were, however, three distinct regions of absorption as shown below. The thermochemical data have also been noted.

Beginning of the first region of absorption. 4129 Å.

Beginning of the second region of absorption 3759 Å.

Beginning of the third region of absorption 2883 Å.

Latent heat of vaporisation of tin ( $L_M$ ) 85.5 k. cal.

Heat of formation of the salt (Q) 80.8 k. cal.

Latent heat of vaporisation of  $\text{SnCl}_2$  ( $\lambda_{MX_2}$ ) 46.8 k. cal.

R=Atomic heat of formation.

$$= Q + D\text{Cl}_2 + L_M - \lambda_{MX_2}$$

$$= 176.5 \text{ k. cal.}$$



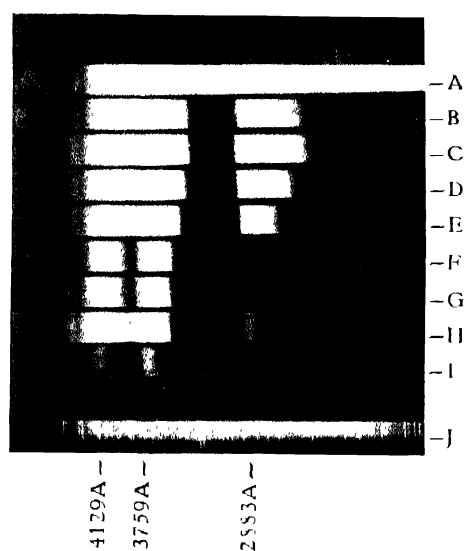


Fig. 1.

A—Continuous spectrum of hydrogen tube.

B—I—Absorption spectra of  $\text{SnCl}_2$  vapour at various temperatures

J—Spectrum of copper arc for comparison



#### 4. Interpretation of the Results—The Spectrum of SnCl.

Before trying to interpret these results, we shall consider the emission spectrum of SnCl, as studied by Jevons<sup>7</sup> and Ferguson.<sup>8</sup> For this purpose we shall have to construct the Franck-Condon diagram for SnCl from data supplied by the above workers.

Jevons classified two systems which he called  $\alpha$  and  $\beta$ . The frequencies of the band-heads were given by

$$\nu_{\alpha} = 31262.5 + 431.3n' - 1.2n'^2 - 353.5n'' + 1.0n''^2$$

$$\nu_{\beta} = 33622.6 + 431.3n' - 1.2n'^2 - 351.4n'' + 1.2n''^2$$

We can now calculate the energy of dissociation of the molecule in the upper and lower (normal) states by using the Birge-Sponer<sup>9</sup> formula

$$D_e = \frac{\omega_e^2}{4x_e\omega_e} \text{ cm}^{-1}$$

For the upper state of the  $\alpha$ -band, we have  $\omega_e' = 432.5 \text{ cm}^{-1}$ ,  $x_e'\omega_e' = 1.2 \text{ cm}^{-1}$ , hence  $D_e' = 38837.4 \text{ cm}^{-1}$

For the lower state,  $\omega_e'' = 354.5 \text{ cm}^{-1}$ ,  $x_e''\omega_e'' = 1.0 \text{ cm}^{-1}$  hence  $D_e'' = 31240 \text{ cm}^{-1}$

The upper state of the  $\beta$ -band is the same as that of the  $\alpha$ -band, the lower level is, however, different. For it,  $\omega_e'' = 352.6 \text{ cm}^{-1}$ ,  $\omega_e''x_e'' = 1.2 \text{ cm}^{-1}$ , hence  $D_e'' = 25725.4 \text{ cm}^{-1}$

The frequencies of the heads of the bands classified by Ferguson are given by the formulae :

$$\lambda \text{ 3800 group (a) : } \nu = 26579.1 + 297.5n' - 4.1n'^2 - 349.5n'' + 1.0n''^2$$

$$\lambda \text{ 3500 group (b) : } \nu = 28665.3 + 296.2n' - 4.2n'^2 + 350.7n'' + 1.1n''^2$$

Ferguson, himself, remarked that the lower states of his bands were identical with the lower states of Jevon's bands. This is

<sup>7</sup> Proc. Roy. Soc., A, Vol. 110, p. 365 (1926)

<sup>8</sup> Phys. Rev., Vol. 32, p. 607 (1926).

<sup>9</sup> W. Jevons, 'Report on Band-Spectra of Diatomic Molecules', p. 27 (1932).

apparent from a reference to the above formulae. The energies of dissociation of the molecule in the lower states of Ferguson's bands are,  $D_e'' = 30713 \text{ cm}^{-1}$  for bands of group (a) and  $28128 \text{ cm}^{-1}$  for the bands of group (b). For the upper states the value for  $D_e'$  is  $5546.5 \text{ cm}^{-1}$  for bands of group (a) and  $5371.5 \text{ cm}^{-1}$  for bands of group (b). It is found that the value of  $D_e''$  for the  $\alpha$ -bands calculated from both Jevons' and Ferguson's bands are almost the same, but for the  $\beta$ -bands they come out to be different.

The distances between the nuclei cannot be determined, as the rotational structure of the bands could not be investigated. But looking at the values of  $\omega_e$  for the upper and lower states we find that  $\omega_e' = 431.3 \text{ cm}^{-1}$  and  $\omega_e'' = 353 \text{ cm}^{-1}$  (approx.) for states giving rise to Jevons' bands. In view of the empirical formula ( $r_e^2 \omega_e = \text{constant}^*$ ) connecting  $\omega_e$  and  $r_e$ , the equilibrium internuclear distance, we see that the equilibrium distance between the nuclei is smaller in the upper state and  $r_e$  for the lower state is 1.105 times the  $r_e$  for the upper one. For Ferguson's states the case is just the reverse. The upper states have  $\omega_e' = 300 \text{ cm}^{-1}$  and the lower ones have  $\omega_e'' = 353 \text{ cm}^{-1}$ . The internuclear distance for the upper states is 1.084 times larger than that for the lower.

Let us now suppose that the binding in the  $\text{SnCl}$  molecule is ionic and it is composed of  $\text{Sn}^+$  and  $\text{Cl}^-$ .  $\text{Sn}^+$  has two states ( $5s^2 5p, {}^2P_{\frac{1}{2}}$ ) and ( $5s^2 5p, {}^2P_{\frac{3}{2}}$ ). The lowest curve corresponding to lowest state involved in the production of the  $\beta$ -bands of Jevons' and  $\gamma$  3500 group of Ferguson is assumed to represent the potential energy of  $\text{Sn}^+ ({}^2P_{\frac{1}{2}}) \text{Cl}^-$  combination and the curve corresponding to the lowest state of the  $\alpha$ -bands of Jevons and  $\lambda$ 3800 group of Ferguson is the corresponding curve for

\* The value of the constant could have been known definitely only if an analysis of the rotational structure of  $\text{SnCl}$  bands had been made. In absence of any such analysis the value of the constant remains unknown, and we can know only the ratio between the values of  $r_e$  for different electronic states of the molecules.

$\text{Sn}^+ (^1\text{P}_{1/2}) \text{Cl}$ . A confirmation of this assumption is found in the fact that the difference in limiting energies of the two states (at  $r=\infty$ ) is given by

$$\begin{aligned}\Delta\nu &= D_e''(a) - D_e''(b) + \nu^{(0,0)}(b) - \nu^{(0,0)}(a) \\ &= 30713 - 28128 + 28665.3 - 26579.1 \\ &= 4671 \text{ cm}^{-1}\end{aligned}$$

This is very nearly equal to  $^2\text{P}_{1/2} - ^2\text{P}_{3/2}$  of  $\text{Sn}_{\text{II}}^+$  which according to Lang<sup>10</sup> has the value  $4253 \text{ cm}^{-1}$

The next higher curves are those representing the upper states of Ferguson's bands, a set of two very close curves with very shallow minima. When the potential energy of these upper states of Ferguson's bands is calculated according to Birge and Sponer's method,\* we obtain, as shown before,  $5546$  and  $5371 \text{ cm}^{-1}$  respectively. This added to  $26579$  and  $28665 \text{ cm}^{-1}$  gives the limiting potential energy to be  $34036 \text{ cm}^{-1}$ . This is practically the same as the limiting energy of  $\text{Sn}^+ (^2\text{P}_{1/2}) \text{Cl}$ . Hence it may be assumed that the upper states arise from the same constituents, *viz.*,  $\text{Sn}^+ (^2\text{P}_{1/2})$  and  $\text{Cl}$  but coupled in a different way so as to give different states.

The next higher curve is the one representing the upper state of Jevons' bands. Its limiting energy at  $r=\infty$  amounts to  $72460 \text{ cm}^{-1}$ . The difference between this and that for the lowest set of molecular states is  $72460 - 28128 = 44332 \text{ cm}^{-1}$ . This approximately corresponds to the difference  $\text{Sn}^+ 5s^3 5p, ^2\text{P}_{1/2} - 5s 5p^2, ^4\text{P}_{1/2}$ , hence we can assume that the photochemical

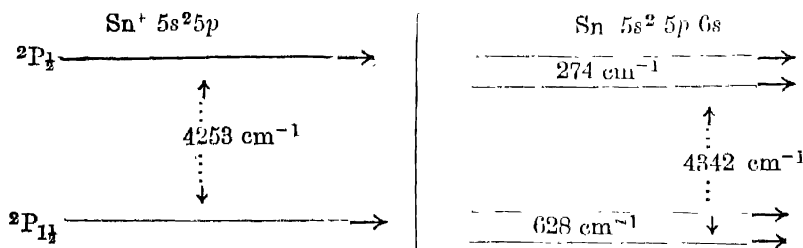
<sup>10</sup> Phys. Rev., Vol. 35, p. 446 (1930).

\* Objection may be taken that the Birge-Sponer method of extrapolation in calculating the energy of dissociation is not applicable to ionic molecules. This objection is based on the fact that  $\omega_e x_e$  curve has not been determined experimentally. In those cases, however, where this determination has been made, *e.g.*, alkali halides, (Sommermeyer, Z. Physik; Vol. 56 p. 548, 1929,) this method of calculation has been found to give quite correct results. There is, further, no strong argument against the use of Birge-Sponer method of calculating the heat of dissociation in the case of ionic molecules, simply because the constituents are ions.

process giving rise to Jevons' bands is the excitation of  $\text{Sn}^+$  from  $5s^2 5p, {}^2P$  to  $5s 5p^2, {}^4P$ .

### 5. Assignment of the Electronic Quantum Numbers to Tin Monochloride Molecule.

Coming to the question of assignment of electronic quantum number to the  $\text{SnCl}$  molecule in its various states we should first note that when a  $6s$ -electron is brought to the  $\text{Sn}^+$  core ( $5s^2 5p$ ) forming  $\text{Sn} (5s^2 5p 6s)$  the coupling is known to be not of the Russell Saunders type but of the  $jj$  type, *i.e.*, we obtain four terms as follows



It may thus seem that the coupling between ' $l$ ' and ' $s$ ' in the  $5p$  electron of  $\text{Sn}^+$  is so strong as to be undisturbed by the imposition of the electric field brought about by the presence of the  $6s$ -electron, whose energy of binding<sup>11</sup> is  $25049 \text{ cm}^{-1}$ .

The  $\text{SnCl}$  molecule is supposed to consist of  $\text{Sn}^+$  and  $\text{Cl}^-$  and the energy of binding of the constituents is calculated to be of the order  $33000 \text{ cm}^{-1}$ . For the upper state of Ferguson's bands, it is only of the order of  $5500 \text{ cm}^{-1}$ . In the first case the energy of binding is very great. According to Hund<sup>12</sup> and Mulliken<sup>13</sup> the coupling between ' $L$ ' and ' $S$ ' vectors is broken in presence of such strong fields. We get the Russell-Saunders type of binding. Hence we may suppose that the molecule in the lower state

<sup>11</sup> Green and Loring, *Phys. Rev.*, Vol. 30, p. 574 (1927).

<sup>12</sup> *Z. Physik*, Vol. 63, p. 726 (1930).

<sup>13</sup> *Reviews Mod. Phys.*, Vol. 4, p. 8 (1932).

corresponds to Hund's 'a' type, or one intermediate between 'a' and 'c'. But for the upper state of Ferguson the electric field is too small, hence the coupling between '*L*' and '*S*' vectors is presumably not broken <sup>14</sup> and we get Hund's case 'c'.

It has been shown by Hund <sup>15</sup> that all the closed shells of an atom remain as closed shells when it combines with another to form a molecule. The valence electrons combine in some way to form the chemical bond. The binding energy of any electron of a closed shell is not changed, no matter how many electrons are placed outside that shell. This has been shown by Moseley from his study of X-ray characteristic lines. It would, thus, appear that the chemical bond and in fact all characteristic molecular properties, *e.g.*, band spectrum, are due to the electrons which do not form closed shells. In the present case the electrons which influence the binding are  $5s^2 5p$  electrons of  $\text{Sn}^+$ , and all the molecular states should be ascribed only to these electrons. In  $\text{Cl}$  all the electrons form closed shells and their quantum characteristics cannot be affected by the presence of a strong electric field. The three electrons of  $\text{Sn}^+$ ,  $5s^2 5p$  will on being perturbed along the electric axis become  $(z\sigma)^2(y\pi)$ , where  $z$  and  $y$  are analogous to total quantum numbers. The states resulting from this configuration will be  ${}^2\pi_{\frac{1}{2}}$  and  ${}^2\pi_{\frac{3}{2}}$ .

Yet a different electronic configuration is possible with the same states ( ${}^2P_{\frac{1}{2}}$ ,  ${}^2P_{\frac{3}{2}}$ ) of  $\text{Sn}^+$ . This is  $(z\sigma)^2(y\sigma)$  and the resulting state is  ${}^2\Sigma_{\frac{1}{2}}$ . On dissociation the states  ${}^2\pi_{\frac{1}{2}}$  and  ${}^2\pi_{\frac{3}{2}}$  (A and B), as well  ${}^2\Sigma_{\frac{1}{2}}$  will break into the same constituents, *viz.*,  $\text{Sn}^+$  ( ${}^2P_{\frac{1}{2}, \frac{3}{2}}$ ) and  $\text{Cl}$  ( ${}^1S_0$ ). But as we see from Fig. 2, the Ferguson's upper states, which ought to have been identified with  ${}^2\Sigma_{\frac{1}{2}}$ , forms a doublet. This can be explained if we assume that the coupling changes from 'a' type of Hund to the 'c' type, as has been pointed out above. Thus in the combination presented by Ferguson's bands, the coupling being of the 'c'

<sup>14</sup> Phys. Rev., Vol. 36, p. 699 (1930).

<sup>15</sup> Z. Physik, Vol. 73, pp. 1,565 (1931); Vol. 74, pp. 1,429 (1932).

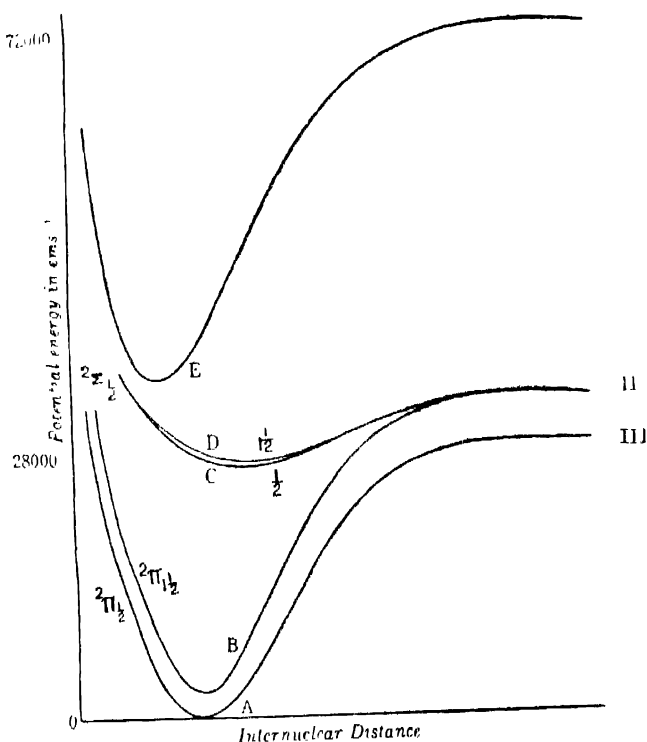
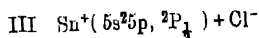
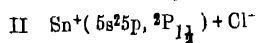
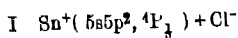


FIG. 2.



type, the  $j$ -vector of  $\text{Sn}^+({}^2P_{1/2})$  precesses about the molecular axis and gives rise to two states with  $\Omega$  (projection of ' $J$ ' on the molecular axis) equal to  $1\frac{1}{2}$  and  $\frac{1}{2}$ . These two states are denoted by C and D. They converge ultimately, at  $r=\infty$ , to the same limit. For small values, they merge into a single level, *viz.*,  ${}^2\Sigma_{1/2}$ , where the binding again changes to the type 'a' of Hund.<sup>16</sup>

<sup>16</sup> In many molecules we often have pairs of states in one of which a  $p\sigma$ , in the other a corresponding  $p\pi$  electron is present. In most of these cases the  $p\pi$  is above  $p\sigma$ .  $\text{CaH}$  is an exception. In this case  $p\sigma$  is above  $p\pi$ . (R. S. Mullikan, *Rev. Mod. Phys.* Vol. 4, p. 24, 1932).  $\text{SnCl}$  appears to be similar to  $\text{CaH}$  in this respect. In the present state of theory there is no method known by which it can be found out without much difficulty which of the two electrons in a molecule is a bonding one,  $\psi\sigma$  or  $\psi\pi$ .



The  $U:r$  curves representing these ( $\frac{1}{2}, 1\frac{1}{2}$ ) states will be as in the Fig. 2. Originating on the left from the same state  $[\text{Sn}^+(^2P_{1/2}) + \text{Cl}^-(^1S_0)]$  they will get separated with a separation equal to  $286 \text{ cm}^{-1}$  at their shallow minima. On the right these curves will again coalesce into a single curve. This part of the curve will represent the  $^2\Sigma_3$  state of the molecule if by any means the atoms could be brought nearer and interatomic field thereby increased to such an extent that the molecule no longer behaves as one of 'c' type, but as a type where Russell-Saunders coupling predominates.<sup>17</sup>

The difference  $286 \text{ cm}^{-1}$ , which Ferguson finds in his upper levels and which he attributes to  $^2\Delta$  separation is nothing but the difference between  $\frac{1}{2}$  and  $1\frac{1}{2}$  levels of  $\text{SnCl}$  when it behaves like Hund's 'c' type. A rotational analysis of the bands of  $\text{SnCl}$  can tell us if these states are  $^2\Delta$  as suggested by Ferguson or  $1\frac{1}{2}, \frac{1}{2}$  as suggested above. In absence of any such analysis we have to rely on other considerations, which have been advanced above. Ferguson's assignment was based on inferences made from results of a very imperfect measurement of the intensity of bands. His assignment is extremely doubtful. Until the theory of transitions from levels of a molecule of 'c' type to one of an 'a' type be fully worked out, the interpretation of the rotational analysis will be doubtful.

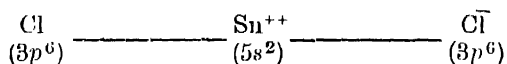
With the data at hand one cannot be very definite about the designation of the upper level of Jevons' bands, except that in that state the molecule will belong to Hund's type 'a'.

## 6. *Interpretation of the Absorption Spectrum of Tin Dichloride.*

We can now interpret the absorption spectrum of tin dichloride. As we have seen above,  $\text{SnCl}_2$  is diamagnetic. It

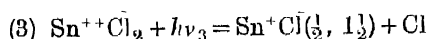
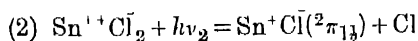
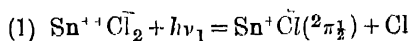
<sup>17</sup> We will get yet one more molecular electronic state from  $\text{Sn}^+(^2P_{3/2})\text{Cl}^-$ , where the molecule behaves as one of Hund's type 'c.' Its  $\Omega$  quantum number will have the value  $\frac{1}{2}$ . Such a state is, however, not obtained experimentally and its absence may be explained by assuming it to be a repulsive state.

means that the molecule has no magnetic moment. This will be the case when each of the constituent atoms has its extranuclear electrons only in closed shells. In  $\text{SnCl}_2$  this state of affairs can be represented as



Each one of the three units has got only closed shells. This kind of ionic binding explains fully the diamagnetic character of the molecule.

When this molecule is optically dissociated,  $\text{SnCl}$  is produced. This process can be expressed by the following equations : <sup>18</sup>



This process of optical dissociation amounts virtually to a passage of an electron from Cl part of  $\text{SnCl}_2$  molecule to  $(\text{Sn}^{++}\text{Cl}^-)$  part. The Cl, relieved of the electron, suffers a repulsive force and flies off, leaving the residue as  $(\text{Sn}^{++}\text{Cl}^-)^-$ . The only form, that it will take, will be  $\text{Sn}^+\text{Cl}^-$ . If it be in its various electronic states, we will get several regions of continuous absorption. The difference between the long wave-length beginnings of the first two absorption regions is  $2384 \text{ cm}^{-1}$ . The difference between the term values of  $^2\pi_{\frac{1}{2}}$  and  $^2\pi_{1\frac{1}{2}}$  states of  $\text{SnCl}$  at  $v=0$  is  $2360 \text{ cm}^{-1}$ . This correspondence between these differences shows that  $\text{SnCl}_2$  breaks on optical dissociation into  $\text{SnCl}$  ( $^2\pi_{\frac{1}{2}}$  and  $^2\pi_{1\frac{1}{2}}$ ) and Cl. The  $\text{SnCl}$  molecule thus produced is the same as gives rise to Ferguson's and Jevons' bands. Since the binding in the molecule which gives rise to these bands is ionic and the  $\text{SnCl}$  molecule obtained by the dissociation of  $\text{SnCl}_2$  is the same as this, we can say that the binding is ionic in both the  $\text{SnCl}$  molecules. We can assume that only one of the bonds

<sup>18</sup> States  $^2\pi_{\frac{1}{2}}$ ,  $^2\pi_{1\frac{1}{2}}$ ,  $\frac{1}{2}$ ,  $1\frac{1}{2}$  are represented in Fig. 2 by A, B, C and D curves.

of  $\text{Cl}^- - \text{Sn} - \text{Cl}^-$  molecule is affected by the optical dissociation and the rest of it is left intact, and that both the bonds are similar. As  $(\text{SnCl})$  portion of  $\text{SnCl}_2$  molecule has ionic binding, we can say, in view of the above arguments, that the whole of  $\text{SnCl}_2$  has ionic binding.

It can further be assumed that the third region of continuous absorption signifies the dissociation of  $\text{SnCl}_2$  molecule into  $\text{Cl}$  and  $\text{SnCl}$  in states  $\frac{1}{2}$  and  $1\frac{1}{2}$  (states C, D). These are the next higher electronic states of  $\text{SnCl}$ . The difference between these two states, equal to  $286 \text{ cm}^{-1}$ , is so small that they will not give rise to two distinct regions of continuous absorption. The difference between the beginnings of the second and third regions of continuous absorption, however, does not correspond to the difference between the energies of the  ${}^2\pi_{1\frac{1}{2}}$  and  $\frac{1}{2}$  states of  $\text{SnCl}$ .

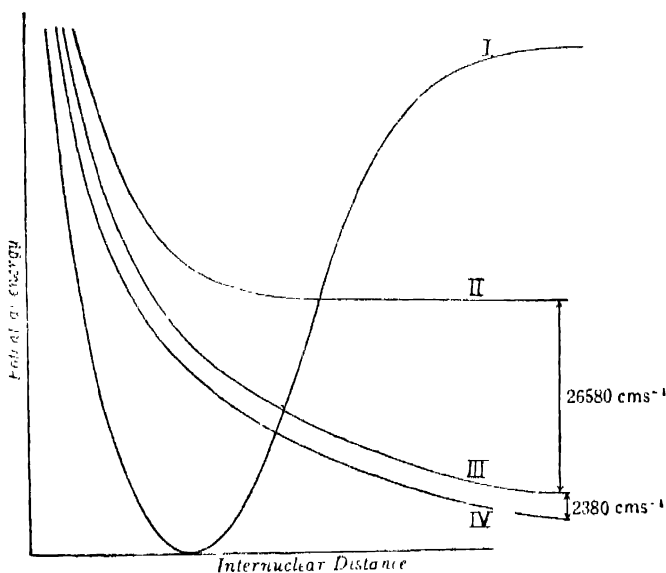


FIG. 3.

- I  $\text{Sn}^{++} + \text{Cl}_2^-$
- II  $\text{SnCl}(\frac{1}{2} \text{ or } 1\frac{1}{2}) + \text{Cl}$
- III  $\text{SnCl}({}^2\pi_{1\frac{1}{2}}) + \text{Cl}$
- IV  $\text{SnCl}({}^2\pi_{1\frac{1}{2}}) + \text{Cl}$

It is much less. This is probably due to the potential energy curves of  $\text{SnCl} ({}^2\pi) - \text{Cl}$  being very steep, whereas the curve for  $\text{SnCl} ({}^1\Sigma) - \text{Cl}$  is comparatively flat, as is shown in Fig. 3. These curves explain only qualitatively the appearance of the third region of absorption so near to the second region.

This point can, however, be substantiated by a study of the fluorescence spectrum of  $\text{SnCl}_2$ . The  $\text{SnCl}_2$  molecule, if illuminated by a light of wave-length smaller than the beginning of the third region of continuous absorption, i.e., 2883 Å. U., will give rise to  $\text{SnCl}$  molecule in its normal and excited states. These excited molecules in falling back to their normal state will give rise to Ferguson's bands.

The region where these bands are expected is  $\lambda\lambda$  3100-3900. This experiment was actually tried.  $\text{SnCl}_2$  was taken at a vapour pressure of 0.001 mms. As the fluorescence spectrum under investigation is also expected to be in the same region, the intensity of the fluorescence spectrum, already very weak, would be still reduced by the absorption of  $\text{SnCl}_2$  molecules lying in the passage. It was to reduce such a weakening of the fluorescence spectrum that the pressure of the  $\text{SnCl}_2$  vapour was reduced. But the more its pressure was reduced, the more feeble became the fluorescence spectrum, because of the smaller number of molecules coming in the path of the exciting radiation. The 0.001 mms. actually chosen was a compromise between the two conflicting requirements. The exposure was 50 hours and the plates used were Ilford Golden Iso-zenith, speed 1400 H & D.

Even after such a long exposure all that was obtained was two faint patches at 3450 Å. U. and 3750 Å. U. They are just at the position expected for Ferguson's bands, but on account of the small dispersion used, no structure was discernible. The experiment is not very much decisive and it is being repeated with better conditions.

It might be supposed that in the case of  $\text{SnCl}$  there are yet one or more curves lying between C and B which correspond to the dissociation of the  $\text{SnCl}$  molecule into Sn and Cl. If

such were the case, the third region of continuous absorption in the case of  $\text{SnCl}$ , would correspond to the dissociation of  $\text{SnCl}_2$  into  $\text{Cl}$  and  $\text{SnCl}$  in the state which is represented by these curves lying between B and C. The existence of such curves is, however, very much improbable as can be seen from the following consideration. The curve A leads on dissociation to  $\text{Sn}^+$  ( $5s^25p$ ,  $^2P_{\frac{1}{2}}$ ) and  $\text{Cl}$ . The energy of formation of  $\text{Sn}^+$  ( $5s^25p$ ,  $^2P_{\frac{1}{2}}$ ) from  $\text{Sn}$  is given by  $I_p = 59192 \text{ cm}^{-1}$ <sup>19</sup> and the energy of

formation of  $\text{Cl}$  from  $\text{Cl}$  is again given by  $E_c = 86.5 \text{ kcal} = 30415 \text{ cm}^{-1}$ <sup>20</sup>. The portion of the potential energy curve for the molecule composed of  $\text{Sn}$  and  $\text{Cl}$ , which corresponds to large internuclear distance, must be  $I_p + E_c = 89607 \text{ cm}^{-1}$  below the similar portion of curve A. Even if this curve is supposed to be very much steep, it is hardly probable that it will ever cross the curve A above the minimum. For the depth of the minimum below that portion of the curve A which correspond to the molecule formed of two atoms  $\text{Sn}^+$  and  $\text{Cl}$  at a large distance, is about 28000 in  $\text{cm}^{-1}$  units. It can thus be safely supposed that there is no intervening curve between B and C.

Thus it appears that the  $\text{SnCl}$  molecule obtained as a result of the optical dissociation of  $\text{SnCl}_2$  when it is subjected to light of proper wave-length, is the same as that which gives rise to various bands. The binding in both  $\text{SnCl}$  and  $\text{SnCl}_2$  is ionic. The  $\text{SnCl}$  molecule obtained by the dissociation of  $\text{SnCl}_2$  is in one of its electronic states,  $^2\pi_{\frac{1}{2}}$ ,  $^2\pi_{\frac{3}{2}}$ ,  $^1\Sigma$  and  $1^1\Sigma$ .

### 7. Acknowledgment.

My sincere thanks are due to Prof. M. N. Saha, F.R.S., for his valuable guidance throughout the work.

<sup>19</sup> Bacher and Goudsmidt, 'Atomic Energy States,' p. 439.

<sup>20</sup> *Zs. f. Phys.*, 75, 17, 1931



# The Surface-force Theory of Rectification in Ionic Crystals

By

S. R. KHASTGIR, D.Sc.

*Reader in Physics, Dacca University*

*(Received for publication, December 13, 1934)*

## 1. *Unbalanced Electrostatic Force on the Surface of an Ionic Crystal.*

In ionic crystals, there is an array of net positive and negative charges which may be considered to be situated at the lattice points. If we take a crystal-plane where *similar* sets of ions are placed at regular intervals, it is evident, when we consider the surface layer and the next, that any ion on the surface layer will experience an unbalanced electrostatic force. If the first layer contains *all positive* ions, the next will have *all negative* ions. The unbalanced electrostatic force will then be directed towards the interior of the crystal. Alternatively, if the first layer contains *all negative* ions, the direction of the surface-force will be the other way. If again, a crystal-plane contains oppositely charged ions alternately, the electrostatic forces will act in opposite directions alternately. Applying the problem to the (100) face of a crystal of the NaCl type, Lennard-Jones, Taylor and Dent<sup>1</sup> have calculated the values of the electrostatic force for various points on the crystal surface.

<sup>1</sup> Lennard-Jones, Taylor and Dent., Trans. Faraday Soc., Vol. XXIV, 1928.

## 2. *The Cause of Rectification in Ionic Crystals.*

Of the two features of the current-voltage characteristic curves for rectifying crystals, namely, (1) asymmetry and (2) curvature, the first can be explained in the case of the ionic crystals in terms of the electrostatic surface-force. The surface-force retards electrons which flow in the same direction as and accelerates those flowing in a direction opposite to the electrostatic force. Thus when an alternating voltage is applied to the surface of such a crystal, the surface-force gives rise to a unidirectional current. The direction of the current depends on the direction of the electrostatic force on the crystal-surface. Considering the crystal-planes which contain *similar* sets of ions, if the first layer has all *positive* ions, the direction of the rectified current will be towards the interior of the crystal. If on the other hand, the first layer contains all *negative* ions, the rectified current will flow from the crystal to the "whisker" which is in contact with the surface of the crystal. If we call the rectified current positive, when it flows from the crystal to the "whisker," we would have negative rectification in the former case and positive rectification in the latter case. Both negative and positive rectification effects are therefore possible. In the planes which contain oppositely charged ions alternately, the "whisker" which is in contact with a large number of such ions, gives on an average, no rectification. In the case of a natural crystal, made up of many tiny crystals, the "whisker" may rest on any kind of planes exhibiting thereby positive, negative or no rectification. This is what has been actually observed, when several natural crystals of irregular form have been studied by the author in collaboration with Mr. A. K. Das Gupta. Only crystals of good crystalline form have shown rectification effects in the same direction.

To explain the curvature of the current-voltage characteristic curves, we should consider first the *local heating at the junction*,



As pointed out by Eccles,<sup>2</sup> the contact-resistance would gradually diminish with the increase of the voltage applied to the crystal due to the gradually increasing local heating at the junction. The increase of current due to this fall of contact-resistance can be more than proportionate with the increase of the applied voltage. The effect of this Joulean heating at the contact-point is the main cause of the curvature in the current-voltage characteristic curve.

*The effect of strain on the crystal* may also produce a slight curvature. The applied voltage causes a displacement of the ions from their positions of equilibrium. When the opposing elastic force is overcome by the applied field, the ions are set free. A part of the applied voltage is necessary to overcome the opposing elastic force and the rest is expended in driving the current through the crystal. All the ions are not however, set free at a definite voltage. There must always be a certain range of voltage within which all the different ions are liberated. This will evidently cause a bend in the current-voltage curve over this range of voltage. Dowsett<sup>3</sup> analysed the current-voltage characteristic curves for carborundum in a similar way.

Thus the electrostatic surface-force together with the heating effect at the contact-point and the effect of strain on the crystal can satisfactorily explain the two features in the phenomenon of rectification in the ionic crystals which do not show volume rectification.

### 3. *Different Degrees of Rectification on the same Surface.*

On a strictly plane surface of a good single crystal, the rectification effect must be more or less the same. The surface however is never plane. Invariably there are cracks and crevices

<sup>2</sup> Eccles, Proc. Phys. Soc. Vol. 22, 1914.

<sup>3</sup> Dowsett, Wireless Telephony and Broadcasting, Vol. II, Chap. II, p. 29.

and sometimes impurities, causing thereby varying degrees of asymmetry in the current-voltage characteristic curve. Again, the contact resistance may vary from point to point depending on the surface condition. These different values of the contact-resistance would result in different amounts of local heating. The curvature of the current-voltage curve is therefore expected to be different for different contact points ; for the curvature has been mainly attributed to the Joulean heating at the contact-point.

#### 4. *Necessity of a small Contact Area for Rectification in the Ionic Crystals which do not show Volume Rectification.*

A small contact area for rectification is necessary in the case of the ionic crystals which do not show volume rectification. A large contact area means a large number of contact-points of varying degrees of rectification and the average gives a small effect. Besides, for some points, the contact resistance may be extremely small, causing more or less a short circuit. When the crystal is soldered on one side and a "whisker" is pressed at a point on the other side, we really observe the difference in the rectification effects for an extremely small and for a very large area of contact. The small area of the point contact controls the rectification.

#### 5. *Variation of Resistance and Rectification Ratio with the Applied Voltage.*

How the resistance in either positive or negative direction changes with the increasing applied voltage depends on the shape of the current-voltage characteristic curve. In all our experiments, the resistance has been found to decrease with the increase in the applied voltage. This is explicable, for with the increase in the voltage, the Joulean heating at the junction is increased and the contact-resistance falls. Besides, the fall of

resistance may be expected, if the number of ions liberated increases<sup>4</sup> at a rate more than proportionate with the applied voltage. The rate of decrease of resistance is not the same for the two opposite directions. It is however, not possible to say definitely how the rectification ratio (the ratio of the difference in the rectified currents in the two opposite directions to the current in the low-resistance direction) should change with the increase of the applied voltage. In our experiments, the ratio has been found to increase in some cases and in some cases to decrease with the applied voltage. In some cases again, there has been an initial increase followed by a slight continuous decrease.

6. *Rectification observed with the Ionic Crystals (which do not show Volume Rectification) in contact with Pointed Crystals of the same Composition.*

The electrostatic surface-force is increased or decreased as the corresponding force at the pointed end is in the same as or opposite to that on the surface. Again a dipole induced in the pointed crystal reduces the electrostatic force on the surface of the crystal, thus decreasing the rectifying power. A small or sometimes a moderate value of rectification is thus expected. This is what has been found in our experiments. Eccles'<sup>5</sup> thermoelectric theory or Schottky's<sup>6</sup> electronic theory of rectification cannot explain the results of these experiments.

7. *Effect of Heating the Contact-point on the Rectifying Power.*

The interplanar distance in the upper layers of the crystal surface increases in the region of the contact, when the junction

<sup>4</sup> This is contrary to Joffe's idea. According to Joffe, Ohm's law holds in crystals. Hevesy, however, thinks that the degree of dissociation increases as the applied field is increased. *Vide Joffe's Physics of Crystals*, p. 94.

<sup>5</sup> Eccles, *Proc. Phys. Soc.*, Vol. 15, 1915.

<sup>6</sup> Schottky, *Zeit f. Physik.*, 14, 1923.

is heated. The electrostatic surface-force is therefore slightly reduced in value. A slight diminution of the rectification effect in the ionic crystals (which do not show volume rectification) on heating the contact point is thus expected. The effect of the thermionic emission from the heating coil may have some effect, especially when the heating current is large. In the crystals, which show negative rectification, the first layer on the surface has been supposed, according to the surface-force theory, to contain only positive ions. The negative charges due to the thermions would cause a force in a direction opposite to that of the surface-force at the contact-point. This may reduce the rectification effect to a certain extent. When the heating current is large, it may sometimes be possible for the emitted thermions to cause a force larger than the surface-force, so that there may be a change in the direction of the rectified current on heating the contact point. In the case of the crystals which show positive rectification, the negative ions are on the first layer. The thermions get repelled and cannot produce any appreciable effect.

The experiments with Mr. Das Gupta have shown these features. Usually there is a decrease in the rectifying power when the contact-point is heated. With iron-pyrites (which shows negative rectification) in some experiments, a change in the sign of the rectified current on heating the contact-point has been observed, when the rectified current has been small.

#### 8. *Effect of Heating the Crystal on Rectification.*

On heating a crystal there is an atmosphere of free ions in the crystal lattices. The photo-electrons which are normally embedded among the different lattices are set free, making the crystalline medium a better conductor. The electrostatic force on the surface layer of the crystal will thus be reduced. When the medium becomes sufficiently conducting, the surface-force may be extremely small. The rectifying power of some

crystals may thus be practically lost on sufficiently heating the crystals. Our experimental results and those of Flowers<sup>7</sup> showing complete or partial loss of the rectifying power of crystals on heating, can thus be explained. Frenkel-Jeffe's<sup>8</sup> theory can also explain the decrease in the rectifying property on heating.

### 9. *Effects of Ultra-violet Light and X-rays.*

Ultra-violet light produces electronic conductivity in dielectric crystals and liberates electrons inside the lattice. This internal photoelectric effect does not necessarily lead to an external effect. When the energy of the incident ultra-violet light is sufficient to produce the internal photoelectric effect, the surface electrostatic force will then be slightly reduced as the conductivity of the crystal is slightly increased owing to the electronic conductivity. When there is external photoelectric effect, the electrons emitted outside the surface tend to further reduce the surface electrostatic force in crystals which show negative rectification. With crystals which show positive rectification, the photoelectrons emitted outside are only repelled by the negative ions on the first layer and do not produce any effect. There will be a small decrease in rectification due to the internal photoelectric effect only which slightly increases the conductivity of the crystal.

The effect of X-rays will be similar and more pronounced. Inside and outside the crystal, the recoil electrons are produced by scattering. The conductivity of the crystal may thus be increased, reducing considerably the electrostatic force which determines the rectification effect.

The reduction in the rectifying property on exposure to ultra-violet light has been extremely slight in our experiments. There has been a very pronounced decrease in the rectification

<sup>7</sup> Flowers, *Phys. Rev.*, 1909.

<sup>8</sup> Frenkel-Jeffe, *Phys. Rev.*, 39, 1932.

effect on exposure to X-rays. The results of Jackson's <sup>9</sup> experiments and our own experiments can therefore be explained.

#### 10. *Rectification in Crystals having no Centres of Symmetry.*

The existence of volume rectification in carborundum, zincite and silicon and the absence of it in the symmetrical crystals (*e.g.*, iron pyrites, galena, molybdenite, pyrolusite, bornite, etc.) which have been observed in the experiments with Mr. Dasgupta have suggested the classification of crystal-detectors into two groups : (1) ionic crystals having centres of symmetry, and (2) ionic or non-ionic crystals having no such symmetry. In the symmetrical ionic crystals, we observe the rectification due to the surface force and this is associated with point contacts. *The surface-force theory given in this paper refers to the symmetrical ionic crystals.* In the case of the ionic crystals having no centres of symmetry, we have to consider the volume rectification in addition to the rectification due to the surface force. The volume rectification can be tentatively attributed to the asymmetry in crystal structure as suggested by R. de L. Krönig <sup>10</sup> in his theory. According to Krönig, the crystal rectification is due to asymmetrical binding of the ions into positions of equilibrium by restoring forces not symmetrical for equal and opposite displacement. We can however explain the volume rectification in this way.

#### 11. *Summary.*

A theory based on the existence of an unbalanced electrostatic force on the surface of an ionic crystal has been proposed in this paper to explain the phenomenon of contact-point rectification in symmetrical ionic crystals. It has been shown how this electrostatic force together with the heating effect at the contact point and the effect of strain on the crystal can satisfactorily

<sup>9</sup> Jackson, *Phil. Mag.*, May, 1929.

<sup>10</sup> Krönig, *Nature*, March 2, Vol. 123, 1929.

explain the asymmetry and the curvature of the current-voltage characteristic curves for the symmetrical ionic crystals. The different degrees of rectification for the different point on the surface and the necessity of a point-contact have been explained. The following experimental results obtained with *symmetrical ionic crystals* are explicable according to the proposed surface-force theory.

(1) The positive, negative and no rectification effects observed in the natural poly-crystals.

(2) The fixed direction of the rectified current in crystals of good crystalline form.

(3) Rectification observed with crystals in contact with pointed crystals of the same composition.

(4) The effect of heating the contact-point on rectification.

(5) The effect of heat, ultra-violet light and X-rays on rectification.

In crystals having no centres of symmetry, the volume rectification has to be considered. There is evidence of very pronounced volume rectification in carborundum, zincite and silicon which can be explained according to Krönig as due to asymmetric binding of the ions, the restoring forces not being symmetrical for equal and opposite displacements.\*

\* An outline of the surface-force theory of rectification is recently published in *Nature*. Vol. 135, 1935, p. 148.





## On Some Characteristics of the Long and Short Spectral Lines

By

S. DATTA, D.Sc. (LONDON)

*Professor of Physics Presidency College, Calcutta*

AND

KEDARNATH CHATTERJEE, B.Sc.

*Research Student.*

(Plate IX.)

(Received for publication, March 12, 1935.)

### 1. *Introductory.*

In an electric arc the space from pole to pole, *i.e.*, the core of the arc is filled with the vapour of the substance under experiment. The temperature as well as the density in the core is very high as compared to those in the sides. If an image of the arc in the transverse position is thrown on the slit of an instrument for spectroscopic analysis, the spectrum obtained is that of a section of the arc normal to its length. In such a spectrum (see Plate IX, A) some lines stretch right across the core from side to side while others seem to originate from the core alone and thus appear to have a length much shorter than the former. These were designated as the *long* and *short* lines respectively by Lockyer.<sup>1</sup>

Though this nomenclature is known to spectroscopists from a very long time no attempt at a systematic classification of the long and short lines with a view to trace their significant differentiating features seem to be on record. In the first

<sup>1</sup> Spectroscopy by E. C. C. Baly, p. 514, 1918; Phil. Trans., 164, 479 (1874).

instance the long and short lines of copper have been classified. On a scrutiny of these, a striking regularity has been observed, that if the relative orientation of the resultant  $l$  and  $s$  vectors in the initial and final states are compared, then those, for which the change in the orientation is large are invariably short lines; whereas those for which the orientation change is small come to the category of long lines. Besides these, transitions which indicate a change of the  $s$  vector, also come out as short lines; this, however, is not without exception.

Experiments have also been performed with the arc at reduced pressures (Plate IX, B) and the following interesting features have been noticed :—

1. Lines which are short in the arc at atmospheric pressure are further shortened in length.

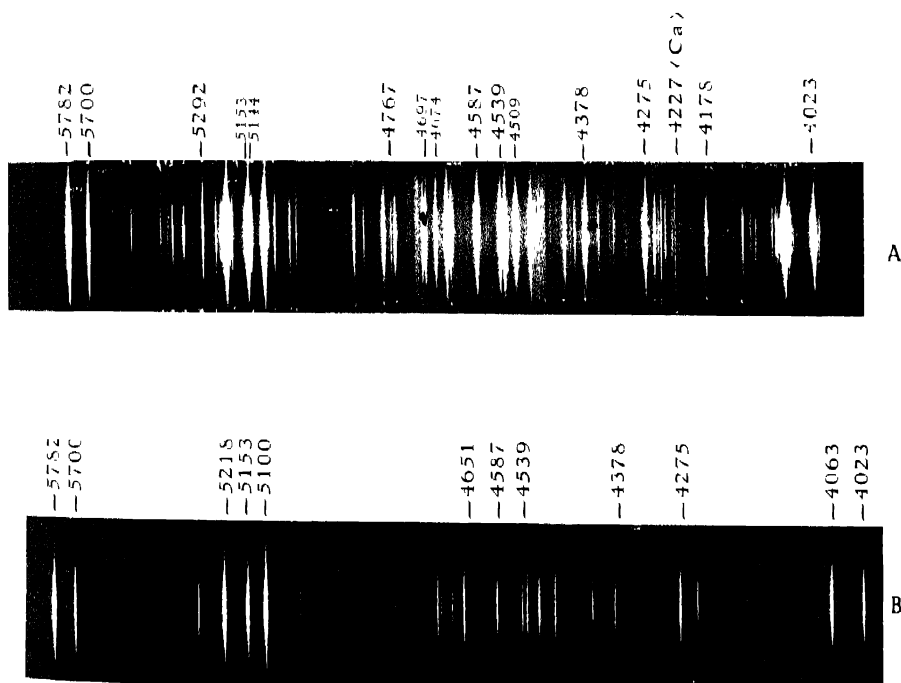
2. Lines which are ordinarily long and for which the orientation change is small but not zero appear as short lines.

3. Long lines for which the orientation change is zero generally persist as long lines even at comparatively low pressures

Experiments are in progress with other metals, such as silver, zinc, iron, etc.

## 2. *Experimental.*

With the arc at atmospheric pressure, the arrangement consists in photographing the spectrum with the enlarged image of the arc in a horizontal position, focussed on the vertical slit of a large two-prism spectrograph with Littrow mounting giving a dispersion of 8 A. U. per mm. at  $\lambda 4023$ . The entire length of the slit (2 cm. long) was thus illuminated so that each part of the spectral image on the photographic plate, neglecting astigmatism, which is rather small in a prism spectrograph, may be regarded as corresponding to different points of the arcs along a normal to its length.





The chief difficulty in this experiment that had to be surmounted was to make the arc steady, which is essential in the present case to obtain any reliable results. This was done by the method adopted by H. Nagaoka and Y. Sugiura<sup>3</sup> and consisted in the introduction of a large capacity and self-inductance between the electrodes. A capacity of 3 micro-farad and a solenoid with a bundle of soft iron wires in the core were used.

For the best working, the current had also to be suitably adjusted. With copper arc, a current of about 5 amps. gave the best results.

Each time a photograph was taken, the ends of the rods of the metal were cut down into the form of a cone and this helped in keeping the arc still more steady.

In the visible region, high speed Ilford Panchromatic plates were used and an exposure of one and a half minutes was sufficient.

For experiments at low pressures, the electrodes were held horizontally, by some mechanical arrangement, inside a metal case provided with a small circular quartz window for letting out the light. The metal case was made air-tight by screwing on it a heavy lid provided with rubber pad round the four edges. The arc could be struck and the gap adjusted from outside by means of an electromagnetic arrangement. The pressure in the chamber was then reduced by a Cenco-Hyvac air pump.

### 3. *Experimental Results.*

Long and short lines of copper have been classified in three separate tables. Table I contains lines of the P—D and F—D combination. Transitions from various initial levels to a particular final level have been grouped together so as to show at a glance how the lengths vary as the orientations between the L

<sup>3</sup> Jap. Journ Phys., 3, 45 (1924).

and  $S$  vectors change. The orientation changes  $\Delta \theta$  have been entered into the seventh column and has been calculated from the difference in the value of  $\theta$ , *i.e.*, the angle between the  $l$  and  $s$  vectors of the terms involved in the translation as obtained from the equation

$$\cos \theta = \frac{l^2 + S^2 - j^2}{2ls}.$$

The configurations of the atoms and the types of the various terms arising therefrom, as also their values have been obtained by reference to A. G. Shenstone, *Phys. Rev.*, 28, 449 (1926), and Bacher and Goudsmit, "Atomic Energy States," pp. 175-179. First Edition, 1932.

TABLE I.

Final level.		Initial level.					
Configura- tion.	Symbol.	Configura- tion.	Symbol.	$\lambda$	Nature	$\Delta \theta$ in degrees.	Remarks.
$3d^9 4s^2$ .	$2D_{2\frac{1}{2}}$	$3d^{10} 4p$	$2P^\circ_{1\frac{1}{2}}$	5106	Long	0	Long at low pressures.
		$3d^9 4s 4p$	$4P^\circ_{2\frac{1}{2}}$	3594	Short	0	$s$ changes
		$3d^9 4s 4p$	$4P^\circ_{1\frac{1}{2}}$	3456	Short	70	" "
$3d^9 4s^2$ .	$2D_{4\frac{1}{2}}$	$3d^{10} 4p$	$2P^\circ_{\frac{1}{2}}$	5782	Long	0	Long at low pressures.
		"	$2P^\circ_{1\frac{1}{2}}$	5700	"	180	Shortened at low pressures.
		$3d^9 4s 4p$	$4P^\circ_{1\frac{1}{2}}$	3720	Short	70	$s$ changes.
		"	$4P^\circ_{\frac{1}{2}}$	3609	Short	0	"
		"	$4F^\circ_{2\frac{1}{2}}$	3530	Long	55	"
		"	$4F^\circ_{1\frac{1}{2}}$	3440	Short	0	"
$3d^{10} 4p$ .	$2P^\circ_{\frac{1}{2}}$	$3d^{10} 4d$	$2D_{1\frac{1}{2}}$	5153	Long	0	Long at low pressures.
		$3d^{10} 5d$	$2D_{1\frac{1}{2}}$	4023	Long	0	"

TABLE I.—(Contd.)

Final level.		Initial level.					
Configura- tion.	Symbol.	Configura- tion.	Symbol.	$\lambda$	Nature.	$\Delta\theta$ in degrees.	Remarks.
3d <sup>9</sup> 4s 4p.	<sup>2</sup> P° 1½	3d <sup>10</sup> 4d.	<sup>3</sup> D <sub>2½</sub>	5218	Long	0	Long at low pressures.
		3d <sup>10</sup> 5d.	<sup>2</sup> D <sub>2½</sub>	4063	Long	0	"
		3d <sup>10</sup> 6d.	<sup>2</sup> D <sub>2½</sub>	3687	Long	0	"
	<sup>4</sup> P° 2½	3d <sup>9</sup> 4s(3D)5s	<sup>4</sup> D <sub>2½</sub>	4178	Short	90	"
		"	<sup>4</sup> D <sub>3½</sub>	4275	Long	0	
	<sup>4</sup> P° 1½	"	<sup>4</sup> D <sub>1½</sub>	4259	Short	62	
		"	<sup>4</sup> D <sub>½</sub>	4104	Short	110	
		"	<sup>4</sup> D <sub>2½</sub>	4378	Long	20	
	<sup>4</sup> P° ½	"	<sup>4</sup> D <sub>1½</sub>	4415	Short	48	Short at low pressures.
		"	<sup>4</sup> D <sub>½</sub>	4248	Long	0	}
	<sup>4</sup> F° 4½	"	<sup>4</sup> D <sub>3½</sub>	4651	Long	0	
		"	<sup>4</sup> D <sub>2½</sub>	4587	Long	6	
	<sup>4</sup> F° 3½	"	<sup>4</sup> D <sub>3½</sub>	4704	Short	84	
		"	<sup>4</sup> D <sub>3½</sub>	4797	Short	124	
	<sup>4</sup> F° 2½	"	<sup>4</sup> D <sub>2½</sub>	4674	Short	34	
		"	<sup>4</sup> D <sub>1½</sub>	4539	Long	8	"
	<sup>4</sup> F° 1½	"	<sup>4</sup> D <sub>2½</sub>	4842	Short	90	
		"	<sup>4</sup> D <sub>1½</sub>	4697	Short	48	
	<sup>2</sup> F° 2½	"	<sup>4</sup> D	4500	Long	0	
		"	<sup>4</sup> D <sub>3½</sub>	5352	Long	180	
		"	<sup>4</sup> D <sub>2½</sub>	5201	Short	90	
		"	<sup>4</sup> D <sub>1½</sub>	5034	Short	48	

Table II contains a set of short lines which do not follow the general rule laid down in the introductory section regarding the length of lines and their orientation changes. They however, all arise from a particular type of transition, *viz.*, D°→D, P, F, G, whose peculiarities have been discussed in a subsequent section.

TABLE II.

Final Level.		Initial Level.			
Configura- tion.	Symbol.	Configuration.	Symbol.	$\lambda$	Nature.
$3d^9 4s 4p$	$4D^0 3\frac{1}{2}$	$3d^9 4s (3D) 5s$	$4D \frac{1}{2}$	5292	Short.
		"	$4D$	5144	"
		$3d^9 4s (1D) 5s$	$2D$	4231	"
		$3d^9 4s (3D_3) 4d$	$2G_4$	3655	"
		"	$2D$	3624	"
	$4D^0 3\frac{1}{2}$	"	$2F$	3620	"
		$3d 4s (3D_3) 4s$	$4P 2\frac{1}{2}$	3613	"
		"	$4D 3\frac{1}{2}$	3602	"
		"	$4F$	3599	"
		$3d^9 4s (D_2) 4d$	$4G 4\frac{1}{2}$	3512	"
	$4D^0 2\frac{1}{2}$	"	$4F 3\frac{1}{2}$	3498	"
		$3d^9 4s (3D_3) 5s$	$4D 3\frac{1}{2}$	5555	"
		"	$4D 2\frac{1}{2}$	5392	"
		$3d^9 4s (1D) 5s$	$2D 2\frac{1}{2}$	4397	"
		"	$2D 1\frac{1}{2}$	4242	"
	$4D^0 2\frac{1}{2}$	$3d^9 4s (3D_3) 4d$	$4S 1\frac{1}{2}$	3759	"
		"	$2D 2\frac{1}{2}$	3745	"
		"	$2F 3\frac{1}{2}$	3741	"
		"	$4P 2\frac{1}{2}$	3734	"
		$3d^9 4s (3D_2) 4d$	$4D 2\frac{1}{2}$	3614	"
	$4D^0 1\frac{1}{2}$	"	$4F 3\frac{1}{2}$	3610	"
		$3d 4s (3D_1) 4d$	$4G 3\frac{1}{2}$	3483	"
		"	$4G 2\frac{1}{2}$	3472	"
		$3d^9 4s (3D) 5s$	$4D 2\frac{1}{2}$	5432	"
		"	$4D 1\frac{1}{2}$	5250	"
	$4D^0 1\frac{1}{2}$	"	$4D \frac{1}{2}$	5016	"



TABLE II.—(Contd.)

Final Level.		Initial Level.			
Configura- tion.	Symbol.	Configuration.	Symbol.	$\lambda$	Nature.
$3d^9 4s 4p$	$^4D_{1\frac{1}{2}}$	$3d^9 4s(^1D)5s$	$^2D_{1\frac{1}{2}}$	4267	Short.
		$3d^9 4s(^3D_2)4d$	$^4D_{1\frac{1}{2}}$	3	"
	$^4D^0_{1\frac{1}{2}}$	$3d^9 4s(^3D_1)4d$	$^2S_{\frac{1}{2}}$	3500	"
		"	$^4G_{2\frac{1}{2}}$	3488	"
		"	$^4F_{2\frac{1}{2}}$	3475	"
	$^4D^0_{\frac{1}{2}}$	$3d^9 4s(^1D)5s$	$^2D_{1\frac{1}{2}}$	4336	"
		$3d^9 4s(^3D_1)4d$	$^2S_{\frac{1}{2}}$	35	"
		"	$^4F_{1\frac{1}{2}}$		"
	$^2D^0_{1\frac{1}{2}}$	$4d^9 4s(^3D)5s$	$^2D_{2\frac{1}{2}}$	5400	"
		$3d^9 4s(^1D)5s$	$^2D_{2\frac{1}{2}}$	4767	"
		$3d^9 4s(^3D_1)$	$^2S_{\frac{1}{2}}$	3712	"
		$3d^9 4s(^3D)5s$	$^2D_{2\frac{1}{2}}$	5536	"
	$^2D^0_{2\frac{1}{2}}$	$3d^9 4s(^1D)5s$	$^2D_{2\frac{1}{2}}$	4867	"
		$3d^9 4s(^3D_2)4d$	$^2D_{2\frac{1}{2}}$	4080	"
		"	$^2F_{3\frac{1}{2}}$	4075	"
		$3d^9 4s(^3D_1)4d$	$^4G_{3\frac{1}{2}}$	3772	"
		$3d^9 4s(^1D)4d$	$^2P_{1\frac{1}{2}}$	3487	"

Table III consists of lines corresponding to transitions involving an  $s$  level in which case the value of  $l$  being zero the angle between the  $l$  and  $s$  vectors becomes incomprehensible. It will be seen from this table that lines due to transition from energy levels higher than  $3d^{10} 6s$  are short. Below this all lines are long.

TABLE III.

Final Level.		Initial Level.		$\lambda$	Nature.
Configura- tion.	Symbol.	Configuration.	Symbol.		
$3d^{10}4s$	$4S_{\frac{1}{2}}$	$3d^{10}4p$	$2P^0_{\frac{3}{2}}$	3274	Long.
		$3d^{10}4p$	$2P^0_{\frac{1}{2}}$	3248	"
$3d^{10}4p$	$2P^0_{\frac{1}{2}}$	$3d^{10}6s$	$2S_{\frac{1}{2}}$	4481	"
		$3d^{10}7s$	$2S_{\frac{1}{2}}$	3825	Short.
		$3d^{10}8s$	$2S_{\frac{1}{2}}$	3566	"
		$3d^{10}6s$	$2S_{\frac{3}{2}}$	4530	Long.
$3d^94s4p$	$2P_{\frac{1}{2}}$	$3d^{10}7s$	$2S_{\frac{3}{2}}$	3861	Short.
	$4D^0_{\frac{3}{2}}$	$3d^94s(3D_3)4d$	$4S_{\frac{1}{2}}$	3759	"
		$3d^94s(3D_1)4d$	$2S_{\frac{1}{2}}$	3500	"
	$4D^0_{\frac{1}{2}}$	"	$2S_{\frac{3}{2}}$	3546	"
	$4D^0_{\frac{5}{2}}$	$3d^94s(3D_3)4d$	$4S_{\frac{1}{2}}$	3665	"
	$2F^0_{\frac{3}{2}}$	$3d^94s(3D_1)4d$	$2S_{\frac{1}{2}}$	3671	"
	$2D^0_{\frac{1}{2}}$	$3d^94s(3D_1)4d$	$2S_{\frac{3}{2}}$	3712	"

Besides the lines tabulated in the above three tables, there are other lines which arise out of transitions between levels of very high energy content. They come out as comparatively weak and short lines, and this is what one would expect, remembering the fact that according to the laws of probability, number of such atoms is very small.

#### 4. Observations.

From Table I it is clear that lines for which the change in the orientation is large are short in the arc at atmospheric pressure. With a reduction in pressure they either disappear or

are considerably reduced in length. Whereas the lines for which  $\Delta\theta$  is small but not negligible and which have been classed as long lines, under reduced pressure appear as short lines, the lines at  $\lambda\lambda$  4587, 4539, 4378 being examples in point; but lines for which  $\Delta\theta$  is zero remain fairly long even at a comparatively low pressure. As examples, the lines at  $\lambda\lambda$  5782, 5218, 5153, 5106, 4651, 4275, 4063 may be mentioned. These lines remain unaffected in length even at a pressure of 30cm. (Plate IX, B) and all these lines have their orientation change equal to zero. The lines at  $\lambda\lambda$  4509, 4248 and 4023 are only slightly diminished in length at this pressure. It would thus mean that the *a priori* probability of a particular transition is, to a great extent, determined by  $\Delta\theta$ , being larger the smaller the value of  $\Delta\theta$ ; so that in the cases of transitions involving  $\Delta\theta=0$ , a very small quantity of vapour is sufficient to produce the line, hence it appears long even at a reduced pressure. Incidentally it may be pointed out that the persistent lines of De Gramont also belong to this category. Some of the lines, however, appear not to follow this rule, and as in their cases there is a spin change, their shortening may be due to the latter cause. The line at  $\lambda$  3530 seems to be an exception. A few words might be necessary for the line at  $\lambda$  5700, one of the most heavy lines in the arc spectrum of copper. The length of this line lies intermediate between those of the long and short lines so that its classification in the present system might seem to be uncertain. But the question is at once settled from its behaviour at low pressure where it is considerably shortened in length like all other short lines. Thus, it should rather be called a short line than a long one.

In the case of  $D^\circ$  transitions, lines of which are all short, attention may be drawn to an interesting feature, *viz.*,  $D^\circ$  type is obtained as a result of synthesis of  $l$  vectors of orbits which are apparently not parallel but inclined to one another. For instance the configuration  $3d^\circ(4s4p)$  gives rise to doublet and quartet terms of  $F^\circ D^\circ P^\circ$  type. Now, of them  $F^\circ$  ( $l=3$ ) and

$P^{\circ} (l=1)$  are obtained by the sum and difference of the  $l$  value of  $3d^0$  ( $\equiv 3d^1$ ) and  $3p$  orbits,  $4s$  not contributing at all ( $\because l=0$ ). This, *a priori*, means that the  $l$  vectors are either parallel or anti-parallel, whereas in the type  $D^{\circ} (l=2)$  they must be inclined. It may be suggested that this latter type of synthesis is not generally favoured and therefore comparatively larger quantity of vapour would be necessary for their production.

As early as 1874 Lockyer<sup>3</sup> observed, and this has been confirmed in case of the present experiment, that many weak lines are longer than some very strong lines and among lines of equal intensity some are considerably longer than the others. They, however correspond to cases where there is a little or no change in the orientation of the  $l$  and  $s$  vectors. Some of these lines have been selected and their lengths have been measured by

TABLE IV.

$\lambda$	Designation.	Intensity.	Length in mm.	$\Delta\theta$	Remarks.
4275	$^4P_{2\frac{1}{2}} - ^4D_{3\frac{1}{2}}$	6	17.4	$0^{\circ}$	
4378	$^4P_{1\frac{1}{2}} - ^4D_{2\frac{1}{2}}$	6u	15.2	$20^{\circ}$	
4674	$^4F_{2\frac{1}{2}} - ^4D_{2\frac{1}{2}}$	6u	14.2	$34^{\circ}$	
4509	$^4F_{1\frac{1}{2}} - ^4D_{\frac{1}{2}}$	4	16.7	$0^{\circ}$	
4539	$^4F_{2\frac{1}{2}} - ^3D_{1\frac{1}{2}}$	4u	16.7	$8^{\circ}$	
4697	$^4F_{1\frac{1}{2}} - ^4D_{1\frac{1}{2}}$	4u	13.6	$48^{\circ}$	
4178	$^4P_{2\frac{1}{2}} - ^4D_{2\frac{1}{2}}$	4u	12.2	$90^{\circ}$	
5292	$^4D_{3\frac{1}{2}} - ^4D_{3\frac{1}{2}}$	4	14.0	$0^{\circ}$	$D^{\circ}$ combination.
4767	$^2D_{1\frac{1}{2}} - ^2D_{2\frac{1}{2}}$	2u	10.0	$180^{\circ}$	"
5144	$^4D_{3\frac{1}{2}} - ^4D_{2\frac{1}{2}}$	1u	11.5	$90^{\circ}$	"

<sup>3</sup> See Spectroscopy by E. C. C. Baly, p. 514, 1918 and reference given there.

means of a low power travelling telescope. Such lines have been collected in Table IV, which shows their lengths and intensities<sup>4</sup> as also their  $\Delta\theta$  values.

From the above table it is apparent that there is no very close relation between lengths of lines and their intensities. The lengths in these cases are rather consistent with the generalisations laid down before.

The fact that the length of a line is not always regulated by its intensity is very clearly brought out by the line at  $\lambda$  4226.79 [ $4s^2(^1S)$ — $4s4p(^1P_1)$ ] due to calcium as impurity (see plate IX, A). Although weak, this line stretches from edge to edge with about undiminished intensity, whereas many stronger lines of copper appear much shorter than this.

From the above results it is evident that near the edge of the flame of the arc, some weak lines are present although some equally intense lines or even some comparatively stronger lines, are absent at the point. A similar phenomenon was observed by M. Kimura and G. Nakamura.<sup>5</sup> They observed that in the spectrum of the light emitted from the neighbourhood of the salt cathode of copper in a discharge tube some heavier lines in the arc and spark spectra of copper such as  $\lambda\lambda$  5700, 4587, etc., are absent. It is interesting to note that if in these cases also, the synthesis of the  $l$  and  $s$  vectors taking part in the scheme of level transition be scrutinised, then it is seen that these lines correspond to cases where there is a change in the relative orientation of the  $l$  and  $s$  vectors. The results obtained by Kimura and Nakamura have been collected in Table V. The 2nd, 6th and the 7th columns have been introduced by the writers.

Thus the cathode spectrum of the  $\text{CuCl}_2$  discharge tube resembles that of a vacuum arc of copper.

<sup>4</sup> Intensities have been taken from Shenstone's paper : *Phys. Rev.*, 28, 449 (1926), *Jap. Journ. Phys.*, 3, 29 (1924).

TABLE V.

$\lambda$	Designation.	Arc.	Intensity Spark.	Cathode space of $\text{CuCl}_2$ .	$\Delta\theta$	Lines as they appear in the low pressure arc.
5782	$^2\text{D}_{1\frac{1}{2}} - ^2\text{P}_{\frac{1}{2}}$	50	10	3	$0^\circ$	Long.
5700	$^2\text{D}_{1\frac{1}{2}} - ^2\text{P}_{1\frac{1}{2}}$	30	8	0	$180^\circ$	Short.
5220	$^2\text{P}_{1\frac{1}{2}} - ^2\text{D}_{1\frac{1}{2}}$	20	8	0	$180^\circ$	Short.
5218	$^2\text{P}_{1\frac{1}{2}} - ^2\text{D}_{2\frac{1}{2}}$	200	200	10	$0^\circ$	Long.
5153	$^2\text{P}_{\frac{1}{2}} - ^2\text{D}_{1\frac{1}{2}}$	100	100	5	$0^\circ$	Long.
5106	$^2\text{D}_{2\frac{1}{2}} - ^1\text{P}_{1\frac{1}{2}}$	50	20	9	$0^\circ$	Long.
4704	$^4\text{F}_{3\frac{1}{2}} - ^4\text{D}_{3\frac{1}{2}}$	8	2	0	$84^\circ$	Short.
4651	$^4\text{F}_{4\frac{1}{2}} - ^4\text{D}_{3\frac{1}{2}}$	20	10	8	$3^\circ$	Long.
4587	$^4\text{F}_{3\frac{1}{2}} - ^3\text{D}_{2\frac{1}{2}}$	20	20	0	$6^\circ$	Short.

# The Band Spectrum of Aluminium Bromide

By

P. C. MAHANTI.

(Plate X.)

(Received for publication, March 28, 1935.)

## ABSTRACT.

The spectrum of  $\text{AlBr}$  has been photographed with moderately high dispersion. The vibrational analysis of the bands is in agreement with that given by Crawford and Ffolliott. Approximate values of the vibrational constants have been calculated from the Q head data. The identity of the emitter is confirmed by the close agreement between the calculated and observed isotopic displacements. Predissociation has been found to be operating at the upper state above  $v'=3$  and is attributed to the interaction of a Heitler-London level whose products of dissociation are probably a normal aluminium atom ( $3^2P_{\frac{1}{2}}$ ) and an excited bromine atom ( $5^2D_{1\frac{1}{2}}$ ).

## 1. Introduction.

No band spectrum associated with the molecule of aluminium bromide was recorded by the early investigators. But in the discharge through the vapour of aluminium tri-bromide,  $\text{AlBr}_3$ , Crawford and Ffolliott<sup>1</sup> reported the existence of a system of red-degrading bands in the region  $\lambda 2745 - \lambda 3065$ . They ascribed them to the diatomic molecule,  $\text{AlBr}$ , and gave an equation of their R heads measured from low dispersion spectrograms. More recently these bands have also been observed by Miescher.<sup>2</sup>

As far as the author is aware, no further account of the spectrum has been published by any of these investigators.

The present paper confirms in main the analysis of the bands given by Crawford and Ffolliott. But the photograph obtained by the author with a moderately high dispersion spectrograph shows the band system in greater detail than theirs as it includes in most cases not only the R and Q heads of each band of the lighter molecule,  $\text{AlBr}^{70}$ , but also those associated with the heavier isotope of bromine. This is a further confirmation of the fact that the band system in question is due to the diatomic molecule of aluminium bromide,  $\text{AlBr}$ .

The similarity of appearance of these bands with those of  $\text{AlCl}^3$  suggests that they originate in a  ${}^1\pi \rightarrow {}^1\Sigma$  transition. An analogous band system has also been recorded in the spectra of gallium<sup>4</sup>-, indium<sup>5</sup>- and thallium<sup>6</sup>-halides.

### *Experimental.*

The bands were photographed by passing an uncondensed discharge through the vapour of aluminium tri-bromide. The pyrex glass discharge tube was of the ordinary H-form with the capillary portion about 2mm. in diameter. At one end it was provided with a quartz window through which the light of the discharge could be focussed on the slit of the spectrograph by means of a quartz lens. The electrodes were of aluminium foils rolled into cylindrical forms. A test tube with ground stopper was sealed to the discharge tube at the end farther from the window and contained anhydrous aluminium tri-bromide. At the window end the discharge tube was connected to the pump through a number of towers containing caustic soda and anhydrous calcium chloride for absorbing bromine which is evolved during discharge. The condensation of the bromine vapour on the window was avoided by removal of the same by the pump. During exposure wet cotton wool was also wrapped round the



tube nearest to the window end and the vapour was further prevented from reaching it. It was found that even when the discharge was run for about three hours, the window was perfectly transparent.

The discharge tube was worked at 5000 volts by means of a step-up 4 kw transformer designed in the laboratory. It was completely filled up with the aluminium bromide vapour by gently heating the test tube containing the solid tri-bromide. The colour of the discharge changed to pale green when the air inside the tube was displaced by the vapour. There was no difficulty in maintaining a fairly constant pressure by continuous pumping and appropriate heating of the bromide.

To photograph the spectrum, Hilger E. 1. quartz spectrograph and Ilford special rapid plates were used. Iron arc was employed for recording the comparison spectra. With this spectrograph the dispersion ranges from 3.5Å per mm. at  $\lambda 2730$  to 5.5Å per mm. at  $\lambda 3100$ . An exposure of about an hour was sufficient to get the bands well developed on the plates and no further extension of the system was recorded by increasing the time of exposure. A Gaertner precision comparator was used for measurements. In view of the fact that there is usually some uncertainty in the correct setting of the cross-wire on the heads of bands, the wave-lengths are given only to two decimal places. They represent the mean of several measurements made on different plates. In no case the individual measurements are found to differ from the mean value by more than  $\pm 0.03\text{\AA}$ .

### 3. *Description of the Spectrum.*

The bands of aluminium bromide possess in most cases sharply defined heads and are all degraded towards the red. The principal band heads occur in pairs and are due to the lighter molecule,  $\text{AlBr}^{79}$ . As one proceeds towards the red end of the spectrum, these pairs of heads are in most cases duplicated by equally intense pairs associated presumably with the heavier

molecule,  $\text{AlBr}^{\text{Al}}$ . These features are easily discernible from an examination of the photographs (Fig. 1). The general appearance of the double-headed bands at once suggests that the shorter wave-length components represent R heads while those lying on the longer wave-length side, their Q heads. Due to greater condensation of lines, the R heads appear in general stronger than those of Q. But the lines of the R branch extend only up to a short distance from the head whereas the Q and P branches extend further and are in places partially resolved.

#### 4. *Vibrational Analysis.*

From an inspection of the photographs the bands could easily be arranged into groups belonging to different sequences of the system. The consideration of intensity of the bands and the variation of interval between their R and Q heads suggested that the group at  $\lambda 2789$  was to be associated with  $v' - v'' = \Delta v = 0$  sequence. The assignment of vibrational quantum numbers to the bands of the remaining groups was then readily made. This was subsequently confirmed by the close agreement between the calculated and observed magnitudes of the isotopic displacements wherever available. Table I contains the particulars of the observed band heads together with the assignment of their  $v'$ ,  $v''$  values.

It is noticed that when the Q heads are arranged in a Deslandres table, the values of  $\Delta G'_{(v'+\frac{1}{2})}$  and  $\Delta G''_{(v''+\frac{1}{2})}$  in the same vertical column or horizontal row are very uniform. This indicates that the Q heads are rather close to the origins of the bands. On the other hand, such uniformity is not noticeable in the case of R heads on account of their varying distance from the band origins. Assuming, therefore, that the Q heads represent band origins, the equation representing them is found to be as follows :

$$\begin{aligned}
 v = 35875.8 + \{301.62(v' + \tfrac{1}{2}) - 0.18(v' + \tfrac{1}{2})^2 - 0.095(v' + \tfrac{1}{2})^3\} \\
 - \{377.94(v'' + \tfrac{1}{2}) - 1.30(v'' + \tfrac{1}{2})^2\} \quad \dots \quad (1)
 \end{aligned}$$

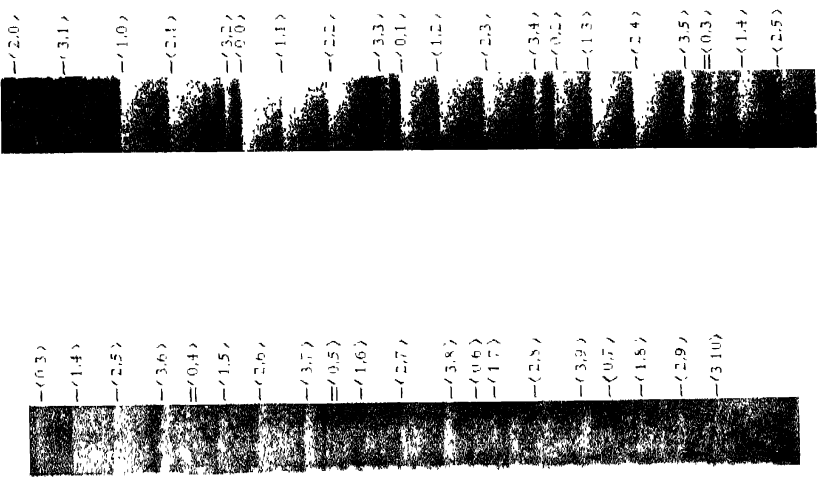


Fig. 1.

The band spectrum of aluminium bromide



TABLE I.

Data of band heads and their classification.

$\lambda$ (in air) and intensity.	$\nu$ (in vacuo).	Classification.	$\lambda$ (in air) and intensity.	$\nu$ (in vacuo).	Classification.
27 17.53 (16)	36385.6	R (2, 0)	2844.33 (31)	35147.4	R' (3, 4)
47 67 (16)	383.7	Q (2, 0)	41 57 (32)	144.4	R (3, 4)
57.47 (26)	251.4	R (3, 1)			& Q' (3, 4)
67.47 (37)	123.1	R (1, 0)	44.82 (32)	141.3	Q (3, 4)
67.77 (37)	119.5	Q (1, 0)	48.22 (33)	099.4	R' (0, 2)
76.07 (36)	011.5	R (2, 1)	48.44 (34)	096.7	R (0, 2)
76.31 (36)	008.4	Q (2, 1)	48.92 (34)	090.7	Q' (0, 2)
86.06 (34)	35882.4	R (3, 2)	49.14 (35)	088.0	Q (0, 2)
86.22 (34)	880.4	Q (3, 2)	55 50 (35)	009.9	R' (1, 3)
89.18 (40)	842.3	R (0, 0)	55.74 (36)	006.9	R (1, 3)
89 65 (39)	836.3	Q (0, 0)	56.02 (36)	003.5	Q' (1, 3)
96.13 (38)	719.2	R (1, 1)	56.26 (37)	000.6	Q (1, 3)
96.82 (37)	714.1	Q (1, 1)	63.98 (34)	31906.2	R' (2, 4)
105.06 (36)	610.1	R (2, 2)	64.23 (35)	902.2	R (2, 4)
105.33 (35)	635.0	Q (2, 2)	64.48 (35)	900.1	Q' (2, 4)
15.06 (28)	512.8	R' (3, 3)	64.76 (36)	896.7	Q (2, 4)
15.18 (29)	511.3	R (3, 3)	74.02 (31)	784.3	R' (3, 5)
18.60 (39)	468.2	R (0, 1)	74.36 (33)	780.2	R (3, 5)
19.18 (38)	461.1	Q (0, 1)			& Q' (3, 5)
25.78 (38)	377.8	R' (1, 2)	74.69 (33)	776.1	Q (3, 5)
25.95 (38)	375.9	R (1, 2)	78.39 (27)	732.4	R' (0, 3)
26.25 (37)	372.2	Q' (1, 2)	78.65 (98)	728.3	R (0, 3)
26.40 (37)	370.3	Q (1, 2)	79.25 (27)	721.1	Q' (0, 3)
34.29 (35)	271.9	R' (2, 3)	79.59 (28)	717.0	Q (0, 3)
34.44 (36)	269.7	R (2, 3)	85.70 (27)	643.5	R' (1, 4)
34.69 (35)	266.9	Q' (2, 3)	86.05 (28)	639.3	R (1, 4)
34.85 (35)	264.9	Q (2, 3)	86.30 (28)	636.3	Q' (1, 4)

TABLE I—(continued).

$\lambda$ (in air) and intensity.	$\nu$ (in vacuo).	Classification.	$\lambda$ (in air) and intensity.	$\nu$ (in vacuo).	Classification.
2886.65 (29)	34632.1	Q (1, 4)	2947.73 (13)	33914.5	R (1, 6)
94.10 (30)	543.0	R' (2, 5)	47.95 (14)	912.0	Q' (1, 6)
94.47 (31)	538.5	R (2, 5)	48.51 (14)	905.6	Q (1, 6)
94.64 (31)	536.5	Q' (2, 5)	55.63 (21)	823.9	R' (2, 7)
95.02 (32)	532.0	Q (2, 5)	56.26 (22)	816.7	R (2, 7) }
2901.14 (33)	423.5	R' (3, 6)			& Q' (2, 7) }
04.57 (34)	418.5	Q' (3, 6) }	56.92 (21)	809.1	Q (2, 7)
		& R (3, 6) }	65.62 (21)	709.9	R' (3, 8)
04.98 (34)	413.6	Q (3, 6)	66.14 (20)	704.0	Q' (3, 8)
09.02 (17)	365.8	R <sub>2</sub> (0, 4)	66.29 (22)	702.3	R (3, 8)
09.43 (17)	361.0 <sub>2</sub>	R (0, 4)	66.81 (23)	696.4	Q (3, 8)
10.00 (18)	354.2	Q' (0, 4)	72.16 (6)	635.8	R (0, 6)
10.41 (18)	349.0	Q (0, 4)	73.35 (5)	622.3	Q (0, 6)
16.20 (21)	281.2	R' (1, 5)	78.62 (6)	562.8	R' (1, 7)
16.67 (22)	275.7	R (1, 5)	79.30 (7)	555.0	R (1, 7)
16.91 (22)	272.8	Q' (1, 5)	80.20 (7)	545.0	Q (1, 7)
17.37 (23)	267.4	Q (1, 5)	87.01 (12)	468.6	R' (2, 8)
24.64 (27)	182.3	R' (2, 6)	87.75 (13)	460.3	Q' (2, 8) }
25.14 (28)	176.4	R (2, 6)			& R (2, 8) }
25.73 (28)	169.5	Q (2, 6)	88.52 (13)	451.7	Q (2, 8)
34.66 (28)	065.6	R' (3, 7)	97.03 (16)	356.7	R' (3, 9)
35.21 (29)	059.2	R (3, 7)	97.53 (16)	350.6	Q' (3, 9)
35.70 (29)	053.5	Q (3, 7)	97.81 (17)	348.0	R (3, 9)
40.00 (10)	003.7	R' (0, 5)	98.37 (18)	341.8	Q (3, 9)
40.56 (11)	33997.2	R (0, 5)	3004.28 (2)	276.2	R (0, 7)
41.10 (10)	991.0	Q' (0, 5)	05.60 (2)	261.6	Q (0, 7)
41.64 (11)	984.7	Q (0, 5)	11.35 (4)	198.0	R (1, 8)
47.14 (13)	921.3	R' (1, 6)	12.30 (4)	187.6	Q (1, 8)

TABLE I—(continued).

$\lambda$ (in air) and intensity.	$\nu$ (in vacuo).	Classification.	$\lambda$ (in air) and intensity.	$\nu$ (in vacuo).	Classification.
3018.80 (7)	33116.1	R <sup>+</sup> (2, 9)	3030.03 (8)	32990.1	Q (3, 10)
19.66 (8)	106.7	Q <sup>+</sup> (2, 9)	43.81 (2)	844.0	R (1, 9)
		& R (2, 9)	41.83 (2)	833.0	Q (1, 9)
20.51 (8)	097.4	Q (2, 9)	52.03 (6)	755.6	R (2, 10)
28.80 (6)	006.8	R <sup>+</sup> (3, 10)	52.93 (6)	745.7	Q (2, 10)
29.42 (6)	000.0	Q <sup>+</sup> (3, 10)	62.02 (6)	648.7	R (3, 11)
29.72 (8)	32996.8	R (3, 10)	62.71 (7)	641.4	Q (3, 11)

TABLE II.  
O—C Values of Q Heads.

$v', v''$	O—C ( $\text{cm}^{-1}$ )	$v', v''$	O—C ( $\text{cm}^{-1}$ )	$v', v''$	O—C ( $\text{cm}^{-1}$ )
2,0	0.9	1,4	-1.4	1,8	-1.7
1,0	0.3	2,5	-0.1	2,9	-1.0
2,1	0.9	3,6	-0.3	3,10	-0.4
3,2	1.5	0,4	-1.5	1,9	-1.8
0,0	0.1	1,5	-1.1	2,10	-0.7
1,1	0.5	2,6	-0.3	3,11	0.2
2,2	1.2	3,7	-0.7	...	...
0,1	0.2	0,5	-0.8	...	...
1,2	-0.9	1,6	-0.6	...	...
2,3	0.3	2,7	-1.0	...	...
3,4	0.1	3,8	-0.6	...	...
0,2	-0.2	0,6	-0.9	...	...
1,3	-0.4	1,7	-1.5	...	...
2,4	-0.4	2,8	-1.2	...	...
3,5	-0.1	3,9	-0.7	...	...
0,3	-1.0	0,7	-1.9	...	...

The wave numbers calculated from equation (1) are in close agreement with their observed values. The differences between the observed and calculated values for the Q heads are collected in Table II. For the thirty-eight heads, algebraical mean deviation is  $-0.5\text{cm}^{-1}$ .

### 5. Separation of R and Q Heads.

The spectrum of AlBr exhibits very clearly the nature of variation of the interval between R and Q heads of bands with increasing values of  $v'$  or  $v''$ . This is shown in  $v', v''$  scheme in Table III. As one would expect normally for a band system degraded towards the red and having  $3B' > B''$ , the observed RQ interval<sup>7</sup> increases with increasing  $v''$  ( $v'$  constant) and with diminishing  $v'$  ( $v''$  constant).

TABLE III.

R Q interval.

$v' \backslash v''$	0	1	2	3	4	5	6	7	8	9	10	11
0	6.0	7.1	8.7	11.3	12.0	12.5	13.5	14.6	...	...	...	...
1	3.9	4.8	5.6	6.3	7.2	8.3	8.9	10.0	10.4	11.0	...	...
2	1.9	3.1	4.1	4.8	5.9	6.5	6.9	7.6	8.6	9.3	9.9	...
3	...	...	2.0	...	3.1	4.1	4.9	5.7	5.9	6.2	6.7	7.3

### 6. The Isotope Bands.

With the dispersion used the isotope bands lying only on the longer wave-length side of the system-origin are discernible. The bands due to the heavier molecule, AlBr<sup>81</sup>, are displaced from those of the lighter one, viz., AlBr<sup>79</sup>, in the direction of the system-origin in accordance with the theory of isotope effect.

To confirm the identity of the emitting molecule and the assignment of vibrational quantum numbers to the bands, it is of importance to compare the observed displacements of the bands of



the heavier molecule with those calculated from theory. To a fair degree of approximation, the vibrational isotopic displacement,  $\Delta\nu$ , of a  $v'$ ,  $v''$  band can be evaluated from the following equation : <sup>8</sup>

$$\begin{aligned}\Delta\nu &= \nu^i(v', v'') - \nu(v', v'') \\ &= (\rho - 1) \left\{ \omega'_{\nu} (v' + \tfrac{1}{2}) - \omega''_{\nu} (v'' + \tfrac{1}{2}) \right\} \quad \dots \quad (2)\end{aligned}$$

where the superscript  $i$  refers to the heavier molecule.  $\omega'_{\nu}$  and  $\omega''_{\nu}$  are the half-intervals between two alternate levels of the lighter molecule. The constant,  $\rho$ , is given by

$$\rho = \sqrt{\mu/\mu^i} \quad \dots \quad (3)$$

where  $\mu$  and  $\mu^i$  are the reduced masses of the two isotopic molecules. If  $M_1$ ,  $M_1^i$  and  $M_2$  represent the masses of the atoms concerned, then

$$\mu = \frac{M_1 M_2}{M_1 + M_2} \quad \text{and} \quad \mu^i = \frac{M_1^i M_2}{M_1^i + M_2} \quad \dots \quad (4)$$

In the case of AlBr, we have

$$M_1 = 78.93 \text{ (Br}^{79}\text{)}$$

$$M_1^i = 80.93 \text{ (Br}^{81}\text{)}$$

$$\text{and } M_2 = 26.97 \text{ (Al),}$$

on the scale of O=16, so that  $\rho = 0.99637$  and  $\rho - 1 = -0.00363$ .

It should be noted, however, that the values of  $\Delta\nu$  calculated according to equation (2) represent only the vibrational displacements. Strictly speaking they should be corrected for rotational displacements for an accurate comparison with the observed values. But the following considerations would show that these corrections are well within the limits of experimental error in the present case. The Q heads being rather close to the band-origins, are practically unaffected by the rotational effect.

But the  $R'$  heads are displaced towards the origin of the respective bands by amounts nearly proportional to the interval between their  $R$  and  $Q$  heads. The amount of displacement is given approximately by  $2(\rho-1)(\nu_R-\nu_Q)$ . In the case of the bands under consideration, it is nearly one three-hundredth of the  $RQ$  interval given in Table III. Hence the observed isotopic displacements for the  $R$  heads may be compared with the calculated vibrational displacements without any serious error.

The observed isotopic separations are given in Table IV. They represent in each case the mean of the measured intervals  $R'$   $R$  and  $Q'$   $Q$  when both have been observed ; when only one has been measured, the tabulated  $\Delta\nu$  is followed by the letter  $R$  or  $Q$  as the case may be. It will be seen that the agreement between the calculated and observed displacements is very close for nearly all the bands.

TABLE IV.  
Isotopic displacements.

$\nu', \nu''$	$\Delta\nu$ (calc.)	$\Delta\nu$ (obs.)	$\nu', \nu''$	$\Delta\nu$ (calc.)	$\Delta\nu$ (obs.)
3,3	+1.7	+1.5	1,5	+5.8	+5.5
1,2	1.9	1.9	2,6	6.2	5.9 (R)
2,3	2.4	2.1	3,7	6.8	6.4 (R)
3,4	3.0	3.0	0,5	6.7	6.4
0,2	2.8	2.7	1,6	7.0	6.6
1,3	3.2	3.0	2,7	7.5	7.4
2,4	3.7	3.5	3,8	8.0	7.6
3,5	4.3	4.1	1,7	8.3	7.8 (R)
0,3	4.1	4.1	2,8	8.7	8.4
1,4	4.5	4.2	3,9	9.2	8.7
2,5	4.9	4.5	2,9	9.9	9.4
3,6	5.5	5.0	3,10	10.4	10.0
0,4	5.4	5.0	...	...	...

7. *Distribution of Intensities.*

Numbers representing the order of intensities on a scale of 40 are given in parentheses after the wave-lengths in the first column of Table I. They have been obtained from uncorrected ordinates of the micro-photometric trace and are not therefore proportional to the intensity. They enable us, however, to estimate the intensities on a more finely divided scale than any eye-estimates and allow a more accurate correlation of widely separated bands. The intensity distribution among the Q heads is shown in a Deslandres scheme in Table V. It will be seen that the locus of the stronger bands is a parabola with (0, 0) band at the vertex. Along each horizontal row there are two intensity maxima in accordance with the prediction of Franck-Condon theory<sup>9</sup> that in general for a given vibrational level,  $v'$ , in the upper state, there are two preferred vibrational levels,  $v''$  in the lower state of the band system.

TABLE V.

Intensity distribution of Q heads

$\sqrt{v}$	0	1	2	3	4	5	6	7	8	9	10	11
0	39	38	35	28	18	11	6	2	x	x	x	x
1	37	37	37	37	29	23	14	7	4	2	x	x
2	16	36	35	35	36	32	28	21	13	8	6	x
3	x	26	34	29	32	33	34	29	23	18	8	7

It is further noticed that in general the intensities of the heads associated with the lighter and heavier molecules, *viz.*, AlBr<sup>70</sup> and AlBr<sup>81</sup> for a given  $v'$ ,  $v''$  value are equal in accordance with the known abundance ratio of the bromine isotopes (1:1). Only in a few cases their intensities are slightly different from

one another. Such discrepancies are, however, not unusual in emission bands in which the relation between the abundance ratio and intensity ratio is a complicated one. It has in fact been observed that the intensity of the isotopic bands changes not only from one condition of excitation to another but also from band to band.

### 8. *Predissociation.*

A striking feature of the spectrum is the limitation of the number of  $v''$ -progressions owing to an unexpected sharp cut off of the intensity of the bands in each sequence above  $v' = 3$ . This is in common with some of the band systems of the halides of the metals of the third group of the periodic table. No bands with  $v' > 10$  appear in the spectrum of  $\text{AlCl}$ .<sup>3</sup> The C system of gallium<sup>4</sup> and of indium<sup>5</sup> chloride also exhibits such an abrupt termination of the band progressions. As an explanation of this phenomenon, Kaplan<sup>10</sup> suggested that in such cases the  $U : r$  curve for the upper electronic state of the band system is crossed by that of an unstable Heitler-London level repulsive in nature. A strong inter-combination with the latter either prevents the excitation of the higher vibrational states or if they are excited, it quenches them. Thus predissociation sets in and accounts for the failure of the band system to agree with the Franck-Condon theory.

In the present case one may, therefore, reasonably infer that the  $U : r$  curve of a Heitler-London level crosses that of the upper electronic state of the band system at a point just above the energy corresponding to  $v' = 3$  and having a vibrational energy,  $D'_s = 0.18 \pm 0.01$  volts. Assuming further that the lower state is derived from a normal Al-atom ( $3^2P_{3/2}$ ) and an excited Br-atom ( $5^2P_{1/2}$ ), the nature of the atoms which combine to form the Heitler-London level may be ascertained by evaluating  $E_{\text{atom}}$ .

Within the limits of experimental error, the relation between  $\omega''$ , and  $v''$  is linear for the lower state of the band system, so

that the actual dissociation energy,  $D''$ , can be approximately determined by the extrapolation method of Birge and Sponer.<sup>11</sup> This is found to be 3.37 volts.  $E_{\text{mol.}}$  corresponding to  $Q(0, 0)$  is 4.42 volts. Hence  $E_{\text{atom}}$  evaluated from the relation, *viz.*,  $E_{\text{atom}} = E_{\text{mol.}} + D' - D''$ , is 1.23 volts. From the analysis of the line spectrum of normal bromine atom, the interval between  $5^2D_{1\frac{1}{2}} - 5^2P_{1\frac{1}{2}}$  is 1.25 volts.<sup>12</sup> It is, therefore, probable that the dissociation products of the Heitler-London level are a  $3^2P_{\frac{1}{2}}$ -atom of aluminium and a  $5^2D_{1\frac{1}{2}}$ -atom of bromine.

It may here be noted that from the difference between the dissociation energies of the upper and lower states of the band system of  $\text{AlCl}$ , Holst<sup>8</sup> was led to infer that in the excited state the molecule has a heteropolar binding and dissociates into an  $\text{Al}^+$  and a  $\text{Cl}^-$  atom. The electron affinity of chlorine calculated from the data derived from the band analysis is in fair agreement

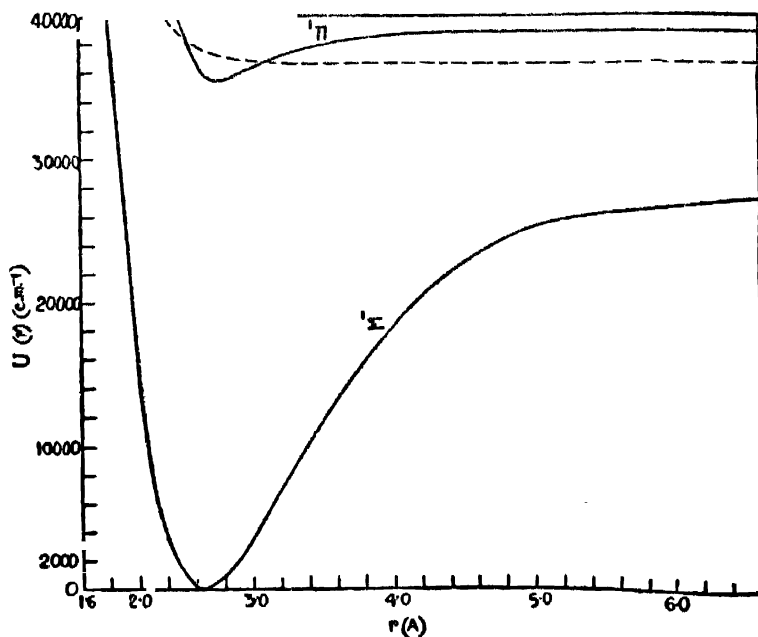


FIG. 2

Potential energy curves.

with the value determined recently by Knipping.<sup>13</sup> It is, therefore, of interest to ascertain the nature of binding of AlBr in its excited state. The value of the actual dissociation energy,  $D'$ , which is, however, very uncertain owing to long extrapolation, is  $0.28 \pm 0.01$  volts. The electron affinity of bromine calculated from the data of  $D'$ ,  $D''$ ,  $E_{\text{mol}}$  and  $I_{(\text{Al})}$ , is 4.63 volts whereas Knipping's value is 3.66-3.00 volts. This discrepancy is large enough to allow any definite conclusion. On the other hand,  $E_{\text{atom}}$  calculated in the usual way is found to be 1.33 volts and is in better agreement with the interval  $5^2D^{\circ}_{2\frac{1}{2}} - 5^2P_{1\frac{1}{2}}$ , which is 1.40 volts.<sup>12</sup>

To illustrate the interpretation of predissociation in the band system under consideration, it was thought desirable to draw the  $U:r$  curves of the different states. For this purpose the value of  $r_c$  for AlBr was approximately estimated from that of AlCl by applying the relationship which exists between the nuclear separations of HCl and HBr.

The author wishes to express sincere thanks to Prof. Dr. P. N. Ghosh for offering all the facilities to carry out this investigation.

#### References.

- 1 F. H. Crawford and C. F. Ffolliott, *Phys. Rev.*, **44**, 953 (1933).
- 2 E. Miescher, *Helv. Phys. Acta*, **7**, 462 (1934).
- 3 P. C. Mahanti, *Zeits. f. Phys.*, **88**, 550 (1934); B. N. Bhaduri and A. Fowler, *Proc. Roy. Soc., Lond. (A)*, **155**, 321 (1934); W. Holst, *Zeits. f. Phys.*, **93**, 55, (1934).
- 4 E. Miescher and M. Wehrli, *Helv. Phys. Acta*, **7**, 331 (1934).
- 5 M. Wehrli and E. Miescher, *Helv. Phys. Acta*, **7**, 293 (1934).
- 6 K. Butkow, *Zeits. f. Phys.*, **58**, 232 (1929).
- 7 W. Jevons, *Report on Band Spectra* (1932), p. 54.
- 8 W. Jevons, *Report on Band Spectra* (1932), p. 213.
- 9 W. Jevons, *Report on Band Spectra* (1932), p. 70.
- 10 J. Kaplan, *Phys. Rev.*, **37**, 1406 (1931).
- 11 R. T. Birge and H. Sponer, *Phys. Rev.*, **28**, 259 (1926).
- 12 R. F. Bacher and S. Goudsmit, *Atomic Energy States* (1932), p. 93.
- 13 P. Knipping, *Zeits. f. Phys.*, **7**, 328 (1921).

#### Note added in proof :

After the communication of the paper to the *Indian Journal of Physics* the author noticed the publication of a paper on the band spectrum of AlBr by H. G. Howell in the February number of the *Proc. Roy. Soc. A*, Vol. 148, and also Mr. Howell kindly forwarded to the author a reprint of the same on the 27th April. In essential details, the results of both the investigations are in fair agreement.

# Researches on the Gyromagnetic Effect of some Ferromagnetic Compounds.\*

By

D. P. RAY CHAUDHURI, D.Sc.

(Received for publication, 3rd April, 1935.)

## ABSTRACT.

The ratio of angular momentum to magnetic moment of the elementary carriers of ferromagnetism in a number of ferrites is determined by the resonance method due to Einstein and de Haas. The 'g' value (Landé factor) falls below the orthodox value of 2 for all cases by about 3 p.c. which is outside the limits of experimental error. The result may be explained on the assumption that the  $l$ -moment also contributes to ferromagnetism.

## 1. INTRODUCTION.

An electron of charge  $e$  and mass  $m$  moving in a circular orbit of radius  $r$  about the positive nucleus of an atom, has a magnetic moment  $M = \pi n e r^2$  and an angular momentum  $J = 2\pi n m r^2$  where  $n$  is the number of revolutions per second. The ratio  $R = J/M = 2m/e = 1.136 \cdot 10^{-7}$ .<sup>1</sup> This ratio of angular momentum to magnetic moment also holds in the general case of an elliptic orbit. It has been shown from various sources that the elementary magnets consist of such electrons. A mechanical moment is thus always associated with a magnetic moment, and when the magnetisation of a body is suddenly changed, there will appear an angular momentum in the direction of this change

\* Read before the Inaugural Meeting of the Indian Physical Society on 29th September, 1934.

<sup>1</sup> With the latest spectroscopic value of  $e/m$ .

owing to the electronic magnets tending to turn their axes in the direction of the applied field. Now, according to the law of conservation of angular momentum, the angular momentum of an isolated system always remains constant. A reactional mechanical force, therefore, appears, to compensate for the change in the intrinsic angular momentum, and causes a rotational motion of the body as a whole, provided the molecules are not free to turn owing to the presence of neighbouring molecules.

This rotational motion accompanying sudden change in magnetisation was first predicted by Richardson.<sup>2</sup> He, however, failed to detect the effect experimentally. Einstein and de Haas<sup>3</sup> first succeeded in detecting the effect and confirmed the above ratio for  $R=J/M$ . Later Beck,<sup>4</sup> finding in it a method of determining  $e/m$  and the sign of the rotating electron, made a very careful observation, and found that for iron and nickel the ratio is not  $2m/e$ , but half the value. Later investigators confirmed Beck's results.

This discrepancy between theoretical and observed values was called the gyromagnetic anomaly, and could not be successfully explained till the advent of the spinning electron. For an electron spinning about its axis and with no orbital motion the ratio is given as  $m/c$ . In his attempt to explain the magnetic properties of the ions of the first transition group, Bose<sup>5</sup> suggested that the  $l$ -moments of the electrons were inoperative. This exclusion which means that the spin alone is effective in producing magnetic properties, gives the value of the ratio as  $m/c$  and thus explains the gyromagnetic anomaly.

It follows from the above result that it is the spin of the electron which plays the role of elementary magnets in ferromagnetics.

<sup>2</sup> Richardson, *Phys. Rev.*, Vol. 26, p. 248 (1908).

<sup>3</sup> Einstein and de Haas, *Verh. d. Deut. Phys. Gess.*, Vol. 17, p. 152 (1915); *Do.*, 18, p. 173 (1916).

<sup>4</sup> Beck, *Ann. d. Phys.*, 60, '09 (1919); *Phys. Zeit.*, 20, 490 (1919).

<sup>5</sup> Bose, *Zeit. f. Phys.*, Vol. 43, p. 864 (1927).



On the other hand, all the ferromagnetics on which gyromagnetic test has been made are metallic conductors and possess two kinds of electrons of which the spin can participate in magnetic phenomena. They are the so-called free electrons carrying electric current, and the electrons attached to metallic ions and moving in orbits about the atoms. The question now is which of these two kinds of electrons play the elementary rôle. No decisive answer can be obtained from theoretical points of view.

From Heisenberg's well-known work on the origin of the Weiss molecular field it appears that ferromagnetism is caused by interaction between the spins of valence electrons<sup>6</sup> which also function as conducting electrons in some incomprehensible way. Heisenberg based his calculations on a model corresponding to Heitler and London's model for the hydrogen molecule, in which each electron is at first thought to be bound to a definite atom. Such a model gives a very small probability for electrical conduction. Bloch<sup>7</sup> bases his considerations on the model of Sommerfeld's free electrons, which gives electrical conduction and he finds the conditions under which it is possible for such a model to give rise to ferromagnetism. A necessary but not sufficient condition for this is that the electrostatic energy of the electrons shall exceed the null-point energy. When there is one free electron eq per atom, the atom-rest forming a closed configuration, and when the temperature is below the critical degeneracy temperature, the above condition requires that the side of the unit cell  $a > 0.6 \cdot 10^{-7}$  cm. This is not fulfilled for the alkali metals, which are not ferromagnetic. Bloch shows that it is quite possible for free electrons to give rise to ferromagnetism. Stoner,<sup>8</sup> however, shows that if ferromagnetism were due to free electrons, the Curie point would

<sup>6</sup> Heisenberg considers the electrons to be in  $S$  states; *Zeit. f. Phys.*, Vol. 49, p. 619 (1928).

<sup>7</sup> Bloch, *Zeit. f. Phys.*, Vol. 52, p. 555 (1928).

<sup>8</sup> Stoner, *Proc. Leeds. Phil. Soc.*, Vol. 2, p. 50 (1930).

have to be higher than the critical temperature of Sommerfeld's conduction theory, and this would require absurdly high temperatures.

Dorfman<sup>9</sup> at one time tried to prove that the magnetic electrons are the conducting electrons, while Ghosh<sup>10</sup> showed that all conducting electrons are not magnetic. Dorfman arrived at his conclusion by studying the magnitude of the sudden change at Curie point of the electrical specific heat of nickel; but, as shown later by Stoner<sup>11</sup> his results are marred by an error in sign, which invalidates the whole conclusion.<sup>12</sup> Others<sup>13</sup> showed that for nickel there is a sudden change in the secondary emission of electrons at the Curie point.<sup>14</sup> All these facts make one inclined to think that "free" electrons play an important rôle in ferromagnetic phenomena. But from the theory of metallic states developed by Bloch, Peierls, Brillouin, Wilson and others<sup>15</sup> it is clear that too sharp a distinction cannot be made between "free" electrons and electrons in atoms or ions in the metal. We have mentioned that Heisenberg's theory requires the interacting electrons to be in S states. But Van Vleck<sup>16</sup> shows that in order that Heisenberg's considerations may apply it is only necessary to suppose that the orbital moment of the electrons in question has been quenched.

Dorfman and Jaanus, *Zeit. f. Phys.*, Vol. 54, p. 277 (1929).

<sup>10</sup> Ghosh, *Zeit. f. Phys.*, Vol. 68, p. 566 (1931).

<sup>11</sup> Stoner, *Nature*, p. 125, 1930.

<sup>12</sup> Nevertheless, the significance of Dorfman's work seems still to be shrouded in mystery. Thomson Effect cannot be understood by an elementary hypothesis of a specific heat of electricity, as has been done by both Dorfman and Stoner. The facts are much more complex, and a detailed theory in Lorentz or Sommerfeld's form requires a very minute consideration of a number of factors. (See N. H. Frank, *Zeit. f. Phys.*, 63, 604, 1930). It is found difficult to establish a relation between Thomson effect and specific heat of electrons. (See L. Brillouin, Report of the Solvay Congress, 1931. Gauthier Villars p. 267.)

<sup>13</sup> Tartakowsky and Kudrjawzewa, *Zeit. f. Phys.*, Vol. 75, p. 137, (1932).

<sup>14</sup> The facts observed by Dorfman and collaborators may be due to secondary processes connected with changes at Curie point.

<sup>15</sup> *Erg. d. ex. Naturwiss.*, Vol. 11, p. 264 (1932).

Wilson, *Proc. Roy. Soc.* Vol. 133, p. 458 (1931), and subsequent papers.

<sup>16</sup> *Theory of Electric and Magnetic Susceptibilities*, p. 324.

The mechanism of this quenching has been explained by him<sup>17</sup> and is due to the effect of an internal asymmetric electrical field. This theory has been applied by Van Vleck and his collaborators<sup>18</sup> to explain the paramagnetic properties of the salts of the iron and rare earth families. Their works in conjunction with other considerations<sup>19</sup> lead us to assume that the electrons of which the interaction is responsible for ferromagnetism are those belonging to the incomplete 'd' shell of the atoms. Paramagnetic phenomena<sup>20</sup> show that though most of the orbital moment is quenched there is still an amount left. The counterpart of this in ferromagnetic phenomena is claimed to have been observed by Barnett<sup>21</sup> who finds that the 'g' value for the ferromagnetic elements is less than the ideal value for the spinning electron by amounts varying from 4% for iron to 7% for cobalt. This is in direct contradiction with the results of British physicists<sup>22</sup> who find  $g=2$  (the value for the spinning electron) exactly, within very narrow limits of experimental error. Barnett's value may be explained as due to a participation of the *l*-moment in ferromagnetic phenomena. Stoner<sup>23</sup> has put forth evidence to prove that the *l*-moment does participate in ferromagnetic phenomena, at the least near about the Curie point. In consideration of these facts, *viz.*, (i) Barnett's low value of 'g,' and (ii) the possibility of participation of an *l*-moment, we have set ourselves to gather as many data as possible for the gyromagnetic ratio of ferromagnetic substances both near to and away from their Curie points. As almost all gyromagnetic measurements have been made on the metals we have started with ferromagnetic

<sup>17</sup> *Ibid*, p. 287.

<sup>18</sup> Penney and Schlapp, *Phys. Rev.*, 42, 666 (1932).

Jordahl, *Phys. Rev.*, Vol. 42, p. 901 (1932).

<sup>19</sup> See e. g., Slater, *Phys. Rev.*, 35, 509 (1930); Stoner, *Phil. Mag.*, 15, 1018 (1932).

<sup>20</sup> Bose, *loc. cit.*; Van Vleck and Collaborators, *loc. cit.*

<sup>21</sup> Barnett, *Proc. Amer. Acad.*, Vol. 66, p. 273 (1931).

<sup>22</sup> See references to Chattock, Bates and Sucksmith; *Proc. Roy. Soc. and Phil. Trans.*

<sup>23</sup> Stoner, *Phil. Mag.*, Vol. 12, p. 737 (1931).

compounds like  $\text{Fe}_2\text{O}_3$ ,  $\text{Fe}_3\text{O}_4$  and the ferrites, some of which are reported to have low Curie points.

Moreover, the ferromagnetic behaviour of these compounds<sup>24</sup> is different in many respects from that of the metals. They, therefore, offer possibilities of an interesting study.

The following is a description of the gyromagnetic test made on some of these compounds.

## 2. THEORY OF THE METHOD.

Owing to the rather low magnetic susceptibility of the materials we had to adopt the resonance method of Einstein and de Haas. The substance, contained in a thin-walled cylindrical tube, is axially hung by means of a glass fibre in a strong magnetic field produced by a cylindrical coil. A sudden reversal of the direction of magnetisation produces a torque on the specimen, which shows a slight rotation. There are disturbing forces

<sup>24</sup> (i) The curves in reduced co ordinates of the spontaneous magnetisation against temperature of different ferromagnetics may be grouped into two classes, one comprising the metals Fe, Co, Ni and the other the compounds magnetite, pyrrhotite, etc.

(ii) The paramagnetic moments above the Curie point of the metals are always much higher than the ferromagnetic moments, while for the ferrites they are practically the same. The following figures are given by Mlle. Serres, Thèse, Strasbourg, 1931.

	Fe	Co	Ni	$\text{Fe}_2\text{O}_3$	$\text{NiO.Fe}_2\text{O}_3$	$\text{CuO.Fe}_2\text{O}_3$
Para-Mom. (in Weiss magnetons)	15.0	16.0	8.0	9	5.2	5.4
Ferro-Mom. (in Weiss magnetons)	11.0	9.0	3.0	10	5.5	5.4

(iii) The ferromagnetic Curie point ( $\theta_f$ ) of the first group lies lower than the paramagnetic Curie point ( $\theta_p$ ), while for the second group the two are very close together or  $\theta_p$  lies lower than  $\theta_f$ . See Forrer., Jour. de. Phys, Serie 7, 62, 312 (1931.)

	Fe	Ni	$\text{PbO.Fe}_2\text{O}_3$	$\text{CuO.Fe}_2\text{O}_3$	$\text{NiO.Fe}_2\text{O}_3$	$\text{MgO.Fe}_2\text{O}_3$
$\theta_f$	770°C	357	442	455	590	339
$\theta_p$	810	378	453	498	597	324

The above figures are taken from Serres' work (*loc. cit.*). Some  $\theta_f$  and  $\theta_p$  values for ferrites are given by the present author in a succeeding paper to appear in the Ind. Jour. Phys.

which often completely mask this effect. To eliminate these and to make measurement of the very small rotation possible a resonance method is employed in which the period of reversal of the current in the magnetising coil coincides with the natural period of torsional oscillation of the specimen. The equation of motion of a suspended system acted on by a couple is

$$I\ddot{\theta} + \nu\dot{\theta} + C\theta = T$$

[where  $I$  = moment of inertia of the system;

$\nu$  = a damping factor ;

$C$  = torsion constant of the suspension ;

$T$  = turning moment

$$T = \frac{1}{g} \cdot \frac{2m}{c} \cdot \chi m_o \frac{dH}{dt}, \text{ where}$$

$\chi$  = mass susceptibility of the specimen.

$m_o$  = mass of the specimen.

$H$  = strength of the magnetic field.]

The current-time form of the magnetising current is not sinusoidal, but can be represented by

$$H = \sum_{n=1}^{n=\infty} H_o \sin n\omega t.$$

As the measurements are taken at resonance, it is easy to show that only the fundamental is effective, which for a perfect square wave has the magnitude

$$\frac{4}{\pi} H_o \sin \omega t.$$

$$T = \frac{1}{g} \cdot \frac{2m}{c} \cdot \chi m_o \frac{4}{\pi} \cdot H_o \omega \cos \omega t.$$

The resonance amplitude

$$\theta_m = \frac{4}{\pi} \cdot \frac{2m}{c} \cdot \frac{1}{g} \frac{\chi m_o H_o}{\nu}$$

But

$$\nu = \frac{2I\lambda}{t}$$

where  $\lambda$  = logarithmic decrement, being given by  $\lambda = \log. \frac{a_1}{a_2}$ , where  $a_1$  and  $a_2$  are two successive amplitudes in the same direction ; and  $t$  = time period of oscillation of the system.

The method, therefore, consists in measuring the resonance amplitude when the disturbing forces have been reduced to a minimum.

### 3. ARRANGEMENT AND APPARATUS.

The experimental arrangement is very nearly the same as that used by Sucksmith.<sup>25</sup>

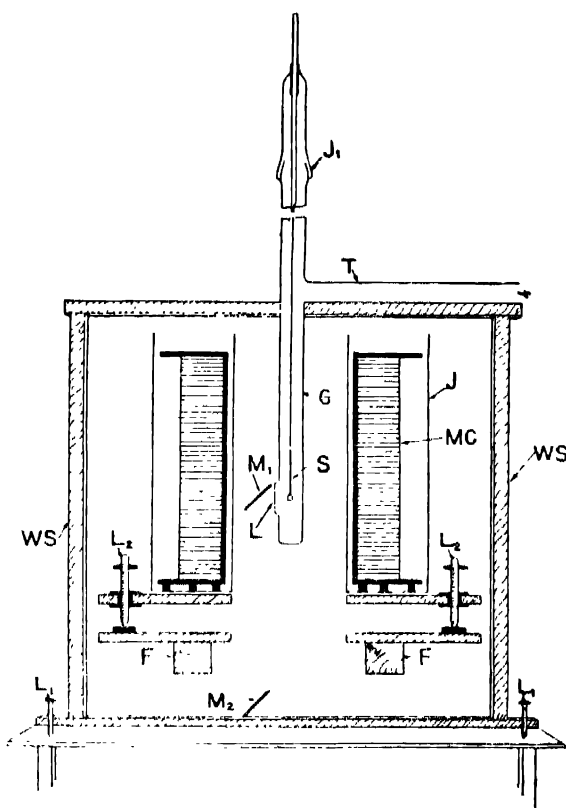


FIG. 1.

<sup>25</sup> Sucksmith, Proc. Roy. Soc.(A), Vol. 128, p. 276 (1930).

(i) *Magnetic Field.*

The magnetic field is produced by a cylindrical coil MC (Fig. 1) of 26 layers with a total of 3,341 turns of No. 14 S.W.G. double cotton covered copper wire wound on a brass former. The mean diameter of the coil is about 23 cm. and the length about 30 cm. Field produced at the centre is 110·0 gauss per ampere. The coil was surrounded by a jacket J of thin brass sheet and was kept cool by circulating oil around it. Current was taken from a storage battery of 144 volts, each unit of which had a capacity of 150 ampere-hours.

(ii) *Preparation of the Material.*

$\text{Fe}_3\text{O}_4$ —Welo's method<sup>26</sup> of preparation was used. To a solution of  $\text{FeSO}_4 \cdot 7\text{H}_2\text{O}$  was added a solution of NaOH and  $\text{KNO}_3$  of given concentration. The green precipitate was allowed to stand for 24 hours when it became black. It was carefully washed, dried and powdered. Analysis gave 98·5% of  $\text{Fe}_3\text{O}_4$ .

$\text{Fe}_2\text{O}_3$ —Heating the above compound at 220°C in a stream of oxygen for 12 hours converted it into ferromagnetic  $\text{Fe}_2\text{O}_3$ . Analysis gave 99·3% of  $\text{Fe}_2\text{O}_3$ .

$\text{NiO} \cdot \text{Fe}_2\text{O}_3$ —To a solution containing equimolecular proportions of  $\text{NiCl}_2$  and  $\text{FeCl}_3$  was added a solution containing requisite quantity of NaOH in boiling. The precipitate was washed, dried and heated to a high temperature to get a ferromagnetic of sufficient intensity.

The ferrites of Mn, Cu, Co and Zn were prepared by the dry method. The metallic oxide and paramagnetic ferric oxide were taken in requisite proportions and heated in an electric furnace to about 1000°C. in a platinum vessel for about 20 hours.

The material under test was finely powdered in an agate mortar, after which a part was taken for susceptibility measurement, while another was used to fill a very thin-walled glass

<sup>26</sup> Welo, *Phil. Mag.*, Vol. 50, p. 899 (1925).

tube of length about 6 cm. and diameters varying between 1·4 and 2·2 mm. The thickness of the walls was from '04 to '06 mm. This glass tube filled with the material forms the specimen to be tested.

(iii) *Suspension.*

This offered a problem ; but finally Chattock and Bates' <sup>27</sup> method was adopted. V's (V, Fig. 2) and hooks (H, Fig. 2) of glass, as shown in the figures, were prepared. This preparation offered some difficulty as the usual method of bending over heated platinum wires proved unsuitable for the rather thicker V's and hooks which was necessary for the purpose. After some practice it was found possible to make good specimens by careful manipulation over a small flame. The junction (S, Fig. 2) between the V and hook was filled with shellac. The arms of the V were inside the tube (T). The suspending glass fibre was attached with shellac. At the top the fibre was fixed at two places at a distance of about 2 cm, the lower one of which was melted to enable the fibre to keep taught under the weight of the specimen.



FIG. 2.

\* Phil. Trans., 223, 257 (1922).



A thin mirror (2 mm.  $\times$  3 mm.) (M, Fig. 2) was attached to the bottom of the glass tube containing the material. The incident light reached the mirror from the bottom of the coil by reflection at two mirrors ( $M_1$  and  $M_2$ , Fig. 1) inclined at  $45^\circ$ , and went out the same way. The source of light was a 6 volt 25 watt lamp producing an intense illumination. A thin wire stretched before the source was focussed on a ground glass scale by means of a lens (L, Fig. 1) attached to the wall of the wider glass tube (G, Fig. 1) containing the specimen. The distance between scale and mirror was over one metre.

*(iv) Mounting.*

The specimen was mounted in a glass tube (G, Fig. 1), of  $1\frac{1}{4}$ " inner diameter, closed at both ends and provided with a ground joint ( $J_1$ , Fig. 1) which helped in the repeated taking off and examination of the specimen (S, Fig. 1) and could also give the specimen a slight rotation when necessary. A side tube (T, Fig. 1) below the ground joint was connected with a pump. The whole thing was mounted on an wooden stand (WS, Fig. 1) provided with levelling screws ( $L_1$ , Fig. 1) and the stand placed on an isolated pillar (P, Fig. 1) whose foundation was 12 feet deep. A wooden frame (F, Fig. 1) spanned the pillar, and on this was placed the magnetising coil, which was provided with levelling screws ( $L_2$ , Fig. 1).

*(v) System for producing Resonance.*

The pendulum of an electrical clock was removed and replaced by one (P, Fig. 3) with adjustable time period. The range of variation obtained was from 1.6 to 3.0 secs. A stiff wire (W) attached to the pendulum rod just closed a circuit when the pendulum was at rest, by contact with a cup of mercury (M), the cup being placed on a stand provided with levelling screws. For one-half the period the circuit was closed,

and for the other half open. The current in this circuit actuated an electromagnet (E M) which again closed another relay circuit by drawing a piece of soft iron (I) attached to one arm of a polarising relay. When the electromagnet was not in action, the loaded arm closed another circuit by contact with a mercury pool.

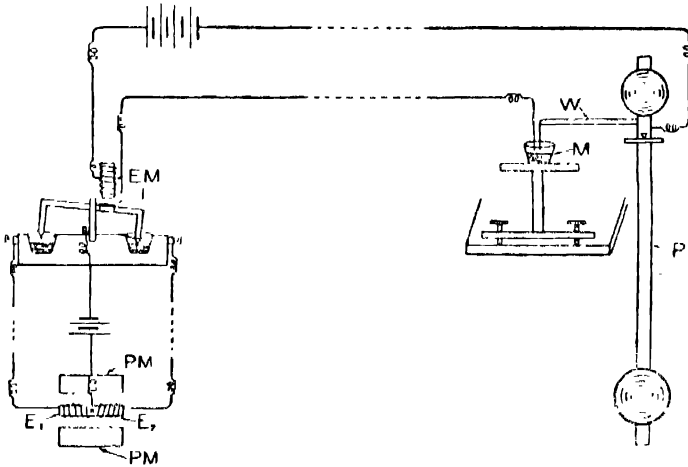


FIG. 3.

These two circuits on their parts actuated two electromagnets ( $E_1$ ,  $E_2$ , Figs. 3 and 4) placed in the field of a strong permanent magnet (PM, Fig. 4). These were so made and mounted that while one exerted a clockwise turning couple on a horizontal rod (R, Fig. 4) which carried them both, the other exerted an opposite one. To this rod was attached the rocker (C) of a commutator whose conductors ( $C_1$ ,  $C_2$ ) were cross-connected. The commutator was of a special design there being two channels ( $L_1$ ,  $L_2$ )  $9'' \times 1'' \times 1''$  in the place of the usual four mercury cups, and served the purpose of reversing the current in the magnetising coil. This arrangement for producing resonance is essentially the same as used by Sucksmith. Later on the relay was done away with, and the current worked by the pendulum actuated an electromagnet which turned the

rocker of the commutator against the pull of a spring. To minimise sparking all the mercury surfaces were covered with light oil and sometimes with glycerine and in all the circuits the minimum potential applied. It was found that with these precautions all the contacts worked regularly for the period necessary.

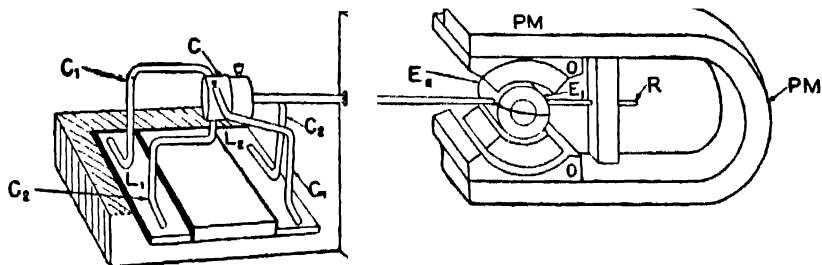


FIG. 4.

To test how far the synchronisation has been perfect a mirror and a long focus lens was attached to the pendulum rod, which served to reflect and focus the light from a distant source on the same scale on which the light from the mirror of specimen under test fell. This spot of light moved with the motion of the pendulum and synchronisation could be tested easily.

#### 4. DISTURBING EFFECTS.

There are disturbing effects whose magnitudes may be hundred to thousand times greater than the effect to be measured, or even more. Their nature as also the method of elimination are given below.

##### (i) *Error due to Earth's Field :*

The earth's magnetic field has three components :

- (i) The north-south horizontal component.
- (ii) The east-west horizontal component.
- (iii) The vertical component.

The compensations are more difficult than they appear to be, because the earth's field is continually varying both in direction and magnitude and because the work had to be done in a building which contains iron and, therefore, disturbs the uniformity of the field.

The first harmonics of the vertical and horizontal magnetic moments of the specimen may be assumed to be

$$M_v = M' \sin \omega t, \quad M_h = M'' \sin (\omega t - \alpha)$$

(a) The induced horizontal component of the magnetisation of the specimen may be acted on by the earth's horizontal component  $H_e$  and produce an axial torque whose magnitude is given by

$$T_h = CH_e, \quad M_h = C' \sin (\omega t - \alpha)$$

If the torsion head is turned through  $180^\circ$  this torque is reversed.

(b) The specimen may have a permanent horizontal magnetic moment  ${}_hM_h$  which when acted on by the earth's horizontal field produces a steady displacement of zero.

(c) The earth's vertical component may produce magnetostriuctive torques of which we shall speak later on.

(ii) *Errors due to Horizontal Component of the Field of the Magnetising Coil :*

(d)  ${}_hM_h$  {see (b) above} may be acted on by it and produce a torque which will nearly be in phase with  $M_v$ , and we may put it as

$$T_e = C'' \sin (\omega t + \beta)$$

where  $\beta$  is small. This may be eliminated by turning the torsion head through  $180^\circ$  when the torque is reversed. It is often of considerable magnitude and special care has to be taken to reduce both the magnitudes,  ${}_hM_h$  and the horizontal component of the field coil.

(e) The alternating field acting on the induced horizontal moment produces a torque of twice the natural frequency.

(iii) *Errors due to Inequality of Half-cycles of the Magnetising Current.*

(f) When the two half cycles are unequal there is a residual torque on the specimen of the same frequency. This may have any phase relation with the gyromagnetic torque, and may be written

$$T' = K \sin (\omega t + \gamma)$$

(iv) *Effects due to Magnetostriction, etc.*

Since the change in dimension due to magnetostriction is independent of the direction of magnetisation, no magnetostrictive torque of the same period as that of the first harmonic of the magnetisation can arise if the two half cycles of magnetisation are exactly similar. When the half cycles are dissimilar or when there is a residual vertical magnetic moment there will be an elongation with a first harmonic of the period of the magnetisation. The error due to the presence of a residual vertical moment may be eliminated by working with fields capable of producing saturation.

## 5. ELIMINATION OF ERRORS.

(i) *Error due to Earth's Horizontal Field.*

The specimen usually had a horizontal magnetic moment which caused a lot of trouble, and required the greatest attention. To eliminate the action of the earth's field, it was neutralised by a current flowing through two rectangular coils  $3' \times 2'$  at a distance apart of about 20". The coils had 32 turns each and required a current of about 54 ampere for neutralisation. The degree of perfectness of neutralisation was tested by a small

magnet suspended by a silk fibre. As the east-west component of the field was small it could be neutralised by a slight rotation of the coils. While working it was found that the direction of the field underwent small changes at times. Instead of altering the position of the rectangular coils it was found more convenient to add two coils of 5 turns each placed parallel to the magnetic meridian at a distance of 22". Current through this coil could be adjusted to perfect neutralisation.<sup>28</sup>

(ii) *Error due to Horizontal Component of the Magnetising Coil.*

The magnetising coil was provided with three levelling screws with which the field could be adjusted to the vertical. But as long as the horizontal moment of the specimen was appreciable the disturbance due to even a very small horizontal field was great. It was, therefore, imperative to bring down the

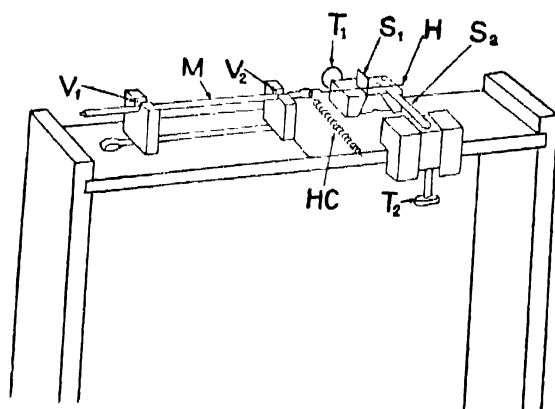


FIG. 5.\*

<sup>28</sup> As the earth's magnetic field underwent changes both in magnitude and direction it was useless to work with a value of the neutralising field obtained at any one time. But the knowledge of such a value is essential as indicating the order of such values. The actual procedure adopted was to vary the north-south component of the neutralising field till a minimum value is obtained for the resonance amplitude, and with that value of the field to vary the strength of the east-west component till a second minimum for the resonance amplitude is observed.

horizontal moment of the specimen to the lowest value possible. This was done as follows : <sup>29</sup>

The specimen (M) was laid down on two metal V grooves ( $V_1, V_2$ , Fig. 5). To the base on which these V's stood were attached two steel strips ( $S_1, S_2$ ) one of which could be moved horizontally and the other vertically by means of two screws ( $T_1$ ), ( $T_2$ ) with a small pitch (32 turns to the inch). To the heads of these screws were attached arms about five inches long (not shown in the figure), so that the steel edges could be adjusted to a few thousandths of a millimetre. After the specimen is laid on the grooves, the screws are adjusted so that the steel edges just touch the hook (H) to which the specimen is attached. There is a small heating coil (H C) below the point where the hook is attached to the V. A small current is sent which is sufficient to soften the shellac in the joint. The screws are moved by small amounts at a time after the shellac has softened. This moves the point of suspension relative to the specimen. After the shellac has solidified the specimen is taken and suspended in a horizontal magnetic field of about 60 gauss supplied by a vertical coil which could be rotated about a vertical axis. The magnitude and direction of the horizontal moment of the specimen could be judged from the direction and degree of deflection resulting.<sup>30</sup> The adjustment

<sup>29</sup> The method is similar to that used by Chattock and Bates, (Phil. Trans., 223, 257, 1922).

The presence of a horizontal moment is due to the magnetic axis of the specimen not coinciding with the axis of suspension. The procedure adopted is to make them identical.

The magnetic axis is generally not identical with the geometrical axis. The correction for horizontal moment, therefore, raises the moment of inertia of the specimen. This may be seen from the calculated and observed values of the moment of inertia for the specimen.

<sup>30</sup> Whenever such a horizontal magnetic field is applied the necessary co-ercive field is also subsequently applied to eliminate the effect of the first field. The magnitude of the co-ercive field depends on (i) nature of the substance, (ii) density of packing and (iii) the intensity of the field first applied. The correct value for the co-ercive field is determined while making the susceptibility measurements.

By co-ercive field is here meant the reverse field which after application and removal leaves zero residual moment.

is to be carried to such a degree that for two positions of the coil inclined at  $90^\circ$  to each other there is practically no deflection of the specimen. This requires that the specimen should always be laid down in the identical position relative to the V's and the steel strips. To ensure this the mirror attached to the specimen is always made to reflect the light from a distant source at a definite spot both being fixed relative to the V's.

It is found that for zero horizontal moment of the specimen the geometrical asymmetry is not generally appreciably large.

### (iii) *Asymmetry in the Alternating Current.*

It is necessary that the duration of the current in the coil in both directions shall be the same, as any want of symmetry will have the frequency of the pendulum and will make itself felt at resonance. To check this the current through the coil was passed through a voltmeter and the gas liberated at the two electrodes was collected. When the current was symmetrical the volumes of the gas in the two tubes were the same. In practice it was found that such a method took time. The water voltmeter was, therefore, removed and replaced by a siphon recorder. The current while passing through one of the small electromagnets of the recorder, pulled a piece of soft iron to which was attached a nib. The continuous line left on the recording paper was thus marked by transverse lines corresponding to the reversals in the current. The adjustment was made by means of levelling screws with which the mercury cup (M, Fig. 3) in which dipped the rod from the pendulum, was provided. This mercury surface was also covered with oil.

### (iv) *Mechanical Disturbances.*

Traffic in the street often caused a vibratory motion of the specimen to be set up, which was more troublesome while working in vacuum. Though the isolated pillar mounting



reduced this effect greatly, it was found that regular working could only be obtained between 1 A.M. and 5 A.M. in the night when all traffic had stopped.

(v) *Heating Effect of the Coil.*

A current of 4 amps. sent through the coil raises the temperature of the bath at the rate of  $2^{\circ}\text{C}$  per hour. A thermocouple inserted at the position occupied by the specimen within the glass tube records a rise of temperature of  $0.2^{\circ}\text{C}$  per hour. It may, therefore, safely be concluded that temperature changes due to heating effect of magnetising current produces no appreciable effect on the specimen.

(vi) *Form of the Magnetising Current.*

This was investigated with an oscillograph. The time taken by the current to change from maximum in one direction to maximum in the other, was a minimum and corresponded to that required by the self-induction of the coil. This duration was less than  $\frac{1}{10}$  of the average time period of the specimens used in the experiment. Sucksmith (Proc. Roy. Soc., 128, 276, 1930) has shown that even when this duration is 3.5% of the time period, the departure from square wave form does not introduce a correction in the const.  $\frac{4}{\pi}$  (see p. 389) by more than 0.1 %. We, therefore, neglected this correction.

## 6. PROCEDURE.

The field within the magnetising coil was explored and standardised. The susceptibility of the material is determined for values of the field strength which are to be used as also for different densities of packing. A suitable thin-walled tube having been found, it is filled with the material. The mirror is attached to the bottom as much possibly, axially to keep the

moment of inertia lowest. To the mirror is attached a very small hook which helps to measure the moment of inertia of the specimen. A suspension fibre is so chosen that the period of torsional oscillation of the specimen falls within the range of periods of which the pendulum is capable, *viz.*, 1.6 to 3.0 secs. in our case. The specimen is suspended in a horizontal magnetic field of 60 gauss and adjusted for zero horizontal moment (see page 399). The moment of inertia of the specimen is determined by loading it with small aluminium discs of known moment of inertia. The correct value of the earth's field neutralising current having been previously obtained, the specimen is put in position and the reflecting mirrors adjusted. The pendulum is then synchronised with the free period of the specimen after fully exhausting the system. The applied field is adjusted to the vertical by means of levelling screws with which the coil is provided. This adjustment is better tested by using a specimen with a horizontal magnetic moment. As long as the coil has a horizontal component the period of oscillation of the specimen with a steady field acting will be different from its natural period. The levelling screws are adjusted till the two periods are the same, the test being made by the pendulum. Accurate centring<sup>31</sup> of the specimen is extremely necessary to avoid pendulum like oscillations of the specimen as a whole as also oscillations about its centre of gravity. When the adjustment is complete the specimen shows no appreciable motion when the current through the coil is put on or reversed. The duration of the current through the coil in either direction is adjusted to be the same by means of levelling screws with which the mercury cup (M, Fig. 3) in the pendulum relay

<sup>31</sup> For this purpose the frame carrying the glass tube containing the specimen, was provided with an arrangement by means of which it could be moved in two mutually perpendicular directions. The motion was given by a screw with a big head and a small pitch. (This arrangement has not been shown in the figure.) Thus the axis of suspension of the specimen could be made to coincide with the axis of the magnetising coil. To make the centres of the coil and the specimen coincide the latter was moved up or down with the help of the glass rod from which it was suspended.

circuit is provided. All these adjustments being complete, the pendulum is started and the magnetising current put on. Sufficient time is allowed to pass for the resonance amplitude to attain 98%<sup>1</sup> its maximum value, and the amplitudes noted every half a minute for a run extending from 20 minutes to half an hour. The earth's field neutralising current is slightly altered by small steps at a time (see page 398) and the corresponding resonance amplitude noted. There is a critical value of this current for which the amplitude is a minimum. This critical value is not a fixed one, but changes from day to day and time to time, though the change is slight and lies within  $\pm 0.1$  ampere of the value for perfect neutralisation which has been fixed previous to mounting the specimen. For higher and lower values of the neutralising current the amplitude increased. Variations of temperature from day to day affects the viscosity of the material of the suspension fibre, glass in this case, and the time period of the specimen changes slightly. It is then necessary to alter the period of the pendulum and readjust it. Sometimes this temperature effect causes more trouble, the time period showing a marked change in a period of 2 hours. The most consistent results are obtained on those nights when the temperature shows no sudden and large change. Any possible departure of the field from the vertical is tested by slight alterations of levelling screws of the coil and noting the effect on the amplitude. In all cases the minimum amplitude<sup>2</sup> is sought. After one series of readings the specimen is turned through  $180^\circ$  and another series of readings taken.

When working in vacuum the pump is started after resonance has been obtained at atmospheric pressure. This is

<sup>2</sup> The reason for this is that all the disturbing torques are in quadrature with the gyromagnetic torque. The former can, therefore, only increase the amplitude due to the latter alone. *Vide* Sucksmith, Proc. Roy. Soc. 128, 276, 1930.

convenient for the fact that at times there are irregular vibrations at the start, which die away more quickly at higher pressures. At the end of the observations the logarithmic decrement is noted with the field on.

## 7. MEASUREMENT.

### (i) *Field Strength.*

This was measured by means of a ballistic galvanometer which has been standardised by a coil of known dimensions. The exploring coil was wound on a piece of copper rod of about the same diameter as the specimens, *viz.*, 2 mm. and had a length of 6 cm., the same as that of the specimens. This was placed in about the same position as was later on occupied by the specimen. The average value of the field over the specimen was thus obtained, and was 109.4 gauss per ampere. A small coil also explored the field axially. The results are given in the Table.<sup>33</sup>

TABLE.

Distance from the Centre of the Coil.	Field Strength in gauss.
0 cm.	110.0
3 "	108.5
5 "	105.7
10 "	90.4

<sup>33</sup> The value of the field at any point as also the average value over the specimen when the latter is placed at the centre of the magnetising coil, may be computed from the known dimensions and the number of turns of the coil. The value thus obtained is about 0.3% higher than the value obtained experimentally. We prefer the latter to the computed value obtained because of the errors introduced by the rather large diameter of the copper wire used (No. 14 S. W. G.).

*(ii) Susceptibility of the Substance.*

The B-H curve of the substance was obtained by a magnetometer method and from it the susceptibility for the field strength used was calculated. Details are given in a separate paper.

*(iii) Moment of Inertia.*

This was measured in the usual way by loading the specimen with aluminium discs of known moment of inertia. A number of discs of values of moment of inertia varying from  $16.14.10^{-4}$  to  $31.66.10^{-4}$  C.G.S. units were used. These were hung from the hook attached to the specimen by means of very short silk loops so that the axis of rotation passed centrally through the disc perpendicular to its axis. The position of the hook had to be slightly altered to secure this. The time period is a minimum when the adjustment is correct.

The accuracy with which 'I' could be measured is manifested by the fact that with care any one of these discs gave the moment of inertia of any other within 0.5 per cent.

## 8. DATA.

Results of measurement are given below in a tabulated form. For notations please turn to pp. 389 and 411.

*Detailed Data for one successful run.*

Material—Copper ferrite. ( $\text{CuO} \cdot \text{Fe}_2\text{O}_3$ )

Date and duration—26th June to 1st July, 1933.

Diameter of glass tube for filling with material :

Diameters in mutually perpendicular directions at

Top.	Middle.	Bottom.	} mean value 1.71 mm.
1.72 mm.	1.70	1.70	
1.70 „	1.71	1.72	

Thickness of wall = .04 mm.

Length of tube filled = 6.6 cm.

Weight of material = .3098 gm.

Density of packing = 2.25 gm/cm<sup>3</sup>.

Determination of moment of inertia (I)

Free period = 2.468 secs. (mean of 550 oscillations)

Time period when loaded with aluminium disc (A) = 3.435 secs. } of moment of inertia = 16.14. 10<sup>-4</sup> c.g.s.u.

Time period with disc (B) (I = 22.34.10<sup>-4</sup> c.g.s.u.)  
= 3.743 secs.

Time period with disc (C) (I = 24.96.10<sup>-4</sup> c.g.s.u.)  
= 3.869 secs.

I from (A), (B), (C) respectively = 17.22.10<sup>-4</sup>, 17.18.10<sup>-4</sup> and 17.12.10<sup>-4</sup>

Mean value of I = 17.17.10<sup>-4</sup> c.g.s.u.

Actual run :

Free period = 2.468 secs.

Magnetising current at start = 2.303 amps.

„ „ „ end = 2.302 amps.

Resonance amplitude = 8.19/2 cm.

Resonance amplitude with

specimen turned through 180° = 8.27/2 cm.

Mean Resonance amplitude = 8.23/2 cm.

*Logarithmic Decrement ( $\lambda$ ).*

No. of Oscillations.	Ratio of Amplitudes.	Log $a_1/a_2$
25	69/40	·009468
25	90/52	·009528
25	112/65	·009452
25	122/71	·009404
25	86/50	·009420
25	138/80	·009468
25	140/81	·009504
25	81/47	·009456
25	93/54	·009444
25	117/68	·009428
25	129/75	·009420
25	143/86	·009445
25	126/73	·009484
25	100/58	·009464

Mean value = ·009465.

$$\lambda = \cdot 009465 \times \log_e 10 = \cdot 02180.$$

$$\text{Field strength} = 2\cdot303 \times 109\cdot4 \text{ gauss} = 252\cdot2 \text{ gauss.}$$

Magnetic susceptibility for this field strength and density of packing  $2\cdot25 \text{ gm/cm}^3 = \cdot 0824$ .

$$\text{Scale distance} = 130\cdot2 \text{ cm.}$$

$$'g' \text{ calculated from these data} = 1\cdot940.$$

Here we have not considered the demagnetising factor, which reduces the field by 5 parts in 1000 in this instance. In the data which follow in pages 408-410 the demagnetising factor has different magnitudes in different cases. The total effect is in the direction of reducing the 'g' value by amounts varying between 1 part in 1000 and 5 parts in 1000 in rare cases.

Substance.	Mass (gm.)	$\chi$	H (gauss.)	$t$ (secs.)	D (cm.)	$I \cdot 10^4$ (C. G. S. U.)	$\lambda$	$d$ (cm.)	$g$	REMARKS.
$Fe_3O_4$	.2372	.072	226.6	2.229	130.2	21.72	.1161	.64	2.013	Only the damping is varied.
	.2373	.072	226.6	2.229	130.2	21.72	.0322 <sub>9</sub>	2.39	1.936	
	.2372	.072	227.7	2.232	130.2	21.83	.1161	.67	1.924	Do. do.
	.2372	.072	227.7	2.232	130.2	21.83	.0334 <sub>9</sub>	2.28	1.961	
	.1062	.0705	219.1	1.882	105.5	6.26	.1192	.62	2.036	Do. do.
	.1062	.0705	219.1	1.882	105.5	6.26	.0825 <sub>6</sub>	2.30	2.009	
	.2313	.0697	215.2	1.683	130.2	23.02	.0324	1.90	1.954	Do. do.
	.2313	.0697	215.4	1.682	130.2	23.02	.0640 <sub>7</sub>	.95	1.976	
	.1763	.0840	210.0	1.772	130.2	14.4 <sub>2</sub>	.114	.64	1.967	Do. do.
	.1763	.0840	210.4	1.772	130.2	14.4 <sub>2</sub>	.0865	.82	2.032	
$Fe_3O_3$	.1763	.0840	210.3	1.773	130.2	14.4 <sub>2</sub>	.0314	2.31	1.986	Other conditions have changed slightly.
	.0998	.0825 <sub>5</sub>	120.6	1.863	130.2	4.32	.0321	2.57	1.953	
	.0998	.0837	123.2	1.863	130.2	4.32	.0319 <sub>6</sub>	3.38	1.954	Field strength varied.
	.0998	.0840	219.8	1.864	130.2	4.32	.0315 <sub>7</sub>	4.94	1.920	
	.2346	.0840 <sub>5</sub>	228.5	2.414	130.2	22.4 <sub>3</sub>	.114 <sub>3</sub>	.81	1.963	Damping varied.
	.2346	.0840 <sub>5</sub>	229.2	2.413	130.2	22.4 <sub>3</sub>	.0324	2.90	1.943	



Substance	Mass (gm.)	$\chi$	H (gauss)	$t$ (sec.)	D (cm.)	$I \cdot 10^4$ (O. G. S. U.)	$\lambda$	$d$ (cm.)	$g$	REMARKS.
$\text{NiO} \cdot \text{Fe}_2\text{O}_3$ (Nickel ferrite.)	1074	0381	232.8	2.188	129.4	7.33	0291 <sub>3</sub>	1.90	1.923	Taken down and remounted after fresh adjustment.
	1074	0381	232.5	2.192	129.4	7.38	0298 <sub>2</sub>	1.82	1.948	
	1074	0381	234.0	2.180	129.2	7.38	0331 <sub>4</sub>	1.63	1.957	Setting on different nights
	1074	0381	235.8	2.180	129.7	7.38	0292 <sub>5</sub>	1.90	1.924	
$2\text{ZnO} \cdot 3\text{Fe}_2\text{O}_3$ (Zinc ferrite.)	1061	0381	245.0	2.082	130.8	6.47	0248 <sub>4</sub>	2.49	1.956	Taken down and remounted after adjustment. Field different.
	1061	0381	265.2	1.926	130.8	6.52	0239 <sub>2</sub>	2.57	1.948	
	1061	0380 <sub>5</sub>	271.4	2.563	130.8	6.58	0286 <sub>5</sub>	3.57	1.912	Do.
	1165	0154	235.2	2.236	132.3	5.08	0257 <sub>2</sub>	1.45	1.906	Do.
	1165	0153	279.6	1.635	132.3	5.12	0261 <sub>5</sub>	1.20	1.942	
	1165	0153	278.3	1.623	132.3	5.02	0283 <sub>0</sub>	1.13	1.920	Do.
	3416	0161	265.3	2.462	131.8	19.4 <sub>2</sub>	0243 <sub>2</sub>	1.51	1.921	Do. Setting on different days.
	3416	0161	273.4	2.348	131.8	19.2 <sub>3</sub>	0236 <sub>5</sub>	1.51	1.957	
	3416	0161	274.2	2.348	131.8	19.2 <sub>3</sub>	0284 <sub>9</sub>	1.54	1.941	

Substance.	Mass (gm.)	$\chi$	H (gauss)	t (sec.)	D (cm.)	I. 10 <sup>4</sup> (C. G. S. U.)	$\lambda$	d (cm.)	g	REMARKS.
MnO.Fe <sub>3</sub> O <sub>3</sub> (Manganese ferrite.)	.4352	.0657	221.6	2.324	128.6	25.5 <sub>g</sub>	.0246 <sub>3</sub>	4.48	1.941	Measurements on different nights. Field different.
	.4352	.0656	230.6	2.326	128.6	25.5 <sub>g</sub>	.0246 <sub>4</sub>	4.69	1.938	
	.4352	.0656	235.2	2.208	128.6	26.4 <sub>7</sub>	.0248 <sub>2</sub>	4.46	1.924	
										Taken down and remounted after fresh adjustment.
	.2361	.0650	254.2	2.196	128.8	14.5 <sub>g</sub>	.0225 <sub>6</sub>	5.02	1.935	Do.
	.2361	.0648	260.5	2.342	128.8	14.4 <sub>2</sub>	.0243 <sub>1</sub>	5.10	1.945	
CuO.Fe <sub>3</sub> O <sub>3</sub> (Copper ferrite.)	.2361	.0646	266.7	2.293	128.8	14.4 <sub>g</sub>	.0222 <sub>4</sub>	5.35	1.957	Do.
	.3098	.0836	225.3	1.946	130.2	17.0 <sub>g</sub>	.0225 <sub>6</sub>	5.78	1.923	Same setting. Measurements on different nights.
	.3098	.0832	234.2	1.946	130.2	17.0 <sub>g</sub>	.0235 <sub>g</sub>	5.61	1.930	
	.3098	.0824	252.0	2.468	130.2	17.1 <sub>7</sub>	.0218 <sub>6</sub>	8.23	1.940	Do.
	.2572	.0873	141.3	2.342	130.2	14.6 <sub>g</sub>	.0225 <sub>7</sub>	4.34	1.942	Only the field strength is varied, other conditions remaining the same. The first value of the field corresponds to the maxi- mum of $\chi$ .
	.2572	.0854	182.6	2.342	130.2	14.6 <sub>g</sub>	.0223 <sub>5</sub>	5.54	1.954	
	.2572	.0843	219.7	2.342	130.2	14.6 <sub>g</sub>	.0224 <sub>g</sub>	6.61	1.934	

## 9. THE ESTIMATION OF PROBABLE ERROR.

(i) *Errors in Reading.*

Measurements of quite a number of different quantities are involved in the determination of  $g$  by the method here adopted. They are : the mass of the material ( $m$ ), the moment of inertia of the specimen ( $I$ ), time period of oscillation of the specimen ( $t$ ) the magnetic susceptibility ( $\chi$ ), logarithmic decrement ( $\lambda$ ), field strength ( $H$ ), distance between scale and mirror ( $D$ ) and the deflection on the scale ( $d$ ). The probable error in the measurement of each of the above quantities is given below :

Probable error in % .

$m$	0.05
$I$	0.5
$t$	0.05
$\chi$	0.5
$\lambda$	0.5
$H$	0.1
$D$	0.1
$d$	0.2

From the above it follows that even if all the component errors are in the same direction the total probable error is 2.0%. The departure from the mean of the final values of  $g$  is, with only one exception (*viz.*, second set of readings in  $\text{Fe}_3\text{O}_4$ ), less than this value.

$\text{Fe}_3\text{O}_4$  was the substance with which the experiment began, and it was not possible to attain the degree of accuracy as obtained later. This makes itself particularly felt in the small values of ' $d$ ' which, for the smallest values, may be in error by as much as 1%. Considering these larger probable errors in ' $d$ '

the total probable error for  $\text{Fe}_3\text{O}_4$  is placed at 3.0%. For  $\text{Fe}_2\text{O}_3$  similar considerations lead to a maximum probable error of about 2.5%. For the rest what is said earlier holds good.

For nickel, manganese, copper and zinc ferrites the values obtained for  $g$  differ from the orthodox value for the spinning electron by more than the experimental error, the  $g$  values obtained being lower than 2. The individual  $g$  values for all these ferrites are less than 2 in all cases, while for  $\text{Fe}_3\text{O}_4$  and  $\text{Fe}_2\text{O}_3$  only three and one, out of eight readings each, are higher than 2. After duly weighing all the results the author is of opinion that for  $\text{Fe}_3\text{O}_4$  and  $\text{Fe}_2\text{O}_3$  also the  $g$  values do differ from that of the spinning electron.

#### (ii) *Errors due to Adjustment.*

The possibility of a systematic error is discounted by the fact that the sources of error mentioned in pp. 395-97 have been attended to properly and the elimination made by taking the readings in two azimuths by turning the specimen through  $180^\circ$ . The only possible source of error not considered is that due to magnetostrictive effects and non-compensation of the earth's vertical field. The first has a harmonic of the natural frequency of the specimen only when the two half cycles of magnetisation current are unequal. But we have taken special care to make the two cycles equal. The only error may arise from the earth's vertical field; but this only when there is a residual vertical magnetisation. At no time was the specimens subjected to a vertical field outside the coil except that of the earth. Moreover, we took special care to make the axis of suspension of the specimen pass through the magnetic axis. Under such circumstances it is hard to believe that an error can arise from the earth's vertical field. In addition, nickel ferrite is characterised by a very low value of remanent magnetisation. The possibility of a large permanent vertical magnetisation is in this case, therefore, to be discounted.

## 10. SUMMARY AND DISCUSSION OF RESULTS.

The results of the above experiments show that the value of the gyromagnetic ratio for the substances investigated, substances which are poor conductors of electricity, is a few per cent smaller than the orthodox value for the spinning electron. This shows that though electron spin supplies the majority of the interaction causing ferromagnetism, there are also other contributing factors to consider. One of them may be a participation of the *l*-moment (the orbital moment). This is in agreement with the observations of Barnett.

*Summary.*

(1) The ratio of angular momentum to magnetic moment of the elementary carriers of ferromagnetism in the following substances is determined by the method of resonance due to Einstein and de Haas :

- |                                |                                            |                                             |
|--------------------------------|--------------------------------------------|---------------------------------------------|
| (i) $\text{Fe}_3\text{O}_4$ ,  | (iii) $\text{NiO}.\text{Fe}_2\text{O}_3$ , | (v) $\text{MnO}.\text{Fe}_2\text{O}_3$ ,    |
| (ii) $\text{Fe}_2\text{O}_3$ . | (iv) $\text{CuO}.\text{Fe}_2\text{O}_3$ .  | (vi) $2\text{ZnO}.3\text{Fe}_2\text{O}_3$ . |

(2) The *g* and *R* values with the probable error are given below :—

	<i>g</i>	<i>R</i>	Probable Error
$\text{Fe}_3\text{O}_4$	1.96	$1.02 \frac{m}{e}$	3%
$\text{Fe}_2\text{O}_3$	1.96	1.02 ..	2.5%
$\text{NiO}.\text{Fe}_2\text{O}_3$	1.94	1.03 ..	2%
$\text{nO}.\text{Fe}_2\text{O}_3$	1.94	1.03 ..	2%
$\text{uO}.\text{Fe}_2\text{O}_3$	1.94	1.03 ..	2%
$\text{nO}.3\text{Fe}_2\text{O}_3$	1.92	1.04 ..	2%

(3) It is concluded that  $g$  is in each case less than 2 (the value for the spinning electron). The difference may be explained as due to participation of an  $l$ -moment.

(4) The value of  $g$  for all the substances is very nearly the same as that for pure iron as found by Barnett, showing that it is principally the  $\text{Fe}^{+3}-\text{Fe}^{+3}$  interaction that gives most of the ferromagnetism in these cases.

My heartiest thanks are due to Prof. D. M. Bose who kindly suggested this problem, gave me every facility to work in his laboratory, and took a constant interest during its progress.

UNIVERSITY COLLEGE OF SCIENCE,  
92, UPPER CIRCULAR ROAD,  
CALCUTTA.

## The Late Dr. Ganesh Prasad

We regret to announce the death of Dr. Ganesh Prasad one of the oldest Life Members and a Vice-President of the Indian Association for the Cultivation of Science on Sunday, March 10th at the age of 59. At the time of his death Dr. Prasad held the chair of the Hardinge Professor of Mathematics of the University of Calcutta.

Dr. Prasad studied in Cambridge and Göttingen and was a favourite pupil of the famous mathematician Prof. Felix Klein. He was the pioneer mathematical investigator in India and his first original contribution on the treatment of the problem of heat conduction elicited admiration even from Klein. His work on the theory of potential of ellipsoids with non-uniform distribution of mass in which he utilised the happy idea of expansion of arbitrary functions in series of spherical harmonics, has found place in standard text-books, the latest being that of Bateman's well-known work on Differential Equations. Dr. Prasad is the author of several well-written text-books for students and of a number of volumes embodying his own researches on theory of summation of Fourier Series.

Having lost his wife and only child in early youth and left alone in the world with none to call his own, he found consolation in his mathematical studies. He was easily approachable by his students and by strangers and was loved by all who came in contact with him. He lived the life of a true *brahmachari* refusing himself the commonest luxuries and at times even the barest necessities of life which practically hastened his end.

A public meeting in honour of his memory was held at the Association Hall on Tuesday the 9th April, 1935, at 6 P.M. Dr. L. L. Fermor, D.Sc., F.R.S., President of the National Institute of Sciences presided over the meeting which was attended by a good number of friends, colleagues, admirers and pupils of the late professor. The president paid tributes to Dr. Prasad, and recalled his various activities, particularly his work in the Academy Committee appointed by the Indian Science Congress to take necessary steps for bringing the National Institute of Sciences into existence. He was also a foundation fellow of the National Institute, and the president recalled that an important paper was read by him in the first meeting of the Institute. The president expressed his desire that some friend or colleague of Dr. Prasad should take upon himself the task of arranging the publication of that work in the transactions of the National Institute.

Dr. S. C. Bagchi, Prof. N. C. Roy, Mr. Panchanan Ghose and Mr. S. C. Ghosh also spoke dwelling upon the various aspects of the achievements, activities and personality of Dr. Prasad.





## Magnetometric Measurement of Susceptibility of Ferro-magnetic Powders.\*

By

D. P. RAYCHAUDHURI.

*(Received for publication, 25th April, 1935).*

### ABSTRACT.

Description is given of a convenient magnetometric method for the measurement of the susceptibility of ferromagnetics in a powdered form. Results of measurements on some ferrites are also given. Under certain circumstances the phenomenon of magnetic viscosity is observed for nickel ferrite.

In connection with gyromagnetic experiments on some ferrites, which are available only in a powdered form, it was necessary to measure the magnetic susceptibility of specimens formed by filling a thin walled glass tube about 6 cm long and from 1.4 to 2 mm in diameter under the exact conditions of the experiment.

It was found that unlike case of ferromagnetics obtainable in the form of rods or wires, a definite value cannot be assigned to magnetic constants like maximum permeability, coercive field etc., in the case of ferromagnetics in the form of a powder. The size and shape of the grains, the density of packing, as also

\* Read before the Indian Physical Society on 24th April, 1935.

previous magnetic history, play an important role for the latter; and so also the shape of the specimen as a whole. In experiments where the magnetic susceptibility values  $\chi$  of such substances are required, a very cautious procedure is to be adopted, as otherwise the final results may very largely be vitiated by the uncertainty of these  $\chi$  values. For rather loosely packed specimens the magnetometric and the ballistic methods generally give different values of  $\chi$ . In the following a magnetometric method due to Bozorth<sup>1</sup> is described by which  $\chi$  values for thin cylindrical specimens may very conveniently be determined under conditions exactly similar to those of the main experiment. Some results of measurements are also given.

Two parallel magnets of equal moment and opposite direction, about 6 cm apart, form an astatic pair, which may be used even under unfavourable laboratory conditions. The specimen is so placed that both of its induced poles produce upon the suspended magnetic system equal torques in the same sense about the axis of suspension.

The adjoining Fig. 1 is a diagram of the magnetometer with its electrical connections. The magnets are made of thin steel strips 6 mm x 2 mm x 0.4 mm. They are made to have almost the same magnetic moment and are attached to the ends of a light but rigid frame provided with oil damping. The suspension fibre is of glass. The magnetising-solenoids, 25 cm long and 7 cm in diameter are placed with axes vertical on opposite sides of the needle system. The axis of suspension of the needle system lie in the same vertical plane, the needle system lying exactly midway between the solenoids. These latter are mounted on bases capable of motion towards or away from the needles along horizontal rails fixed to the walls. The carrier for the needle system is also fixed. The solenoids have

the same dimensions and number of turns, and are so connected in series as to exert equal and opposite torques on the needles. In one of the solenoids is placed the specimen accurately centred.

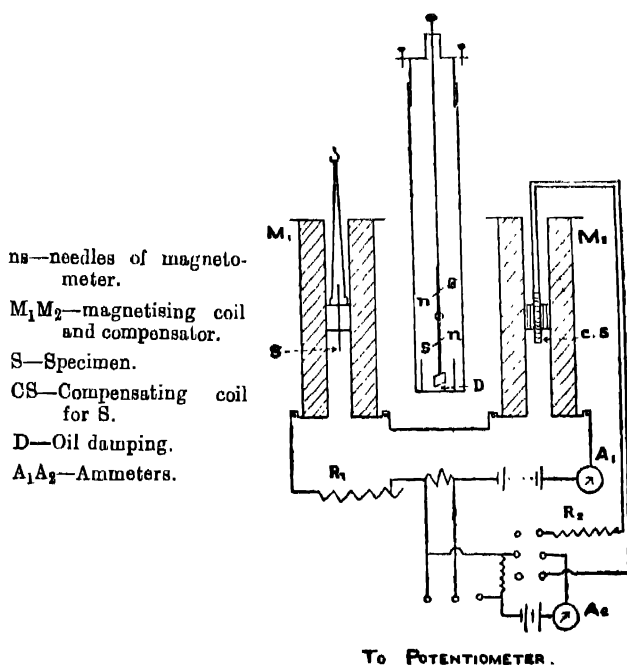


FIG. 1.

For purposes of measurement a current is sent through the magnetising solenoids, which are then adjusted so as to give no deflection of the needles. The zero is checked each time the magnetising current is altered. The deflections are read with a scale and telescope arrangement. Susceptibility is obtained by comparison with a small solenoid having the same dimensions as the specimen, hung exactly at the same place, of known number of turns and with a known current flowing through it. Current is measured with a potentiometer and a standard cell.

*Calculation of constants.*

The average magnetic field over the specimen may be calculated in the ordinary way from the dimension of the magnetising coil and the length of the specimen. Let

$2l$  = length of the solenoid.

$r_1, r_2, r$  = the inner, outer and average radii of the solenoid respectively.

$n$  = number of turns of the solenoid.

$d$  = length of the specimen.

The coil may be considered as an infinite solenoid with two magnetic poles  $\pm \frac{n i a}{10}$  at the two end surfaces, ( $a$  = area of the end). The field at an axial distance from the middle of the coil is

$$H_z = 0.4\pi n i - \frac{n i a}{10} \left[ \frac{1}{(l+x)^2} + \frac{1}{(l-x)^2} \right]$$

This expression on averaging over the length of the specimen gives

$$H = 0.4\pi n i \left[ 1 - \frac{2r^2}{4l^2 - d^2} \right]$$

which on averaging again over the radial thickness gives

$$H = 0.4\pi n i \left[ 1 - \frac{r_1^2 + r_1 r_2 + r_2^2}{4l^2 - d^2} \right]$$

This is the expression for the average magnetic field over the specimen.

The balancing coil may be considered as a long thin solenoid, the effect of a single layer of which on the astatic system is the

same as that of a magnet of pole strength

$$m_o = \frac{\pi n i l}{10} \cdot \frac{\rho^2}{(l^2 + \rho^2)^{\frac{1}{2}}}$$

where  $2l$  = length of the coil and  $\rho$  its radius, and polar distance

$$l_o = (l^2 + \rho^2)^{\frac{1}{2}}$$

For multiple layer

$$m_o = \frac{\pi n i l}{10} \cdot \frac{\sum_1^p \rho_m^2}{(l^2 + \rho_m^2)^{\frac{1}{2}}}$$

$$\text{and } l_o = \frac{\sum_1^p \rho_m^2 (l^2 + \rho_m^2)^{\frac{1}{2}}}{\sum_1^p \rho_m^2}$$

the summation extending over all the layers,  $p$  in number.

Let the effect of the specimen at the needle be approximated by a pair of poles  $m'_o$  at a mutual distance of  $2l'_o$ . Under the condition of the experiment the horizontal field produced at the needles by  $m_o$  and  $m'_o$  are equal. If  $l_o = l'_o$  then  $m_o = m'_o$ . In such a case the intensity of magnetisation of the specimen  $I = m_o/A$  where  $A$  = cross sectional area of the cylindrical specimen.

The value of  $l'_o$  is uncertain and changes with the intensity of magnetisation. The error due to it is minimised by placing the specimen at a distance from the needle where the torque exerted is a maximum, the dimensions being so chosen as to give a flat maximum. At the position of maximum torque the rate of change of torque with change of position of pole is zero, while for positions near by the change of torque is very small. The position for the specimen was calculated<sup>2</sup> for different di-

<sup>2</sup> Bozorth, *loc. cit.*

mensions of the needles and their distance apart so as to give a flat maximum.

The effect of the compensating solenoid at the specimen was calculated and taken account of.

The above instrument was used for measuring the magnetic susceptibility of a number of ferrites in connection with gyro-magnetic tests made on them. The ferrites of Mn, Co, Cu and Zn were prepared by Holgerson's dry method in which the oxides are taken in the requisite proportion and heated to a high temperature for a sufficient length of time. In our case the temperature was about  $1000^{\circ}\text{C}$  and duration of heating 20 hours.  $\text{Fe}_3\text{O}_4$  and  $\text{NiO} \cdot \text{Fe}_2\text{O}_3$  were prepared by the wet method.

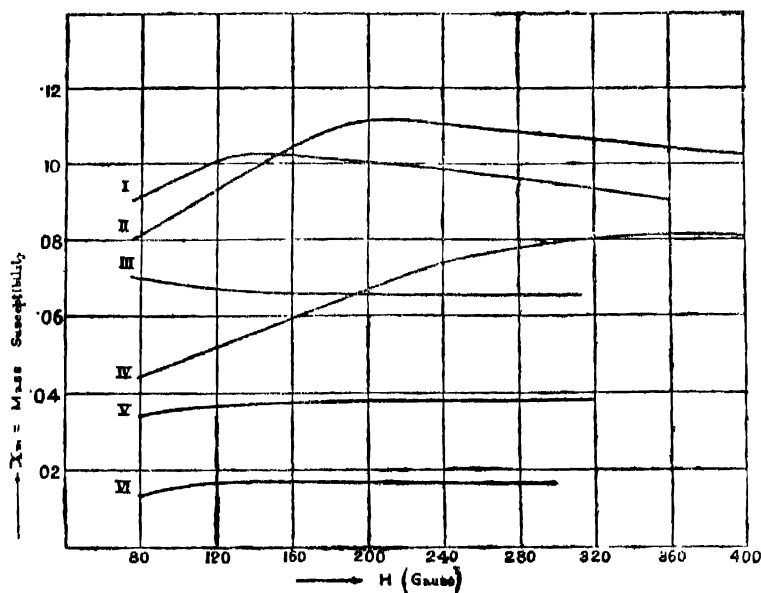


FIG. 2.

- |                                                 |               |
|-------------------------------------------------|---------------|
| I. $\text{CuO} \cdot \text{Fe}_2\text{O}_3$ ,   | $\rho = 2.65$ |
| II. $\text{Fe}_2\text{O}_3$ ,                   | $\rho = 1.42$ |
| III. $\text{MnO} \cdot \text{Fe}_2\text{O}_3$ , | $\rho = 2.45$ |
| IV. $\text{Fe}_3\text{O}_4$ ,                   | $\rho = 1.08$ |
| V. $\text{NiO} \cdot \text{Fe}_2\text{O}_3$ ,   | $\rho = 1.42$ |
| VI. $2\text{ZnO} \cdot \text{Fe}_2\text{O}_3$ , | $\rho = 2.48$ |

It is found that  $\chi$  depends on quite a large number of factors. Higher temperature and longer heating raises the value of  $\chi$ . After a sample has been prepared the effective  $\chi$  depends on the size of particles and density of packing. For tight packing particle size has lesser effect. Different samples prepared by the same wet process do not give identical values of

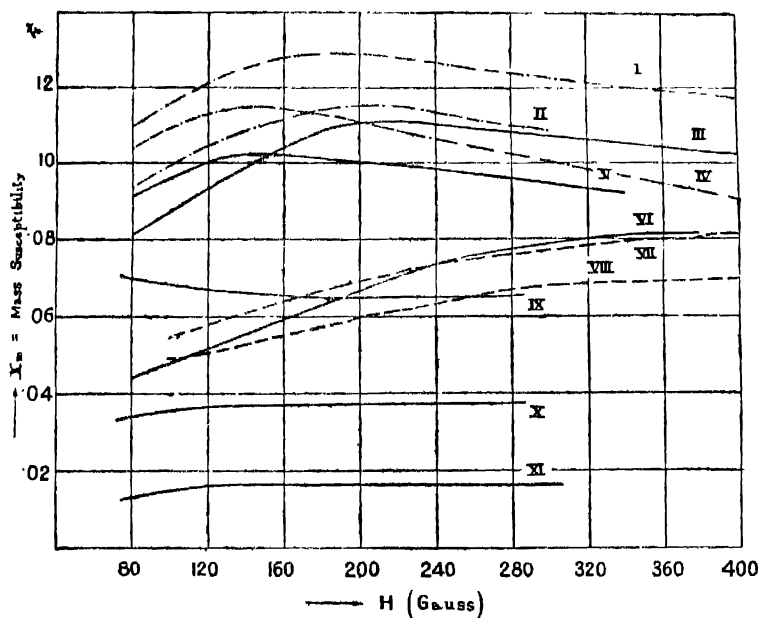


FIG. 3.

I. $\text{Fe}_2\text{O}_3$ ,	$\rho=1.67$ (H. & W.)	VII. $\text{Fe}_3\text{O}_4$ ,	$\rho=1.68$ (W. & B.)
II. $\text{Fe}_3\text{O}_4$ ,	$\rho=1.73$ „	VIII. $\text{Fe}_3\text{O}_4$ ,	$\rho=1.07$ „
III. $\text{Fe}_2\text{O}_3$ ,	$\rho=1.42$ (D. R.)	IX. $\text{MnO} \cdot \text{Fe}_2\text{O}_3$ ,	$\rho=2.45$ (D. R.)
IV. $\text{CuO} \cdot \text{Fe}_2\text{O}_3$ ,	$\rho=3.02$ (H. & W.)	X. $\text{NiO} \cdot \text{Fe}_2\text{O}_3$ ,	$\rho=1.42$ „
V. $\text{CuO} \cdot \text{Fe}_2\text{O}_3$ ,	$\rho=3.65$ (D. R.)		(4 hrs. heating at $500^\circ\text{C}$ )
VI. $\text{Fe}_3\text{O}_4$ ,	$\rho=1.08$ „	XI. $2\text{ZnO} \cdot 3\text{Fe}_2\text{O}_3$ ,	$\rho=2.48$ (D. R.)

$\rho$ =packing density.

H. & W.=Heroun and Wilson, Proc. Roy. Soc., 41, 100 (1928).

W. & B.=Welo and Baridich, Phys. Rev., 25, 58 (1925).

D. R.=This author.

$\chi$  even when the details of the process and other conditions remain the same. Generally there are small variations due

apparently to undetermined causes. The larger the size of the microcrystals formed on precipitation and the higher the temperature of precipitation, the higher is  $\chi$  generally.

For the purpose of gyromagnetic experiments the substance, finely powdered in an agate mortar, was packed to different degrees of tightness in a thin-walled copper tube about 2 mm in diameter and 6.5 cm in length. The value corresponding to the packing density of the specimen used in the gyromagnetic experiment could be found from these data by interpolation.

The results of some of the measurements are represented graphically in the adjoining figures. Some of the results of other authors are incorporated for comparison.

An observation made on nickel ferrite may be mentioned. This substance was investigated at different stages of formation. When heated to 550°C for 4 hours, the maximum  $\chi$  value attained was about .034. When this powder was taken in a tube of diameter 8 mm it showed magnetic viscosity for all degrees of packing. The same phenomenon was not observed when it was heated to a higher temperature, or when the diameter of the specimen was much smaller, say, 2 mm. The connection between magnetic viscosity and the formation of microcrystals is being further investigated.

In finding  $\chi$  the demagnetising factor  $N$  was taken to be constant, and equal to that for a long thin ellipsoid of ratio of axes = 65 : 2. Owing to the small value of intensity of magnetisation this produces no perceptible error.



## On the Formation and the Magnetic Properties of some Ferrites.\*

By

D. P. RAYCHAUDHURI.

*(Received for publication, 25th April, 1935).*

### ABSTRACT.

It is shown that the magnetic properties of ferrites depend largely on their method of preparation. For the dry method the deciding factors are the duration of heating and the temperature. This leads to clearing of the disagreements among different observers. Some magnetic data are given for a number of ferrites.

Ferrites have the general formula  $\text{MeO} \cdot \text{Fe}_2\text{O}_3$  where Me is a bi-valent metal. Hilpert<sup>1</sup> has shown that the relative proportions of MeO and  $\text{Fe}_2\text{O}_3$  may be varied and new ferrites formed having the formula  $n\text{MeO} \cdot m\text{Fe}_2\text{O}_3$  where n and m are small integers. A number of the ferrites shows ferromagnetic properties, while the others are paramagnetic. The structure is cubic (magnetite type) or hexagonal (haematite type), while some belong to an undetermined type. Attempts at correlating crystal structure and ferromagnetism<sup>2</sup> have not been successful, all of the cubic type and some amongst the other two showing ferromagnetism.

There are three methods available for the preparation of the ferrites.

(1) Heating the iron oxide with the base in requisite proportions to a high temperature preferably with addition of KCl.<sup>3</sup>

(2) Equimolecular proportions of salts of iron and some other element are taken and NaOH, KClO or some other material added to precipitate the sesquioxide of iron and the oxide of the other. After dessication the hydroxides are calcined, when the compound becomes ferromagnetic.

If instead of calcining the solution be kept for 12 hours in a sealed tube in an oil bath at 120°C, the precipitate becomes ferromagnetic. Further calcination does not appreciably increase the co-efficient of magnetisation.<sup>4</sup>

(3) Replacing Na in  $\text{Na}_2\text{O} \cdot \text{Fe}_2\text{O}_3$  with metal by heating the sodium ferrite and metallic chloride at high temperatures. Sodium ferrite is prepared by heating  $\text{Fe}_2\text{O}_3$  and  $\text{Na}_2\text{CO}_3$  in requisite proportions at high temperatures.<sup>1</sup>

Though all the three methods give the same compound the magnetisability of the products formed may differ considerably. Even the Curie points and the magneton numbers above the curie point show differences. This is due to the microcrystals and the crystalline aggregates not getting time and opportunity enough for their full growth. The present author has studied the effect of time and temperature of the magnetisability of the ferrites, some of the results of which are given below.

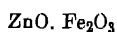
TABLE 1.

 $\text{CoO} \cdot \text{Fe}_2\text{O}_3$ . $\chi_{\text{CoO}} = 28.8 \cdot 10^{-6}$ ;  $\chi_{\text{Fe}_2\text{O}_3} = 32.5 \cdot 10^{-6}$ .

Field = 600 Gauss.

T°C	Time of heating.	$\chi \cdot 10^6$ .	Colour	Remarks.
30	...	...	Blue	
800	20 hours.	56.6	Blue as before	
900	"	330	Green	
950	"	1570	Dull green	Ferromagnetic
980	"	3096	Dull green	Do.

TABLE 2.



$\chi_{\text{ZnO}} = -54 \cdot 10^{-6}; \quad \chi_{\text{Fe}_2\text{O}_3} = 32 \cdot 5 \cdot 10^{-6}.$

Field = 600 gauss

Temp.	Time of heating.	$\chi \cdot 10^6$ .	Colour.	Remarks.
800	20 hrs.	147	Brick	
880	2 "	171	Darkening towards brown	
"	8 "	253		
"	16 "	378		
"	20 "	456		
950	10 "	632	Dark brown	Attractable by magnet
"	18 "	723		Ferromagnetic
1000	5 "	1272	Brownish black	"
"	10 "	4286		"
"	18 "	...		Strongly ferromagnetic

Above  $950^\circ\text{C}$  crystals grew larger in size and formed into lumps. When rapidly cooled  $\chi$  was lower than when slowly cooled.

The formation of  $2\text{ZnO} \cdot 3\text{Fe}_2\text{O}_3$  was also studied. The results are in general agreement with Hilpert's.<sup>1</sup> 20 hours heating at  $600^\circ\text{C}$  gave  $\chi = 1013 \cdot 10^{-6}$ , the material containing ferromagnetic particles attractable by a magnet. Two hours' heating at the same temperature gave  $\chi = 214 \cdot 10^{-6}$ .

The results of different investigators on the ferrite of zinc of composition  $\text{ZnO} \cdot \text{Fe}_2\text{O}_3$  do not agree amongst themselves. Thus Forestier and Chaudron<sup>5</sup> find no discontinuity of magnetisation with temperature. The curves are perfectly reproducible even after long heating at  $1200^\circ\text{C}$ . Value of  $\chi$  between 0 and 100 gauss is  $160 \cdot 10^{-6}$ . Forestier<sup>2</sup> states that the compound is paramagnetic Mlle Serres<sup>6</sup> says that "this is the only ferrite

known in the paramagnetic state alone. Even at liquid air temperatures it is not attractable by a magnet. This holds both for the product obtained by Chaudron and Forestier's wet method and for the one obtained by Holgersson's dry method. It behaves as a normal paramagnetic salt of iron obeying Curie-Weiss law between  $0^{\circ}\text{C}$  and  $700^{\circ}\text{C}$  with a Weiss magneton number of 24 and  $25\cdot5$ ." Against these Hilpert<sup>1</sup> observes that the substance obtained by the dry method at  $1200^{\circ}\text{C}$  is slightly ferromagnetic. Our data show that the compound obtained by heating the mixture of  $\text{ZnO}$  and  $\text{Fe}_2\text{O}_3$  above  $900^{\circ}\text{C}$  is ferromagnetic. The intrinsic magnetisation-temperature curve shows that  $\text{ZnO}\cdot\text{Fe}_2\text{O}_3$  has a Curie point of  $522^{\circ}\text{C}$ . Heat treatment changes its properties as shown below.

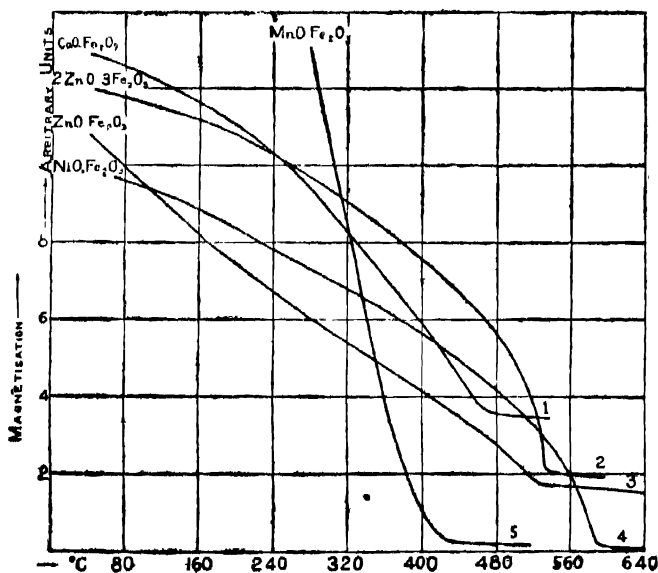


FIG. 1.

Curves 1, 2 and 3 are shifted upwards with respect to 4 and 5.

TABLE 3.

Paramagnetic Susceptibility Values.

Before heating.		After heating.	
Temp. (0°C)	$\chi \cdot 10^6$	Temp. (0°C)	$\chi \cdot 10^6$
539.5	38.1	543	38.4
615	22.6	617	35.2
639.7	18.2	638	33.0
		672	31.7

In the ferromagnetic part of the curve heat treatment lowers the  $\chi$  values, the Curie point remaining unchanged. The Curie point of  $\text{ZnO} \cdot \text{Fe}_2\text{O}_3$  and  $2\text{ZnO} \cdot 3\text{Fe}_2\text{O}_3$  are very nearly the same.

Ferromagnetic  $\chi$  values of  $\text{ZnO} \cdot \text{Fe}_2\text{O}_3$  before and after heat treatment. Field applied about 6,000 gauss.

TABLE 4.

Before heating.		After heating.	
(Temp. (0°C))	$\chi \cdot 10^6$	(Temp. (0°C))	$\chi \cdot 10^6$
80	548	80	290
196	358	196	184
288	267	288	92.2
373	195	373	70.6
468	106	468	66.0

$\chi$ 's in the paramagnetic region of the above compound are not quite independent of field strength.

TABLE 5.

Temp. (°C).	Ratio of $\chi$ 's.	Ratio of field strengths.
293	1'00; '67 : '35	1'00 : '58; '28 (Maximum field about 6,000 gauss)
470	1'00 : '59 : '29	
545	1'00; '56 : '26	
616	1'00 : '55: '24	

In the above the magnetisation-temperature curve showed no discontinuity at the Curie points of  $\text{Fe}_2\text{O}_3$  and iron. Hence ferromagnetic  $\text{Fe}_2\text{O}_3$  or free iron was absent.

The accompanying table gives the maximum value of  $\chi$  and the Curie point of a number of ferrites. Where possible X-ray data have also been included.  $\chi$  values show very large variations, the maximum value observed by particular observers being given.

TABLE 6.

Compound.	Curie point. (°C).	Magnetisability.	X-ray Structure.
$\text{NaO.Fe}_2\text{O}_3$	Much lower than $-70^\circ$ (1)	4 at liquid air temp. (1) (a)	Undetermined type (1)
$\text{CaO.Fe}_2\text{O}_3$	170 (1) 425 (5)	1 (1) (a) $\chi = '0425$ (5)	Undetermined type (1) (2)
$\text{SrO.Fe}_2\text{O}_3$	420 (1)	8 (1) (a)	Hexagonal close pack $\frac{c}{a} = 1'8$ (2) Undetermined type (1)
$\text{BaO.Fe}_2\text{O}_3$	435 (1) 440 (5)	10 (1) (a) $\chi = '0099$ (5)	Hexagonal close pack $\frac{c}{a} = 1'8$ (2) Undetermined type (1)

(a) The numbers are relative to the magnetisability of reduced iron powder which is taken as 1000.

TABLE 6—Continued.

Compound.	Curie point. (°C)	Magnetisability.	X-ray Structure.
ZnO.Fe <sub>2</sub> O <sub>3</sub>	70 to 80 (1) No discontinuity of magnetisation with temp (5) $\theta_f = 522^*$	20.3 (1) (a) $\chi = .00016$ (5) $\chi = .005^*$	Magnetite type (1)
PbO.Fe <sub>2</sub> O <sub>3</sub>	320 (1) 435 (5) $\theta_f = 442.2$ (6) $\theta_p = 453.1$ (6)	49 (1) (a) $\chi = .0012$ (5)	Hexagonal close pack $\frac{c}{a} = 1.8$ Undetermined type (1)
CuO.Fe <sub>2</sub> O <sub>3</sub>	450 (1) $\theta_f = 455$ (6) $\theta_f = 453^*$ $\theta_p = 438.1$ (6) $\theta_p = 436^*$	300 (1) (a) $\chi = .102^*$ $\chi = 115$ (8)	Magnetite (1) (2) $a = \text{parameter} = 8.44$ $A^\circ$ (7)
FeO.Fe <sub>2</sub> O <sub>3</sub>	581 (6) $\theta_f = 582^*$	460 (1) (a) $\chi = 11^*$ $\chi = 12$ (8)	Cubic (7) $a = 8.42$
NiO.Fe <sub>2</sub> O <sub>3</sub>	$\theta_f = 590$ (6) $\theta_f = 591^*$ $\theta_p = 597$ (6)	$\chi = .078^*$	Cubic (7) $a = 8.41$
MnO.Fe <sub>2</sub> O <sub>3</sub>	$\theta_f = 304^*$	$\chi = .072^*$	Cubic (7) $a = 8.57$
CoO.Fe <sub>2</sub> O <sub>3</sub>	$\theta_f = 463^*$	$\chi = .079^*$	Cubic (7) $a = 8.39$
MgO.Fe <sub>2</sub> O <sub>3</sub>	$\theta_f = 339$ (6) $\theta_f = 324.1$ (6) 315 (5) 361.8 (6)	$\chi = .035$ (8) $\chi = .054$ (5)	Cubic (7) $a = 8.34$
CdO.Fe <sub>2</sub> O <sub>3</sub>	250 (5)	.....	Hexagonal close pack $\frac{c}{a} = 1.64$ Face centred cube. $a = 8.45$ (2) $a = 8.73$ (7)
Fe <sub>2</sub> O <sub>3</sub>	675 (5) 690 (10)	$\chi = .25$ (9) $\chi = .13$ (8) $\chi = .11^*$	.....
2ZnO.3Fe <sub>2</sub> O <sub>3</sub>	529 *	$\chi = .016^*$	Cubic (1)

 $\theta_f$  = Ferromagnetic Curie Point. $\theta_p$  = Paramagnetic Curie Point.

\* Observed by the present author.

*References.*

- <sup>1</sup> S. Hilpert and A. Wille, *Zeit. f. Phys. Chem.*, B, 18, p. 291 (1932).
- <sup>2</sup> Hilpert and Wille, l. c., also H. Forestier, *Compt. Rend.*, 192, p. 842 (1931).
- <sup>3</sup> S. Holgerason, *Lunds Univ. Arsskrift*, 23, p. 58 (1927).
- <sup>4</sup> H. Veil, *Compt. Rend.*, 188, p. 1293 (1929).
- <sup>5</sup> H. Forestier and M. Chaudron, *Compt. Rend.*, 182, p. 777 (1926).
- <sup>6</sup> Mlle. Serres, *These*, Strasbourg, pp. 65-67 (1931).
- <sup>7</sup> *Struktur Berichte*, Ewald and Hermann
- <sup>8</sup> Herroun and Wilson, *Proc. Phys. Soc. (Lond.)*, 41, p. 100 (1928).
- <sup>9</sup> Sachse, *Zeit. f. Phys. Chem. B.*, 148, p. 401 (1930).
- <sup>10</sup> Honda and Soné, *Sc. Rep. Tokoku Univ.* 3, p. 228 (1914).



## Investigations in the Infra-Red.\*

### *Part I. Absorption Spectrum and Molecular Structure of Borates*

By

M. K. SEN AND A. K. SEN GUPTA.

*(Received for publication, 1st May, 1935).*

#### ABSTRACT.

A study of the near infra-red absorption spectra of a few borates has been made in the region  $5\mu$ - $15\mu$ . The results are in agreement with the predictions of Cassie. The magnitude of the true force constant of the radical under investigation in comparison to that of  $\text{CO}_3$  and  $\text{NO}_3$  shows that the bond is not localised as in  $\text{BCl}_3$ . The slightly positive value of true rigidity reveals further that its plane configuration is not due to repulsion of the oxygen ions alone and follows the central quantisation more closely than  $\text{NO}_3$  or  $\text{CO}_3$  radical.

#### 1. Introduction.

It is now well known that a radical or a molecule of the type  $\text{XO}_3$  may possess either a pyramidal or a planar configuration, and has six vibrational degrees of freedom but only four distinct fundamental frequencies. One of these corresponds to oscillation of the X atom relative to the  $\text{O}_3$  triangle along the

\* Read before the meeting of the Indian Physical Society on the 24th April, 1935.

line through the median point and normal to its plane. There are two fundamentals of double frequencies corresponding to the motion of the four atoms in the equilibrium plane. Another is due to simultaneous vibration of the three O atoms in phase towards or away from the X atom. This frequency plays an important role in deciding between the pyramidal and planar configurations. For a radical or molecule with the planar configuration it is inactive whereas in the case of a pyramidal one it is active.

A planar configuration has been ascribed to the nitrates, carbonates as well as the borates from crystal lattice data. In the case of the first two radicals, support to this view has been obtained from a study of their infra-red and Raman spectra. Pauling<sup>1</sup> however suggested that these radicals are slightly pyramidal in structure and the apparent planar configuration is due to the vibration of the N or C nuclei through the oxygen plane. From a consideration of their rigidity Cassie<sup>2</sup> has shown that the nitrate radical has a greater tendency to become pyramidal than the carbonate and that the plane configuration is maintained not through the central quantisation but through the repulsion of the oxygen ions. It is therefore, of interest to calculate the rigidity of  $\text{BO}_3$  as well as its force constants which will indicate the type of link in the BO bond. For this purpose a study of the infra-red and Raman spectra of the radical has been considered to be desirable.

The present paper deals with the infra-red investigations on a few inorganic borates. In view of the fact that the fundamentals of the carbonate<sup>3</sup> and nitrate<sup>4</sup> radicals lie between  $5\mu$  to  $15\mu$ , our observations are also confined to this region of the spectrum. Three fundamental frequencies have been located at  $7.5\mu$ ,  $11\mu$  and  $14\mu$ . The fourth fundamental which from a

<sup>1</sup> Pauling, Jour. Amer. Chem. Soc., Vol. 53, p. 1982 (1931).

<sup>2</sup> Cassie, Proc. Roy. Soc., "A" Vol. 148, p. 87 (1935).

<sup>3</sup> Brester, Zeits. f. Phys. Vol. 24, p. 324 (1924.).

<sup>4</sup> Schafer and others, Zeits. fur. Phys. Vol. 45, p. 493 (1927).

comparison of the data for the above two radicals may be expected to be at about  $9\mu$  is definitely absent. This would correspond to the inactive fundamental frequency and would prove that the  $\text{BO}_2$  radical has a planar configuration. The true rigidity of the radical as distinct from its strain rigidity is slightly positive. Hence its planar configuration is not due to repulsion of the oxygen ions alone and follows the central quantisation more closely than  $\text{CO}_2$  and  $\text{NO}_2$ . The evaluation of the true force constant reveals further that the bond is not localised as in  $\text{BCl}_2$  investigated by Cassie (*loc. cit.*).

## 2. Experimental.

The source of radiation is a linear Nernst filament. A steady current from a battery of 72 storage cells of 250 amp.-hours capacity has been used to heat the filament. The current through the filament is maintained at 0.50 amps. with the help of a suitable resistance in series.

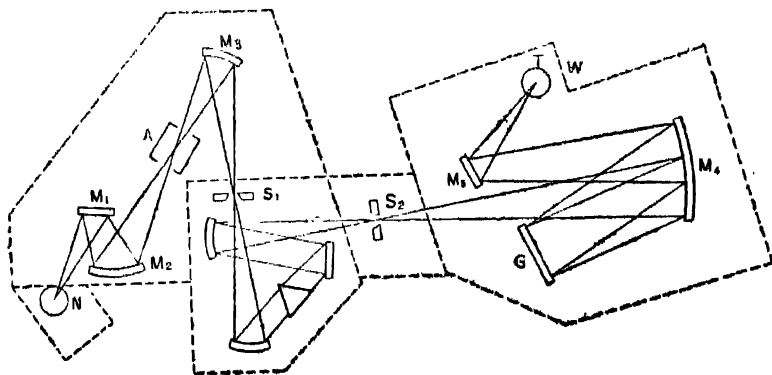


FIG. 1.

The general optical arrangement of the dispersive system is given in Fig. 1. This consists of three parts. The first part contains the condensing mirrors and the absorption chamber. Radiation from the source  $N$  after reflection at a plane mirror

$M_1$  is focussed at A within the absorption chamber by the concave mirror  $M_2$ . The beam then diverges and is again brought to a focus by the mirror  $M_3$ , on the slit  $S_1$  which is the entrance slit of the prism spectrometer. The second part consists of the prism spectrometer which is a Leiss monochromator having a rock salt prism, two concave mirrors placed at right angles and a prism table with a Wadsworth mirror mounted on it and capable of rotation from outside by worm wheel and pinion. The scale on the drum is directly graduated in wavelengths corresponding to rock salt prism.

The second slit  $S_2$  of the monochromator is the collimator slit of the grating spectrometer which constitutes the third part in the diagram.  $M_4$  is a single long focus concave mirror functioning both as the collimator and telescope. The last mirror  $M_5$  which is a plane one brings the focus to a convenient position for the thermopile T. The grating G is mounted on a goniometric table. In the present investigation, the grating spectrometer has not however been used.

A thermopile in conjunction with a Paschen galvanometer has been used for the detecting system and is of Hilger bismuth silver junction type. It has a symmetrical slit in its front and an eyepiece behind it. The latter along with a cross wire inserted in place of the pile is used for visual calibration. The Downing type Paschen galvanometer has a resistance of 13.56 ohms and gives a deflection of 1600 mms. per microampere on a scale placed at a distance of 1 meter. The sensitivity of the galvanometer can be varied by means of its control magnets. It has been made free from mechanical vibrations as far as possible by placing it on a concrete pillar on a foundation of about 9 ft. below the floor of the laboratory. Underneath the foundation there are shock absorbers consisting of 2 sheets of lead placed under 5 sheets of India rubber. The annular space around the pillar is filled with sand. To overcome the electrical disturbances on the connecting wires they are enclosed in composition tubing carefully earthed. Even with this arrangement the galvanometer vibrates

due to outside mechanical disturbances such as the passing of a heavy vehicle in the neighbourhood. The observations had therefore to be taken in the calm hours of the night.

The different sections of the apparatus are enclosed in separate boxes as indicated by dotted lines in Fig. 1. The Nernst filament with its asbestos housing is kept outside the chamber containing the absorption cells and the condensing mirrors. The enclosing chamber is provided with shutters to screen the rock salt prism from the influence of moist draughts while the instrument is not in operation. The box containing the grating spectrometer and the thermopile has its walls lined with asbestos. The open spaces are all packed with cotton wool to ensure a constancy of temperature inside.

The absorption chamber has been designed to hold vertically a rock salt plate on one side of which a thin layer of the solid under investigation is spread in the form of fine powder. Previous to this the rock salt plate is well ground and polished. To prevent moisture from depositing on the rock salt plates, the chamber, A is provided with a heater which consists of a small resistance coil carefully insulated. This enables us to maintain a slightly higher temperature than that of the room, the difference being nearly  $3^{\circ}\text{C}$ . A similar precaution is also taken to keep the monochromator prism dry. Drying agents are also placed inside the boxes to ensure further that the general atmosphere is free from moisture.

As the drum of the monochromator is calibrated in wave-length scale, it is expected that wave-length of any monochromatic radiation could be directly obtained, only if the prism is set in its minimum deviation for any known radiation. The green and yellow lines of mercury have been used for this purpose. A further check on the accurate setting of the prism spectrometer was made by identifying the fundamental bands of  $\text{BaCO}_3$ .

### 3. Experimental Results.

Merck's chemicals of extra pure quality were used in the investigation. Curves showing the absorption maxima for compounds are given in Fig. 2. It will be seen that in each case there are a number of absorption regions, some of which are evidently due to the presence of combination tones. In view of their intensities the mean band centres at  $7.5 \mu$ ,  $11 \mu$  and  $14 \mu$  select themselves as the active fundamentals. From an analogy with  $\text{CO}_2$  and  $\text{NO}_2$  radicals they have been ascribed to  $\nu_2$ ,  $\nu_1$  and  $\nu_3$  respectively, while the remaining fundamental  $\nu_4$  which is optically inactive is assumed to lie at about  $9 \mu$ . The band centres of the observed fundamentals for the different compounds are collected in Table I.

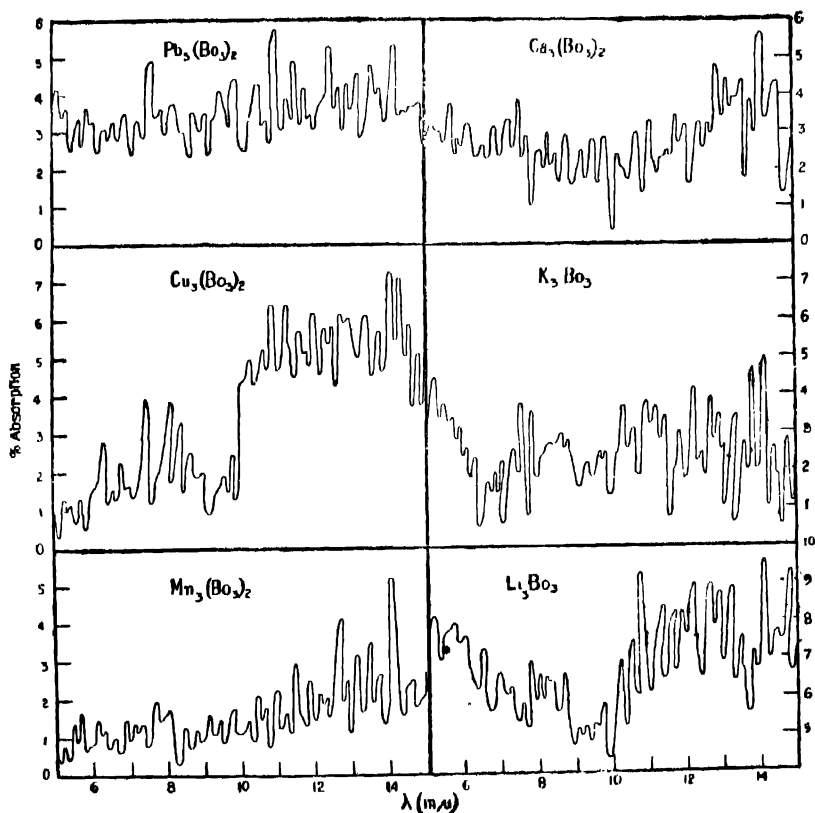


FIG. 2.

TABLE I.

Compound.	Bands.		
	$\nu_2$ ( $\mu$ )	$\nu_1$ ( $\mu$ )	$\nu_3$ ( $\mu$ )
Lithium Borate	7.6	10.7	14.0
Potassium Borate	7.5	10.9	14.1
Calcium Borate	7.5	11.0	14.1
Manganese Borate	7.6	10.3	14.0
Copper Borate	7.5	10.8	14.2
Lead Borate	7.6	11.0	14.1

#### 4. Evaluation of Force Constants.

Formulae showing the relationships between the fundamental frequencies and force constants of the  $\text{XO}_3$  type radical or molecule have been given by Nielson<sup>5</sup> and later by Menzies.<sup>6</sup> It may here be pointed out that their results are not in agreement due probably to approximation involved in transforming the potential function,

$$V = F(r) + f(a) + F'(r)(q_4 + q_5 + q_6) + \frac{1}{2}F''(r)(q_4^2 + q_5^2 + q_6^2) + f'(a)(q_1 + q_2 + q_3) \\ + \frac{1}{2}f''(a)(q_1^2 + q_2^2 + q_3^2) \quad \dots \quad \dots \quad \dots \quad (1)$$

where  $r$  is the normal distance of X from O atom;  $a$ , the length of the side of the triangle in the undisplaced state;  $q_1$ ,  $q_2$  and  $q_3$ , the mutual displacements of O atoms in pairs;  $q_4$ ,  $q_5$  and  $q_6$ , the relative displacements of the X and the O atoms.

Menzies' expression for the frequencies are

$$\nu_1 = \frac{1}{2\pi} \sqrt{\frac{k}{m}} \sqrt{\beta_\mu} \quad \dots \quad (2)$$

<sup>5</sup> Nielson, Phys. Rev., Vol. 32, p. 773 (1928).

<sup>6</sup> Menzies, Proc. Roy. Soc. "A," Vol. 134, p. 265 (1931).

$$\nu_{2,3} = \frac{1}{2\pi} \sqrt{\frac{k}{m}} \sqrt{\frac{1}{4}[\mu(1+\beta) + (1+3\alpha)] \pm \sqrt{\left[\frac{1}{4}\mu(1+\beta) + \frac{1}{4}(1+3\alpha)\right]^2 - \frac{1}{4}\mu \times [(1+3\alpha)(1+\beta) - (1-\beta)^2]}} \quad \dots \quad (3)$$

$$\nu_4 = \frac{1}{2\pi} \sqrt{\frac{k}{m}} \sqrt{(1+3\alpha)} \quad \dots \quad \dots \quad \dots \quad (4)$$

where  $\mu = \frac{M+3m}{M}$  ( $M$  is the mass of X atom;  $m$ , the mass of O atom)

$$k = F''(r); \quad \alpha = \frac{f'''(a)}{F''(r)}; \quad \beta = \frac{F'(r)/r}{F''(r)}$$

The value of  $F''$  is found out by eliminating  $\alpha$  and  $\beta$  from equations (3) and (4) as follows:—

$$[(v_2^2 + v_3^2)^2 - (v_2^2 - v_3^2)^2]\mu - \gamma(v_4^2\mu - \gamma)]\Lambda^2 - 4\mu\gamma\Lambda + 4\mu^2 = 0 \quad \dots \quad (5)$$

$$\text{where } \gamma = [2(v_2^2 + v_3^2) - v_4^2]$$

Hence “A” can be evaluated by solving the above quadratic equation and is related to  $F''$  as  $A = \frac{4\pi^2 m}{F''}$ . Corresponding to the two values of “A” we have  $F'' = 4.3 \times 10^5$  and  $1.8 \times 10^6$  dynes/cm. Now substituting these values in equations (3) and (4)  $f''$  and  $F'$  are found to be as follows:

$f''$	$F'$
dynes/cm.	dynes.
$2.4 \times 10^5$	$1.9 \times 10^{-3}$
$3.4 \times 10^5$	$5.5 \times 10^{-3}$

On the other hand the value of  $F'$  corresponding to  $\nu_1$  is  $2.0 \times 10^{-8}$  dynes. This shows that  $F' = 1.9 \times 10^{-3}$  dynes corresponds to the case when the planar configuration could be maintained in the absence of repulsion between the atoms while  $F' = 5.5 \times 10^{-3}$  dynes to the case when the repulsion alone simulates its plane configuration.



The force constant  $F''$  of any link calculated as above from the observed vibrational frequencies should be corrected for deviation from the minimum of the potential energy curve to give its true value. It may here be noted that the value of  $F'' = \frac{d^2V}{dr^2}$  measures the curvature of the  $V:r$  curve for the link at its equilibrium separation and corresponds to the minimum in the curve for diatomic and non-closed triatomic molecules. But if the link is under strain as in the present case the equilibrium separation does not represent this minimum and the curvature measured by  $F''$  may be very different from that of the same link joining the same atoms in a diatomic molecule. The analytical expression for the potential energy curve of a diatomic molecule as given by Morse is

$$F = D e^{-2a(r-r_0)} - 2D e^{-a(r-r_0)} \quad (6)$$

where  $D$  is the energy of dissociation of the bond,  $r_0$  the separation of the nuclei at the position of the minimum potential and  $a = 0.245 \sqrt{M_0 \omega_0 x}$  in  $\text{\AA}^{-1}$ ,  $\omega_0 x$  being the anharmonicity factor

$$\text{and } M_0 = \frac{Mm}{M+m}$$

$$\text{Putting } b = e^{-a(r-r_0)}$$

$$F' = -2aDb^2 + 2aDb \quad (7)$$

$$F'' = 4a^2Db^2 - 2a^2Db \quad (8)$$

For  $r=r_0$  the true force constant,

$$F_0'' = 2a^2D \quad (9)$$

Now  $D$  can be determined from equations (7) and (8) as follows :—

$$D = \frac{(4F' + F'')^2}{8(2F' + F'')} \quad \dots (10)$$

Corresponding to  $F'' = 4.3 \times 10^5$  dynes/cm and  $F' = 1.9 \times 10^{-3}$  dynes the energy of dissociation  $D$  is 13.7 volts. Substituting the value of  $D$  in equation (9) one can evaluate the true force constant  $F''_0$  provided " $a$ " is known. From the analysis of the bands associated with the diatomic molecule of boron monoxide<sup>7</sup> one finds that in the ground state,  $^2\Sigma$ , of the molecule,  $\omega_0 x$  is  $10.7 \text{ cm.}^{-1}$  so that  $a$  comes out to be nearly  $2\text{\AA}^{-1}$  and the true force constant  $F''_0$  is  $17.4 \times 10^5$  dynes/cm.

### 5. Calculation of Rigidity.

Of the four fundamental frequencies  $\nu_1$  is assumed to arise only from the strain of the radical and as we have already remarked it corresponds to motion of the B atom in the perpendicular plane. On the other hand, the frequencies  $\nu_2$ ,  $\nu_3$  and  $\nu_4$  involve only motions in the plane of the triangle. Hence  $\beta$  should have two different values, their difference giving a measure of the rigidity of the plane configuration which can be calculated as follows from the observed fundamental frequencies:—

If  $\theta$  is the angle between the displaced link and its equilibrium position, the potential energy associated with a deviation of one BO bond from the plane configuration is given by,

$$V = \frac{1}{2} K_\theta (\tau^2 \theta^2) \quad \dots (11)$$

where  $K_\theta$  is the tangential restoring force constant,  $\nu_1$  is then given by

$$4\pi^2 \nu_1^2 = \frac{1}{m} K_\theta \mu \quad \dots (12)$$

But from Menzies' expression,

$$4\pi^2 \nu_1^2 = \frac{1}{m} \cdot \frac{F'}{r} \cdot \mu \quad \dots (13)$$

<sup>7</sup> Jevons, Report on Band Spectra of Diatomic Molecules.

Hence assuming  $r$  to be  $1.35\text{\AA}$  as found by Zachariasen<sup>8</sup> one can calculate from the above relation the value of  $F'/r$  and thus of  $K_\theta$  which must be corrected for the strain of the radical. The frequencies of the normal modes confined to the plane of the radical give  $F'/r$  as  $1.4 \times 10^5$  dynes/cm. and this is due to strain alone. On the other hand  $F'/r$  calculated from  $\nu_1$  is  $1.5 \times 10^5$  dynes/cm. This shows that the true rigidity of each bond is given by tangential restoring force constant of approximately  $1 \times 10^4$  dynes/cm; in other words the rigidity associated with the central B atom in  $\text{BO}_3$  radical is  $3 \times 10^4$  dynes/cm.

### 6. Conclusions.

The results are in agreement with the prediction of Cassie. The magnitude of the true force constant of the radical under investigation in comparison to that of  $\text{CO}_3$  and  $\text{NO}_3$  shows that the bond is not localised as in  $\text{BCl}_3$ . The slightly positive value of true rigidity reveals further that its plane configuration is not due to repulsion of the oxygen ions alone and follows the central quantisation more closely than  $\text{NO}_3$  or  $\text{CO}_3$  radical.

The authors acknowledge their gratefulness to Prof. P. N. Ghosh for suggesting the problem and guidance during the course of the investigation.

APPLIED PHYSICS DEPARTMENT,  
UNIVERSITY COLLEGE OF SCIENCE,  
92, UPPER CIRCULAR ROAD,  
CALCUTTA.

<sup>8</sup> Zachariasen, Jour. Amer. Chem. Soc., Vol. 53, p. 2124 (1931).



## Influence of Magnetic Field on the Co-efficient of Viscosity of Liquids.\*

P. K. RAHA AND S. D. CHATTERJEE.

(Received for publication, 11th May 1935).

### ABSTRACT.

The paper gives a preliminary account of the results of the investigation on the influence of magnetic field on the co-efficient of viscosity of liquids. The following results have been noted :

(i) Liquids with long chain aliphatic molecules, *e.g.*, acetone and propyl alcohol (normal), show diminution of viscosity in a magnetic field.

(ii) Liquids of the aromatic class, *e.g.*, nitro-benzene and toluene and an alcohol with side chains, *e.g.*, iso-amyl alcohol, show increase of viscosity in a magnetic field.

(iii) Carbon tetrachloride, water and aqueous solution of cerium nitrate show no change of viscosity.

For nitro-benzene, the change  $d\eta/\eta$  increases linearly with increase of magnetic field, no indication of saturation being observed. The thermal variation of  $d\eta/\eta$  for the same liquid is also recorded.

The influence of electric and magnetic field on the so-called transference processes in liquids and gases, *viz.*, on the co-efficients of viscosity, conductivity and diffusion, has been the subject of many investigations in recent years. A concise summary of these investigations will be found in a paper by Trautz and Fröschel in the *Ann. d. Phys.* Bd. 22, p. 223, 1935. Most of the changes observed by the previous investigators lay within the limits of experimental error, and no definite conclusions could be drawn from them. Recently Senftleben<sup>1</sup> and

\* Communicated by the Indian Physical Society.

his fellow-workers have investigated the influence of a magnetic field on the conductivity of paramagnetic gases, and have obtained definite results, *viz.*, a diminution of conductivity of  $O_2$  in a magnetic field of maximum value of the order of 1.1%. Owing to the close relation between the diffusion and conduction in a gas, Engelhardt and Sack<sup>2</sup> investigated and found a definite diminution in the value of the co-efficient of viscosity of  $O_2$ , of the order of 0.4%, in a magnetic field of strength 6-8 K. G. Similar results have been found by Trautz and Fröschel.<sup>3</sup> On reading accounts of these investigations of Senftleben, Sack and Trautz, it appeared worth while to us to try similar experiments with liquids.

It is known that organic liquids like nitrobenzene exhibit strong magnetic birefringence (Cotton-Mouton effect), which shows that molecules of such liquids possess a large degree of magnetic and optical anisotropy. These molecules are also highly anisotropic in shape, and it appeared reasonable to us to expect that due to the orientation of these molecules in a magnetic field, the co-efficient of viscosity of the liquid containing these molecules will be altered. After a large number of preliminary investigations, it has been possible for us to detect a definite change in the co-efficient of viscosity of different liquids, in magnetic fields of the order of 25-35 K. G. We have also investigated the effect of such a field on the viscosity of a solution of cerium nitrate, whose magnetic birefringence has been observed by Chinchalkar<sup>4</sup> and Haenny.<sup>5</sup> We could not observe any measurable change of viscosity in this solution, which is in agreement with the negative result obtained by König, on the effect of a magnetic field (much weaker in strength as compared to ours) on the viscosity of a solution of manganese sulphate.

In the present paper a preliminary account of the results obtained so far will be given; theoretical discussion of the effects observed will be postponed till a large amount of accurate results have been obtained.

*Experimental Method.*

The method used was to measure the time of flow of a given volume of liquid through a capillary tube, placed between the pole-pieces of a powerful electromagnet. The change in the time of flow, when the given volume of liquid falls through a constant height, is taken to be proportional to the change in the viscosity of the liquid under the influence of the given magnetic field; it being assumed that there has not been any appreciable change of temperature. The electromagnet used was of Rutherford type, by means of which a magnetic field of about 34 K. G., was produced, between the prismatic-shaped pole pieces, over a volume of 17 cms.  $\times$  0.4 cm.  $\times$  0.4 cm. This type of electromagnet has no arrangement for water cooling. Special arrangement had to be made, to keep the temperature of the pole-pieces and of the liquid flowing through the capillary tube constant, during the period of the experiment. The necessity of ensuring the constancy of temperature will be apparent from the following consideration: For nitrobenzene we obtained an increase of viscosity of 0.2% in a field strength of 36 K. G. and temperature 23.5C. The time of flow was 25 minutes. The temperature change of viscosity of nitrobenzene is  $3\frac{1}{2}\%$  per degree, so that an increase in temperature of 0.1C would completely mask the increase in viscosity in the magnetic field.

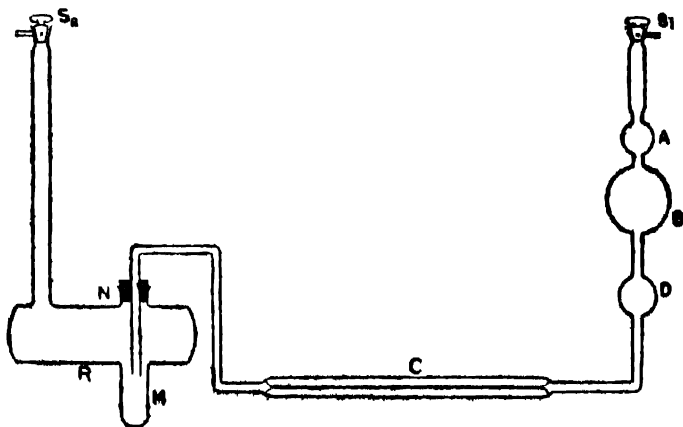


FIG. 1

The apparatus consisted essentially of a horizontal capillary tube C, (Fig. 1) of length 17 cms., and internal bore 0.5 mm., with two vertical limbs. One of these comprised of three glass bulbs, A, B, D, interconnected by means of slender glass tubes, while the other communicated with a receiving bulb R through a cork. A projecting glass tube M sealed to the lower end of the receiver, vertically below the cork N, allowed freedom of adjustment of the difference of level through which the liquid volume contained in A and B was intended to fall. The time of flow of the liquid could thus be regulated to a certain extent. Usually the time taken by the meniscus of the liquid head to flow across two specified marks on the narrow stems of the middle bulb B (about 1 inch in diameter) was observed. When, however, the viscosity of the liquid was large (*e.g.*, for iso-amyl alcohol and normal propyl alcohol), the time taken by the meniscus to travel across two marks on the narrow stems of the uppermost bulb A (about  $\frac{1}{4}$  the size of the middle bulb)

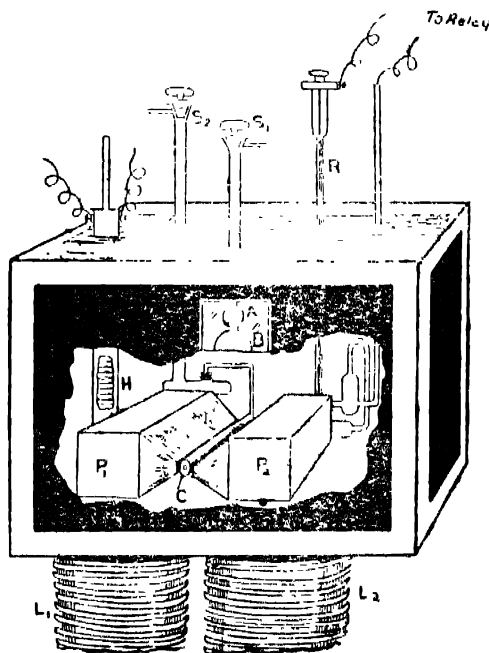


FIG. 2.



was observed. Two sides of the capillary tube were ground flat to a thickness of 2 mm. to enable its being placed in the narrow rectangular gap between the pole-pieces  $P_1$  and  $P_2$ , leaving sufficient space between the ends of the latter and the sides of the tube for the circulation of water. By means of the stop-cock  $S_1$ , the apparatus could be connected through a calcium chloride tower, either to air or to a rotary oil pump.  $S_2$  is connected to outside air through another calcium chloride tower. After each experiment, the liquid is sucked back to the bulbs A and B by connecting  $S_1$  to the air pump and opening  $S_2$ .

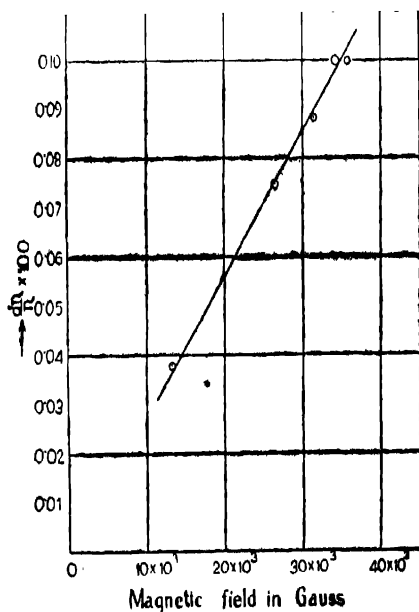
The electromagnet consisted of two vertical limbs  $L_1$  and  $L_2$ , (Fig. 2) round which the field coils were wound. On the top of these two limbs a thick brass plate was supported, through which the two rectangular ends of the cores of  $L_1$  and  $L_2$  project out and support the prism-shaped pole-pieces  $P_1$  and  $P_2$ . On this brass-plate a thermostat, of dimensions  $21'' \times 19'' \times 13''$ , is built up. The bottom of the thermostat is fixed water tight on the brass plate by means of white paint, while the protruding corners are supported by suitable wooden supports. The bottom has two rectangular openings through which the cores of  $L_1$  and  $L_2$  project out. The outside of the thermostat, which is made of copper sheet, is covered with asbestos board fixed to a wooden frame. The front side is provided with a glass window to enable an observer to watch the motion of the liquid meniscus in the glass bulbs A and B, by means of a telescope and a metal filament lamp, the latter being placed above the thermostat. The glass apparatus is placed in the thermostat, with the capillary portion C between the pole-pieces  $P_1$  and  $P_2$ , and only the stop-cocks  $S_1$  and  $S_2$  project above the level of water in the thermostat. The latter also contains a heater H, a toluene thermostat-regulator R, a sensitive relay and a thermometer whose bulb lies above the capillary tube. With vigorous stirring, the temperature fluctuation is found not to exceed  $0^\circ.02$  C. The most accurate measurements are made, when the temperature of the bath is made equal to that of the surrounding air; then

over the period of a series of observations there is no perceptible variation of temperature. Most of the observations are made under this condition.

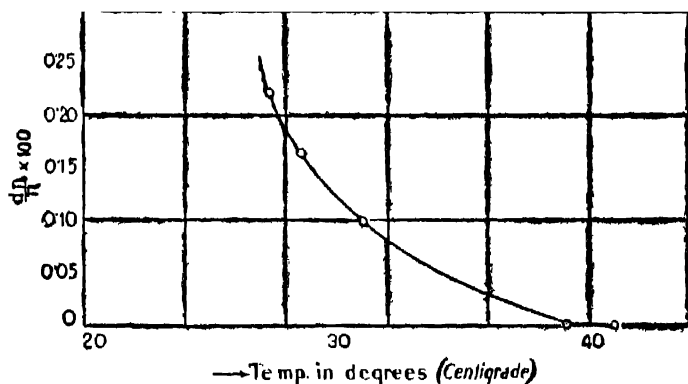
The procedure adopted for taking a set of readings, is as follows: First a set of readings are taken for the time of flow, without putting on the magnetic field. When the steady temperature state is reached, it is found that the consecutive readings do not vary by more than 0.1 sec. in 25 minutes. Then alternate readings are taken with the magnetic field on and off. Though the capacity of the thermostat is about 3 cubic feet, it is found that after taking two readings with the field on, the temperature of the pole-pieces and of the capillary tube rises and the percentage change in the time of flow in the magnetic field begins to diminish. So that in any set of observations, not more than two readings with the magnetic field on, are recorded.

### *Experimental Results.*

In Table I is given the values of the readings taken for the time of flow of nitrobenzene through the given capillary tube,



with and without a magnetic field. This gives an idea of the accuracy with which the time of flow can be observed. The variation of  $d\eta/\eta$  of nitrobenzene with field strength is given in Table II and the graph in Fig. 3. It will be seen that  $d\eta/\eta$  increases directly with  $H$ , and there is no indication of saturation. With a given field strength, the variation of  $d\eta/\eta$  with temperature of the same liquid is shown in Table III and in Fig. 4, apparently  $d\eta/\eta$  becomes zero at about  $35^\circ\text{C}$ . That  $d\eta/\eta$  diminishes with increase of temperature is definite, as the first three readings which were taken with thermostat working at the room temperature on different days indicate. Owing to the difficulty of keeping the temperature of the thermostat constant within the required range, when kept at temperature several degrees higher than the room-temperatures not much value can be attached to the readings taken at  $35^\circ\text{C}$  and  $37^\circ\text{C}$ . Table IV contains the values of  $d\eta/\eta$  for different organic liquids, water, and a solution of cerium nitrate in water, of concentration 0.3 gms. per cc.



Only a limited number of liquids have been tried, but still indications of some regularity in the results appear.

(I) Liquids with long chain aliphatic molecules show a diminution of viscosity in a magnetic field.

(II) Liquids of the aromatic series and an alcohol with side chains show increase of viscosity in a magnetic field. Benzene monochloride seems to be an exception.

(III) Carbon tetrachloride, water and aqueous solution of cerium nitrate show no change in viscosity. The result is to be expected for a non-polar symmetrical liquid like  $\text{CCl}_4$ . Water has a dipole moment but has not a large molecular dimension. Cerium nitrate in aqueous solution shows magnetic birefringence of the same order of magnitude as organic liquids of the aromatic class. Evidently the mechanism of the production of birefringence is different in the case of liquid containing molecules belonging to the aromatic group and in aqueous solutions containing paramagnetic molecules.

TABLE I.

Temperature of the thermostat— $27^\circ\text{C}$ .

H—31 kilo-gauss.

Number of observations.	Field.	Time.
1	off	24 mins. 55.6 secs.
2	off	24 mins. 55.6 secs.
3	off	24 mins. 55.6 secs.
4	on	24 mins. 57.0 secs.
5	off	24 mins. 55.6 secs.
6	on	24 mins. 56.9 secs.
7	off	24 mins. 55.4 secs.

TABLE II.

Relation of  $d\eta/\eta$  with H.

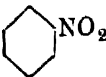

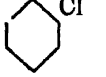
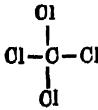
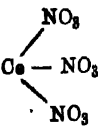
Substance	Temp.	Magnetic field in Gauss.	$d\eta/\eta \times 100$
Nitrobenzene	$27^\circ\text{C}$	13,750	+0.0372
"	"	26,740	+0.0744
"	"	31,700	+0.0879
"	"	34,760	+0.100
"	"	36,400	+0.099

TABLE III.

Thermal variation of  $d\eta/\eta \times 100$ .

Substance	Magnetic field	Temp.	$d\eta/\eta \times 100$
Nitrobenzene	36 K.G.	23°5C	+0.202
"	"	24°6C	+0.160
"	"	27°0	+0.100
"	"	35°C	Inappreciable
"	"	37°C	"

TABLE IV.

Substance	Structural Formula	Temp.	$d\eta/\eta \times 100$
Nitro benzene		27°C	+0.10
Toluene		25.°5C	+0.0703
Benzene monochloride		[29.°5C 26.°30	Zero
Acetone	$\text{CH}_3-\text{CO}-\text{CH}_3$	25.°5C	-0.085
Iso-amyl alcohol	$\text{CH}_3 \begin{smallmatrix} \text{OH}_3 \\ \text{CH}_3 \end{smallmatrix} \text{CH}-\text{CH}_2-\text{CH}_2-\text{OH}$	26.°5C	+0.089
Propyl alcohol (normal)	$\text{CH}_3-\text{CH}_2-\text{CH}_2-\text{OH}$	26.°5C	-0.12
Carbon tetra-chloride		27°C	Zero
Water	$\text{H}-\text{O}-\text{H}$	27°C	Zero
Cerium nitrate solution		27°C	Zero

In conclusion, the authors desire to express their grateful thanks to Prof. D. M. Bose for his suggesting this problem and for his guidance during the progress of the work.

PALIT PHYSICAL LABORATORY,  
UNIVERSITY COLLEGE OF SCIENCE,  
CALCUTTA.

*References.*

- <sup>1</sup> H. Senftleben u. Mitarbeiter; *Ann. d. Physik*, 6, p. 109, (1930);  
*Phys. Zeit.* 30, p. 177 (1932); *Ann. d. Physik*, 16, p. 907 (1933);  
*Phys. Zeit.* 34, p. 834 (1933).
- <sup>2</sup> H. Engelhardt u. H. Sack. *Phys. Zeit.* 33, p. 724 (1932); *Leipziger Vorträge*  
(1933).
- <sup>3</sup> M. Trautz u. E. Fröschel. *Ann. d. Physik*, 22, p. 223 (1935).
- <sup>4</sup> S. W. Chinchalkar, *Ind. Jour. Phys.* 6, p. 580, (1931).
- <sup>5</sup> Haenny, *Compt. Rend.* 194, p. 931 (1931).
- <sup>6</sup> W. König, *Wied. Ann.*, 25, p. 618 (1885).

# Fine Structure Analysis of the Red Bands of Magnesium Oxide and Isotope Effect.

BY

P. C. MAHANTI.

(Received for publication, 5th June, 1935.)

## ABSTRACT.

Measurements of the structure lines in the (0,1), (0,0), (1,0) and (2,0) bands of the red bands of magnesium oxide,  $\text{MgO}$ , are reported. Each band has two strong *P* and *R* branches associated with the main molecule,  $\text{Mg}^{24}\text{O}$ , and in most cases they are accompanied by fainter components which are definitely attributed to the two isotopic molecules,  $\text{Mg}^{25}\text{O}$  and  $\text{Mg}^{26}\text{O}$ . The two main *P* and *R* branches are strictly single and their continuity in the vicinity of the band origin is interrupted by the absence of one line. This structure characterises the system as due to a  $^1\Sigma \rightarrow ^1\Sigma$  transition.

The principal molecular constants evaluated from rotational term differences are as follows:—

Upper  $^1\Sigma$  state.

$$B_e' = 0.7625 \text{ cm.}^{-1}$$

$$B_0' = 0.7594$$

$$B_1' = 0.7538$$

$$B_2' = 0.7470$$

$$\alpha' = 0.0062$$

$$D_e' = -2.62 \times 10^{-6}$$

$$\tau_e' = 1.510 \times 10^{-8} \text{ cm.}$$

$$I_e' = 36.27 \times 10^{-40} \text{ gm. cm.}^2$$

Lower  $^1\Sigma$  state.

$$B_e'' = 0.6852 \text{ cm.}^{-1}$$

$$B_0'' = 0.6815$$

$$B_1'' = 0.6740$$

$$\alpha'' = 0.0075$$

$$D_e'' = -2.57 \times 10^{-6}$$

$$\tau_e'' = 1.543 \times 10^{-8} \text{ cm.}$$

$$I_e'' = 40.36 \times 10^{-40} \text{ gm.cm.}^2$$

*Introduction.*

Two band systems<sup>1</sup> are known for magnesium oxide. Both of them lie in the visible region, one in the green and the other in the red, extending however in the shorter wave-length region as far as  $\lambda 4700$ . The distinctive feature about them is that while the band systems so far known for the other alkaline earth oxides are all degraded to the red, they are shaded towards the violet. Of the two systems the green bands are easily excited while the red bands are not of perceptible intensity in the usual flame surrounding the magnesium arc in air, but become fairly intense in processes where higher temperature is available for excitation. From this observation it would appear that although they lie on the longer wave-length side of the green bands, the energy of excitation of the red bands is much higher than those of the green. This would indicate that the levels involved in the emission of the former are different from those necessary for the appearance of the latter.

In the case of the oxides of beryllium,<sup>2</sup> calcium,<sup>3</sup> strontium,<sup>4</sup> and barium,<sup>5</sup> the rotational structure analysis for at least one of their band systems has been worked out thus enabling one to evaluate their more important molecular constants and to ascertain the nature of electronic states involved in the emission of the band systems. It is, therefore, of interest to study the fine structure of the bands of magnesium oxide with a view to complete our knowledge of the oxides of the alkaline earths and also to investigate the nature of isotope effect of magnesium, which is known to consist of three isotopes of masses 24, 25 and 26 and of relative abundance<sup>6</sup> of about 8 : 1 : 1.

The green system is of the familiar type in which the vibrational frequency and the moment of inertia are only slightly changed by the electron transition. The vibrational intensity distribution is also characteristic of this type resembling that of the green bands of beryllium oxide. It consists of only three



sequences, viz.,  $\Delta v = v' - v'' = 0, \pm 1$ . Of these the zero-sequence is the most intense, while the two others are very weakly developed. In each sequence the successive members are very closely spaced but the interval between their heads increases with increasing  $v', v''$  values since while  $\omega_o' > \omega_o''$ ,  $\omega_o' x_o' < \omega_o'' x_o''$ . Even under the highest dispersion available, the (0,0) band is but partially resolved. Moreover owing to the low intensity of (1,0) and (0,1) bands, it did not seem encouraging to take up the rotational structure analysis of the system under question as one would not get sufficient data for a verification of the combination principle and to arrive at the correct assignment of the rotational quantum numbers to the lines of the (0,0) band.

On the other hand the red system consists of a large number of sequences and the intense bands lie on a wider Condon parabola. They are more open in structure than those of the green system and are thus more suitable for an investigation of their rotational structure. The object of the present investigation is to present the results of such a study. The bands (0,1), (0,0), (1,0), and (2,0) have been chosen for the purpose.

### *Measurements.*

For the purpose of measurement, photographs of the selected bands were taken in the first orders of a 15 ft. and a 21 ft. concave grating set up on Paschen mounting and having dispersions of about 3.55 Å/mm. and 1.25 Å/mm. respectively. To secure the best definition of the structure lines, fine grained panchromatic plates were employed. Several plates were taken for each of the four bands under investigation, the best ones being selected for the final measurement. For each band at least four sets of independent measurements were carried out and in no case the individual measurements differed from one another by more than  $\pm 0.01$  Å. Neon lines and iron arc lines recommended as standards were used for comparison. Reduction

to wave-numbers in vacuo were made with the aid of Kayser's "Tabelle der Schwingungszahlen."

### *The Structure of the Bands.*

In each band the resolution is complete except for a few lines at the head. The bands consist in main of two strong series of lines which are pretty long due to the high temperature of the source. Each of these series is in most cases accompanied by two comparatively fainter series of lines until the next band of the sequence is encountered and is superposed by the branches of the latter. Even then the two main series can be followed very far with certainty as the succeeding bands are very weak in intensity. The analysis given in the next section reveals that while the two strong series are but the *P* and *R* branch lines associated with the main molecule,  $\text{Mg}^{24}\text{O}$ , the fainter series are due to the isotopic molecules  $\text{Mg}^{25}\text{O}$  and  $\text{Mg}^{26}\text{O}$ .

### *Analysis of Band Structure.*

The band heads are single, indicating that the band system is due to a transition between two similar electronic states. There is no sign of splitting into finer components even for the last lines of the two strong series, evidently the *P* and *R* branch lines, found in each band. This indicates that the levels involved are singlets. It also excludes levels with  $\Lambda=1$  as in this case one would expect each line of the series to be a narrow doublet on account of the  $\Lambda$ -type doubling of each rotational energy level in both electronic states. Further no lines, which could be associated even with a short  $\tilde{Q}$  branch, are observed in any of the bands investigated, thus showing that only the levels with  $\Lambda=0$  are responsible for the emission of the band system. It may here be pointed out that the theoretical intensities to be expected in transition between two singlet electronic levels

both of which have the same value of  $\Lambda$  are given by the equations.

$$i_{Q(K)} = \frac{a(2K+1)\Lambda^2}{K(K+1)} \quad \dots \quad (1)$$

$$i_{P(K)} = \frac{a(K^2 - \Lambda^2)}{K} \quad \dots \quad (2)$$

$$i_{n(K)} = \frac{a(K+1)^2 - \Lambda^2}{K+1} \quad \dots \quad (3)$$

In these equations the Boltzmann factor has been assumed to be unity. It is readily seen that if  $\Lambda=1$ , *i.e.*, in a  $^1\pi \rightarrow ^1\pi$  transition, the bands should have a weak  $Q$  branch and the intensity of the first  $Q$  line is three times as great as that of the first  $R$  line, while the intensities of the other  $Q$  lines decrease rapidly for higher values of  $K$ . Similarly for  $\Lambda=2$ , *i.e.*, in a  $^1\Delta \rightarrow ^1\Delta$  transition the first  $Q$  line is very much stronger, and the intensities of the other lines decrease less rapidly. These considerations lead one to associate the band system under question to a  $^1\Sigma \rightarrow ^1\Sigma$  transition. Further evidence is secured from the criterion of missing lines, *viz.*, the first line of the  $R$  branch in the (0, 0) band begins definitely from  $K=0$ .

After sorting out the two main series of lines in each band, the next step was the identification of each series and the assignment of quantum numbers to the lines belonging to it. As the bands are degraded towards the shorter wave-length side, the series of lines starting from their heads evidently belong to the  $P$  branch in each case. Proceeding away from the head, one can unerringly identify the neighbouring lines as belonging either to  $P$  or  $R$  branch merely from a visual inspection of their relative intensities except in the regions where the lines of the two series coalesce into one. In many cases lines from the  $P$  and  $R$  branches dispose themselves in a manner as to appear like close

doublets, the doublets becoming single lines as they approach the head. It should, however, be noted that from the relative intensities of these apparent doublets, one can easily distinguish them from what would occur either when the electronic levels are doublets or when the rotational levels possess  $\Lambda$ -type doubling. Thus after identifying the two main  $R$  and  $P$  branches of the bands, it was only a matter of trial to find out the proper combination relationship between them and thereby to arrive at the unique assignment of quantum numbers to the lines of the two series. The correctness of their  $K$ -numbering was further confirmed from the close agreement between the calculated and observed magnitudes of the isotopic displacements of the rotational lines wherever available.

It is well known that the lines of the  $R$  and  $P$  branches are given theoretically by,

$$R(K) = T'(K+1) - T''(K) \quad \dots (4)$$

$$P(K) = T'(K-1) - T''(K) \quad \dots (5)$$

So that,

$$\triangle_2 T'(K) = R(K) - P(K) \quad \dots (6)$$

$$\triangle_2 T''(K) \equiv R(K-1) - P(K+1) \quad (7)$$

According to the combination principle all bands having the same upper vibrational state should yield sets of values of  $\triangle_2 T'(K)$ , which are numerically identical; and similarly all bands having the same lower vibrational state should give identical sets of values of  $\triangle_2 T''(K)$ .

The wave-lengths and wave-numbers of the lines of  $P$  and  $R$  branches of each analysed band due to the main molecule,  $\text{Mg}^{24}\text{O}$ , together with their  $K$ -numbering are given in Tables I-IV.

TABLE I.

*Structure of the (0, 0) band at  $\lambda 6060\cdot31$ .*

K	R		P	
	$\lambda(\text{\AA.})$	$\nu(\text{cm.}^{-1})$	$\lambda(\text{\AA.})$	$\nu(\text{cm.}^{-1})$
0	6057.70	16503.36		
1	57.06	05.10		
2	56.35	07.04		
3	55.58	09.14		
4	54.75	11.40		
5	53.85	13.85		
6	52.89	16.47		
7	51.85	19.31		
8	50.79	22.21		
9	49.73	25.10		
10	48.62	28.13	6060.31	16496.25
11	47.46	31.30	60.25	96.41
12	46.30	34.47	60.20	96.55
13	45.12	37.70	60.13	96.64
14	43.87	41.12	59.98	97.15
15	42.55	44.74	59.77	96.72
16	41.16	48.54	59.48	98.51
17	39.71	52.51	59.19	99.46
18	38.20	56.65	58.72	16500.58
19	36.63	60.96	58.24	01.89
20	34.99	65.46	57.70	03.38
21	33.28	70.16	57.06	05.10
22	31.51	75.02	56.39	06.93
23	29.68	80.04	55.65	08.94
24	27.80	85.22	54.86	11.10
25	25.85	90.58	54.00	13.44

TABLE I (contd.).

K	R		P	
	$\lambda$ (I.A.)	$\nu$ (cm. <sup>-1</sup> )	$\lambda$ (I.A.)	$\nu$ (cm. <sup>-1</sup> )
26	6028·84	16596·12	6053·06	16616·01
27	21·77	16601·82	52·06	18·74
28	19·64	07·70	51·00	21·63
29	17·46	13·71	49·89	24·66
30	15·23	19·87	48·73	27·83
31	12·96	26·15	47·52	31·14
32	10·64	32·57	46·26	34·58
33	08·28	39·10	44·96	38·14
34	05·86	45·80	43·59	41·89
35	03·39	52·65	42·17	45·78
36	00·88	59·62	40·71	49·77
37	5998·33	66·70	39·20	53·91
38	05·73	73·93	37·64	58·19
39	98·08	81·30	36·02	62·63
40	00·37	88·85	34·36	67·19
41	87·62	96·51	32·64	71·81
42	84·82	16704·32	30·85	76·83
43	81·96	12·31	28·99	81·94
44	79·02	20·53	27·07	87·22
45	76·05	28·84	25·10	92·65
46	73·03	37·30	23·08	98·21
47	69·96	45·90	21·02	16603·89
48	66·84	54·66	18·90	09·74
49	63·67	63·57	16·72	15·76
50	60·45	72·62	14·47	21·97
51	57·18	81·83	12·18	28·30
52	53·85	91·21	09·87	34·79
53	50·46	16800·78	07·41	41·51

TABLE I (contd.).

K	R		P	
	$\lambda$ (I.A.)	$\nu$ (cm. <sup>-1</sup> )	$\lambda$ (I.A.)	$\nu$ (cm. <sup>-1</sup> )
54	5947.01	16810.53	6004.93	16648.38
55	43.52	20.40	02.40	55.40
56	39.98	30.42	5999.81	62.69
57	36.39	40.60	97.17	69.92
58	32.75	50.93	94.47	77.43
59	5929.05	61.45	91.70	85.14
60	25.29	72.15	88.87	93.03
61	21.48	83.00	85.99	16701.06
62	17.64	93.96	83.05	09.27
63	13.76	16905.04	80.06	17.62
64	09.83	16.28	77.05	26.04
65	05.88	27.60	74.00	34.58
66	01.88	39.07	70.90	43.27
67	5897.82	50.73	67.72	52.19
68	93.69	62.61	64.52	61.18
69	89.49	74.70	61.19	70.54
70	85.24	86.96	57.84	79.97
71	80.95	99.35		
72	76.62	17011.88		
73	72.25	24.54		
74	67.34	37.34		
75	63.39	50.27		
76	58.90	63.33		

TABLE II.

*Structure of the (0,1) band at  $\lambda$  6311.65.*

K	R		P	
	$\lambda$ (Å.)	$\nu$ (cm. <sup>-1</sup> )	$\lambda$ (Å.)	$\nu$ (cm. <sup>-1</sup> )
5	...	...	6311.65	15899.35
6	...	...	11.38	40.03
7	...	...	11.10	40.73
8	...	...	10.78	41.53
9	...	...	10.42	42.43
10	...	...	10.04	43.39
11	...	...	09.69	44.42
12	...	...	09.18	45.55
13	...	...	08.70	46.75
14	...	...	08.17	48.09
15	6268.95	15896.62	07.60	49.52
16	87.14	15901.10	06.98	51.08
17	85.28	05.80	06.31	52.76
18	83.36	10.66	05.58	54.60
19	81.38	15.68	04.78	56.61
20	79.35	20.82	03.93	58.74
21	77.27	26.10	03.03	61.01
22	75.14	31.50	02.08	63.40
23	72.95	37.07	01.06	65.97
24	70.70	42.78	6209.98	68.69
25	68.40	48.63	98.85	71.53
26	66.04	54.64	97.56	74.53
27	63.62	60.80	96.40	77.71
28	61.12	67.15	95.07	81.07
29	58.57	73.69	93.66	84.62
30	55.93	80.42	92.18	88.36



TABLE II (*contd.*).

K	R		P	
	$\lambda$ (I.-A.)	$\nu$ (cm. <sup>-1</sup> )	$\lambda$ (I.-A.)	$\nu$ (cm. <sup>-1</sup> )
31	6253.23	15987.32	6290.62	15892.30
32	50.46	94.41	88.99	96.42
33	47.63	16001.65	87.30	15900.69
34	44.75	09.03	85.55	05.13
35	41.81	16.57	83.74	09.70
36	38.80	24.30	81.86	14.46
37	35.73	32.19	79.92	19.38
38	32.62	40.19	77.92	24.45
39	29.46	48.32	75.87	29.65
40	26.25	56.60	73.76	35.01
41	22.97	65.06	71.59	40.52
42	19.63	73.69	69.35	46.22
43	16.24	82.45	67.05	52.07
44	12.78	91.41	64.69	58.08
45	09.27	16100.51	62.26	64.27
46	06.70	09.77	59.76	70.64
47	02.07	19.20	57.20	77.18
48	6198.39	28.77	54.58	83.87
49	94.65	38.51	51.90	90.72
50	90.84	48.44	49.15	97.76
51	86.97	58.54	46.33	16004.98
52	83.04	68.81	43.44	12.39
53	79.06	79.23	40.50	19.94
54	75.02	89.81	37.49	27.66
55	70.93	16200.54	43.04	35.53
56	66.79	11.42	31.30	43.59
57	62.59	22.47	28.11	51.80
58	58.34	33.66	24.87	60.16

TABLE II (*contd.*).

K	R		P	
	$\lambda$ (I. A.)	$\nu$ (cm. <sup>-1</sup> )	$\lambda$ (I. A.)	$\nu$ (cm. <sup>-1</sup> )
59	6154.04	16245.00	6221.57	16068.68
60	49.69	56.50	18.21	77.36
61	45.29	68.14	14.79	86.21
62	40.86	79.87	11.30	95.25
63	36.40	91.70	07.78	16104.37
64	31.85	16303.79	04.23	13.59
65	27.30	15.90	00.64	22.92
66	22.67	28.23	6196.95	32.52
67	17.98	40.75	93.23	42.21
68	13.26	53.37	89.46	52.14
69	08.47	66.19	85.57	62.20
70	03.60	79.25	81.64	72.47
71	6098.70	92.41	77.64	82.94
72	93.72	16405.81	73.57	93.61
73	88.70	19.33	69.47	16204.38
74	83.62	33.04	65.30	15.33
75	78.50	46.88	61.07	26.47
76	73.29	60.99	56.74	37.88
77	68.08	75.13	52.40	49.33
78	62.80	89.47	47.98	61.02
79	57.48	16503.96	43.52	72.82
80	52.11	18.60 •	...	...

TABLE III.

*Structure of the (1, 0) band at  $\lambda$  5775.25.*

K	R		P	
	$\lambda$ (Å.)	$\nu$ (cm. <sup>-1</sup> )	$\lambda$ (Å.)	$\nu$ (cm. <sup>-1</sup> )
10	...	...	5775.25	17310.48
11	...	...	75.00	11.23
12	...	...	74.72	12.07
13	...	...	74.41	13.00
14	5759.41	17358.09	74.08	13.99
15	58.09	62.06	73.73	15.04
16	56.73	66.17	73.35	16.18
17	55.39	70.21	72.94	17.41
18	54.00	74.41	72.49	18.76
19	52.60	78.64	72.05	20.08
20	51.17	82.96	71.57	21.52
21	49.70	87.40	71.06	23.05
22	48.19	91.97	70.54	24.61
23	46.64	96.66	69.97	26.32
24	45.07	17401.42	69.35	28.18
25	43.45	06.32	68.65	30.28
26	41.77	11.42	67.94	32.42
27	40.04	16.66	67.21	34.61
28	38.26	22.07	66.42	36.99
29	36.43	27.62	65.57	39.54
30	34.55	33.34	64.67	42.25
31	32.61	39.24	63.73	45.08
32	30.62	45.29	62.73	48.09
33	28.59	51.47	61.68	51.25
34	26.48	57.90	60.56	54.62
35	24.35	64.40	59.41	58.09

TABLE III (contd.).

K	R		P	
	$\lambda(\text{\AA.})$	$\nu(\text{cm.}^{-1})$	$\lambda(\text{\AA.})$	$\nu(\text{cm.}^{-1})$
36	5722.16	17471.08	5758.18	17361.80
37	19.94	77.86	56.89	65.69
38	17.67	84.80	55.57	69.67
39	15.35	91.90	54.20	73.80
40	12.99	99.12	52.78	78.09
41	10.59	17506.48	51.30	82.56
42	08.14	13.90	49.78	87.16
43	05.63	21.70	48.19	91.97
44	03.05	29.62	46.54	96.96
45	00.45	37.62	44.82	17402.17
46	5697.83	45.68	43.07	07.48
47	95.18	53.85	41.29	12.87
48	92.47	62.20	39.48	18.36
49	89.70	70.76	37.62	24.01
50	86.89	79.44	35.70	29.84
51	84.04	88.25	33.74	35.80
52	81.16	97.17	31.74	41.88
53	78.25	17606.19	29.72	48.03
54	75.27	15.43	27.63	54.40
55	72.25	24.81	25.48	60.95
56	69.18	34.35	23.25	67.75
57	66.08	44.00	20.99	74.65
58	62.95	53.76	18.72	81.59
59	59.77	63.67	16.40	88.69
60	56.57	73.67	14.02	95.97
61	53.32	83.88	11.61	17503.85
62	50.01	94.19	09.15	10.89

TABLE III (contd.).

K	R		P	
	$\lambda(\text{\AA.})$	$\nu(\text{cm.}^{-1})$	$\lambda(\text{\AA.})$	$\nu(\text{cm.}^{-1})$
63	5546.66	17704.68	5606.66	1718.53
64	43.27	15.32	64.12	26.34
65	39.83	26.12	61.52	34.33
66	36.35	737.07	98.87	542.48
67	32.83	48.15	96.16	50.83
68	29.26	59.40	93.39	59.37
69	25.65	70.80	90.58	68.04
70	22.00	82.34	87.72	76.87
71	18.30	94.05	84.84	85.78
72	14.57	17805.87	...	...
73	10.80	17.84	...	...
74	06.98	29.97	...	...
75	03.12	42.26	...	...
76	5599.24	51.62	...	...
77	95.32	67.13	...	...
78	91.38	79.72	...	...
79	87.40	92.46	...	...
80	83.39	17905.31	...	...
81	79.32	18.37	...	...
82	75.20	31.61	...	...

TABLE IV.

*Structure of the (2, 0) band at  $\lambda$  5518.70.*

K	R		P	
	$\lambda$ (I.A.)	$\nu(\text{cm.}^{-1})$	$\lambda(\text{I.A.})$	$\nu(\text{cm.}^{-1})$ .
14	5505.86	18157.44		
15	04.95	60.44		
16	03.93	63.80	5518.70	18115.19
17	02.88	67.27	18.61	15.49
18	01.78	70.90	18.41	16.14
19	00.63	74.70	18.17	16.93
20	5499.45	78.60	17.88	17.88
21	98.23	82.63	17.55	18.97
22	96.96	86.83	17.19	20.15
23	95.64	91.20	16.78	21.49
24	94.28	95.71	16.32	23.01
25	92.89	10200.31	15.81	24.68
26	91.47	05.02	15.26	26.49
27	90.02	09.82	14.67	28.43
28	88.51	14.73	14.05	30.47
29	87.03	19.75	13.39	32.64
30	85.47	24.93	12.69	34.94
31	83.86	30.28	11.95	37.37
32	82.21	35.77	11.18	39.91
33	80.52	41.39	10.37	42.57
34	78.79	47.15	09.51	45.41
35	77.02	53.05	08.61	48.37
36	75.21	59.08	07.67	51.47
37	73.35	65.29	06.69	54.70
38	71.45	71.63	05.67	58.06

TABLE IV (contd.).

K	R		P	
	$\lambda(\text{\AA.})$	$\nu(\text{cm.}^{-1})$	$\lambda(\text{\AA.})$	$\nu(\text{cm.}^{-1})$
39	5469.53	18278.04	5504.61	18161.56
40	67.58	81.56	03.52	65.16
41	65.59	291.21	02.40	168.8
42	63.56	98.01	01.23	72.72
43	61.48	18304.98	00.02	76.72
44	59.34	12.16	5498.75	80.91
45	57.14	19.54	97.43	85.28
46	54.90	27.06		
47	52.63	34.69		
48	50.32	42.46		
49	47.97	50.37		
50	45.59	58.39		

*Calculation of Molecular Constants.*

The next step was to calculate the rotational constants of the molecule from the combination differences, which are given in Tables V-VIII for the different vibrational states. The mean value of the combination differences,  $\triangle_2 T(K)$ , has been taken in cases where there was more than one datum available for a particular pair of rotational levels. Since the rotational energy of a molecule in a  ${}^1\Sigma$  state is  $T(K)$ , where,

$$T(K) = B_v(K+1) + D_v K^2(K+1)^2 + \quad (8)$$

the combination differences can be expressed thus :

$$\begin{aligned}\triangle_2 T(K) &= T(K+1) - T(K-1) \\ &= 4B_v(K + \tfrac{1}{2}) + 8D_v(K + \tfrac{1}{2})^3 + \dots\end{aligned}\quad (9)$$

where terms small in comparison with  $8D_v(K + \tfrac{1}{2})^3$  are dropped. Both  $B_v$  and  $D_v$  depend upon  $v$  according to the relations

$$\begin{aligned}B_v &= B_e - \alpha(v + \tfrac{1}{2}) \\ &= B_0 - \alpha v \quad \dots \quad \dots \quad \dots \quad \dots\end{aligned}\quad (10)$$

and

$$\begin{aligned}D_v^{\frac{3}{2}} &= D_e + \beta(v + \tfrac{1}{2}) \\ &= D_0 + \beta v \quad \dots \quad \dots \quad \dots \quad \dots\end{aligned}\quad (11)$$

Here  $B_e$  and  $D_e$  are the extrapolated values of  $B_v$  and  $D_v$  corresponding to the non-vibrating molecule.

For each vibrational level, the values of  $\triangle_2 T(K)$  were plotted against  $K$ . It was found that for low values of  $K$  the points lay approximately on a straight line, whose slope gave a good approximation to the value of  $4B_v$  in each case. The approximate value of  $D_v$  was calculated from the theoretical relation,

$$D = 4B^3/\omega^2 \quad (12)$$

Then by successive approximation and repeated trials, values are finally assigned to  $B_v$  and  $D_v$ . The variation of  $D_v$  with  $v$  was of negligible magnitude, so that  $D_e$  was taken equal to  $D_v$ . The final values of the different constants thus evaluated are collected in Table IX.

To ensure the correct valuation of  $B_v$  and  $D_v$  values,  $\triangle_2 T(K)$  values were calculated from equation (2) for each vibrational state. To illustrate their agreements with the observed  $\triangle_2 T(K)$  values, they have been included in Tables V and VII only for the vibrational states  $v'=0$  and  $v''=0$ .



TABLE V.  
*Combination differences,  $\Delta_2 T'(K)$ , in the upper state,*  
 $v=0$ .

K	$\Delta_2 T' (K)$ (Obs.)			$\Delta_2 T' (K)$ (Calc.)	O-C.
	(0, 0)	(0, 1)	Mean		
10	31.88		31.88	31.87	+0.01
11	34.89		34.89	34.90	-0.01
12	37.92		37.92	37.93	-0.01
13	40.96		40.96	40.96	0.00
14	43.97		43.97	43.99	-0.02
15	47.02	47.00	47.01	47.00	+0.01
16	50.03	50.02	50.03	50.03	0.00
17	53.05	53.04	53.05	53.05	0.00
18	56.07	56.06	56.07	56.07	0.00
19	59.07	59.07	59.07	59.08	-0.01
20	62.10	62.08	62.09	62.09	0.00
21	65.06	65.09	65.08	65.10	-0.02
22	68.09	68.10	68.10	68.11	-0.01
23	71.10	71.10	71.10	71.11	-0.01
24	74.12	74.09	74.11	74.11	0.00
25	77.14	77.10	77.12	77.11	+0.01
26	80.11	80.11	80.11	80.11	0.00
27	83.08	83.09	83.09	83.09	0.00
28	86.07	86.08	86.08	86.08	0.00
29	89.05	89.07	89.06	89.07	-0.01
30	92.04	92.06	92.05	92.06	-0.01
31	95.01	95.02	95.02	95.02	0.00
32	97.99	97.99	97.99	98.00	-0.01
33	100.96	100.96	100.96	100.97	-0.01
34	103.91	103.91	103.91	103.94	-0.03
35	106.87	106.87	106.87	106.89	-0.02

TABLE V (*contd.*).

K	$\Delta_2 T' (K)$ (Obs.)			$\Delta_2 T' (K)$ (Calc.)	O - C.
	(0, 0)	(0, 1)	Mean		
36	109.85	109.84	109.85	109.85	0.00
37	112.79	112.81	112.80	112.80	0.00
38	115.74	115.74	115.74	115.75	-0.01
39	118.67	118.67	118.67	118.69	-0.02
40	121.66	121.69	121.68	121.68	0.00
41	124.60	124.64	124.57	124.56	+0.01
42	127.49	127.47	127.48	127.49	-0.01
43	130.37	130.38	130.38	130.40	-0.02
44	133.31	133.33	133.32	133.32	0.00
45	136.19	136.24	136.22	136.24	-0.02
46	139.09	139.13	139.11	139.14	-0.03
47	142.01	142.02	142.02	142.04	-0.02
48	144.92	144.90	144.91	144.93	-0.02
49	147.81	147.79	147.80	147.82	-0.02
50	150.65	150.68	150.67	150.69	-0.02
51	153.53	153.56	153.55	153.57	-0.02
52	156.42	156.42	156.42	156.43	-0.01
53	159.27	159.29	159.28	159.30	-0.02
54	162.15	162.15	162.15	162.16	-0.01
55	165.00	165.01	165.01	165.01	0.00
56	167.83	167.83	167.83	167.84	-0.01
57	170.68	170.67	170.68	170.67	+0.01
58	173.50	173.50	173.50	173.50	0.00
59	176.31	176.32	176.32	176.32	0.00
60	179.12	179.14	179.13	179.13	0.00
61	181.94	181.93	181.94	181.93	+0.01
62	184.69	184.62	184.66	184.73	-0.07

TABLE V. (contd.).

K		$\Delta_2 T' (K)$ (obs.)		$\Delta_2 T' (K)$ (calc.)	O-C
	(0, 0)	(0, 1)	Mean		
63	187.42	187.33	187.38	187.52	-0.14
64	190.24	190.20	190.22	190.30	-0.08
65	193.02	192.98	193.00	193.07	-0.07
66	195.80	195.71	195.76	195.84	-0.08
67	198.54	198.54	198.54	198.59	-0.05
68	201.43	201.23	201.33	201.34	-0.01
69	204.16	203.99	204.08	204.07	+0.01
70	206.99	206.78	206.89	206.80	+0.09
71		209.47	209.47	209.53	-0.06
72		212.20	212.20	212.24	-0.04
73		214.95	214.95	214.94	+0.01
74		217.71	217.71	217.63	+0.08
75		220.41	220.41	220.32	+0.09
76		223.11	223.11	223.00	+0.11
77		225.80	225.80	225.65	+0.15
78		228.45	228.45	228.31	+0.14
79		231.14	231.14	230.96	+0.18

TABLE VI.

Combination difference,  $\Delta_2 T' (K)$ , in the upper state,  
 $v'=1$  and  $v'=2$

K	$\Delta_2 T' (K)$ $v'=1$ (1, 0)	$\Delta_2 T' (K)$ $v'=2$ (2, 0)	K	$\Delta_2 T' (K)$ $v'=1$ (1, 0)	$\Delta_2 T' (K)$ $v'=2$ (2, 0)
14	44.10		17	52.80	51.78
15	47.02		18	55.65	54.76
16	49.99	48.61	19	58.56	57.77

TABLE VI (contd.).

$K$	$\Delta_2 T' (K)$ $v'=1$ (1, 0)	$\Delta_2 T' (K)$ $v'=2$ (2, 0)	$K$	$\Delta_2 T' (K)$ $v'=1$ (1, 0)	$\Delta_2 T' (K)$ $v'=2$ (2, 0)
20	61.44	60.72	46	138.20	
21	64.35	63.66	47	140.98	
22	67.36	66.68	48	143.84	
23	70.34	69.71	49	146.75	
24	73.24	72.70	50	149.60	
25	76.04	75.63	51	152.45	
26	79.00	78.53	52	155.29	
27	82.05	81.39	53	158.16	
28	85.08	84.26	54	161.03	
29	88.08	87.11	55	163.86	
30	91.09	89.99	56	166.60	
31	94.16	92.91	57	169.35	
32	97.20	95.86	58	172.17	
33	100.22	98.82	59	174.98	
34	103.28	100.74	60	177.70	
35	106.31	104.68	61	180.48	
36	109.28	107.61	62	183.30	
37	112.17	110.59	63	186.15	
38	115.13	113.57	64	188.98	
39	118.10	116.48	65	191.79	
40	121.03	119.04	66	194.59	
41	123.92	122.36	67	197.32	
42	126.83	125.29	68	200.08	
43	129.73	128.26	69	202.76	
44	132.66	131.25	70	205.47	
45	135.45	134.26	71	208.27	

TABLE VII.

*Combination differences,  $\Delta_2 T''$  (K), in the lower state,  $v''=0$ .*

K	$\Delta_2 T''$ (K) (obs.)				$\Delta_2 T''$ (K) (calc.)	O-C
	(0,0)	(1,0)	(2,0)	Mean		
9	25.96			25.96	25.88	+0.08
10	28.69			28.69	28.60	+0.09
11	31.58			31.58	31.32	+0.26
12	34.56			34.56	34.04	+0.52
13	37.32			37.32	36.75	+0.57
14	39.98			39.98	39.47	+0.51
15	42.61	41.91	42.25	42.26	42.17	+0.09
16	45.28	44.65	44.95	44.90	44.89	+0.07
17	47.96	47.41	47.66	47.68	47.60	+0.08
18	50.62	50.18	50.34	50.36	50.30	+0.06
19	53.20	52.89	53.02	53.07	53.01	+0.06
20	55.86	55.59	55.73	55.73	55.70	+0.03
21	58.53	58.35	58.45	58.44	58.41	+0.03
22	61.22	61.08	61.14	61.15	61.11	+0.04
23	63.92	63.79	63.82	63.84	63.79	+0.05
24	66.60	66.38	66.52	66.50	66.49	+0.01
25	69.21	69.00	69.22	69.14	69.17	-0.03
26	71.84	71.71	71.88	71.81	71.86	-0.05
27	74.49	74.43	74.55	74.49	74.54	-0.05
28	77.16	77.12	77.18	77.15	77.21	-0.06
29	79.87	79.82	79.79	79.83	79.89	-0.06
30	82.57	82.54	82.38	82.50	82.56	-0.06
31	85.29	85.25	85.02	85.19	85.23	-0.04
32	88.01	87.99	87.71	87.90	87.89	+0.01
33	90.68	90.67	90.36	90.57	90.55	+0.02
34	93.32	93.38	93.02	93.24	93.21	+0.03
35	96.08	96.10	95.68	95.94	95.86	+0.08

TABLE VII (contd.).

K	$\Delta_2 T''$ (K) (obs.)				$\Delta_2 T''$ (K) (calc.)	O-C
	(0,0)	(1,0)	(2,0)	Mean		
36	98.74	98.71	98.35	98.60	98.50	+0.10
37	101.43	101.41	101.02	101.29	101.15	+0.14
38	104.07	104.06	103.73	103.95	103.78	+0.17
39	106.74	106.71	106.47	106.64	106.41	+0.23
40	109.39	109.34	109.19	109.31	109.03	+0.28
41	112.02	111.96	111.84	111.94	111.66	+0.28
42	114.57	114.51	114.49	114.52	114.28	+0.24
43	117.10	117.03	117.10	117.08	116.89	+0.19
44	119.66	119.53	119.70	119.63	119.50	+0.13
45	122.32	122.14		122.23	122.09	+0.14
46	124.95	124.76		124.85	124.69	+0.16
47	127.46	127.32		127.30	127.29	+0.10
48	130.14	129.84		129.99	129.86	+0.13
49	132.69	132.36		132.53	132.45	+0.08
50	135.27	134.96		135.12	135.01	+0.11
51	137.83	137.56		137.70	137.58	+0.12
52	140.32	140.22		140.27	140.14	+0.13
53	142.83	142.77		142.80	142.69	+0.11
54	145.38	145.24		145.31	145.24	+0.07
55	147.94	147.68		147.81	147.77	+0.04
56	150.48	150.16		150.32	150.31	+0.01
57	152.99	152.76		152.88	152.84	+0.04
58	155.46	155.81		155.39	155.35	+0.04
59	157.90	157.79		157.85	157.87	+0.02
60	160.39	160.32		160.36	160.37	-0.01
61	162.88	162.78		162.83	162.87	-0.04
62	165.38	165.80		165.34	165.36	-0.02
63	167.92	167.85		167.89	167.83	+0.06

TABLE VII (contd.).

K	$\Delta_2 T'' (K)$ (obs.).				$\Delta_2 T'' (K)$ (Calc.)	O - C.
	(0, 0)	(1, 0)	(2, 0)	Mean.		
64	170.46	170.35		170.41	170.81	+0.10
65	173.01	172.84		172.98	172.77	+0.16
66	175.41	175.29		175.35	175.23	+0.12
67	177.89	177.70		177.80	177.69	+0.11
68	180.19	180.11		180.15	180.12	+0.08
69	182.64	182.53		182.59	182.56	+0.08
70		185.02		185.02	184.97	+0.05

TABLE VIII.

Combination differences,  $\Delta_2 T''(K)$ , in the lower state,  
 $v'' = 1$ .

K	$\Delta_2 T''(K)$ (0, 1)	K	$\Delta_2 T''(K)$ (0, 1)	K	$\Delta_2 T''(K)$ (0, 1)
16	43.76	27	73.57	38	102.54
17	46.50	28	76.18	39	105.18
18	49.19	29	78.79	40	107.80
19	51.92	30	81.39	41	110.38
20	54.67	31	84.00	42	112.99
21	57.42	32	86.63	43	115.61
22	60.13	33	89.29	44	118.18
23	62.81	34	91.95	45	120.77
24	65.54	35	94.57	46	123.33
25	68.25	36	97.19	47	125.90
26	70.92	37	99.85	48	128.48

TABLE VIII (contd.).

$K$	$\Delta_2''(K)$ (0, 1)	$K$	$\Delta_2 T''(K)$ (0, 1)	$K$	$\Delta_2 T''(K)$ (0, 1)
49	131.01	59	156.30	69	180.90
50	135.53	60	158.79	70	183.25
51	136.05	61	161.25	71	185.64
52	138.60	62	163.77	72	188.03
53	141.15	63	166.28	73	190.48
54	143.70	64	168.78	74	192.80
55	146.23	65	171.27	75	195.16
56	148.74	66	173.69	76	197.55
57	151.26	67	176.09	77	199.97
58	153.79	68	178.55	78	202.31

TABLE IX.

*Rotational Constants.*Upper  ${}^1\Sigma$  state.

$$B_e' = 0.7625 \text{ cm}^{-1}.$$

$$B_0' = 0.7594$$

$$B_1' = 0.7538$$

$$B_2' = 0.7470$$

$$\alpha' = 0.0062$$

$$D_e' = -0.262 \times 10^{-6}$$

$$r_e' = 1.510 \times 10^{-8} \text{ cm.}$$

$$I_e' = 36.27 \times 10^{-40} \text{ gm. cm.}^2$$

Lower  ${}^1\Sigma$  state.

$$B_e'' = 0.6852 \text{ cm}^{-1}.$$

$$B_0'' = 0.6815$$

$$B_1'' = 0.6740$$

$$\alpha'' = 0.0075$$

$$D_e'' = -2.57 \times 10^{-6}$$

$$r_e'' = 1.593 \times 10^{-8} \text{ cm.}$$

$$I_e'' = 40.36 \times 10^{-40} \text{ gm. cm.}^2$$

*Isotope Effect.*

The theory of the isotope separations in band spectra was developed for vibration-rotation bands by Loomis<sup>7</sup> and by Kratzer.<sup>8</sup> The first evidence of the isotope effect was found by them in Ime's data on the infra-red spectrum of HCl. Later



on, Mulliken<sup>9</sup> worked out in detail the theory of isotopic separations for electronic bands and obtained confirmation of the theoretically predicted effects in the band systems of several diatomic molecules. Further points in the theory have however been elucidated in recent years chiefly by Gibson,<sup>10</sup> Birge<sup>11</sup> and by Patkowski and Curtis.<sup>12</sup> It may be noted here that in addition to the isotopes whose existence had already been established by Aston by means of the mass spectrograph, rare isotopes notably of O, N, C and H have been discovered by the band-spectrum method.

For magnesium there are three isotopes of masses 24, 25 and 26 in order of abundance 8 : 1 : 1. Their effects in band spectra have been detected by Watson and Rudnick<sup>13</sup> in the green system of MgH and by Pearse<sup>14</sup> in the ultra-violet bands of MgH<sup>+</sup>. Considering the relative masses of oxygen and magnesium atoms the band systems of magnesium oxide may reasonably be expected to bring out the effects of magnesium isotopes more favourably.

It is well known that in the spectrum of a mixture of two or more isotopic molecules the bands of the less abundant ones are similar to, but displaced from, the weaker than those of more abundant molecule. The lines of the latter are adopted as points of reference on account of their intensity and being more easily measurable. Using the notation suggested by Birge in which the corresponding quantities for two isotopic molecules are distinguished by affixing a superscript 'i' to all symbols for the less abundant molecule and keeping those for more abundant unaltered, we have the isotopic displacement of a line in an electronic band ( $\nu'$ ,  $\nu''$ ) given by

$$\nu^i - \nu = (\nu_e^i - \nu_e) + (\nu_v^i - \nu_v) + \nu^i - \nu_r \quad (13)$$

For practical purposes, the electronic isotope displacement may be left out of account owing to its negligibly small magnitude. The exact expression for the vibrational isotope displacement is given approximately by

$$\nu_v^t - \nu_v \equiv (\rho - 1) \left\{ \omega_e' (v' + \frac{1}{2}) - \omega_e'' (v'' + \frac{1}{2}) \right\} \\ - (\rho^2 - 1) \left\{ x_e' \omega_e' (v' + \frac{1}{2})^2 - x_e'' \omega_e'' (v'' + \frac{1}{2})^2 \right\} + \dots \quad (14)$$

It is evident from the above equation that the vibrational isotopic displacement is constant for all lines of a given band. But it increases in magnitude from band to band of a system almost linearly with the interval,  $\nu_v$ , from the system origin,  $\nu_o$ , to the band origin and extrapolates to zero at the system origin. It would therefore be zero in any band whose origin happens to coincide with the system origin but it is not zero in the (0,0) band.

The rotational isotope displacement is approximately given by

$$\nu_r' - \nu_r = (\rho^2 - 1) \times \begin{array}{ccccccc} \text{the wave-number interval between the} \\ \text{line, whose isotope shift is to be calculated and the band origin,} \\ \nu_o & \dots & \dots & \dots & \dots & \dots & \dots \end{array} \quad (15)$$

It is also evident from equation (15) that the rotational displacement vanishes at the band origin.

Thus for any line of a given band the observed isotopic displacement is the algebraic sum of the constant vibrational and the varying rotational displacement given respectively by equations (14) and (15). If there are more than two isotopes, we may expect as many components of the band lines as there are isotopes, whose relative masses determine the positions of the corresponding lines in the spectrum. It may here be noted that in the preceding expressions,  $\rho$  is given by

$$\rho = \sqrt{\mu/\mu'} \quad \dots \quad \dots \quad \dots \quad (16)$$

where  $\mu$  is the reduced or effective mass of the molecule so that if  $M_1$  stands for the mass of the isotopic atom and  $M_2$  for the non-isotopic atom, we have

$$\mu = \frac{M_1 M_2}{M_1 + M_2} \quad \text{and} \quad \mu' = \frac{M_1' M_2}{M_1' + M_2} \quad \dots \quad (17)$$

For the bands under consideration, if we assume that the lines associated with the rare isotopes of oxygen would be too faint to be observed, we can treat the oxygen atom as non-isotopic, so that taking  $\text{Mg}^{24}$  as the main isotope of magnesium, we have

	$\text{Mg}^{25}\text{O}$	$\text{Mg}^{26}\text{O}$
$\rho - 1$	-0.00803	-0.01552
$\rho^2 - 1$	-0.01600	-0.03080

Using these values of  $(\rho - 1)$  and  $(\rho^2 - 1)$  together with the calculated origins of the bands analysed, the isotopic displacements for each stronger line are calculated by means of equations (14) and (15). Fainter series of lines due to the less abundant molecules  $\text{Mg}^{25}\text{O}$  and  $\text{Mg}^{26}\text{O}$  were found in most cases in their calculated positions within the errors of measurement. Definite evidence of their presence was secured by accounting for the lines which lie in the region not superposed by the lines of the succeeding band and which are not included in the two main *P* and *R* branches. The data for the (0,0) band are given in Table I to illustrate the agreement between the calculated and observed positions of the lines of the less abundant molecules. This establishes further the correctness of the *K*-numbering of the lines of the different bands in addition to confirming the identity of their emitter.

TABLE X.  
Isotope Effect in  $(0, 0)$  band.  
*R*-branch lines.

K	Mg <sup>25</sup> O			Mg <sup>26</sup> O		
	$R' (K)$	$\Delta\nu$ (obs.)	$\Delta\nu$ (calc.)	$R' (K)$	$\Delta\nu$ (obs.)	$\Delta\nu$ (calc.)
9	16524.66	0.44	0.35	16524.96	0.74	0.68
10	27.83	0.30	0.40	27.40	0.79	0.77
11	30.78	0.52	0.45	30.34	0.96	0.87
12	34.01	0.46	0.50	35.57	0.90	0.97
13	37.10	0.60	0.56	36.63	1.07	1.07
14	40.60	0.52	0.61	39.94	1.18	1.17
15	44.10	0.64	0.67	43.39	1.35	1.29
16	47.83	0.71	0.73	47.09	1.45	1.40
17	51.67	0.84	0.79	51.01	1.50	1.52
18	55.78	0.87	0.86	55.01	1.64	1.65
19	59.94	1.02	0.93	59.07	1.89	1.79
20	64.44	1.02	1.00	63.54	1.92	1.92
21	68.97	1.19	1.07	67.96	2.20	2.07
22	73.80	1.22	1.15	...	...	2.22
23	78.78	1.26	1.23	77.65	2.39	2.37
24	83.90	1.32	1.32	82.72	2.50	2.53
25	89.04	1.54	1.40	...	...	2.70
26	94.50	1.62	1.49	...	...	2.87
27	16600.17	1.65	1.58	98.91	2.91	3.04
28	06.07	1.63	1.68	16604.42	3.28	3.22
29	11.05	1.76	1.77	10.29	3.42	3.41
30	17.83	2.04	1.87	(arc line)	...	3.60
31	(arc line)	...	1.97	22.33	3.82	3.79
32	30.46	2.11	2.07	28.67	3.90	3.99
33	36.83	2.27	2.18	34.79	4.31	4.19

TABLE X (*contd.*).

K	Mg <sup>25</sup> O			Mg <sup>26</sup> O		
	R <sup>i</sup> (K)	$\Delta\nu$ (obs.)	$\Delta\nu$ (calc.)	R <sup>i</sup> (K)	$\Delta\nu$ (obs.)	$\Delta\nu$ (calc.)
34	16643.53	2.27	2.28	16641.51	4.29	4.40
35	50.27	2.38	2.39	48.02	4.63	4.61
36	57.09	2.53	2.51	54.79	4.83	4.82
37	64.01	2.69	2.62	61.67	5.09	5.04
38	71.12	2.81	2.73			
39	78.52	2.78	2.85			
40	85.70	3.15	2.97			
41	93.39	3.12	3.10			
42	16701.06	3.26	3.22			
43	08.85	3.46	3.35			
44	17.06	3.47	3.48			
45	25.20	3.64	3.61			
46	33.40	3.90	3.75			
47	42.09	3.81	3.89			
48	50.59	4.07	4.03			
49	59.43	4.14	4.17			
50	68.23	4.39	4.31			
51	77.41	4.42	4.46			
52	86.59	4.52	4.61			
53	96.15	4.63	4.76			
54	16805.53	5.00	4.92			
55	15.14	5.26	5.08			

TABLE X (contd.).  
P-branch lines.

K	Mg <sup>25</sup> O			Mg <sup>26</sup> O		
	P <sup>1</sup> (K)	$\Delta\nu$ (obs.)	$\Delta\nu$ (calc.)	P <sup>1</sup> (K)	$\Delta\nu$ (obs.)	$\Delta\nu^{\dagger}$ (calc.)
29	16524.36	0.30	0.35	16523.08	0.68	0.67
30	27.40	0.43	0.40	26.98	0.85	0.76
31	30.78	0.36	0.45	30.34	0.80	0.87
32	34.01	0.57	0.51	33.57	1.01	0.97
33	87.70	0.44	0.56	37.10	1.04	1.08
34	41.12	0.77	0.62	40.60	1.20	1.20
35	45.01	0.77	0.68	44.59	1.20	1.32
36	49.01	0.76	0.75	48.24	1.53	1.44
37	53.09	0.82	0.81	52.27	1.64	1.57
38	57.17	1.02	0.88	56.44	1.75	1.70
39	61.67	0.96	0.95	60.96	1.67	1.84
40	66.12	1.07	1.03	65.19	2.00	1.98
41	...	...	1.10	69.64	2.27	2.12

The author acknowledges his gratefulness to Prof. P. N. Ghosh for offering all facilities to carry out this investigation.

#### REFERENCES.

- (1) P. C. Mahanti, Phys. Rev., 42, 609 (1932).
- (2) E. Bengtsson, Ark. f. Math., Astr. Och. Fys., 20A, 28 (1928).  
J. E. Rosenthal and F. A. Jenkins, Phys. Rev., 33, 163 (1929).  
L. Herzberg, Frankfurter Dissertation; Zeits. f. Physik, 84, 571 (1933).
- (3) K. Mahla, Erlangener Dissertation; Zeits. f. Physik, 81, 625 (1933).
- (4) P. H. Brodersen, Zeits. f. Physik, 79, 613 (1932).
- (5) P. C. Mahanti, Proc. Phys. Soc., 46, 51 (1934).
- (6) F. W. Aston, Mass Spectra and Isotopes, p. 236 (1933).
- (7) F. W. Loomis, Astrophys. Jour., 52, 248 (1920).
- (8) A. Krutzer, Zeits. f. Physik, 3, 460 (1920).
- (9) R. S. Mulliken, Phys. Rev. 25, 119 (1925).
- (10) G. E. Gibson, Zeits. f. Physik., 60, 692 (1933).
- (11) R. T. Birge, Trans. Far. Soc., 25, 718 (1929).
- (12) J. Patkowski and W. E. Curtis, Trans. Far. Soc., 25, 725 (1929).
- (13) W. W. Watson and P. Rudnick, Phys. Rev., 29, 413 (1927).
- (14) R. W. B. Pearse, Proc. Roy. Soc., 125, 157 (1929).

# On the Measurement of Quantity of Light by the Photo-Electric Cell.

By

D. V. GOGATE AND D. S. KOTHARI.

(Received for publication, 4th June, 1935.)

The application of the photo-electric cell in the measurement of intensity of light is well-known. The present paper deals with the use of the cell for the determination of the quantity of light. These two uses of the photo-electric cell correspond to the use of a galvanometer for measuring current and quantity of electricity respectively.

If a source of candle power (C.P.) be placed at a distance  $r$  from a cell of area  $A$ , the luminous flux received by the cell will be  $\frac{(\text{C.P.})}{r^2}A$  lumens. If this causes a galvanometer deflection of  $\theta$  divisions, then we have,

$$K \frac{(\text{C.P.})}{r^2} A = S_c \theta \quad (1)$$

where  $S_c$  represents the current sensitivity of the galvanometer and  $K$  is a constant.

If light from the source of candle power (C.P.) be allowed to fall on the cell for a time  $\Delta t$ , then,

$$S_q \theta' = K' Q = K' A I \Delta t$$

where  $S_q$  denotes the ballistic sensitivity of the galvanometer,  $\theta'$ , the kick observed,  $Q$ , the quantity and  $I$ , the intensity of light. Therefore,

$$S_q \theta' = K' A \frac{(\text{C.P.})}{r^2} \Delta t \quad \dots \quad (2)$$

The cell used is the Westinghouse Photo-electric cell (Type P.A. I). It consists of a disc of copper oxidised on one side by a special treatment to cuprous oxide.

To test the relation (1) the cell was placed at different distances from a 16 volt 32 watt lamp and the corresponding deflection  $\theta$  in the galvanometer was observed in each case. It was found that  $r^2\theta$  was nearly constant and we obtained for K the value  $7.5 \times 10^{-6}$  amperes per lumen.

The relation (2) was verified by allowing the lamp to fall vertically from different heights in front of the photo-electric cell and noting the corresponding kicks in the galvanometer. For this purpose the lamp was fixed in a thick card-board sheet which was allowed to fall smoothly in a vertical plane distant about 10 cms. from the photo-electric cell by means of pulleys and falling weights. The illumination of the photo-electric cell by the falling lamp is maximum when it is just in front of it, but even when it is a couple of centimetres away from this position, on either side, the cell receives an appreciable amount of light. The "effective value"  $\Delta x$  of this range was determined by plotting a graph between the steady deflection in the galvanometer and the height of the lamp. The area enclosed by this graph divided by the maximum value of the deflection gives the value for  $\Delta x$ . The duration of exposure  $\Delta t$  was then calculated from the relation,

$$\Delta t = \frac{\Delta x}{\sqrt{2fx}}$$

where,  $f$  is the acceleration of the system (lamp, weights, etc.) and  $x$  denotes the height of the lamp from the cell. Thus finally, we have,

$$S_s \theta' = K' A \frac{(\text{C.P.})}{r^2} \cdot \frac{\Delta x}{\sqrt{2fx}} \quad \dots (3)$$

Our experiments gave the value for  $K'$  to be  $6 \times 10^{-6}$  coulombs per lumen-second. From the known properties of the photo-electric cell one should expect this value to agree with the value



of  $K$  in equation (I). Our experiments show that  $K'$  is slightly less than  $K$ .

For these experiments the cell was connected directly to the galvanometer. We now propose to introduce an amplifier in between and then use the cell for measuring the quantity of light in lightening discharge and other similar phenomena.

It may be of interest to note here that the internal resistance of the photo-electric cell, as given by the makers, is 1800 ohms. It is, however, found to vary with the current passing in the cell.\* When the direction of the current is from copper to cuprous oxide (the same as the direction of the photo-electric current),† the resistance is found to increase with the current and varies from about 350 to 1700 ohms. The latter value corresponds to a current of about 1.5 milli-amperes in the cell. On further increase in the current through the cell, its resistance begins to decrease and is unsteady. When the direction of the current in the cell is from cuprous oxide to copper (the same as the direction of the rectified current),† the resistance decreases with increase of current and varies from about 300 to 140 ohms.

PHYSICS LABORATORY,  
UNIVERSITY OF DELHI.

\* The current was always kept less than about two milli-amps. in accordance with the instructions of the manufacturers.

† The direction of the generated current in the photo-electric cell is from copper to cuprous oxide, *i.e.*, opposite to the direction of the rectified current, when the combination  $\text{Cu-Cu}_2\text{O}$  is used as a rectifier.



# On the Absorption Spectra of Some Complex Ions

(Contributions to the Theory of Co-ordinate Linkage VII \*).

By

R. SAMUEL, MOHD. ZAMAN AND A. W. ZUBAIRY.

(Received for publication, 9th May, 1935.)

In continuation of earlier investigations (III and VI) we have measured the absorption spectra of some complex salts, in solutions containing different salts like KCl, KBr. etc., *i.e.*, under the influence of the varying electric fields of the surrounding positive and negative ions. The experimental method was the same as described earlier (I). The absorption coefficient  $k$  is defined by  $I = I_0 \times 10^{-kcd}$ ,  $I_0$  and  $I$  being the intensities of light entering the medium and emerging from the medium,  $c$  and  $d$  standing for concentration of the solution and the thickness of the layer respectively.

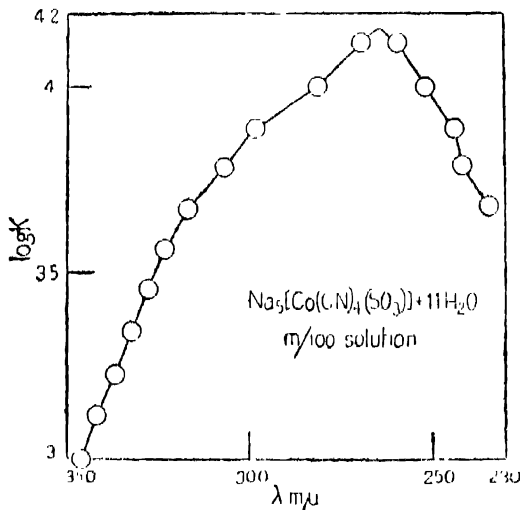


FIG. 1.

\* Earlier papers of this series are : (I) R. Samuel, *Z. Physik*, **70**, 49, 1931; (II) R. Samuel and Advi Rao R. Deshpande, *ibid*, **80**, 395, 1933; (III) R. Samuel, A. Hafiz Khan and Nazir Ahmad, *Z. Physik. Chem. (B)* **22**, 431, 1933; (IV) R. Samuel and Mohd. Jan Khan, *Z. Physik*, **84**, 87, 1933; (V) Must. Karim and R. Samuel, *Bull. Ac. Sc. Unit. Prov. (Allahabad)*, **3**, 157, 1934; (VI) R. Samuel and Mumtaz Uddin, *Trans. Farad. Soc.*, **31**, 423, 1935: Quoted as I, II, etc.

$K_4[Cr (CN)_6]$ . The absorption spectrum was observed in normal solutions of KCl, KBr. and NaCl. The various maxima are represented in Fig. 1 and in the following Table 1, together with those of the solution in water only, measured previously (II).:—

TABLE 1.

	1st maximum		2nd maximum		3rd maximum	
	$\lambda$ (m $\mu$ )	log k	$\lambda$ (m $\mu$ )	log k	$\lambda$ (m $\mu$ )	log k
In water ...	383	2.0	307	2.0	261	3.9
In solutions of NaCl. ..	376	2.0	306	1.9	262	4.0
KCl. ...	376	2.0	307	2.0	265	4.0
KBr. ...	382	2.0	310	1.7	265	3.5

The second and third maxima show a slight variation of wave-length only, but a distinct variation of their log k values in the different solvents; this indicates, as was pointed out earlier (III and VI), a molecular Stark effect. The variation of wave-length of the first maximum, however, is considerably larger, the log k value being almost constant, thus indicating a deformation of the molecule. That is exactly the behaviour as found in the case of other complex cyanides. It has been seen that those maxima which seem to be characteristic for all of them and the only existing ones of the diamagnetic cyanides, show the molecular Stark effect only, whereas those which appear additionally at longer wave-lengths in the paramagnetic cyanides, indicate a deformation of the molecule. It is, however, surprising, that both these effects are similar in the presence of KCl and NaCl, but different in the presence of KBr. In analogy to previous results we expected, that the exchange of the positive ion would be more observable, because positive ions will surround and approach closer the negatively charged complex ion.

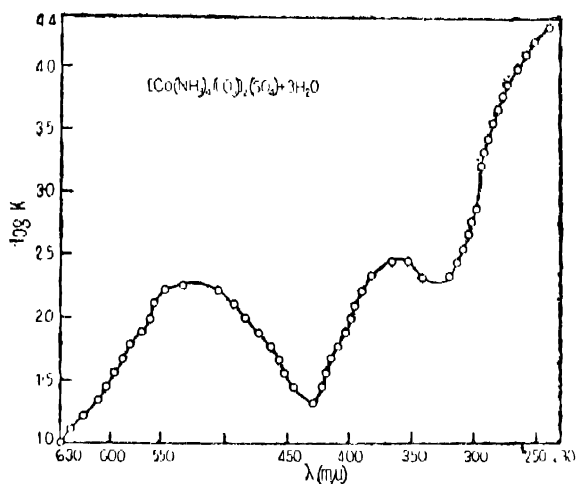


FIG. 2.

$K_2 [Pd (CN)_4]$  (Fig. 2.) In the presence of foreign ions, the absorption maxima are as is often the case more diffuse than in water only. Still, the maximum found in (I) at  $239 m\mu$  ( $\log k = 3.0$ ) appears as a point of inflection of the curve at almost the same wave-length. Also the  $K$  value remains the same in the presence of  $NaCl$  and  $Na_2CO_3$ , but increases to  $\log k = 3.3$  in the presence of  $KCl$ . The absorption curve indicates a molecular Stark effect only, and this is due to the presence of the positive ion.

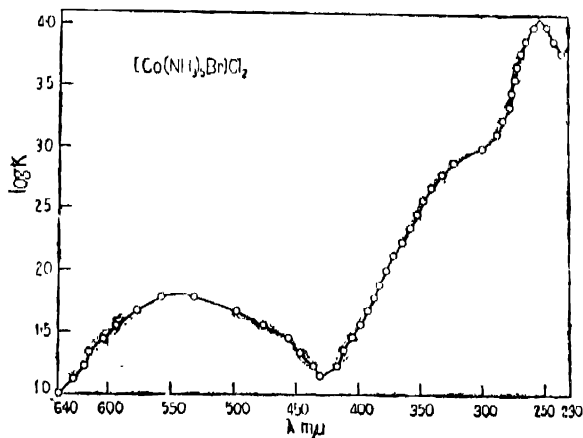


FIG. 3.

K [Cu (CN)<sub>2</sub>] (Fig. 3.). The absorption spectrum of this salt was not previously measured. It shows two maxima which agree fairly well with those three, shown by other diamagnetic cyanides. The third one at short wave-lengths is missing. The results of the measurements in various solvents are as follows :—

TABLE 2.

In solutions of	Maximum I		Maximum II	
	$\lambda$ (m $\mu$ )	log k	$\lambda$ (m $\mu$ )	log k
NaCl ... ..	297	1.8	284	2.0
KCl ... ..	303	1.7	275	1.9
Na <sub>2</sub> CO <sub>3</sub> ... ..	302	1.9	279	2.2

Since the maxima are rather diffuse and mostly shown as inflexions of the curve only their interpretation is more difficult. The salt appears to show a molecular Stark effect only, produced by the presence of positive ions, surrounding the negative complex ion.

Thus it can be seen, that all the cyanides, investigated till now, *i.e.* K<sub>3</sub> [Co (CN)<sub>6</sub>], K<sub>3</sub> [Fe (CN)<sub>6</sub>], K<sub>2</sub> [Ni (CN)<sub>4</sub>] (*cf.* III) K<sub>4</sub> [Cr (CN)<sub>6</sub>], K<sub>2</sub> [Pd (CN)<sub>4</sub>] and K [Cu (CN)<sub>2</sub>] behave very similarly indeed. These measurements indicate, that they represent a type of co-ordination of great stability, probably the most stable type yet known.

The absorption curves of K<sub>2</sub> [Pd Cl<sub>4</sub>], K<sub>2</sub> [Pt Cl<sub>4</sub>], and Na<sub>3</sub> [Rh Cl<sub>6</sub>] underwent a complete change in the presence of bromine but not of chlorine ions (III and IV). Therefore it seemed to be of interest, to extend these measurements to chloroplatinic acid H<sub>2</sub> [Pt Cl<sub>6</sub>]. The results are represented in Fig. 4 and in the following Table 3 :—

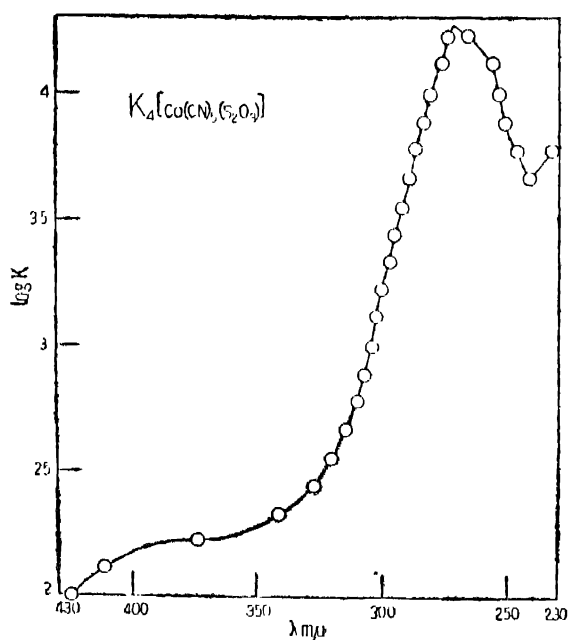


FIG. 4.

TABLE 3.

	Maximum I		Maximum II		Maximum III	
	$\lambda$ (m $\mu$ )	$\log k$	$\lambda$ (m $\mu$ )	$\log k$	$\lambda$ (m $\mu$ )	$\log k$
In water ...	455	1.7	375	2.8	262	4.4
In solution of NaCl. ...	430	1.7	340	2.8	262	4.65
M/10 HCl ...	430	1.7	345	2.8	265	4.65
M/10 H Br ...	430	1.9	340	2.8	262	4.3

The absorption curve remains rather constant, the displacements, which occur, are slight and by no means comparable to those of  $K_2[PtCl_4]$  or  $Na_3[RhCl_6]$ . Wherever distinct variations occur, they are produced again by bromine ions. Furthermore, compared with the values obtained in water only,

TABLE 4.\*

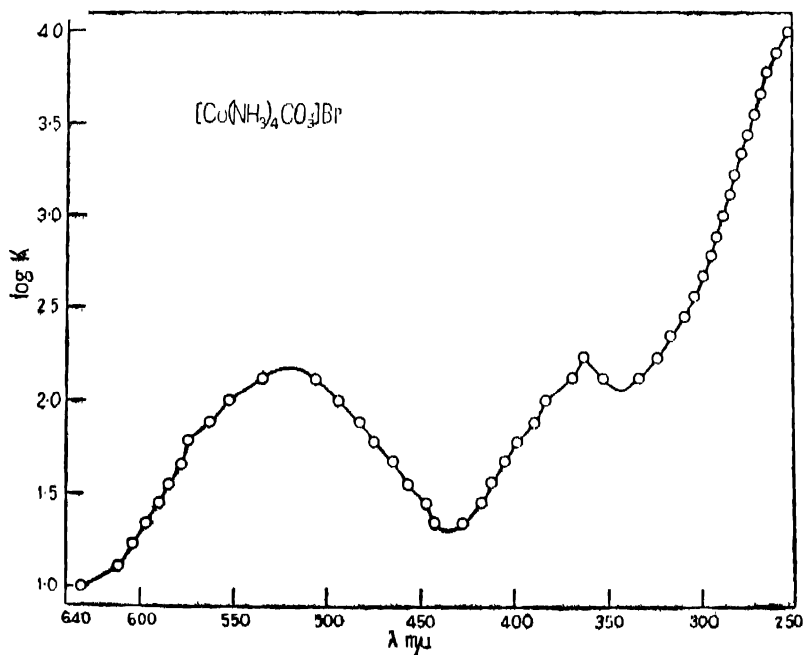
[Co en <sub>3</sub> ] Cl <sub>3</sub> (I) (III)	.....	497	467	434	.....	347	.....
[Co en <sub>3</sub> ] Cl <sub>3</sub> .....	.....	502	468	438	.....	339	.....
[Co (NH <sub>3</sub> ) <sub>5</sub> Cl] Cl <sub>2</sub> (I) (III)	565	528	460	.....	.....	345	(265) (280) (245)
[Co (NH <sub>3</sub> ) <sub>5</sub> Cl] SeO <sub>4</sub>	.....	(545) 512	.....	440	390 360	.....	(265)
[Co (NH <sub>3</sub> ) <sub>5</sub> Br] Cl <sub>2</sub>	616	545	455	.....	.....	320	252
[Co en <sub>2</sub> Cl <sub>2</sub> ] Cl + HCl + H <sub>2</sub> O (crystal)	565	510	.....	.....	.....	.....	.....
[Co (NH <sub>3</sub> ) <sub>4</sub> Cl <sub>2</sub> ] Cl (I)	.....	545 512 492	.....	.....	.....	.....	.....
[Co (NH <sub>3</sub> ) <sub>4</sub> (NO <sub>2</sub> ) <sub>2</sub> ] Cl (I)	.....	.....	490	445	(375)	349	(268) 251
[Co (NH <sub>3</sub> ) <sub>4</sub> (NO <sub>2</sub> ) <sub>2</sub> ] Cl	.....	.....	495	440	390	349	271 252
[Co (NH <sub>3</sub> ) <sub>4</sub> (NO <sub>2</sub> ) <sub>2</sub> ] NO <sub>3</sub>	.....	.....	496	442	.....	347	253.5
[Co (NH <sub>3</sub> ) <sub>4</sub> CO <sub>3</sub> ] Br .....	575	520	451	.....	380 360	.....	.....
[Co (NH <sub>3</sub> ) <sub>4</sub> CO <sub>3</sub> ] NO <sub>3</sub>	568	525	493	.....	392 360	.....	(250)
[Co (NH <sub>3</sub> ) <sub>4</sub> CO <sub>3</sub> ] SO <sub>4</sub>	575	518	462	(408)	359	.....	(260)
N <sub>2</sub> S [Co (CN) <sub>5</sub> (SO <sub>3</sub> ) <sub>2</sub> ]	.....	.....	.....	.....	.....	.....	.....
K <sub>4</sub> [Co (CN) <sub>5</sub> (S <sub>2</sub> O <sub>3</sub> )]	.....	.....	.....	.....	.....	508	264 (244)
K <sub>3</sub> [Co (CN) <sub>5</sub> ] (I) .....	.....	.....	.....	.....	374	.....	281 270 252
N <sub>2</sub> S SO <sub>3</sub>	.....	.....	.....	.....	.....	348 328 309	287 267
N <sub>2</sub> S S <sub>2</sub> O <sub>3</sub>	.....	.....	.....	.....	.....	300	(245)
.....	.....	.....	.....	.....	.....	no selective	absorption.

\* Main maxima in bold figures, subsidiary maxima in ordinary figures, weak or doubtful subsidiary maxima in brackets.  
For the absorption of the sulphite and thiosulphate ions cf. S. M. KARIM and R. SAMUEL, Proc. Ind. Ac. Sci. (Bangalore), 1, 398, 1934.



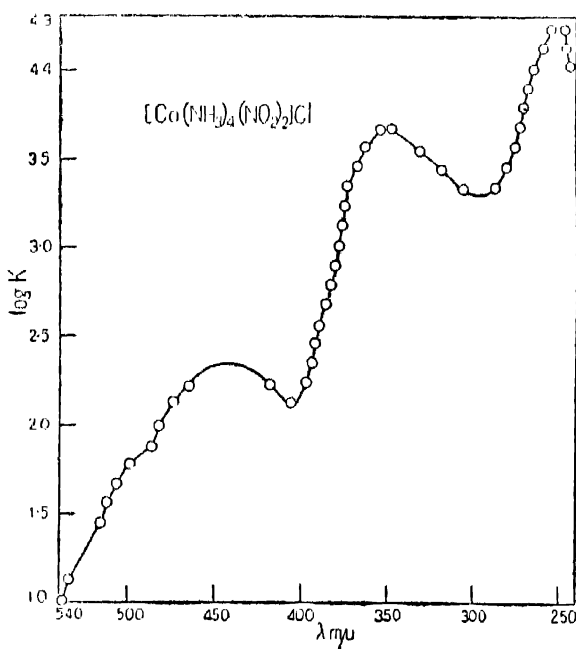
the long wave-length maxima, characteristic for co-ordinated chlorine, show a very considerable shift towards shorter wave-length. Still, the complex  $[\text{Pt Cl}_6]^{2-}$  seems to be, considerably more stable than the other three, mentioned above. Whereas it is doubtful, if  $\text{K}_2 [\text{Pt Cl}_4]$  and  $\text{Na}_3 [\text{Rh Cl}_6]$  form true complex salts, or have to be considered as linked by electrostatic forces as  $(\text{Pt Cl}_2 + 2 \text{KCl})$ , etc., the chloroplatinic acid seems to belong to the same class of genuine complex salts as the hexammines or hexacyanides formed by the trivalent cobaltium ion.

We have further measured the absorption curve of a number of complex salts in water. Most of them have not been measured previously and a few of them have been repeated, for in (I) a quartz spectrograph only was used and the data for the visible region required confirmation by an instrument with higher resolving power. In these measurements a grating spectrograph with a dispersion of about 40 AU per mm. was

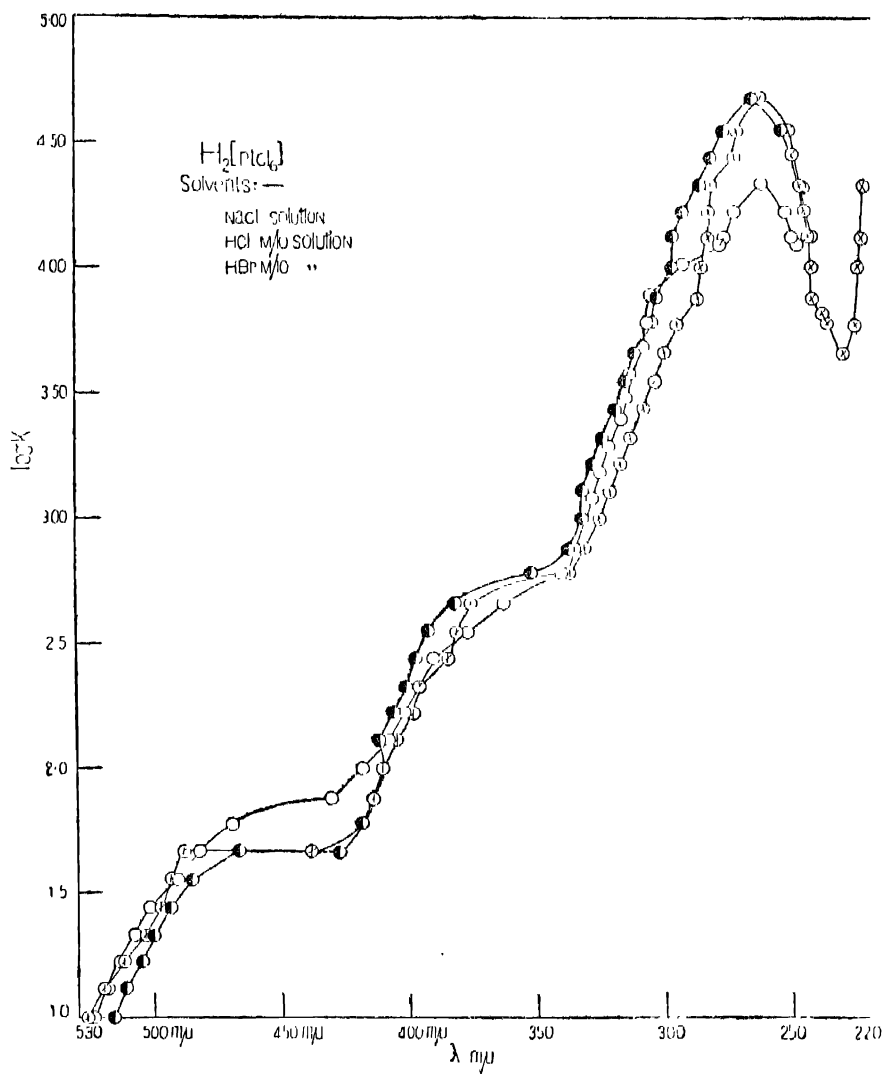


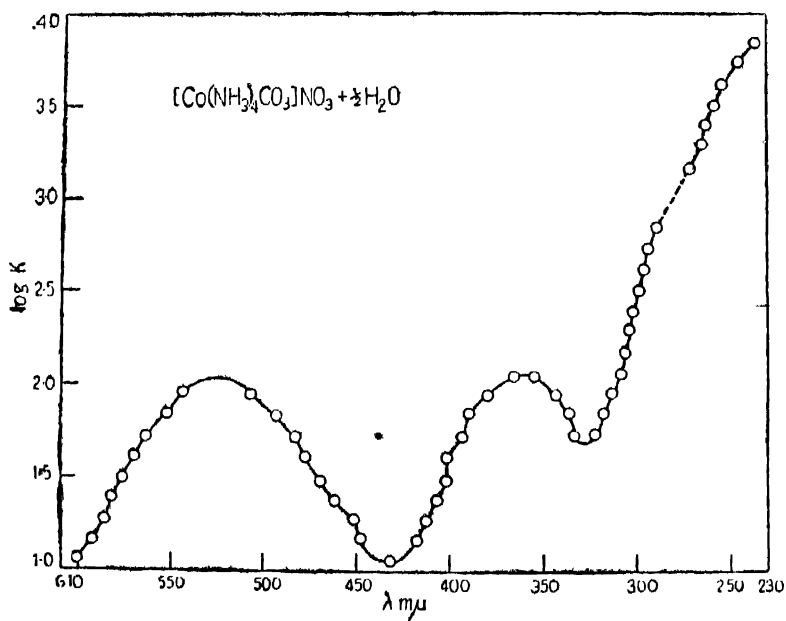
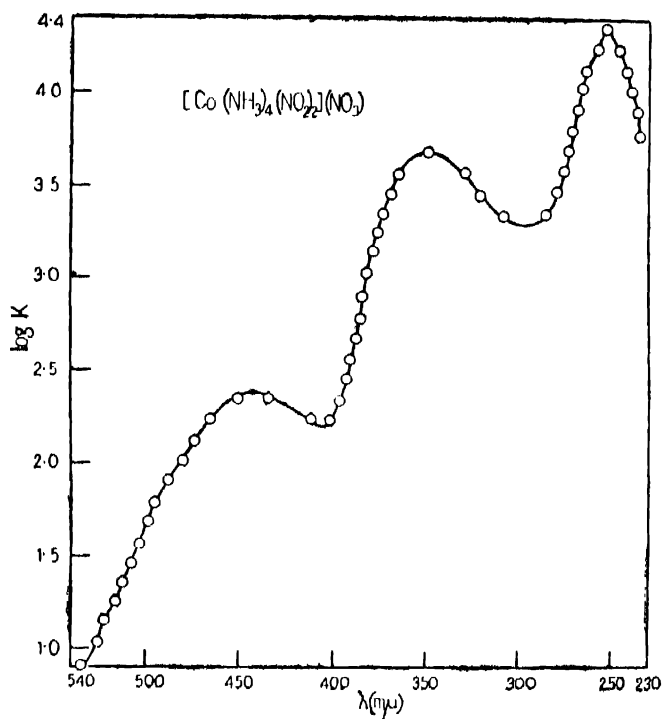
used.<sup>1</sup> The results are given in the following diagrams 5 to 13 and in Table 4 where we have added certain figures of previous papers for the sake of comparison. The visible absorption band of praseo  $[\text{Co en}_2 \text{Cl}_2]\text{Cl}$  was remeasured in the solid state with the help of a recording photometer.

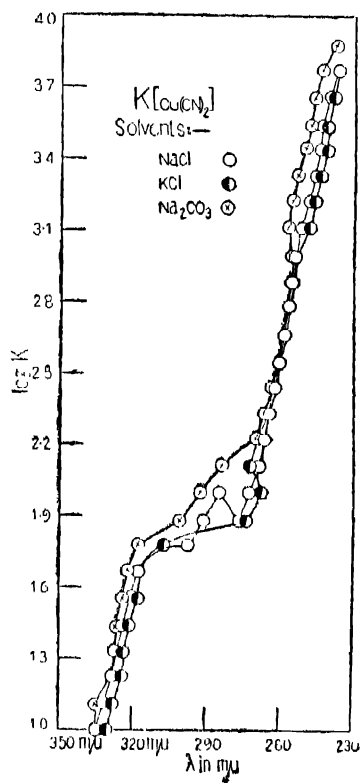
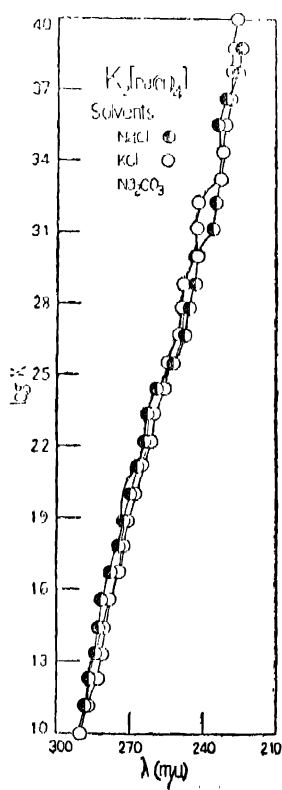
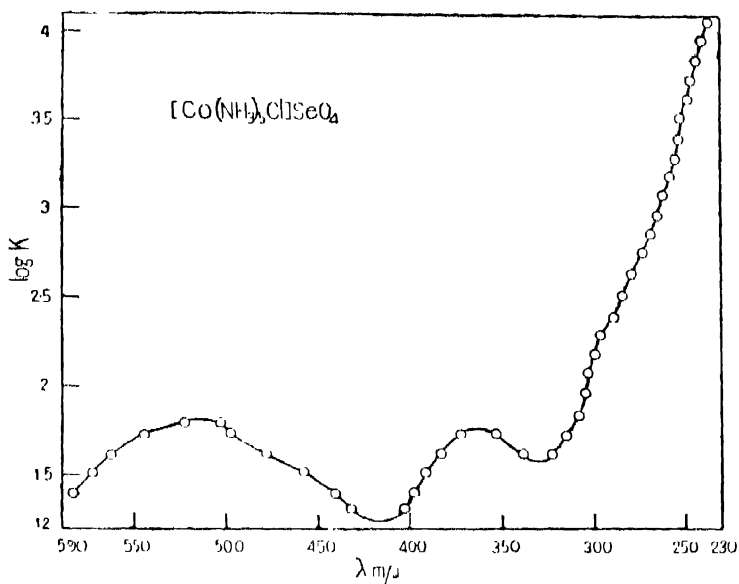
We consider at first a number of salts for which the complex remains the same whereas the ions of the second sphere are changed. Since the addition of foreign ions to the solution produces certain changes in the absorption curve, the exchange of the ions of the second sphere should give similar even if smaller displacements, since the surrounding ions are different.

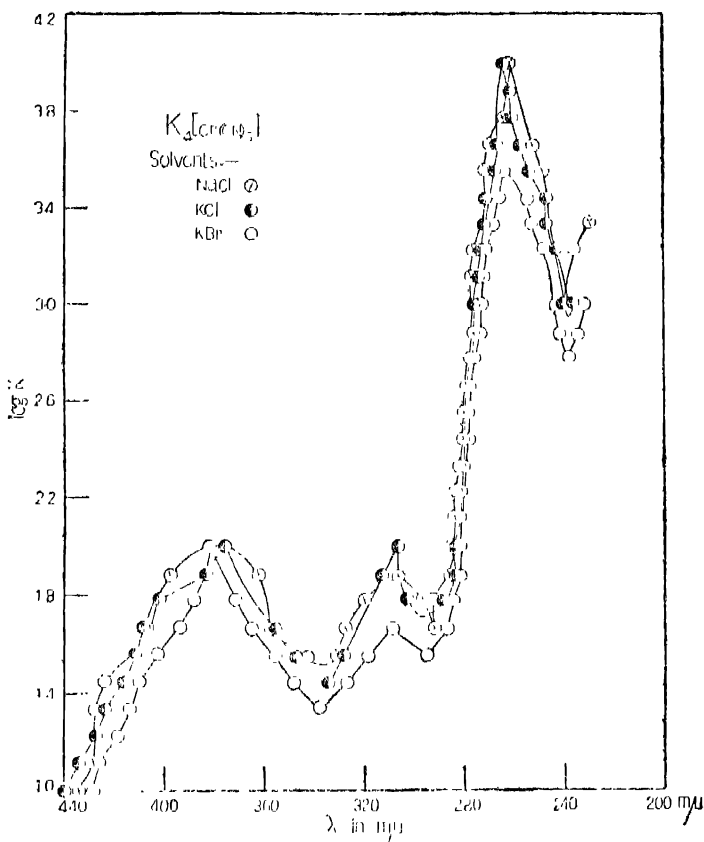


<sup>1</sup> F. W. Beyer (Zs. f. Phys. 1933, 83, 806) tries to improve on some of the measurements in the first paper of this series. He has overlooked that the data for the visible region are clearly characterised as temporary, because only a quartz spectrograph with low dispersion in the yellowgreen region was at our disposal. (cf. I page 46). The first measurements with a glass spectrograph, published simultaneously with his paper (cf. III) agree indeed as regard to the main maximum with his controlling measurements by means of a Koenig—Martens photometer at least as well as his own. The reference of Luther and Niclopolar Zs. Phys. Chem. 82, 361 1913, was not quoted in (I) since the article of H. Ley, Handb. d. Phys. XXI was given as general reference of all previous work. According to the tables in the Beyer's paper a comparison of the wavelengths of the main maxima of the two salts measured by him gives the following results:—









Indeed the maxima of  $[Co(NH_3)_6Cl]Cl_2$  and  $[Co(NH_3)_5Cl]SeO_4$ , of  $[Co(NH_3)_4(NO_2)_2]Cl$  and  $[Co(NH_3)_4(NO_2)_2]N(O)^3$  and of  $[Co(NH_3)_4CO_3]Br$ ,  $[Co(NH_3)_4CO_3]NO_3$ , and  $[Co(NH_3)_4CO_3]_2(SO_4)$  show different values, the differences being mostly very slight, but sometimes quite remarkable. It is noticeable, that the shift of the absorption curves does not run in the same

		$[Co(NH_3)_6]Cl_3$	$[Coen_3]Cl_3$
Beyer (Koenig-Martens)	...	481.1 mμ	467.9 mμ
Beyer (new photographic method)	..	473.8 mμ	477.4 mμ
Samuel & Collaborators (III)	..	482 mμ	467 mμ

There seems to be no reason to assume, that his new method is in any way more accurate than ours.

sense for the various maxima. The position of the first maximum of the chloro-pentammino complex shifts towards shorter wave-lengths, if the chloride and the selenate are compared ; the ultra-violet maximum, however, shifts in the opposite sense. The same holds good in the other cases, indicating, that the two maxima might correspond to different parts of the molecule with different polarity. In any case it is clear that also the ions of the second sphere are not without influence on the absorption curve and since in certain conditions even a slight shift of wave-length will produce a great difference of colour, this accounts for certain well-known changes of colour of apparently closely connected salts. The difference between solution and crystal seems to be very slight only.

Naturally the effect is more distinct, when changes take place inside the complex proper, *i.e.*, inside the first sphere of the molecule, as it is shown by the exchange of chlorine against the bromine ion in the pentammine complex. This exchange shifts the first maximum considerably towards the red. The maximum lies at about  $470\text{ m}\mu$ , if no halogen ion is present, at about  $510$  to  $520\text{ m}\mu$  when one or two chlorine ions are linked in the first sphere and at  $545\text{ m}\mu$  if the chlorine ion is replaced by a bromine ion. The subsidiary maximum at the long wave side is displaced even more, *i.e.*, to  $618\text{ m}\mu$ . whereas the subsidiary maximum on the short wave-length side is shifted very slightly only with the result, that this part of the absorption curve becomes broadened by the introduction of bromine. The pentammino-bromo-cobaltic chloride is definitely violet, but this change is not due to a constitutional change in the complex and even not so much to the displacement of the maxima as to this broadening of the curve ; besides the blue and green regions of the spectrum also the yellow and orange regions are absorbed. The ultra-violet maximum is shifted to  $320\text{ m}\mu$ , *i.e.*, towards shorter wave-length. At the same time a third maximum appears at  $252\text{ m}\mu$ , *i.e.*, at the same wave-length, where

it appears in those complexes, containing Cl or NO<sub>2</sub> ions in the first sphere.

The replacement of one NH<sub>3</sub> molecule of the hexammino complex by carbonate ion gives nearly the same results as the introduction of chlorine ions. The first maximum lies at about 520 mμ, the second one at about 360 mμ. The maxima at still shorter wave-length appears only as slight inflexions of the curves as in the case of a single chlorine ion being introduced in the complex.

If we take the hexammino complex as the normal substance, we see that its first maximum is displaced towards longer wave-length by the introduction of chlorine, bromine, and carbonate ions, but towards shorter wave-length by the introduction of one or more NO<sub>2</sub> ions. The maximum at about 450 mμ remains also in the complex Na<sub>3</sub> [Co (NO<sub>2</sub>)<sub>6</sub>], in which no NH<sub>3</sub> molecule is present at all, showing that also in the case of the NO<sub>2</sub> group it is the nitrogen which is co-ordinated to the Co ion (*cf.* I). In the NO<sub>2</sub> ion itself, however, the nitrogen atoms is clearly the centre of positive polarity. In the carbonate ion the carbon atom itself forms the centre of the group and since all its electrons take part in the linkage with oxygen, co-ordination takes place most probably between the Co ion and one of the oxygens, which all charged and uncharged, are centres of negative polarity, and the remaining chlorine and bromine ions are negatively charged in any case. The above result therefore can be expressed as follows :—If in the hexamino complex one of the NH<sub>3</sub> molecules is replaced in such a way, that co-ordination takes place between Co and a negative ion or a centre of negative polarity, the first maximum is displaced towards longer wave-length; if, however, a centre of positive polarity takes the place of the nitrogen atom of NH<sub>3</sub>, the maximum is shifted towards shorter wave-length. How far such a generalisation is possible and how far there exist connection to the experiments of Scheibe and von-Halban<sup>2</sup> and Eisenbrandt on

<sup>2</sup> Ber. 58, 612, 1925; Z. Phys. Chem. 132, 433, 1928.



the deformation of chromophores by foreign ions has to be investigated further experimentally.

The results obtained with  $\text{Na}_5 [\text{Co} (\text{CN})_4 (\text{SO}_3)_2]$  and  $\text{K}_4 [\text{Co} (\text{CN})_6 (\text{S}_2 \text{O}_3)]$  seem to be of special interest \*). Instead of the marked maxima of  $\text{K}_3 [\text{Co} (\text{CN})_6]$  the absorption curve shows a broad region of selective absorption in which one main maximum is marked and the other ones form points of inflections only. By an independent measurement of the absorption curve by means of a micro-photometer this result was controlled; obviously the maxima of the selective absorption have become much more diffuse by the exchange of CN ions with sulphide or thiosulphate ions. Since the thiosulphate ion does not possess any selective absorption in the near ultra-violet, the absorption curve of  $\text{K}_4 [\text{Co}(\text{CN})_5(\text{S}_2\text{O}_3)]$  can hardly be considered as a mere superposition of the different absorption curves of the constituent ions, but appears to be the characteristic absorption curve of a true complex salt. On the other hand,  $\text{Na}_5 [\text{Co} (\text{CN})_4 (\text{SO}_3)_2]$  does not follow Beer-Lamberts Law, and the subsidiary maximum at  $308 \text{ m}\mu$  may be due to the selective maximum of the  $\text{SO}_3$  ion. But the maximum at  $264 \text{ m}\mu$  cannot be accounted for by a superposition of different curves. If we have to classify these salts ultimately as genuine complex salts and not as mere associations due to electrostatic attractions, the co-ordinate bond here is considerably weakened as compared to that in the hexacyanides. Further investigations, however, are necessary to decide this question definitely.

We have to thank Prof. P. Rây, who very kindly has put these salts at our disposal.



# The State of Polarisation of Continuous X-rays from a Thin Aluminium Anti-cathode

BY H. P. DE, CALCUTTA.

*(Received for publication, 17th June, 1935.)*

## ABSTRACT.

An experimental method has been described for observing the state of polarisation of the continuous X-rays from a thin aluminium anti-cathode along different directions of emission. The X-rays emitted from a thin anti-cathode was allowed to pass through a Wilson chamber and the initial direction of ejection of the photo-electrons was observed. From such observations the state of polarisation has been found to be 52% along 90° with the line of flight of the cathode particles; 12.5% along 30° with the line of flight and 4% along 0°, i.e., along the direction of motion of the cathode particles. The results obtained have been discussed in the light of the experimental results of other observers and the theoretically expected values of Sommerfeld and Sugiura.

Above 25 years back Sommerfeld<sup>1</sup> put forward a theory to account for the production of continuous X-rays. The fundamental assumption of this theory was, that an electron during its impact with the anticathode material suffers a rectilinear retardation. On this assumption Sommerfeld deduced an expression for the intensity distribution of the X-rays emitted along different directions. If  $J$  denotes the intensity along a particular direction, then

$$J = \frac{e^2 \dot{v}}{16 \pi c^2 r^2} \cdot \frac{\sin^2 \theta}{\cos \theta} \cdot \left[ \frac{1}{(1 - \beta \cos \theta)^4} - 1 \right]$$

where,

$e$  = electronic charge

$c$  = velocity of light

$\dot{v}$  = accel. of the electron

$\beta$  = ratio of the velocity of the electron to that of light.

$\theta$  = angle between the line of flight of the electron and the direction of observer.

$r$  = distance of the point of observation from the anticathode.

According to this theory radiation was expected to be completely polarised. But Barkla and others found that the continuous radiation was only partially polarised, and the characteristic radiation unpolarised. Therefore, to account for the observed facts, the further plausible assumption was made, that the electron suffered scattering and nuclear deflection before the actual stopping took place, and as such it gave rise to an unpolarised radiation. Ross carrying on his investigation for the short wavelength limit of the continuous radiation from thick anticathodes found it to be completely polarised, as was to be expected on Sommerfeld's theory.

Sommerfeld<sup>2</sup> later attempted to explain the production of continuous X-rays from thin anticathodes, from wave mechanical standpoint, where thinness has the implication of reducing the scattering and bending of the cathode particles in the anticathode material to a minimum. Results deduced on this theory were found to be corroborated by the experimental findings of Kulenkampff. Sommerfeld in this theory expected a partial polarisation of the continuous X-rays from thin anticathode in any direction, though a complete polarisation for the short wavelength limit.

Duane,<sup>3</sup> in 1929, experimentally attempted to study the state of polarisation of X-rays generated by the impact of the cathode rays with a stream of mercury vapour; such a process might be regarded to be analogous to the production of X-rays from a thin anticathode, in which the scattering of the cathode particles

might be expected to be nil. Duane in his arrangement was specially careful to keep the voltage much below that required to produce the "L"-radiation of mercury. The observation was made at right angles to the cathode rays, and the X-rays generated were allowed to fall on a carbon block and the scattered photons were measured with a point counter. It was found, that the number of photons registered at right angles to the line of flight of the cathode rays was much larger than those along the cathode ray stream. Now if  $I_1$  and  $I_2$  are the values of the scattered photons recorded in a given period along the former and the latter directions, then the state of polarisation might be given by the formula

$$P = \frac{I_1 - I_2}{I_1 + I_2} \times 100$$

In this case the state of polarisation for the total radiation at right angles to the cathode ray beam was found out to be 47%. Dasanacharya<sup>4</sup> experimentally measured the state of polarisation of the continuous X-rays from a thin aluminium anti-cathode, for various accelerating potentials. He also measured the state of polarisation of the total radiation. In his arrangement the radiation from an anti-cathode,  $64\mu$  thick, was scattered from a suitable carbon block, and the measurements of the scattered radiation was made with an ionisation chamber and an electrometer. His results were similar to those of Duane, the state of polarisation being about 53% for the radiation at right angles to the cathode ray beam.

Sugiura<sup>5</sup> worked out a theory of the distribution of the intensity and the state of polarisation of the continuous radiations using the method of retarded current matrix. In his theory, an expression has been deduced for the angular distribution of intensity of the continuous X-rays from thin anti-cathode, and also for the state of polarisation for different directions. The distribution curve for the state of polarisation, as put forward by Sugiura, is given below.

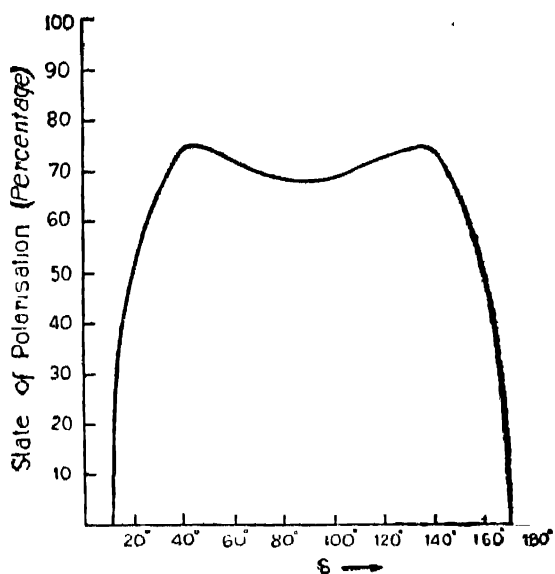


FIG. 1.

As the figure shows, one should expect complete polarisation for the radiation along  $0^\circ$  and  $180^\circ$ , and a partial polarisation along other directions, and the state of polarisation would be a function of the angle of the direction of observation, and vary according to the manner shown in the graph; and further from the theory, it is expected that the state of polarisation would depend on the exciting voltage.

Later Sommerfeld<sup>6</sup> again has attacked this problem, regarding the state of retarded electron responsible for the generation of continuous X-rays, to be represented by a plane wave in contra-distinction to the assumption of Sugiura and others; and according to this theory, the intensity distribution resembles closely the experimental findings of Kulenkampff. In this connection it might be stated, that Kulenkampff<sup>7</sup> studied the state of polarisation for different spectral regions by sorting out the general radiation by means of suitable filters; he found a complete polarisation for the short wave-length limit.

In the present paper the degree of polarisation of the continuous radiation emitted by a thin anti-cathode along different directions of emission has been studied by means of a Wilson chamber. It is well-known, that when a polarised beam of X-rays is sent through an expansion chamber, the initial direction of ejection of the photo-electron tracks tend to lie along the direction of the electric vector in the radiation. It is also known that at right angles to the direction of propagation of X-rays the photo-electrons are distributed around the electric vector according to a  $\cos^2 \theta$  law, where  $\theta$  is the angle between the normal to the radiation and any direction lying in the plane containing the direction of emission of X-Rays and the electric vector ; of course here the effect of the forward momentum in the radiation is ignored. Now in our case the distribution of the initial direction of ejection of the photo-electrons were measured in a transverse plane,\* a plane which is normal to the direction of propagation of the X-rays in the chamber. In this transverse plane two directions were chosen one vertical and the other horizontal, the horizontal in fact was a direction parallel to the line of flight of the cathode particles in the X-ray tube when the emission was examined along  $90^\circ$  to the line of motion of the cathode particles, and the vertical was at right angles to the horizontal. The photo-electrons lying in the transverse plane were divided into two groups, one group lying along the vertical in the transverse plane between  $45^\circ$  on either side, and the rest will naturally lie around  $45^\circ$  on the either side of the horizontal. Here it was legitimately assumed that those electrons, whose initial direction of ejection was found to lie within  $45^\circ$  on the either side of the vertical, had a bias for the vertical direction, and this bias was due to the presence of the electric vector in the radiation along that specific direction. Therefore, a preponderance of the initial direction of ejection

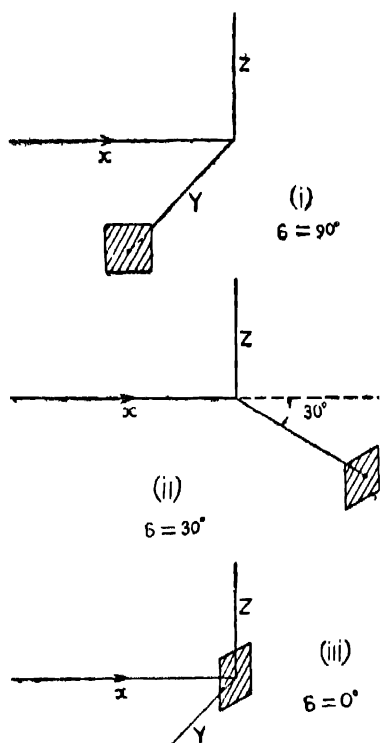
\* In the three diagrams, Figure 2, 'x' represents the line of flight of the parent cathode particles in the horizontal plane and 'Z' represents the vertical. The shaded plane represents the transverse plane in each case.

along any direction either horizontal or vertical would determine the state of polarisation. Here polarisation might be defined as

$$P = \frac{H - V}{H + V} \times 100$$

where  $H$  = number of tracks for which the initial directions of ejection were found to lie between  $45^\circ$  on the either side of the horizontal in the transverse plane.

$V$  = number of tracks for which initial directions were found to lie between  $45^\circ$  on either side of the vertical in the transverse plane.



(i) In this case the direction of emission of the X-rays lies along the Y axis and the transverse plane is identical with the (x, Z) plane.

(ii) In this case the direction of emission makes an angle of  $30^\circ$  with the 'x' axis and therefore the transverse plane makes  $60^\circ$  with the 'x' axis.

(iii) In this case the direction of emission coincides with the 'x' axis, i.e., with the line of flight of the cathode particles, and the transverse plane coincides with the (Y, Z) plane.

FIG. 2.



In this experiment the X-ray tube employed consisted of two portions, the cathode portion of the tube was identical with ordinary Hadding gas filled metal tubes with porcelain insulator, and therefore needs no description; the anti-cathode portion of that tube was removed and in its place an iron tube B was soldered. the diameter of its inner bore was about 2 mm. and the external diameter was about 4 cm. Iron was employed in the construction, with the object of screening the effect of the stray magnetic field on the cathode particles passing through the tube.

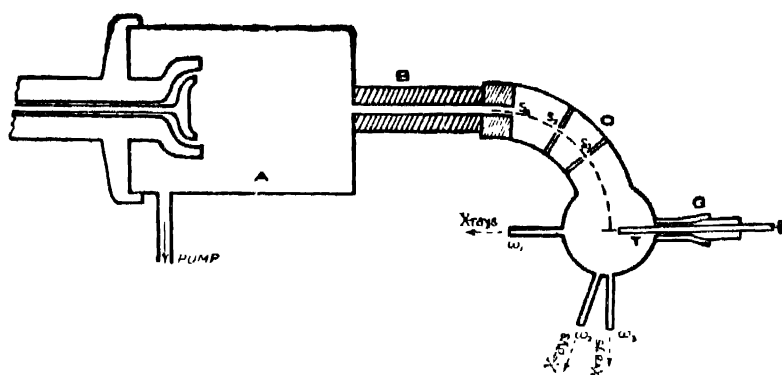


FIG. 3.

A = cathode portion of the tube.

B = iron tube with 2mm bore.

C = brass box with proper slit systems.

T = thin anti-cathode mounted on a ground joint.

$W_1$  = window at right angles to the cathode ray beam.

$W_2$  = window at  $30^\circ$  with the incident cathode ray beam.

$W_3$  = window making  $0^\circ$  with the incident cathode ray beam.

The cathode rays entered the brass box, placed in a uniform magnetic field at right angles to the plane of the paper. It was provided with a system of slits  $S_1$ ,  $S_2$ , etc., to define the cathode-ray beam; just after emerging out of the magnetic field the beam impinged on the thin anti-cathode ( $66\mu$ ). The latter was mounted on a rod fixed to a ground joint G so that it would be placed in the path of the cathode rays when required, and that only for a few seconds. Vacuum inside the system was maintained by a mercury pump with a proper backing oil pump; a

stabilising arrangement was used in order to maintain the vacuum constant for a long time ; when the tube ran hard, a side tube containing charcoal was connected to the vacuum circuit for a fraction of a second, and at once the desired value of the vacuum could be obtained. The electron current through the anti-cathode was measured with a galvanometer, one terminal of which was connected to T and the other was earthed ; it was found to be of the order of a micro-ampere.

The X-rays generated were allowed to enter the Wilson chamber, which was protected by lead screens from stray radiations ; only the X-rays from the thin anti-cathode were allowed to enter the chamber through one of the windows  $w_1$ ,  $w_2$ , etc. From control experiments it was found, that no electron tracks were produced in the chamber when the thin anti-cathode was absent, the other conditions remaining the same in the discharge tube. A stereo-camera was used to photograph the tracks. It was mounted with the axis horizontal coinciding with the direction in which the X-rays were incident. In order to photograph the tracks with best possible definition, a small vertical plane, near the camera end of the chamber was illuminated, and during each expansion, tracks formed in that plane were photographed. During each expansion the number of tracks formed were found to be restricted to four or five only. In measuring the initial direction of ejection, a Zeiss stereo-micrometer was employed and the measurements were taken as stated before.

The slit-system which admitted the cathode ray beam, though sufficiently narrow were of finite width, and due to this a dispersion of the velocity of the cathode particles were introduced, and the amount of dispersion was found to be 3% of the mean velocity.

In this experiment the lengths of the photo-electron tracks were found to range from 4 mm. to 15 mm., of which about 60% were found to have lengths between 6-7 mm. The voltage corresponding to the short wave-length limit was found out to be 25.8 K.V.

Direction of emission.	Number of photo-electrons.		State of polarisation.
	within 45° on either side of the vertical.	within 45° on either side of the horizontal.	
90°	86	26	52
30°	165	212	12.5
*0°	229	242	4

\* In this direction the largest number of plates were taken to secure an accurate value of the degree of polarisation, as a preliminary observation showed that the degree of polarisation is least in this direction.

From the given data the state of polarisation as shown in the last column was calculated according to the formula

$$P = \frac{H - V}{H + V} \times 100$$

where H and V represent the number of photo-electron tracks ejected along the horizontal and vertical directions respectively.

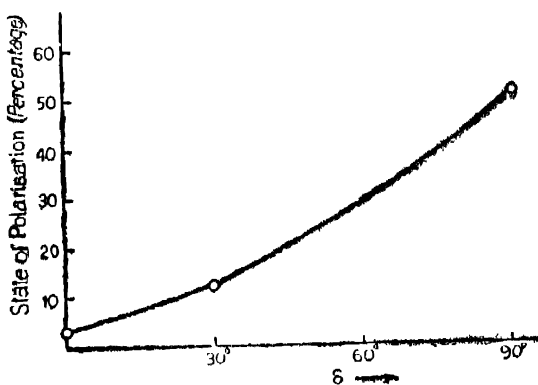


FIG. 4.

$\delta$  is the angle between the direction of motion of the particle and the line of observation.

From the graph it is seen that the state of polarisation decreases as  $\delta$  decreases. According to the classical theory of emission from an infinitely thin anti-cathode, one would expect to find no radiation emitted along the line of flight of the cathode particles. We find that radiation is emitted in that direction and the latter shows a slight degree of polarisation.

The experimental results obtained can only be satisfactorily compared with the predictions of theory after corrections are made for (i) the want of uniformity in the thickness of the anti-cathode, (ii) scattering of the cathode particles in the cathode, (iii) error in measuring the initial direction of ejection of the photo-electrons. The last mentioned error can be reduced by taking a much larger number of observations. In spite of these possible errors it is remarkable how our value for the degree of polarisation at  $90^\circ$  agrees with those of other observers.

The writer's best thanks are due to Prof. D. M. Bose for his keen interest and helpful suggestions during the progress of the work.

UNIVERSITY COLLEGE OF SCIENCE,  
CALCUTTA.  
MAY 15, 1935.

#### REFERENCES.

1. Sommerfeld—*Physik. Zeit.* 10 (969). 1909.
2. „ —*Proc. Nat. Acad. Sciences*, May, 1929.
3. Duane— „ „ Nov., 1929.
4. Dasanacharya—*Physical Review*, Vol. 35, 1930.
5. Sugiyara—*Scientific papers of the Institute of Physical and Chemical Research* (Japan), p. 251 (1929), April (1930).
6. Sommerfeld—*Ann. d. Phys.* 11, 257 (1931).
7. Kulenkampff—*Phys. Zeit.* 30, 513 (1929).

## Potential Energy Curves and Structure of the Alkaline Earth Oxides

By

P. C. MAHANT.

### ABSTRACT.

The potential energy curves for the different electronic states of the alkaline earth oxides have been drawn after Morse. The electronic configuration, dissociation energy and the products of dissociation in each state are discussed and the similarities in the spectra of the different members have been traced as far as possible.

In the ground state of the alkaline earth oxides, the metal atom has been supposed to be in an excited  $^3P$  state with outermost electrons in a  $s p$  configuration and the oxygen atom in its normal  $^3P$  state with  $p^4$ -configuration, the linkage in the molecule being due to a  $p p$ -type of binding between the constituent atoms.

### *Introduction.*

The data obtained from the analysis of the spectra of a diatomic molecule can be utilised to construct  $U(r)$  curves for its various electronic states. A study of these curves supplies us with many interesting informations about the nature of the molecules in question. From the data so far accumulated in literature, one finds that molecules with the same number of electrons and not differing too much in their nuclear charges, the so-called iso-electronic molecules, are closely similar to one another, in the order of binding of different types of electrons as

is evident from the nature of potential energy curves, and also in respect to the positions of their different electronic energy levels for  $r=r_e$ . Where the nuclear charges are very unequal, (as in hydrides), the order of binding and arrangement of electron levels are essentially those of the atom with the same number of electrons (*i.e.*, united atom) except for the  $\lambda$  and  $\Lambda$  subdivision.

Furthermore, certain diatomic molecules show homologous characteristics as are found to exist between atoms occurring in the same column of the periodic table. These features are manifested in the existence of marked similarities between the energy level diagrams of molecules, one of whose atoms varies from one element to another in the same column of the periodic table, while the other remains fixed; or else both vary, each within a given column of the table. As yet, the data on such series of molecules are not extensive enough to show how far these similarities can be followed. For homologous hydride molecules, the similarities between their energy level diagrams can be explained from the consideration of their homologous united-atoms. In the case of non-hydride homologous molecules, it has been found that in most cases their resemblance to the united-atom is not close enough to be of any direct interest except in only a few aspects. They have, however, a relationship to their separated atoms, which is rather interesting. The object of the present paper is, firstly to trace the relationships which exist between the energy levels of different alkaline earth oxides with those of their separated atoms, from a study of the energy level diagrams and  $U(r)$  curves, and secondly to determine the nature of the electronic structure in the different states.

#### *Construction of $U(r)$ Curves.*

For each electronic state of a diatomic molecule there is a function  $U(r)$  representing the relation between the potential energy and the internuclear distance which has a single minimum

corresponding to an equilibrium value,  $r_e$ , of the distance  $r$  between the nuclei. If  $U(r)$  is taken as zero, then  $U(r)$  represents the total potential energy of a molecule whose nuclei are momentarily at rest at distance  $r$  apart. The variation of  $U(r)$  with  $r$  can be graphically represented by means of a curve, called the  $U(r)$  curve for that electronic state. Thus each electronic state has its own  $U(r)$  curve.

Kratzer<sup>1</sup> was the first to work out a potential energy function of an anharmonic oscillator composed of a dipole and showed that  $U(r)$  curves of molecules can be constructed with the help of this function. He gave the following expansion of  $U(r)$  in terms of  $\rho = r/r_e$ .

$$U(\rho) = -a^* \left[ -\frac{1}{2} + 1/\rho - \frac{1}{2}\rho^2 + b^*(\rho-1)^3 + c^*(\rho-1)^4 + \right] \quad (1)$$

which is convergent for values of  $r$  not far from  $r_e$ .

From the analysis of band spectra if  $\omega_e$ ,  $x_e\omega_e$ ,  $B_e$  and  $a$  are known, one can compute  $r_e$ ,  $a^*$ ,  $b^*$ , and  $c^*$  from the following equations.

$$B_e = \frac{27.7 \times 10^{-40}}{\mu r_e^2}, \text{ where } \mu \text{ is the effective mass of the molecule.}$$

$$\omega_e = \frac{1}{2\pi c} \left( \frac{a^*}{\mu r_e^2} \right)^{\frac{1}{2}},$$

and

$$\bar{a} = (6B_e/\omega_e)(2b^* + 1),$$

$$x_e\omega_e = 3B_e \left\{ 1 + 5b^* + c^* + \frac{5}{2}b^{*2} \right\}$$

There are, however, several objections to the series form used by Kratzer. Firstly, the effect of all the terms in  $(r-r_e)$  to the power three or higher can only be approximately calculated. Secondly, it is only applicable over a restricted range of  $r$ . Thirdly, it does not take into account the relative magnitudes of the anharmonic co-efficients.

In 1929 Morse<sup>2</sup> pointed out that the above objections can

be met by a series form, which would satisfy the following requirements, *viz.*,

- (1) It should come asymptotically to a finite value  $r \rightarrow \infty$
- (2) It should have its only minimum point at  $r=r_e$
- (3) It should become infinity at  $r=0$
- (4) It should exactly give the allowed energy levels as the finite polynomial,

$$W(v) = h\omega_e \left[ \left(v + \frac{1}{2}\right) - x_e \left(v + \frac{1}{2}\right)^2 \right]$$

From the above considerations, he gave essentially the following function, *viz.*,

$$U(r) = D_e \left\{ 1 - e^{-a(r-r_e)} \right\}^2 \quad \dots \quad (2)$$

where,

$$a = \left\{ \frac{2\pi^2 \mu_e \omega_e^2}{h D_e} \right\}^{\frac{1}{2}}$$

$D_e$  may be determined independently or evaluated from the relation,  $D_e = \frac{\omega_e^2}{4x_e \omega_e} \text{ cm}^{-1}$ . This function has a minimum of 0 at  $r=r_e$  and comes asymptotically to  $D_e$  at  $r=\infty$ . It does not, however, satisfy strictly the requirement (3). Morse's function permits, therefore, the construction of  $U(r)$  curves, which are qualitatively correct, though not quantitatively, from  $r=0$  to  $r=\infty$  except in the region close to  $r=0$ , which is of no practical importance.

More recently Rydberg<sup>3</sup> has proposed for the  $U(r)$  function an expression slightly different from that of Morse. This is given by,

$$U(r) = D_e \{ a(r-r_e) + 1 \} e^{-a(r-r_e)} \quad \dots \quad (3)$$

where,

$$a = \left\{ \frac{(0.1735 \omega_e)^2 \mu_e}{D_e} \right\}^{\frac{1}{2}}$$



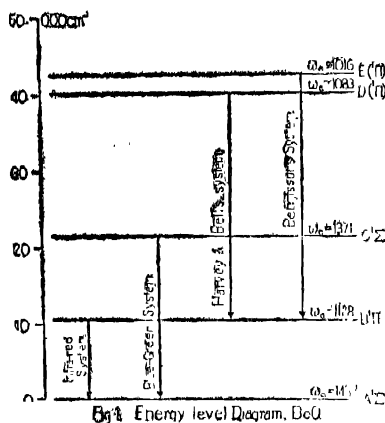
He constructed the  $U(r)$  curves for a few molecules on the basis of the above equation and found them to be in better agreement with the theoretically calculated curves than those drawn after Morse's function.

In the present paper the  $U(r)$  curves for the different electronic states of the molecules have been drawn according to Morse's function, which is generally used by different investigators till now. Hence we are to know the values of  $r_e$ ,  $\omega_e$  and either  $x_e\omega_e$  or  $D_e$  for each state. In many cases, however,  $r_e$  is not known owing to the lack of rotational analysis of the bands involving the given electronic level but the value of  $\omega_e$  is known from their vibrational analysis. It may here be noted that when  $\omega_e$  is known, the corresponding  $r_e$  can be estimated with fair accuracy by means of one of the two empirical relations, *viz.*,  $\omega_e r_e^2 = \text{const.}$ , or  $\omega_e r_e^3 = \text{const.}$  as given by Birge<sup>4</sup> and Morse<sup>2</sup> respectively. Both relations, especially the first, hold fairly well for different states of a molecule if the value is known for one state. The second relation, with the constant as  $3000 \times 10^{-21} \text{ cm.}^2$  is fairly applicable for a wide variety of states, even of different molecules, provided the masses of the two atoms are not too unequal. For our purpose the relation of Birge has been preferred since the value of the constant is known from at least two of the electronic states of each molecule under discussion.

### BeO.

Excitation of the BeO molecule has so far been found to emit four band systems. Two of these have been analysed in detail and have been shown to be due to  $^1\Sigma \rightarrow ^1\Sigma$  and  $^1\pi \rightarrow ^1\Sigma$  transitions respectively, one lying in the blue-green<sup>5</sup> and the other in the near infra-red.<sup>6</sup> The other two band systems<sup>7</sup> lie in the near ultra-violet region and it has been suggested that both of them are due to  $^1\pi \rightarrow ^1\pi$  transitions. The energy level diagram correlating the different electronic states of the molecule is given after Harvey and Bell in Fig. 1. The ultra-violet band

system recently analysed by the above investigators has a peculiarity, *viz.*, that it consists of a strong 0-sequence with two very faint ones, *viz.*,  $\Delta v = \pm 1$ .



There have been of late interesting discussions by Mulliken,<sup>8</sup> G. Herzberg,<sup>9</sup> Lessheim and Samuel,<sup>10</sup> L. Herzberg,<sup>6</sup> and others on the electronic configurations and products of dissociation of BeO molecule corresponding to the two states of  $C^1\Sigma \rightarrow A^1\Sigma$  band system. According to Mulliken since BeO and  $C_2$  are isoelectronic, it is expected that their spectra would be similar. Their  $r_e$  values also indicate that one is nearly as stable as the other. He is of opinion that the  $C^1\Sigma \rightarrow A^1\Sigma$  bands of BeO probably correspond to  $\sigma\pi^4\sigma \rightarrow \sigma^2\pi^4$ , the energy interval between the two  $^1\Sigma$  states being about the same as that predicted for the corresponding interval in  $C_2$ .

Turning to the question of dissociation products, Mulliken has pointed out that since the two normal atoms Be ( $1s^2 2s^2$ ,  $^1S$ ) + O( $^3P$ ) give only a  $^3\Sigma$  and a  $^1\pi$  state, they must almost certainly be identified with the molecular states  $\sigma^2\pi^3\sigma$ ,  $^3\pi$  and  $\sigma^2\pi^2\sigma^2$ ,  $^3\Sigma$ . But these states are of relatively higher energy content in BeO than in  $C_2$  and are thus of low stability or possibly even repulsive. Hence  $\sigma^2\pi^4$ ,  $^1\Sigma$  the lower state of the  $C^1\Sigma \rightarrow A^1\Sigma$  system, is the normal state of BeO, and is derived from Be(S) + O( $^1D$ ),

which is the lowest energy pair of states capable of giving  $^1\Sigma$  state.

On the other hand G. Herzberg was of opinion that the normal state,  $\sigma^2\pi^4$ , of BeO is obtained from  $\text{Be}(^3\text{P}) + \text{O}(^3\text{P})$  while its excited state,  $\sigma\pi^4\sigma$ , from  $\text{Be}(^3\text{S}) + \text{O}(^3\text{P})$ .

Lessheim and Samuel have recently pointed out that if the normal state of BeO corresponding to the lower state of  $\text{C}^1\Sigma \longrightarrow \text{A}^1\Sigma$  system, is taken to be derived from  $\text{Be}(2s^2, ^1\text{S}) + \text{O}(2s^22p^4, ^1\text{D})$  as suggested by Mulliken, one can then assume that in the excited state, the molecule dissociates either into an excited Be atom and a normal oxygen atom in the metastable  $^1\text{D}$  state, or into a normal Be atom and an excited oxygen atom. With the first alternative, one finds that the energy interval between  $(2s^2) ^1\text{S}$  and the next higher term, *viz.*,  $(2s2p) ^3\text{P}, ^1\text{P}, (2s3s) ^3\text{S}$  of the Be atom, is 2.70, 5.25 and 6.43 volts respectively, while with the second alternative the energy interval between  $(2s^22p^4)^1\text{D}$  and the next higher terms, *viz.*,  $(2s^22p^4) ^1\text{S}, (2s^22p^33s)^3\text{S}$  of the oxygen atom, is 2.21 and 7.64 volts respectively. But the  $E_{\text{norm}}$  calculated from the data of the band system in question is 4.46 volts and is thus at large variance with any of the above values. They further point out that  $\text{Be}(1s^22s^2, ^1\text{S})$  as a dissociation product is to be excluded, since the closed shell of two s-electrons giving rise to a  $^1\text{S}$  state may act similarly as in He-configuration such that the resulting molecular states would have either no minima in their potential curves or the curves would be very flat. Their internuclear distances would also be very large. These states would thus be repulsive or slightly attractive in nature. This view is substantiated from Hund's theory of crystal lattice for BeO.<sup>11</sup> The continuous absorption spectra<sup>12</sup> of a number of molecules which are known to be of this configuration also support the above view.

Furthermore if one assumes the nature of the dissociation products in the two states of BeO molecule to be that ascribed by Herzberg, the energy interval between  $(2s3s)^3\text{S} - (2s2p)^3\text{P}$  of Be atom is 3.72 volts and it is not in agreement with the experi-

mental data. It has also been remarked that in accordance with either of the above electronic configurations of BeO, one would expect the heat of dissociation in the excited state,  $\sigma\pi^4\sigma$ , to be lower than that of the normal state of completed shells with  $\sigma^2\pi^4$  configuration. This is in contradiction to actual data, since the dissociation energy in the normal state is 5.66 volts and in the excited state 7.50 volts.

From the above considerations, Lessheim and Samuel were led to suggest that the ground level of BeO does not start with the configuration ( $s^2$ ) of Be atom as assumed by Mulliken but probably starts from the first excited term of the metal atom with the configuration ( $sp$ ) as proposed by Herzberg. Thus one may assume that the chemical linkage in BeO is due to a  $pp$ -binding between a  $p$ -electron of Be and a  $p$ -electron of oxygen atom. If the  $p$ -electron is excited we get a molecular state which has a decreased heat of dissociation and which dissociates adiabatically, yielding a metal atom in its ordinary excited state. The  $s$ -electron of the metal would not then take part in the linkage but would only disturb it. If on the other hand this electron is excited, the heat of dissociation would increase in the excited level and the molecule dissociates adiabatically yielding a metal atom in an anomalous excited state. The above authors were, therefore, led to suggest that in the lower  $A'\Sigma$  state of the band system, the electronic configuration of BeO corresponds to

$$k_1 k_2 2s\sigma^2 (2s) 2p\pi^4 (2p) 3p\sigma (2s) : d\sigma (2p),$$

dissociating into Be( $k_2 s 2p$ ,  $^3P$ ) and O( $k_1 s^2 2p^4$ ,  $^3P$ ), i.e., into an excited Be atom and a normal oxygen atom.

In the upper  $C'\Sigma$  state of the band system, since the energy of dissociation is larger, leading evidently to stronger binding force, it may be assumed that this state is derived by the excitation of a  $s$ -electron in the molecule, so that a complete shell is formed in place of two incomplete ones in the ground state. Such an assumption leads to the following configuration, viz.,

$$k_1 k_2 2s\sigma^2 (2s) 2p\pi^4 (2p) 3d\sigma^2 (2p).$$

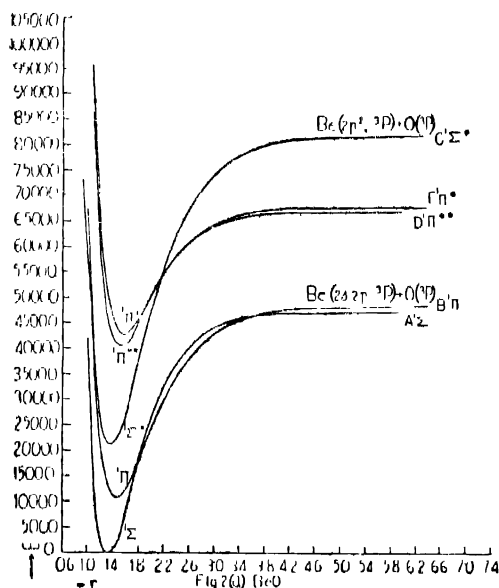
This dissociates into  $\text{Be}(k2p^2, {}^3\text{P})$  and  $\text{O}(k2s^22p^4, {}^3\text{P})$ , that is, into a Be atom in an anomalous excited state and a normal O-atom. The energy interval  $(2p^2){}^3\text{P} - (2s2p){}^3\text{P}$  is 4.66 volts and is in fair agreement with the calculated value of  $E_{\text{atom}} = 4.46$  volts from the data of the band system.

The problem of the electronic configuration and the products of dissociation of BeO molecule has further been discussed by L. Herzberg. She has worked out the electronic configuration in each state after the "Aufbau" principle of Mulliken and Hund and has identified the different states of the infra-red, the blue-green and Bengtsson's ultra-violet band systems with the molecular states  $\sigma^2\pi'(A^1\Sigma)$ ,  $\sigma^2\pi'\sigma(B^1\pi)$ ,  $\sigma\pi'\sigma(C^1\Sigma)$  and  $\sigma\pi^3\sigma^2(E^1\pi)$ . She has also drawn the potential energy curves for each of these four states. From the course of these curves, L. Herzberg was led to infer that for large values of  $r$ , the curves for  $A^1\Sigma$  and  $B^1\pi$  and those for  $C^1\Sigma$  and  $E^1\pi$  merge into one another indicating that each pair dissociates into identical atoms. She was thus of opinion that while the molecular states of the former pair are derived from either  $\text{Be}(^1\text{S}) + \text{O}(^1\text{D})$  or  $\text{Be}(^3\text{P}) + \text{O}(^3\text{P})$ , those of the latter are probably obtained from  $\text{Be}(^3\text{S}) + \text{O}(^3\text{P})$  or  $\text{Be}^+(^2\text{S}) + \text{O}^-(^2\text{P})$ . This assumes that the excited  $C^1\Sigma$  state dissociates into  $\text{Be}^+(^2\text{S}) + \text{O}^-(^2\text{P})$ , which is an ionic binding, explaining the higher value for the heat of dissociation in this state than that in the normal  $A^1\Sigma$  state. The assumption of L. Herzberg of an ionic binding in the excited  $C^1\Sigma$  state does not seem justifiable as one finds that the value of electron affinity of oxygen calculated from the band analysis data is at wide variance with that directly measured by Mayer and Maltbie, while the value of  $E_{\text{atom}}$  evaluated from the same data, is in fair agreement with the energy interval  $(2p^2){}^3\text{P} - (2s2p){}^3\text{P}$  of Be atom as has already been pointed out.

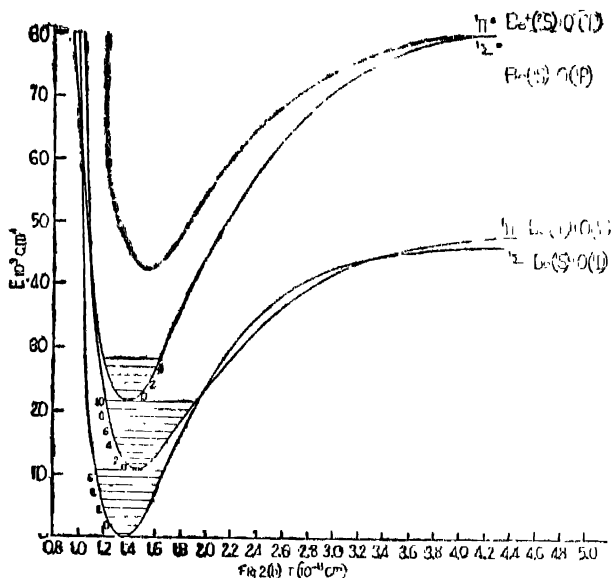
It may further be noted that the assumption of an ionic binding, would lead one to expect a higher value of heat of dissociation in the  $E^1\pi$  state than that in the  $B^1\pi$  state of Bengtsson's ultra-violet band system. But the value calculated from band

head data is lower. This means, therefore, that the products of dissociation in  $C^1\Sigma$  and  $E^1\pi$  states are not probably identical, so that their  $U(r)$  curves would not merge into one another as shown by L. Herzberg in her paper. In fact she has herself noted that the  $U(r)$  curve for the  $E^1\pi$  state does not represent its actual course calculated from the available data. The  $U(r)$  curve for the  $D^1\pi$  state was not included as the analysis of the  $D^1\pi \rightarrow B^1\pi$  band system was not then published.

The potential energy curves for the different states of BeO have been drawn in Fig. 2(a), those of L. Herzberg being reproduced in Fig. 2(b) for a comparison. From both these figures, it is evident that allowing for small inaccuracy in the experimental data, the  $U(r)$  curves for  $A^1\Sigma$  and  $B^1\pi$  states coalesce into



one another for larger  $r$  values, indicating that their products of dissociation are identical as has been suggested by the above author. On the other hand, the  $U(r)$  curve for  $E^1\pi$  does not merge into that for  $C^1\Sigma$  (Fig. 2b) but it runs together with the one for the  $D^1\pi$  state (Fig. 2a). From this, one can reasonably suggest that  $D^1\pi$  and  $E^1\pi$  states would be derived from identical



atoms. Further definite information regarding the electronic configuration and products of dissociation of BeO in these two states can be had only when more accurate data on the analysis of the ultraviolet band systems will be available.

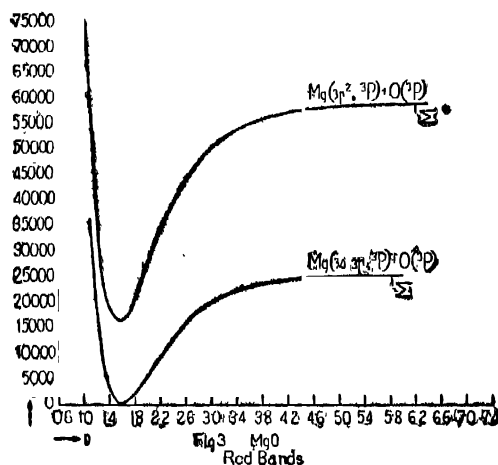
In our view we agree with Lessheim and Samuel in their assignment of electronic configuration and identification of the products of dissociation of the  $A^1\Sigma$  and  $C^1\Sigma$  states. The  $B^1\pi$  state, whose  $U(r)$  curve coalesces into that of the normal  $A^1\Sigma$  state, dissociates also into Be ( $k\ 2s\ 2p$ ,  $^3P$ ) and O ( $k\ 2s^2 2p^4$ ,  $^3P$ ), *i.e.*, into a normal oxygen atom and an excited Be atom. Since the dissociation energy decreases in this state, one is to consider only those configurations of the excited molecule in which the excitation is due to a  $p$ -electron contributing to the linkage. This  $p$ -electron will, therefore, be excited to the next  $\pi$ -group,  $3d\pi$  ( $2p$ ). Hence the electronic configuration of BeO in this state would correspond to

$$k^1\ k_2\ 2s\sigma^2\ (2s)\ 2p\pi^4\ (2p)\ 3p\sigma\ (2s)3d\pi\ (2p).$$

So it is different from what has been assigned by L. Herzberg.

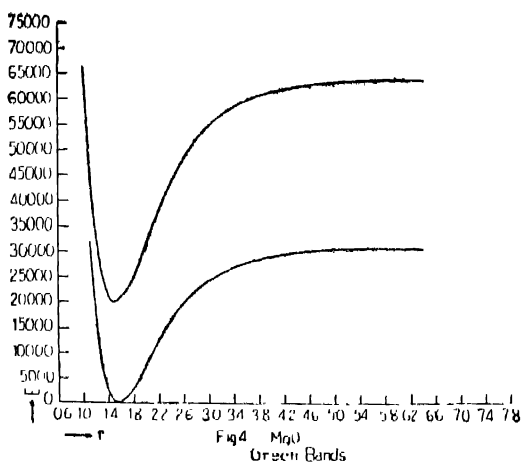
*MgE.*

For MgO two band systems<sup>13</sup> are known, one lying in the green and the other in the red. The analysis<sup>11</sup> of the red system reveals that it is due to a  ${}^1\Sigma \rightarrow {}^1\Sigma$  transition. The green system is very similar in appearance to the ultra-violet system of Harvey and Bell for BeO, *viz.*, having a strong zero sequence with two faint sequences  $\Delta v = \pm 1$  and has also  $\omega_e'$  and  $\omega_e''$  value nearly equal in magnitude. From the high dispersion photographs of these bands, it appears that the higher members of the P and R series, are probably double, which may be attributed to  $\Delta$ -type doubling. In view of the superposition of the higher members of the sequence and in the absence of a rotational analysis, this cannot be over-emphasised. One can, however, assume that these bands are analogues of ultra-violet bands of Harvey and Bell while the red systems are analogues to the blue-green system of BeO. The potential energy curves are given in Figs. 3 and 4.



With a view to ascertain the atomic states from which the electronic levels corresponding to the two states of the red bands





of MgO are derived,  $E_{\text{atom}}$  was calculated. Since  $E_{\text{mol.}} = 2.03$ ,  $D' = 5.09$  and  $D'' = 3.06$  volts, we have

$$\begin{aligned} E_{\text{atom}} &= E_{\text{mol.}} + D' - D'' \\ &= 4.06 \text{ volts.} \end{aligned}$$

From the line spectrum data of Mg, the energy interval between  $(3s^2) {}^1S$  and  $(3s3p) {}^1P$  is about 4.3 volts while that between  $(3s3p) {}^3P$  and  $(3p^2) {}^3P$  is nearly 4.4 volts. Both these values are in fair agreement with the value of  $E_{\text{atom}}$  calculated above from the band analysis data. We are thus presented with two possibilities.

If we adopt the view of Mulliken that the linkage in MgO starts also with the configuration  $(s^2)$  of the metal atom as in the case of BeO molecule, then the lower  $\Lambda^1\Sigma$  state of the red system, which is probably the ground state of MgO, may be supposed to be derived from Mg  $(3s^2, {}^1S) + O (2s^2 2p^4, {}^1D)$ . Hence we are to identify the products of dissociation of the upper  $C^1\Sigma$  state with Mg  $(3s 3p, {}^1P) + O (2s^2 2p^4, {}^1D)$ . One would, therefore, expect the heat of dissociation in the upper state,  $\sigma\pi^4\sigma$ , to be less than that of the lower,  $\sigma^2\pi^4$ , which consists of only completed shells. This is, however, in contradiction to the actual data. We may further exclude this possibility from the consideration which has

already been made with reference to BeO that the helium-like configuration ( $s^2$ ) usually gives rise only to repulsive or slightly attractive states of diatomic molecules.

On the other hand if we assume that the linkage in the ground level of the molecule is due to a  $pp$ -binding and thus starts from the first excited term of the metal atom with the configuration ( $sp$ ) as has been suggested by G. Herzberg as well as by Lessheim and Samuel, then the lower ( $A^1\Sigma$ ) and upper ( $C^1\Sigma$ ) states of the red system may be taken to be derived from Mg ( $3s\ 3p, {}^3P$ ) + O ( $2s^2\ 2p^4, {}^3P$ ) and Mg ( $3p^2, {}^3P$ ) + O ( $2s^2\ 2p^4, {}^3P$ ) respectively. It is thus possible to explain the higher value of heat of dissociation in the excited  $C^1\Sigma$  state. As in the case of BeO, we may here suppose that the  $p$ -electron of magnesium together with a  $p$ -electron of oxygen are responsible for the chemical linkage in the molecule in its ground state and that the upper  $C^1\Sigma$  state has been derived by the excitation of the  $s$ -electron in the molecule. Hence the heat of dissociation increases in the excited level.

From analogy with BeO, one obtains the following configuration for the ground and excited levels of MgO according to Weizel's correlation scheme.<sup>16</sup>

$$\pi^2\sigma\sigma, A^1E : k_1k_2\ 2s\sigma^2(2s)\ 3p\sigma^2(2s)\ 3d\sigma^2(2p)\ 4f\sigma^2(2p)\ 2p\pi^4(2p) \\ 3d\pi^2(2p)\ 3s\sigma(3s)\ 4d\sigma(3p).$$

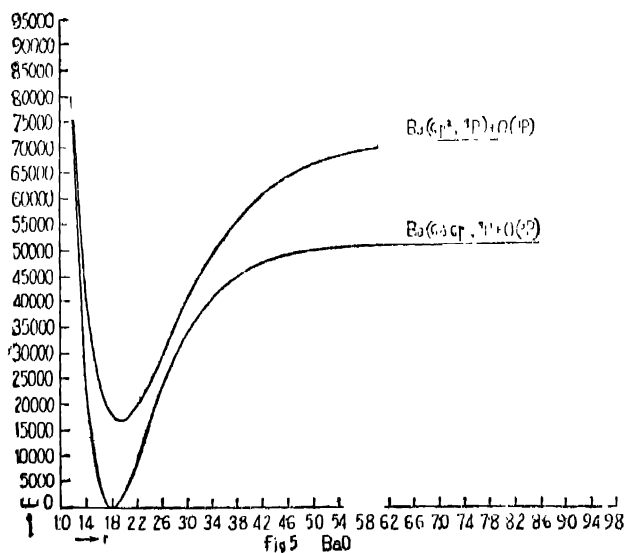
$$\pi^2, C^1E : k_1\ k_2\ 2s\sigma^2(2s)\ 3p\sigma^2(2s)\ 3d\sigma^2(2p)\ 4f\sigma^2(2p)\ 2p\pi^4(2p) \\ 3d\pi^2(2p)\ 4d\sigma^2(3p).$$

The products of dissociation in the two states of the green system can be fairly ascertained by calculating also the value of  $E_{\text{atom}}$  from the band analysis data. This is found to be 4.05 volts, since  $E_{\text{mol.}} = 2.46$ ,  $D' = 5.36$  and  $D'' = 3.77$  volts. Comparing this value with that evaluated from the red system, it seems likely that the products of dissociation of the lower states of the two systems are identical and so also of their upper states. But the values of  $\omega_e$  and  $x_e\omega_e$  in the band head equation

of the green system are a bit uncertain as they have been evaluated only from  $\Delta v=0$  and  $-1$  sequences. This renders the values of  $D'$  and  $D''$  also unreliable. Hence the above statement regarding the nature of the products of dissociation in the two states of the green system cannot be over-emphasised. In the absence of a rotational structure analysis of these bands, the electronic configuration of MgO in these states cannot also be ascertained with certainty. But it seems most likely that a transition between two similar states, probably  ${}^1\pi$ , is responsible for the emission of the band system. It may be noted that the molecular states derivable from combination of an unexcited O-atom ( ${}^3P$ ) with a Mg-atom in ( $3s\ 3p, {}^3P$ ) or in ( $3p^2, {}^3P$ ) state are two quintets, triplets, singlets  $\Sigma$  and  $\pi$ -states and one quintet, triplet, and singlet  $\Delta$  state in each case.

### BaO.

Excitation of the BaO molecule has so far been found to give rise to a single extended band system<sup>15</sup> lying in the region  $\lambda\ 8000 - \lambda\ 4300$ . From its fine structure analysis it has been



attributed to be due to a  ${}^1\Sigma \rightarrow {}^1\Sigma$  transition.  $U(r)$  curves for the two states are given in Fig. 5. This system is in all probability analogous to the blue-green bands of BeO and the red bands of MgO, so that it is schematically represented as due to a transition between  $C^1\Sigma$  and  $A^1\Sigma$  states. It is further noticed that the heat of dissociation in its upper state is also greater than that in the lower, which is possibly the ground state of the molecule. Hence from considerations, similar to those of BeO and MgO, we can here also assume that the linkage in the ground state of BaO is due to a  $pp$ -binding which starts from the first excited term of Ba atom with the  $(sp)$  configuration, and that the  $s$ -electron is excited to give rise to the upper state of the band system. Thus the ground state  $A^1\Sigma$  is derived from Ba  $(6s\ 6p, {}^3P) + O(2s^2 2p^4, {}^3P)$  while the upper state,  $C^1\Sigma$ , from Ba  $(6p^2, {}^3p, P) + O(2s^2 2p^4, {}^3P)$ . The energy interval between  $(6p^2) {}^3P - (6s\ 6p) {}^3P$  of Ba is 2.74 volts, which is in sufficiently close agreement with the value of  $E_{\text{atom}}$  2.52 volts, calculated from band analysis data. It may here be pointed out that the interval between  $(6s\ 6p) {}^1P - (6s^2) {}^1S$  of Ba is 2.23 volts. Although this value may be considered to be in fair agreement with the calculated value of  $E_{\text{atom}}$ , we have excluded this possibility for reasons which have already been given in connection with BeO and MgO.

In this case, however, we cannot be certain of the quantum numbers of the molecule. But adopting Weizel's correlation scheme we can derive the configuration of BaO in each state analogous to that of BeO or MgO.

### *CaO and SrO.*

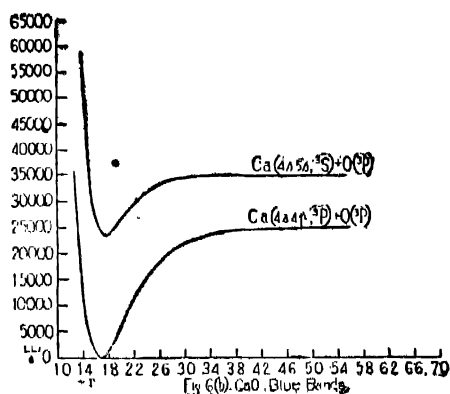
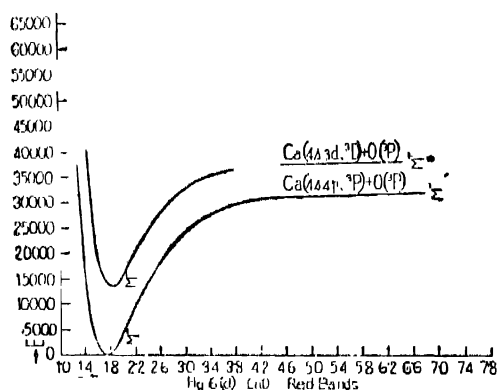
Three band systems are known for each of these molecules. One of these lies in the near infra-red,<sup>16</sup> another in the blue and a third in the ultra-violet.<sup>13</sup> Comparing the co-efficients,  $\omega_0$  and  $x_0 \omega_0$  in the band head equations of the different systems, it is found that there is no state in common amongst them.

The rotational analysis of the infra-red bands reveals that they are due to  ${}^1\Sigma \rightarrow {}^1\Sigma$  transitions, and are probably analogous to the  $C^1\Sigma \rightarrow A^1\Sigma$  band system of the oxides of the remaining alkaline earth metals. It is further noticed that the heat of dissociation in the upper state of the infra-red system is less than that of the lower which may be supposed to be the ground state of the molecule concerned. If we now assume that the linkage in each of these two molecules is also due to a  $pp$ -binding with the metal atom in the ( $sp$ ) configuration and that the  $p$ -electron is excited to give rise to the upper state of the infra-red systems, we can explain the decreased heat of dissociation in the excited states of the molecules. Thus the ground state,  $A^1\Sigma$ , is derived from  $\text{Ca } (4s\ 4p, {}^3P) + \text{O}(2s^2\ 2p^4, {}^3P)$  in the case of  $\text{CaO}$  and from  $\text{Sr } (5s\ 5p, {}^3P) + \text{O}(2s^2\ 2p^4, {}^3P)$  in the case of  $\text{SrO}$ . The products of dissociation of their upper  $C^1\Sigma$  states may then be associated with  $\text{Ca}(4s\ 3d, {}^3D) + \text{O}(2s^2\ 2p^4, {}^3P)$  and  $\text{Sr } (5s\ 4d, {}^3D) + \text{O } (2s^2\ 2p^4, {}^3P)$  respectively. The energy interval between  $(4s\ 3d)\ {}^3D - (4s\ 4p)\ {}^3P$  of  $\text{Ca}$  is 0.64 volts while  $E_{\text{atom}}$  calculated from the data of Brodersen is 0.75 volts. In the case of strontium, the interval between  $(5s\ 4d)\ {}^3D - (5s\ 5p)\ {}^3P$  is 0.47 volts. From Mahla's data one finds that  $E_{\text{atom}}$  gives a negative value, which may, however, be attributed to error in extrapolation.

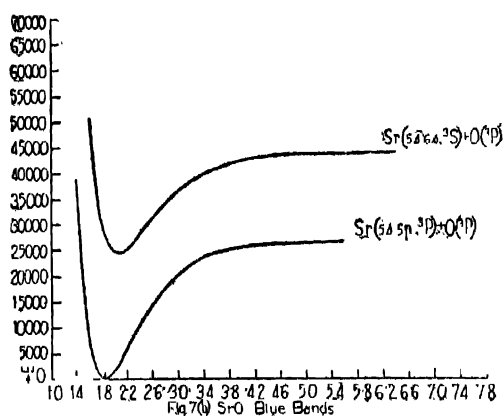
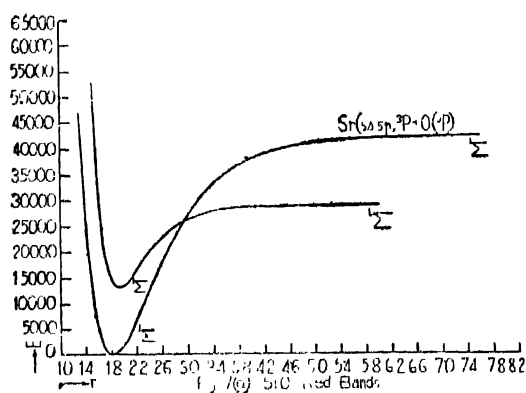
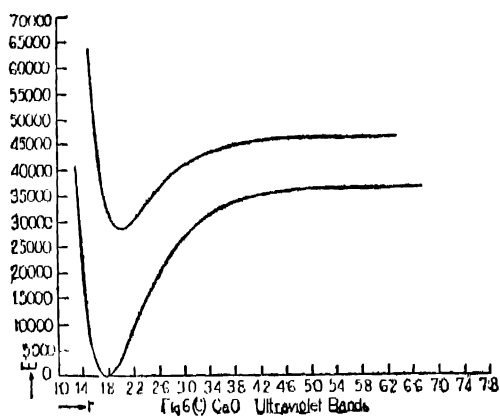
The blue systems of calcium and strontium oxides consist of single headed bands and are probably analogous to the ultra-violet  $D^1\pi \rightarrow B^1\pi$  system of  $\text{BeO}$ . The heats of dissociation of their upper states are also less than those of their lower, which may be assumed to be derived from atoms, identical with the products of dissociation of the lower states of the infra-red bands of each molecule. It may here be noted that a  ${}^3P$  term of the excited metal atom with  $sp$ -configuration and  ${}^3P$  term of the normal oxygen atom combine to give a number of molecular states other than the  $A^1\Sigma$  state of the red bands. These possible molecular terms have already been noted in the case of  $\text{MgO}$  molecule. As in the case of the infra-red bands, we may also assume that the  $p$ -electron is excited to give rise to the upper

state of each of the blue systems. Hence the products of dissociation in these states may be identified with  $\text{Ca } (4s \ 5s, {}^3S) + \text{O } (2s^2 \ 2p^4, {}^3P)$  and  $\text{Sr } (5s \ 6s, {}^3S) + (2s^2 \ 2p^4, {}^3P)$  for  $\text{CaO}$  and  $\text{SrO}$  respectively. In the case of  $\text{Ca}$  the interval between  $(4s \ 5s) {}^3S - (4s \ 4p) {}^3P$  is 2.0 volts while the  $E_{\text{atom}}$  calculated from band analysis data is 1.3 volts, the discrepancy between the two values being attributed to an error in extrapolation. Similarly the interval between  $(5s \ 6s) {}^3S - (5s \ 5p) {}^3P$  of  $\text{Sr}$  is 1.8 volts while the calculated value of  $E_{\text{atom}}$  is 2.1 volts and is thus in fair agreement.

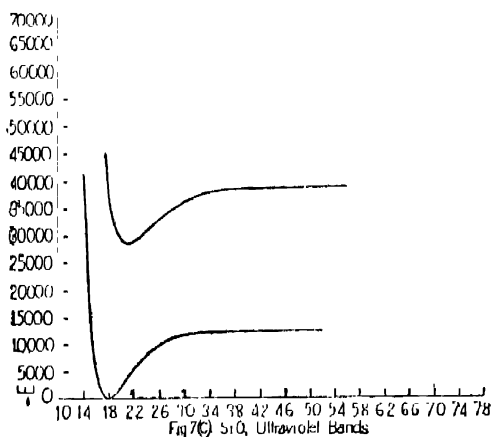
Finally the ultra-violet systems of these two molecules may be assumed to be analogous to Bengtsson's ultra-violet system in the case of  $\text{BeO}$  molecule. In view of their uncertain vibrational analysis, it is preferable to postpone any further discussion on these bands.



The  $U(r)$  curves for the different electronic states of CaO and SrO are given in Figs. 6 and 7. It may be noted further



that the electronic configuration of these molecules in the different states will be similar to those of the analogous states of BeO or MgO.



The author acknowledges with pleasure his gratefulness to Prof. P. N. Ghosh for many helpful discussions on the subject.

- <sup>1</sup> A. Kratzer, *Zeits. f. Physik*, 3, 289 (1920).
- <sup>2</sup> P. M. Morse, *Phys. Rev.*, 34, 57 (1929).
- <sup>3</sup> R. Rydberg, *Zeits. f. Physik*, 73, 376 (1931).
- <sup>4</sup> R. T. Birge, *Phys. Rev.* 25, 240, (1925); R. Mecke, *Zeits. f. Physik*, 32, 823 (1925).
- <sup>5</sup> E. Bengtsson, *Ark. Mat. Astro. Och. Fysik*, 20F, No. 28, (1928); J. E. Rosenthal and F. A. Jenkins, *Phys. Rev.* 33, 163 (1929).
- <sup>6</sup> L. Herzberg, *Zeits. f. Physik*, 84, 571 (1933).
- <sup>7</sup> E. Bengtsson, *Ark. Mat. Astro. Och. Fysik*, 20A, No. 38 (1928); W. Jevons, *Proc. Roy. Soc.* 122, 211 (1923); A. Harvey and H. Bell, *Proc. Phys. Soc.* 47, 415 (1935).
- <sup>8</sup> S. Mulliken, *Rev. Mod. Phys.* 4, 1 (1932).
- <sup>9</sup> G. Herzberg, *Zeits. f. Physik*, 75, 601 (1930).
- <sup>10</sup> H. Leesheim and R. Samuel, *Zeits. f. Phys.* 84, 637 (1933).
- <sup>11</sup> F. Hund, *Zeits. f. Physik*, 74, 1 (1932).
- <sup>12</sup> P. K. Sen Gupta, *Proc. Roy. Soc.* 143A, 433 (1934).
- <sup>13</sup> P. C. Mahanti, *Phys. Rev.* 42, 509 (1932).
- <sup>14</sup> P. C. Mahanti, *Ind. J. Phys.* 9, 455 (1953).
- <sup>15</sup> P. C. Mahanti, *Proc. Phys. Soc.* 46, 51 (1934).
- <sup>16</sup> P. H. Brodersen, *Zeits. f. Physik*, 19, 613, (1932); K. Mahla, *Zeits. f. Physik*, 61, 625 (1933).



## Spectrum of Doubly Ionised Zinc

By

SUDHENDU BASU,

*Department of Physics, Science College, Patna.*

*(Received for publication, 2nd July, 1935.)*

### ABSTRACT

The spectrum of doubly ionised zinc has been analysed in the region between  $\lambda 5513$  to  $\lambda 2387$ . Twenty three new terms have been obtained, mostly derived from the configuration  $3d^9 4d$ , and over one hundred lines are accounted for.

The spectrum of doubly ionised zinc described here is an extension of the analysis carried out by Otto Laporte<sup>1</sup> and R. J. Lang in the region between  $\lambda 1432$  to  $\lambda 1839$ . These authors photographed the spectra by means of a two-metre grating having 30,000 lines per inch. As a source of light sparks in vacuum between two electrodes of metallic zinc were passed. L. & E. Bloch<sup>2</sup> have recently published a list of the spectra of zinc in various stages of excitation by using sparks of varying intensities in air and in vacuum between zinc electrodes, and by passing electrodeless discharge in vaporised metal. This complete and

<sup>1</sup> Phys. Rev., 30, p. 378 (1927).

<sup>2</sup> L. & E. Bloch, Jour. de. Phys. et le Radium, 5, p. 289 (1934).

valuable list contains over 550 lines definitely assigned to Zn III, and ranges from  $\lambda$  5757 to  $\lambda$  2229, and has been utilized by the author in the present work.

The normal state of Zn III is represented by  $3d^{10}$  electrons giving  $^1S_0$ . This was established by Laporte and Lang by its combination with the terms of the configuration  $3d^9 4p$ , giving three lines about the region  $\lambda$  700. The lines about  $\lambda$  1600 are all due to  $3d^9 4s - 3d^9 4p$  transitions. The complexity of the spectrum in the visible and the ultra-violet is presumably due to the presence of two electron jumps, which are quite frequent and strong in the analogous spectrum of nickel.

Table I gives a list of calculated terms obtainable from some of the most probable configurations in Zn III.

TABLE I

$3d^{10}$	$^1S_0$
$3d^9 4s$	$^3D \ ^1D$
$3d^9 4p$	$^3(PDF) \ ^1(PDF)$
$3d^9 4d$	$^3(GFDPS) \ ^4(GFDPS)$
$3d^8 4s^2$	$^3(PF) \ ^1(SGD)$
$3d^8 4s 4p$	$^5^3(DFG) \ ^5^3(SPD)$

Approximate positions for the  $3d^9 (4p-4d)$  can be deduced by applying the Irregular Doubtlet Law, but these at best can only be approximate, since the nomenclature of the terms for  $3d^9 4d$  configuration in Cu II is not exactly known, though they have been determined for Ni by K. Bechert<sup>3</sup> and L. A. Sommer and by Russell.<sup>4</sup> In all these spectra deviations from Russell-Saunders coupling are great and therefore definite multiplet assignments cannot be made without ambiguity. The spectrum of Cu II has

<sup>3</sup> K. Bechert and L. A. Sommer, Ann. der. Phys. 77, p. 351 (1925).

<sup>4</sup> H. N. Russell, Phys. Rev. 34, p. 821 (1929).

been classified by Shenstone<sup>5</sup> and by Kruger<sup>6</sup> in addition to others, and in this the exact identifications of the K values of the terms originating from the configuration  $3d^9 4d$  have not been made. Table II gives the approximate positions of the lines from the combination  $3d^9 (4p-4d)$  as deducible from the Irregular Doublet Law.

TABLE II

	Ni I	Cu II	Zn III
$3d^9 (4p-4d)$	20,000	26,000	32,000 (?)

The tables as provided by L & E Bloch cover this region and there are a large number of lines recorded by them about this approximate position. Unfortunately the method of horizontal comparison is also of no use as the data are not available.

The analysis as put forth in this paper accounts for over a hundred lines, and there are about 400 more lines to be analysed. It seems therefore clear that  $3d^8 4s^2$ ,  $3d^8 4s 4p$ , etc., configurations would also be present strongly. Though an attempt was made to obtain these terms, it was felt during the present analysis that more accurate measurements of the recorded lines would be necessary to bring out further details of the spectrum. The author proposes to repeat the observations of L & E Bloch with a three metre concave grating.

The new terms obtained are given in Table III. It will be seen that in many cases it has not been possible to identify their natures and these are therefore marked by the letters A, B, C .....etc., pending further investigation.

<sup>5</sup> A. G. Shenstone, Phys. Rev. 28, p. 392 (1927).

<sup>6</sup> P. G. Kruger, Phys. Rev. 34, p. 1122 (1929).

TABLE III

Configuration.	Notation.	Value.
$3d^9 4d \rightarrow$	$^3S_1$	100621.0
	$^3P_0$	117528.2
	$^3P_1$	112972.0
	$^3P_2$	117209.5
	$^3D_1$	114733.0
	$^3D_2$	115258.1
	$^3D_3$	115113.6
	$^3F_2$	121949.7
	$^3F_3$	122233.0
	$^3F_4$	118361.8
	$^3G_3$	117105.9
	$^3G_4$	117689.0
	A	119697.3
	B	118742.0
	C	118162.1
	D	117679.0
	E	116985.1
	F	116186.8
	G	115239.8
	H	113086.9
	K	113012.0
	L	112746.3
	M	112704.9

Table IV contains all the lines which have been analysed during the present analysis.

TABLE IV

$\lambda$ I. A.	I	$\nu$ (vac.)	Combination.
5513.33	0	18132.8	$3d^9 4p \ ^3P_1 - 3d^9 4d \ ^3F_8$
5499.93	0	18177.0	$3d^9 4p \ ^3P_2 - A$
5423.87	2	18431.9	$3d^9 4p \ ^3F_3 - 3d^9 4d \ ^3F_3$
5233.55	3	19102.1	$3d^9 4p \ ^3F_4 - 3d^9 4d \ ^3F_3$
4866.84	6	20541.4	$3d^9 4p \ ^3F_2 - 3d^9 4d \ ^3F_2$
4836.06	4	20672.3	$3d^9 4p \ ^3P_2 - 3d^9 4d \ ^3P_2$
4609.21	3	21689.6	$3d^9 4p \ ^3P_2 - F$
4605.57	3	21706.8	$3d^9 4p \ ^3P_0 - A$
4487.55	2	22277.6	$3d^9 4p \ ^3D_3 - 3d^9 4d \ ^3F_3$
4482.73	4	22301.6	$3d^9 4p \ ^3F_3 - 3d^9 4d \ ^3F_4$
4442.50	3	22503.0	$3d^9 4p \ ^3F_3 - C$
4431.47	2	22559.5	$3d^9 4p \ ^3D_3 - 3d^9 4d \ ^3F_2$
4424.04	3	22592.8	$3d^9 4p \ ^3F_4 - B$
4419.61	0	22620.1	$3d^9 4p \ ^3P_2 - 3d^9 4d \ ^3D_2$
4416.66	0	22635.2	$3d^9 4p \ ^3P_2 - G$
4412.05	2	22658.8	$3d^9 4p \ ^3P_0 - B$
4392.22	3	22761.1	$3d^9 4p \ ^3P_2 - 3d^9 4d \ ^3D_3$
4385.66	3	22795.5	$3d^9 4p \ ^3F_2 - A$
4370.47	4	22874.4	$3d^9 4p \ ^3P_1 - 3d^9 4d \ ^3P_2$
4351.71	4	22973.0	$3d^9 4p \ ^3F_4 - 3d^9 4d \ ^3F_4$
4351.11	4	22976.2	$3d^9 4p \ ^3F_3 - 3d^9 4d \ ^3G_4$
4349.47	2	22984.8	$3d^9 4p \ ^3F_3 - D$
4343.14	1d	23018.3	$3d^9 4p \ ^3D_2 - 3d^9 4d \ ^3F_3$
4328.32	4	23097.1	$3d^9 4p \ ^3P_1 - E$
4314.07	1	23173.4	$3d^9 4p \ ^3F_4 - C$
4302.62	1	23235.1	$3d^9 4p \ ^3P_0 - C$
4260.98	2	23462.2	$3d^9 4p \ ^3F_3 - 3d^9 4d \ ^3P_2$
4243.67	2	23557.8	$3d^9 4p \ ^3F_3 - 3d^9 4d \ ^3G_3$
4228.08	1d	23644.7	$3d^9 4p \ ^3F_4 - 3d^9 4d \ ^3G_4$

TABLE IV—*contd.*

$\lambda$ I. A.	I	$\nu$ (vac.)	Combination.
4226.10	2	23655.8	$3d^9 4p \ ^3F_4 - D$
4214.25	1	23722.3	$3d^9 4p \ ^3P_0 - D$
4209.67	2	23748.1	$3d^9 4p \ ^3F_2 - B$
4187.82	3	23872.0	$3d^9 4p \ ^3P_0 - 3d^9 4d \ ^3P_0$
4183.70	1	23895.5	$3d^9 4p \ ^3P_1 - F$
4126.02	0	24229.6	$8d^9 4p \ ^3F_4 - 3d^9 4d \ ^3G_3$
4094.48	2	24416.2	$3d^9 4p \ ^3P_0 - E$
4020.19	00	24811.9	$3d^9 4p \ ^3D_3 - A$
4027.68	0	24821.2	$3d^9 4p \ ^3P_1 - 3d^9 4d \ ^3D_2$
3978.39	1	25128.6	$3d^9 4p \ ^3P_2 - L$
3971.48	5	25172.4	$3d^9 4p \ ^3P_2 - M$
3965.47	3d	25210.5	$3d^9 4p \ ^3P_0 - F$
8944.65	0	25343.6	$3d^9 4p \ ^3P_1 - 3d^9 4d \ ^3D_1$
3938.51	2	25383.1	$3d^9 4p \ ^3F_2 - 3d^9 4d \ ^3G_3$
3935.06	3	25405.4	$3d^9 4p \ ^3F_3 - 3d^9 4d \ ^3D_2$
3912.12	3	25554.3	$3d^9 4p \ ^3F_3 - 3d^9 4d \ ^3D_3$
3830.51	4	26098.8	$2d^9 4p \ ^3F_4 - G$
3823.01	2	26150.0	$3d^9 4p \ ^3D_3 - 3d^9 4d \ ^3F_4$
3812.75	4	26220.3	$3d^9 4p \ ^3F_4 - 3d^9 4d \ ^3D_3$
3794.24	00	96348.2	$3d^9 4p \ ^3D_3 - C$
3770.94	3	26511.0	$3d^9 4p \ ^3D_2 - B$
3748.72	4	26668.2	$3d^9 4p \ ^3P_0 - 3d^9 4d \ ^3D_1$
3703.55	4	26993.4	$3d^9 4p \ ^3P_1 - H$
8693.47	5	27067.1	$3d^9 4p \ ^3P_1 - K$
3689.99	0	27092.6	$3d^9 4p \ ^3D_2 - C$
3688.01	4	27107.2	$3d^9 4p \ ^3P_1 - 3d^9 4d \ ^3P_0$
3668.23	9	27253.3	$3d^9 4p \ ^3F_2 - G$
3661.13	1	27306.2	$3d^9 4p \ ^3D_3 - 3d^9 4d \ ^3P_2$

TABLE IV—*contd.*

$\lambda$ I. A.	I	$\nu$ (vac.)	Combination.
3657.05	1	27333.3	$3d^9 4p\ ^3P_1 - L$
3651.76	1	37376.2	$3d^9 4p\ ^3P_1 - M$
3647.09	4	27406.8	$3d^9 4p\ ^3D_3 - 3d^9 4d\ ^3G_3$
3632.02	7	27525.0	$3d^9 4p\ ^3D_3 - E$
3620.43	5	27613.1	$3d^9 4p\ ^1F_3 - 3d^9 4d\ ^3F_4$
3615.26	3	27652.6	$3d^9 4p\ ^3P_2 - K$
3601.20	2	27760.6	$3d^9 4p\ ^3F_2 - 3d^9 4d\ ^3D_1$
3595.25	2	27806.5	$3d\ 4p\ ^3D_1 - A$
3580.74	6	27919.2	$3d^9 4p\ ^3F_3 - L$
3575.89	1	27957.1	$3d^9 4p\ ^3F_3 - M$
3539.11	4	28247.6	$3d^9 4p\ ^3F_4 - H$
3536.89	5	28265.3	$5d^9 4p\ ^3D_2 - E$
3530.82	6	28313.9	$3d^9 4p\ ^3P_0 - H$
3529.40	4	28325.3	$3d^9 4p\ ^3D_3 - F$
3492.43	5	28625.1	$3d^9 4p\ ^3F_4 - M$
3488.70	0	28655.8	$3d^9 4p\ ^3P_0 - L$
3484.35	1	28691.5	$3d^9 4p\ ^3P_0 - M$
3415.32	1d	29271.4	$3d^9 4p\ ^3D_3 - G$
3407.02	0	29342.7	$3d^9 4p\ ^3D_1 - C$
3386.42	00	29521.2	$3d^9 4p\ ^3F_2 - 3d^9 4d\ ^3P_1$
3361.34	1	29741.5	$3d^9 4p\ ^3F_2 - L$
3354.86	3	29977.6	$3d^9 4p\ ^3D_1 - 3d^9 4d\ ^3P_0$
3339.18	1	29992.7	$3d^9 4p\ ^3D_2 - 3d^9 4d\ ^3D_2$
3326.54	1	30052.6	$3d^9 4p\ ^1P_1 - 3d^9 4d\ ^3P_0$
3317.12	2	30137.9	$3d^9 4p\ ^3D_2 - 3d^9 4d\ ^3D_3$
3288.73	1	30398.2	$3d^9 4p\ ^1D_2 - 3d^9 4d\ ^3P_0$
3253.33	1	30731.7	$3d^9 4p\ ^1F_3 - G$
3101.00	0	32238.3	$3d^9 4p\ ^3D_2 - K$
3100.15	0	32247.1	$3d^9 4p\ ^3D_1 - 3d^9 4d\ ^3D_2$

TABLE IV—*contd.*

$\lambda$ I. A.	I	$\nu$ (vac.)	Combination.
3098.35	2	32265.8	$3d^9 4p \ ^3D_1 - G$
3097.15	1	32278.4	$3d^9 4p \ ^3D_2 - 3d^9 4d \ ^3P_1$
3091.69	2d	32335.3	$3d^9 4p \ ^1P_1 - G$
3071.40	1	32549.0	$3d^9 4p \ ^3D_2 - M$
3060.05	0	32669.7	$3d^9 4p \ ^1D_2 - 3d^9 4d \ ^3D_2$
3058.48	1	32686.5	$3d^9 4p \ ^1D_2 - G$
3050.43	4	32772.7	$3d^9 4p \ ^3D_1 - 3d^9 4d \ ^3D_1$
3048.60	3	32845.3	$3d^9 4p \ ^1P_1 - 3d^9 4d \ ^3D_1$
3039.82	1	32887.1	$3d^9 4p \ ^1F_3 - H$
2875.94	4	34761.0	$3d^9 4p \ ^3D_1 - L$
2872.35	1	34804.5	$3d^9 4p \ ^3D_1 - M$
2869.29	2	34841.6	$3d^9 4p \ ^1D_2 - H$
2866.55	2	34874.9	$3d^9 4p \ ^1P_1 - M$
2860.07	0	34953.9	$3d^9 4p \ ^1D_2 - 3d^9 4d \ ^3P_1$
2683.11	5	37259.1	$3d^9 4p \ ^3P_2 - 3d^9 4d \ ^3S_1$
2533.33	3d	39461.8	$3d^9 4p \ ^3P_1 - 3d^9 4d \ ^3S_1$
2451.52	2?	40778.6	$3d^9 4p \ ^3P_0 - 3d^9 4d \ ^3S_1$
2387.62	0	41869.9	$3d^9 4p \ ^3F_2 - 3d^9 4d \ ^3S_1$

I am very thankful to Prof. J. B. Seth, for his hospitality during my stay at the Physics Laboratory, Government College, Lahore, and to Dr. P. K. Kichlu, for the help in completing this work.



## Raman Spectra of Cis and Trans Decalines

By

S. K. KULKARNI JATKAR.

According to Sachse-Mohr strainless multiplaner ring structure cyclohexane should exist as a 'chair and cradle' form. However, neither cyclohexane nor its derivatives show the isomerism. Hückel has pointed out the small energy difference between the coplaner and multiplaner models as the cause of the difficulty in distinguishing among the possible derivatives of the isomers and chemists are content to regard cyclohexane as plane ring for all practical purposes or if the classical tetrahedral theory is to be maintained the two forms are regarded as easily interconvertible.

Cyclohexane ring in decaline, however, cannot lie in one plane for it is impossible to construct a model out of two plane cyclohexane rings.

It was originally shown by Mohr<sup>1</sup> that two forms of decahydronaphthalene can be constructed from tetrahedral models. One is the trans form which shows the symmetry of a cubic lattice (diamond) and the other cis form which has hexagonal symmetry. Both forms seem to be stable and can be converted one into the other with some difficulty.

Zelinskii and Trovapolak<sup>2</sup> have shown that if decaline is kept in contact with aluminium chloride for twenty-four hours it was converted into trans. This method has been used in the present investigation.

Recently Waterman, Clausen and Tullemers<sup>3</sup> have shown

<sup>1</sup> J. Prakt. Chem. (2), **98**, 318 (1918).

<sup>2</sup> Ber., **65B**, 1299 (1932).

<sup>3</sup> Rec. Trav. Chim. Phys. Bas., **4**, III, 827 (1934).

that prolonged contact with nickel catalyst tends to produce more of the trans decaline.

It was thought that Raman spectra of these compounds would throw some light on the problem, especially the line  $800\text{ cm.}^{-1}$  which is supposed to be due to the cyclohexane ring, should be different in cis and trans forms and similarly the line  $752\text{ cm.}^{-1}$  characteristic of the two fused rings in deca-hydronaphthalene should show a difference. It has been observed that this shift is slightly broad in the spectra of cis-trans mixture.

The technical decaline which is usually prepared by catalyst hydrogenations is supposed to be a mixture containing about 70% of trans. This is borne out by the present investigation by the visual intensity of the characteristic Raman lines. It was considered that for a preliminary investigation it was enough if one could get two substances one having a predominance of one form and the other a mixture of the two forms.

A previous experiment having shown appreciable differences in the relative intensities of the Raman lines of purified technical decaline as such and of that treated with aluminium chloride, a sample containing more (36%) of cis form was prepared by fractional distillation and also a sample representing mostly trans was prepared by the method of Zelinskii (*loc. cit.*). The physical properties of the substances are given below :—

*Physical properties.*

	B. P.	M. P.	Density.	$n_D^{20^\circ}$ .
<i>Cis Decaline.</i>				
Landolt and Bornstein	193	$-51^\circ$	$\cdot 895\ 20/4$	1.4828
Author	73.5 (15 mm)	$-60^\circ$	$\cdot 878\ 21/4$	1.4749 (21°)
<i>Trans Decaline.</i>				
Landolt and Bornstein	187-188	$-36^\circ$	$\cdot 870\ 20/4$	1.4706
Author	71.5 (15 mm)	$-45^\circ$	$\cdot 868\ 21/4$	1.4705 (21°)

From the physical properties of the samples especially the density and refractive index it appears that the fraction collected is a mixture of 36% cis and 64% trans.

TABLE I.

*Cis Decalin.*

No.	Wave-length.	Intensity.	Wave number.	Shift.
1	4436.9	5	22532	406
2	4453.9	3	22446	492
3	4463.1	0	22400	539
4	4474.4	3	22343	595
5	4505.4	5 b	22188	751
6	4514.6	1	22141	794
7	4525.6	3	22090	848
8	4531.2	1	22063	875
9	4555.3	0	21947	992
10	4565.4	2	21898	1040
11	4569.1	3	21890	1058
12	4574.6	8 b	21854	1085 or c2857
13	4590.5	10 b	21778	1160 or c2928
14	4610.8	5	21682	1256
15	4613.7	5	21669	1270
16	4630.2	3 b	21592	1347
17	4633.2	3 b	21578	1361
18	4651.9	8	21491	1447
19	4977.0	5 b	20087	2351
20	4994.9	5 b	20016	2922

*Experimental.*

A Fuess spectrograph with a dispersion of 28 A.U. at  $\lambda$  4358 was used. The tube containing the liquid was 15 cm.  $\times$  1.2 cm. with a fused on jacket to hold the filter solution. This consisted of a 4 per cent. solution of *m*-dinitro-benzene in benzene (recommended by Bär) to cut off the excitation by  $\lambda$  4046. Another jacket was put on this with waxed metal ends to circulate tap water. The tube was aligned on the axis of the spectrograph in the usual way and a lens was used to focus the scattered light

TABLE II.  
*Trans Decaline.*

No.	Wave-length.	Intensity.	Wave number cm. <sup>-1</sup> .	Shift cm. <sup>-1</sup> .
1	4437.9	5	22527	410
2	4454.6	5	22442	496*
3	4506.5	4	22184	754
4	4525.8	3	22089	849
5	4531.4	3	22057	881
6	4548.2	1	21981	957
7	4556.1	2	21943	996
8	4569.2	8	21880	1059
9	4575.3	8	21850	1088 or $\epsilon$ 2856
10	4586.4	3	21798	1141
11	4591.8	8	21772	1166 or $\epsilon$ 2932
12	4606.1	1	21704	1234
13	4611.2	5	21680	1258
14	4615.4	1	21661	1277
15	4633.7	5 b	21575	1363
16	4652.7	10 b	21487	1451
17	4976.4	5	20089	2849
18	4995.2	8 b	20014	2925

emerging from a small aperture. Owing to the considerable continuous spectrum of Heraeus quartz mercury arc used, it was absolutely essential to cut off all stray light even at the sacrifice of scattered light. This made the spectra rather weak even after 24 hours' exposure but the results were considered sufficient for a preliminary report. The results of the wave-length measurements are given in the Tables I and II.

TABLE III.  
*Decaline.*

Cis. Trans.	Trans.	Bonino.
406 (5)	400 (5)	402 (4)
492 (3)	496 (5)	490 (4)
539 (0)		554 (4)
595 (3)		593 (5)
751 (5b)	751 (4)	753 (6)
794 (1)	849 (3)	804 (3)
848 (3)	881 (3)	851 (5)
875 (1)	957 (1)	
992 (0)	996 (2)	990 (2)
1040 (2)	1059 (8)	4046 (7)
1058 (3)	1145 (3)	
1160 (10b)	1166 (8b)	1165 (2)
1256 (5)	1234 (1)	
1270 (5)	1258 (5)	1260 (8)
1347 (3b)	1277 (1)	
1361 (3b)	1363 (5b)	1360 (4)
1447 (8)	1451 (10b)	1448 (10)
2851 (5b)	2840 (5)	2856
2922 (5b)	2925 (8b)	2922

From Table III showing the comparison of the data with that of Bonino<sup>4</sup> (with his visual intensities multiplied to bring up in line with those of the author given within brackets) it is clear that the shifts 539 (0), 595 (3), 794 (1), 1040 (2), 1270 (5), 1347(3b) are characteristic of cis and 495 (5), 881 (3), 957 (1), 996 (2), 1145 (3), 1234 (1), 1363 (5b) are characteristic of trans decaline. A most striking comparison of these observations with the data of Miller and Piaux<sup>5</sup> for cis and trans ortho dimethyl cyclohexane lies in the fact that the shifts 537  $\text{cm}^{-1}$  and 593  $\text{cm}^{-1}$  occur in their cis and 498 in trans compounds. 1053  $\text{cm}^{-1}$  and 1260  $\text{cm}^{-1}$  occur in cis and 1164 and 1355 in trans. That there is a resemblance in the structure of these compounds is at once apparent from the fact that decaline ring is ortho substituted cyclohexane, the cis trans positions in which are also similiary configured to that of dimethyl cyclohexane. In view of the persistence of group frequencies<sup>6</sup> with increasing complexity of compounds it appears that the compounds isolated by Miller and Piaux are more likely to be the 'cradle and chair' forms of the cyclohexane derivative in addition to being space isomers.

The smaller number of frequencies for the trans compound in the region of short shifts which are usually due to oscillation of the ring is in harmony with the idea that the trans compound is more symmetrical.

The fact that the shift 750  $\text{cm}^{-1}$  is broad in the spectra of the mixture of cis and trans decaline shows that the characteristic frequencies of two fused rings for the two decalines are apparently slightly different, that of cis being smaller than the shift due to trans.

Attempt is being made to find evidence for the existence of the two possible forms of cyclohexane by studying the Raman

<sup>4</sup> Atti. Accad. Lincei., **43**, 784 (1931).

<sup>5</sup> Comptes Rendus, **197**, 412 (1933).

<sup>6</sup> Recently Mukerjee (*Nature*, **134**, 811, 1934) has reported several weak lines in the Raman spectrum of decaline which correspond to some of the shifts observed in cyclohexane.

effect of pure cyclohexane (m.p.  $6.4^{\circ}$ ) and the same treated with aluminium chloride as suggested by Zelinskii.<sup>7</sup> Although such treatment converts cyclohexane into methyl pentane, it should be possible to stop the transformation to trans stage provided such stage exists. Study of Raman effect should prove most useful in this direction, particularly in view of the conclusion of Wierl<sup>8</sup> based upon electron interference measurements, that cyclohexane is an equilibrium mixture of the cis and trans forms.

The experimental work was done by the author when he was temporarily transferred to Physics Department and the thanks of the author are due to Sir C. V. Raman for the facilities given.

DEPARTMENT OF GENERAL-CHEMISTRY,  
INDIAN INSTITUTE OF SCIENCE,  
BANGALORE.

<sup>7</sup> Ame. Chem. Abstr., 2429, 1933.

<sup>8</sup> Ann. der Physik, 8, 559, 1931 ; 13, 453, 1932.





## A Bibliography of the Raman Effect. Part III.

By

S. C. SARKAR AND DWIJESH CHAKRAVARTY.

*Palit Laboratory of Physics, University of Calcutta.*

### *Plan of the Bibliography.*

This bibliography is in continuation of the earlier one (Ind. J. Phys., **7**, 431, 1932), which again was in continuation of a still earlier one (Ind. J. Phys., **5**, 257, 1931). A few of the papers published in 1931 and during the first half of the year 1932, which were not included in the second part of this series of bibliographies through oversight, have now been included in the present one.

The plan adopted in the classification of the various papers under different subject headings is the same as in the earlier bibliographies but a single alteration has been made regarding the subject headings. The subject heading in the section Y in the earlier bibliographies was "Incoherence" but in the present one it is "Isotope Effect."

In the author index, against the name of each author are given the letters of the alphabet indicating the sections in which his name appears.

An index of all the substances studied is also given. The inorganic substances are arranged alphabetically and the organic ones are arranged, as far as possible, according to the plan adopted in the "International Critical Tables."

**A****Special Monographs.**

1. BOURGUEL, M. Application of the Raman effect in organic chemistry. Bull. Soc. Chim. de France, **53**, 1 (1933).
  - I. Introduction. Spectra of mixtures, empirical classification of frequencies. Frequencies characteristic of groups. Enol form, oxylacton form, mixtures of isomers. Quantitative spectral analysis.
  - II. Structure of molecules (carbon dioxide, nickel carbonyl, isonitrile, isocyanate, thioisocyanate, allen, CO<sub>3</sub> ion, CO<sub>2</sub>, NO<sub>2</sub> groups). Influence of constitution. C—H frequencies, benzene.
  - III. Experimental technique.
2. KOHLRAUSCH, K. Quantum effects in scattering of light. Die Physik, **2**, 177 (1934).  
W. F.
3. SIRKAR, S. C. A bibliography of the Raman effect. 1930-32. Ind. J. Phys., **7**, 431 (1932).
4. PLACZEK, G. Rayleigh scattering and Raman effect. Marx, Handbuch der Radiologic, **6**, Part II 2nd Edition, 1934.

## B

## Journal Articles.

1. BHAGAVANTAM, S. Light scattering and Raman effect. *Current Science*, **3**, 526 (1933).
2. HIBBEN, J. H. The Raman effect. Applications and present limitations in petroleum chemistry. *Indust. Eng. Chem.*, **26**, 646 (1934).
3. KOHLRAUSCH, K. W. F. Smekal-Raman effect and molecular structure. *Naturwiss.*, **22**, 161 (1934).
4. " " " " " **22**, 181 (1934).
5. " " " " " **22**, 196 (1934).
- 6<sub>2</sub> " Raman spectra and organic chemistry. *Z. f. Elektrochem.*, **40**, 429 (1934).
7. WEIGLE, J. Raman effect of polyatomic molecules. *Arch. des. Sc.*, **14**, 82 (1932).
8. WEILER, J. Raman effect of inorganic substances. *Naturwiss.*, **23**, 125 (1935).
9. " " " " " **23**, 139 (1935).
10. ——— Raman spectra and chemistry. (Report on the discussions held by the Chemical Society.) *Nature*, **131**, 263 (1933).

## D

## Experimental Technique.

1. BALMOKAND ANAND      A modified apparatus for Raman effect.      Jour. Scient. Instr., **8**,  
258 (1931).
2.        „                        „                        „                        „                        „      Jour. Scient. Instr., **9**,  
324 (1932).
3. PFUND, A. H.      Filter for the study of Raman effect.      Phys. Rev., **42**, 581  
(1932).
4. RANK, D. H.      Raman spectrum of tetramethyl methane.      Jour. Chem. Phys., **1**,  
572 (1933).
5. RAO, I. R.      Structure and polarisation of Raman bands      Z. f. Phys., **90**, 658  
of water.      (1934).
6. TIMM, B. AND MECKE, R.      Investigations on the Raman effect of      Z. f. Phys., **94**, 1 (1935).  
organic molecules.

**E****Character of the Lines; Continuous Spectrum.**

1. BÄR, R.                      Existence of a continuous Raman effect in liquids.      *Z. f. Phys.*, **79**, 455 (1932).
2.     „                      Raman effect in glycerine.                      *Z. f. Phys.*, **81**, 785 (1933).
3. BLOCH, L. AND E.      Structure of principal Raman line of benzene.      *Compt. Rend.*, **196**, 1787 (1933).
4. BOLLA, G.                Raman spectrum of ethyl alcohol.              *Z. f. Phys.*, **89**, 513 (1934).
5. CARRELLI, A. AND CENNAMO, F.      On the intensity of Raman effect in water.      *Il Nuovo Cimento*, **10**, 329 (1933).
6. CARRELLI, A. AND WENT, J. J.      On the Raman effect in liquids.                  *Z. f. Phys.*, **80**, 232 (1933).
7. EMBIRIKOS, N.            Influence of ions on the Raman bands of water.      *Physikal. Z.*, **33**, 946 (1932).
8. GRASSMANN, P.          Width of the Raman line  $\Delta\nu=992\text{ cm}^{-1}$  of benzene.      *Z. f. Phys.*, **82**, 767 (1933).
9. GROSS, E.                Modification of light quanta by elastic heat oscillations in scattering media.      *Nature*, **129**, 722 (1932).
10. GROSS, E. AND KHVOSTIKOV, J.      Variation of the structure of scattered lines with the frequency of the primary light.      *Phys. Rev.*, **42**, 579 (1932).
11. GROSS, E. AND VUKS, M.      The phenomenon of wings and the vibrational Raman effect in benzene and naphthalene crystals.      *Nature*, **135**, 431 (1935).
12.                      Quasi-crystalline structure of liquids and the Raman effect.      *Nature*, **135**, 100 (1935).
13. HORLUTI, J.              On the vibration structure in carbontetrachloride spectrum.      *Z. f. Phys.*, **84**, 380 (1933).
14. HOWDEN, O. H. AND MARTIN, W. H.      Continuous spectrum in the light scattered by glycerin and other liquids.      *Trans. Roy. Soc. Canada*, **27**, 91 (1933).
15. HOWLETT, L. E.          Raman effect in benzene and toluene under high dispersion and resolving power.      *Canad. J. of Research*, **5**, 572 (1931).

**E—Contd.**

16. KHVOSTIKOV, J. A.      Modification of frequency of scattered light due to elastic heat waves in liquids.      *Phys. Z. Sowjet Union*, **6**, 343 (1934).
17. LANDEN, L. AND PLACZEK, G.      Structure of the undisplaced scattered line.      *Phys. Z. Sowjet Union*, **5**, 172 (1934).
18. MEYER, E. H. L.      Kerr constant and Raman effect.      *Physikal. Z.*, **37**, 212 (1935).
19. MITRA, S. M.      On the continuous band in glycerine.      *Z. f. Phys.*, **93**, 141 (1935).
20. MITRA, S. M. AND MEHTA, S.      Splitting up of spectral lines by scattering in liquids.      *Ann. d. Phys.*, **22**, 311 (1935).
21. ORNSTEIN, L. S. AND VAN CITTERT, P. H.      On the explanation of fine structure of Rayleigh line, II.      *Physica*, **2**, 499 (1935).
22. ORNSTEIN, L. S. AND WENT, J. J.      Overtone  $\Delta\nu=1539$  in the Raman spectrum of carbon tetrachloride.      *Proc. K. Akad. Amsterdam*, **35**, 1024 (1932).
23. RAMM, W.      Fine structure of Rayleigh radiation.      *Physikal. Z.*, **35**, 111 (1934).
24.      „      Fine structure of lines of Rayleigh scattering in liquids.      *Physikal. Z.*, **35**, 756 (1934).
25. RAO, B. V. R.      Examination of molecularly scattered light with Fabry Perot etalon, Part I.      *Proc. Ind. Acad. Sc., A*, **1**, 216 (1934).
26.      „      Examination of molecularly scattered light with a Fabry-Perot etalon, Part II.      *Proc. Ind. Acad. Sc., A*, **1**, 473 (1935).
27.      „      The Doppler effect in light scattered by liquids, Part I. Variation with temperature.      *Proc. Ind. Acad. Sc., A*, **1**, 765 (1935).
28. RAO, I. R.      Raman effect for water in different states.      *Proc. Roy. Soc.*, **145**, 489 (1934).
29. ROUSSET, A.      Molecular diffusion of light.      *Jour. de Phys.*, **3**, 555 (1932).
30. TRUMPY, B.      Intensity distribution and polarisation of Rayleigh lines.      *Kong. Norske Vidensk. Selsk. Forh.*, **5**, 183 (1933).

**E—Contd.**

31. TROMPY, B. Depolarisation of the continuous radiation accompanying the Rayleigh line in liquids. Kong. Norske Vidensk. Selsk. Forh., **6**, 169 (1933).
32. Raman effect and constitution of molecule. VI. Raman frequencies of  $\text{CH}_2\text{Cl}_2$  and their polarisation. Z. f. Phys., **88**, 226
33. Structure of Rayleigh line. Kong. Norske Vidensk. Selsk. Forh., **6**, 665 (1932).

## F

## Intensity.

1. BAUER, E., Raman spectrum of calcium nitrate. *Compt. Rend.*, **197**, 313  
MAGAT, M. (1933).  
AND SILVEIRA,  
A. DA
2. BHAGAVANTAM, Intensity relations in the Raman spec- *Ind. J. Phys.*, **7**, 549  
S. trum of hydrogen, II. (1933).
3. BHAGAVANTAM, Rotational Raman effect in liquids, Part *Ind. J. Phys.*, **8**, 437  
S. AND RAO, I. Benzene. (1934).  
A. V.
4. „ Rotational Raman effect in gases: carbon *Nature*, **135**, 150 (1935).  
dioxide and nitrous oxide.
5. Distribution of intensity in the rotational *Proc. Ind. Acad. Sc., A*  
Raman spectra of gases. **1**, 419 (1935).
6. CRAWFORD, F. Raman spectrum of fluoro benzene. *Jour. Chem. Phys.*, **2**,  
W. AND NIEL- 567 (1934).  
SEN, J. R.
7. CRIGLER, E.A. Relative intensities of lines in the Raman *Jour. Amer. Chem. Soc.*,  
spectra of benzene toluene mixtures. **54**, 4307 (1932).
8. DAMASCHUN, I. Measurement of relative intensities of *Z. f. Phys. Chem., B.*  
H. Raman lines of inorganic complexes. **22**, 97 (1933).
9. DHAR, J. Relative intensities of Rayleigh and *Ind. J. Phys.*, **9**, 189  
Raman lines in light scattering. (1934).
10. HABERL, K. Intensity measurements of Raman lines. *Ann. d. Phys.*, **21**, 285  
(1934).
11. HANSON, I. Intensity measurements in the Raman *Phys. Rev.*, **46**, 122  
spectrum of carbon dioxide. (1934).
12. LANGSETH, A. Polarisation and intensity measurements *Phys. Rev.*, **46**, 1057  
AND NIELSEN, in the Raman spectrum of carbon  
J. R. dioxide. (1934).
13. LANGSETH, A. Raman effect of the triatomic molecules, *Z. f. Phys. Chem., B.*, **27**,  
AND WALLEs, VI. On the constitution of nitrate ion. 209 (1934).  
E.



**F—Contd.**

14. LANGSETH, A., Raman spectrum of carbon disulphide. Jour. Chem. Phys., **2**, 402  
SØRENSEN, J. (1934).  
U. AND NIELSEN, J. R.
15. ORNSTEIN, L. Overtone  $\Delta\nu=1539$  in the Raman spec- Proc. K. Akad. Amster-  
S. AND WENT, trum of  $\text{CCl}_4$ . dam, **35**, 1024 (1932).  
J. J.
16. ORNSTEIN, L. Dependence of the intensity of the Raman Z. f. Phys., **82**, 750 (1933).  
S., WENT J. scattered radiation of quartz on the  
J., AND ATEN, exciting frequency.  
A.H. W. (JR.)
17. RANGANADHAM, Molecular rotation in liquids. Ind. J. Phys., **7**, 353  
S. P. (1932).
18. RAO, A. V. Rotational Raman effect in liquids. Proc. Ind. Acad. Sc., **1**,  
274 (1934).
19. RAYCHAUDHURI, Correction to my work: the angular dis- Z. f. Phys., **74**, 574 (1932).  
D. P. tribution of intensities of Raman lines.
20. SIRKAR, S. C. Influence of ultra-violet absorption on the Ind. J. Phys., **8**, 67 (1933).  
relative intensities of Stokes and anti-  
Stokes lines in the Raman spectrum.
21. Rotational Raman scattering in benzene Nature, **134**, 850 (1934).  
vapour.
22. Ind. J. Phys., **9**, 295  
(1935).
23. SIRKAR, S. C. Rotational Raman scattering in benzene Ind. J. Phys., **9**, 323  
AND MAITI, B. at different temperatures. (1935).  
B.
24. WENT, J. J. Investigations on Raman effect in crystals. Diss. Amsterdam (1935).

## G

## Polarisation.

1. BÄR, R.           Existence of continuous Raman effect in liquids.   *Z. f. Phys.*, **79**, 455 (1932)
2. BHAGAVANTAM, S.   Intensity relations in the Raman spectrum of hydrogen, II.   *Ind. J. Phys.*, **7**, 549 (1933).
3. CABANNES, J.   Raman spectrum of  $\text{SO}_4^{''}$  in gypsum.   *Compt. Rend.*, **195**, 1353 (1932).
4.                   Depolarisation of light scattered by a uniaxial crystal when the optic axis and the scattered ray are parallel.   *Compt. Rend.*, **196**, 977 (1933).
5. CABANNES, J.   Anomalous depolarisation of Raman lines in uniaxial crystals.   *Compt. Rend.*, **193**, 1410 (1931).  
AND OSBORNE, D.
6. CABANNES, J.   Raman spectrum of water.   *Compt. Rend.*, **198**, 30 (1934).  
AND RIOLS, J. DE
7. CABANNES, J.   Depolarisation of Raman lines in liquids.   *Ann. d. Phys.*, **19**, 229 (1933).  
AND ROUSSET, A.
8. DAURE, P.       The State of circular polarisation of Raman lines in pinene excited by circularly polarised light and observed longitudinally.   *Compt. Rend.*, **198**, 725 (1934).
9. GRASSMANN, P.   Raman effect of aqueous nitrate solutions.   *Z. f. Phys.*, **77**, 616 (1932).
10. HANLE, W.       Circular polarisation of Raman lines, Part II.   *Ann. d. Phys.*, **15**, 345 (1932).
11. HANLE, W.       The broadening of the Rayleigh line.   *Physikal. Z.*, **35**, 1008 (1934).  
AND HEIDENREICH, F.
12. LANGSETH, A.   Polarisation and intensity measurements in the Raman spectrum of carbon dioxide.   *Phys. Rev.*, **46**, 1057 (1934).  
AND NIELSEN, J. R.
13.                Raman spectra of  $\text{N}_3^-$ ,  $\text{NCS}^-$  and  $\text{CO}_2$ .   *Phys. Rev.*, **47**, 198 (1935).

## G—Contd.

14. LANGSETH, A. Raman effect of  $\text{N}_3^-$  and  $\text{NCS}^-$  ions. *Z. f. Phys. Chem., B.*,  
NIELSEN, J. 27, 100 (1934).  
R. AND SØRENSEN, J. V.
15. „ Raman spectrum of carbon disulphide. *Jour. Chem. Phys.*, 2, 402  
(1934).
16. LANGSETH, A. Raman effect of triatomic molecules, VI. *Z. f. Phys. Chem., B.*, 27,  
AND WALLES, E. 209 (1934).
17. MURRAY, J. W. The Raman spectrum of fluorobenzene. *Jour. Chem. Phys.*, 2,  
AND ANDREWS D. H. 890 (1934).
18. ORNSTEIN, L. S. Depolarisation of Raman radiation in *Z. f. Phys.*, 85, 754 (1933).  
AND STOUTENBEEK, P. liquids.
19. PAULSEN, O. Studies in Raman effect, XL. On the *Z. f. Phys. Chem., B.*,  
Raman spectra of cis-trans isomers. 28, 123 (1935).
20. RANGANADHAM, S. P. Molecular rotation in liquids. *Ind. J. Phys.*, 7, 353  
(1932).
21. RAO, I. R. Structure and polarisation of Raman bands *Z. f. Phys.*, 90, 658 (1934).  
of water.
22. ROUSSET, A. The scattering of light and rotation of *Compt. Rend.*, 197, 1033  
molecules in liquids. (1933).
23. SIMONS, L. On the polarisation of the Raman lines of *Soc. Sc. Fenn. Comm.*  
some organic substances. *Phys. Math.*, 6, 58  
(1932).
24. SIRKAR, S. C. Dispersion of polarisation of Raman Lines. *Current Science*, 1, 347  
(1933).
25. „ Effect of electric field on the polarisation of Raman lines. *Ind. J. Phys.*, 8, 377  
(1934).
26. „ Dispersion of polarisation of Raman lines. *Ind. J. Phys.*, 8, 415  
(1934).
27. TRUMPY, B. Depolarisation of the continuous radiation *Kong. Norske Vidensk.*  
accompanying the Rayleigh line in *Selsk. Forh.*, 6, 169  
liquids. (1933).

**G—Contd.**

- |     |                   |                                                         |                                                            |
|-----|-------------------|---------------------------------------------------------|------------------------------------------------------------|
| 28. | ,,                | Intensity distribution and polarisation of Raman lines. | Kong. Norske Vidensk. Selsk. Forh., <b>5</b> , 183 (1933). |
| 29. | TRUMPY, B.        | Raman effect and constitution of molecules, VI.         | Z. f. Phys., <b>88</b> , 226 (1934).                       |
| 30. | ,,                | Raman effect and constitution of molecules, VII.        | Z. f. Phys., <b>90</b> , 133 (1934).                       |
| 31. | VENKATESWARAN, S. | Polarisation of light scattering, Part II.              | Phil. Mag., <b>15</b> , 263 (1933).                        |

## H

## Rotation and Vibration-Rotation Spectra.

1. AMALDI, E.      On the Raman effect in carbon monoxide.    Z. f. Phys., **79**, 492 (1932).
2. AMALDI, E. AND      On the Raman spectrum of gaseous am-    Z. f. Phys., **81**, 253 (1933).  
PLACZEK, G.      monia.
3. ANDERSON, T.      Raman spectrum of deuterium.      Jour. Chem. Phys., **3**, 242  
F. AND YOST,      (1935).  
D. M.
4. BENDER, D.      The rotational Raman spectrum of nitrous    Phys. Rev., **45**, 732  
oxide.      (1934).
5. BHAGAVANTAM,      Anomalous behaviour of methane in the    Nature, **130**, 740 (1932).  
S.      Raman effect.
6.      Raman effect in gases.      Phys. Rev., **42**, 437 (1932).
7.      Rotational Raman effect in liquids.      Ind. J. Phys., **8**, 197  
    (1933).
8. BHAGAVANTAM,      Rotational Raman effect in gases: carbon    Nature, **135**, 150 (1935).  
S. AND RAO,      dioxide and nitrous oxide.  
A. V.
9.      „      Distribution of Intensity in the rotational    Proc. Ind. Acad. Sc., A.,  
    Raman spectra of gases.      **1**, 419 (1935).
10.      „      Rotational Raman effect in liquids, Part I. Ind. J. Phys., **8**, 437  
    Benzene.      (1934).
11. FERMI, E.      On the oscillation and rotation band of    Il Nuovo Cimento, **9**, 277  
    ammonia.      (1932).
12. GLOCKLER, G.      Raman effect of acetylenes, I.      Jour. Chem. Phys., **2**, 881  
AND DAVIS, H.      (1934).  
M.
13. LANGSETH, A.      Raman and infra-red spectra of carbon    Z. f. Phys. Chem., B.  
AND NIELSEN,      dioxide.      **19**, 35 (1932).  
J. R.
14.      On the Raman spectrum of carbon dioxide.    Z. f. Phys. Chem., B., **19**,  
    427 (1932).

**H—Contd.**

15. LEWIS, C. M. Raman effect in ammonia and other gases. *Phys. Rev.*, **44**, 903 (1933),  
AND HOUSTON, W. V.
16. MAGAT, M. Raman spectrum of water (liquid), I. *Jour. de Phys.*, **5**, 347 (1934).
17. NIELSEN, J. R. Rotational structure of the Raman band  $(0000) \rightarrow (020 \pm 2)$  in linear symmetrical molecules  $YX_2$ . *Phys. Rev.*, **44**, 326 (1933)
18. „ „ *Phys. Rev.* **44**, 911 (1933).
19. RAO, A. V. Rotational Raman effect in liquids. *Proc. Ind. Acad. Sc., A*, **1**, 274 (1934).
20. ROUSSET, A. Scattering of light and rotation of molecules in liquids. *Compt. Rend.*, **197**, 1033 (1933).
21. SCHEIB, W. AND LUEG, P. The rotation oscillation spectrum of ethylene. *Z. f. Phys.*, **81**, 764 (1933).
22. SIRKAR, S. C. Rotational Raman scattering in benzene vapour. *Nature*, **134**, 850 (1934).
23. SIRKAR, S. C. Rotational Raman scattering in benzene at different temperatures. *Ind. J. Phys.*, **9**, 323 (1935).  
AND MAITI, B. B.
24. TRUMPY, B. The Rotational Raman spectrum of oxygen at high pressure. *Z. f. Phys.*, **84**, 282 (1933).
25. WILLIAMS, J. W. Molecular scattering of light from ammonia solutions. Fine structure of a vibrational Raman band. *Phys. Rev.*, **42**, 379 (1932).  
AND HOLLAENDER, A.

## I

## Relation to Infra-red Absorption.

1. ADEL, A. Raman spectrum of gaseous carbon dioxide. *Phys. Rev.*, **44**, 691 (1933).
2. ANDANT, A., LAMBERT, P. AND LECOMITE, J. Raman and infra-red absorption spectra of isomeric hexanes. *Compt. Rend.*, **189**, 1316 (1934).
3. BHAGAVANTAM, S. Raman effect in gases. *Phys. Rev.*, **42**, 437 (1932).
4. CASSIE, A. B. D. Investigations in the infra-red region, Part XI. *Proc. Roy. Soc., A*, **148**, 87 (1935).
5. CASSIE, A. B. D. AND BAILY, C. R. Infra-red and Raman band of carbon dioxide, carbonoxysulphide and carbonyl disulphide molecules. *Z. f. Phys.*, **79**, 35 (1932).
6. COSTEANU, G., FREYMAN R. AND NAHERNIAC, A. Study of absorption spectra of liquid, gaseous and dissolved ammonia at the near infra-red. *Compt. Rend.*, **200**, 819 (1935).
7. ELLIS, J. W. AND SORGE, B. W. The Infra-red absorption spectrum of water containing deuterium. *Jour. Chem. Phys.*, **2**, 559 (1934).
8. EUCKEN, A. AND AHRENS, H. Normal oscillations of sulphur hexafluoride. *Z. f. Phys. Chem., B*, **26**, 297 (1934).
9. GRASSMANN, P. AND WEILER, J. The complete Raman spectrum of benzene from 4100 to 5100  $\text{\AA}^{\circ}$ . *Z. f. Phys.*, **86**, 321 (1933).
10. HENRI, V. AND CARTWRIGHT, C. H. Absorption spectra of benzene at high temperature. *Compt. Rend.*, **200**, 1532 (1935).
11. HOWARD, J. B. On the normal vibration frequencies of  $\text{NH}_3$ ,  $\text{PH}_3$  and  $\text{AsH}_3$ . *Journ. Chem. Phys.*, **3**, 207 (1935).
12. LANGSETH, A. AND NIELSEN, J. R. Raman and Infra-red spectra of  $\text{CO}_2$ . *Z. f. Phys. Chem., B*, **19**, 35 (1932).

## I—Contd.

- |                     |                                                            |                                                                                                               |                                           |
|---------------------|------------------------------------------------------------|---------------------------------------------------------------------------------------------------------------|-------------------------------------------|
| 15. L               | 13. LANGSETH, A.                                           | Raman spectrum of carbondioxide.                                                                              | Z. f. Phys. Chem., B.,<br>19, 427 (1932). |
|                     | AND NIELSEN,<br>J. R.                                      |                                                                                                               |                                           |
| 16. M               | 14. „                                                      | Raman spectra of $N_3^-$ , $NCS^-$ and $CO_2$ .                                                               | Phys. Rev., 47, 198,<br>(1935).           |
|                     | 15. MAGAT, M.                                              | On two new Raman bands of water.                                                                              | Compt. Rend., 196, 1981<br>(1933).        |
| 17. NI              | 16. MILLER, O. AND<br>LECOMITE, J.                         | Infra-red absorption spectra of the stereo-<br>isomers of ortho-dimethyl cyclohexane.                         | Compt. Rend., 198, 812<br>(1934).         |
| 18.                 | 17. PAI, N. G.                                             | Raman spectra of iodides, Part I.                                                                             | Ind. J. Phys., 7, 285<br>(1932).          |
| 19. RA              | 18. PARANJPE, G.<br>R. AND SAVA-<br>NUR, K. S.             | Raman effect in organic esters.                                                                               | Ind. J. Phys., 8, 503<br>(1934).          |
| 20. RO              | 19. RANK, D. H.,<br>LARSEN, K. D.<br>AND BORDNER,<br>E. R. | Raman spectrum of heavy water vapour.                                                                         | Jour. Chem. Phys., 2, 464<br>(1934).      |
| 21. SOI<br>L        | 20. RAO, I. R.                                             | Raman effect for water in different states.                                                                   | Phil. Mag., 17, 1113<br>(1934).           |
| 22. SIR             | 21. SARKAR, S. C.                                          | Raman spectra of dimethyl ether, diethyl<br>ether and heptane.                                                | Ind. J. Phys., 7, 257<br>(1932).          |
| 23. SIR<br>AN<br>B  | 22. WEILLER, J.                                            | Raman effect and benzene problem.                                                                             | Z. f. Phys., 89, 58 (1934).               |
| 24. TRU             | 23. WILSON, E. B.<br>(JR.).                                | Normal modes and frequencies of vibra-<br>tion of the regular plane hexagon<br>model of the benzene molecule. | Phys. Rev., 45, 706 (1934).               |
| 25. WII<br>AN<br>DE | 24. „                                                      | A partial interpretation of the Raman<br>and infra-red spectrum of benzene.                                   | Phys. Rev., 46, 146 (1934).               |
|                     | 25. WU, TA-YOU.                                            | The infra-red spectra of the chlorine deri-<br>vatives of ethylene.                                           | Phys. Rev., 46, 465 (1934).               |



# **K**

## **Resonance Radiation, Fluorescence and Phosphorescence.**

1. BAILEY, V. A.    Light absorption, the Raman effect and    Phil. Mag., **13**, 993 (1932).  
                                         the motions of electrons in gases.

- |                                                            |                                                                                                                 |                                                        |
|------------------------------------------------------------|-----------------------------------------------------------------------------------------------------------------|--------------------------------------------------------|
| 1. BLACKMAN, M.                                            | The Raman spectrum of rocksalt.                                                                                 | Naturwiss., <b>21</b> , 367 (1933).                    |
| 2. CABANNES, J.                                            | Depolarisation of light scattered by a uniaxial crystal when the optic axis and the scattered ray are parallel. | Compt. Rend., <b>196</b> , 977 (1933).                 |
| 3. CABANNES, J. AND OSBORNE, D.                            | Anomalous depolarisation of Raman lines in uniaxial crystals.                                                   | Compt. Rend., <b>193</b> , 1410 (1931).                |
| 4. CALLIHAN, D. AND SALANT, E.O.                           | Modified scattering by crystalline HCl and HBr.                                                                 | Jour. Chem. Phys., <b>2</b> , 317 (1934).              |
| 5. FERMI, E.                                               | Raman effect in molecules and crystals.                                                                         | Mem. Real. Acc. Ital., <b>3</b> , 22 (1932).           |
| 6. FERMI, E. AND RASETTI, F.                               | Raman effect in rock-salt.                                                                                      | Z. f. Phys., <b>71</b> , 689 (1931).                   |
| 7. GANESAN, A.S.                                           | Raman effect in selenic acid and selenates.                                                                     | Proc. Ind. Acad. Sc., A., <b>1</b> , 156 (1934).       |
| 8. NAVAR, M. R. AND SHARMA, P. N.                          | Constitution of iodic acid and its salts, II (Raman spectrum).                                                  | Z. f. Anorg. Chem., <b>220</b> , 169 (1934).           |
| 9. NISI, H.                                                | Raman spectra of alkali metal nitrates.                                                                         | Proc. Phys.-Math. Soc., Japan, <b>15</b> , 114 (1933). |
| 10. ,,                                                     | Raman spectra of anhydrite and anglesite.                                                                       | Proc. Phys.-Math. Soc., Japan, <b>15</b> , 463 (1933). |
| 11. ORNSTEIN, L. S., WENT, J. J. AND ATEN, A. H. W. (JR.). | Dependence of the intensity of Raman scattering on the exciting frequency with quartz.                          | Z. f. Phys., <b>82</b> , 750 (1933).                   |
| 12. PAI, N. G.                                             | Raman spectra of iodides, Part I.                                                                               | Ind. J. Phys., <b>7</b> , 285 (1932).                  |
| 13. RAO, C. S.                                             | Raman effect in oxalic acid under different conditions.                                                         | Z. f. Phys., <b>94</b> , 536 (1935).                   |
| 14. RAO, I. R.                                             | Study of electrolytic dissociation by the Raman effect, II. Nitrates.                                           | Proc. Roy. Soc., A., <b>144</b> , 159 (1934).          |

**L—Contd.**

15. RAO, I. R. AND RAO, C. S. Raman frequency of ammonium group. *Z. f. Phys.*, **88**, 127 (1934).
16. RASETTI, F. Raman effect and structure of the molecules and crystals. *Leipziger Vorträge*, **59**, (1931).
17. SALANT, E. O. AND CALLIHAN, D. Modified scattering by crystalline halides. *Phys. Rev.*, **43**, 590 (1933).
18. *Jour. Chem. Phys.*, **2**, 317 (1934).
19. SUTHERLAND, G. B. B. M. Raman effect at very low temperatures. *Proc. Roy. Soc., A.*, **141**, 535 (1933).
20. THATTE, V. N. AND GANESAN, A. S. The Raman effect of inorganic nitrates. *Current Science*, **1**, 345 (1933).
21. VENKATESWARAN, C. S. The Raman spectra of some metallic halides. *Proc. Ind. Acad. Sc., A.*, **1**, 850 (1935).
22. WEILER, J. Fundamental frequencies of the group  $\text{SiO}_4$  in quartz crystals. *Nature*, **130**, 893 (1932).
23. WENT, J. J. Investigations on Raman effect in crystals. *Diss. Amsterdam* (1935).

## M

## Effect of Change of State.

1. BENDER, D. Raman effect of water vapour. *Phys. Rev.*, **47**, 252 (1935).
2. BHAGAVANTAM, S. Raman effect in liquid CO<sub>2</sub>. *Current Science*, **1**, 9 (1932).
3. BRAUNE, H. AND ENGELBRECHT, G. On the Raman effect in a few halogen compounds in liquid and gaseous state. *Z. f. Phys. Chem., B.*, **19**, 303 (1932).
4. CABANNES, J. AND RIOLS, J. DE Raman spectrum of water. *Compt. Rend.*, **198**, 30 (1934).
5. CALLIHAN, D. AND SALANT, E.O. Modified scattering by crystalline HCl and HBr. *Jour. Chem. Phys.*, **2**, 317 (1934).
6. EPSTEIN, H. AND STEINER, W. Raman spectra of benzene and hydrogen iodide in the liquids and solid state. *Nature*, **133**, 910 (1934).
7. Raman effect at low temperatures. *Z. f. Phys. Chem., B.*, **26**, 131 (1934).
8. GRASSMANN, P. Raman effect of aqueous nitrate solutions. *Z. f. Phys.*, **77**, 616 (1932).
9. IMANISHI, S. Raman spectrum of gaseous carbon disulphide. *Nature*, **135**, 396 (1935).
10. McLENNAN, J. C. AND SMITH, H. D. Raman effect for liquid and solid carbon dioxide. *Canad. J. of Research*, **7**, 551 (1932).
11. BANK, D. H. Raman spectrum of water vapour. *Jour. Chem. Phys.*, **1**, 504 (1933).
12. RAO, A. V. Rotational Raman effect in liquids. *Proc. Ind. Acad. Sc.*, **A-1**, 274 (1934).
13. RAO, I. R. Raman effect of water for different states. *Nature*, **132**, 480 (1933).
14. „ Constitution of water in different states. *Proc. Roy. Soc., A.*, **145**, 489 (1934).
15. Raman frequencies of sodium nitrate in different states. *Z. f. Phys.*, **90**, 650 (1934).
16. SALANT, E. O. AND CALLIHAN, D. Modified scattering by crystalline halides. *Phys. Rev.*, **43**, 590 (1933).

**M—Contd.**

17. SALANT, E.O. Modified scattering by crystalline halides. Jour. Chem. Phys., **2**,  
AND CHALLI- 317 (1934).  
HAN, D.
18. SALSTROM, E. Raman spectra of fused salts, Jour. Chem. Phys., **3**,  
J. AND 241 (1935).  
HARRIS, L.
19. THATTE, V. N. The Raman effect of inorganic nitrates. Current Science, **1**, 345  
AND GANESAN, (1933).  
A. S.
20. „ „ „ Ind. J. Phys., **8**, 341  
(1934).
21. VENKATESWA- Raman spectrum of sulphur in solid and Proc. Ind. Acad. Sc., A.,  
RAN, C. S. liquid states. **1**, 120 (1934).
22. WOOD, R. W. Raman spectrum of heavy water vapour. Phys. Rev., **45**, 732  
(1934).
23. YOST, D. M., Raman spectra and molecular constants of Jour. Chem. Phys., **2**,  
STEFFENS, hexafluorides of sulphur, selenium and 311 (1934).  
C. C. AND tellurium.  
GROSS, S.T.

## N

## Effect of Solution and Electrolytic Dissociation.

1. ADERHOLD, H. Raman effect in nitric acid. Z. f. Phys., **88**, 83 (1934).  
AND WEISS, H.  
E.
2. BAUER, E., Raman spectrum of calcium nitrate. Compt. Rend., **197**, 313 (1933).  
MAGAT, M. AND  
SILVEIRA, A. DA
3. BELL, R. M. AND Raman spectra of sulphuric acid solutions. Journ. Chem. Phys., **2**,  
JEPPESEN, M. A 711 (1934).
4. BRAUNE, H. AND Raman effect of certain inorganic halides Z. f. Phys. Chem., B,  
ENGELBRECHT, in the liquid and gaseous states. **19**, 303 (1932).  
G.
5. BRUNETTI, R. Separation of the  $^2F$  levels in Raman spectra of Ce, IV. Z. f. Phys., **75**, 415  
AND OLLANO, (1932).  
Z.
6. FADDA, P. Raman spectrum test for sodium bisulphite Il Nuovo Cimento, **9**,  
in solution. 227 (1932).
7. „ Raman effect of the ions  $SO_4$  and  $SO_3$  and Il Nuovo Cimento, **9**,  
electrolytic dissociation of sulphuric 168 (1932).  
and sulphurous acids.
8. GANESAN, A. S. Raman effect in selenic acid and selenates. Proc. Ind. Acad. Sc., A.,  
**1**, 156 (1934).
9. GERLACH, W. On the two phenomena observed with the Münch. Ber. Nr., **1**, 39  
help of Raman effect (1933).
10. GLOCKER, G. AND Raman effect in di-iod acetylene. Journ. Chem. Phys., **2**,  
MORRELL, C. 349 (1934).
11. GOUBEAU, J. Influence of dissolved metal perchlorate on Naturwiss, **21**, 468  
the Raman frequency of alcohols. (1933).
12. GRASSMANN, P. The Raman effect of aqueous nitrate solutions Z. f. Phys., **77**, 616  
(1932).
13. Z. f. Phys., **82**, 765  
(1933).
14. GUÉRON, J. Raman spectrum of stannic chloride. Compt. Rend., **199**, 945  
(1934).

## N—Contd.

15. HAYASHI, T.      Application of the Raman effect to the investigation of the molecular constitution in organic chemistry, Part I.      Sc. Pap. Inst. Phys. Chem., Res. Tokyo, **21**, 69 (1933).
16. HIBBEN, J. H.      An investigation of intermediate compound formation by means of the Raman effect.      Proc. Nat. Acad. Amer. **18**, 532 (1932).
17. LAIRD, E. R. AND FRANKLIN, D. A.      The Raman spectra of sodium nitrate, sodium acetate and acetic acid.      Phys. Rev., **45**, 738 (1934).
18. LANGSETH, A. AND NIELSEN, J. R.      Raman spectra of some linear triatomic molecules.      Phys. Rev., **44**, 326 (1933).
19. LANGSETH, A., NIELSEN, J. R. AND SPØRRESEN, J. U.      Raman effect of  $\bar{N}_3$  and  $NCS^-$  ions.      Z. f. Phys. Chem., B., **27**, 100 (1934).
20. ME'DARD, L.      The Raman effect in sulphuric acid.      Compt. Rend., **197**, 582
21.      Raman effect in binary mixtures of sulphuric and nitric acids.      Compt. Rend., **199**, 1615 (1934).
22. ME'DARD, L. AND PETITPAS, T. H.      Raman effect in solutions of ammonium nitrate in nitric acid.      Compt. Rend., **197**, 1221 (1933).
23. ME'DARD, L. AND VOLKINGER, H.      Raman effect in nitric acid.      Compt. Rend., **197**, 833 (1933).
24. NAYAR, M. R. AND SHARMA, P. N.      Constitution of iodic acid and its salts, II (Raman spectrum).      Z. f. Anorg. Chem., **220**, 169 (1934).
25. NISI, H.      Raman spectra of alkali metal nitrates.      Proc. Phys-Math. Soc., Japan, **15**, 114 (1933).
26. OLLANO, Z. AND FRONGIA, G.      Multiplicity of certain Raman frequencies of the radical  $NO_3$  in nitrates of valency greater than one.      Il Nuovo Cimento, **10**, 306 (1933).
27. RAO, C. S.      Raman effect in oxalic acid under different conditions.      Z. f. Phys., **94**, 544 (1935).

## N—Contd.

- |                                                              |                                                                                                                               |                                                        |
|--------------------------------------------------------------|-------------------------------------------------------------------------------------------------------------------------------|--------------------------------------------------------|
| 28. RAO, I. R.                                               | Evidence for electrolytic dissociation in sulphuric acid from Raman effect.                                                   | Ind. J. Phys., <b>8</b> , 123 (1933).                  |
| 29.                                                          | Raman frequencies of sodium nitrate in different states.                                                                      | Z. f. Phys., <b>90</b> , 650 (1934).                   |
| 30.                                                          | Study of electrolytic dissociation by the Raman effect, II. Nitrates.                                                         | Proc. Roy. Soc., A., <b>144</b> , 159 (1934).          |
| 31. RAO, I. R.<br>AND RAO, C. S.                             | Raman frequencies of ammonium group.                                                                                          | Z. f. Phys., <b>88</b> , 127 (1934).                   |
| 32. RICCA, V.                                                | On the Raman spectrum of sulphuric acid.                                                                                      | Il Nuovo Cimento, <b>8</b> , 199 (1931).               |
| 33. SILVEIRA, A.<br>DA.                                      | Raman effect in salt solutions.                                                                                               | Compt. Rend., <b>195</b> , 521 (1932).                 |
| 34. „                                                        | Raman effect in solutions of cupric salts.                                                                                    | Compt. Rend., <b>195</b> , 652 (1932).                 |
| 35. „                                                        | Raman effect in aluminium salts.                                                                                              | Compt. Rend., <b>197</b> , 1035 (1933).                |
| 36. SILVEIRA, A.<br>DA. AND BAUER,<br>E.                     | Raman effect in salt solutions.                                                                                               | Compt. Rend., <b>195</b> , 416 (1932).                 |
| 37. SIMONS, L.                                               | Raman effect—measurements of electrolytic solution.                                                                           | Sc. Fenn. Comm. Phys-math. Soc., <b>7</b> , 24 (1934). |
| 38. THATTE, V. N.<br>AND GANESAN,<br>A. S.                   | Raman effect of inorganic nitrates.                                                                                           | Current Science, <b>1</b> , 345 (1933).                |
| 39. VENKATESWARAN, C. S.                                     | The Raman spectra of metallic halides.                                                                                        | Proc. Ind. Acad. Sc., A., <b>1</b> , 850 (1935).       |
| 40. VOGEL, H. H.                                             | Raman spectra of compounds containing carbon-bromine bonds. Possible changes of the vibration frequencies in ionic solutions. | Jour. Chem. Phys., <b>2</b> , 264 (1934).              |
| 41. VOLKINGER,<br>A. TCHAKIRIAN,<br>A. AND FREY-<br>MANN, M. | Raman spectra and structure of metallo-chloroforms.                                                                           | Compt. Rend., <b>199</b> , 292 (1934).                 |



**N—Contd.**

42. WEST, WM. AND Raman spectra of HCl in non-ionizing Jour. Chem. Phys., **2**,  
ARTHUR, P. solvents. 215 (1934).
43. WILLIAMS, J. W. Molecular scattering of light from ammonia Phys. Rev., **42**, 379  
AND HOLLAEN- solutions. Fine structure of a vibra- (1932).  
DER, A. tional Raman band.
44. WOODWARD, Raman effect and the complexity of the Phil. Mag., **18**, 823  
L. A. mercurous and thallous ions. (1934).
45. WOODWARD, Changes in the Raman spectrum of sulphu- Roy. Soc. Proc., A., **144**,  
L. A. AND ric acid on dilution. 129 (1934).  
HORNOR, R. G.

## O

**Effect of Molecular Association, Polymerisation and Intermolecular Field.**

1. ADERHOLD, H. Raman effect in nitric acid. Z.f. Phys., **88**, 83 (1934).  
AND WEISS, H. E.
2. EMBIRIKOS, N. Influence of ions on the Raman bands of Physikal. Z., **33**, 946  
water. (1932).
3. LEITMAN, S. I. Combination-scattering and association of Jour. Chem. Phys., **2**,  
AND UKHOLIN, molecules. 825 (1934).  
S.A.
4. LUCAS, R. Light scattering and molecular polymor- Compt. Rend., **198**, 721  
phism. (1934).
5. MAGAT, M. New Raman bands of water. Compt. Rend., **196**, 1981  
(1933).
6. RAO, C. S. Influence of dissolved electrolytes on the Current Science, **3**, 154  
constitution of water. (1934).
7. RAO, I. R. Raman effect for water in different states. Nature, **132**, 480 (1933).
8. ROUSSET, A. Molecular scattering of light. Jour. de Phys., **3**, 555  
(1932).
9. THORNE, A. M. Raman spectra of two liquid phases of Phys. Rev., **41**, 376  
AND BAYLEY, nitrobenzene. (1932).  
P. L.

## P

## Liquids and Liquid Mixtures.

1. ANGUS, W. R. Raman spectrum of nitrosyl sulphuric acid. *Nature*, **134**, 572 (1934).  
AND LECKIE,  
A. H.
2. BIRCHENBACH, L. Raman effect as the foundation of organic Ber. Deuts. Chem.  
AND GOUBEAU, spectral analysis. Gesell., **65**, 1140  
J. (1932).
3. BOLLA, G. Raman band in water. *Il Nuovo Cimento*, **9**, 290  
(1932).
4. „ „ New Raman bands of water. *Il Nuovo Cimento*, **10**,  
101 (1933).
5. Raman spectrum of ethyl alcohol. *Z. f. Phys.*, **89**, 513  
(1934).
6. „ „ New frequencies in the Raman spectrum *Z. f. Phys.*, **90**, 607  
of ethyl alcohol. (1934).
7. BRODSKY, A. E., Raman effect of arsenic trichloride in solu- *Phys. Z. Sowjetunion*,  
SACK, A. M. AND tion. **5**, 146 (1934).  
BESUGLI, S. F.
8. CABANNES, J. AND Raman spectrum of water. *Compt. Rend.*, **198**, 30  
RIOLS, J. DE (1934).
9. CARRELLI, A. AND On the intensity of Raman effect in water. *Il Nuovo Cimento*, **10**,  
CENNAMO, F. 329 (1933).
10. CHEDIN, J. On the Raman effect in sulphonitric mix- *Compt. Rend.*, **200**, 1397  
tures. (1935).
11. CRIGLER, E. A. Relative intensities of lines in the Raman *J. Am. Chem. Soc.*, **54**,  
spectra of benzene toluene mixtures. 4207 (1932).
12. CUJUMZELIS, Contribution to the Raman effect. *Praktika*, **7**, 242 (1932).  
TH.
13. GLOCKLER, G. AND Fundamental frequencies of acetylene. *Phys. Rev.*, **46**, 233  
MORRELL, C. (1934)<sub>s</sub>.
14. HIBBEN, J. H. An investigation of intermediate compound *Proc. Nat. Acad. Amer.*,  
formation by means of Raman effect. **18**, 532 (1932).
15. HOWDEN, O. H. Continuous spectrum in light scattered by *Trans. Roy. Soc., Canada*,  
AND MARTIN, glycerine and other liquids. **27**, 91 (1933).  
W. H.

**P—Contd.**

- |                                             |                                                                                |                                                       |
|---------------------------------------------|--------------------------------------------------------------------------------|-------------------------------------------------------|
| 16. HOWLETT,<br>L. E.                       | Raman effect in benzene and toluene under high dispersion and resolving power. | Canad. J. of Research,<br><b>3</b> , 572 (1931).      |
| 17. LEITMAN, S. I.<br>AND UKIOLIN,<br>S. A. | Combination scattering and association of molecules.                           | Jour. Chem. Phys., <b>2</b> ,<br>825 (1934).          |
| 18. MAGAT, M.                               | Raman spectrum of liquid water, I.                                             | Jour. de Phys., <b>5</b> , 347<br>(1934).             |
| 19. MÈDARD, L.                              | Raman effect of hydroxyl group.                                                | Compt. Rend., <b>198</b> , 1407<br>(1934).            |
| 20. MIZUSHIMA, S.<br>AND MORENO, Y.         | Investigations on the Raman spectrum of dichloroethylene in benzene.           | Jour. Chem. Soc., Japan<br><b>55</b> , 131 (1934).    |
| 21. PARTHASA-<br>RATHY, S.                  | Raman effect in the study of chemical reactions.                               | Phil. Mag., <b>17</b> , 471 (1934).                   |
| 22. TURPAIN, A.                             | Discovery of molecular diffraction of light in pure liquids.                   | Comp. Rend., <b>197</b> , 1107<br>(1933).             |
| 23. VOGEL, H. H.                            | Raman spectra of compounds containing carbon-bromine bonds.                    | Jour. Chem. Phys., <b>2</b> ,<br>264 (1934).          |
| 24. WEILER, J.                              | Sensitivity of Raman effect in spectral analysis.                              | Verh. Dents. Phys. Ges.<br>(3), <b>13</b> , 5 (1932). |
| 25. WOOD, R. W.                             | Raman spectrum of heavy water.                                                 | Science, <b>78</b> , 588 (1933).                      |
| 26.     "                    "          "   |                                                                                | Nature, <b>132</b> , 970 (1933).                      |
| 27.     "                    "          "   |                                                                                | Nature, <b>133</b> , 106 (1934).                      |
| 28.     "                    "          "   |                                                                                | Phys. Rev., <b>45</b> , 392<br>(1934).                |
| 29.     "                    "          "   |                                                                                | Phys. Rev., <b>45</b> , 565<br>(1934).                |